STALL/SPIN PROBLEMS OF MILITARY AIRCRAFT

ADVISORY GROUP FOR
AEROSPACE RESEARCH AND DEVELOPMENT

JUNE 1976

AGARD-CP-199

AGARD

ADVISORY GROUP FOR AEROSPACE RESEARCH & DEVELOPMENT

7 RUE ANCELLE 92200 NEUILLY SUR SEINE FRANCE

AGARD CONFERENCE PROCEEDINGS No. 199

on

Stall/Spin Problems of Military Aircraft

NORTH ATLANTIC TREATY ORGANIZATION

DISTRIBUTION AND AVAILABILITY
ON BACK COVER

REPORT DOCUMENTATION PAGE			
1. Recipient's Reference	2. Originator's Reference AGARD-CP-199	3. Further Reference ISBN 92-835-0169-1	4. Security Classification of Document UNCLASSIFIED
5. Originator	Advisory Group for Aerospace Research and Development North Atlantic Treaty Organization 7 rue Ancelle, 92200 Neuilly sur Seine, France		
6. Title	STALL/SPIN PROBLEMS OF MILITARY AIRCRAFT		
7. Presented at	the Flight Mechanics Panel Specialists' Meeting held at the Von Kármán Institute, Rhode Saint Genèse, Belgium, 18–21 November 1975.		
8. Author(s) Various			9. Date June 1976
10. Author's Address Various			11. Pages 245
12. Distribution Statement	This document is distributed in accordance with AGARD policies and regulations, which are outlined on the Outside Back Covers of all AGARD publications.		
13. Keywords/Descriptors Military aircraft Stalling Spinning (aerodynamics) Flight maneuvers Aerodynamic stability Flight tests Design			14. UDC 533.6.013.66:533.6.013.7: 623.746

15. Abstract

These proceedings consist of 23 unclassified contributions to the Flight Mechanics Panel Specialists' Meeting on STALL/SPIN PROBLEMS OF MILITARY AIRCRAFT which was held in November 1975. There were 5 technical sessions in which the state-of-the-art in the high angle of attack regime was reviewed under the titles: the Stall/Spin Problem; Analysis and Design Techniques; Test Techniques; and Full Scale Flight Experience. There was a concluding discussion which examined the contemporary problem areas in this important aspect of aircraft design and operation. The findings and recommendations are summarized in the Preface to the proceedings.

AGARD-CP-199

NORTH ATLANTIC TREATY ORGANIZATION

ADVISORY GROUP FOR AEROSPACE RESEARCH AND DEVELOPMENT

(ORGANISATION DU TRAITE DE L'ATLANTIQUE NORD)

AGARD Conference Proceedings No. 199

STALL/SPIN PROBLEMS OF MILITARY AIRCRAFT

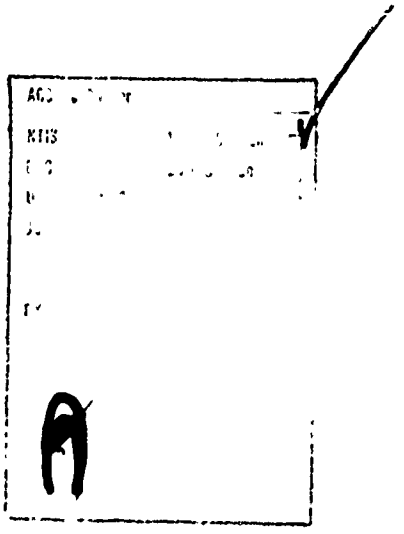

Unclassified papers presented at the Flight Mechanics Panel Specialists' Meeting
held at the Von Kármán Institute, Rhode Saint Genèse, Belgium, 18–21 November 1975

THE MISSION OF AGARD

The mission of AGARD is to bring together the leading personalities of the NATO nations in the fields of science and technology relating to aerospace for the following purposes:

- Exchanging of scientific and technical information;
- Continuously stimulating advances in the aerospace sciences relevant to strengthening the common defence posture;
- Improving the co-operation among member nations in aerospace research and development;
- Providing scientific and technical advice and assistance to the North Atlantic Military Committee in the field of aerospace research and development;
- Rendering scientific and technical assistance, as requested, to other NATO bodies and to member nations in connection with research and development problems in the aerospace field;
- Providing assistance to member nations for the purpose of increasing their scientific and technical potential;
- Recommending effective ways for the member nations to use their research and development capabilities for the common benefit of the NATO community.

The highest authority within AGARD is the National Delegates Board consisting of officially appointed senior representatives from each member nation. The mission of AGARD is carried out through the Panels which are composed of experts appointed by the National Delegates, the Consultant and Exchange Program and the Aerospace Applications Studies Program. The results of AGARD work are reported to the member nations and the NATO Authorities through the AGARD series of publications of which this is one.

Participation in AGARD activities is by invitation only and is normally limited to citizens of the NATO nations.

Published June 1976

ISBN 92-835-0169-1

533.6.013.66:533.6.013.7:623.746

Printed by Technical Editing and Reproduction Ltd
Harford House, 7–9 Charlotte St, London, W1P 1HD

PREFACE

The objectives of this Flight Mechanics Panel Specialists' Meeting on Stall/Spin Problems of Military Aircraft, held at the Von Kármán Institute, Rhode St. Genèse, Belgium in November 1975, were:

to review the state of the art in stall/spin aspects of aircraft design, ground and flight tests, and aircraft operation.

- to discuss the limitations and deficiencies of current design and test methods.

to propose follow-on actions for technological improvements.

to bring together, as is rarely possible, operational pilots, test pilots, flight-test engineers, and specialists involved in design and windtunnel testing.

With the increased emphasis on air-superiority, air defence and tactical fighters, and on advanced trainers, the classic stall/spin demonstration and recovery procedure has broadened to a comprehensive survey of all aircraft behaviour in flight at high angles of attack. The range of interest now extends from the angle of attack where a degradation of flying qualities appears (such as pitch-up, nose slice yaw-off, wing-rock etc.) to the fully developed spin. There are an increasing number of aircraft designs capable of sustained, controlled flight at ultra-high angles of attack.

Thus, the papers presented at the meeting discussed the following important aspects related to the high angle of attack problem area:

- Stall/spin characteristics of military aircraft in service in various NATO countries (France, FRG, Holland, UK, US).

  Operational requirements concerning stall/spin behaviour and, more generally, desirable high angle of attack characteristics of fighters and trainers.

- The importance of stall and departure resistance in combat aircraft. It was pointed out that flight demonstrations of spins and recovery are needed but alone are insufficient as showing compliance with criteria, as, in many cases, excessive altitude is lost during recovery. In this respect, updating the Milspecs to give more detailed and quantitative requirements would be useful.

- The options open to the design team to trade performance, manoeuverability, and good stall/spin characteristics.

- Analytical and experimental design methods and criteria for departure and spin resistance. Interesting applications of Cn_{β}dynamic and LCDP (Lateral Control Divergence Parameter) concepts were shown in various papers. The influence of aircraft configuration (wing planform and position, forebody and afterbody shapes, nose strakes etc ...) was described, as was the correlation of the effect of pitching moment due to sideslip on the departure characteristics with flight tests.

- Analytical spin prediction methods, their validity and limitations (Nonlinearities, asymmetric yawing moments at zero sideslip, unrepresentative aerodynamic coefficients, etc ...).

- Rotary balance techniques for the measurement of static and dynamic aerodynamic coefficients for refined analytical spin studies, (Rotary balance measurements are necessary to represent the proper flow conditions in steady spins).

- Free flight horizontal and vertical tunnel model testing techniques, respectively for stall/departure and steady spin.

- Large scale remotely piloted or preprogrammed models dropped from helicopters or aircraft. Use of sophisticated instrumentation and telemetry coupled with modern parameter identification techniques giving a good aerodynamic description of the high angle of attack characteristics.

- Use of catapults for remotely controlled models for high angle of attack studies.

- Full scale stall-spin flight test techniques and results (In addition to a detailed description of specialized instrumentation and results, a computer graphics display was presented, giving a rapid visualization of the aircraft motion).

- Stall/spin characteristics of some of the new generation fighters and trainers.

- Automatic stall/departure and spin prevention systems.

- Groundbased simulators and pilot-vehicle analysis application to stall/spin.

- Training of student pilots in spinning and recovery techniques.

These subjects were comprehensively covered, and, in addition, many papers were illustrated by films showing full-scale or model tests. An important part of the meeting was the one-day visit to the "Institut de Mécanique des Fluides de Lille", specialized in dynamic testing. In the 4 m diameter vertical tunnel of the Institute, the spin characteristics of a number of aircraft were demonstrated to the visitors.

The main conclusions resulting from the presentation of 28 papers and the subsequent discussions are:

The basic tool for spin studies is still the vertical tunnel; however, the general high angle of attack problem requires the use of many other techniques. Moreover, on some configurations, due to significant scale effect, the interpretation of the results obtained can be difficult. In this respect the experience gained by the European and US specialists is not entirely similar. The differences can certainly be reduced by some cooperative effort.

Many aircraft of the sixties presented high angle of attack deficiencies which led to a significant number of accidents; now, a better understanding of the complex interference phenomena and of the departure/spin mechanism, more comprehensive model testing, and the use of better design methods result in substantial improvements for the new generation fighters, enhancing their manoeuvering capability.

- High angle of attack behaviour can also be improved by control systems designed for the automatic prevention of stall/departure and spin. In this respect the CCV concept offers some promising opportunities.
- From the operational viewpoint it was indicated that:

  (a) comprehensive flight tests must be carried out to explore the high angle of attack behaviour in the whole flight envelope, including representative external store configurations. This is the condition to allow the full operational use of the performance potential of the aircraft. (One of the papers presented describes some problems encountered in this area in the latest development stage of a fighter).

  (b) the availability of aircraft for spin training is highly desirable.

Written comments were solicited from the participants, and the meeting ended with a round table discussion with the theme: *Design Methods for Spin Prevention and Spin Control*

It was observed that the meeting had been an excellent opportunity to review the present knowledge in this relatively new area and, more importantly, to identify problems where more research and development is needed. It was shown that, on a modern combat aircraft, the stall/spin characteristics must be considered from the preliminary design stage, and the prediction of those characteristics, using both analytical and experimental methods, must be refined progressively in the design development. The difficulties of achieving a proper balance between various possibilities, including the cost/effectiveness viewpoint, have been recognized. In particular, ways must be found to simplify and to reduce the cost of the promising RPRV technique.

The following actions have been recommended:

- Active cooperation between European and US specialists, in particular in the area of vertical tunnel testing and free flight models. Contacts have been arranged for the near future.
- Application of departure/spin criteria to various aircraft and exchange of information about the results.

  Promotion of refined analytical flight dynamic studies of high angle of attack behaviour. (The data input to these studies would be based on extensive static and dynamic wind tunnel tests up to 90° of angle of attack and 30 to 40° of sideslip). The difficulties created by the highly nonlinear aerodynamic characteristics and by scale effect must be solved by the development of adequate testing facilities, specialized testing equipment, and testing methods.
- Periodic review of the high angle of attack problems either through the medium of similar specialists' Meetings or by Working Groups sponsored by AGARD.

G.P. BATES, Jr
Member
Flight Mechanics Panel

J. CZINCZENHEIM
Member
Flight Mechanics Panel

CONTENTS

	Page
PREFACE	iii
	Reference
THE STALL/SPIN PROBLEM by R.J. Woodcock and R. Weissman	1
THE STALL/SPIN PROBLEM – AMERICAN INDUSTRY'S APPROACH by C.A. Anderson	2
SOME EUROPEAN SPIN EXPERIENCE	
(A) COMPARISON OF THE SPIN AND A LOW INCIDENCE AUTOROTATION OF THE JAGUAR STRIKE AIRCRAFT by R.J. Blamey	3A
(B) A FEW REMARKS CONCERNING SOME STALL/SPIN EXPERIENCE IN THE NETHERLANDS by J. Hofstra	3B
(C) GERMAN AIR FORCE OPERATIONAL SPIN EXPERIENCE by D. Thomas	3C
A COMPARISON OF MODEL AND FULL SCALE SPINNING CHARACTERISTICS OF THE LIGHTNING by B.R.A. Burns	4
DESIGN TECHNOLOGY FOR DEPARTURE RESISTANCE OF FIGHTER AIRCRAFT by A. Titiriga, Jr, J.S. Ackerman and A.M. Skow	5
RESULTS OF RECENT NASA STUDIES ON SPIN RESISTANCE by J.R. Chambers, W.P. Gilbert and S.B. Grafton	6
APPLICATION DES MESURES DE COEFFICIENTS AERODYNAMIQUES STATIQUES ET DYNAMIQUES A DES RECOUPEMENTS PAR CALCUL DES VRILLES OBTENUES EN SOUFFLERIE par M. Vanmansart	7
STALL BEHAVIOUR AND SPIN ESTIMATION METHOD BY USE OF ROTATING BALANCE MEASUREMENTS by E. Bazzocchi	8
STABILITY OF HELICOIDAL MOTIONS AT HIGH INCIDENCES by F.C. Haus	9
EVOLUTION DES CARACTERISTIQUES DE LA VRILLE EN FONCTION DE L'ARCHITECTURE DES AVIONS par J. Gobeltz	10
LIMITING FLIGHT CONTROL SYSTEMS by D.K. Bowser	11
ASYMMETRIC AERODYNAMIC FORCES ON AIRCRAFT FOREBODIES AT HIGH ANGLES OF ATTACK – SOME DESIGN GUIDES by G.T. Chapman, E.R. Keener and G.N. Malcolm	12
STALL/SPIN TEST TECHNIQUES USED BY NASA by J.R. Chambers and J.S. Bowman, Jr	13
ACTION SUR LA VRILLE, PAR MOMENT 'STATIQUE', DE FUSEES ET DE CHARGEMENTS DISSYMETRIQUES par J. Gobeltz et L. Beaurain	14

Reference

UNE NOUVELLE ANALYSE DE LA VRILLE BASEE SUR L'EXPERIENCE FRANCAISE SUR LES AVIONS DE COMBAT
par C. la Burthe 15A

SPIN INVESTIGATION OF THE HANSA JET
by H. Neppert 15B

METHODES D'ESSAIS DE VRILLES EN VOL
par J.P. Duval 16

F-14A STALL AND SPIN PREVENTION SYSTEM FLIGHT TESTS
by C.A. Sewell and R.D. Whipple 17

ESSAIS DE VRILLES DU JAGUAR, DU MIRAGE F1 ET DE L'ALPHA-JET
par J. Differ, J.P. Duval et J. Plessy 18

YF-16 HIGH ANGLE OF ATTACK FLIGHT TEST EXPERIENCE
by J.P. Lamers 19

U.S. NAVY FLIGHT TEST EVALUATION AND OPERATIONAL EXPERIENCE AT HIGH ANGLE OF ATTACK
by A.F. Money and D.E. House 20

THE STALL/SPIN PROBLEM

by

Robert J. Woodcock
Principal Scientist
Control Criteria Branch
Flight Control Division
Air Force Flight Dynamics Laboratory
Wright-Patterson AFB, Ohio 45433

Robert Weissman
Chief, Stability and Control Branch
Aeromechanics Division
Aeronautical Systems Division
Wright-Patterson AFB, Ohio 45433

SUMMARY

Stall/spin problems, as old as the history of airplane flight, still plague aircraft designers. Aircraft configurations are driven by performance demands, while at high angle of attack our capability to analyze potential problems - or to devise solutions - has remained limited. Simple prediction methods are not always enough, and data inadequacies impair the usefulness of more sophisticated analysis. The development of spin tunnel and free-flight model testing techniques is traced, prospects of improved aerodynamics indicated, and some flight control system capabilities outlined, with reference to experience with some recent airplanes. We retain interest in recovery from spins and post-stall gyrations, but see a need for more emphasis on designing for resistance to loss of control.

The early glider flights of the Wright brothers often ended by dropping off on one wing, out of control, with a wingtip eventually striking the Kitty Hawk, North Carolina, sand in a rotary motion. While the low altitude of these flights prevented motion from developing fully, it seems clear that these were departures into incipient spins.

In those early days of manned flight the spin was as dangerous as it is today. When the Wright brothers first tried warping the wings to roll into a turn, they found that the banking was accompanied by a dangerous tendency to diverge in yaw at high angle of attack[1]. Adding a fixed vertical fin helped stabilize the 1902 glider, but the loss-of-control problem persisted. Orville Wright reasoned that a hinged vertical rudder could produce a counter yawing moment to keep the yaw from starting and thus enable the flyer to remain under control. This was tried first with rudder deflection connected to the wing-warp control, then with the pilot controlling the rudder separately. The fix was effective but required the pilot's constant attention. Proper spin recovery controls were not generally known until 1916, when flight test experiments on spin recovery procedures were conducted at the Royal Aircraft Factory, Farnborough, in an F E 8[2]. Wing Commander Macmillan is responsible for a fascinating early history of the spin in Aeronautics, 1960-62 issues. For early airplanes the spin recovery technique was at least rational if not instinctive: forward stick and rudder opposing the yawing motion should stop the rotation and install the wing. Once these recovery controls were known, WWI pilots used the spin as a maneuver to lose altitude without gaining airspeed[3]. Then in the 1920s some of the more peculiar spin modes were recognized as problems. Accident summaries from that era[4,5,6] show spins involved in about three percent of all accidents reported and in twenty to thirty percent of the fatal accidents.

Analytical studies and dynamic wind tunnel testing to reduce the stall/spin problem were reported in England as early as 1917. Autorotation was observed in the wind tunnels, and the first analytical prediction methods were developed by Glauert and Lindemann. Gates and Bryant presented a comprehensive survey of spinning[7] in 1927. About 1930, a method of determining the flight path and altitude of a spinning aircraft was put into use[8]. Rotation rates about and accelerations along the principal axes, as well as vertical velocity were measured and recorded photographically. This information was used to define the motion of the aircraft, which could then be used in conjuction with the analytical prediction methods.

In the 1920s and 1930s several forms of testing were being performed. One safety measure used in full-scale testing was to attach external ballast, which when released would cause the center of gravity of the airplane to move forward, thus returning the airplane to a controllable configuration[9]. Because of the hazards involved in stall/spin flight testing, researchers hesitant to use full-scale aircraft tried free-flight models. One of the early spin models was dropped from the top of a 100-foot balloon hangar at Langley Field. This proved an inadequate means of obtaining data, and soon vertical wind tunnels were being built to investigate spinning (1930 in the United States, 1931 in England). In 1945 the U.S. Army Air Force dropped an instrumented model from a Navy blimp to study spin entry and recovery.

As jet aircraft were developed, the inertial characteristics of fighters in particular were changed to the point that spins and other post-stall motions became more troublesome and even required different recovery techniques. By the time of the 1957 Wright Air Development Center Spin Symposium[10], most stall/spin problems were identified, some analysis methods had been developed, and the electronic digital computer provided a useful tool with which to examine the stall/spin problem[11].

Then suddenly the emphasis was shifted to space. With little management interest and rather poor expectations of improvement, resources for stall/spin research were quite limited. Instead our Air Force tended to concentrate on performance improvements, which often have aggravated stability and control problems at high angles of attack. Today, a large and costly Air Force accident record and a renewed emphasis on maneuver capability have led to a larger concentrated effort to solve the problems associated with aircraft operating in the stall/spin flight regime[12].

Large aircraft have also experienced stall/spin problems. For example, several B-58s were lost in spins. Automatic trimming of the control-stick force was mechanized in such an insidious way that an inattentive pilot might not be aware of a slowdown to stall speed. Trouble with fuel management could result in an extreme aft center of gravity, at which B-58 stability and control were deteriorated. The C-133, on long flights, would climb to an altitude approaching its absolute ceiling. Poor stall

warning and a vicious stall while trying to fly there are thought to have caused the disappearance of several C-133 aircraft. It has become customary to require analysis and spin tunnel testing of all U.S. military airplanes even though flight demonstration of large, low-maneuverability types is limited to stalls with only moderate control abuse[13].

The military specification[14] for flying qualities defines good high-α characteristics in terms that are qualitative rather than quantitative. The airplane must exhibit adequate stall warning, and in addition the stall must be easily recoverable. We now emphasize resistance to violent departures from controlled flight, while retaining requirements for recovery from attainable post-stall motions. The definitions of good high-angle-of-attack characteristics will differ for the various classes of aircraft; but with respect to fighter aircraft, a pilot should not have to worry about loss of control while flying within his useful maneuver envelope. We shall need quantitative requirements that will be of more use in the design stage for all classes of airplanes.

Generally post-stall design and testing have emphasized spins and spin recovery, taking the point of view that assurance of recoverability from the worst possible out-of-control situation guarantees safety. This philosophy falls short in several respects. Resistance to departure has not been emphasized adequately. The motions can be disorienting, and recovery control inputs such as ailerons with the spin are unnatural. And as airplanes grow larger and heavier, altitude loss becomes excessive. F-111 instructions, for example, are to eject if spin recovery has not commenced upon reaching 15,000 feet altitude. Spins and spin recovery should not be neglected, but emphasis needs to shift to departure resistance and early recovery.

STATUS OF TECHNOLOGY

Recent studies of current Air Force fighters have developed additional insight into their high-angle-of-attack problems. Also, initial F-14 and F-15 flight results show that substantial improvements can be secured by concentrated design attention. But design effort is very large, trade-offs are uncertain, and confidence is unsure until after thorough flight demonstration. There remains the need to establish definitive requirements and develop a greatly expanded basis for aerodynamic and flight control design. To that end, improved design methods and criteria are being sought for the high-α characteristics of present and future aircraft.

Except for a few rules of thumb, analytical stall/spin work is based on the mathematical equations that describe the motion of an aircraft. The general equations of motion involve both inertial and aerodynamic nonlinearities. For the large-amplitude motions associated with stall/post-stall flight, linearization of the equations is of limited value, while using the nonlinear equations makes generalization difficult. The primary reason for inaccurate prediction of high-angle-of-attack characteristics is the insufficient quality of the available aerodynamic data. Analysis of the three-dimensional separated flow field is most difficult.

The principal U.S. source of high-α static aerodynamic data at high Reynolds number has been the National Aeronautics and Space Administration Ames 11-foot and 12-foot wind tunnels. (Figure 1) Although flow irregularities and mount limitations there have limited the validity of data taken, these deficiencies are to be rectified. The Arnold Engineering Development Center 16-foot transonic tunnel also has a high Reynolds number capability, but no existing facility can reach the flight Reynolds numbers of full-scale airplanes. Still, exceeding critical Reynolds number appears to be the most important test requirement. NASA has had a small rotary balance in the spin tunnel and now is employing a new rotary balance in the Langley 30-foot by 60-foot tunnel. Rotary and oscillatory dynamic testing are expected to produce different aerodynamic results[15]. NASA Ames is also working on improved dynamic wind tunnel testing apparatus.

The steady spin and recovery can be investigated in a vertical wind tunnel, but the dynamically scaled spin tunnel aircraft models are rather small. Moreover, a more fundamental limitation is that the models are tossed into the tunnel much as a Frisbee is launched; it takes more skill than we possess to determine entry characteristics, although Gobeltz has shown some capability in his spin tunnel at Lille. Also at NASA Langley, models of about 3-foot span are flown in the 30-foot by 60-foot tunnel, with power and control signals transmitted through an umbilical cord. (Figure 2) This method enables 1-g stalls and initial departures to be studied in conditions resembling free flight.

Free-flight model testing has also taken the forms of catapulted models (recorded by multiple-exposure photos), (Figure 3) and radio-controlled models dropped from blimps, lightplanes, or helicopters. In the U.S., Bowman has done much of this at Langley. Free-flight model test results have been found generally to agree qualitatively with full-scale results despite Reynolds number differences. But from cost and time considerations most of these tests have followed, rather than preceded, full-scale tests at high angle of attack.

In design development, drop model testing can be coupled with recently developed parameter identification techniques to supply both the aerodynamic description and an indication of the real airplane behavior at high angles of attack. A large-scale model can allow both a better match of Reynolds number and the internal volume required for extensive telemetry equipment and sensors. Telemetry is used to gather detailed data for later analysis and possibly also for modeling an active flight system. The model can enter stall/departure from maneuvers as well as from 1-g flight, and the entire motion from onset through recovery can be experienced. The quickened time scale, however, will not permit a direct pilot evaluation of flying qualities. The model can be used to provide information at extreme flight conditions, with no danger to the pilot. Variations of this technique are currently being pursued by the NASA Flight Research Center (F-15), Air Force Flight Dynamics Laboratory and Flight Test Center (YF-16), NASA Langley Research Center (various models), and the Royal Aircraft Establishment, Bedford. In another program at Langley, smaller models with simpler instrumentation and controlled with hobby equipment are being investigated to see how much can be learned from a minimum-cost drop model program aimed at general aviation. Figure 11 shows a 0.30-scale YF-16 drop model ready for installation on a helicopter in preparation for stall/spin testing at the Air Force Flight Test Center.

The analysis of high-angle-of-attack flight characteristics has been a subject of increased interest and importance over the past few years. No one here needs to be reminded that uncontrollable yaw and/or roll divergence at or near the stall prevents unrestricted use of an airplane's full maneuvering capability and occasionally results in the loss of an airplane and crew. In military service not only fighter type aircraft but bomber and cargo aircraft too have experienced stall/spin problems. The stall/spin problem has also been responsible for a great many losses of life and equipment in the civil aviation field.

During the past decade we have seen the development of numerous configurations of jet-powered fighter and transport airplanes. Transport aircraft, in general, have been characterized by a moderately swept-back wing of medium aspect ratio in combination with innovations such as fuselage-mounted engines and tee-tails, all leading to a fundamental change in stall characteristics. High-performance fighter aircraft design has only recently emphasized the need for good flying qualities at high angles of attack. Unfortunately, definition of the configuration features which contribute favorably to those flying qualities is far from complete.

The potential for conducting meaningful analytical investigations to determine stability and control characteristics at high angle of attack is considerably better today than in the past. Computers have been developed to the point where solution of the six-degree-of-freedom equations of motion poses few problems of cost, programming, computation time, etc. There is a consensus that, in the design process, dynamic characteristics should be investigated at angles of attack to and beyond stall on every aircraft and at even higher angles of attack (i.e., up to 90 degrees) and also high sideslip angles (i.e., up to 30-40 degrees) on some types of aircraft. It is generally agreed that a full statement of aerodynamic characteristics obtained in the wind tunnel provides a good basis at least for near-stall stability and control analysis, but that there are many unresolved problems associated with the validity of data at much higher angles of attack.

Analytical studies are being conducted with these data, for example Reference 16, and results correlated with free-flight model and full-scale flight test results. Attempts at correlation have had varying degrees of success. The analytical technique most commonly employed to study stall/spin problems involves a simultaneous solution of the equation of motion and associated formulas. Near-stall stability and control analysis using this technique correlates better with experimental test results than does analysis of developed spin modes. Good matching of spin modes and recovery characteristics with free-flight model and full-scale flight test results is seldom obtained with a computer solution. On the other hand, spin tunnel and free-flight dynamically similar scale model test results correlate reasonably well with full-scale airplane test results. If we are to resolve problems associated with the validity of data and analysis, a continuing effort is needed which includes research as well as work on aircraft now under development.

ANALYSIS AND DESIGN TECHNIQUES

A considerable amount of work has been completed, and more is being planned, to identify configuration features which either promote or delay departures from controlled flight and which contribute favorably toward spin recovery [17-22]. The influence of wing planform and position have been investigated with symmetrical fuselage shapes as well as on specific airplane configurations. Wind tunnel investigations are needed to determine the integrated effects of forebody and afterbody shapes, inlet ducts, vertical wing position, wing leading edge flaps, single and twin vertical fins, horizontal stabilizer position, and strakes on lateral-directional static stability characteristics at high angles of attack. Identification of those features which are stabilizing and/or provide favorable interference effects on other components can provide guidelines for the design of new aircraft (or the modification of existing aircraft) with inherently good high angle of attack flight characteristics, and design data needs to be compiled. Examples of some such work on lateral-directional stability characteristics are shown in Figures 4 through 7[17].

Figure 4 shows the effect of forebodies with elliptical cross sections on directional stability. For the fuselage alone, both forebodies exhibit a destabilizing characteristic up to about 30 degrees angle of attack. However, the horizontal elliptical forebody (forebody A) shows a stable break and then becomes stable above 30 degrees.

Figure 4 also shows the effect of forebody shape when a vertical tail is added. Forebody A exhibits good directional stability over a large range of angles of attack as compared to the forebody shaped as a vertical ellipse (forebody B).

The effect of wing position on forebody A, which now includes a ventral inlet as well as a vertical tail, is shown in Figure 5. At high angles of attack the low wing produces significantly better lateral-directional stability than does the high wing. Apparently the low wing has less adverse effect on the body and a more favorable effect on vertical tail effectiveness.

One final example has to do with the effect of forebody strakes on lateral-directional stability. It was found that a forebody strake contributes favorably to lateral-directional stability, as indicated in Figure 6, and that the length of the strake affects the degree of improvement. Because of their location, these forebody strakes produce a longitudinal destabilizing effect as shown in Figure 7. The effect is minimal for the short strake (the one most effective from a lateral-directional standpoint).

Flow visualization tests are invaluable for obtaining an understanding of the nature of flow phenomena causing aerodynamic pro-spin moments at developed spin angles of attack or a loss of lateral-directional stability at stall. Flow visualization studies have been conducted on several fighter-type aircraft[21,22] after lateral-directional stability problems were encountered during flight testing. But then even if a seemingly minor aerodynamic modification will correct the problem often it cannot be accomplished because of high cost, impact on production schedules, etc., a situation that some of us here have been faced with. Flow visualization studies at high angle of attack can be considered a necessity for design of an air superiority aircraft, and they can be a great help in designing other aircraft.

The problems experienced with analytical studies of stall/post-stall/spin characteristics seem to be associated with the aerodynamic model. If the aerodynamic model is based on wind tunnel data at low Reynolds number then the results obtained may be misleading for some configurations. The use of dynamic stability derivatives (as determined from forced-oscillation tests) to compute developed spin motions has met with limited success in matching the motions obtained from free-flight models or spin tunnel tests. The aerodynamic moments generated in a developed spin due to steady rotational flow appear to be significant. A rotation-balance is required to obtain data while the model is rotating and under the same local flow conditions that exist in an actual spin[23].

Analytical studies with the objective of matching model and full-scale departure characteristics have had some success, though fudging of the data is not uncommon. Exact matching is seldom if ever achieved, but there has been good correlation with respect to the degree of spin susceptibility and the type of departure-that is, a strong yaw divergence or a rolling departure. In any case there must be a fully defined statement of aerodynamic characteristics. Dynamic derivatives may be obtained with the forced-oscillation technique, rotary derivatives obtained with the use of a rotation-balance, and data measured in increments as small as one or two degrees in angle of attack and sideslip at near stall angles of attack.

Over the past few years there have been several studies conducted to investigate initial design criteria for predicting departure characteristics and spin susceptibility of fighter-type aircraft. These criteria use static aerodynamic characteristics since static-force test data are among the first data obtained during the initial design stages. The designer has available basic data early in preliminary design from which stability and control analysis can be started, in order to determine whether or not the airplane might experience problems at near-stall angles of attack. A main objective of these studies has been to verify or extend existing stability criteria, and possibly develop new criteria which can be used with a reasonable degree of confidence for a first-out prediction of full-scale aircraft departure characteristics and spin susceptibility as early as possible in the design stage.

Some of the parameters developed for predicting aircraft departure characteristics and spin susceptibility[24-29] are shown in Figure 8. There has been a considerable amount of effort to correlate the dynamic directional stability parameter $Cn_{\beta DYN}$ and the lateral control divergence parameter, LCDP, with experimental data as well as with results of analytical studies. The studies described in References [25] and [26] are recent examples. Figure 9 illustrates the use of the $Cn_{\beta DYN}$ and LCDP parameters for predicting departure characteristics and spin susceptibility[27-28]. The parameters are calculated for a range of near-stall angles of attack. Then depending upon where values of the criteria plot, a judgment can be made regarding departure and spin susceptibility.

Another criterion for predicting departure angle of attack is the "β plus δ Axis Stability Indicator" (Figure 8, equations 4 and 5). A detailed derivation and explanation of this criterion can be found in Reference[29]. Figure 10 illustrates the use of this criterion. In order to predict aircraft departure angles of attack, $\alpha_{-\beta}$ and α_{δ} are plotted over the desired range of aircraft angles of attack. If the α_{δ} line is above the $\alpha_{-\beta}$ line at a given angle of attack or if $\alpha_{-\beta} < 0$, then a tendency toward instability can be expected at the lower of these angles of attack. Because of the direct relationship between $Cn_{\beta DYN}$ and $\alpha_{-\beta}$, when $\alpha_{-\beta} = 0$ then $Cn_{\beta DYN} = 0$. Also, when $\alpha_{-\beta} = \alpha_{\delta}$ then LCDP = 0.

Generally the stability derivatives used in calculating these various criteria are applicable over only a small sideslip angle range, for example ±5°. The higher the angle of attack, the more nonlinear Cn and Cl versus β become and it is possible to calculate positive values for, say $Cn_{\beta DYN}$ over a small β range and negative values over a larger β range (e.g., ±10°). Consequently, the aerodynamic data used in calculations should also take into account nonlinearities over the large as well as over the small β range. The uncertainty of determining dynamic response of a nonlinear system in terms of linear parameters is one significant shortcoming of these methods, the other being a degree of oversimplification even for aerodynamics that are linear with sideslip. Nevertheless, these rules of thumb can give valuable early indication of potential problems.

Despite the problems that have been and will continue to be encountered regarding correlation of analytical and experimental results, analytical studies can play an important role in exploring the overall spin problem. Reference[30] extends closed-loop pilot-vehicle analysis to coupled longitudinal and lateral-directional motion at combined angles of attack and sideslip. Reference[20] is an example of a program now in progress to investigate the stall/spin characteristics of a CCV fighter aircraft and to establish configuration design guidelines.

Although much progress has been made in analyzing and understanding the effects of configuration features on aerodynamic characteristics at high angle of attack, analytical studies cannot and should not be considered a substitute for full-scale flight test programs. However, they can augment the knowledge gained from such programs as well as providing important information either during preliminary design or for possible configuration changes to existing aircraft.

THE OUTLOOK

The increased attention now given to stall/spin characteristics is in itself a major step forward. Relatively simple fixes have been found which, while not eliminating stall spin problems, have provided significant improvement. Such a fix is the F-111 Stall Inhibitor System, which has been flown. While the flight-test program stopped short of extreme maneuvers, the combination of additional directional stability augmentation and a high stick force gradient in pitch near the limit angle of attack appears to be an effective departure deterrent. For one thing, the stability augmentation forces the airplane to roll more about its flight path than about its body X axis. On the F-4, leading-edge slats now delay both buffet onset and departure to a higher angle of attack. Also, Air Force Flight Dynamics Laboratory's Tactical Weapon Delivery (TWeaD) program demonstrated the effectiveness of improved stability augmentation at angles of attack below departure for a standard F-4. On a simulator, Calspan Corporation has demonstrated[31] that a somewhat more sophisticated change in the flight control system can essentially eliminate A-7D departures, and Vought independently has derived an aerodynamic modification, a wing leading-

edge extension next to the fuselage, that gives significant improvement. The F-14 also uses the flight control system to improve departure resistance: "The magnitude of the yawing moment required for a spin cannot be developed when the stick is laterally centered at spin angles of attack."[32] A highly successful example of effective control-limiting is the T-38/F-5, which has a potential unrecoverable flat spin mode. While stabilizer authority is adequate for other uses, it is limited to the extent that, in flight test, only abrupt full aft stick held for a long time would develop a spin. Spins have not been encountered at all in T-38/F-5A, B operational use.

We feel strongly that, despite the possible capabilities of a flight control system, there is no substitute for careful aerodynamic design. Nevertheless, other factors may dictate use of the flight control systems to prevent departure from controlled flight. Air combat effectiveness, excessive altitude loss, possible pilot disorientation, and perhaps an unnatural recovery technique are some considerations in further limiting airplane motions.

It can be said that in order to improve aerodynamic design capability, better tools are needed. High-α aerodynamic theory is a long-term project, although intermediate results will be helpful we look for progress in the form of fundamental flow theory including viscid-inviscid interaction, with highly instrumented wind tunnel models to provide data and validation; new dynamic model mounts for wind tunnel testing; and free-flight models improved at both ends of the cost spectrum. Simple, less expensive free-flight testing of relatively small models can be helpful early in design, while the effects of stability augmentation, etc., can be investigated with larger, more elaborate free-flight models in time to aid the full-scale flight tests.

Although flying qualities in the normal flight regime can be specified quantitatively in great detail, the complications of non-linearities and coupled motions near the stall region have precluded the statement of criteria that could be very helpful to the designer. Qualitative statements of general aircraft behavior at the stall region are of limited help. Groundbased simulators with enhanced visual or motion capability, or both, offer a safe, efficient way to conduct preliminary pilot evaluations. Pilot-vehicle analysis has been instrumental in recasting dynamic requirements for lower angles of attack, and now we may be able to extend these techniques to the stall/spin region. The goal of the flying-qualities efforts is to derive and quantify motion and vehicle parameters and to develop analysis techniques that can be related directly to airplane design.

On the other hand, we realize that "design trade-off" is a synonym of "compromise." Thus, we will never be rid of stall/spin problems even if we should come to understand the phenomena thoroughly. But there are several approaches that need to be followed in order to make these design trade-offs possible on a basis approaching rationality.

REFERENCES

1. Wright, O., Stability of Aeroplanes, Journal of the Franklin Institute, September 1914. Reprinted by the Smithsonian Institution, 1915.

2. Glauert, A., The Investigation of the Spin of an Aeroplane, ARC R&M, No. 618, June 1919.

3. Sutton, N.A., Tail Spins, paper presented at the 18th National Meeting of the SAE, August, 1930.

4. Analysis of Aircraft Accidents, Air Corps Information Circular, Vol. 4, No. 340, 1 May 1922.

5. Analysis of Aircraft Accidents, Air Corps Information Circular, Vol. 7, No. 633, 24 November 1928.

6. Statistical Studies of Aircraft Accidents and Forced Landings, Air Corps Information Circular, Vol. 7, No. 652, 28 June 1930.

7. Bryant, L.W., and Gates, S.B., The Spinning of Aeroplanes, Jour. Royal Aeronautical Society, Vol. XXXI No. 199, July 1927.

8. Weick, F.E., The Present Status of Research on Airplane Spinning, paper presented at the 18th National Meeting of the SAE, August 1930.

9. Sutton, op. cit.

10. Wright Air Development Center Airplane Spin Symposium, February 1957.

11. Wykes, J.H., An Analytical Study of the Dynamics of Spinning Aircraft, WADC TR-58-381, February 1960.

12. AFFDL/ASD Stall/Post-Stall/Spin Symposium, December 1971 (hereafter cited as AFFDL/ASD Symposium).

13. MIL-S-83691A, Military Specification, Stall/Post-Stall/Spin Flight Test Demonstration Requirement for Airplanes, 15 April 1972.

14. MIL-F-8785B (ASG) Amendment 2, Military Specification, Flying Qualities of Piloted Airplanes (Amendment 2 to be published shortly).

15. Tobak and Schiff, L.G., A Nonlinear Aerodynamic Moment Formulation and Its Implications for Dynamic Stability Testing, AIAA paper 71-275, March 1971.

16. Adams, W.M., Analytical Predictions of Airplane Equilibrium Spin Characteristics, NASA-TN D-6926, November 1972.

17. Brassard, J.A., Robinson, L.D., Strong, K.L., Configuration Effects on Lateral/Directional Stability at High Angles of Attack, LTV Aerospace Corp. (VSD), 2-53363/4R-3171, July 1974.

18. Skow, A.M., F-5E/F Yaw Departure Analysis, Northrop Aircraft Div., AR 75-5, May 1975.

19. Grafton, S.B., Chambers, J.R., Coe, P.L., Jr. Wind Tunnel Free-Flight Investigation of a Model of a Spin-Resistant Fighter Configuration, NASA TN D-7716, June 1974.

20. Watson, J.H., Kouri, B.G., Wilson, J.W., Stall/Spin Susceptibility Characteristics of CCV Fighter Aircraft, General Dynamics ERR-FW-1606, December 1974.

21. Chambers, J.R., Bowman, J.S., Anglin, E.L., Analysis of the Flat-Spin Characteristics of a Twin-Jet Swept-Wing Fighter Airplane, NASA TN D-5409, September 1969.

22. Bell, M.A. Etheridge, J.D., A-7 Accelerated Stall Departure Study, LTV Aerospace Corp. (VSD), 2-53310/IR-3598, April 1971.

23. Bihrle, W., Jr., Barnhart, B., Effects of Several Factors on Theoretical Predictions of Airplane Spin Characteristics. NASA CR-132521, August 1974.

24. Moul, M.T., Paulson, J.W., Dynamic Lateral Behavior of High Performance Aircraft, NACA RM L58F16, August 1958.

25. Greer, H.D., Summary of Directional Divergence Characteristics of Several High Performance Aircraft Configurations. NASA TN D-6993, November 1972.

26. Weissman, R., Criteria for Predicting Spin-Susceptibility of Fighter-Type Aircraft, ASD-TR-72-48, June 1972.

27. Weissman, R., Preliminary Criteria for Predicting Departure Characteristics/Spin Susceptibility of Fighter-Type Aircraft, AIAA Journal of Aircraft, Vol. 10, No. 4, April 1973.

28. Weissman, R., Status of Design Criteria for Predicting Departure Characteristics and Spin Susceptibility, AIAA Paper 74-791, Anaheim, CA, August 5-9, 1974.

29. Pelikan, R.J., Evaluation of Aircraft Departure Divergence Criteria with a Six Degree-of-Freedom Digital Simulation Program, AIAA Paper 74-68, Washington, DC., February 1974.

30. Johnston, D.E., Ashkenas, I.L., Hogge, J.R., Investigation of Flying Qualities of Military Aircraft at High Angles of Attack, AFFDL-TR-74-61, June 1974.

31. Chen, R.T.N., Newell, F.D., Schelhorn, A.E., Development and Evaluation of an Automatic Departure Prevention System and Stall Inhibitor for Fighter Aircraft, AFFDL-TR-73-29, April 1973.

32. AFFDL/ASD Symposium, p. 115.

Figure 1 - An F-4E model with leading-edge slats is tested at high angle of attack in the 12-foot wind tunnel at NASA Ames Research Center.

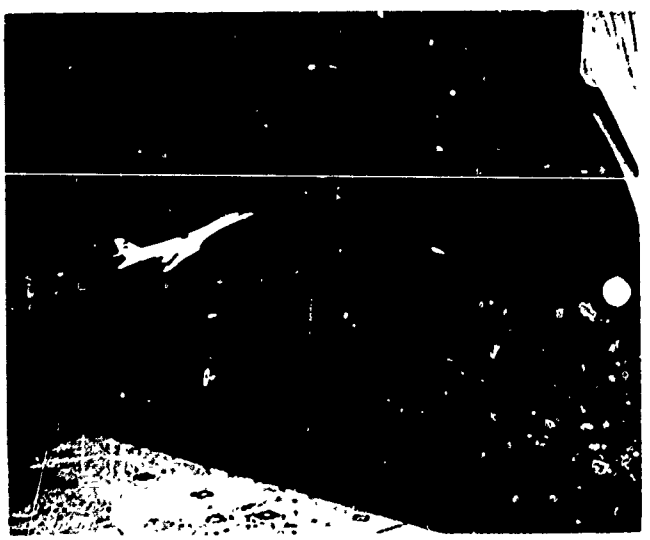

Figure 2 - A B-1 free-flight model being tested in the 30 x 60-foot wind tunnel at NASA Langley Research Center.

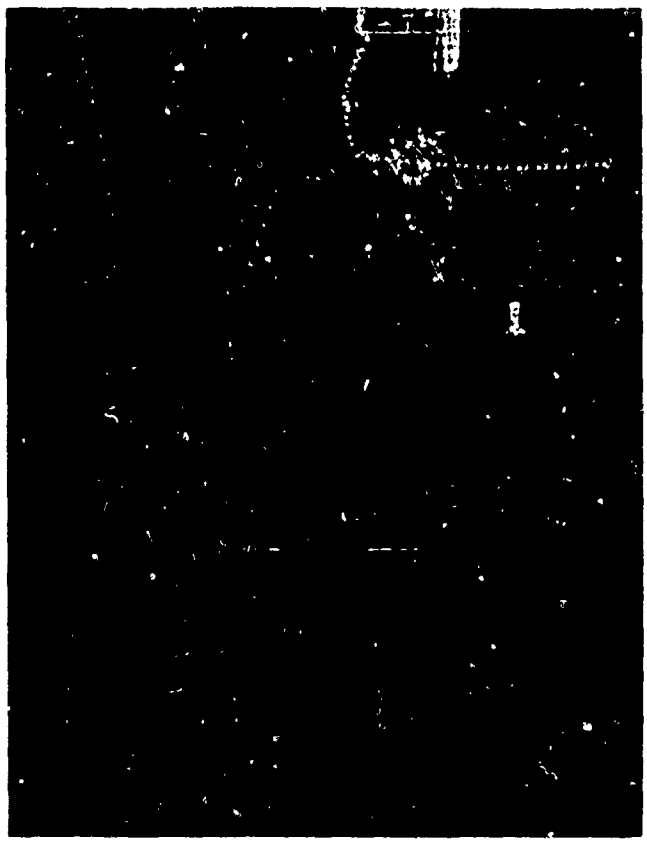

Figure 3 - Multiple-exposure photograph provided data for analyzing the stall/spin characteristics of a model aircraft being tested at the catapult facility of the Flight Dynamics Laboratory at Elizabeth City, NC.

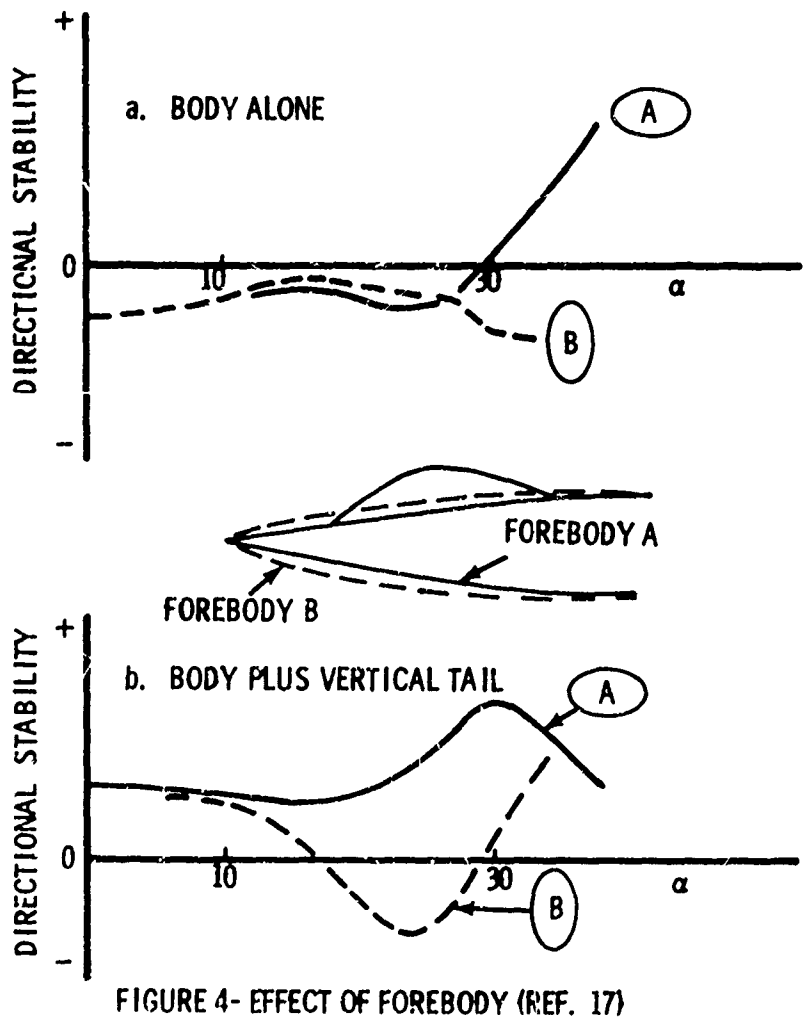

FIGURE 4- EFFECT OF FOREBODY (REF. 17)

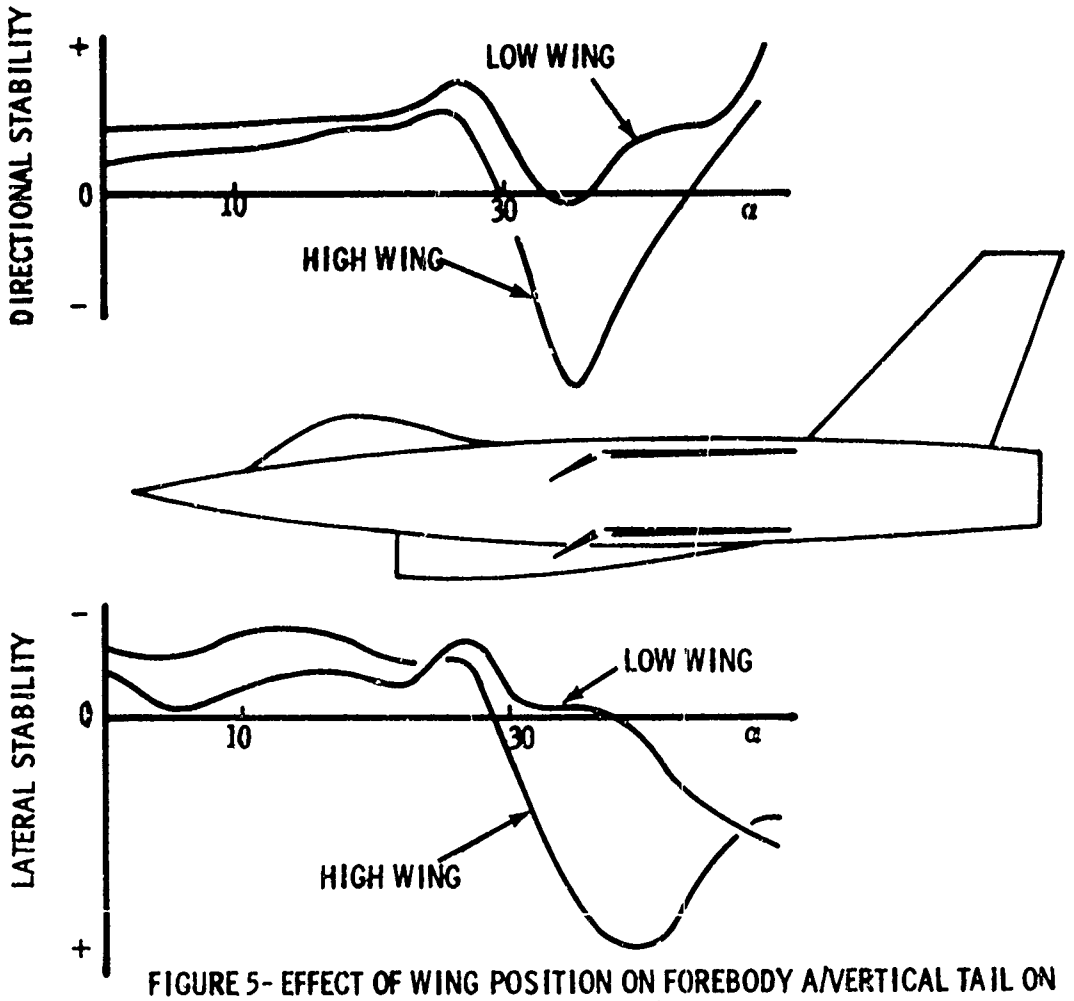

FIGURE 5- EFFECT OF WING POSITION ON FOREBODY A/VERTICAL TAIL ON AND VENTRAL INLET (REF. 17)

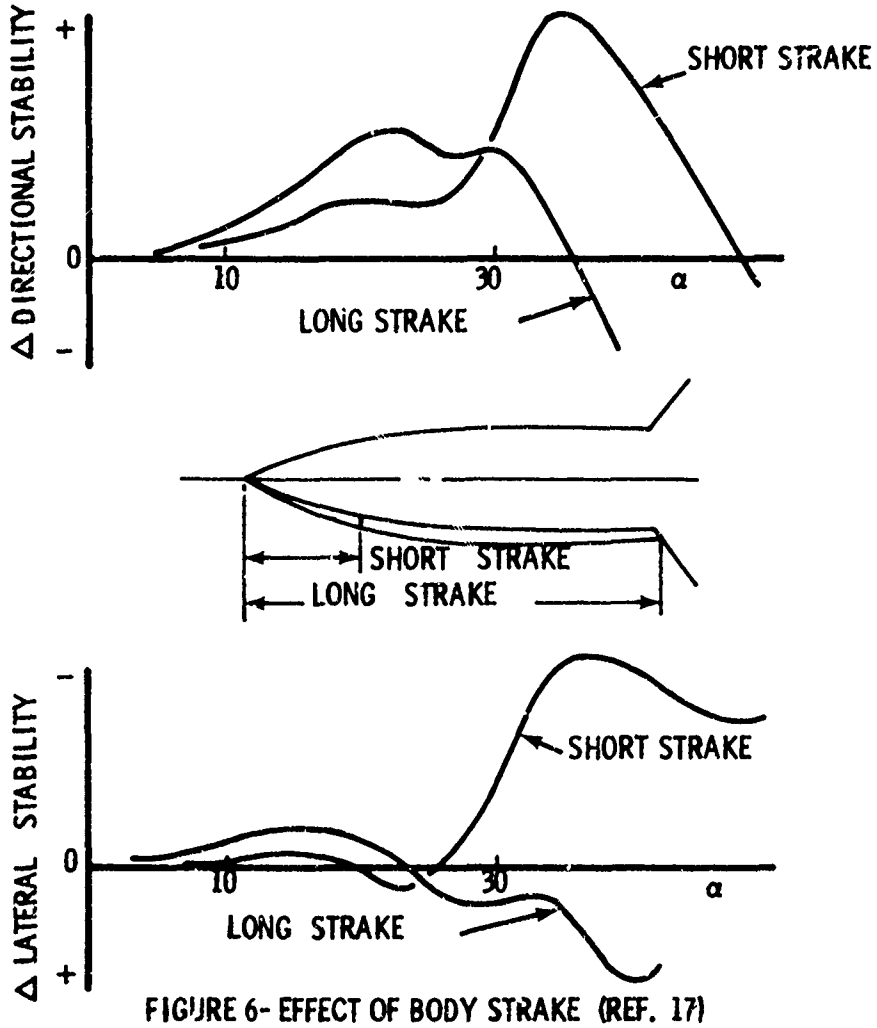

FIGURE 6- EFFECT OF BODY STRAKE (REF. 17)

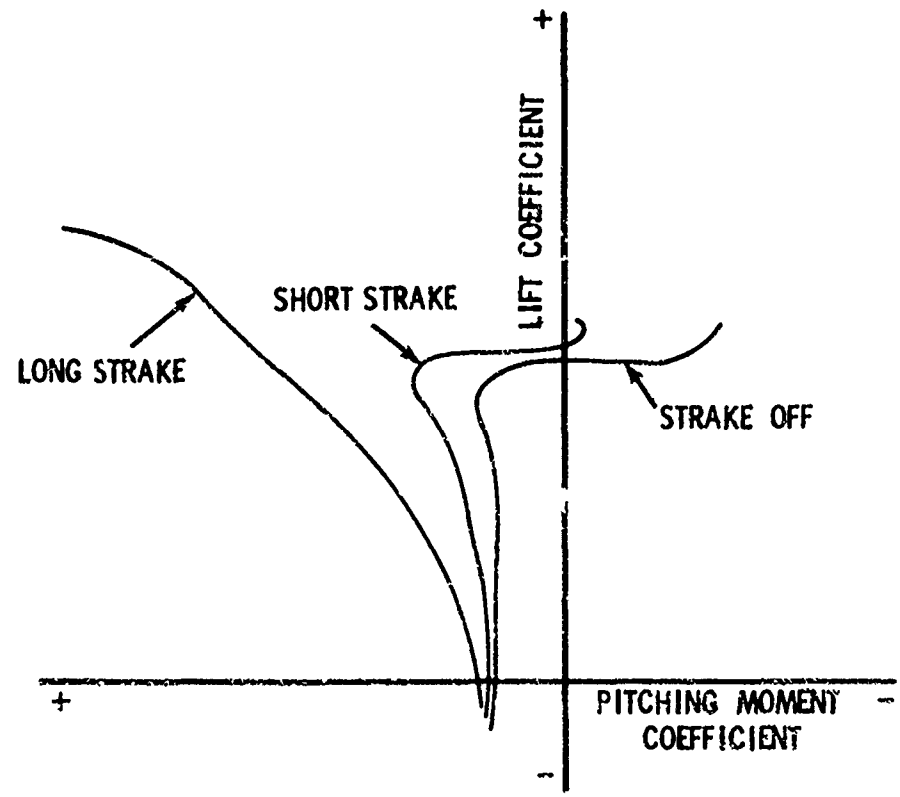

FIGURE 7- EFFECT OF BODY STRAKE ON LONGITUDINAL STABILITY (REF. 17)

$$Cn_{\beta DYN} = Cn_\beta \cos\alpha - (Iz/Ix)\, C\ell_\beta \sin\alpha > 0 \qquad (1)$$

$$LCDP = Cn_\beta - C\ell_\beta \frac{Cn_{\delta a}}{C\ell_{\delta a}} > 0 \qquad (2)$$

AILERON + RUDDER PROPORTIONAL TO AILERON:

$$LCDP = Cn_\beta - C\ell_\beta \frac{Cn_{\delta a} + K_2 Cn_{\delta r}}{C\ell_{\delta a} + K_2 C\ell_{\delta r}} > 0 \qquad (3)$$

$$K_2 = \delta r / \delta a$$

β PLUS δ AXIS STABILITY INDICATOR:

$$\alpha_{-\beta} = \alpha - \tan^{-1}\left(\frac{Cn_\beta}{C\ell_\beta}\frac{Ix}{Iz}\right) \qquad (4)$$

$$\alpha_{\delta} = \alpha - \tan^{-1}\left(\frac{Cn_\delta}{C\ell_\delta}\frac{Ix}{Iz}\right) \qquad (5)$$

FOR STABILITY: $\alpha_{-\beta} > \alpha_\delta$ AND $\alpha_{-\beta} > 0$

FIGURE 8- PARAMETERS FOR PREDICTING DEPARTURE AND SPIN SUSCEPTIBILITY

REGION A: NO DEPARTURE
REGION B: MILD INITIAL YAW DIVERGENCE FOLLOWED BY ROLL REVERSAL (MILD ROLLING DEPARTURE) LOW SPIN SUSCEPTIBILITY
REGION C: MODERATE INITIAL YAW DIVERGENCE FOLLOWED BY ROLL REVERSAL (MODERATE ROLLING DEPARTURE) MODERATE SPIN SUSCEPTIBILITY
REGION D: STRONG DIRECTIONAL DIVERGENCE WITH ROLL REVERSAL HIGH SPIN SUSCEPTIBILITY

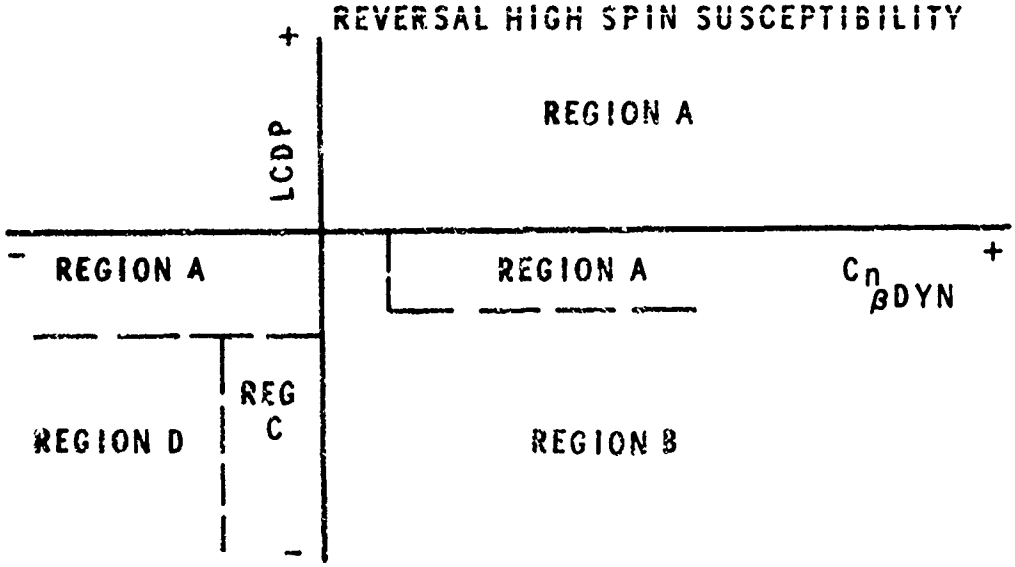

FIGURE 9- DEPARTURE AND SPIN SUSCEPTIBILITY CRITERIA (REF. 27, 28)

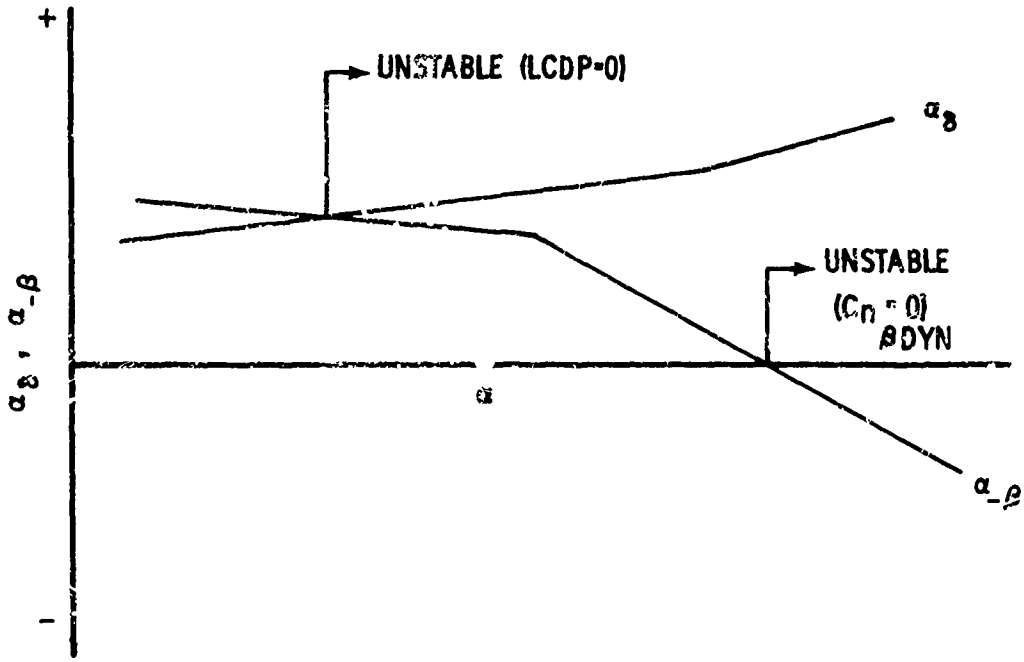

FIGURE 10 β PLUS δ STABILITY INDICATOR (REF. 29)

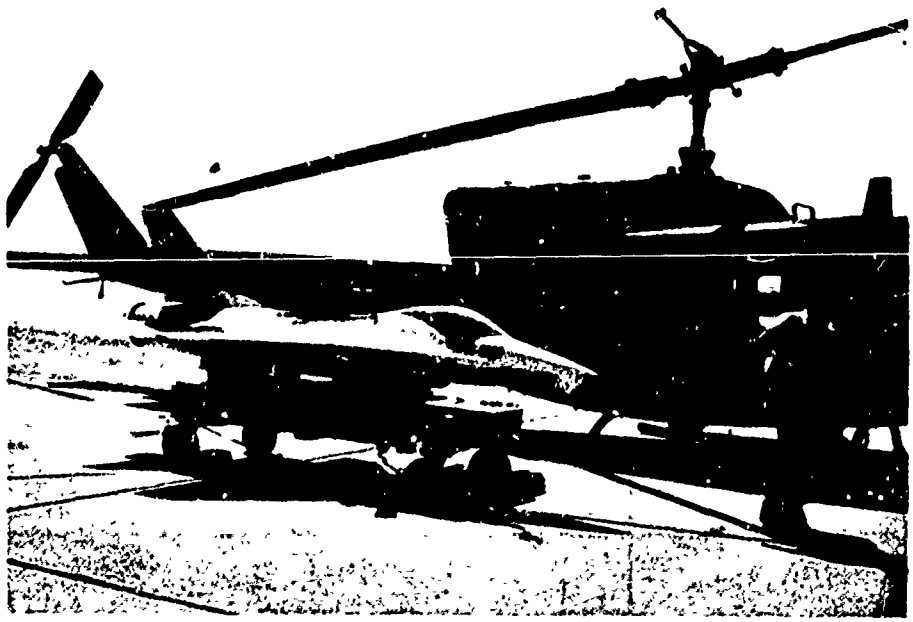

Figure 11 - An Air Force Flight Dynamics Laboracory YF-16 drop . . el is readied for stall/ spin tests at the Flight Test Center, Edwards AFB, CA.

THE STALL/SPIN PROBLEM - AMERICAN INDUSTRY'S APPROACH

by

Charles A. Anderson
Fighter CCV Program Manager
General Dynamics' Fort Worth Division
P.O. Box 748, Fort Worth, Texas 76101

SUMMARY

In this paper the stall/spin problem as viewed by American industry is reviewed. An attempt is made to detail what has caused us to have stall/spin problems, what options are open to the aircraft designer to reduce stall/spin susceptibility, and some of the current evaluation criteria that are available. Also, the various analytical and experimental tools and flight test techniques available today are reviewed. An assessment is then made of the usefulness of each of these guidelines, tools, and techniques. Finally, a recommended procedure for determining the stall/spin susceptibility and characteristics is presented.

LIST OF SYMBOLS

A_1	area forward of center of gravity, ft^2
A_2	area aft of center of gravity, ft^2
BA	body axis
I_x	inertia about x-axis, $slug\text{-}ft^2$
I_y	inertia about y-axis, $slug\text{-}ft^2$
I_z	inertia about z-axis, $slug\text{-}ft^2$
LCDP	lateral control departure parameter
L_1	distance from centroid of A_1 to center of gravity, ft
L_2	Distance from centroid of A_2 to center of gravity, ft
NACA	National Advisory Committee for Aeronautics
RN	Reynolds number, per ft
S	wing area, ft^2
US	United States
V	velocity, ft/sec
b	wing span, ft
$\bar{c}$	mean aerodynamic chord, ft
dyn	dynamic
g	normal load factor, ft/sec^2
m	mass, slugs
α	angle of attack, deg
β	angle of sideslip, deg
ρ	density of air, $slug/ft^3$
Δ	delta
Λ	wing sweep, deg

C_L	lift coefficient
C_m	pitching moment
C_l	rolling moment coefficient
C_n	yawing moment coefficient
C_{n_β}	yawing moment coefficient due to sideslip
$C_{n_{\delta_a}}$	yawing moment coefficient due to aileron
C_{l_β}	rolling moment coefficient due to sideslip
$C_{l_{\delta_a}}$	rolling moment coefficient due to aileron
δ_a	aileron deflection, deg
δ_r	rudder deflection, deg
δ_{H_a}	differential horizontal tail deflection, deg.

INTRODUCTION

The stall/spin problem has been with us for a long time and is one of the last to receive a great deal of attention. Ever since the Wright Brothers flew their first aircraft, the stall/spin phenomenon has relentlessly taken its toll of aircraft and lives. As we in industry expanded the boundaries of aircraft performance, we also expanded the stall/spin susceptibility problem. With the help of the old NACA organization, much work was accomplished in the 1930-1940 time period to understand the stall/spin problem and how to design aircraft that were not so susceptible to it.

With the advent of the jet engine and the concentration of large quantities of mass and inertia along the centerline of the aircraft, a whole new set of stall/spin characteristics emerged. With our zeal to increase the aircraft performance through ever expanding performance envelopes, we introduced configurations that were designed to meet performance goals only (drag and maneuverability) and, therefore, very little attention was given in the early design phase to assure that the aircraft had good stall/spin characteristics. In general, the aircraft configurations were driven mainly by drag considerations, and stall/spin analysis was very limited, being confined mainly to a determination of the characteristics of the configuration already being built.

Consequently, most of the U.S. high-performance aircraft built in the 1950's and 1960's demonstrated less-than-desirable stall/spin characteristics. This is evidenced in the fact that between 1966 and 1970 we lost approximately 225 military aircraft, which resulted in a material loss of approximately 360 million dollars and 110 lives.

DISCUSSION

In order to understand the current stall/spin problems, one must first try to understand how we got where we are, what options are open to the aircraft design team to reduce stall/spin susceptibility, and what are the current methods of determining stall/spin characteristics.

How We Got Where We Are

Up to the late 1950's, most high-performance aircraft were limited to subsonic speeds and were designed primarily for air-to-air combat. This meant that they had relatively low wing loadings, airfoils designed for maneuver, and moderate sweep angles with most of the aircraft lift carried on the wings. For this type of aircraft the wing generally stalled before an angle of attack at which directional stability went to zero was reached. This is illustrated in Figure 1. For this type of aircraft, stall was characterized by the classic "g" break with the nose falling through. To get these types of aircraft in a spin, you generally had to really want to.

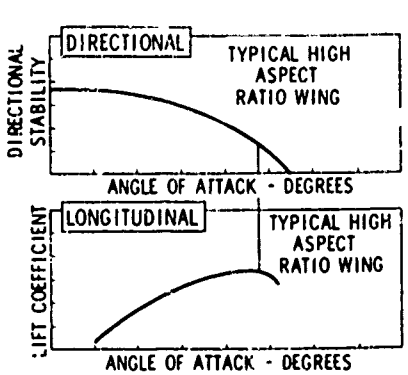

FIG 1 RELATIONSHIP BETWEEN DIRECTIONAL STABILITY AND LIFT COEFFICIENT AS A FUNCTION OF ANGLE OF ATTACK

In the late 1950's and early 1960's, the age of the missiles and sophisticated fire control systems came into being and the emphasis in air-to-air combat switched from close-in gun firing to stand-off missile firing. With this philosophy driving the aircraft designs and the tremendous improvements in jet engines, aircraft designs were now aimed at obtaining high maneuverability, low drag, and large speed envelopes. This led to thin wings with sharp leading edges and high sweep angles, large flat fuselages that continues to lift after the wing had stalled, and large horizontal tails to obtain the desired supersonic maneuverability. With the advent of this type of configuration, the aircraft could be maneuvered to higher and higher angles of attack in the subsonic flight regime since more-than-adequate horizontal tail power was available as a result of the supersonic maneuver requirements.

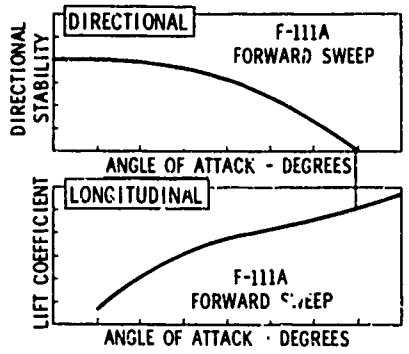

FIG 2 RELATIONSHIP BETWEEN DIRECTIONAL STABILITY AND LIFT COEFFICIENT AS A FUNCTION OF ANGLE OF ATTACK

We now encounter the type of stall most representative of today's aircraft - yaw divergence. No longer was the classic stall with its "g" break experienced; a new condition now existed in which the aircraft continues to generate lift and thus passes the angle of attack at which directional stability goes to zero. This is illustrated in Figure 2. For this type of configuration, stall comes very suddenly in the form of uncommanded yaw and/or roll excursions and usually results in loss of control before the pilot is aware of it. Because directional stability is already zero at the time of stall, the aircraft is very prone to enter a spin unless the pilot takes immediate and correct action.

Also during the late 1950's and early 1960's, little was accomplished in the way of specification changes, development of analytical prediction methods or detailed criteria for stall/spin prevention. Most of what was accomplished was mainly confined to determining the characteristics of the configurations being built. As a result of the above philosophy and the lack of specifications, methods, and criteria, most U.S. high-performance aircraft designed between 1950 and 1965 exhibited less-than-desirable stall/spin characteristics, which resulted in limiting the performance of the aircraft. Today we still have no specifications, standard analysis methods, or detailed criteria available to assure that an aircraft in the design phase will have acceptable stall/spin characteristics.

As a result of the past three major world conflicts, in which air power played a predominant role, it became quite obvious that the concept of stand-off missile battles only has given way to close-in air-to-air dog fights with both guns and missiles. During this time it also became obvious that the stall/spin characteristics of our first-line fighters were far from optimum and in some cases actually limited maneuvering performance. In a fighter aircraft, stall-/spin-free performance to at least the maximum usable maneuvering angle of attack is essential. It is also important to understand when one talks about performance for this type of aircraft that handling qualities be included rather than just drag and thrust to weight. It does no good for a pilot to be able to pull or sustain high "g" levels and not be able to track well enough to use his gun.

As a result of the rapid growth of our industry and our failure to recognize that the missile is not the ultimate weapon that would send the air-to-air dog fight into the history books, we arrived in the late 1960's at a point where the aircraft loss rate due to stall/spin accidents was large. It was during this time that both industry and various U.S. government agencies started to really look at the problem. Symposiums were organized, study contracts were let, ad hoc committees were formed, and, most important of all, requirements for good stall/spin characteristics were included in the requirements for new aircraft. These new requirements, plus the work done by government and industry specialists in pulling together the available evaluation criteria to assist the designer, resulted in later production aircraft like the F-14, F-15, and F-16 possessing good stall/spin characteristics.

Some of the current evaluation criteria that are available to assist the aircraft designer in assessing good stall/spin characteristics are presented in Figures 3 and 4. The characteristics indicating good spin resistance are shown in Figure 3 and those indicating good spin recovery characteristics are shown in Figure 4. As mentioned above, these data represent evaluation criteria only and, unfortunately, do not give the design guidelines necessary to assure the designer that he is obtaining the characteristics depicted in these figures. It is in these areas of establishing new specifications, design guidelines, and analysis methods that much work needs to be done to ensure that good stall/spin characteristics are obtained.

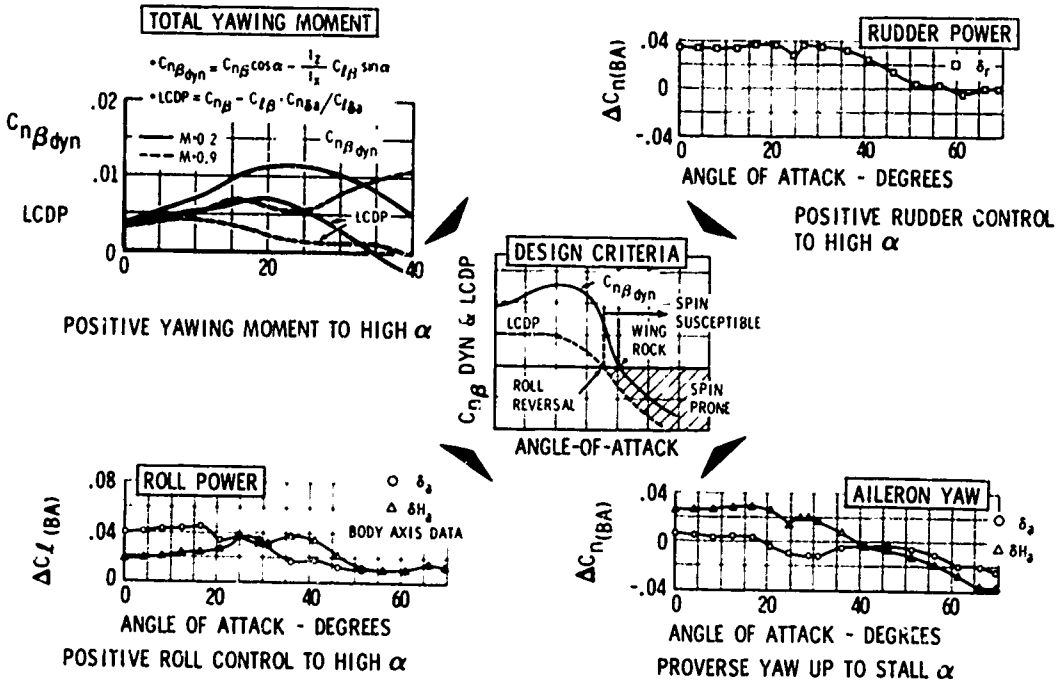

FIG 3 CHARACTERISTICS FOR GOOD SPIN RESISTANCE

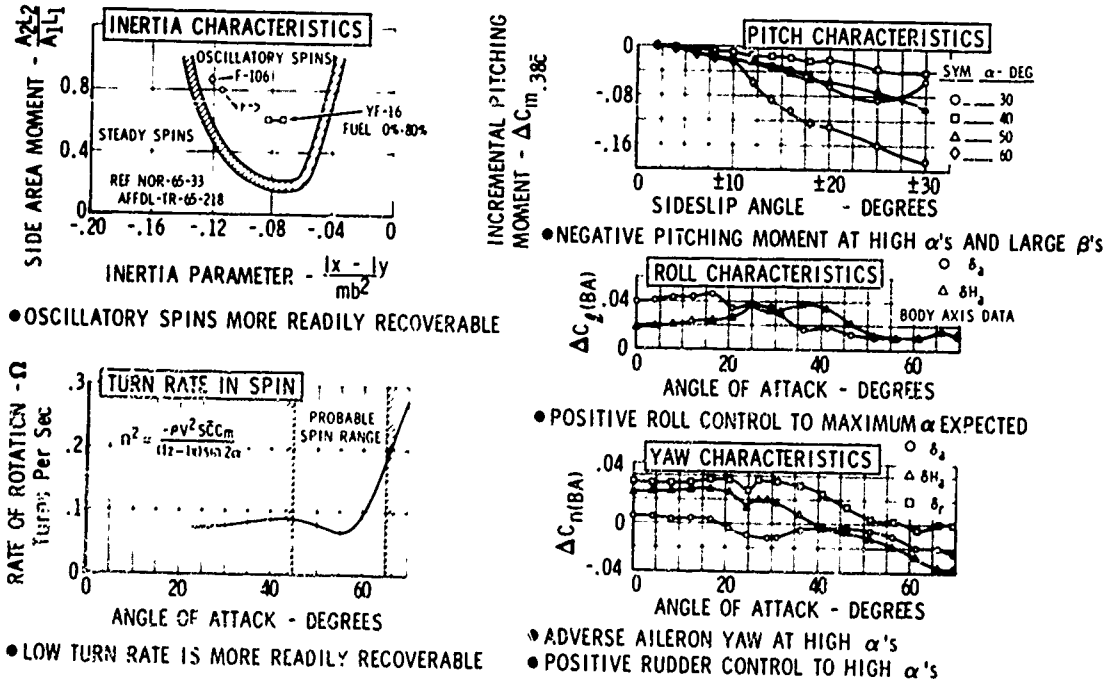

FIG 4 CHARACTERISTICS FOR GOOD SPIN RECOVERY

What Options Are Open To The Designer

Now that we have looked at a bit of history and the limited evaluation available for assuring that good stall/spin characteristics are available, let's look at the options open to the aircraft design team. The term "design team" is used here because the design of today's aircraft is really more of a team effort than ever before because of the inclusion of more flying qualities and stall/spin analysis in the design selection process.

The first basic option open to the design team is to allow the aircraft configuration to be driven by speed and maneuverability considerations only. Although speed and maneuverability are paramount in any design, they are usually achieved by compromising good high-angle-of-attack flying qualities. A traditional fighter design approach has been to concentrate on speed and maneuverability at the expense of high-angle-of-attack qualities, conduct stall/spin testing, install a stall warning device in the aircraft, and provide appropriate precautions in the flight handbook. Continuing stall/spin losses testify to the shortcomings of this approach.

Departure prevention can be designed into an aircraft in a variety of ways. For example, a combination of limited control power plus high basic airframe stability can be used to prevent attainment of departure angle of attack; however, maneuverability would be severely compromised. If the design team does not wish to compromise maneuverability, it could supply the departure resistance through high basic airframe stability, which would result in a severe performance compromise. If the design team does not wish to compromise maneuverability or performance, then it could design the aircraft with very low basic airframe stability and supply the required departure resistance through the control system. If the control surfaces are designed for maximum maneuverability and performance, that is, using the smallest tail size that will meet the high-q maneuver requirements, then the operating envelope of the aircraft will probably be compromised by control power limiting at low-q conditions.

It is quite obvious that there has to be a middle ground or optimum compromise that will allow the maximum values of performance, maneuverability, and operational flight envelope to be obtained. But what is the magic by which we achieve the best compromise? What are the design criteria? The one suggested is really very simple; it is merely to design the aircraft to have enough basic stability to provide good handling qualities and spin resistance over the operational flight envelope and up to the maximum useful angle of attack, and then use the flight control system to prevent excursions outside this envelope. It should be noted that the term "maximum useful angle of attack" is employed in this suggestion. To understand this term, one must first understand what the maximum useful angle of attack for a fighter would be.

First, since turn performance is one of the main indicators of fighter performance, the relationship between turn performance and angle of attack must be understood. As is quite obvious to everyone, turn performance is a function of both speed and normal acceleration. Further, in turning flight, speed is a function of drag and thrust-to-weight ratio, and normal acceleration is a function of wing loading, angle of attack, and speed. Therefore, for a given configuration, once the desired wing loading and thrust-to-weight ratio have been established, the maximum turning capability can be determined. Increased turn rate can be obtained in maneuvering flight conditions by increasing load factor or by holding load factor and bleeding off speed (energy). In this case the minimum useful speed occurs at that angle of attack where the speed is decreasing faster than the lift is increasing and, consequently, both normal acceleration and turn rate fall off. Increases in angle of attack above this maximum useful value not only result in excessive speed loss, which further reduces turn rate, but put the aircraft in an area in which it is subject to loss of control. Since loss of control appears to have very little tactical usefulness, increasing angle of attack beyond the maximum usable value puts one more task on the pilot that detracts from his ability to visually track his opponent, that is, monitoring angle of attack.

Using the control system to limit the angle of attack to the maximum usable, or slightly above, does not actually limit performance but tends to enhance it by allowing the pilot complete freedom to utilize the aircraft's maximum performance. Moreover, using the control system to limit normal-load-factor capability or sideslip excursions tends to further enhance the pilot's freedom to maneuver and thus to utilize the aircraft's maximum performance. Since most modern-day aircraft have their maximum turning performance capabilities at angles of attack below 30 degrees, little tactical benefit would be obtained by developing an aircraft that can exceed these angles of attack. Therefore, it appears that a good design compromise is to provide good basic stability up to the maximum usable angle of attack and then to use the flight control system to limit excursions in all axes above this angle of attack.

Current Methods for Determination of Stall/Spin Characteristics

Now that we have looked at how the stall/spin problem emerged and what options are open to the design team to assure that acceptable stall/spin characteristics are achieved in a new design, let us look at the various methods currently available to assess stall/spin characteristics.

Vertical Tunnel Tests - This type of testing is generally used to determine the possible spin modes, susceptibility, and predicted recovery controls and to size the spin recovery parachute system. It is generally accomplished by hand launching a model in a stalled condition in a vertical tunnel. Experience shows that, because of scaling, Reynolds number effects, and testing techniques, the results obtained from this type of testing tend to be pessimistic and are difficult to extrapolate to full scale. Also, as a result of the testing techniques, no information can be obtained regarding entry and post-stall characteristics. Therefore, although this type of testing is very useful, it should be limited to prediction of possible spin modes and recovery controls and to the sizing of recovery parachute systems.

Free-Flight Testing - This type of testing is generally used to examine an aircraft's handling qualities up to stall. It is normally accomplished by remotely flying a large-scale model attached to a safety line in a large tunnel. Because the control systems for these tests are usually limited to simple rate feedback systems, it is difficult to simulate an active control system. Experience shows that this type of testing is very useful in determining the stall or divergence characteristics, but that the ability to determine stall or divergence angle of attack for the full-scale aircraft is very questionable. It appears that as a result of the low Reynolds number and Mach number at which the testing is conducted and of the limited simulation of the basic aircraft control system, the results of this type of testing may tend to be either conservative or optimistic, with no way of knowing which of the two were obtained.

Radio Control Model Tests - This is the newest and probably the most promising type of testing available to determine the stall/spin characteristics of a given configuration. This type of testing allows examination of an aircraft's stall/spin characteristics over the entire angle of attack range and, with the installation of high-speed computers and data links in the ground station, allows simulation of the most sophisticated active control system. In this type of testing, a large model is air launched from either a helicopter or an aircraft, and the model's flight control system is used to maneuver it into the desired manner. The beauty of this type of testing is that one can safely look at all kinds of combinations of entry conditions and gross misapplications of controls to determine where the flight test effort should be concentrated. Another by-product of this type of testing is that with the limited amount of instrumentation required for the control systems and for just flying the model (α, β, airspeed, angular rates, linear accelerations, and surface positions) the model's aerodynamic characteristics can be obtained through regression techniques. Thus a data bank can be accumulated for analytical prediction programs.

The advantages of this type of testing over the vertical and free-flight testing techniques are obvious. Not only does it provide information on departure characteristics, but it also allows examination of the post-stall and spin susceptibility characteristics. The basic drawback is the low Mach and Reynolds number conditions at which the data are obtained and the fact that this type of testing by necessity occurs after the configuration is firm and, thus, the results are usually used simply to document the stall/spin characteristics of the configuration.

Flight Test - Flight testing, of course, is the best way to determine an aircraft's stall/spin characteristics. Unfortunately, up until the late 1960's, stall/spin flight testing consisted mainly of attempting to satisfy the old spin specification, MIL-S-25015. Flight testing against this spec was more of a test of endurance than anything else. To satisfy the spec required that the test pilot put the aircraft into a spin at a variety of flight conditions and loadings and allow the aircraft to complete from two to five turns before applying spin recovery controls. This type of testing not only put the aircraft in danger of being lost, but usually resulted in big expensive spin programs that did little to define what to do during the first few critical seconds after control was lost.

As a result of the large numbers of aircraft that were lost in the late 1960's that had been put through just such a spin demonstration, emphasis was shifted from pure spin recovery testing to stall prevention and spin susceptibility determination. As a result of this change in philosophy, the old spin specification was replaced by a new one, MIL-S-83691, which placed the emphasis on the determination of stall/spin prevention and susceptibility. Although testing an aircraft in accordance with this specification

improve its stall/spin characteristics, the information derived from this type of testing is extremely useful in supplying the operational pilot with the necessary information to recover from a stall/spin situation.

The main drawback to this new specification is that the contractor must assume that he will have to perform all phases of the testing required and bid it accordingly. Consequently, the cost of the program is maximized.

Force Model Testing - This type of testing is the only one that can provide information early enough to affect the configuration design from a stall/spin standpoint. A good set of low-speed data covering the desired angle-of-attack range (0^{o} to 70^{o}) and sideslip range (-20^{o} to $+20^{o}$) can be invaluable in assessing the stall/spin susceptibility of a given configuration. It is also very useful in providing the necessary guidance for selecting the direction the configuration should be driven.

Even though this type of data is very useful in evaluating stall/spin characteristics, the data obtained at angles of attack between 30^{o} and 80^{o} is very dependent on configuration and model size. An example of this is shown in Figures 5 and 6, where the

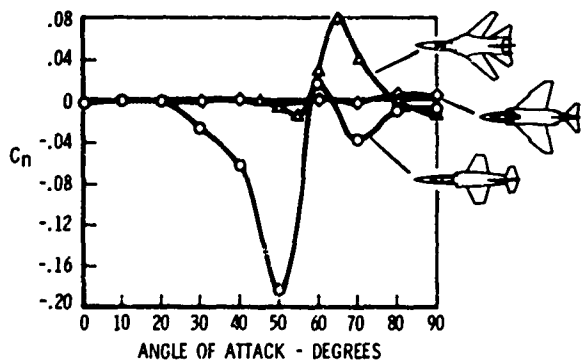

FIG 5 VARIATION OF YAWING-MOMENT COEFFICIENT WITH ANGLE OF ATTACK FOR SEVERAL AIRPLANES

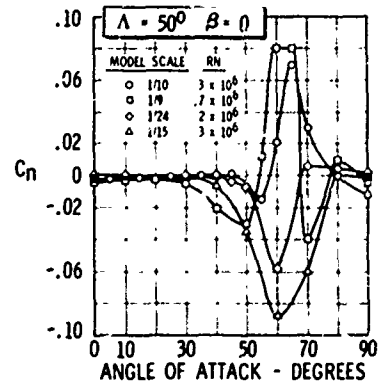

FIG 6 VARIATION OF YAWING-MOMENT COEFFICIENT WITH ANGLE OF ATTACK FOR SEVERAL MODEL SIZES

variation of yawing-moment coefficient is presented for various nose shapes and for a given nose shape with model size as a function of angle of attack. It is not known at this time whether these variations are caused by Mach number, Reynolds number, or other effects. It is very strongly felt that a program should be initiated to resolve this dilemma.

Analytical Programs - With the advent of high-speed computers with large memory storage capability, analytical programs have become a very useful tool in analyzing the stall/spin characteristics of a given configuration. One cannot only obtain a time history of a given type maneuver, but also build his program in such a manner that it will take time-history traces from model test or flight test and allow regression techniques to be used to extract the aerodynamics of the configuration. This type of information, of course, is usually obtained too late to change configuration significantly, but it is very useful in determining the exact stall/spin characteristics of the configuration.

Unfortunately the analytical program is no better than its data and therein lies the problem. Industry and government must establish some clear-cut method of both determining and evaluating a given aircraft design's stall/spin characteristic from an analytical basis.

CONCLUSIONS

Good stall/spin characteristics can be designed into an aircraft if these requirements are written in the initial requirements for a new aircraft and, thus, are allowed to drive the configuration. This fact is evidenced by the good stall/spin characteristics of the last three major fighter aircraft, the F-14, F-15, and F-16.

The design approach taken to provide good stall/spin characteristics can compromise overall performance capability if the control system is not used as an integral part of the aircraft configuration. Use of criteria such as designing the basic aircraft to have good basic stability up to the maximum usable angle of attack and using the control system to limit excursions in all axis above this angle of attack appears to provide the minimum overall performance compromise.

A proven set of design guidelines or prediction techniques is not available today to aid the design team in putting a configuration together that will have acceptable stall/spin characteristics. In general, each company must rely on its past experience and the expertise of its specialists and then go to the wind tunnel and check out the proposed configuration.

Extensive work in the areas of establishing design guidelines, prediction techniques, and reliable testing techniques needs to be undertaken and, in some cases, continued to provide industry with the tools necessary to provide the best aircraft at the least cost.

RECOMMENDATIONS

In view of past experience with stall/spin characteristics on the B-58, F-111, and YF-16, future aircraft should be designed and tested as follows:

1. Design the aircraft to have good closed-loop or natural stability and controllability up to the maximum usable angle of attack and use the control system to limit excursions in all axes above this angle of attack.

2. Conduct sufficient force and dynamic wind tunnel tests to obtain a good data base. Use this data base to continually examine the acceptability of the predicted stall/spin characteristics. Compare predicted configuration characteristics against current evaluation criteria.

3. Conduct vertical tunnel testing to determine possible spin modes, recovery controls, and spin recovery chute size.

4. Conduct drop model and limited flight tests to obtain aerodynamic coefficients to update the data bank.

5. Use analytical programs with updated data banks and drop model tests to determine critical areas where an aircraft is most susceptible to stall/post-stall/spin entries and subsequently demonstrate these areas during flight test.

3. SOME EUROPEAN SPIN EXPERIENCE

3A. COMPARISON OF THE SPIN AND A LOW INCIDENCE AUTOROTATION OF THE JAGUAR STRIKE AIRCRAFT

by

R.J.Blamey, B.Sc.
Aeroplane and Armament Experimental Establishment
Boscombe Down, Salisbury, UK

1. INTRODUCTION

From the extensive flight trials which were carried out by both the aircraft manufacturer and official agencies on Jaguar high incidence and spin behaviour, a number of interesting results emerged. In a short paper it is only possible to present one aspect and I have chosen to compare the classical high incidence spin mode with a rather less common low incidence autorotation which appeared during Jaguar evaluation trials.

2. THE AIRCRAFT

The Jaguar strike aircraft is a two engined, high winged, low altitude combat aircraft which can weigh between 8000 and 15000 kg. The wing area is 25.2 m^2 and the span 8.69 m. Stores are carried externally and the centre of gravity shift for 4000 kg of stores is from 16% to 27% SMC. The aircraft has an all moving tailplane, spoiler plus differential tail roll control and a conventional rudder. The aircraft is fitted with autostabilizers in all 3 axes.

3. THE SPIN

During the test programme a large number of classical spins were deliberately provoked and these are fully described and categorized in Reference 1. Only one inadvertent spin is known to have occurred during development and Service use by RAF and FAF. This case fell into the general pattern described below and the aircraft was recovered safely.

Spins can be, in general, characterised as follows:

Incidence oscillating	$\triangleq$ +30° to +80° nose up
Sideslip oscillating	$\triangleq$ ±50°
Roll rate oscillating	$\triangleq$ ±150°/sec
Yaw rate oscillating	$\triangleq$ 0 to 100°/sec
Pitch rate oscillating	$\triangleq$ 50°/sec nose up to 80°/sec nose down
Normal acceleration	$\triangleq$ 0 to +2g
IAS	< 180 kn

Pilots described the spin as disorientating but found the simple recovery drill easy to apply and entirely satisfactory. Figure 1 shows a typical spin.

4. THE AUTOROTATION

In the early stages of the project a mild, low incidence, stable autorotation was demonstrated on spin recovery and recovery from loss of control when incidence limits were being established.

A much more severe autorotation was then discovered during lift boundary definition tests at high incidence which resulted in the loss of an aircraft. This autorotation is shown in Figure 2 and was described by the pilot as oscillatory and disorientating. It was characterised by:

Incidence oscillating	+5° to + 25° nose up
Sideslip oscillating	±12° (mean value +8°)
Roll rate	$\triangleq$ 200 to 250°/sec (peak 300°/sec)
Yaw rate	$\triangleq$ greater than 20°/sec (off scale)
Pitch rate	$\triangleq$ 10° to 15°/sec nose down
Normal acceleration	0 to 6½ g (mean $\triangleq$ 3 g)
IAS	400 kn

5. THE COMPARISON

5.1 Entry Conditions

Figure 3 (upper insert) shows where spin entries were achievable. Although numerous attempts were made outside this zone using normal flying techniques the aircraft could not be made to spin. If, after control was lost, recovery action was not taken and the aircraft held in a pre spin condition until the speed reduced to values inside the shaded area then the aircraft would enter. Even so, if control was lost in the shaded area and recovery action taken immediately the aircraft recovered more often than not.

The low incidence autorotation was not systematically explored in the same way as the spin and actual test experience is limited to that shown in the lower insert of Figure 3. There is no evidence which indicates probable boundary conditions for entry nor any test evidence on the effects of relevant variables on entry. However, the limited evidence available backed up by a comprehensive mathematical model study by BAC (Ref.2) indicates good correlation between tail plane position and/or movement and entry into autorotation. All entries have occurred with the stick either at mid-position (300 kn trim) or forward of this point. The model (Ref.2) confirmed that rapid forward movement of the stick at the critical point during onset of loss of control was likely to provoke an autorotative motion. It was also shown that in the case described in paragraph 4, the rapid forward stick movement to the forward stop was a direct cause of entry in this particular instance.

5.2 Recovery

A simple and effective recovery technique has been demonstrated for the Jaguar strike version. This technique, "release the controls", proved successful in every case.

Recovery from autorotation has been repeatedly demonstrated in the 150 to 300 kn region by a rearward movement of the stick, the exact amount required being dependent on the flight condition and easily judged by the pilot at the time. In the violently oscillatory autorotation discussed in paragraph 4, the stick was held forward on the forward stop throughout the descent because the aircraft was thought to be in a spin. The theoretical model (Ref.2) showed that a rearward movement of the stick to the trim point for 400 kn IAS would have calmed the autorotation, and a further aft movement of the stick would have stopped it.

6. CONCLUSIONS

Two distinct oscillatory motions which arise from loss of control have been demonstrated for the Jaguar strike aircraft. Satisfactory recovery techniques have been developed and some knowledge of the conditions under which entry can occur has been obtained.

However, several questions still remain – for example

(a) Are there other stable oscillatory modes still to be uncovered?

(b) Are there other means of entry in to the known modes?

(c) Is sufficient investigation being carried out on future projects to ensure that should stable spin and autorotation be possible, satisfactory recovery procedures, as is the case with Jaguar, will be achievable?

(d) Is sufficient emphasis being put upon the development of loss of control prevention devices on future projects?

REFERENCES

1. – AMD Rapport Technique No.277. Aout 19. *Jaguar MO5 Déclenches et Vrilles.*

2. – BAC Report Ae/J/536 *Matching and Investigation of the B1 Flight 236 Autorotational Rolling Accident.*

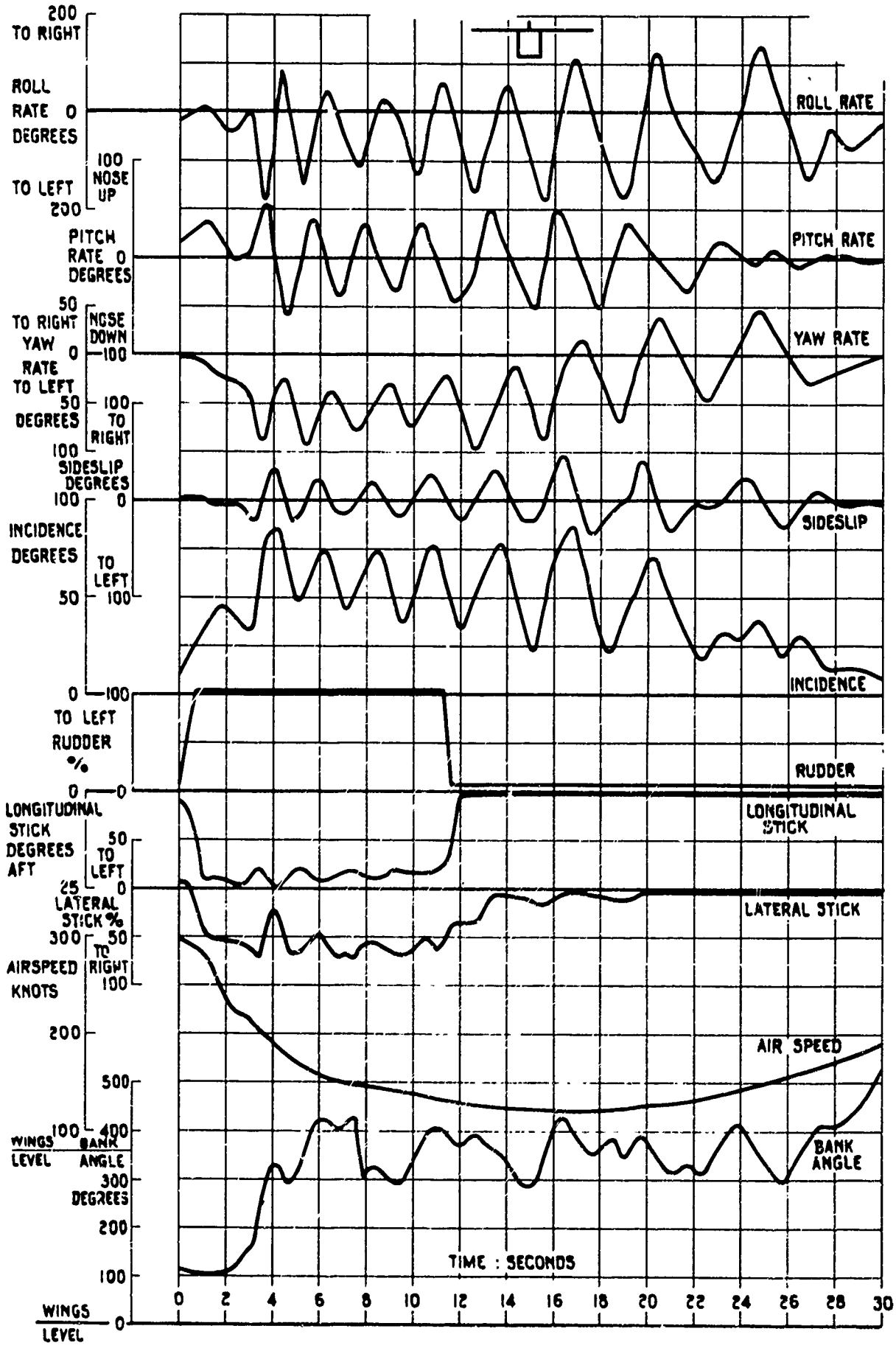

Fig.1 Deliberate spin – clean configuration. (Test 43)

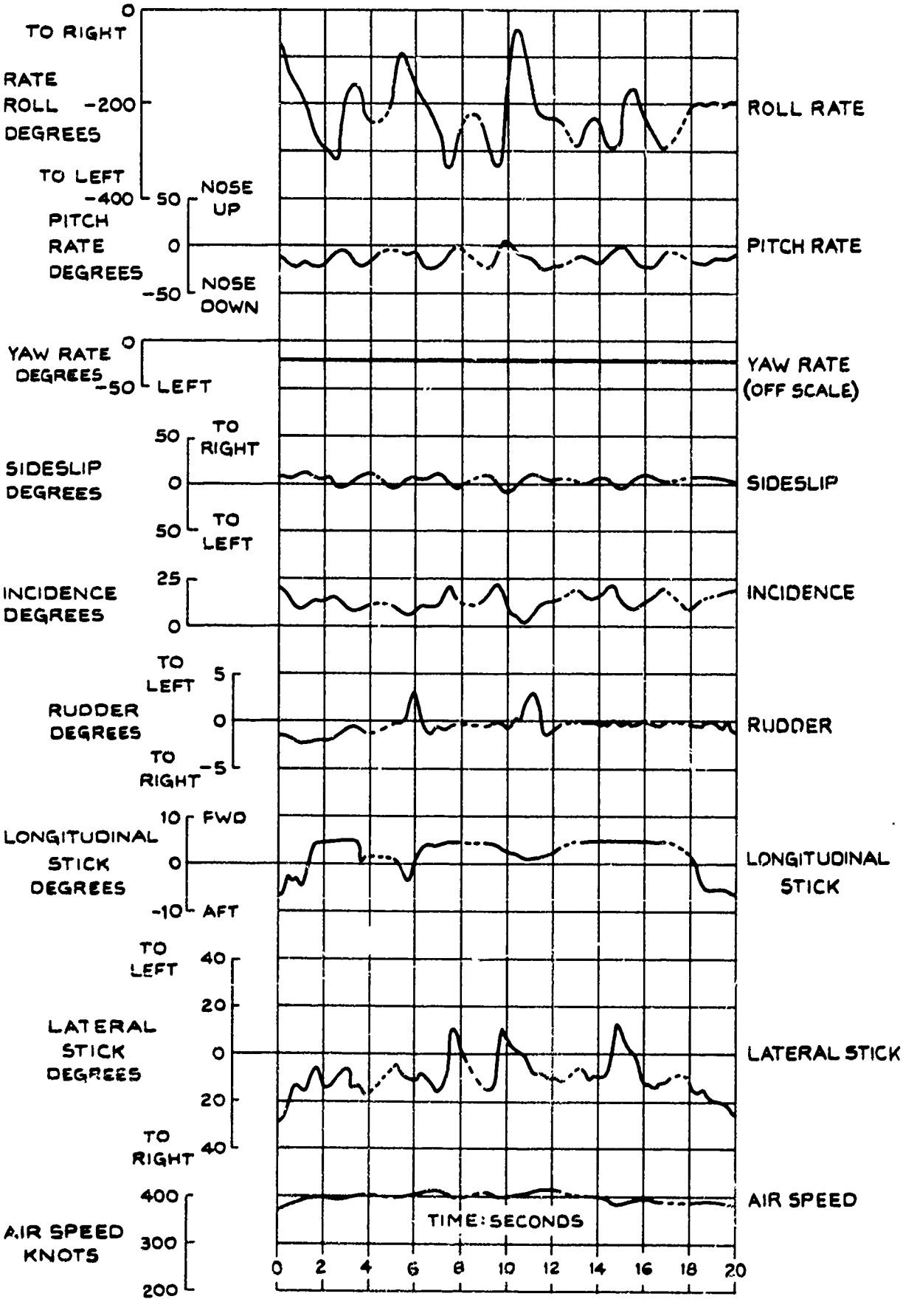

Fig.2 Jaguar - low incidence autorotation

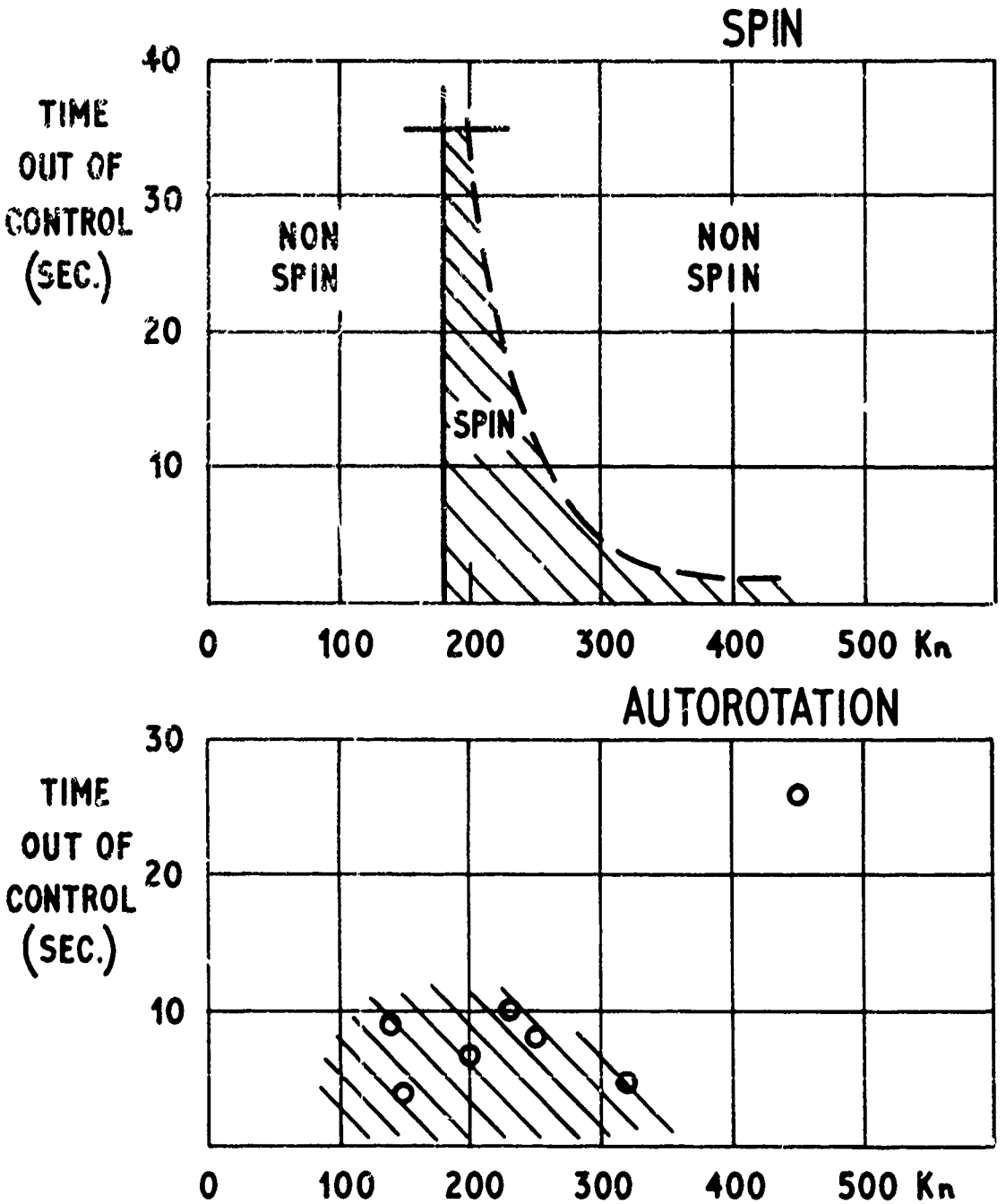

Fig.3 Jaguar G.R. Mk.1

A FEW REMARKS CONCERNING SOME STALL/SPIN EXPERIENCE IN THE NETHERLANDS

by

J. Hofstra

Fortunately I can say that operational spin experience is very limited in the Netherlands, at least over the last 15 years. In my opinion this is mainly due to the fact that the aircraft in use had good stall characteristics and resistance to spin entries. But nevertheless I would like to make some remarks about the stall and spin problem, especially as it is encountered during air combat manoeuvring.

In the past it has been proven that for air combat the spin implies a definite disadvantage, although I remember stories about the early days of aviation that sometimes this manoeuvre was used to escape from critical situations. Together with the normal warning in the flight handbook that intentional spinning is prohibited we can safely say, that we do not want to enter a spin except in certain training aircraft, since in that case it can give a pilot some spin experience which in my opinion is very useful.

One of the important problems is how to stay away from the critical stall/spin area and still use the aircraft to its limits as necessary in air combat, during which high angles of attack often occur. It is well-known that in air combat it is essential to keep the opponent in sight all the time. A short glance in the cockpit will normally give eye focus problems and there is a fair chance you have lost sight of your opponent and then you are in trouble. So if you fly an aircraft where you have to monitor cockpit instruments frequently this will be to your disadvantage.

To illustrate this I would like to compare two types of fighter aircraft, namely the Hawker Hunter and the F-104G Starfighter. This comparison will of course be limited to the high angle of attack region because as far as other potentials are concerned the aircraft differ by about a generation, the Hunter being a typical subsonic fighter and the Starfighter being a supersonic one.

From about 1955 till 1965 the Hunter was part of The Netherlands Air Force inventory. Intentional spinning was prohibited. During manoeuvering in air combat the pilot could look outside the cockpit almost continuously. Especially in high angle of attack flight the aerodynamic behaviour of the aircraft told the pilot to what extent he had penetrated the stall region. If too far, lost control could quickly be recovered with a minimum loss in height and relative position to the opponent. But if this was done too roughly the odds of entering a spin were increasing and personally I know of two occasions where the spin fully developed. In one case the aircraft recovered at lower altitude by releasing the controls and in the other by normal controls when the selected flaps were retracted according to the spin recovery procedures.

The Starfighter is an aircraft equipped with a stick pusher installation to prevent the development of unstable pitch behaviour at high angles of attack, which is normally followed by a tumble and a spin. To prevent unexpected operation of the stick pusher during high angle of attack flight in air combat, it was necessary to monitor the angle of attack indicator frequently. This monitoring inside the cockpit combined with the requirement to keep the opponent in sight as much as possible was a definite disadvantage and compared unfavourably with the Hawker Hunter, again given full credit to the other potentials of the Starfighter.

To conclude I would wish:

1. some type of aerodynamic stall warning which intensifies with increasing angle of attack, so that the pilot can feel how far he is in the stall penetration,
2. the possibility of a quick recovery with minimum height loss once the aircraft is stalled,
3. high resistance against spin entries.

However, with an eye on the future, I believe that the possibilities offered by the lately developed "fly by wire" systems with computer controlled modification of pilot inputs form an even better solution. In all flight conditions these systems allow the pilot to utilize the full instantaneous capability of the aircraft while at the same time they safeguard against stall spin and/or overstress.

GERMAN AIR FORCE OPERATIONAL SPIN EXPERIENCE

D. Thomas
Testpilot
Dornier GmbH
D 799 Friedrichshafen
Germany

SUMMARY

This paper presents the operational spin experience of the German Air Force during the last 20 years.

The G-91, F-104 and F4 flight characteristics at high angles of attack, the spin test program and the number of accidents due to post stall gyrations are discussed.

The training and proficiency program concerning spinning of aircraft are mentioned and a proposal of modifications is made.

1 INTRODUCTION

In this paper I will discuss only the Post Stall Problems encountered during flight operations by the German Air Force (GAF) since its new start in 1956.

Naturally, the spin experience acquired by the Luftwaffe during World War II was quite broad, yet, unfortunately, nobody has ever written a report on this subject.

As a test pilot I am interested not only in the spin experience of all flying services, but also in paragraphs of Military Specifications dealing with spin prevention demonstrations and requirements for airplanes.

It is also of interest to know for each typ of aircraft actually in service with the GAF what type of spin test program was carried out at the manufacturer's as well as to compare the results with the operational experience acquired until now by the Luftwaffe with these aircraft. Naturally a detailed investigation would require quite an effort. Maybe one of the big research organisations would be willing to do this job in the future.

2 AIRWORTHINESS SPECIFICATIONS

In Germany, in the pre- ALPHA-JET and MRCA- phase, we bought all our jet aircraft abroad. The FOUGA MAGISTER came from France, the FIAT G-91 from Italy, an all other training and combat jet aircraft were bought from the USA. The G-91 and the US airplanes had an airworthiness certificate according to the famos MIL SPEC's.

These Specifications are well known to our procurement agency, the BWB-ML. This authority adopted these regulations as standard requirements for all questions referring to post stall and spins. (MIL - S - 83691, stall/post - stall/spin flight test demonstration requirements for airplanes). However, an exception was recently approved for the

ALPHA-JET which has to comply with the French Air Norms, as the FOUGA MAGISTER already did.

3 SPIN TESTING AND FLYING QUALITIES AT HIGH ANGLES OF ATTACK OF PRESENT LUFTWAFFE AIRCRAFT

3.1 Training aircraft

As far as I know, all jet training aircraft at the Luftwaffe have been thoroughly spin tested.

These aircraft were at the beginning the FOUGA MAGISTER and the T-33.

These are now the USAF operated but GAF owned T-37 and T-38.

3.2 Combat aircraft

As far as the combat aircraft actually in service are concerned, the situation is somewhat worse.

G-91

Of this aircraft only the G-91 T model, the two seat version, has been spin tested by the manufacturer, whereas the single seat version never accomplished any official spin test flight.

During the stall, this aircraft has no tendency to enter a spin unless forced to do so by the pilot. The aircraft can be flown with the stick full aft where only a pitch oscillation and a high sink rate can be observed.

F 104

This aircraft was spin tested in the initial light weight configuration.

There was no further spin test program added following the weight increase and the change of the weight distribution for the European version, nor were there any spin tests carried out with heavy external stores. The flying qualities of the aircraft up to stall are very good but will deteriorate abruptly in the post stall region. The aircraft has therefore a very effective stall warning and preventing system (APC).

F 4

The F 4 E has gone through a very extensive spin test program with and without external stores and even with asymetrical loads.

The new fighter version F 4 F now also in GAF service is equipped with leading edge flaps to improve the handling qualities at high angles of attack.

The responsible authorities did not consider this as a major modification, necessitating a new spin test survey.

In general, handling qualities of the F4 deteriorate progressively when angle of attack is increased. As the aircraft has only a passive stall warning system using a warning horn and a rudder pedal shaker, the GAF is watching closely how the fighter pilots will respect the aircraft limitations in future operation.

4 OPERATICNAL SPIN EXPERIENCE

4.1 Spin Training

The student pilot only receives spin training on the T-37 aircraft. With the T-38 and combat aircraft, intentional spins are not allowed.

4.2 Squadron Experience

When a young pilot enters a squadron, his last spin training was 18 months ago. If such a pilot now encounters a spin or a post stall gyration, he may get easily disorientated due to a lack of experience. If this pilot gets out of the trouble, this is most probably due to the fact, that the aircraft recovered itself and not because the"Tiger" stayed calm and executed the prescribed spin recovery procedure.

Unfortunately the squadron will not learn from this pilots spin experience because it must be considered, that before entering the spin, he did something "off limits" and will not mention anything to anybody.

Even, if a pilot returns with an aircraft heavily overstressed by gyration, the accident investigator will have troubles in finding out the reasons, because the pilot will tell him everything but the truth. This is also due to the fact that in Germany a pilot may well be fined a "not too small" amount of money should the investigation board find out that the accident was caused by the pilot not adhering to the mission or flight order.

4.3 Accident Investigation

"General Flugsicherheit", the flight safety service of the Bundeswehr, registers all spin accidents under the headline "Loss of Control".

As this subject covers a vast variety of accidents (ground accidents in high wind conditions are also considered as a loss of control), it is very difficult to sort out and classify separately the real spin or post stall accidents.

In the following are given the figures of accidents that could be clearly identified as being due to post stall gyrations:

G-91

Only one accident was identified as being due to spinning. As the aircraft is operated most of the time at 5oo ft AGL with 35o KIAS, the risk of stalls or spins is small. Should it happen, it will be very difficult for the investigator to find out.

F 104

2,1% of the total accidents were due to post stall gyrations. Most of these accident occured when, for some reason or other, the APC system was not operating.

F 4

The accident rate of this aircraft is very low. The RF 4 E like the G-91 is mainly operated in low level with little risk of stalling. The risk is considerably increased in fighter operations. There was already one accident where the pilot exceeded the operational limits of the aircraft with subsequent loss of control.

5 INOFFICIAL OPERATIONAL SPIN EXPERIENCE

As already mentioned, spins are not allowed in normal Air Force operations.

Nevertheless, it is known that several pilots have encountered spins, but their experiences were only released during a Friday beercall after 11 p.m.

As for the F-104 pilots, their experience always sounds as follows: "I pulled hard to get behind him and suddenly found myself in a terribly disorientating maneuver. I don't know how I made it, but suddenly the gyration stopped and I recovered the airplane".

A very interesting report from a G-91 pilot reads as follows: "I am quite experienced in spinning this airplane, I made spins on the single and two seaters, with and without external tanks, until the day when I made my first spin with the recently adopted large 520 liters external tanks. After the entry I found myself in a normal spin, but when I tried to recover after 5 revolutions - nothing happened. I therefore started "pumping" the elevator fore and aft, but producing only a light pitch oscillation. Then I shut off the engine, and the aircraft recovered, I found myself 3.000 ft above ground, terribly excited in a quiet sailplane".

So much for this pilot's report. As he is not on the incident or accident list of the GAF, it is quite obvious that he managed to restart the engine and to complete his mission as planned.

6 CONCLUSION

The spin experience gained by the German Air Force during the last 20 years is a peacetime operation experience where the aircraft are handled mainly under the aspect of flight safety. Spin experience acquired during this type of operation is very limited and of no use for aircraft designers, nor as a basis of discussion for airworthiness considerations.

If a complete picture on the problems encountered in this field is wanted, the operational experience of nations recently engaged in actual combat operations will have to be analysed. Only during such operations are pilots forced to fight for their lives, and only under these circumstances they won't care anymore about respecting aircraft limitations.

Precisely this fact will have to be taken into consideration by the aircraft manufacturers in the design of new aircraft.

To prepare the crews for combat situations, the operational authorities should provide training for their pilots, even in peacetime, such as to teach how an aircraft will behave when the normal limits are exceeded, especially when flying in the pre-stall buffeting region.

Once a year, a spin training program on a jet airplane should be taken into consideration: An aircraft on which this can be done will be the Luftwaffe's new ALPHA-JET.

If this should not be possible, the minimum requirement must be a training program even on a light acrobatic trainer, which shows all typical spin modes including inverted spins. This aircraft should have self recovery characteristics, but the normal recovery procedure should require a positive pilot action.

A COMPARISON OF MODEL AND FULL SCALE SPINNING CHARACTERISTICS ON THE LIGHTNING

B.R.A.BURNS
Assistant Chief Aerodynamicist
British Aircraft Corporation Limited,
Military Aircraft Division,
Warton Aerodrome,
PRESTON
Lancashire
PR4 1AX

SUMMARY

"Lightning" spinning history is reviewed and a comparison is made of the characteristics as shown by Vertical Wind Tunnel, helicopter drop model and full scale flight trials. The comparison is made in terms of both qualitative interpretation of the spin and recovery behaviour and measured data.

It is shown that the three types of tests exhibited good qualitative agreement in all important respects. Only a limited quantitative comparison is possible because of limitations of the measured data and differences between the test techniques.

The test results are related to Service experience and some observations are made about the interpretation of spinning test results and the need for simplicity in pilot's operating notes.

1. INTRODUCTION

The Lightning (Figure 1) was designed in the early 1950's as a supersonic, high altitude interceptor. A combination of high thrust/weight ratio, in the region of 1, and moderate wing loading - about 65 pounds per sq.foot - conferred outstanding supersonic performance in acceleration and manoeuvre. The same formula has since become fashionable for air superiority fighters.

Throughout the flight development of the early Marks the main emphasis was on supersonic performance and handling, with comparatively little attention devoted to subsonic, high incidence, manoeuvring behaviour. In fact, the Lightning entered Squadron Service in 1960 before full scale stalling and spinning trials had been undertaken.

2. TEST EXPERIENCE

2.1.Helicopter drop models

The overall spinning history of the Lightning is summarised in Figure 2.

Full scale stalling and spinning trials were preceded by model tests using 1/8th scale models (Figure 3) dropped from a helicopter. The models were dropped from a height of about 4,000ft at zero forward speed with pro-spin controls. After a pre-set time interval the tailplane and rudder controls were moved to the "recovery" position by means of spring-loaded mechanisms activated by a clockwork timer. After a further time interval the model recovery parachutes were deployed. Model behaviour was photographed by ground cameras and the flight path and attitudes determined by kine-theodolite records. The results were used mainly to give qualitative information on spin and recovery characteristics, that is spin attitude, steep or flat, calm or oscillatory, recovery or no recovery. This was backed up by limited quantitative information - time per turn, rate of descent, amplitude of oscillations and turns to recover. A typical time history, from kine-theodolite measurements, is shown in Figure 4. A total of 27 successful model drops using 4 models was made in the course of testing 1- and 2-seat variants with a variety of weapon configurations.

2.2.Full Scale Tests

In accordance with U.K. requirements for fighter aircraft, to cater for inadvertent spins only, full scale trials were confined to demonstration of recovery from stalls and 2-turn spins entered in both straight and manoeuvring flight. All tests were monitored from the ground using telemetry. Special cockpit instrumentation was provided to give unambiguous indications of spin direction and attitude, and a spin recovery parachute was carried (but never used).

A total of 128 spins was carried out in Lightning Marks 1, 3, and 4, and a further 130 on the Mark 6. A typical flight record is shown in Figure 5.

2.3. Vertical Wind Tunnel Tests

Although some early tests in the prototype P1A configuration had been made in the RAE Bedford vertical wind tunnel these results were not used to provide handling information on the Lightning, being unrepresentative in fuselage geometry and in mass distribution.

During the period of development of the Lightning Marks 1 to 5 (1957-63) there was no spinning tunnel available in the U.K. and all model spinning tests were carried out on helicopter-drop models. The same technique was used to test the Lightning Mark 6 configuration, with cambered wing leading edges, additional ventral fuel and ventral fins (Figure 6). Helicopter-drop model tests revealed no significant differences from earlier Marks and in fact the Mark 6 entered service before full scale stalling and spinning tests had been made, with instructions in pilots' notes regarding spin and recovery identical to those of the earlier marks. However, during the early Service history of the Mark 6 some inadvertent spins occurred; the pilot descriptions of these suggested a smoother, slightly flatter and faster spin than earlier Marks with prolonged recovery. In the light of this experience and because of favourable impressions of vertical wind tunnel tests formed during BAC involvement in the Jaguar model spinning tests, a programme of vertical wind tunnel tests at IMF Lille, using a Lightning model was undertaken. This preceded full scale trials on the Mark 6.

The Lille programme, using a 1/24th scale model, was divided into two phases :

1. Tests in the Marks 1 and 4 configuration to establish credibility by comparison with full scale and helicopter drop model experience.

2. Tests in the Mark 6 configuration

The same model was used, with interchangeable noses (1- or 2-seat) wing leading edges (plain and cambered) ventral tank (250 or 600 gallon), packs and fins.

Features of the Lightning relevant to its spinning characteristics are :

- A value of B/A ($^{IYY}/_{IXX}$) in the region of 5 or 6
- Unswept rudder, unshielded by tailplane wake at high incidence
- Unswept ailerons
- Low-set all-moving tailplane

Principal differences between the Marks referred to are listed below.

LIGHTNING : PRINCIPAL DIFFERENCES BETWEEN VARIANTS TESTED

	Mark 1.	Mark 4.	Mark 6.
Nose	1-seat	2-seat	1-seat
Fin	130%	130%	145%
Ventral tank	250 gall	250 gall	600 gall
Leading edge	Plain	Plain	Cambered
Ailerons	Horn-balanced ± 8°	Horn-balanced ± 8°	Plain ± 10°

3. TEST RESULTS

3.1. Interpretation of results

In comparing the results of the two types of model tests and full scale tests, the capabilities and limitations of the three types of testing must be recognised.

These are summarised below :

Phase of Spin	Helicopter drop	Vertical W.T.	Full Scale
Entry	Broadly representative of entries in straight flight and moderate manoeuvres	Not representative	
Incipient Spin	Representative	Can be assessed by observing spin development from launches at different combinations of incidence and rate of rotation but gravity terms are incorrect.	
Developed Spin	Not tested generally. Up to 6 turns tested on Mark 6 models.	All types of developed spin, which could result from any type of entry can be assessed.	Not tested (No requirement.)
Recovery (to "rotation ceased")	Representative of recovery from incipient spins.	Representative of recovery from all types of spins.	Recovery from 2-turn spins only.
Post-recovery motions	Not represented (could be done with extension of model techniques).	Representative, as far as motions are contained within the tunnel.	

Overall it can be said that the helicopter drop model tests and full scale trials concentrated on the incipient spin, whereas the vertical wind tunnel yielded information on all possible types of developed spin.

3.2. Qualitative Comparison

Qualitative comparisons of the salient characteristics of the spin and recovery are made in the following tables.

From these tables, it is evident that both helicopter drop and vertical wind tunnel model tests showed good agreement, in most significant respects, with full scale flight results. The only significant differences were :-

(i) The helicopter drop model tests on the Mk.6 failed to reveal an important difference from earlier Marks - the tendency to remain in a persistent spin over a much wider range of control positions - hence greater importance in applying correct recovery control.

(ii) The vertical wind tunnel results did not reveal the phase difference between roll and pitch oscillations between Mks. 1 and 4, observed in the helicopter drop and full scale trials, or the difference in optimum tailplane angles for recovery. However, these are detailed points.

LIGHTNING

MARKS 1 and 4 - QUALITATIVE COMPARISON OF SPIN AND RECOVERY CHARACTERISTICS

TABLE 1

Characteristic	Helicopter-drop models	Vertical wind tunnel	Full scale flight
Spin behaviour	Moderate, regular oscillations about all axes. Period of oscillation ½ turn of spin. Mark 1: Nose high with wings level. Mark 4: Nose high with outer wing down.	Similar Detail difference not reproduced	Similar This detail difference was reproduced in flight.
Time/Turn	4.3 secs	4 secs	5-6 secs
Rate of descent	440ft/sec	400ft/sec	350-400ft/sec
Recommended Recovery Controls	Rudder - full out-spin Ailerons - Neutral Tailplane -7°(Mk.1) -3°(Mk.4) (limited variations only)	Rudder - full out-spin Ailerons - Neutral Exact position not critical -7° best overall	Rudder - full out-spin Ailerons - Neutral Approx.neutral (-3°to -7°);more +ve on Mk.4.
	Recovered in 1 turn	Recovers in 1-2 turns	Recovers in 1-2 turns
Recovery with Controls neutral	Not tested	Good chance of recovery in 2-3 turns	Successful, but delayed, recovery. (3 turns)
Effect of Ailerons	Not tested	IN-SPIN Favours recovery but reversal of spin likely OUT-SPIN Behaviour less predictable.	IN-SPIN Rapid recovery followed by reversal of spin. OUT-SPIN Delays or prevents recovery.

TABLE 2

LIGHTNING

MARK 6 - QUALITATIVE COMPARISON OF SPIN AND RECOVERY CHARACTERISTICS

Characteristics	Helicopter-drop models	Vertical wind tunnel	Full scale flight
Spin behaviour	Oscillatory, as earlier Marks, but with reduced amplitude and steadier rotation rate.	Two types of spin: oscillatory, as earlier Marks, or calm.	Mild oscillations only, between "oscillatory" and "calm" spins found in VWT.
Recommended Recovery Action	Rudder:out-spin Ailerons:Neutral Tailplane:-7° (As Mks. 1 and 4) Recovers in 1 turn.	Rudder out-spin Ailerons:Neutral Tailplane:-7° Recovery in 1-2 turns (As Mks 1 and 4 but more important to observe recovery instructions precisely; spin maintained with wider range of control positions than on Mks 1 and 4).	Rudder:out-spin Ailerons:Neutral Tailplane:forward of neutral. Recovers within 2 turns.
Recovery with Controls neutral	Not tested	Doubtful	Doubtful.(Some sign of incipient recovery after 4 turns)
Effect of Ailerons	Not tested	IN-SPIN Rapid recovery OUT-SPIN Maintains spin - over rides effect of out-spin rudder.	IN-SPIN Rapid recovery followed by reverse spin. OUT-SPIN Generally delayed recovery. Effects somewhat random.

3.3. Quantitative Comparison

Because of differences between the test techniques - control positions, duration of spin etc., comparison of quantitative test results is difficult. For this reason such comparison has been restricted to the Mk.6 configuration in which some more prolonged spins were made in full scale and with helicopter drop models. The quantitative comparison is shown in Figure 7.

This figure shows that there is good agreement between the results of helicopter drop model and vertical wind tunnel tests on time per turn of spin with pro-spin controls. With controls neutral the full scale results agree with the slow extreme of the range of times measured in the vertical wind tunnel.

Rates of descent show reasonable agreement from all types of tests.

Pitch attitudes show good agreement between full scale and helicopter drop models and lie within the range of values corresponding to different spins in the vertical wind tunnel. Pitch oscillations measured on helicopter-drop models and in the vertical wind tunnel were similar. The full scale flight spin exhibited oscillations in both pitch and roll of reduced amplitude compared with the models, being close to the calm spin found in the vertical wind tunnel.

3.4. Comparison : Summary

Overall, the results of the three types of tests showed good qualitative agreement in all important respects. Quantitative results also agree quite well, where direct comparison is possible.

Vertical wind tunnel and helicopter drop model tests are considered to be complementary rather than competitive. The VWT can be used to investigate a very wide range of control positions and configurations within a short time. Helicopter model tests can be used to investigate spin entry and recovery, unconfined by tunnel walls.

4. SERVICE EXPERIENCE

During the 15 years that the Lightning has been in Service, there have been a number of reported inadvertent spins in service, some of which culminated in pilot ejection. The statistics show an average of one aircraft lost due to a spinning accident, per 60,000 hours flying time over the total period in Service with the RAF, RSAF, and Kuwait Air Force.

The common features of these incidents were :

- Pilots were taken completely by surprise; spins usually occurred while doing a "head-up" task, e.g. an evasive combat manoeuvre and the speed had been allowed to decay without the pilot realising it, while manoeuvring beyond the sustained manoeuvre boundary.
- Lack of immediate recognition of the incipient spin. The first indication to the pilot that something is wrong is usually lack of response in roll or rolling against the applied aileron.
- When the spin is recognised and recovery control applied, the pilot is usually surprised by the long time to respond to recovery control.

These points are all related to lack of recent spinning experience by operational pilots. Many of them had not spun since basic training days, perhaps 5 or 10 years before. The latter point is particularly noteworthy. It is important to educate operational combat pilots to expect a long time to respond to controls. Although the Lightning recovers quite quickly (usually within 10 seconds) this may seem an age compared with response times to control in normal flight (of the order of 1 second). In particular the tendency to "try some other control action because nothing seems to be happening" must be resisted.

5. PILOT'S INSTRUCTIONS

The most imporant outcome of a spinning trial is the advice to Service pilots on :

Spin avoidance

Spin recognition

Spin recovery

The advice must be clear and irrelevant information excluded. For example, although in the incipient stage of a spin it is meaningful to differentiate between roll and yaw, once the spin has developed this distinction becomes an academic one: to a pilot who is not in spinning practice, the whole world seems to be rotating and the axis of rotation is not easily identified. Even to talk about pitching motion as opposed to roll and yaw can be misleading because the Service pilot tends to derive motion cues from attitude changes; an aeroplane can change attitude from "nose high" to "nose down" by yaw or by pitch and it is dangerous to translate body axis motions into pilot briefing data in the same terminology. A further point concerns the distinction between "calm" and "oscillatory" spins. In the incipient stage of a spin where the trajectory is changing from the horizontal to the vertical, large apparent changes in pitch attitude occur once per turn even when the rates of rotation, in body axes, are steady. This effect is illustrated in Figure 8 and in the accompanying film.

Subtle changes in behaviour such as may occur due to variation in mass distribution with fuel usage or with external store configuration are irrelevant to the Service pilot, and should be excluded from operating notes. Statements such as "with underwing pylons fitted the spin is less oscillatory and recovery time is prolonged slightly" may be interesting to the test engineer but irrelevent to a Service pilot who, we hope, will spin only once, if at all, in his operational career on the type and cannot therefore, relate that experience to any other incident.

A significant revision made to Lightning Pilot's notes concerning spin recovery at one stage in its Service history was the introduction of a "wait and see" period between initial loss of control and application of recovery controls. On recognising loss of control, instead of immediately trying to identify the motion and apply appropriate control actions, the pilot is instructed to :

1. Centralise controls
2. Confirm that the aircraft is spinning
3. Assess direction of rotation
4. etc (apply recovery controls)

It is believed that in many cases the action of centralising the controls and allowing the natural stability of the aeroplane time to have effect would prevent a spin whereas "fighting the motion" might well provoke a spin. U.S. experience, reported in the 1971 WADC Spin Symposium, reinforces this belief.

6. CONCLUDING REMARKS

In the Lightning, we were fortunate to have an aeroplane with docile spin and recovery characteristics on which to learn and develop the test techniques. This has stood us in good stead for later projects. Perhaps the most important lesson learned is that no single test technique yields completely comprehensive or entirely credible results. it is only by a combination of model testing, full scale flight testing and (on later projects) analytical techniques that a total picture of the spinning behaviour can be built up.

ACKNOWLEDGEMENT is made to the test pilots and engineers who took part in the trials and to the Staff of the I.M.F. Lille for their careful and searching investigations.

FIG. 1

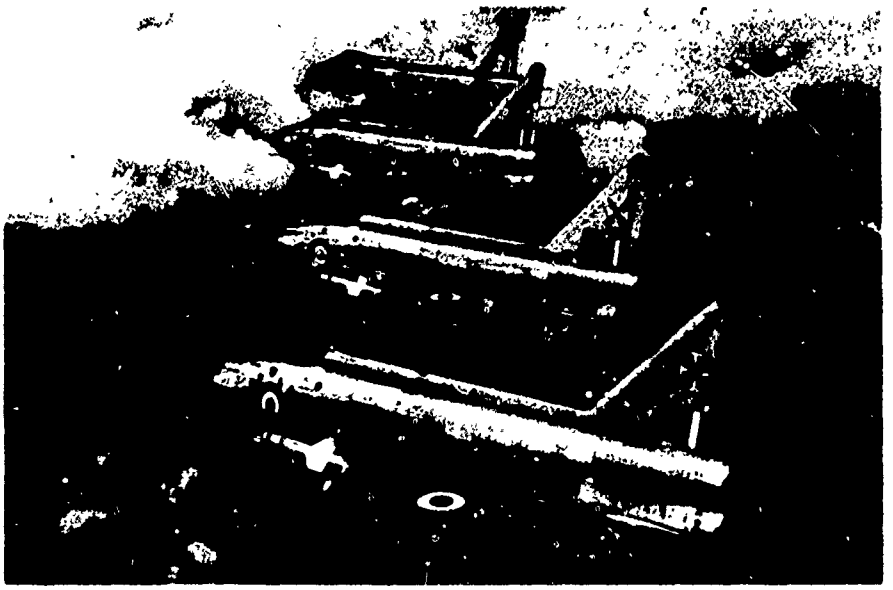

LIGHTNING F. MK 1 (WITH 2 FIRESTREAK MISSILES)

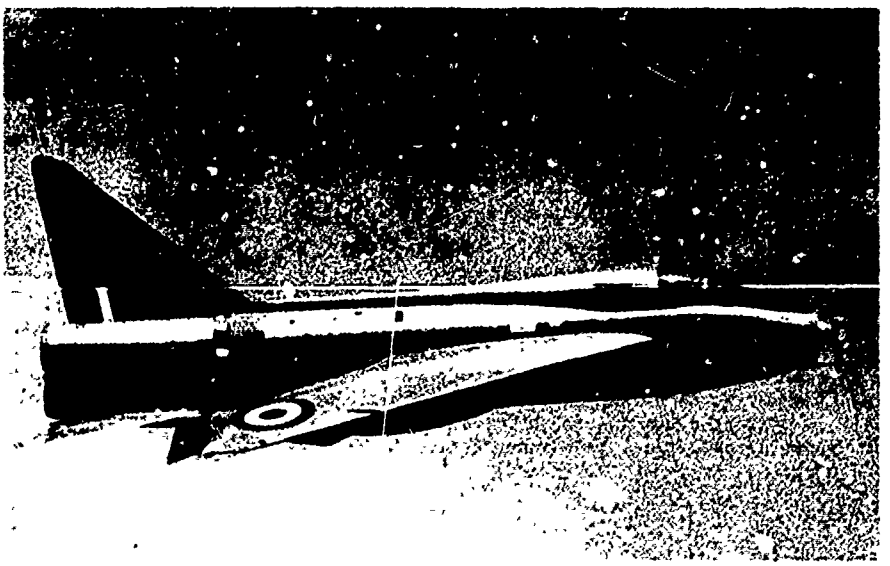

LIGHTNING T. MK 4

FIG. 2.

LIGHTNING SPINNING HISTORY.

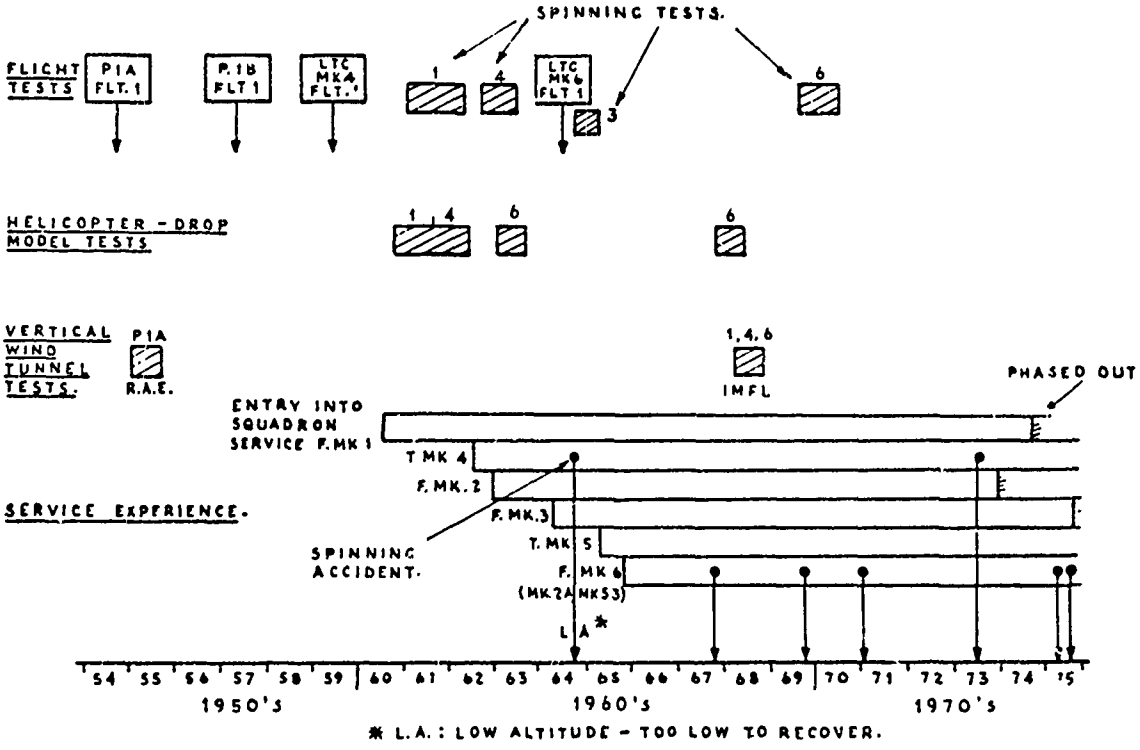

LIGHTNING MK 6 HELICOPTER DROP MODEL FIG. 3.

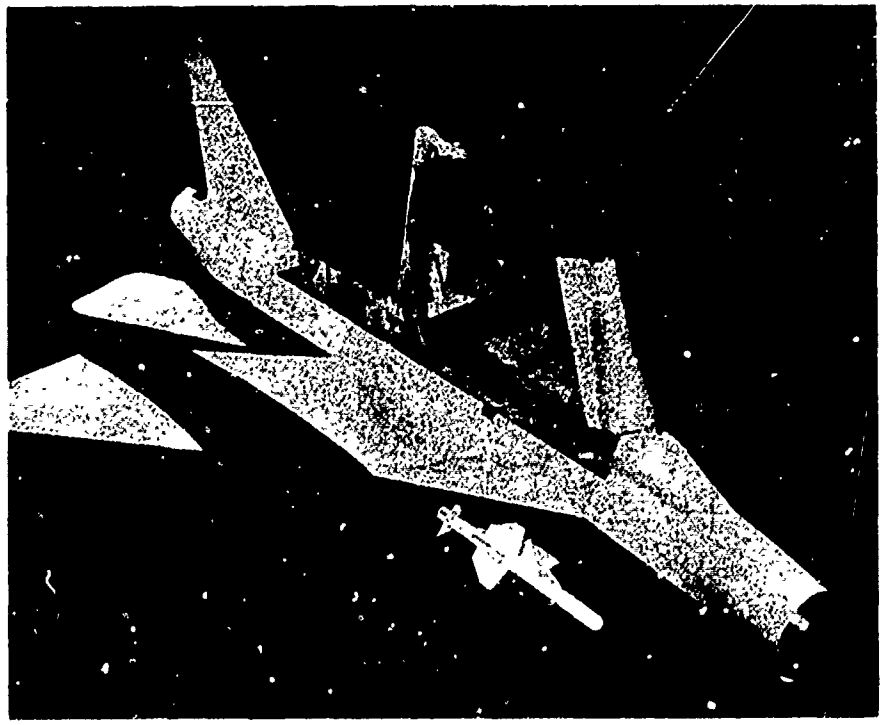

FIG. 4

EXTRACT FROM A TYPICAL HELICOPTER DROP MODEL
SPIN RECORD - LIGHTNING MARK 6.

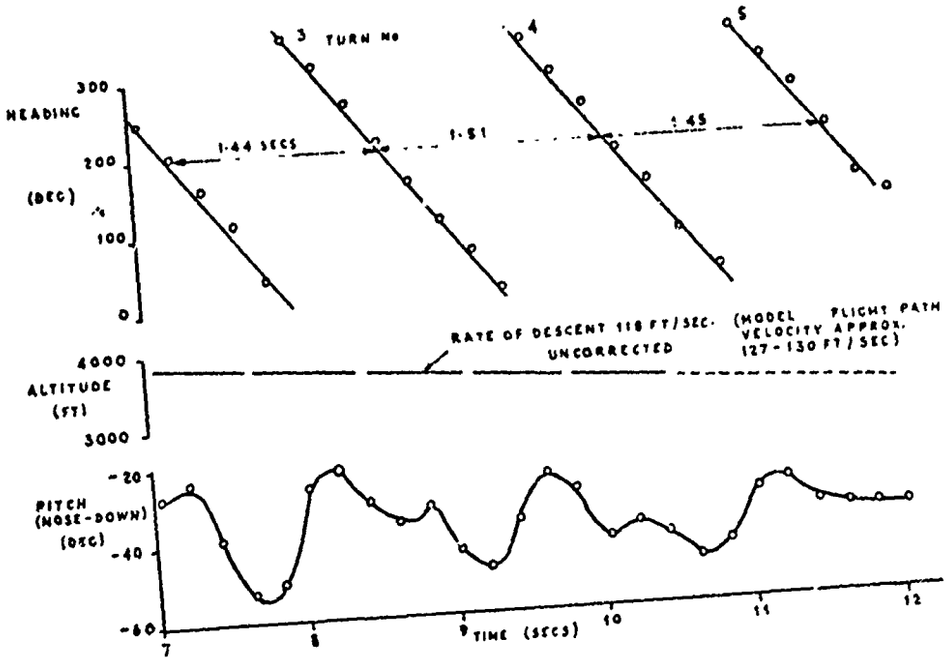

TYPICAL FULL SCALE FLIGHT SPIN RECORD
LIGHTNING MARK 6

FIG 5

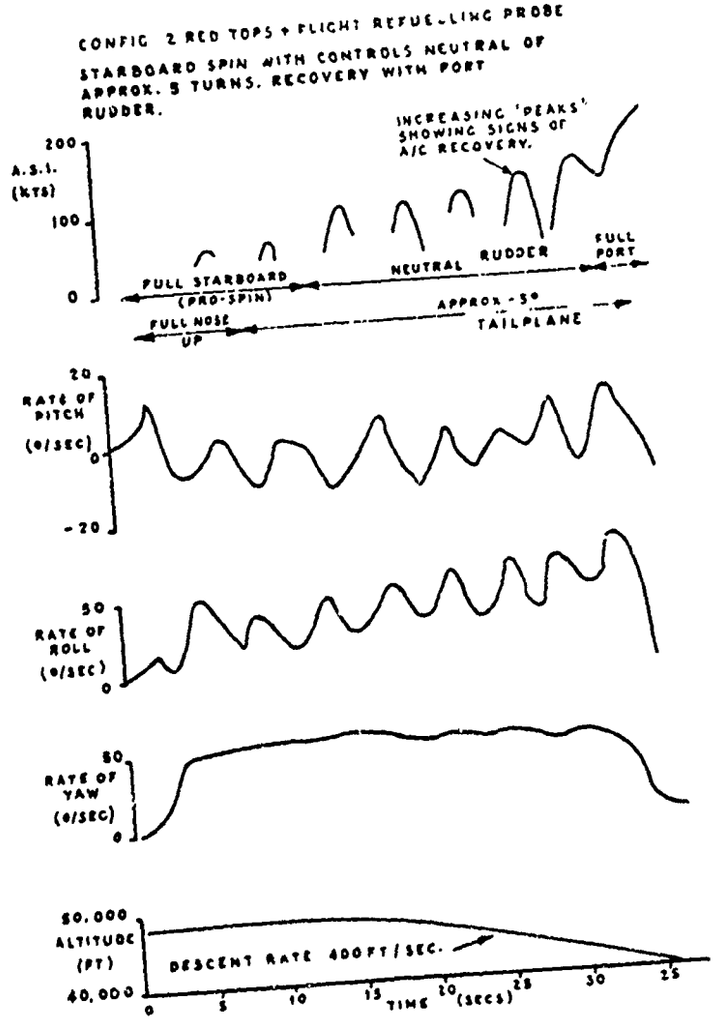

FIG. 6

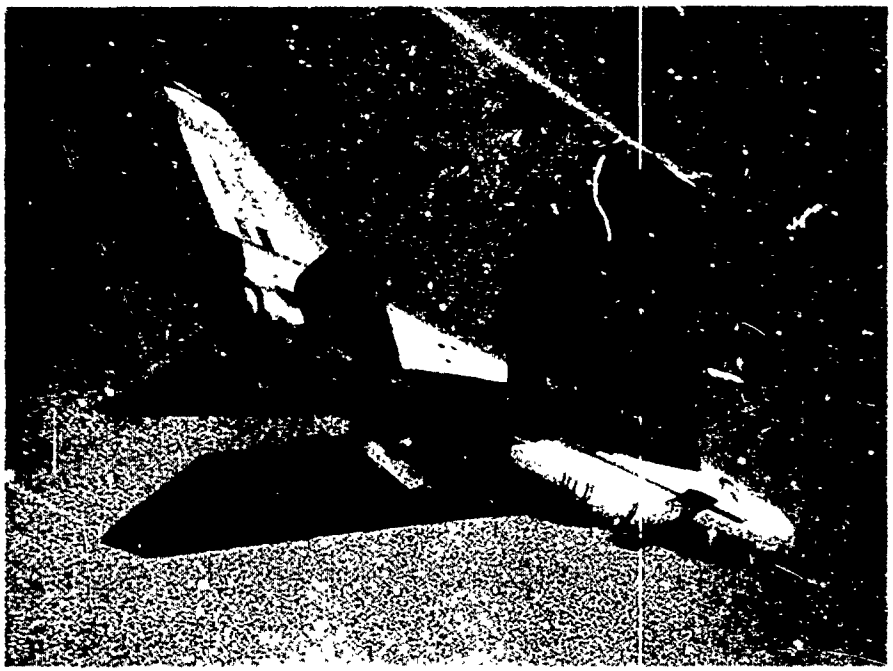

LIGHTNING F. MK.6

LIGHTNING MK 6 SPINNING. COMPARISON OF VERTICAL WIND TUNNEL, HELICOPTER-DROP MODEL & FULL SCALE FLIGHT RESULTS

FIG7

* CORRECTED FULL SCALE

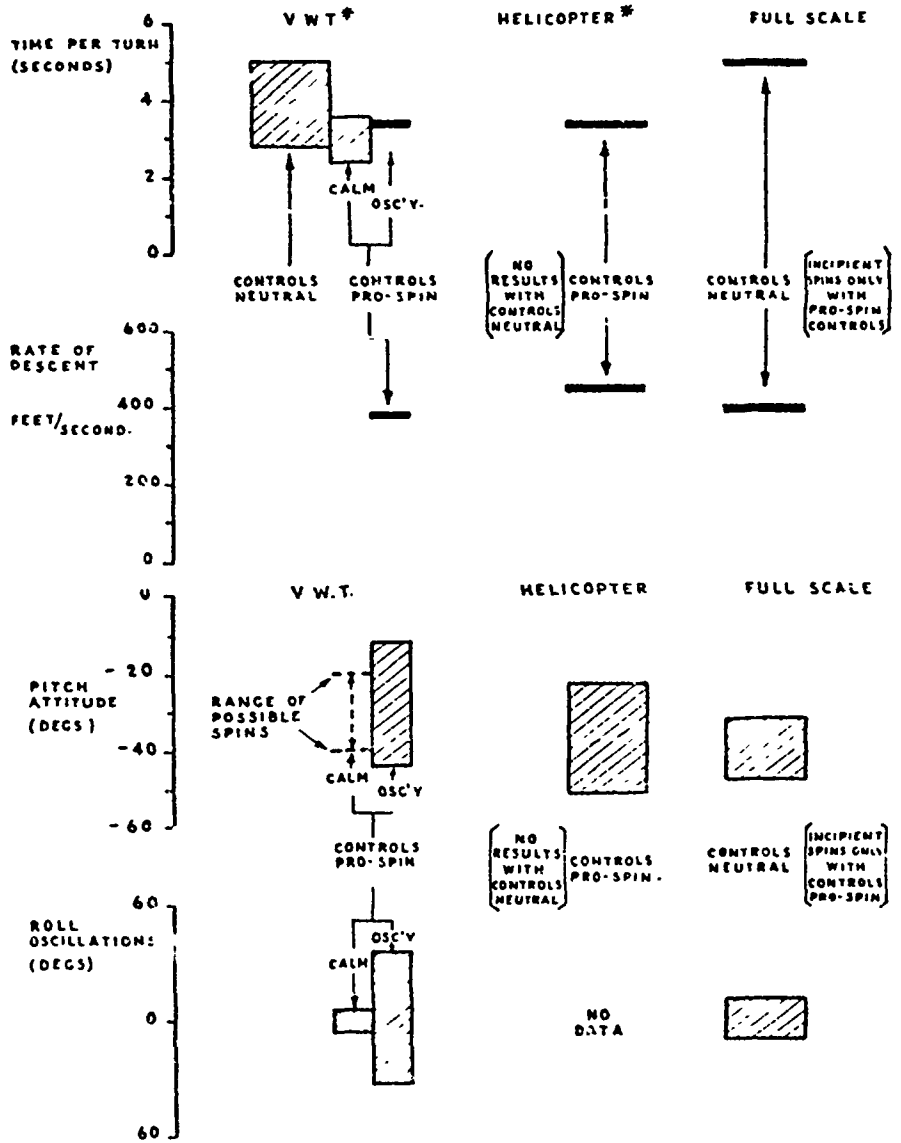

FIG. 8

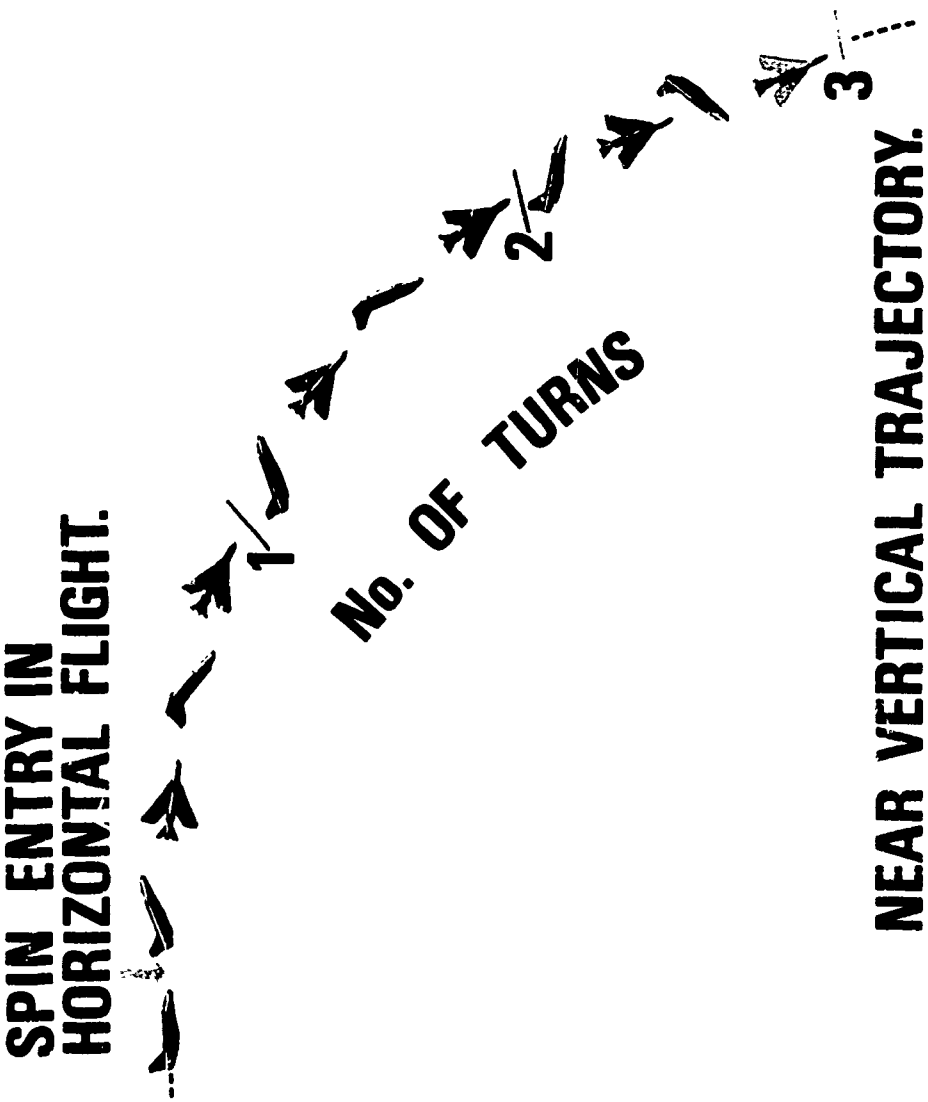
SPIN ENTRY IN HORIZONTAL FLIGHT.
1
2
3
No. OF TURNS
NEAR VERTICAL TRAJECTORY.

DESIGN TECHNOLOGY FOR DEPARTURE RESISTANCE OF FIGHTER AIRCRAFT

by
A. Titiriga, Jr.
J.S. Ackerman
A.M. Skow

Northrop Corporation
Aircraft Division
3901 W. Broadway
Hawthorne, California
90250 U.S.A.

1. SUMMARY

Good stall/post stall characteristics are required for a fighter aircraft in order to fully utilize its potential during air combat. Prediction of these characteristics, prior to flight test, of prototype or first production aircraft is a difficult problem that has received industry-wide emphasis. Because of the current schedules associated with free flight model tests, early stall/post stall predictions using wind tunnel data and computer techniques are necessary in some cases to avoid possible extreme modifications to production aircraft.

Methods are presented for predicting departure characteristics of aircraft during the design stages prior to model or flight tests. The significance of longitudinal pitching moment characteristics with respect to sideslip is discussed and correlated with flight test data. The use of departure parameters is discussed and examples are presented which show good correlation with flight test results.

A computer graphics display of the aircraft driven by actual flight test data has proven to be extremely helpful in visualizing complex motions of an aircraft. In particular this technique shows great promise in aiding both pilots and engineers in describing disorienting post stall gyrations that may be encountered during stall/spin flight testing of an aircraft. A computer graphics display available for on-line testing would contribute substantially to safety of flight during spin test programs.

2. INTRODUCTION

An effective air combat fighter aircraft must be sufficiently free of adverse flying qualities so that the pilot can concentrate his attention on his opponent. This is especially true in the high angle-of-attack region where he may be either tracking at high g's, or executing extreme evasive maneuvers in a defensive posture.

The prediction of high angle of attack characteristics prior to actual flight testing is difficult and is receiving industry wide emphasis. Because of the relatively long lead time necessary to acquire free-flight model data, reliance must be placed on determinations employing wind tunnel six component data and computer techniques. The undesirable alternative is to wait for flight testing to disclose problem areas which may require extensive airframe modifications to correct.

Prediction techniques discussed herein can illustrate an aircraft's behavior more accurately than inflight experience by indicating specific regions of angle-of-attack or sideslip where instabilities may occur. For example, the F-5E flight test program included numerous full aft stick stalls in both air-to-air and air-to-ground configurations and no departure tendencies were exhibited. In spite of these extensive flight tests, two operational aircraft were lost in spins. Subsequently, a thorough flight test investigation was conducted and specific guidelines were formulated to correlate wind tunnel tests with analytical predictions and flight test results.

Part of the problem of high angle-of-attack stall/departure prediction arises from the aerodynamic nonlinearities with both angle-of-attack and sideslip. These aerodynamic nonlinearities arise from flow separation and formation of vortex shedding systems both from the wing and from the body. Evidence of the latter is readily available in examining body alone and wing-body lateral-directional wind tunnel data obtained over an angle-of-attack range at zero sideslip.

Further difficulties arise during the testing phase in attempting to visualize the complex aircraft motions in the stall which are presented to the engineering analyst by means of time histories of the angles, rates and accelerations obtained from an instrumented aircraft. A real breakthrough in this area has been the utilization of a computer graphics display, which includes a three-dimensional image of the aircraft, and which can translate a complex flight test time history into an immediately recognizable mode of aircraft motion. An on-line computer graphics display could also contribute significantly to flight safety by giving the pilot, who may have been disoriented due to violent aircraft dynamics, an accurate description of the motion.

It is the intent of this paper to present the methods employed at Northrop in the preflight determination of high angle-of-attack handling characteristics and the steps that may be taken to deal with specific problems during the aircraft design stage.

3. THE MECHANISM OF DEPARTURE

As an aircraft approaches stall conditions the aerodynamic changes produced by flow breakdown over the wing and tail result in degraded stability and control effectiveness. It is the extent of this degradation which determines whether the aircraft is departure-prone or departure-resistant. Use of controls to prevent departure may not be effective because both aileron and rudder effectiveness are greatly reduced in the stall and, in addition, adverse yaw characteristics may prohibit the use of the aileron.

If the aircraft becomes directionally unstable but still retains a stable dihedral effect of sufficient magnitude, its departure will not be divergent. When both directional stability and dihedral effect become unstable, then any disturbance such as a gust or control input can result in a departure. The departure may be self-terminating or it may result in subsequent spin entry. Once a departure has occurred, an important question arises: Is there any restoring tendency which will impede further uncontrolled excursions and if so, how is it manifested?

If the aircraft has a pitch down at the stall, or if the longitudinal control retains full effectiveness, the departure may be terminated through reduction in angle of attack. There may even be a restoring tendency at large sideslip angles where the vertical tail emerges from the wing-body interference field to restore both directional stability and dihedral effect of sufficient magnitude to attenuate the departure tendency. This effect is characteristic of the F-5.

Working against a self-reducing angle of attack can be a strong nose-up pitching moment at the stall, which is due to sideslip. This effect has been seen in the F-5 at extreme aft c.g.'s and is referred to herein as sideslip/angle of attack coupling. It can be insidious because the pilot usually does not perceive the increase in angle of attack and consequently does not relax stick pressure before excessive pitch attitudes are attained.

When increasing angles of attack and sideslip both result in further degradations in directional stability and dihedral effect and longitudinal control is not effective, (or is not applied!) departure and subsequent spin entry are highly probable.

It is well to mention that probably one of the more important considerations in determining the extent of uncontrolled aircraft motion following a departure is the probability of pilot disorientation. If he is unable to visualize what the aircraft is doing, he will not be able to effectively apply controls which will arrest the motion.

4. WIND TUNNEL TESTING TECHNIQUES

Engineers are confronted with two wind tunnels: The small one on the ground and the big "tunnel" in the sky. Without a correlation between these two it is not possible to accurately predict the stall/spin characteristics of an aircraft. The manner in which wind tunnel data is interpreted is of vital concern to the accurate prediction of aircraft behavior. Techniques have been developed to prove that high attitude wind tunnel data, if obtained and interpreted correctly, can be correlated with flight test results.

It is recognized that the vortices originating from a pointed slender fuselage and those from the wing produce very significant aerodynamic effects in the stall region and beyond (Reference 1, for example). One important point is: These vortices are responsible for the presence of rolling and yawing moments at zero sideslip as seen in Figure 1, and for the aerodynamic hysteresis effects when obtaining sideslip data at constant angle of attack depicted in Figure 2.

These rolling and yawing moments were once considered to be model asymmetries that would not be present on the full scale aircraft; however, this has since been disproven. Interaction of the fuselage vortices and those shed from a wing leading edge extension strongly influence the flow over the wing and tail vicinities. For example, the F-5 fuselage vortex shedding system is asymmetric. The relative motion of the vortex system when the aircraft sideslips is unpredictable in the angle of attack region from stall (24 degrees) to about 30 degrees. These effects appear in lateral directional wind tunnel model force data as asymmetries and greatly complicate the determination of both sideslip and control derivatives. At higher angles of attack the F-5 vortex system appears to be unique in that it produces a stable directional effect. The nose vortex pair separate on the down wind side but on the up wind side they provide a strong suction force on the nose which produces a stabilizing yawing moment. This effect was explored during F-5 tests in the NASA Langley Wind Tunnel (Reference 2).

In determination of the sideslip derivatives for an airplane such as the F-5 which has complex vortex systems it is important to select the most representative sideslip angle from a departure and repeatability standpoint. Consideration should be given to the aerodynamic hysteresis present at sideslip angles from, say, 2 to 5 degrees; a typical hysteresis curve is sketched in Figure 2. Because of these effects,

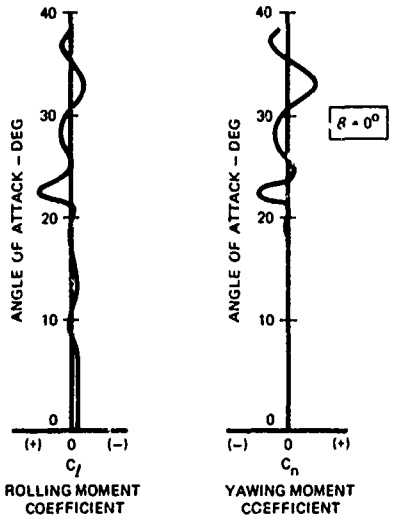

FIGURE 1. ZERO BETA DATA

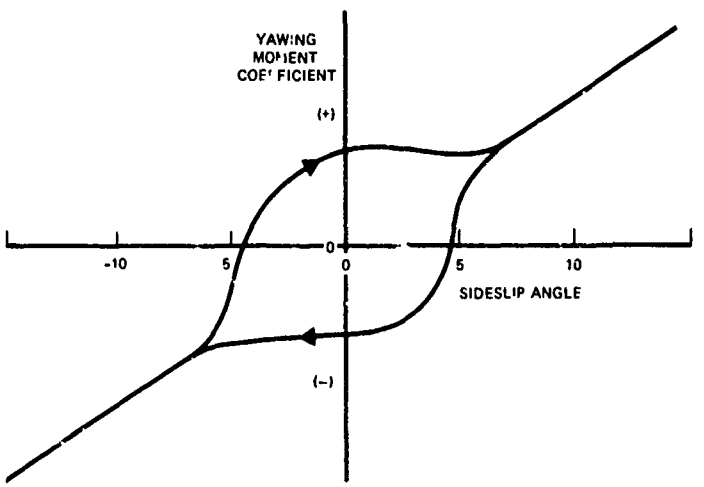

FIGURE 2. AERODYNAMIC HYSTERESIS IN THE STALL REGION

different wind tunnel runs of the same airplane configuration at the same sideslip angle could result in different values for stability derivatives at the stall, depending upon the manner in which sideslip is varied. Consideration should also be given to the apparently less critical stability effects which may occur at the more extreme sideslip angles from 15 to 20 degrees, as presented in Figure 3. At these large sideslip angles, as the vertical tail emerges from the wake of the wing/body combination, directional stability is restored. A kind of lateral/directional stability "wall" exists at extreme sideslip angles which is not pertinent to the aircraft's initial departure characteristics; however, it can act to make a departure self terminating.

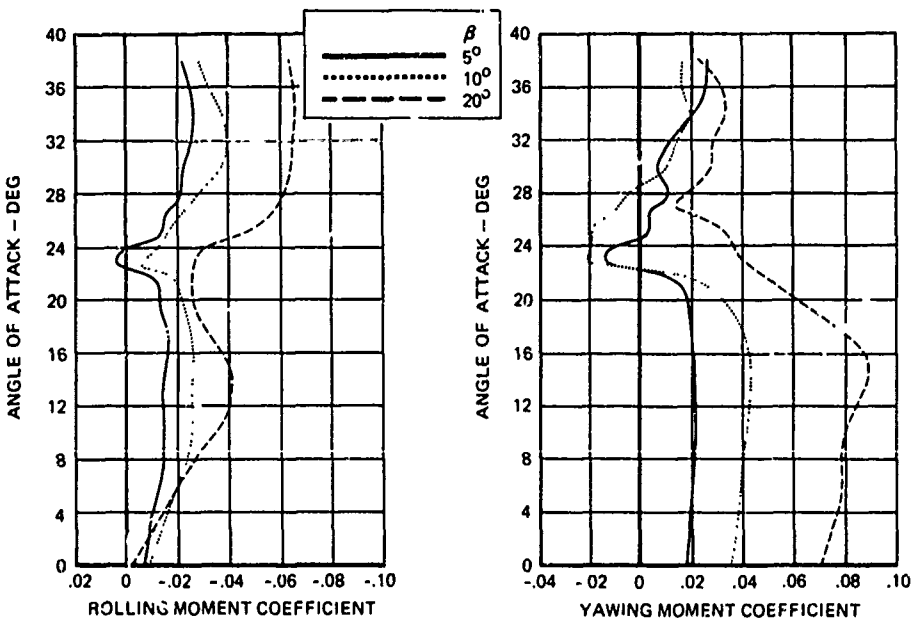

FIGURE 3. EFFECTS OF SIDESLIP ANGLE ON THE SIDESLIP COEFFICIENTS

The wind tunnel technique recommended to determine static sideslip derivatives is to select the appropriate sideslip angle as previously discussed and make pitch runs over a wide angle of attack range. It is important that small angle-of-attack increments of one degree or less be scheduled in the stall region in order to obtain the true stability variations with angle of attack. This effect is presented in Figure 4 which shows the misleading result of testing with too large an increment. In this case the aircraft is indicated to have directional stability and a stable dihedral effect. With smaller increments however, there is a large range of directional instability and the dihedral effect actually approaches zero at the stall.

It is also important to average the sideslip derivatives between positive and negative values of sideslip as presented in Figure 5. It is evident that the zero sideslip curve is not reliable as a zero reference because it lies within the hysteresis band. The zero sideslip values should be utilized, however, as forcing functions when simulating aircraft dynamics at high angle of attack; especially for stall investigations. This will insure that the lateral directional equations are disturbed (in the same manner as the aircraft) without inputs from rudder or aileron, in a six degree-of-freedom simulation.

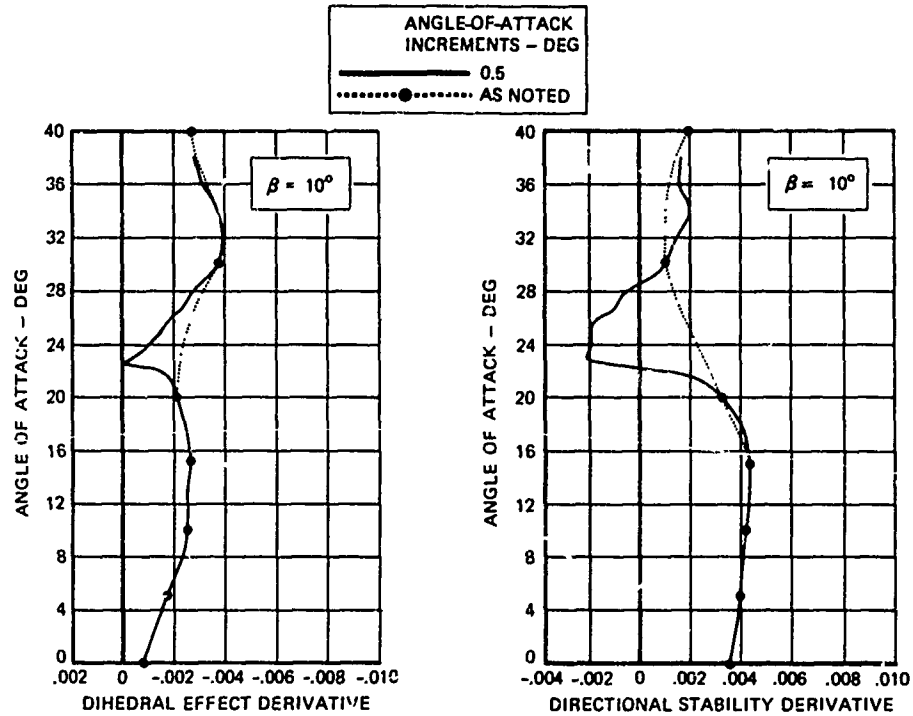

FIGURE 4. EFFECT OF ANGLE OF ATTACK INCREMENTS

The determination of aileron and rudder effectiveness requires a different technique. It is evident from Figure 6 that curves of various rudder deflections do follow the same variation with angle of attack as the zero rudder curve. Therefore the zero rudder curve, rather than the value of zero, should be used as the zero rudder deflection data. This same consideration also holds true for determination of aileron effectiveness. It is also important to perform the pitch runs for each control setting (at zero sideslip) with increasing angle of attack in order to avoid inconsistencies due to hysteresis.

If the curves of various control deflections do not follow the zero deflection curve it may be necessary to run both positive and negative control angles and average the results in the same manner as for the sideslip derivatives.

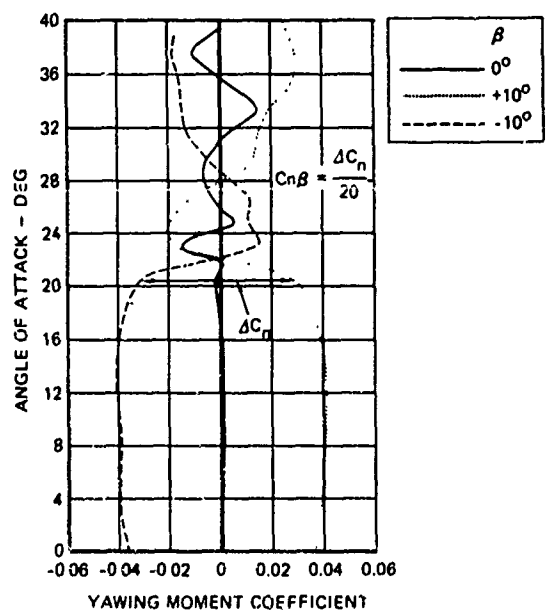

FIGURE 5. DETERMINATION OF SIDESLIP DERIVATIVES

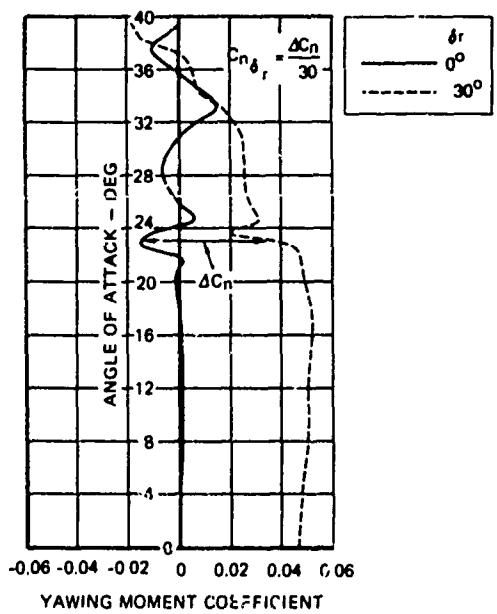

FIGURE 6. DETERMINATION OF CONTROL EFFECTIVENESS AT ZERO SIDESLIP ANGLE

5. AIRCRAFT PREDICTION PARAMETERS

There are three parameters that are useful in predicting aircraft behavior in the stall region. They are all determinable from basic six component wind tunnel data and have proven to be effective in defining regions where the aircraft may be expected to experience departure tendencies.

Directional Departure Parameter:

This parameter is generally known as $C_{n_\beta DYN}$, and has been used successfully to predict the susceptibility of an aircraft to directional departure. It is derived from the open-loop lateral directional quartic equation and represents an approximation of the "C" term. Both the derivation and application of this parameter are presented in Reference 3 where it has been correlated with flight results of 17 different aircraft, ten of which included more than one aerodynamic configuration. A good to fair correlation was obtained for 90 percent of the cases studied, including the F-5A aircraft. The F-5A was the only one to indicate no departure tendencies in both model test and full scale flight test, as well as a positive $C_{n_\beta DYN}$ value to the maximum angle of attack tested, 32 degrees. Possibly the poor correlation obtained on some of the aircraft could be attributed to the wind tunnel testing techniques employed, i.e., the angle-of-attack increment may have been too large.

The expression for $C_{n_\beta DYN}$ is as follows:

Equation 1

$$C_{n_\beta DYN} = C_{n_\beta} \cos\alpha - \frac{I_z}{I_x} C_{l_\beta} \sin\alpha$$

Where: $C_{n_\beta DYN}$ = directional departure parameter ~ per degree

C_{n_β} = directional stability derivative ~ body axes

C_{l_β} = dihedral effect derivative ~ body axes

I_z/I_x = yaw to roll moment of inertia ratio

α = aircraft angle of attack ~ deg

The equation for this parameter may also be derived by expressing the dimensional stability derivative N_β in stability axis and converting to coefficient form:

$$N_{\beta_s} = N_\beta \cos\alpha - L_\beta \sin\alpha$$

Where: N_{β_s} = dimensional directional stability derivative expressed in stability axis

N_β, L_β = dimensional derivatives based on body axis

In this form it is obvious to see that $C_{n_\beta DYN}$ represents the aircraft dynamic directional stability with respect to the flight path rather than the body axis system. If $C_{n_\beta DYN}$ becomes negative, a yaw departure is possible. If it remains negative over a fairly wide range of angle of attack, a yaw departure is highly probable when the aircraft operates in that region.

It is evident from Equation 1 that both the dihedral effect, C_{l_β} and the inertia ratio, I_z/I_x, can contribute significantly to $C_{n_\beta DYN}$. With a stable dihedral effect the dynamic directional stability increases as the inertia ratio increases, and can make up for severe deficiencies in directional stability. The opposite effect occurs, however, with an unstable dihedral effect. Present day fighter aircraft typically have higher inertia ratios than their predecessors as a result of concentrating weight in the fuselage and the trend toward lower aspect ratio wings. This effect can be beneficial from the standpoint of departure resistance improvement through a stable dihedral effect. It can also be highly detrimental if the dihedral effect is not stable.

Figure 7 presents an example of both the aerodynamic and inertia effects when tip mounted missiles are added to the F-5 aircraft. The improvements in both directional stability and dihedral effect overpower the counter effect of a lower inertia ratio and the net result is an increase in $C_{n_\beta DYN}$ in the stall. Below the stall, however, the decrease in inertia ratio is predominant and the aircraft has less $C_{n_\beta DYN}$ with tip mounted missiles.

Although $C_{n_\beta DYN}$ predicts where departure may be expected, it alone does not differentiate between the various modes of motion the aircraft may encounter. The manner in which an aircraft may depart and the dependence upon the individual aerodynamic effects is summed up in Figure 8. It should be noted that

these data are based on F-5 aircraft experience and represent the open-loop lateral-directional characteristics following a stick back and hold maneuver for configurations that experienced a negative directional stability in the stall region.

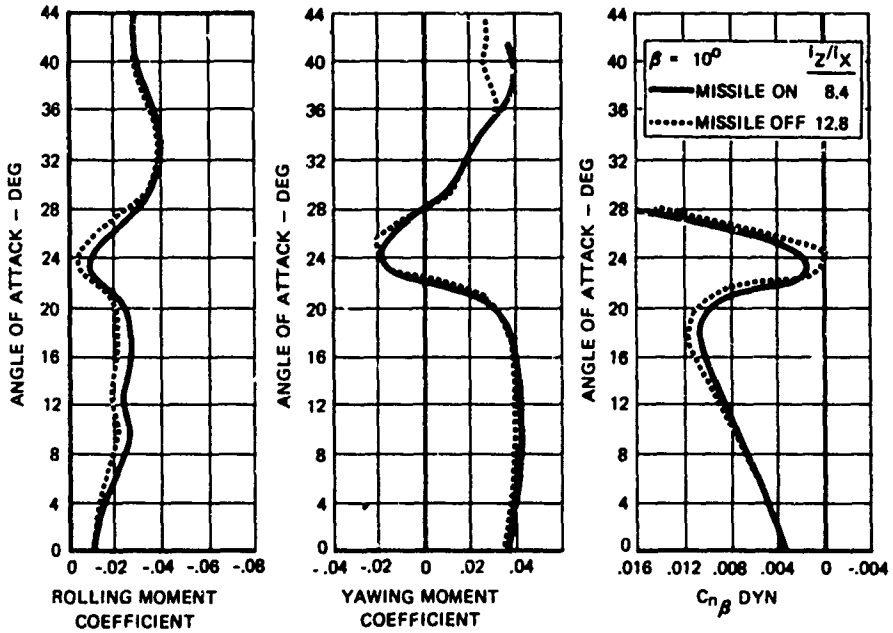

FIGURE 7. THE EFFECTS OF ADDING TIP-MOUNTED MISSILES TO THE F-5E

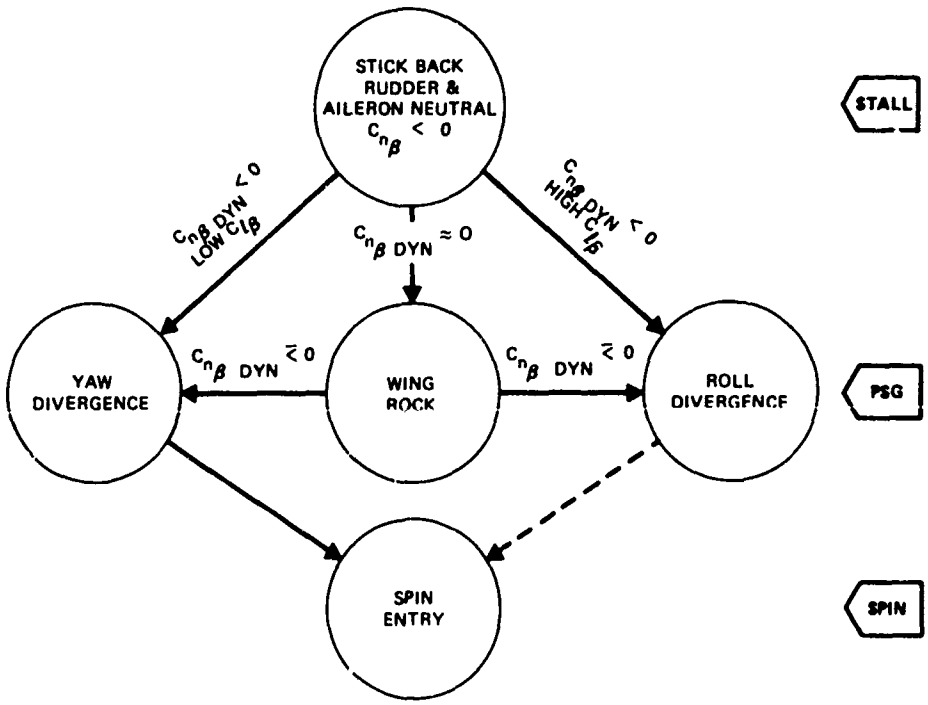

FIGURE 8. AERODYNAMIC EFFECTS ON OPEN-LOOP LATERAL-DIRECTIONAL MODE DEVELOPMENT

For a given value of $C_{n_\beta} < 0$ the motion of the aircraft becomes a function of $C_{n_\beta DYN}$. If $C_{n_\beta DYN}$ is positive, a bounded wing rock, which is primarily a Dutch roll, can result. With the value of $C_{n_\beta DYN}$ near zero or slightly negative the wing rock becomes slowly divergent. Depending on the time spent in this region, and the value of dihedral effect, the aircraft motion can translate to either a roll or a yaw divergence. With directional stability and $C_{n_\beta DYN}$ both negative, an initial yaw develops and the aircraft motion will again depend upon dihedral effect. A yaw divergence can occur with a low dihedral effect while a rolling divergence can be expected with a high dihedral effect.

Lateral Control Departure Parameter:

This parameter has been used in various forms for different uses. It is developed from the simplified rolling and yawing moment equations assuming the aircraft to be laterally and directionally trimmed. As a lateral control departure parameter, LCDP predicts at what angle of attack roll reversal is expected to occur when using ailerons. Reversal in this sense does not mean aeroelastic aileron reversal, but that condition where the rolling moment due to sideslip, resulting from adverse yaw, overpowers the rolling moment commanded by the aileron. To the pilot this condition is known as reverse aileron command or roll reversal.

This parameter has been correlated with spin entry tendency due to aileron adverse yaw for several fighter aircraft (Reference 4, for example, where it is referred to as the aileron alone divergence parameter, AADP). The expression for LCDP also contains the sideslip derivatives and is as follows:

Equation 2

$$LCDP = C_{n_\beta} - \frac{C_{n_{\delta a}}}{C_{l_{\delta a}}} C_{l_\beta}$$

Where: LCDP = lateral control departure parameter

$C_{l_{\delta a}}$ & $C_{n_{\delta a}}$ are the aileron rolling moment and yawing moment derivatives respectively

Aileron reversal occurs when LCDP becomes negative. Note the similarity of the role that dihedral effect plays in this expression relative to its role in $C_{n_\beta DYN}$. It again acts as a "multiplier" and the benefit or detriment in this case depends upon the sign of $C_{n_{\delta a}}$. If the aircraft has adverse yaw due to aileron ($C_{n_{\delta a}}$ is negative), then a stable dihedral effect ($-C_{l_\beta}$) will have an adverse effect. The opposite is true if the aircraft has proverse yaw. If the aircraft has an unstable dihedral effect, then the combined effects of LCDP and $C_{n_\beta DYN}$ will determine the type of departure following an aileron input.

The effect of rudder inputs can also be included in LCDP such as would be present with an aileron rudder interconnect or during a pilot coordinated rolling maneuver. This expression is similar to Equation 2 but introduces the rudder derivatives:

Equation 3

$$LCDP = C_{n_\beta} - C_{l_\beta}\left[\frac{C_{n_{\delta a}} + KC_{n_{\delta r}}}{C_{l_{\delta a}} + KC_{l_{\delta r}}}\right]$$

Where: $C_{n_{\delta r}}$ & $C_{l_{\delta r}}$ are the rudder yawing and rolling moment derivatives respectively and K represents the ratio of rudder to aileron

It can be readily seen that K is the determining factor because $C_{n_{\delta a}}$ is typically small relative to $KC_{n_{\delta r}}$. A negative value of K (right rudder with right stick) is of course required to counter the effects of adverse yaw, or to augment the roll performance, through a stable dihedral effect.

Figure 9 shows the variation of LCDP with angle of attack for aileron alone for the F-5F with and without centerline tank. It is noted that little roll response from aileron should be expected in the region from 18 to 23.5 degrees angle of attack for the centerline tank configuration.

A portion of the time history of a 1g stall is presented in Figure 10 for this same configuration and shows no roll response at an angle of attack of 22 to 23 degrees even though the pilot is commanding 40 degrees of aileron. The sideslip due to adverse yaw is overpowering the ailerons in this case, as predicted by Figure 9. Roll control can still be achieved with rudder, however, through the stable dihedral effect.

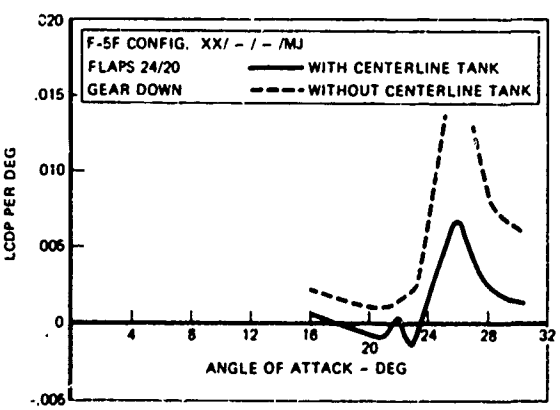

FIGURE 9. LATERAL CONTROL DEPARTURE PARAMETER VS ANGLE OF ATTACK, F-5F WITH MISSILES

Sideslip/Angle of Attack Coupling Parameter:

This parameter is the single aerodynamic derivative which indicates lateral-directional to longitudinal coupling (pitching moment due to sideslip). This phenomenon has been observed during flight test of an F-5E in performing full back stick stalls at the aft c.g. limit. An intentional use of this effect

($+C_{m_{|\beta|}}$) was evidenced when the F-5A went into service. Operational pilots reported they would walk the rudder pedals in a low speed, high attitude maneuver in order to hold the nose up for a longer period of time. The variation of $C_{m_{|\beta|}}$ with α for a typical configuration tested in the wind tunnel is shown in Figure 11.

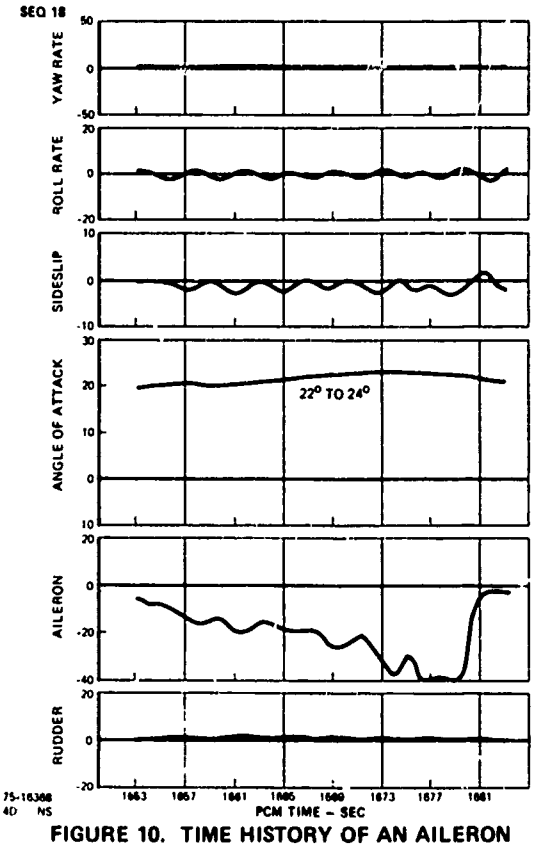

FIGURE 10. TIME HISTORY OF AN AILERON INPUT DURING A 1 G STALL, F-5F 8891, FLT 78

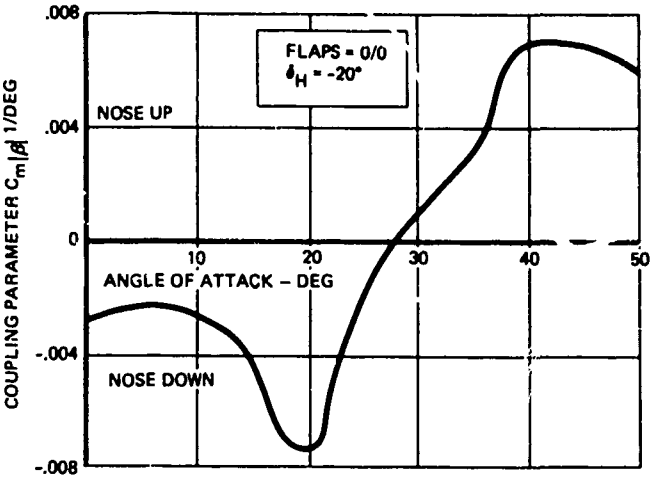

FIGURE 11. VARIATION IN PITCHING MOMENT DUE TO SIDESLIP WITH ANGLE OF ATTACK

6. COMPUTER GRAPHICS

Aircraft motions in the post stall region are sometimes aperiodic and usually quite complex. In order for an engineer to develop a thorough understanding of the mechanism of a departure from controlled flight and the qualitative difference in stall behavior between, for instance, a configuration which exhibits heavy wing rock prior to a rolling departure and one which departs initially in yaw, he must be able to accurately visualize the aircraft motion in 3 dimensions. Time histories of aircraft parameters provide all the necessary information for the engineer, but the process of integrating three angles and three velocities over a particular time span during a complex post stall gyration is more than most engineers can manage. Also, analyzing time histories of departures provides an engineer with very little feeling for the rate at which an uncontrolled motion develops or of the severity of the gyrations.

A method has been developed at Northrop using a small computer and an interactive CRT which provides the engineer with a visualization of a maneuver similar to that which he would receive had he been in a chase aircraft, perfectly located with respect to the test aircraft, while the actual maneuver took place. In fact, the perspective provided is considerably better than a chase pilot could provide: with the computer graphics display the maneuver can be replayed in real time or slower; the position of the test aircraft controls is known; the viewer's vantage point may be relocated to any point in space, and flight test data such as airspeed, angle of attack and sideslip may be monitored.

A sketch of a typical computer graphics display is shown in Figure 12. The basic theory of the method is very straightforward. First, a three-dimensional line drawing of the subject aircraft is constructed in the computer memory. This line drawing can be as simple or as complex as desired, ranging from a basic delta wing and vertical tail up to a multiline wire drawing limited in complexity only by the size of computer memory. This line drawing is then oriented in space according to the direction cosine matrix formulated from aircraft Euler angles θ, ϕ and ψ as determined from actual flight test data. This rotated three-dimensional line drawing is then displayed in two dimensions on a Cathode Ray Tube. The image is updated at every flight test data point to give the drawings time dependent motion. Sample rates as high as 134 times per second and as low as 20 times per second have provided smooth representations of even the most violent departures.

The computer graphics display has been used to date with a great deal of success in the post flight analysis of maneuvers. The accurate visualization of such maneuvers as inverted pitch hangup (IPH), post stall gyrations (PSG), snap roll departures from windup turns and spinning motion has been greatly aided by this method. However, several extensions of the method have been proposed and are being implemented at the present time. In its present configuration, the time delay between the performance of a particularly interesting maneuver and the viewing of that maneuver by the engineer using computer graphics is approximately 48 hours. An order of magnitude increase in the usefulness of the computer graphics would be effected if this time period could be reduced to a matter of minutes, or even seconds; i.e., near-real time.

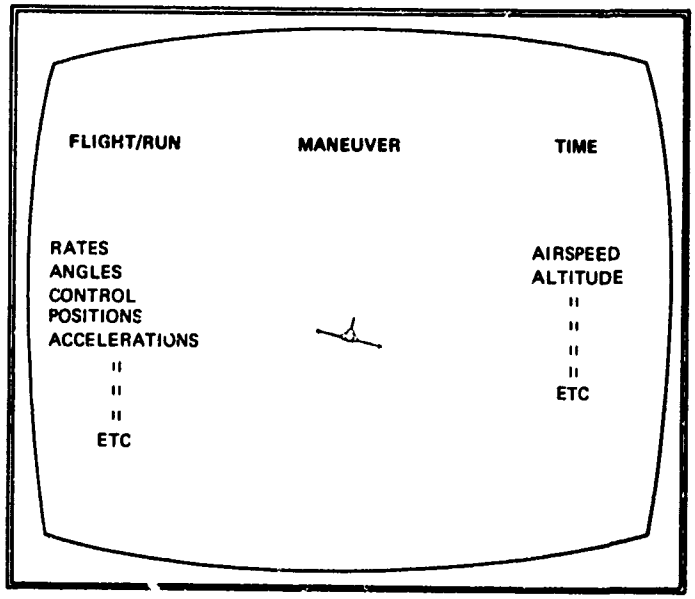

FIGURE 12. COMPUTER GRAPHICS DISPLAY

The nature of certain flight test programs, for example a post stall or a spin investigation, is such that out of control or spin boundaries are approached in careful steps. If a thorough understanding of a test point is grasped quickly, a decision to move to the next point closer to the boundary can be made with confidence and dispatch. In this way, it is felt that the overall efficiency and safety of the test program would be enhanced by the near real time implementation of the computer graphics display.

7. F-5 FLIGHT TEST EXPERIENCE AND CORRELATION WITH PREDICTIONS

This section describes the way in which the prediction techniques, correlation parameters and maneuver visualization methods previously discussed have been applied to the F-5E and F-5F aircraft.

The T-38 and F-5A/B series of aircraft have historically been very resistant to departure from controlled flight. The F-5E differs very subtly from these early aircraft and therefore is also expected to be similarly free from departure tendencies. (A three-view of the F-5A and the F-5E is presented in Figure 13 and shows the high degree of similarity.) This expectation was initially verified by several hundred 1 "g" and accelerated stalls performed during the developmental flight testing of the aircraft during which no departures were noted. After the major portion of the F-5E flight test program was completed, two operational aircraft were lost in spins. Both aircraft were performing full aft stick one g stalls at an aft center of gravity. This precipitated an investigation employing analytical, wind tunnel and flight test efforts in order to reassess the high angle-of-attack handling qualities of the aircraft.

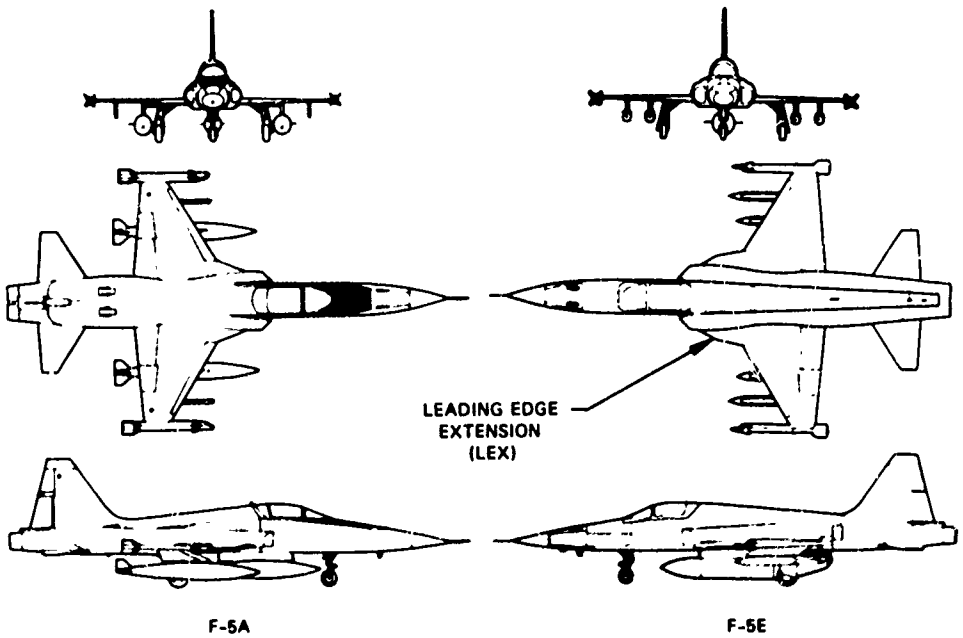

FIGURE 13. F-5A AND F-5E CONFIGURATION COMPARISON

Flight tests conducted on an F-5E performing 1g stalls at an aft center of gravity indicated a strong sideslip/angle of attack coupling effect. A typical time history is presented in Figure 14. This coupling effect was minimized by reducing the maximum horizontal tail deflection from -20 to -17 degrees as shown in Figure 15.

The reduction in maximum angle of attack attained during full aft stick 1g stalls with the limited tail authority, as opposed to the original tail authority, is shown in Figure 16. It should be noted that these curves represent peak values and include dynamic overshoot.

As so often happens, the solution to one problem provided access to another. Limiting the angle of attack through reduced tail authority resulted in the aircraft encountering a more unfavorable region with respect to departure when performing full aft stick stalls. This fact was not evident at the time, but it was clearly demonstrated in flight as will be shown.

It was common knowledge that when $C_{n_\beta DYN}$ was positive the aircraft would be departure-free and if negative would be departure-prone. What was not known was the effect of a local instability such as depicted in Figure 17.

The F-5E with a centerline store and limited tail authority encountered several snap rolls out of accelerated stalls, with maneuver flaps retracted below 300 KCAS. During this same period the F-5F experienced an abrupt nose slice during a 1g stall. This incident also was with the centerline tank configuration.

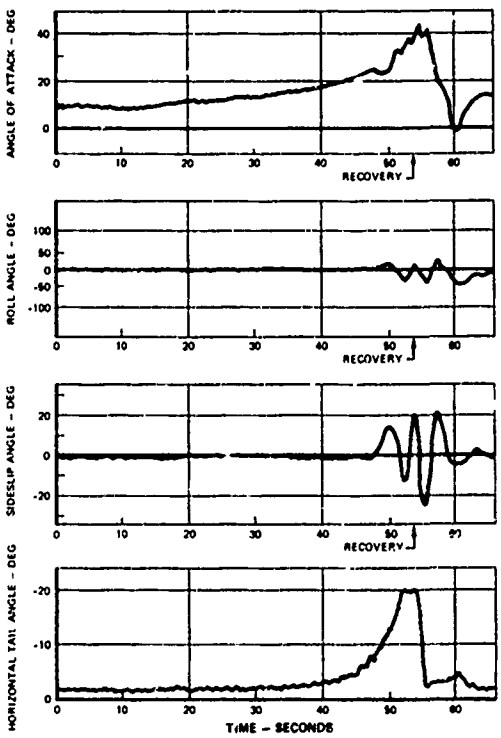

FIGURE 14. EXAMPLE OF SIDESLIP/ANGLE-OF-ATTACK COUPLING

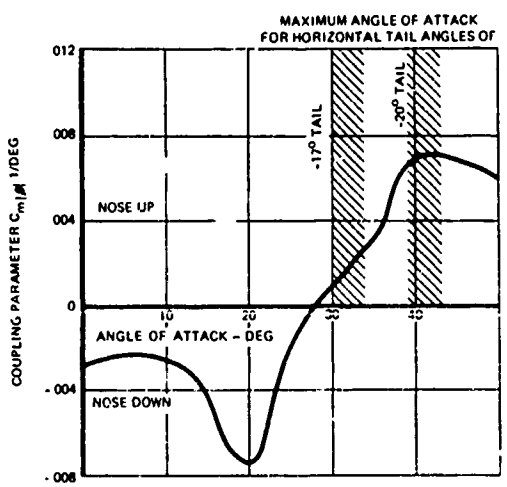

FIGURE 15. EFFECT OF LIMITING TAIL AUTHORITY ON SIDESLIP/ANGLE-OF-ATTACK COUPLING PARAMETER

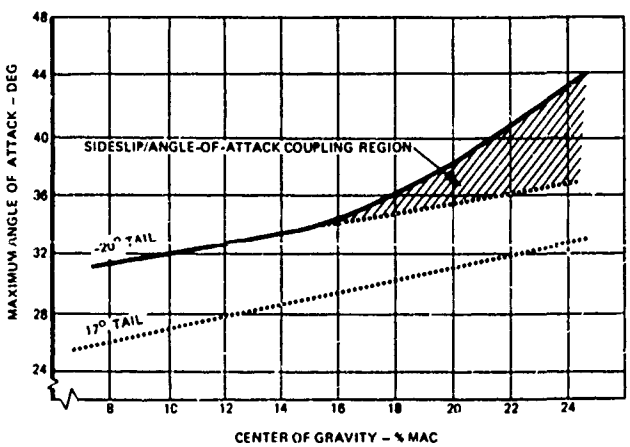

FIGURE 16. EFFECT OF LIMITING TAIL AUTHORITY ON MAXIMUM ANGLE OF ATTACK

The departure parameter, $C_{n_\beta DY_N}$, for the F-5E presented in Figure 18 shows a neutral stability in the stall for the clean aircraft and a locally unstable region for the centerline tank configuration. The F-5F departure parameter indicates an even more severe local instability as presented in Figure 19. The maneuvering flaps are shown to have a strong stabilizing effect as also seen in Figure 19.

At this point, a definitive correlation of flight test results with the departure parameter $C_{n_\beta DYN}$ was accomplished. On the basis of Figure 19 it was predicted that a nose slice tendency could also be expected with the F-5E with flaps up and centerline store during a 1g stall. Review of previous 1g stall data did not reveal this tendency with the F-5E because the pilot pulled through this area due to the greater tail authority. A flight test of the centerline tank configuration was repeated where the pilot very carefully stabilized in the critical angle-of-attack region, and the F-5E did indeed exhibit the departure tendency predicted.

Referring again to limiting of the angle of attack through reduced tail authority for the F-5E, the effect was to lower the maximum 1g trimmed angle of attack attainable during a slow approach to the stall, and consequently, a longer exposure in the departure prone region as shown in Figure 20.

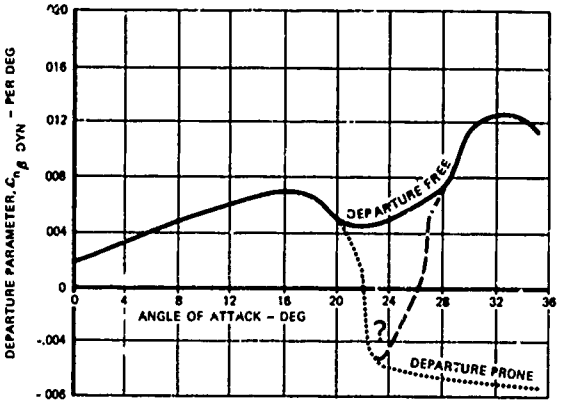

FIGURE 17. DEPARTURE PARAMETER LOCAL INSTABILITY

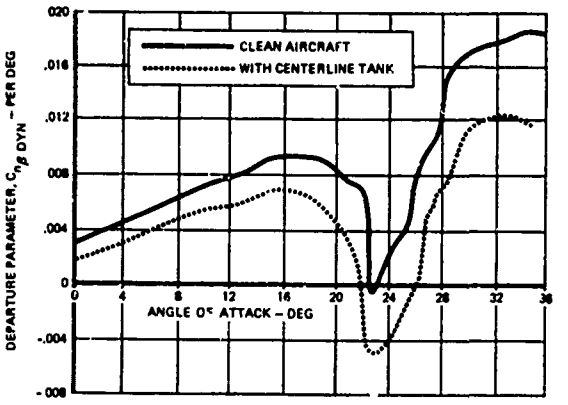

FIGURE 18. EFFECT OF CENTERLINE TANK ON F-5E DEPARTURE PARAMETER (MISSILES)

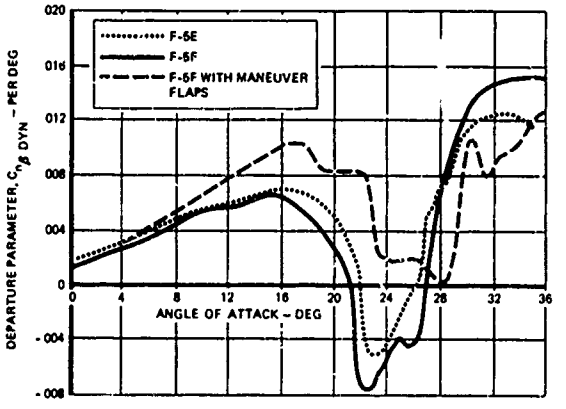

FIGURE 19. COMPARISON OF F-5E AND F-5F DEPARTURE PARAMETER (CENTERLINE TANK AND MISSILES)

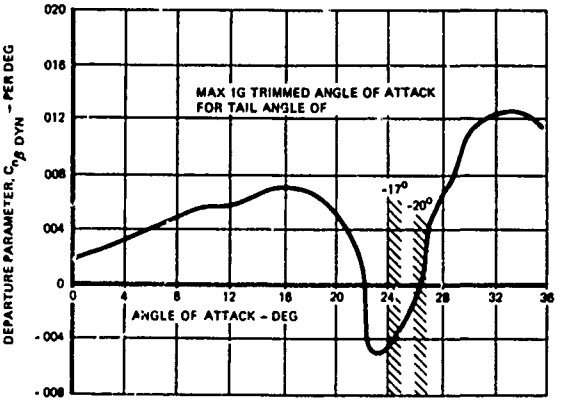

FIGURE 20. EFFECT OF LIMITING TAIL AUTHORITY ON NOMINAL ANGLE OF ATTACK F-5E WITH CENTERLINE TANK AND MISSILES

Utilizing $C_{n_\beta DYN}$ as the primary departure criterion, complete correlation was obtained between flight and wind tunnel data, establishing the following departure trends:

1. F-5F departure tendencies were more severe and more repeatable than those of the F-5E.
2. The centerline stores configured aircraft with flaps up, both "E" and "F", displayed the most severe departures.
3. Maneuver flaps had a large stabilizing effect; no departures were noted with maneuvering flaps down on the F-5E and only random departures on the F-5F.
4. Outboard stores, pylons and landing gear all showed a stabilizing effect.
5. Horizontal tail deflection trailing edge up is destabilizing.

Wind tunnel testing was continued for the purpose of defining modifications which would improve the aircraft handling qualities by increasing $C_{n_\beta DYN}$ in the stall. A large number of configuration modifications were tested and included the following. nose shape modifications, nose strakes, ventral fins, dorsal fins, larger vertical tail, wing fences, wing LEX shape changes, incidence changes, wing leading edge snags, wing vortex generators, inlet duct modifications and various combinations of the above. In addition, the effect of various store loadings and configuration changes such as flaps and gear were further investigated.

The results of the wind tunnel investigation uncovered only a few modifications to the aircraft which produced favorable changes in the lateral/directional stability characteristics. Those modifications which provided sizeable improvements in lateral/directional stability without causing a reduction in $C_{L_{MAX}}$ or an increase in nose-up pitching moment due to sideslip could be grouped into two major areas somewhat independent of each other. Modifications to the fuselage or engine inlet duct were mostly ineffective but when improvements were seen, they were mainly slight improvements in directional stability (C_{n_β}). Modifications to the wing planform outboard of the wing LEX were effective mainly in improving dihedral effect (C_{l_β}), and the larger increments in dynamic stability were obtained here.

Significant directional stability improvements in the stall angle-of-attack region were extremely difficult to achieve since nearly all of the aft fuselage near the vertical tail is immersed in a large wake and has greatly reduced dynamic pressure. The single largest source of aerodynamic energy comes from the vortices generated by the wing LEX and consequently, the largest improvement in directional stability was obtained by the removal of the LEX. This also caused an intolerable reduction in maximum lift coefficient (-. 28). A large and small rectangular LEX (see Figure 21) was also tested and showed that improvements in $C_{n_\beta DYN}$ were only accomplished with significant maximum lift coefficient reductions. These effects of LEX size are presented in Figure 22.

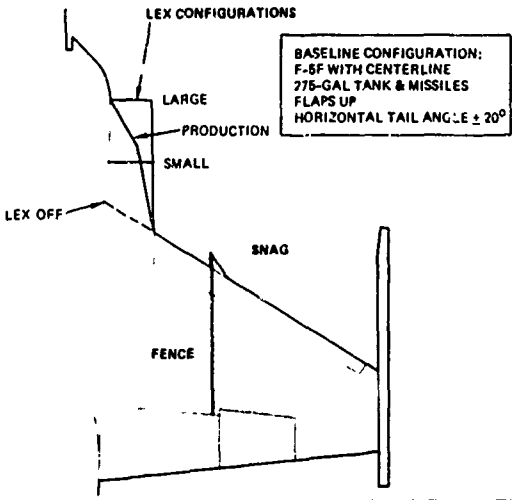

FIGURE 21. SELECTED MODIFICATIONS FROM THE CONFIGURATION STUDY

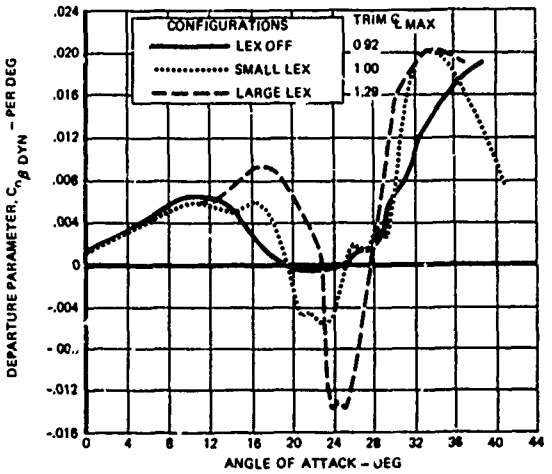

FIGURE 22. EFFECT OF LEX SIZE, F-5F WITH CENTERLINE TANK

Dihedral effect improvements were easier to obtain than directional stability improvements. In the post stall angle-of-attack region the major portion of the wing panel is completely separated. Consequently, most modifications placed on the upper surface of the wing such as vortex generators had no effect. Upper surface wing fences located at approximately mid span resulted in a significant improvement in dihedral effect. The effect of the fence is to reduce the extent of spanwise flow over the wing, allowing the wing to maintain a positive dihedral effect at all angles of attack. The vortex field downstream of the wing also influences the vertical tail resulting in an increase in directional stability in the stall region. These effects, combined with the aircraft's high inertia ratio which multiplies the effect of C_{l_β}, translate to a truly significant improvement in the minimum value of $C_{n_\beta DYN}$ in the stall, as seen in Figure 23.

Another modification which provided improvement in lateral stability was the addition of snags to the leading edge of the wing (see Figure 21). The snag creates a very strong vortex at the inboard juncture at high angles of attack which augments the fence effect, restricting spanwise flow. Like the fences, the optimum location found was approximately mid span.

The effect of combining the snags and fences at the same spanwise location is shown in Figure 24, providing positive dynamic directional stability at all angles of attack for the centerline store configuration.

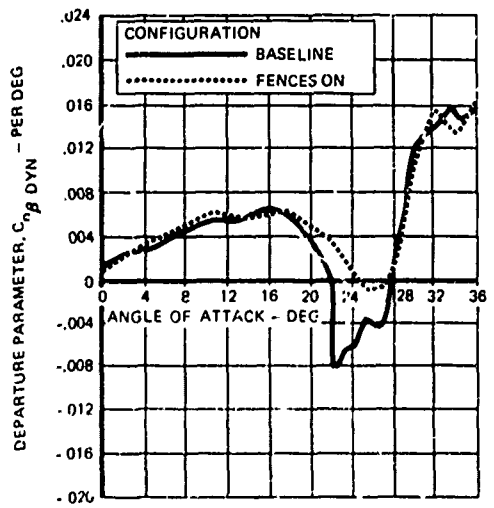

FIGURE 23. EFFECT OF FENCES – F-5F WITH CENTERLINE TANK AND MISSILES

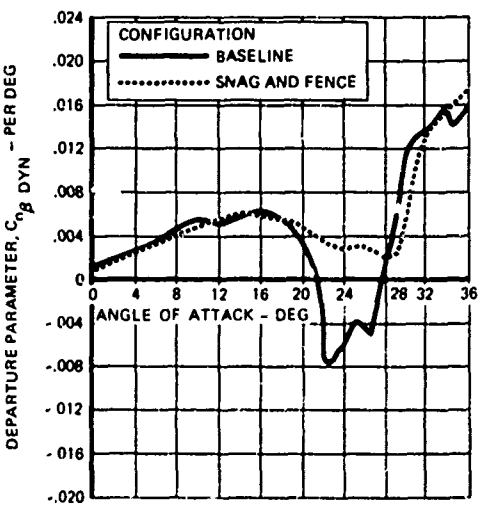

FIGURE 24. EFFECT OF SNAG AND FENCES – F-5F WITH CENTERLINE TANK AND MISSILES

As a result of the wind tunnel program, modifications were fabricated for an F-5F flight test airplane to evaluate the effect of the optimum fence configuration and the fence/sawtooth combination on post stall behavior. Both of these modifications were the same as those tested in the wind tunnel and are depicted in Figure 21.

The configuration with centerline tank and missiles, but without fences or snags, was tested first in order to establish a baseline. The 1g stall time history presented in Figure 25 shows the nose slice tendency in yaw rate which occurs at 20 seconds, just prior to stall recovery. The positive roll rate increase starting at 21 seconds shows a stable dihedral effect because the angle of attack had already been reduced to less than 20 degrees and was decreasing rapidly. In this region the dihedral effect is stable.

The fence configuration was tested next and the 1g stall time history is presented in Figure 26. It is noted that full back stick was held to sustain the 26 degree angle of attack for 20 seconds and no departure tendencies were present. The roll rate and yaw rate traces indicate a mild wing rock, or stable dutch roll motion.

The last test configuration included a fence and snag combination for which the 1g stall time history is presented in Figure 27. The addition of the snag did not appear to be appreciably different than the fence alone even though the wind tunnel data, Figure 24, showed a beneficial effect. The snag also produced an early buffet onset with maneuver flaps deflected and was therefore not included in the modification for the production airplane.

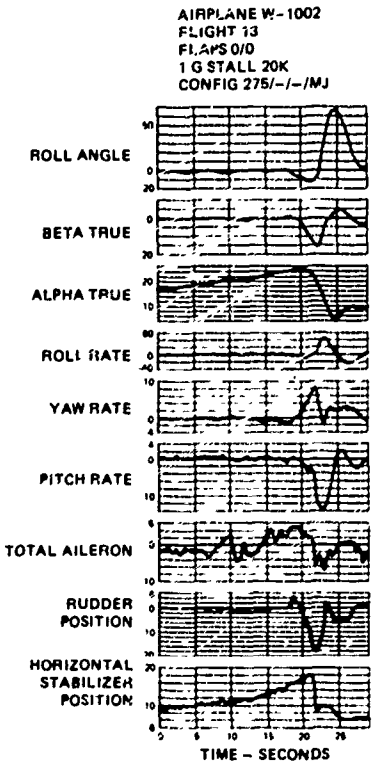

FIGURE 25. BASELINE CONFIGURATION

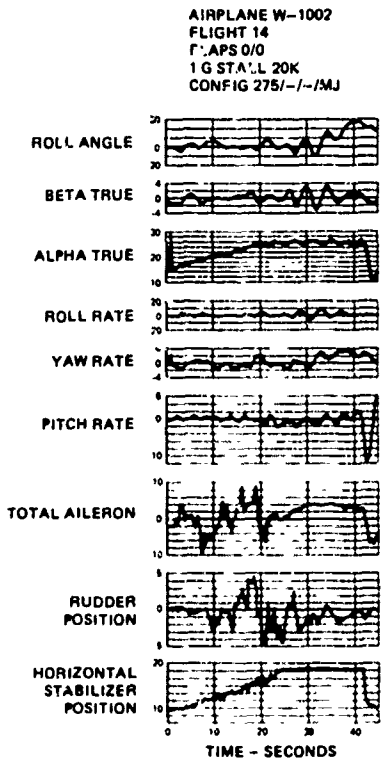

FIGURE 26. FENCE CONFIGURATION

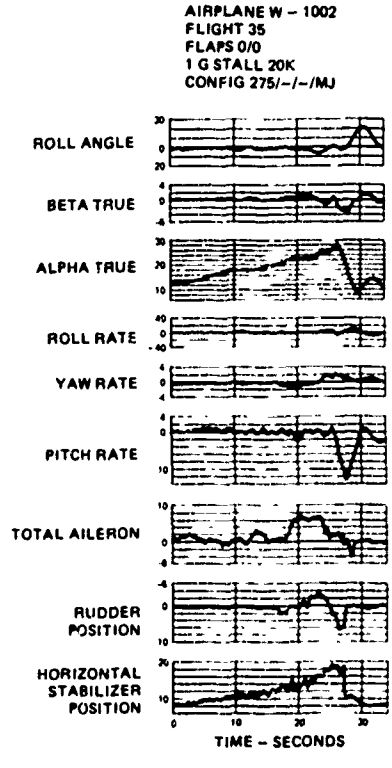

FIGURE 27. FENCE AND SNAG CONFIGURATION

TIME HISTORIES OF AN F-5F 1G STALL

On the basis of these tests it was possible to define various regions of $C_{n_\beta DYN}$ which would result in predictable aircraft behavior in the stall. These regions are shown in Figure 28 along with an explanation of the type of stall and extent of departure tendencies to be expected in each region. Departure tendencies are not always consistent and repeatable, hence the overlap.

Although the flying qualities regions of Figure 28 were derived from F-5E/F flight test results they should be generally applicable to other fighter aircraft. The various boundaries may shift somewhat due to specific directional, dihedral and inertial effects. The boundaries and overlaps will also be dependent upon repeatability of results.

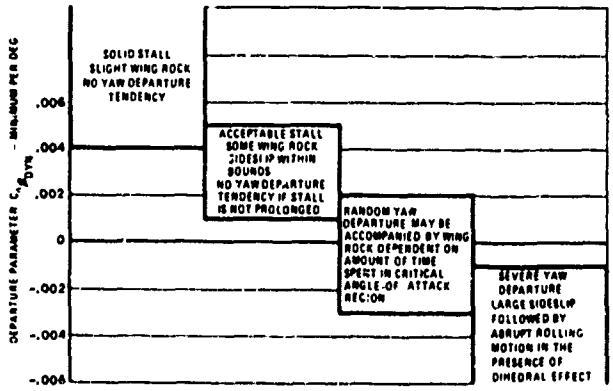

FIGURE 28. EXPECTED STALL BEHAVIOR AS A FUNCTION OF $C_{n_\beta DYN}$

8. CONCLUSIONS

The F-5E/F stall investigation program surfaced some important guidelines for testing as well as for correlating analytical parameters with test results:

1. A definitive correlation of a locally (with AOA) unstable departure parameter, $C_{n_\beta DYN}$ with flight test results has been accomplished.
2. The directional departure parameter was used to determine an effective solution to unacceptable stall characteristics by combining wind tunnel and flight testing efforts.
3. This parameter can also be used to define critical angle-of-attack regions for flight test purposes.
4. Wind tunnel testing in the stall angle-of-attack region must be accomplished using small increments in angle of attack (one degree or less) or the true stall characteristics may not be identified.
5. In determining sideslip derivatives it is best to obtain pitch runs at both a positive and a negative sideslip angle beyond the aerodynamic hysteresis region and average the results. A few preliminary runs made at several constant angles of attack and varying sideslip will determine the extent of the aerodynamic hysteresis.
6. In determining rudder and aileron effectiveness a zero sideslip run should be used to determine the zero control datum.
7. The computer graphics display represents an effective visualization technique for interpreting complex aircraft motions in three dimensions. It also represents a potential enhancement of safety of flight in the conduct of hazardous test programs if provided in an on-line basis.

REFERENCES

1. Effects of a Pointed Nose on Spin Characteristics of a Fighter Airplane Model including Correlation With Theoretical Calculations; J. Chambers, et al; NASA Langley TN D-5921, September 1970.
2. Wind Tunnel Free-Flight Investigation of a Model of a Spin-Resistant Fighter Configuration; Paul L. Coe, Joseph R. Chambers, and Sue B. Grafton; NASA Langley TN D-7716; June 1974.
3. Summary of Directional Divergence Characteristics of Several High-Performance Aircraft Configurations; H. Douglas Greer; NASA Langley TN D-6993, November 1972.
4. Preliminary Criteria for Predicting Departure Characteristics/Spin Susceptibility of Fighter - Type Aircraft; R. Weissman, AIAA Journal of Aircraft, April 1973.

RESULTS OF RECENT NASA STUDIES ON SPIN RESISTANCE

Joseph R. Chambers, William P. Gilbert,
and Sue B. Grafton
Aeronautical Engineers
NASA Langley Research Center
Hampton, Virginia 23665
U.S.A.

SUMMARY

Two approaches to providing spin resistance for highly maneuverable military airplanes are being studied by the National Aeronautics and Space Administration. The approaches consist of: (1) providing inherent spin resistance by proper design of the airframe configuration, and (2) providing automatic spin prevention by use of the avionic and flight control systems. The studies are conducted using free-flight tests of dynamically scaled models and piloted simulator studies.

The results of a recent study conducted to determine some of the factors which contribute to the good stall/spin characteristics of a current fighter configuration indicate that the design of airframe components for inherent spin resistance is very configuration dependent and that few generalizations can be made. Secondary design features, such as fuselage forebody shape, can have significant effects on stability characteristics at high angles of attack.

Recent piloted simulator studies and airplane flight tests have indicated that current automatic control systems can be tailored so as to provide a high degree of spin resistance for some configurations without restrictions to maneuverability. Such systems result in greatly increased pilot confidence and increased tactical effectiveness.

SYMBOLS

b	Wing span, m (ft)
C_ℓ	Rolling-moment coefficient, $\frac{M_X}{qSb}$
ΔC_ℓ	Increment of rolling-moment coefficient, positive for right rolling moment
C_{ℓ_β}	Effective dihedral derivative, $\frac{\partial C_\ell}{\partial \beta}$, per deg
C_n	Yawing-moment coefficient, $\frac{M_Z}{qSb}$
ΔC_n	Increment of yawing-moment coefficient, positive for right yawing moment
C_{n_β}	Directional stability derivative, $\frac{\partial C_n}{\partial \beta}$, per deg
$C_{n_{\beta,dyn}}$	Dynamic directional stability parameter, $C_{n_\beta} - C_{\ell_\beta} \frac{I_Z}{I_X} \sin \alpha$, per deg
$C_{n_r} - C_{n_{\dot\beta}} \cos \alpha$	Damping-in-yaw parameter, per rad
I_X, I_Z	Moments of inertia about X- and Z-body axes, kg-m^2 (slug-ft^2)
q	Free-stream dynamic pressure, N/m^2 (lb/ft^2)
r	Yawing velocity, rad/sec
S	Wing area, m^2 (ft^2)
α	Angle of attack, deg
β	Angle of sideslip, deg
$\dot\beta$	Rate of change of sideslip, rad/sec
M_X, M_Z	Moments about X- and Z-body axes, m-N (ft-lb)

INTRODUCTION

Recent experience has shown that most contemporary fighter airplanes exhibit poor stall characteristics and a strong tendency to spin. They also have poor spin characteristics and recovery from a fully developed spin is usually difficult or impossible. As a result of these unsatisfactory stall and spin characteristics, the developed spin is currently an undesirable and potentially dangerous flight condition which should be avoided. There is, therefore, an urgent need to develop guidelines for use in the design of future military aircraft in order to minimize or eliminate spins and insure good handling qualities at high angles of attack. The National Aeronautics and Space Administration currently has a broad research program underway to provide these guidelines. The program includes conventional static wind-tunnel force tests, dynamic force tests, flight tests of dynamically scaled models, theoretical studies, and piloted simulator studies.

Two approaches to providing spin resistance are currently under consideration. In the first approach, the basic airframe is configured so as to be inherently spin resistant by virtue of good stability and control characteristics at high angles of attack. At the present time, however, a lack of understanding of the major factors affecting stability and control characteristics at high angles of attack for current fighters has prevented the development of detailed design procedures for inherent spin resistance. The second approach to providing spin resistance is through the use of avionics and flight control system elements in automatic spin prevention concepts. Such concepts can be highly effective in preventing inadvertent stalls and spins; however, they must be designed so as not to restrict the maneuverability and tactical effectiveness of the airplane.

The present paper discusses the results of two recent NASA studies on inherent spin resistance and automatic spin prevention. The studies were conducted at the NASA Langley Research Center using free-flight model tests and piloted simulator studies.

INHERENT SPIN RESISTANCE

In view of the limitations imposed on military airplanes by poor stall/spin characteristics, and the lack of understanding of factors which determine these characteristics, it is highly desirable to identify geometric features of airplanes which promote inherent spin resistance. As a step toward providing this information, NASA has recently conducted an investigation (Ref. 1) to provide some insight into the features affecting the lateral-directional stability characteristics of a high-performance twin-engine fighter which in operation has exhibited outstanding stall and spin characteristics. These characteristics, which result in an inherent resistance to spins, include positive directional stability through the stall with no tendency to diverge and no significant adverse yaw due to aileron deflection at high angles of attack.

Description of Configuration

A wind-tunnel investigation was made with the 0.17-scale model shown in Figure 1 in order to define some of the more important geometric and aerodynamic characteristics responsible for the good stall and spin characteristics exhibited by the configuration. The study included wind-tunnel free-flight tests, static force tests, and dynamic (forced-oscillation) force tests.

One airframe component expected to have significant effects on the stability and control of the model at high angles of attack is the wing. Past studies (Refs. 2 and 3) have shown that wing planform characteristics, such as sweep and taper ratio, can have large effects on lateral-directional stability at high angles of attack. In order to evaluate the effects of wing modifications, a swept wing (similar in planform to that employed by the configuration of Ref. 4) and a delta wing were also tested as shown in Figure 2. All wings were of equal area and of relatively equal weights, so that the flight tests were conducted with a constant value of wing loading. Aspect ratio and wing span varied with each wing design. (See Table I.) The location of the 0.25 $\bar{c}$ point was constant for all configurations tested. The additional wings incorporated conventional ailerons for roll control.

Results of Force Tests

The static directional stability characteristics of the basic configuration are presented in Figure 3 in terms of the static stability derivative, C_{n_β}. The data show that C_{n_β} was large and positive (stable) at low angles of attack. The magnitude of C_{n_β} decreased markedly when the wing stalled at an angle of attack near 17°; but C_{n_β} became increasingly stable at post-stall angles of attack, in contrast to trends shown by most current fighter configurations. (See Ref. 4, e.g.) This unusual increase in directional stability at post-stall angles of attack is expected to be a major beneficial factor resulting in the excellent stall characteristics shown by the configuration.

A number of additional component-buildup tests were conducted to determine the airframe component responsible for the pronounced increase in C_{n_β} exhibited by the configuration beyond wing stall. The data shown in Figure 4 indicate the contribution of the vertical tail to C_{n_β}. Two significant results are immediately apparent from these data: First, the tail contribution decreased markedly at angles of attack beyond that for wing stall; and second, when the tail was off, the directional stability continued to increase markedly at angles of attack above 25°, with the result that the model was directionally stable at angles of attack above 31° without a vertical tail. The decrease in tail contribution to directional stability at angles of attack beyond that for wing stall ($\alpha > 17°$) was due to the fact that the tail became immersed in the low energy wake of the stalled wing. The fact that the loss in tail effectiveness was the result of loss of dynamic pressure at the tail was shown by tests to determine rudder effectiveness. Such loss in tail effectiveness at high angles of attack is not unusual. The most remarkable, and more significant, characteristic is the large increase in tail-off directional stability at high angles of attack.

Additional tests were made to determine the wing-fuselage component responsible for the stability at high angles of attack. The component found to be responsible was the fuselage forebody as shown in Figure 5 which presents results of tests conducted with the isolated nose mounted on a balance at a distance ahead of the moment center representative of that for the nose of the basic configuration. The data show that the isolated nose was directionally unstable at low angles of attack, as would be expected. At high angles of attack, however, the isolated nose became directionally stable, and comparison of data for the nose alone and data obtained for the basic configuration with the vertical tail off indicates that virtually all the directional stability of the configuration at angles of attack above 32° was produced by the nose.

The geometric feature probably responsible for the aerodynamic characteristics of the fuselage forebody of the present configuration is the cross-sectional shape indicated in Figure 5. As shown in the sketch, the cross section is an elliptical shape with the major axis horizontal. It has been found in past investigations (Refs. 5 to 7) that a "flattened" nose similar to that of the present configuration tends to produce such stability; the relatively long nose of the present configuration tends to accentuate this effect because of the long moment arm through which side forces produced by the nose can act.

The static-directional stability characteristics of the swept- and delta-wing configurations are compared with those of the basic configuration in Figure 6. As shown in Figure 6, the swept- and delta-wing configurations had levels of directional stability equal to or higher than those of the basic configuration, and the trends of C_{n_β} at high angles of attack were dominated by the characteristics of the nose, as previously discussed for the basic configuration. It should also be noted that the apparent increase in C_{n_β} for the swept- and delta-wing configurations at low angles of attack was caused by the data-reduction procedure, in which the aerodynamic characteristics were based on the geometric characteristics of the individual wings. When compared for equal wing spans, the values of C_{n_β} for the individual wings are about equal at $\alpha = 0°$. The relative unimportance of the large changes in wing planform for the present configuration underlines the complexity of flow phenomena at high angles of attack and the increased importance of what might be assumed to be secondary design features, such as fuselage forebody shape.

The results of force tests conducted to determine the control effectiveness of the ailerons and rudder for the basic and modified configurations are presented in Figures 7 and 8. The data are presented in terms of the incremental values of C_n and C_ℓ produced by a right-roll or right-yaw control input. The data of Figure 7 show that the incremental rolling moment produced by aileron deflection for the basic configuration decreased markedly as wing stall was approached; the ailerons produced relatively small values of ΔC_ℓ at post-stall angles of attack. The incremental yawing moments produced by aileron deflection were favorable (nose-right for right roll input) near stall. These favorable yawing moments are unusual for a high-performance fighter and are another factor producing the known spin resistance of the present configuration. Both the swept and delta configurations exhibited equal or larger increments of ΔC_ℓ at angles of attack above $\alpha = 12°$ than did the basic configuration; however, both wing modifications produced large adverse yawing moments at and beyond wing stall. These adverse values of ΔC_n would be expected to degrade the post-stall control of the configuration considerably.

The rudder effectiveness of the various configurations is shown in Figure 8. Although the results for the three configurations were about equal at $\alpha = 0°$ (when compared for a constant value of b), the swept- and delta-wing configurations exhibited much higher values of rudder effectiveness at high angles of attack than did the basic configuration. This result was probably related to stall patterns on the individual wings and relative location of the stalled-wing wakes. It should be noted, however, that the rudder effectiveness of the basic configuration remains quite high to angles of attack substantially beyond wing stall.

As pointed out in Reference 1, a fuselage forebody which produces a large contribution to static directional stability at high angles of attack will also tend to produce unstable values of damping in yaw. Presented in Figure 9 is the variation of the damping-in-yaw parameter $C_{n_r} - C_{n_{\dot\beta}} \cos \alpha$ for the basic configuration as measured in forced-oscillation tests.

As shown in Figure 9, $C_{n_r} - C_{n_{\dot\beta}} \cos \alpha$ was stable (negative) at angles of attack below stall but became unstable near $\alpha = 28°$ and attained very large unstable values at higher angles of attack. The results of tail-off tests showed that vertical tail had little effect on the unstable values or trends of the data at high angles of attack.

Additional forced-oscillation tests were conducted with components of the model to identify the nose as the cause of the unstable values of $C_{n_r} - C_{n_{\dot\beta}} \cos \alpha$ at high angles of attack. The physical cause of the unstable damping in yaw is illustrated by the sketches shown in Figure 10. In Figure 10(a) the configuration is shown in a steady sideslipped condition with the same value of β at both the nose and the center of gravity. As pointed out previously, for the present configuration, the nose produced a side force which acted through a relatively long moment arm to create a stabilizing yawing moment that tended to reduce the value of β. The sketch in Figure 10(b) illustrates the situation for yawing flight, with zero sideslip at the center of gravity. Because the flight path is curved, the nose of the configuration is subjected to a local sideslip angle which produces a side force in a manner similar to that for the static situation. In this case, however, the resulting yawing moment is in a direction which tends to increase the value of yawing velocity and therefore results in unstable values of $C_{n_r} - C_{n_{\dot\beta}} \cos \alpha$.

Results of Flight Tests

The test setup for the free-flight tests is shown in Figure 11. The model was flown without restraint in the 9- by 18-m (30- by 60-ft) open-throat test section of the Langley full-scale tunnel and was remotely controlled about all three axes by two human pilots. One pilot, who controlled the model about its roll and yaw axes, was stationed in an enclosure at the rear of the test section. The second pilot, who controlled the model in pitch, was stationed at one side of the tunnel. Pneumatic and electric power and control signals were supplied to the model through a flexible trailing cable which was made up of wires

and light plastic tubes. The trailing cable also incorporated a 0.318-cm-diameter (1/8-in.) steel cable that passed through a pulley above the test section. This section of flight cable was used to catch the model when an uncontrollable motion or mechanical failure occurred. The entire flight cable was kept slack during the flights by a safety-cable operator using a high-speed pneumatic winch. A further discussion of the free-flight technique, including the reasons for dividing the piloting tasks, is given in Reference 8.

During the flight tests it was found that the basic model flew smoothly and with little effort by the pilots up to an angle of attack of about 20°. Above $\alpha = 20°$ there was a slight nose wandering, or directional "looseness," noted by the lateral-directional pilot. The nose wandering (although small) increased the pilot effort required to fly the model smoothly. But the pilot was satisfied with the level of stability and considered that the major cause of the increased pilot effort was the rapid decrease in lateral-control effectiveness with increasing angle of attack (see Fig. 7). At an angle of attack of about 30° the model diverged slowly in yaw against full corrective controls. The yawing motion at the divergence appeared to be a fairly slow rotation about the Z body axis. The swept- and delta-wing configurations exhibited the same general flight characteristics as the basic configuration.

The possibility of directional divergence at high angles of attack is normally examined by means of the dynamic directional-stability parameter $C_{n_{\beta,dyn}}$ (Ref. 4), where

$$C_{n_{\beta,dyn}} = C_{n_\beta} - \frac{I_Z}{I_X} C_{\ell_\beta} \sin \alpha$$

Negative values of $C_{n_{\beta,dyn}}$ usually indicate the existence of a directional divergence.

The variations of $C_{n_{\beta,dyn}}$ for the swept- and delta-wing configurations are compared with that for the basic configuration in Figure 12. The values of $C_{n_{\beta,dyn}}$ were large and positive for all configurations, indicating no directional divergence. It appears, therefore, that the slow directional divergence exhibited by the model near $\alpha = 30°$ was not predicted by $C_{n_{\beta,dyn}}$ but is probably associated with the unstable values of $C_{n_r} - C_{n_{\dot\beta}} \cos \alpha$ (Fig. 9) and the low rudder effectiveness (Fig. 8), neither of which is accounted for in the $C_{n_{\beta,dyn}}$ criterion.

Flights were made to determine the effects of various pilot lateral control techniques at high angles of attack by flying the model with rudder and ailerons individually and in an interconnected, or coordinated, mode. The results of these tests showed that at angles of attack above 10°, the pilot could not use ailerons alone for satisfactory lateral control of the basic configuration because of apparently reduced control effectiveness. The results of the lateral-control tests for the modified configurations were similar to those for the basic configuration in that the rudder was the most effective means of roll control at high angles of attack. It was noted, however, that use of the ailerons appeared to be completely unsatisfactory because of noticeable adverse yaw. Some indication of the shortcomings of the aileron control at high angles of attack can be obtained from the aileron-effectiveness parameter given by

$$C_{n_\beta} - C_{\ell_\beta} \frac{\Delta C_n}{\Delta C_\ell}$$

Negative values of this parameter indicate roll reversal; that is, a control input for right roll results in roll to the left. The calculated values of the parameter for the three configurations are presented in Figure 13. The variations in magnitude of the aileron-effectiveness parameter are caused by variations in C_{n_β} and aileron yawing-moment characteristics.

The values of the parameter for the basic configuration were a minimum near $\alpha = 21°$, but the parameter remained positive indicating no roll reversal. On the other hand, the values for the swept- and delta-wing configuration were negative at high angles of attack, indicating roll reversal due to adverse yaw.

Interpretation of Results

The results of the free-flight tests for the basic configuration are in very good agreement with the characteristics exhibited by the full-scale airplane. In particular, within the operational angle-of-attack range, the absence of any divergence, the good rudder effectiveness, and the absence of adverse yaw due to ailerons appear to have been adequately represented by the model. Of course, the low values of Mach and Reynolds numbers associated with the present tests could cause some characteristics, such as wing stall, to occur at slightly different angles of attack. In addition, the confined space available within the wind tunnel, the rapidity of the motions of the model, and the lack of piloting cues cause the evaluation of lateral-control techniques to be qualitative at best. It appears, however, that the results of the tests have identified some of the factors which cause the basic configuration to have outstanding stall and spin characteristics.

It should be pointed out, however, that some of the factors, such as nose shape, which was found to have a large influence on the stability of the present configuration at high angles of attack, may be insignificant for other configurations. The blending of airframe components for good characteristics at high angles of attack is very configuration dependent and there are few general conclusions to be made. Instead, wind-tunnel test techniques and methods of analysis similar to those discussed must be used early in design stages in order to insure good stall characteristics.

AUTOMATIC SPIN PREVENTION

Automatic Control Concepts

Experience has shown that spins can generally be avoided if the proper recovery action is taken immediately after departure from controlled flight while the spin energy is low and the aerodynamic controls are effective. The problem in effecting such early recovery is that the pilot frequently is not able to take immediate corrective action because of disorientation which results from his lack of experience with spins of such aircraft, from the fact that the departure and spin entry occurred unexpectedly when he was intent on another task, and from the violent and confusing nature of the motions during spin entry for many airplanes. This situation would seem to suggest the use of an automatic system which could quickly identify the situation and take the required action. An electronic system capable of this task would have several inherent advantages over the human pilot, including (1) quicker and surer recognition of an incipient spin, (2) faster reaction time for initiation of recovery, (3) application of correct spin-recovery controls, and (4) elimination of tendencies toward spin reversal.

The idea of automatic spin-prevention, or recovery, systems is not new. Stick-pushers that prevent, or discourage, stalling the airplane are, in a sense, spin-prevention systems; but they may restrict the pilot from exploiting the full potential-maneuver envelope of the airplane. The installation of more elaborate automatic spin-prevention, or recovery, systems has, until recent years, involved the addition of complete sensing, logic, and control systems at a time when such devices were not very reliable and would probably not have been maintained in proper operating condition because they were protecting against a very rare occurrence. The fact that modern tactical airplanes already incorporate most of the elements of automatic spin-prevention (or recovery) systems, together with a great increase in the reliability of avionics systems, now makes the use of these automatic systems more practical.

Several approaches to automatic spin prevention have been evaluated by NASA. The types of concepts studied and the area of application of each concept are graphically depicted in Figure 14. Yaw rate and angle of attack are used as the primary variables identifying spin entry. For a particular airplane configuration one can generally identify two important areas in the yaw-rate angle-of-attack plane: the airplane maneuver envelope involving relatively low values of yaw rate and angle of attack, and the developed spin region involving relatively high values of yaw rate and angle of attack. Three types of automatic control concepts have been evaluated: (1) automatic spin recovery, (2) automatic spin prevention, and (3) automatic departure prevention.

In the automatic spin recovery concept, the airplane is allowed to depart from controlled flight, experience the incipient spin, and enter the fully developed spin. Values of yaw rate and angle of attack supplied by the sensors used in the automatic control system are sampled to identify the developed spin condition and actuate the proper recovery controls. The results of a study of the effectiveness and value of such a system (Ref. 9) indicated that the primary benefits of this type of concept were: rapid identification of the spin, input of proper recovery controls, and minimization or elimination of spin reversals following recovery. The concept obviously requires the airplane under consideration to have satisfactory spin recovery characteristics. Inasmuch as most current fighter designs have poor recovery characteristics from developed spins, it would appear that systems of this type would be relatively ineffective. In fact, the concept appears to be working "the wrong end of the problem."

The automatic spin prevention concept indicated in Figure 14 also allows the airplane to depart from controlled flight; however, recovery controls are actuated during the early stages of the incipient spin when recovery characteristics are generally good. By simultaneously sensing angle of attack and yaw rate, a control actuation boundary can be established which limits the attainable magnitudes of these variables, thereby preventing spins. An automatic spin prevention system concept has been studied (Ref. 9) using theoretical studies and flight tests of an unpowered drop-model of a current military configuration. The results of the theoretical studies showed that such a system was extremely effective in preventing developed spins, and that the exact configuration of the automatic system will depend on the stall/spin characteristics of the airplane design under consideration. The model flight tests verified the theoretical results and showed that current flight control components could be used to implement the system.

As might be expected, the control actuation boundary for the automatic spin prevention concept can be designed to be in close proximity to the normal flight envelope, thereby permitting only minimal excursions from controlled flight. It should be pointed out that the concept described does not infringe on the maneuverability of the airplane or restrict the tactical effectiveness of the vehicle. Rather, the system quickly senses an out-of-control condition and impending spin and applies control inputs required of the pilot in a rapid, correct manner.

The automatic spin prevention concept appears to be ideally suited for airplanes which are especially susceptible to inadvertent spins. In particular, configurations which exhibit a severe directional divergence and loss of control power at high angles of attack are appropriate for application of the system if no limit is desired on angle of attack attained during normal flight. Fighter configurations may, however, exhibit a divergence at an angle of attack considerably higher than those used in normal maneuvering flight. In this case, artificial angle-of-attack limiting systems may be more appropriate.

Recently, a number of fighter configurations have been developed which are dynamically stable at high angles of attack with no natural tendency to diverge in yaw. However, the designs are subject to control-induced departures from controlled flight as a result of large values of adverse yaw at high angles of attack. These vehicles are well suited for the application of automatic departure-prevention concepts (Ref. 10) which, as indicated in Figure 14, operate within the normal maneuver envelope of the airplane in order to prevent natural or control-induced departures from controlled flight. It will be shown that the use of such systems does not inhibit maneuvering of the airplane at high angles of attack, and actually increases the usable maneuverability as well as the pilot's confidence during strenuous maneuvers.

Evaluation Procedures

Several techniques have been developed at Langley for the evaluation of automatic departure/spin prevention systems. As previously mentioned, free-flight tests of dynamically scaled models and theoretical studies of flight motions have been extremely valuable in assessing the effectiveness of such systems; however, these techniques do not allow an evaluation of pilot reaction to the effects of automatic systems on maneuverability and tactical effectiveness. The Langley Differential Maneuvering Simulator (DMS) shown in Figure 15 has therefore been used to obtain such information.

The DMS is a fixed-base simulator which has the capability of simultaneously simulating two airplanes as they maneuver with respect to one another, and includes a wide-angle visual display (including the opposing aircraft) for each pilot. Real-time digital simulation techniques are used for the studies. Some of the unique capabilities of the DMS which are utilized for studies of automatic departure/spin prevention are listed in Figure 16. A detailed discussion of the capabilities and operational aspects of the DMS is given in Reference 11.

Previous experience with the simulation of fighter stall/spin characteristics (Ref. 12) has shown that visual tracking tasks which require the pilot to divert his attention from the instrument panel are necessary to provide realism in studying the possibility of unintentional loss of control and spin entry. Furthermore, other studies (Ref. 10) have shown that mild, well-defined maneuvers can produce misleading results inasmuch as a configuration that behaves fairly well in such mild maneuvers may be violently uncontrollable in the complex and pressing nature of high-g, air-combat maneuvering (ACM). Finally, for purposes of evaluation in comparing the performance of the airplane with and without automatic systems, the tasks used must be repeatable. The following test procedures are used in order to account for the foregoing factors.

In order to force the evaluation pilot to fly at high angles of attack, the target airplane is programed to have the same thrust and performance characteristics as the evaluation airplane; however, the target has idealized high angle-of-attack stability and control characteristics. The target airplane is flown by the evaluation pilot through a series of ACM tasks of varying levels of difficulty while the target's motions are tape recorded for playback later to drive the target as the task for the evaluation airplane. In this manner, repeatable tasks ranging from simple tracking tasks to complex, high-g ACM tasks are developed for use in the evaluation. Some of the simulation evaluation maneuvers normally used are listed in Figure 17.

The results of the studies are in the form of time-history records of airplane motions and pilot comments regarding the departure/spin susceptibility of the basic airplane and the effects of automatic prevention systems.

The objectives of such studies are: (1) to determine the controllability and departure resistance of a configuration during 1-g stalls and accelerated stalls, (2) to determine the departure susceptibility of the configuration during demanding air-combat maneuvers, and (3) to identify maneuvers or flight conditions which might overpower the departure-resistant characteristics provided by the automatic control system.

Results of Simulation

At the present time, simulator studies of the application of automatic departure/spin prevention systems have been conducted for four current fighter configurations. The results of the studies show that such systems can be very effective in preventing inadvertent departures from controlled flight during strenuous maneuvering. The resulting improvement in high angle-of-attack characteristics markedly improves handling, maneuverability, and safety. As a result of these improvements, the pilot's confidence in the capability of the vehicle is greatly increased, and the configuration can be used to its full capability. All of the studies show that these automatic systems can be implemented with current flight hardware and avionics technology. As an example of the benefits provided by automatic departure prevention systems, the use of automatic lateral-directional control phasing will be discussed.

Shown in Figure 18 are typical lateral-directional control characteristics for fighter configurations with adverse yaw. The data of Figure 18 show the variation with angle of attack of yawing moments produced by ailerons and rudder for right roll and right yaw control inputs The yawing moments produced by ailerons at low angles of attack are favorable (nose right) for right roll control; however, the moments become adverse (nose left) at high angles of attack. Right rudder input produces a normal nose right moment, but at high angles of attack the rudder loses effectiveness because of impingement of the low energy wake from the partially stalled wing. As can be seen, the magnitudes of the adverse moments due to ailerons are much larger than the corrective moments available from the rudder. When the resulting adverse moments are coupled with low directional stability at high angles of attack, a reversal of roll response occurs wherein the airplane rolls in a direction opposite to that desired by the pilot.

Shown in Figure 19 are calculated time histories which illustrate the roll reversal phenomenon. The roll response of a typical configuration is shown at an angle of attack of 25° for control inputs of rudder alone and ailerons alone for right roll control. The response to the rudder input is seen to be quite normal. The airplane yaws to the right, creating nose-right sideslip. The dihedral effect then rolls the airplane to the right, as desired. In contrast to this result, input of aileron control creates adverse yaw which causes the airplane to yaw to the left and the sideslip created is in the opposite direction, resulting in the dihedral effect opposing the rolling moment produced by the aileron. After a brief time, the airplane rolls to the left in response to the right roll control.

As would be expected, the reversed roll response to normal lateral control stick inputs presents the pilot with a coordination problem in order to avoid unintentional loss of control and spins. Most fighter pilots adapt to the situation by transitioning from lateral stick inputs for roll control at low α to rudder pedal inputs for roll control at high α. The problem becomes one of how to phase these controls in an optimum manner to obtain maximum performance, particularly during the pressure of combat.

Using the simulator at Langley, it has been found that configurations which exhibit such characteristics are susceptible to inadvertent departures during vigorous combat maneuvers. Many proposed solutions to the problem were evaluated, and the most effective system involved the stick-to-rudder interconnect concept shown in Figure 20.

Basically, the control system is modified such that deflection of the control stick laterally produces aileron inputs at low angles of attack and rudder inputs at high angles of attack. As shown in the sketch, the ailerons for the example discussed were phased out by $\alpha = 25°$. At that point, lateral stick inputs produced only rudder inputs. In addition, the yawing moments produced by the ailerons above $\alpha = 25°$ were used to advantage in an additional stability augmentation channel which augmented directional stability. This control scheme essentially eliminated inadvertent spins in the simulator.

The net effect of the automatic interconnect scheme on roll performance is illustrated in Figure 21. With the basic control system, the roll rate produced by lateral deflection of the control stick reversed near $\alpha = 20°$ and the pilot could not maneuver at higher angles of attack with only stick inputs. When the control system was modified with the interconnect, the pilot could maneuver the airplane beyond maximum lift using only stick inputs without fear of unintentional departures.

The preceding illustration of the use of automatic control concepts to prevent inadvertent spins is but one example of the significant gains to be achieved with these systems. The concept of automatic spin prevention is currently widely accepted by industry in the United States, and it is apparent that such systems will be employed by future fighter designs.

CONCLUDING REMARKS

The present paper has attempted to summarize recent NASA studies on spin resistance for military airplanes. The two approaches to providing spin resistance discussed herein are promising methods to achieve this goal. Much of the technology required to utilize the approaches is in hand, particularly for automatic spin prevention. In order to be effective, however, the approaches must be considered early in the design stages of military aircraft.

REFERENCES

1. Grafton, Sue B., Chambers, Joseph R., and Coe, Paul L., Jr.: Wind-Tunnel Free-Flight Investigation of a Model of a Spin Resistant Fighter Configuration. NASA TN D-7716, 1974.

2. Polhamus, Edward C., and Spreeman, Kenneth P.: Subsonic Wind-Tunnel Investigation of the Effect of Fuselage Afterbody on Directional Stability of Wing-Fuselage Combinations at High Angles of Attack. NACA TN 3896, 1956.

3. Goodman, Alex: Effects of Wing Position and Horizontal-Tail Position on the Static Stability Characteristics of Models With Unswept and 45° Sweptback Surfaces With Some Reference to Mutual Interference. NACA TN 2504, 1951.

4. Chambers, Joseph R., and Anglin, Ernie L.: Analysis of Lateral-Directional Stability Characteristics of a Twin-Jet Fighter Airplane at High Angles of Attack. NASA TN D-5361, 1969.

5. Chambers, Joseph R., Anglin, Ernie L., and Bowman, James S., Jr.: Effects of a Pointed Nose on Spin Characteristics of a Fighter Airplane Model Including Correlation With Theoretical Calculations. NASA TN D-5921, 1970.

6. Bates, William R.: Static Stability of Fuselages Having a Relatively Flat Cross Section. NACA TN 3429, 1955. (Supersedes NACA RM L9106a.)

7. Spencer, Bernard, Jr., and Phillips, W. Pelham: Effects of Cross-Section Shape on the Low-Speed Aerodynamic Characteristics of a Low-Wave-Drag Hypersonic Body. NASA TN D-1963, 1963.

8. Parlett, Lysle P., and Kirby, Robert H.: Test Techniques Used by NASA for Investigating Dynamic Stability Characteristics of V/STOL Models. J. Aircraft, Vol. 1, No. 5, Sept.-Oct. 1964, pp. 260-266.

9. Gilbert, William P., and Libbey, Charles E.: Investigation of an Automatic Spin-Prevention System for Fighter Airplanes. NASA TN D-6670, 1973.

10. Gilbert, William P., Nguyen, Luat T., and VanGunst, Roger W.: Simulator Study of Applications of Automatic Departure — and Spin-Prevention Concepts to a Variable-Sweep Fighter Airplane. NASA TM X-2928, 1973.

11. Ashworth, B. R., and Kahlbaum, William M., Jr.: Description and Performance of the Langley Differential Maneuvering Simulator. NASA TN D-7304, 1973.

12. Moore, Frederick L., Anglin, Ernie L., Adams, Mary S., Deal, Perry L., and Person, Lee H., Jr.: Utilization of a Fixed-Base Simulator to Study the Stall and Spin Characteristics of Fighter Airplanes. NASA TN D-6117, 1971.

TABLE I. GEOMETRIC CHARACTERISTICS OF THE WING CONFIGURATIONS

	Basic wing	Swept wing	Delta wing
Wing:			
Span	1.34 m (4.39 ft)	1.17 m (3.85 ft)	1.01 m (3.31 ft)
Area	0.49 m^2 (5.24 ft^2)	0.49 m^2 (5.24 ft^2)	0.49 m^2 (5.24 ft^2)
Root chord	0.59 m (1.95 ft)	0.71 m (2.34 ft)	0.92 m (3.01 ft)
Tip chord	0.15 m (0.48 ft)	0.12 m (0.39 ft)	0.05 m (0.15 ft)
Mean aerodynamic chord	0.41 m (1.34 ft)	0.48 m (1.59 ft)	0.61 m (2.01 ft)
Aspect ratio	3.68	2.82	2.09
Taper ratio	0.25	0.17	0.05
Dihedral	0	3.69°	0
Aileron area (one side)	0.013 m^2 (0.14 ft^2)	0.014 m^2 (0.15 ft^2)	0.013 m^2 (0.14 ft^2)

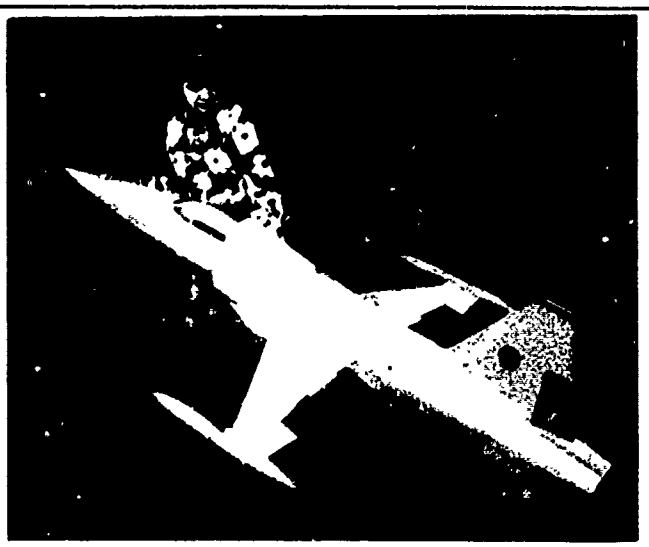

Figure 1. Photograph of model.

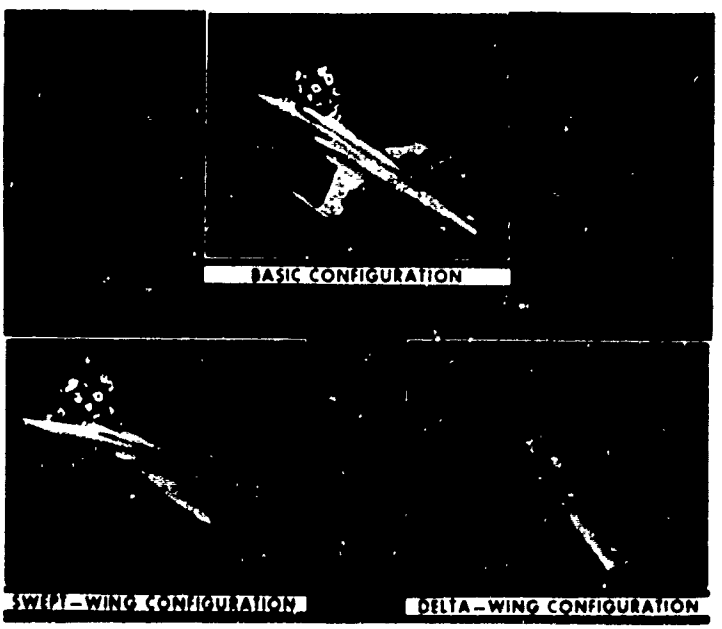

Figure 2. Photographs of model with modified wings.

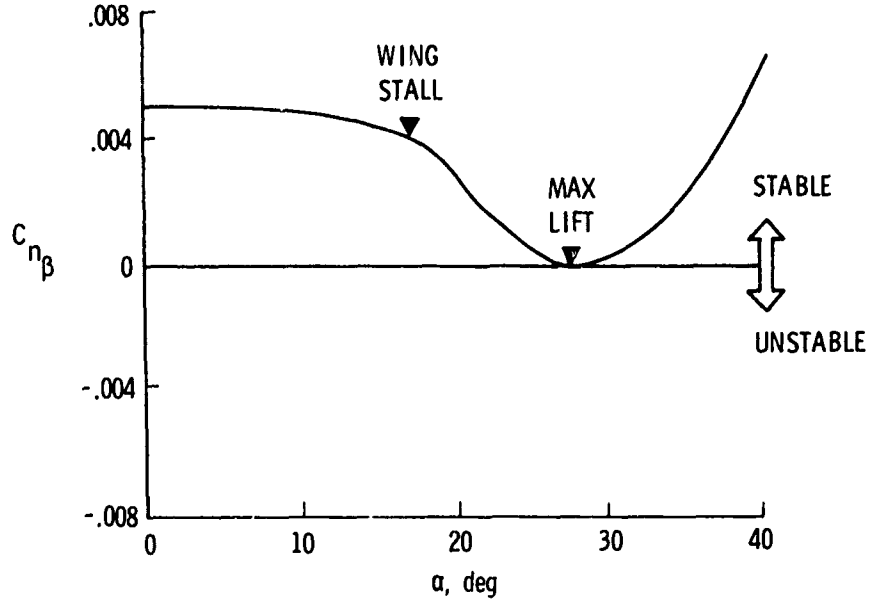

Figure 3. Static directional stability characteristics of the basic configuration.

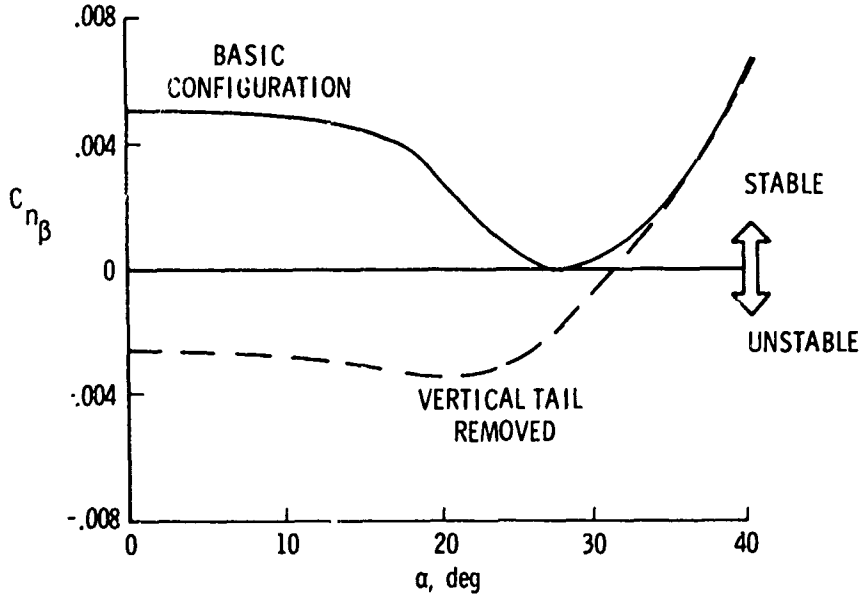

Figure 4. Effect of tail on directional stability of basic configuration.

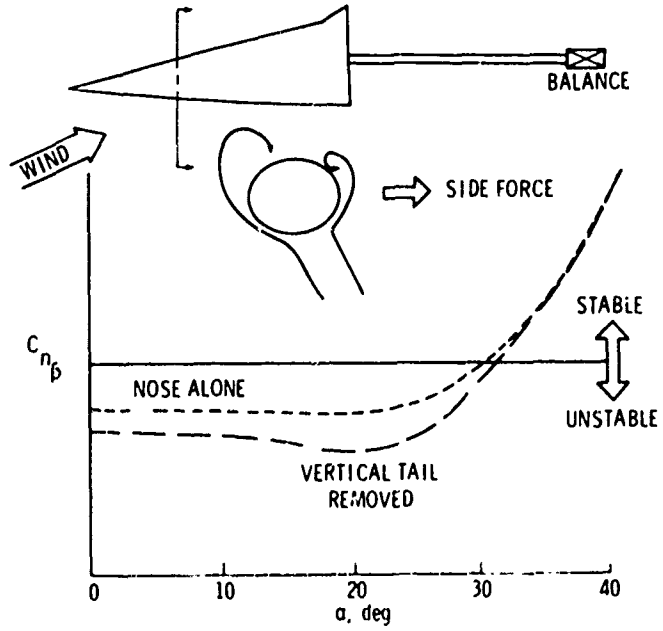

Figure 5. Directional stability characteristics of fuselage forebody.

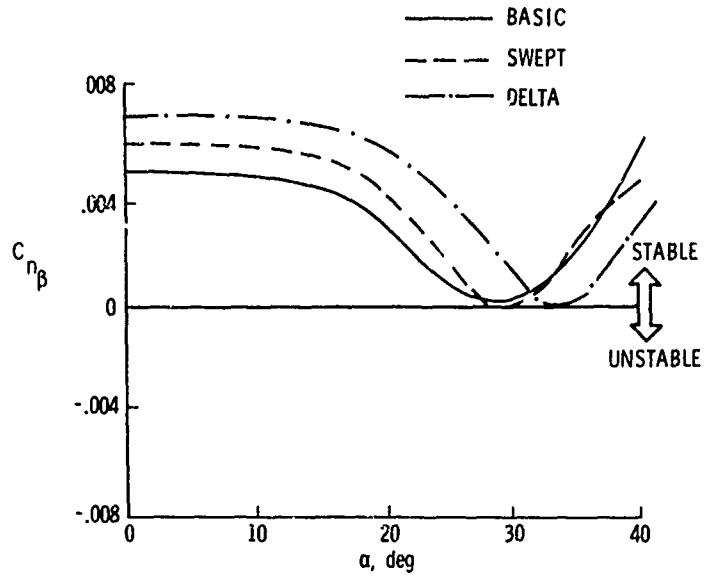

Figure 6. Effect of wing planform on directional stability.

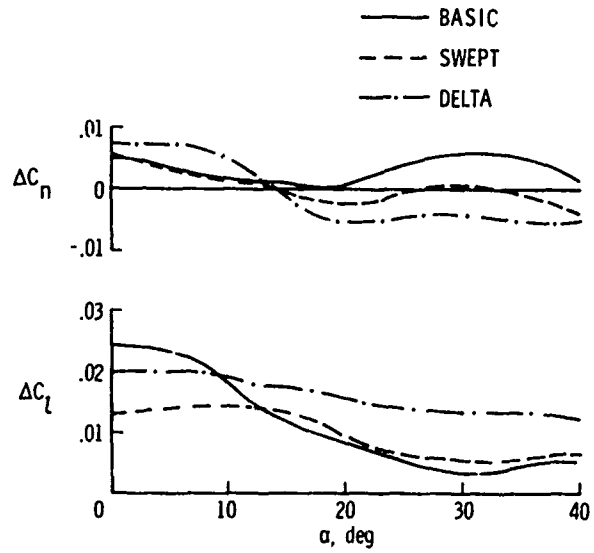

Figure 7. Effect of wing planform on aileron effectiveness.

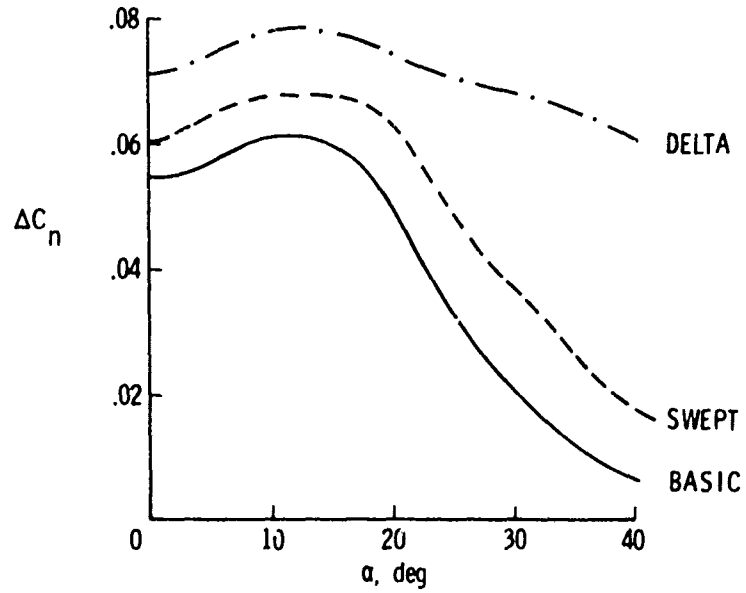

Figure 8. Effect of wing planform on rudder effectiveness.

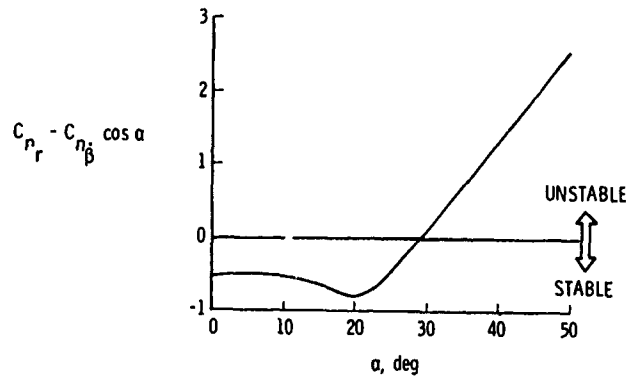

Figure 9. Variation of damping in yaw parameter with angle of attack for basic configuration.

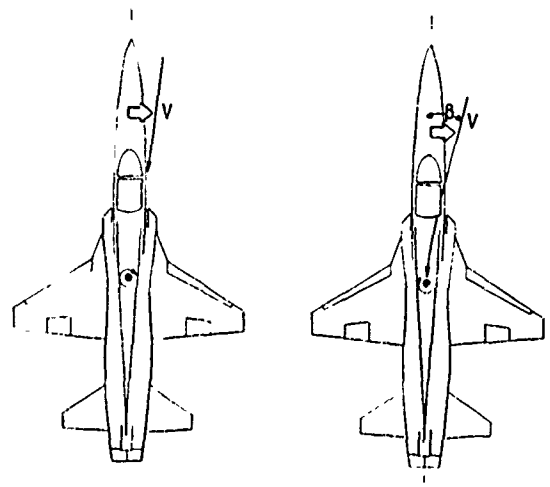

(a) Static, $\beta \neq 0°$. (b) Yawing, $\beta = 0°$

Figure 10. Sketch of cause of unstable damping in yaw.

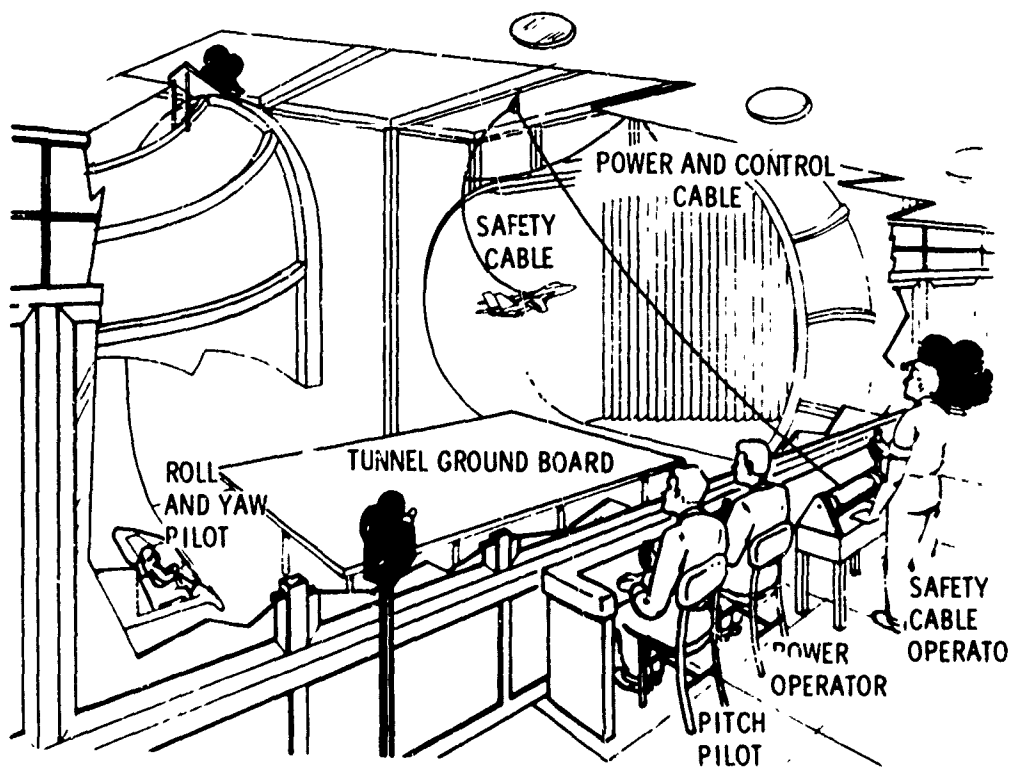

Figure 11. Test setup for free-flight tests.

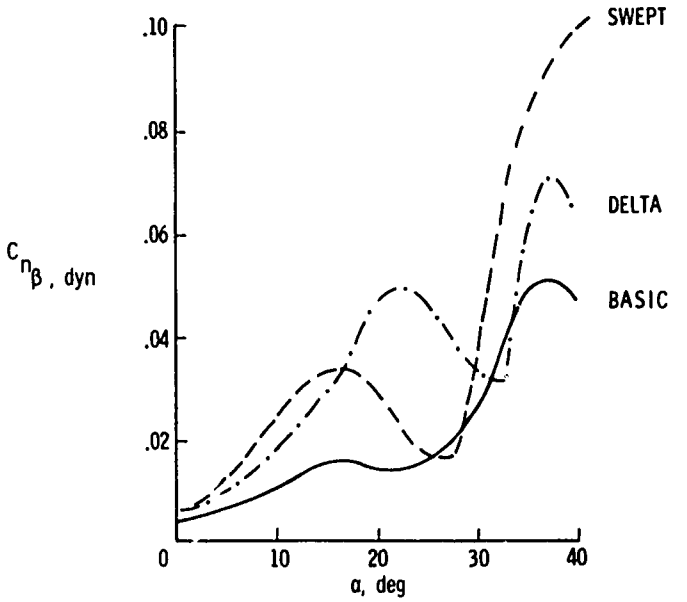

Figure 12. Variation of $C_{n_{\beta,dyn}}$ with angle of attack.

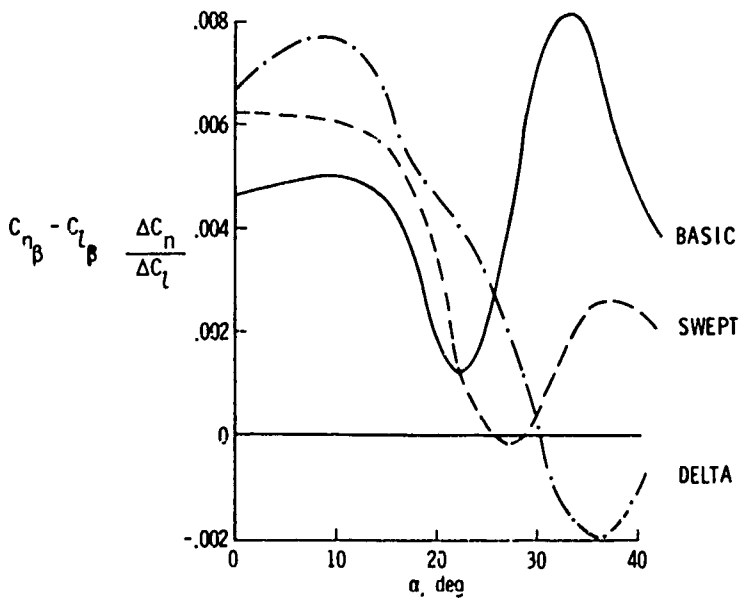

Figure 13. Variation of aileron effectiveness parameter with angle of attack.

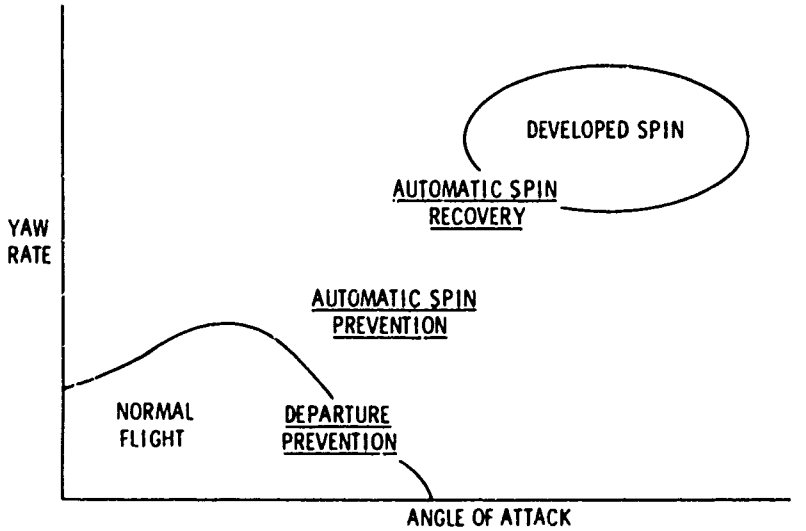

Figure 14. Automatic control concepts for departure/spin prevention.

Figure 15. Sketch of the DMS facility.

ONE-ON-ONE AIR COMBAT MANEUVERING (ACM)

REALISTIC COCKPIT/VISUAL REPRESENTATION

- STICK FORCE/FEEL
- BUFFET
- G SIMULATION (BLACKOUT AND G-SUIT)
- ENGINE/WIND NOISE

REALISTIC EVALUATION TASKS

- ONE-ON-ONE ACM
- TAPED, REPEATABLE TRACKING TASKS

COMPREHENSIVE DATA PACKAGE

Figure 16. Features of the DMS facility.

STALL ENTRIES - 1G AND ACCELERATED

- SYMMETRIC AND WINDUP TURNS
- ADVERSE CONTROLS
- MANEUVER CONTROLS

SPECIAL ENTRY MANEUVERS

- AERODYNAMICALLY COUPLED
- INERTIALLY COUPLED
- VERTICAL

REPEATABLE TRACKING TASKS

- STEADY TURNS
- BANK-TO-BANK REVERSALS
- COMPLEX ACM

Figure 17. Simulation evaluation maneuvers.

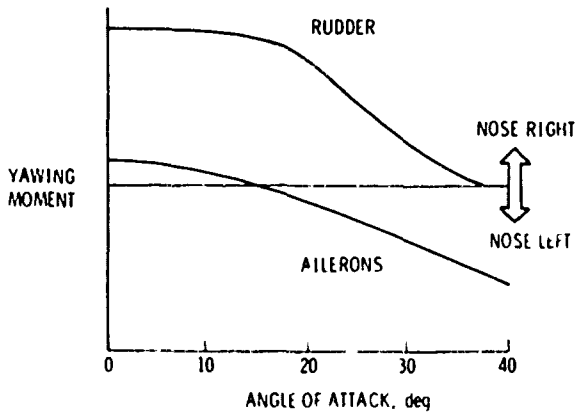

Figure 18. Yawing moments produced by lateral-directional controls.

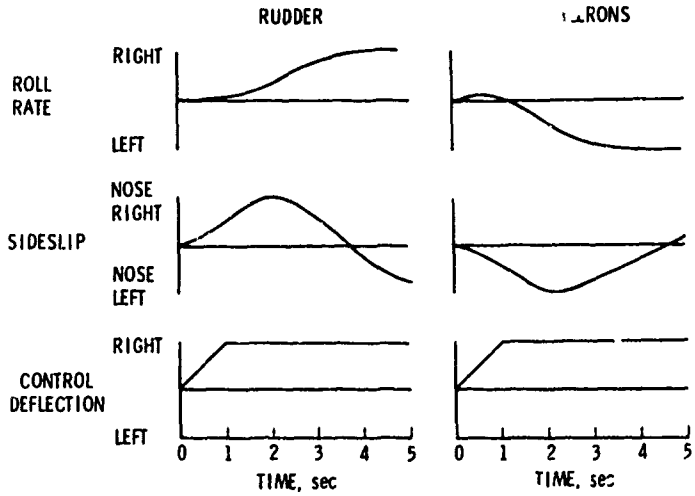

Figure 19. Illustration of roll reversal.

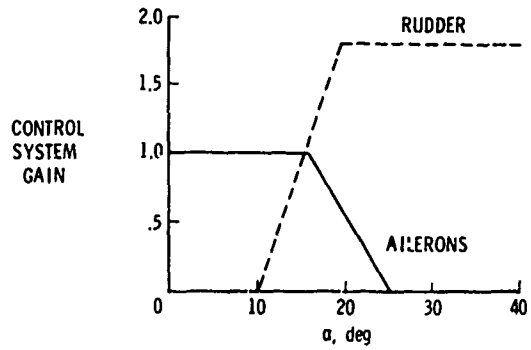

Figure 20. Stick-to-rudder interconnect concept.

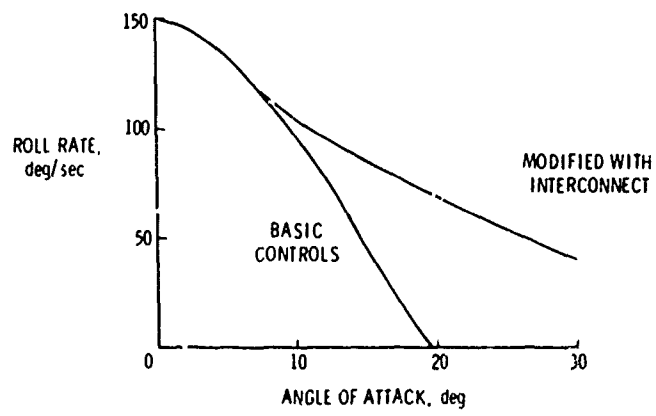

Figure 21. Effect of interconnect on roll response to lateral stick input.

APPLICATION DES MESURES DE COEFFICIENTS AERODYNAMIQUES STATIQUES ET DYNAMIQUES A DES RECOUPEMENTS PAR CALCUL DES VRILLES OBTENUES EN SOUFFLERIE

par Marc VANMANSART
Ingénieur de Recherches
Institut de Mécanique des Fluides de Lille
5,bd Paul Painlevé, 59000 - Lille (France)

1 - INTRODUCTION.-

La présente communication porte sur des travaux relatifs à l'étude du recoupement par le calcul de vrilles réelles, stade indispensable à la validation d'une modélisation de la vrille.

L'expérience acquise à ce sujet jusqu'à ce jour fait apparaître de réelles difficultés de recoupement. Pour nous mettre dans des conditions de recoupement à priori les plus faciles, nous avons choisi, pour nos travaux, le cas d'un avion léger dont la vrille est particulièrement calme et pour laquelle les gouvernes sont très efficaces. Afin d'avoir une très bonne connaissance du vol, nous avons choisi de chercher le recoupement de vrilles obtenues en soufflerie verticale.

Les différentes étapes du travail seront examinées. En premier lieu, sont relatés les calculs effectués avec des coefficients stationnaires et instationnaires mesurés de façon classique, c'est-à-dire maquette fixe montée sur dard dynamométrique en soufflerie horizontale, avec oscillations forcées pour les mesures de dérivées.

Les coefficients, d'abord utilisés bruts, n'ont pas conduit à un recoupement satisfaisant avec la vrille libre de la maquette de cet avion.

Certains coefficients ont alors été retouchés. Cela ne s'étant pas avéré suffisant, nous avons inclus, dans les calculs, d'autres coefficients que, parce que non mesurés, nous avons estimés.

Les résultats n'étant pas suffisants, nous avons alors modifié la méthode de mesures, et nous avons effectué ces dernières en montant la maquette sur bras tournant dans la soufflerie verticale de l'I.M.F.Lille, afin de lui imposer, pendant les mesures, un mouvement semblable à la vrille. Il est apparu que les valeurs des coefficients, mesurés dans ces conditions, étaient sensiblement différentes de celles mesurées par la méthode classique, et leur utilisation, lors du calcul, a sensiblement amélioré le recoupement.

2 - LES RESULTATS DE VOLS LIBRES EN SOUFFLERIE VERTICALE.-

A l'I.M.F.Lille, en soufflerie verticale, il est d'usage de débuter l'étude de la vrille d'un avion par un ensemble de 27 combinaisons de braquages de gouvernes, avec 3 positions de chacune des 3 gouvernes (positions extrêmes et position neutre). C'est donc une étude exploratrice par points discrets. Ce sont les résultats d'une telle exploration qui ont été l'ensemble des données en vol utilisées pour l'étude de recoupement.

La figure 1 représente l'avion qui fut retenu pour les calculs. C'est un avion léger ayant des gouvernes très efficaces tant pour le maintien de la vrille que pour la sortie. Rappelons que c'est pour la bonne efficacité de ses gouvernes et le caractère calme de ses vrilles que cet avion fut retenu pour nos calculs.

Pour cet avion, la consigne pro-vrille est : Direction "Avec", c'est-à-dire braquée à fond pour un virage de même sens que la vrille. Les combinaisons des autres gouvernes ne jouent alors que sur les caractéristiques de la vrille sans en empêcher le maintien. La consigne anti-vrille est : Direction "Contre", les autres gouvernes pouvant être laissées à un braquage quelconque.

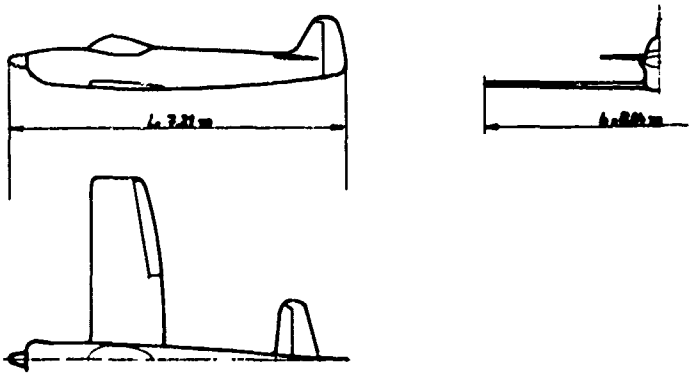

Fig. 1 - Plan 3 vues de l'avion retenu pour l'étude.

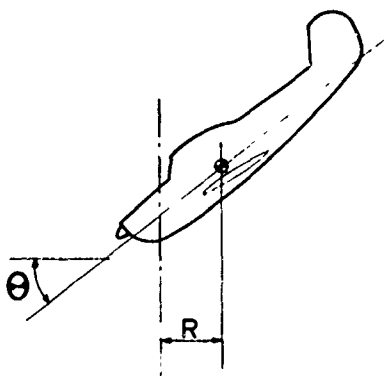

$\theta = -45°$ $\quad \Omega^{-1} = 2.5$ s/tour

$\theta = -70°$ $\quad \Omega^{-1} = 1.7$ s/tour

$R \simeq 1m$

Sur les 27 combinaisons de braquages de gouvernes, environ la moitié permet le maintien de la vrille ; l'autre implique la sortie plus ou moins rapide. Dans le domaine des gouvernes où la vrille se maintient, les principales caractéristiques de la vrille sont comprises, selon le braquage des gouvernes, entre $\theta = -45°$ et $-70°$ avec, respectivement, $\Omega^{-1} = 2.5$ et 1.7 secondes par tour (grandeur avion). Le rayon de vrille est de l'ordre du mètre. L'assiette transversale est comprise dans le domaine d'amplitude $\pm 20°$; la valeur dépend du braquage des ailerons.

Fig. 2 - Attitudes de vrille

3 - LES RESULTATS DE CALCULS (AVEC METHODE CLASSIQUE DE MESURES).-

3.1 - Les coefficients mesurés.

Dans les équations de la mécanique du vol appliquées à la vrille, nous avons choisi de faire apparaître les composantes aérodynamiques sous la forme suivante :

$$C = C_S(\alpha, \beta) + \sum \frac{\partial C_i}{\partial a} a \quad .$$

C_S est la valeur pour α et β constants (terme statique). Il est composé du terme mesuré toutes gouvernes au neutre, et des efficacités de gouvernes utilisées pour le calcul.

Les autres termes sont les actions sur C des vitesses angulaires (termes instationnaires). Ils sont, eux aussi, donnés pour α et β constants.

La figure 3 donne la liste des coefficients mesurés entrant dans la composition des composantes aérodynamiques.

MOMENTS

C_l $C_{l\delta l}$ $C_{l\delta n}$

C_m $C_{m\delta m+}$, $C_{m\delta m-}$

C_n $C_{n\delta l}$ $C_{n\delta n}$

FORCES

C_x $C_{x\delta m+}$ $C_{x\delta m-}$

C_y

C_z $C_{z\delta m+}$ $C_{z\delta m-}$

DERIVEES AERODYNAMIQUES

C_{lp} C_{lr}

C_{mq}

C_{nr} C_{np}

Fig. 3 - Liste des coefficients aérodynamiques mesurés.

Les coefficients stationnaires ont été mesurés à l'I.M.F.Lille dans la soufflerie horizontale de 2,40 m de diamètre. C'est la maquette de vrille initialement essayée en soufflerie verticale qui a servi aux mesures. Son envergure est de 0.74 m. Elle était montée sur un support spécial qui permet de faire varier l'incidence de 0° à 90° et le dérapage de -90° à +90°, en déplaçant à peine le centre de la maquette. Pour chaque couple (α, β), à la suite des mesures faites gouvernes au neutre, et sans arrêt de la soufflerie, les efficacités de gouvernes étaient mesurées après déclenchement de ces gouvernes. Le domaine α β exploré était celui des vrilles libres, soit $20° \leqslant \alpha \leqslant 60°$ et $-20° \leqslant \beta \leqslant 20°$.

En ce qui concerne la mesure des dérivées par oscillations forcées, faite également en soufflerie horizontale, le dispositif imposant les oscillations a été monté sur le support déjà cité. Les dérivées n'ont été calculées - en fonction de α et β - que pour la configuration toutes gouvernes au neutre. A priori, nous avons choisi de mesurer 5 coefficients dérivés : 3 coefficients d'amortissement : C_{lp} , C_{mq} et C_{nr} , et 2 dérivées croisées : C_{lr} et C_{np} .

Notons que toutes les mesures mentionnées dans cette étude ont été faites au même nombre de Reynolds que celui de la vrille libre de la maquette. En effet : c'est la même maquette qui a servi aux essais et aux mesures. De plus, pour les mesures, la vitesse du vent était égale à la vitesse moyenne de chute de la maquette pendant la vrille.

3.2 - Résultats de calculs faits avec les coefficients mesurés.

Dans un premier temps, les coefficients aérodynamiques statiques et dérivés ont été introduits bruts dans le calcul. Dans ces conditions, des sorties énergiques en moins d'un quart de tour ont été obtenues pour la totalité des combinaisons discrètes des gouvernes, sauf pour une seule, pour laquelle la direction - gouverne prépondérante - est pro-vrille. Dans ce cas, le phénomène calculé était une vrille piquée et peu rapide :

Θ = -70° $\quad \Omega^{-1}$ = 2.7 s/tr $\quad R \simeq 5$ m

alors que la vrille libre réelle était :

Θ = -60° $\quad \Omega^{-1}$ = 2.2 s/tr $\quad R \simeq 1.5$ m

Par rapport aux résultats de vrilles libres, il y a donc eu un glissement général très marqué des résultats de calculs. Ce glissement est défavorable au maintien de la vrille.

3.3 - Résultats de calculs faits avec coefficients corrigés.

Afin de tenter de comprendre ce glissement, nous avons essayé de rechercher l'effet de modifications des dérivées dans les calculs. L'action sur la vrille est chiffrée par l'influence sur l'incidence α, les assiettes longitudinale θ et transversale Φ_1, et la vitesse de rotation Ω.

Pour cela, nous avons utilisé comme conditions initiales de calcul la seule vrille obtenue par calcul avec les coefficients utilisés bruts.

Des modifications successives ont été apportées aux valeurs des dérivées, en les multipliant séparément par -1, 0, 1 et 2. Lorsqu'une dérivée était modifiée, les autres dérivées n'étaient pas retouchées. Nous avons fait ceci dans le but d'étudier un large domaine de valeurs.

Les nouvelles caractéristiques de vrilles obtenues sont données à la figure 4, en fonction du coefficient multiplicateur.

Sur cette figure, nous pouvons constater que les dérivées croisées C_{lr} et C_{np} ont un effet nul. Par contre, les termes d'amortissement C_{lp}, C_{mq} et C_{nr} ont une action beaucoup plus nette sur les caractéristiques.

Notons que l'exploration de l'effet du coefficient multiplicateur a été faite par valeurs discrètes de celui-ci. En tout état de cause, cette exploration n'a pas été faite finement, et nous avons peut-être pu ainsi passer au-dessus de certains phénomènes intéressants. Sous cette réserve, et malgré des modifications importantes apportées aux dérivées, les caractéristiques de la vrille maquette n'ont toujours pas été retrouvées.

Il y a eu bien d'autres tentatives de corrections de coefficients mesurés de façon classique, mais sans résultat intéressant.

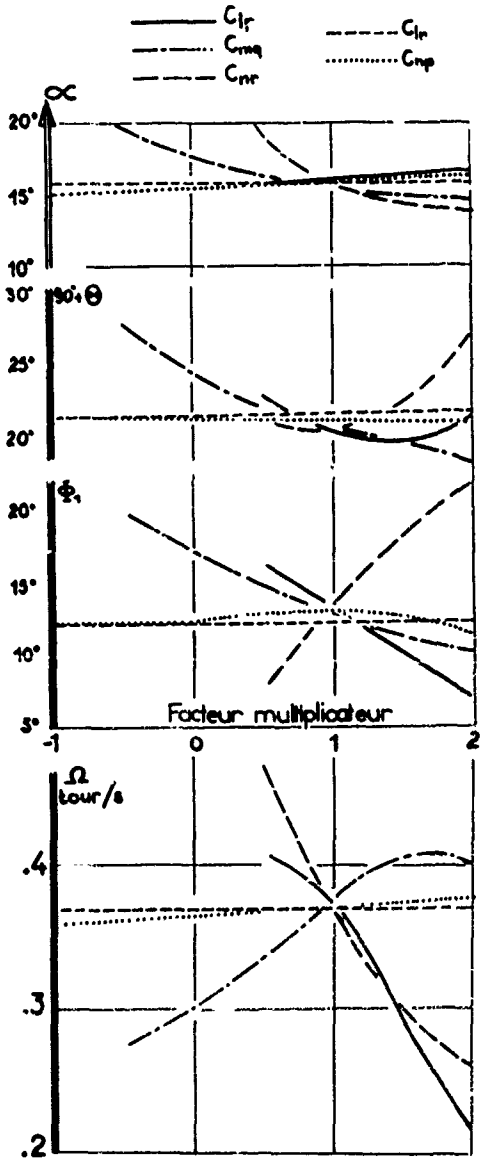

Fig. 4 - Effet séparé des dérivées aérodynamiques sur α, θ, Φ_1 et Ω.

3.4 - Résultats de calculs faits avec termes supplémentaires.

Au vu des résultats obtenus après correction des dérivées, nous sommes passés à la phase suivante des travaux. Les coefficients mesurés ont été remis à leur valeur exacte, et nous avons introduit dans les calculs des coefficients non mesurés, mais que nous avons estimés.

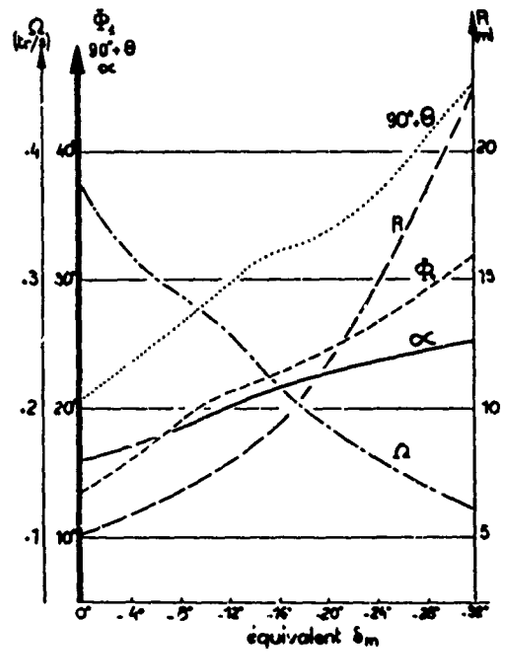

Fig. 5 - Effet du C_{mr} sur les caractéristiques de vrille.

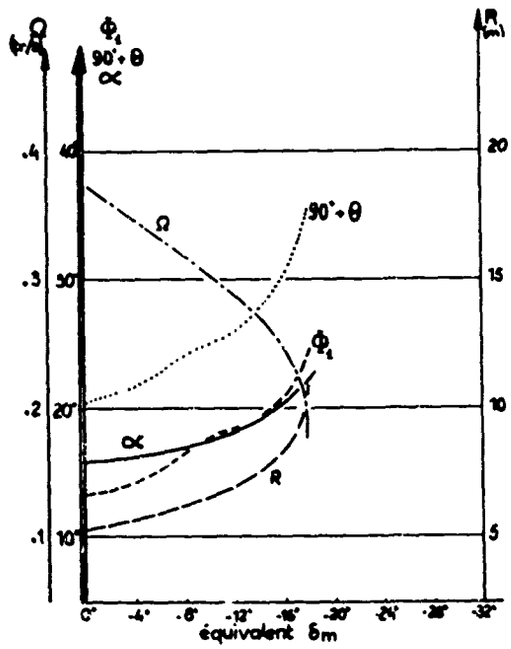

Fig. 6 - Effet du $C_{m\Omega}$ sur les caractéristiques de vrille.

3.1.1 - Introduction d'un C_{mr}

Dans un premier temps, nous avons tenu compte de ce que, pour certains avions ayant des vrilles très plates, cette attitude ne peut être observée en soufflerie verticale que si, simultanément, la vitesse de rotation de vrille est forte. Or, le couple centrifuge de tangage devient négligeable à cette attitude, ce qui montre l'existence d'un C_m aérodynamique cabreur dû à la rotation. Ceci imposerait d'introduire un C_{mr} dans les calculs. Arbitrairement, une valeur équivalente à tel braquage de profondeur lui a été donnée.

Les conditions initiales de calculs effectués avec le C_{mr} sont celles données par la seule vrille obtenue avec les seuls coefficients mesurés et non retouchés. En partant de cette vrille, la figure 5 donne l'influence du C_{mr} sur les caractéristiques principales de vrille.

Rappelons que pour la même combinaison de braquages des gouvernes, la vrille initiale calculée était plus piquée et plus lente que la vrille maquette. Avec l'introduction du C_{mr}, nous sommes parvenus à rectifier l'attitude longitudinale mais, en même temps, d'autres caractéristiques de la vrille se sont détériorées. Ainsi, le rayon de vrille qui était déjà de 5 mètres initialement, s'est trouvé encore augmenté. De plus, la vitesse de rotation a diminué.

Les nouvelles valeurs du rayon et de la vitesse de rotation étaient alors devenues telles que le phénomène ne pouvait plus être assimilé à une vrille réelle.

3.4.2 - Introduction d'un $C_{m\Omega}$

Etant donné que dans une vrille piquée, la composante r de la rotation est plus faible que la composante p, un C_{mp} a ensuite été introduit, en plus du C_{mr}. En fait, les deux coefficients ont été réunis en un seul : le $C_{m\Omega}$.

Sur la figure 6, l'effet du $C_{m\Omega}$, sur les caractéristiques de vrille, est représenté.

Comme nous pouvons le constater, l'amélioration espérée n'a pu être acquise. Les phénomènes obtenus sont encore comparables à ceux trouvés précédemment : descente en hélice à grand rayon et grande incidence.

L'excès de la valeur du rayon fait alors penser que d'autres coefficients seraient encore à ajouter, mais cette fois-ci sur les forces : par exemple un C_{Zr} ou un $C_{Z\Omega}$, un C_{Xp}, etc ...

4 - MESURES DE COEFFICIENTS EN ROTATION CONTINUE.-

4.1 - Les motifs. Les moyens d'essais.

Lors des mesures de coefficients par la méthode classique, le champ aérodynamique environnant la maquette est sensiblement différent de celui qui règne au cours d'une vrille libre : le champ aérodynamique établi présente de très nettes composantes hélicoïdales dans un domaine étendu autour de l'avion.

Il est fondé d'envisager que c'est cette différence qui est la cause principale des impossibilités de recoupement de la vrille libre par le calcul. Si nous voulons que les mesures des coefficients soient représentatives des phénomènes, il faut donc tenir compte de ces champs aérodynamiques. Or, les mesures de dérivées en oscillations forcées sont incapables de cela, attendu que le champ environnant ne peut s'établir alternativement dans les deux sens au cours d'une période.

Afin d'apprécier l'effet de la rotation continue, nous sommes alors passés à des mesures en rotation. La maquette de vrille de l'avion étudié précédemment a été fixée sur un axe en rotation imposée. Les coefficients aérodynamiques globaux ont été mesurés en fonction de la vitesse de rotation. Afin de ne pas parasiter les mesures par la pesanteur, ces essais ont été faits dans la soufflerie verticale de 4 m. de l'I.M.F.Lille.

Il est bien évident que ce n'est pas la rotation elle-même qui doit être prise en compte, mais la forme de l'hélice. Nous utiliserons ici l'angle τ de l'hélice décrite par l'extrémité de l'aile, comme le montre la figure 7.

Les mesures effectuées sont celles des coefficients globaux de forces et de moments. Elles ont toutes été faites gouvernes au neutre.

Toutes les mesures dont il est question ici ont été effectuées avec un rayon de vrille simulé nul.

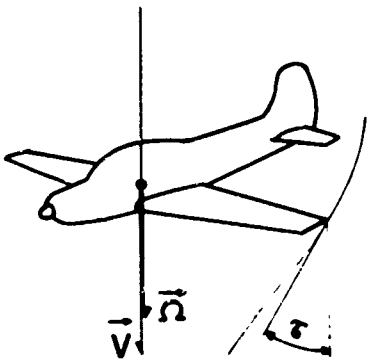

b = envergure

$$\tau = \tan^{-1} \frac{\Omega\, b/2}{V}$$

Fig.7 - Définition de l'angle τ .

4.2 - Les résultats de mesures.

A partir des coefficients stationnaires et des coefficients dérivés dont il a été question dans les chapitres précédents, nous avons reconstitué les coefficients globaux que nous aurions dû avoir au cours d'une rotation continue. Ces coefficients globaux ont été comparés à ceux effectivement mesurés avec la méthode par rotation continue.

La vrille étant, en première approximation, une affaire de moments, nous commencerons la comparaison avec les coefficients de moments. Dans les calculs faits avec les coefficients statiques et dérivés, un amortissement très net de la rotation avait été constaté. Aussi commencerons-nous la comparaison avec le C_n.

4.2.1 - Etude du C_n .

La figure 8 représente le rapport, à β nul, entre, d'une part le C_n mesuré en rotation et, d'autre part le C_n global reconstitué à partir du C_n stationnaire - qui est nul à β zéro - et des coefficients dérivés mesurés par oscillations forcées. Entre les deux bandes grises, se trouve le domaine de l'angle d'hélice τ des vrilles de la maquette. Nous constatons, entre le C_n mesuré et celui reconstitué, un rapport qui peut être très élevé. Par exemple, pour une incidence de 40°, le rapport est de l'ordre de 15 et, pour des attitudes encore plus plates, ce rapport peut atteindre 40.

Nous pouvons également constater que, sur cette composante, les résultats ne sont pas linéaires vis-à-vis de l'incidence.

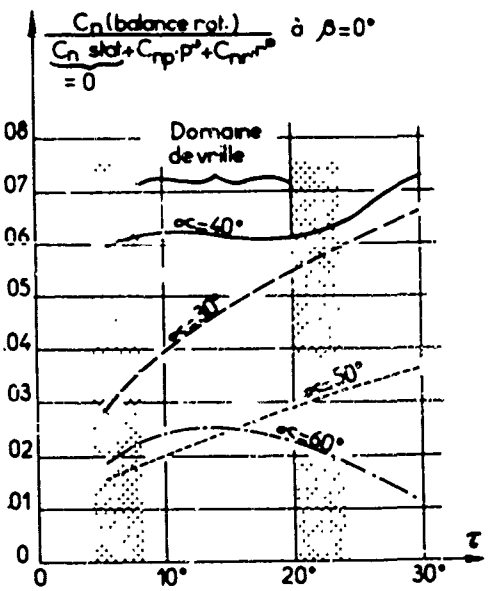

Fig.8 - Rapport des C_n globaux mesuré et reconstitué.

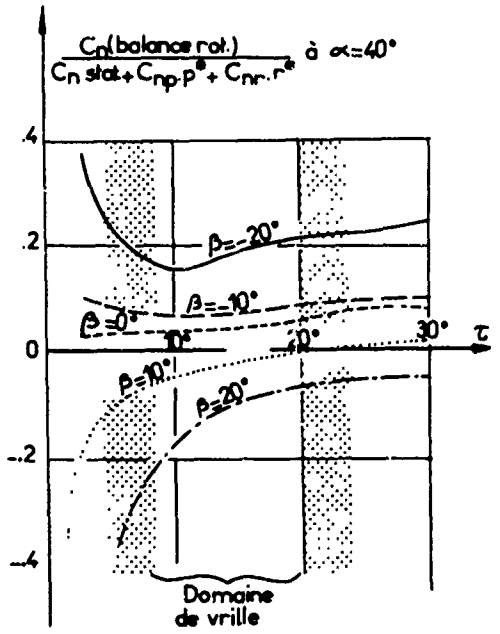

La figure 9 correspond, toujours pour le même coefficient, à une seule incidence, $\alpha = 40°$, pour un domaine de dérapage allant de -20° à +20°. La courbe centrale est la courbe supérieure de la figure précédente. Nous pouvons remarquer que les échelles utilisées ont dû être très différentes. L'ensemble des courbes montre que le rapport des valeurs entre les deux méthodes est très largement fonction du dérapage, de façon quasi-linéaire.

La figure 10 donne l'évolution du C_n en fonction de τ et du dérapage. Sur cette figure, est tracée la courbe iso $C_n = 0$ qui donne la valeur du dérapage en fonction de τ, autour de laquelle le moment de lacet change de signe.

Fig.9 - Rapport des C_n globaux

Enfin, notons qu'à dérapage nul, les valeurs provenant de la méthode classique ne contiennent que celles des dérivées C_{np} et C_{nr} (C_n stationnaire = 0) et qu'il est difficile, pour autant que α est différent de 0° et de 90°, de définir séparément les véritables C_{np} et C_{nr} à partir des données de la balance rotative.

Fig. 10 - Evolution du C_n en fonction de τ et β.

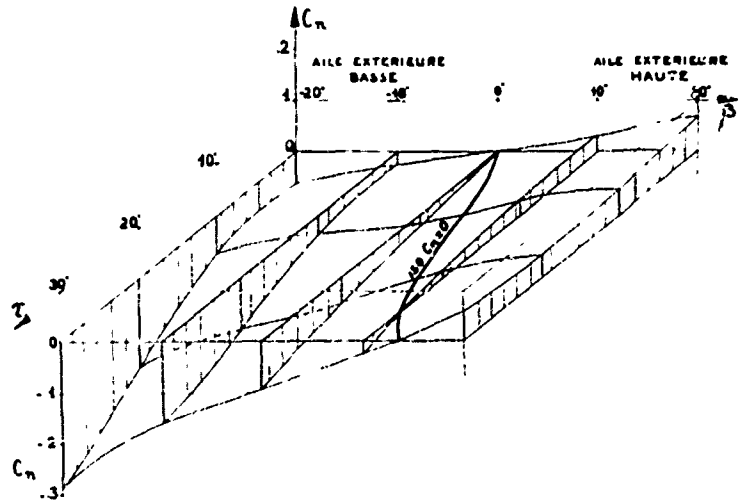

4.2.2 - Etude du C_m.

En ce qui concerne le tangage, la figure 11 représente, à dérapage nul, le rapport entre le C_m mesuré en rotation et le C_m stationnaire. Sur la figure, l'effet de la rotation est comparé à celui de la profondeur lorsque celle-ci passe de "neutre" à "à fond à piquer" pour Ω et ρ nuls.

Nous remarquons que l'effet de la rotation sur le C_m diminue pour $\alpha = 60°$. Il pourrait même vraisemblablement devenir nul, puis changer de signe pour des incidences supérieures, devenant ainsi cabreur.

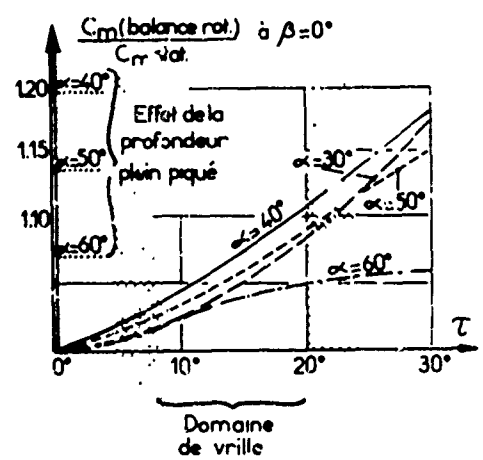

Fig. 11 - Effet de la rotation sur le C_m.

Il faut noter qu'à dérapage nul, l'écart entre le C_m global et le C_m stationnaire correspond à du C_{mp} et du C_{mr} qui n'étaient pas mesurés à priori.

Les différences sont donc beaucoup moins importantes, de façon relative, que précédemment pour le C_n , mais le C_m est loin d'être nul, alors que le C_n était forcément petit.

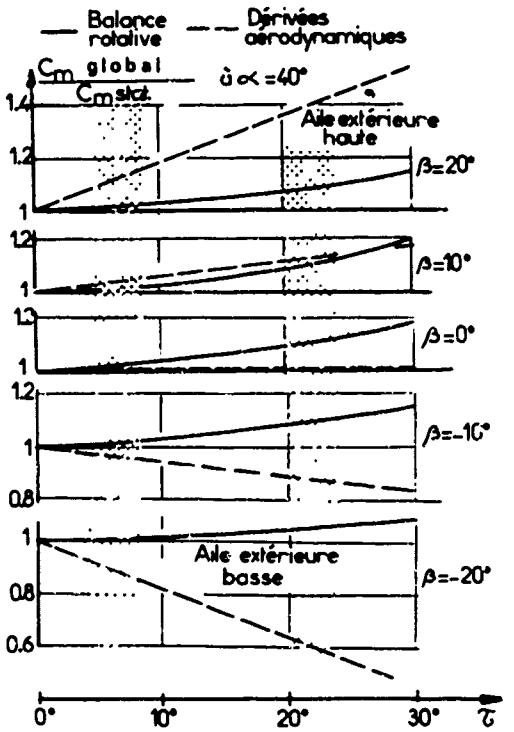

Sur la figure 12, les évolutions des C_m globaux pour différents angles de dérapage ont été comparées au C_m stationnaire, pour une même incidence $\alpha = 40°$. Les courbes correspondant au C_m global reconstitué à partir des mesures classiques sont soit au-dessus, soit au-dessous des courbes des mesures en rotation. Il y a donc des inversions de signe de correction vis-à-vis du dérapage, comme ce fut le cas précédemment avec le C_n .

Fig. 12 - Comparaison des C_m globaux mesuré et reconstitué.

Le figure 13 donne l'évolution du C_m en fonction de τ et du dérapage. Elle fait ressortir une inversion de sens de leurs effets respectifs.

Fig. 13 - Evolution du C_m en fonction de τ et de β .

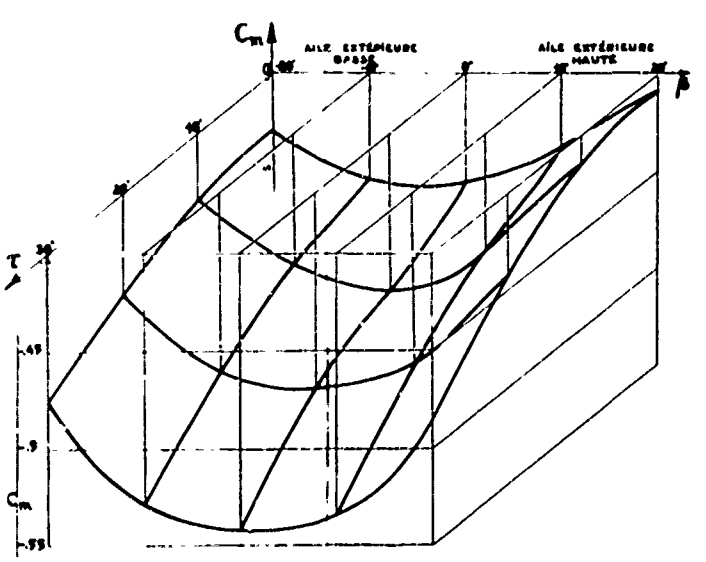

4.2.3 - Etude du C_l .

Enfin, sur le C_l , nous pouvons encore noter, figure 14, des écarts, mais qui paraissent moindres que pour le C_n . Par contre, il y a des inversions de signe, même à dérapage nul, et pour des incidences et des valeurs de τ très vraisemblables pour une vrille.

4.2.4 - Etude du C_X et du C_Z.

Rappelons que la méthode de mesures, dite classique, n'offrait, pour les forces, que des coefficients stationnaires.

Sur la figure 15, apparaissent directement les pourcentages de variation du C_X en fonction de la rotation. Si à 30° d'incidence, les écarts sur le C_X sont en moyenne nuls, par contre, pour une incidence supérieure, le C_X en rotation devient plus faible. Rappelons ici que le trièdre de référence est le trièdre avion.

Sur le C_Z enfin, figure 16, nous observons des variations similaires à celles sur le C_X , mais de sens contraire.

4.3 - Conclusions relatives aux méthodes de mesures.

La comparaison des valeurs de coefficients de moments en fonction de la rotation, les unes provenant de mesures directes, les autres étant de la reconstitution à partir de mesures en stationnaire et en "instationnaire", montre un écart important entre les résultats des deux méthodes. Cela pourrait fournir une explication quant aux impossibilités de retrouver par le calcul - avec coefficients sans rotation - les caractéristiques de la vrille réelle.

D'autre part, la prise en compte simultanée des variations sur le C_X et le C_Z explique directement les écarts dont il a été question plus haut, relatifs aux rayons de vrille.

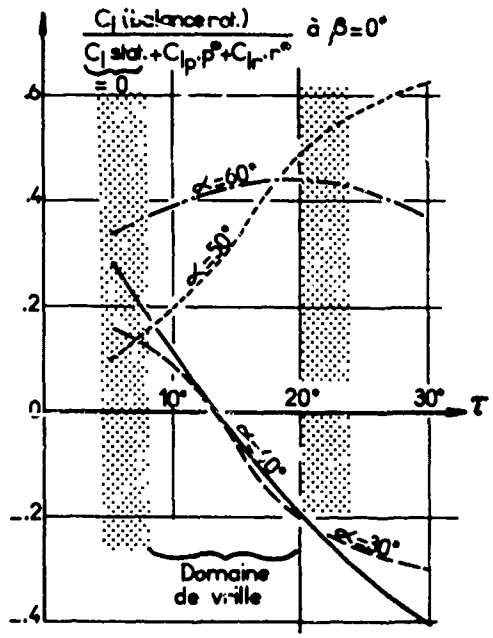

Fig. 14 - Rapport des C_l globaux mesuré et calculé.

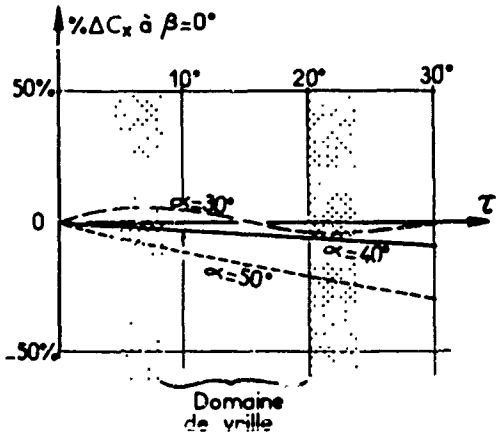

Fig. 15 - Variations du C_X en fonction de la rotation.

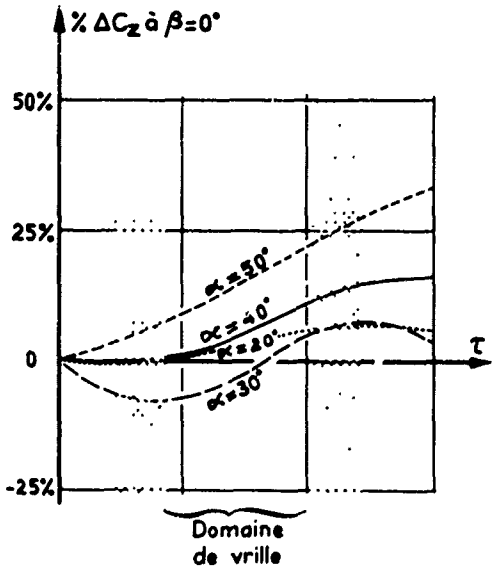

4.4 - Application des mesures en rotation aux calculs.

Rappelons que les mesures en rotation relatées ici ont été faites toutes gouvernes au neutre. Pour cette combinaison de braquages de gouvernes, en soufflerie verticale, à partir d'un lancer de maquette fait avec des conditions initiales très voisines d'une vrille stabilisée, une sortie en 3 tours a été observée.

Fig. 16 - Variations du C_Z en fonction de la rotation.

Pour l'utilisation des mesures en rotation continue dans les calculs, nous avons choisi de donner comme conditions initiales du calcul, celles imposées à la maquette au moment du lancer. Le calcul a alors donné un résultat très voisin de celui de soufflerie. Il y a donc une très nette amélioration du recoupement lorsque, pour le calcul, les coefficients mesurés en rotation sont utilisés, sans même ajouter de nouveaux termes.

Nous avons alors essayé d'introduire le braquage pro-vrille d'une, puis de plusieurs gouvernes afin de recouper des vrilles stabilisées de la maquette. Les seules efficacités de gouvernes pouvant être introduites dans les calculs ont été celles mesurées sans rotation, en stationnaire ; toutefois, nous avons tenu compte de l'incidence et/ou du dérapage géométriques locaux à chaque gouverne pendant la rotation. Dans ces conditions, pour des combinaisons de gouvernes diverses mais toujours pro-vrille, il n'a pas été possible de retrouver exactement le caractère des vrilles libres. Toutefois, la vrille se maintenant, ce qui était une nette amélioration par rapport aux résultats de calculs faits uniquement avec les coefficients provenant de la méthode classique de mesures, avec lesquels, rappelons-le, pour les mêmes conditions de gouvernes, il y avait refus de vrille.

Il y a donc encore une certaine difficulté de recoupement qui semble pouvoir être attribuée au fait que les efficacités de gouvernes n'ont pas été mesurées en rotation continue.

5 - CONCLUSIONS.-

La première conclusion que l'on peut tirer de cette étude est qu'il est nécessaire, pour un calcul correct de la vrille, que les coefficients soient mesurés sur maquette en rotation continue. Ces mesures doivent inclure les efficacités de gouvernes, elles-même très affectées par l'écoulement général.

Toutes ces mesures doivent être impérativement effectuées pour la seule prévision des vrilles très calmes.

Mais ces mesures sont encore insuffisantes si nous voulons prendre en considération tous les types de vrilles possibles. Ainsi, la vrille des avions d'armes est, à l'inverse de celle des avions légers, le plus souvent très agitée. Pour tenir compte des agitations dans les calculs, il faudrait vraisemblablement faire des mesures en oscillations forcées au cours d'un mouvement en rotation continue, comme nous sommes obligés de faire des mesures en oscillations forcées pour étudier les petits mouvements autour d'un vol rectiligne.

Enfin, toutes ces mesures, y compris celles en oscillations forcées, et tous ces calculs, supposent à tout moment l'écoulement permanent général établi. Or, si nous envisageons l'étude d'une vrille très agitée, à agitations amples et rapides, il faudrait encore pouvoir introduire des termes instationnaires, qui tiennent compte de l'établissement des écoulements, comme nous sommes obligés de le faire dans le calcul de la réponse d'un avion à la traversée d'une rafale.

STALL BEHAVIOUR AND SPIN ESTIMATION METHOD BY USE OF ROTATING BALANCE MEASUREMENTS

BY

Dr. Ing. Ermanno BAZZOCCHI
FRAeS
General Manager, Technical
Aeronautica Macchi S.p.A.
Varese, Italy

1. SUMMARY

This paper describes the experimental work carried out at Aeronautica Macchi since 1950 in the field of wind tunnel investigation of stall behaviour, in the evaluation of the characteristics of lateral control devices in the measurement of the aerodynamic coefficients to determine lateral-directional stability and the analytical study of the spin.
This research has required the development of special test equipment, measurement methods and calibration systems.
The purpose of this paper is to provide a description and data on the test equipment adopted, its use and some of the results obtained

2. SYMBOLS

The stability axes system is used as reference for the measurement of the moment coefficients in the wind tunnel
The wind axes system is considered as reference in the study for the determination of the equilibrium of the aircraft moments in the spin.

A, B, C	moments of inertia about aircraft X, Y, Z axes, respectively
A.R.	aspect ratio
b	wing span
C_D	drag coefficient: $\frac{D}{\frac{1}{2}\rho V^2 S}$
C_l	rolling moment coefficient. $\frac{L_a}{\frac{1}{2}\rho V^2 S b}$
C_L	lift coefficient: $\frac{L}{\frac{1}{2}\rho V^2 S}$
C_m	pitching moment coefficient: $\frac{M_a}{\frac{1}{2}\rho V^2 S b}$
C_n	yawing moment coefficient: $\frac{N_a}{\frac{1}{2}\rho V^2 S b}$
C_y	side-force coefficient: $\frac{F_y}{\frac{1}{2}\rho V^2 S}$
D	aerodynamic drag
F_y	force acting along Y body axis
g	acceleration due to gravity
L	aerodynamic lift
L_a, L_i, L_e	rolling moment
M_a, M_i, M_e	pitching moment
N_a, N_i, N_e	yawing moment
m	aircraft mass
p, q, r	components of angular velocity
R	radius of spin
S	aircraft wing area
t	time
U, T, S	spin axes (see figure 14)
V	velocity of aircraft center of gravity (resultant velocity of components u, v, w along X, Y and Z axes, respectively)
W	aircraft weight
X, Y, Z	aircraft body axes

α	aircraft angle of attack
β	angle of sideslip
δ	control surface (or flap) deflection
ρ	air density
ω	rate of rotation around spin axis
$\lambda = \omega b/2V$	spin parameter
γ	helix angle
θ	wing tilt angle

Suffixes:

a	aileron or aerodynamic
e	engine (gyroscopic couple) or elevator
i	inertial
f	flap
r	right or rudder
l	left
sp	spoiler

3. REASONS FOR WIND TUNNEL TESTING WITH ROTATING BALANCES

For the study of the aircraft motion during manoeuvres or in special conditions such as stall and spin, it is necessary that aerodynamic coefficients and their derivatives be known. For the conditions below the stall in the linear or quasi linear range, a theoretical calculation can still be carried out, although the interference phenomena may render these calculations rather doubtful, but as far as the conditions at and beyond the stall are concerned, the theoretical calculations are often unreliable.

Only wind tunnel testing can provide reliable data, though the effects of the Reynolds number and of the transition points may be quite important.

Of particular interest is the determination of the rotary derivatives, which are highly affected by nonlinearities, and whose theoretical determination by the handbook methods can be affected by large errors. To this purpose, the use of a rotating balance allows the experimental determination of the rotary derivatives with a relatively large model and with good accuracy. The independent measurement of the various components is also very important for flight dynamic calculations, while other methods (free flight spin tunnels, remotely controlled models) allow only global verification of the aircraft behaviour. The method is not new (see for example ref. 1 and 2), but the continuous improvements provided by the modern instrumentation and computing equipment may be of interest.

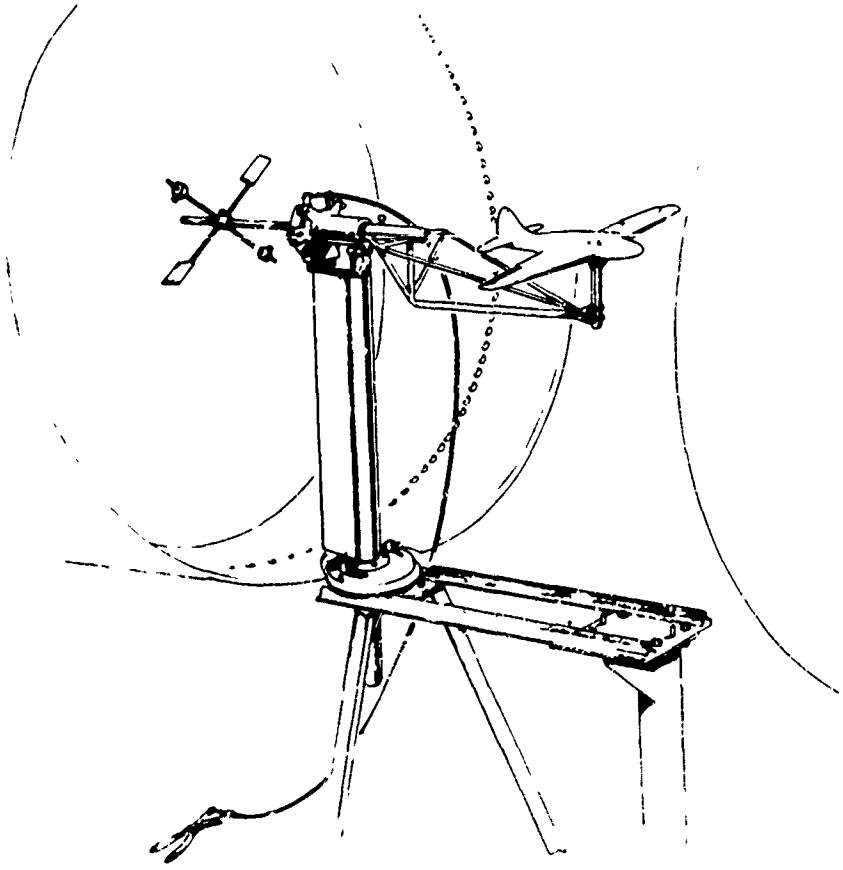

FIGURE 1
WINDMILLING BALANCE
("GIROUETTE")

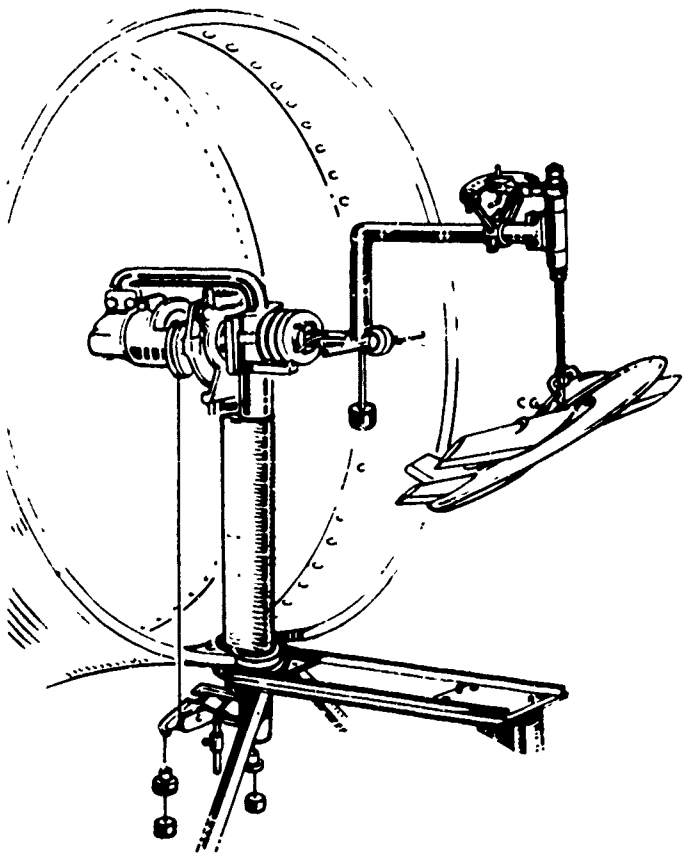

FIGURE 2.
THREE-COMPONENTS
ROTATING BALANCE

4. TESTING EQUIPMENT USED

Since 1950, different types of rotating balances have been successively built at Aeronautica Macchi, from the simple "girouette" (windmill) shown at fig. 1 to the balance capable of measuring all six components, as shown at fig. 5, 6.

With this equipment, continuous experimental work has been developed in past years both on aircraft designed by Aeronautica Macchi and on collaborative programs such as the military transport Aeritalia G222, the MRCA and the Bandeirante EMB-120 on behalf of Embraer - Brasil.

The balance illustrated at fig. 2 was first used in 1956 for the analytical study of the spin. The radius of the spin was reproduced on this balance, and the moments acting around the spin axis and a yaw axis normal to it were measured. The model was mounted with the possibility of variation of pitch and tilt angles. The method adopted for this study is described in paper ref. 3.

Later a new type of rotating balance has been built.

Most of the experimental work has been conducted using this equipment, illustrated at fig. 3, 4. The model has a max. wing span of up to m 1.30, the max. rate of rotation reaches 150 rpm corresponding to a max. value of pb/2V of 0.28.

The wind speed is 40 to 50 m/sec. The Reynolds number is between 600,000 and 750,000.

The rate of rotation can be changed with continuity. The strain gauges in the balance permit the measurement of the coefficient of pitching moment C_m, the rolling moment C_l, the yawing moment C_n and the side-force C_y.

The lift and drag coefficients are assumed to be obtainable with fairly good approximation from fixed model tests.

With this equipment, the tests have always been performed with the roll axis passing through the aircraft C.G. (the radius of spin is not represented).

The sideslip angle has been introduced by means of a sprocket fitted to the model supporting bar. The indication of the strain gauges fitted on the rotating arm are collected via a 36-channel slip ring collector, processed by a measuring chain and perforated on paper tape.

This tape is then processed in a Philips 880 digital computer and the results are directly displayed by a plotter Calcomp Mod. 936. The precision of the measuring system and the repeatability of the results have been confirmed in a fully satisfactory manner.

More recently a new improved rotating balance has been built which permits to measure all six components and to simulate the radius of the spin

The equipment is illustrated at figs. 5 and 6 and has been designed to allow a rather large radius of spin and a pitching attitude up to 90° (flat spin). For this purpose, a circular rail has been provided to react to the centrifugal force on the model. This eliminates the elastic distortion effect of the supporting arm.

5. CALIBRATION METHODS

A comment on the calibration methods adopted may be of interest.

The models used for the tests are built with geometrical similarity only. All measurements are therefore to be corrected for the effect of weight and moments of inertia of the model.

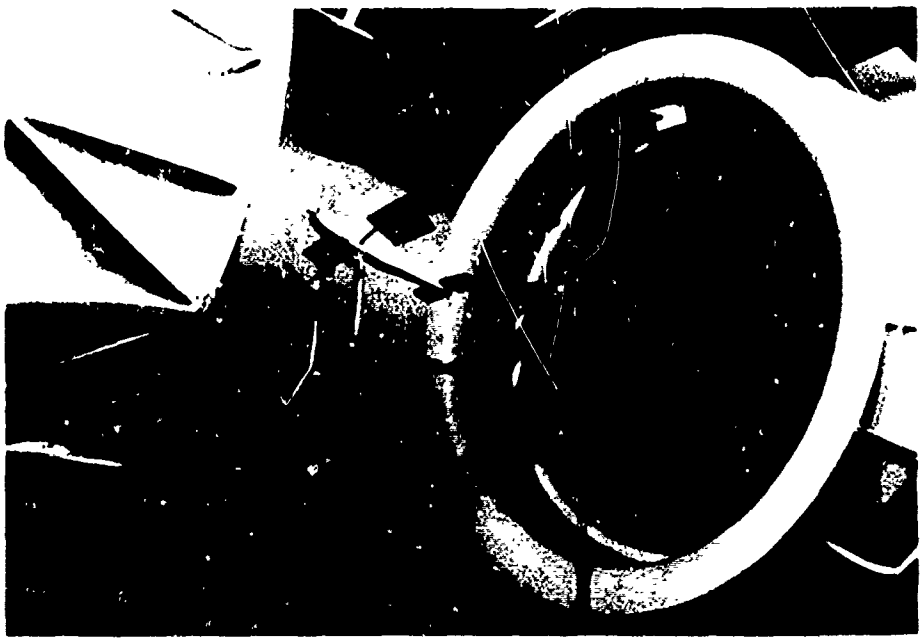

FIGURE 3. FOUR-COMPONENTS ROTATING BALANCE

The effect of the forces due to weight varies sinusoidally during one complete revolution. In order to remove this effect, it is necessary to integrate over one revolution all the balance measurements this is automatically done by the measuring chain

The effect of the model moments of inertia is measured by rotating the model in the absence of wind. These results are however affected by the air moved by the model. This effect can be easily measured both for the roll and yaw axes by rotating the model with no yaw; in this condition the inertial couples around the roll and yaw axis are zero and therefore it is only the aerodynamic effect which is measured.

A particularly critical aspect of the setting up is the calibration of the 6 component balance.

Above all it is necessary to ensure that each component is not affected by mutual influences, viz that the force or moment acting in one plane does not induce false indications in the other planes.

It may be of interest, from the experimental viewpoint, to describe the method and equipment used, as illustrated at figure 7

On the rotating balance, the model is replaced by a sphere on which many meridian planes are carefully traced. To these meridian planes there can be applied tangential forces or moments of which the components along the balance axes are known with precision. An accurate calibration of each single component is thus possible as well as the check of any cross reading on the other axes.

6. VISUALIZATION

An interesting aid to the development and interpretation of the tests proved to be a TV camera fitted on the rotating arm and recording on video tape. This permits a visual analysis of the behaviour of wool tufts applied to the model and the observation of phenomena which would otherwise go undetected.

The visualization of the flow is an efficient means for the interpretation of the complex phenomena that take place in stall conditions and at attitudes beyond the stall.

Visualization has proved to be very useful and sometimes indispensable to identify aerodynamic hysteresis phenomena. In one instance it proved to be of great practical use in revealing the instability conditions existing in the flap slot of a transport aircraft. The instability phenomenon was removed by a minor modification to the slot duct.

7. TYPES OF INFORMATION AND OBTAINABLE DATA

Attitudes below the stall

a. Measurement of C_l and C_n with and without sideslip.

b. Measurement of C_l and C_n due to aileron deflection as function of pb/2V.

c Flow visualization.

All components of the forces and moments can be measured

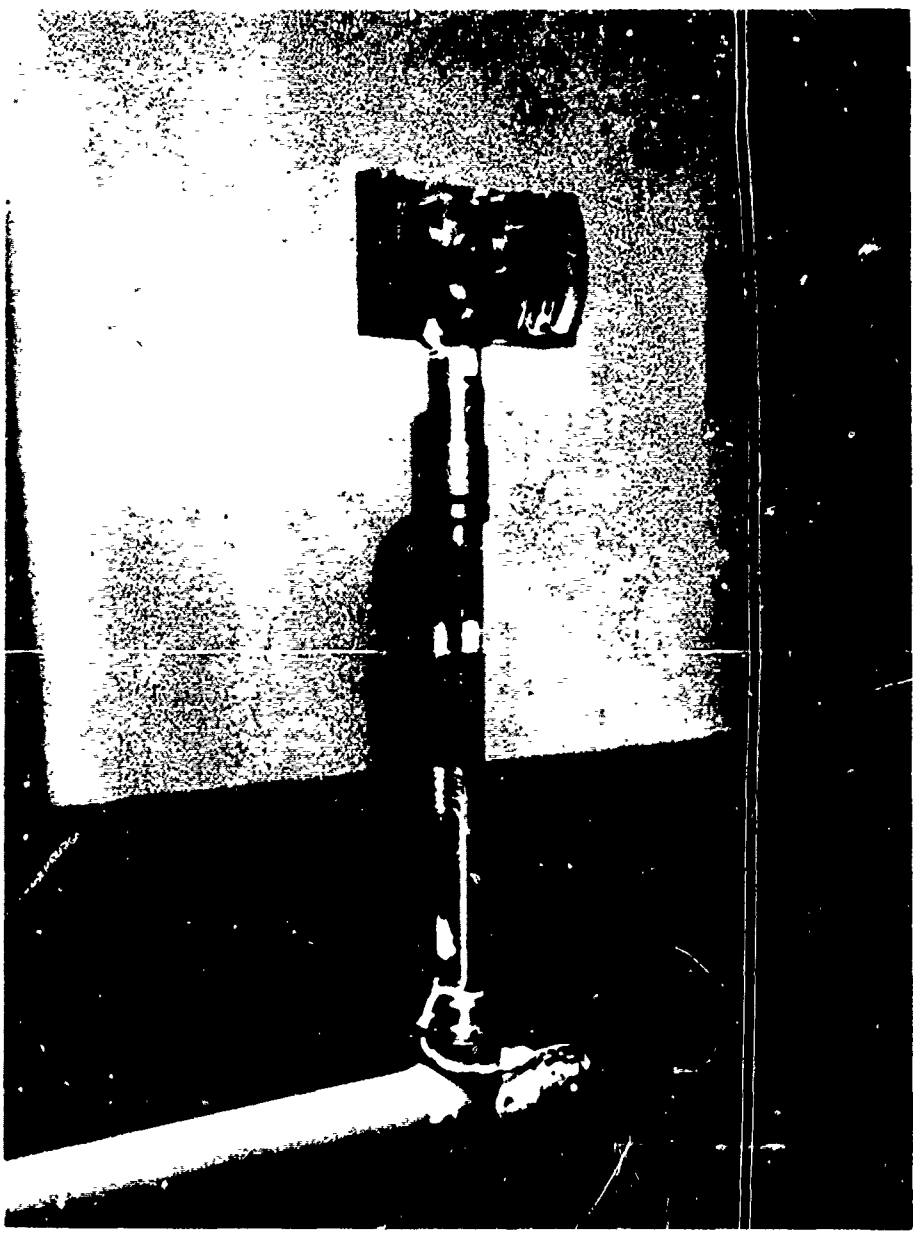

FIGURE 4. MEASURING ARM

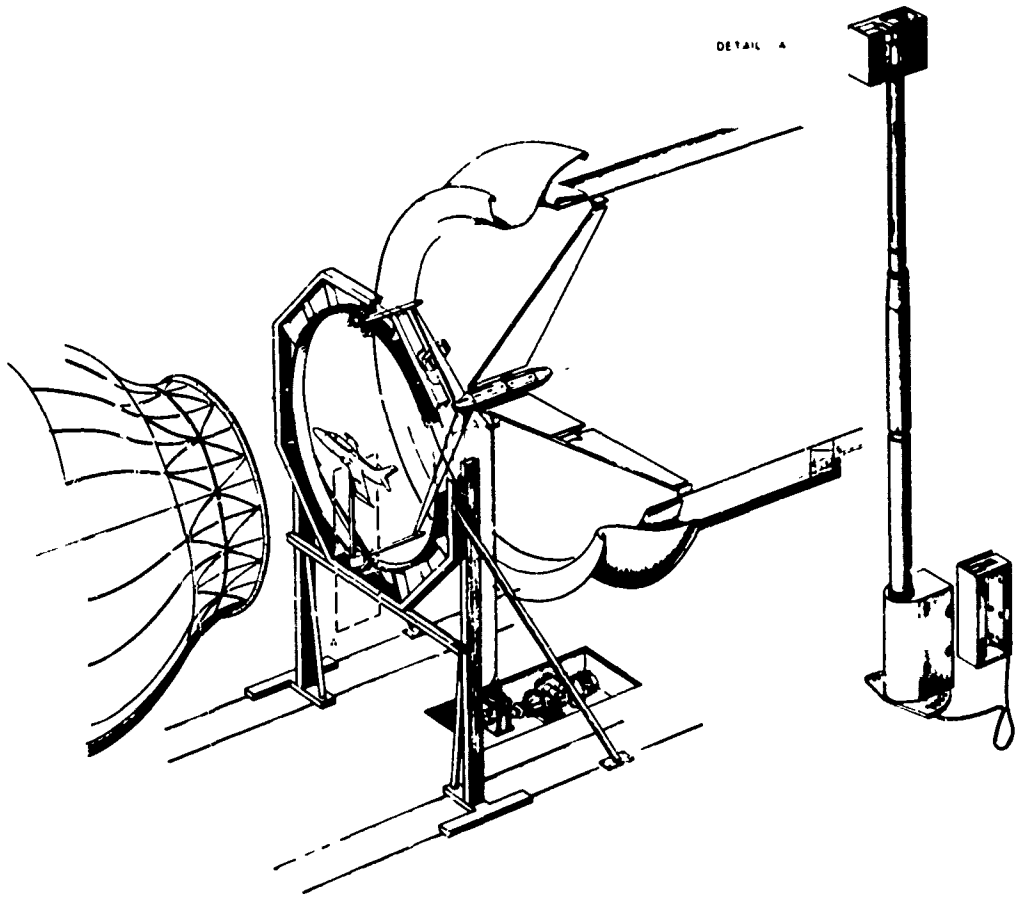

FIGURE 5. SIX-COMPONENTS BALANCE

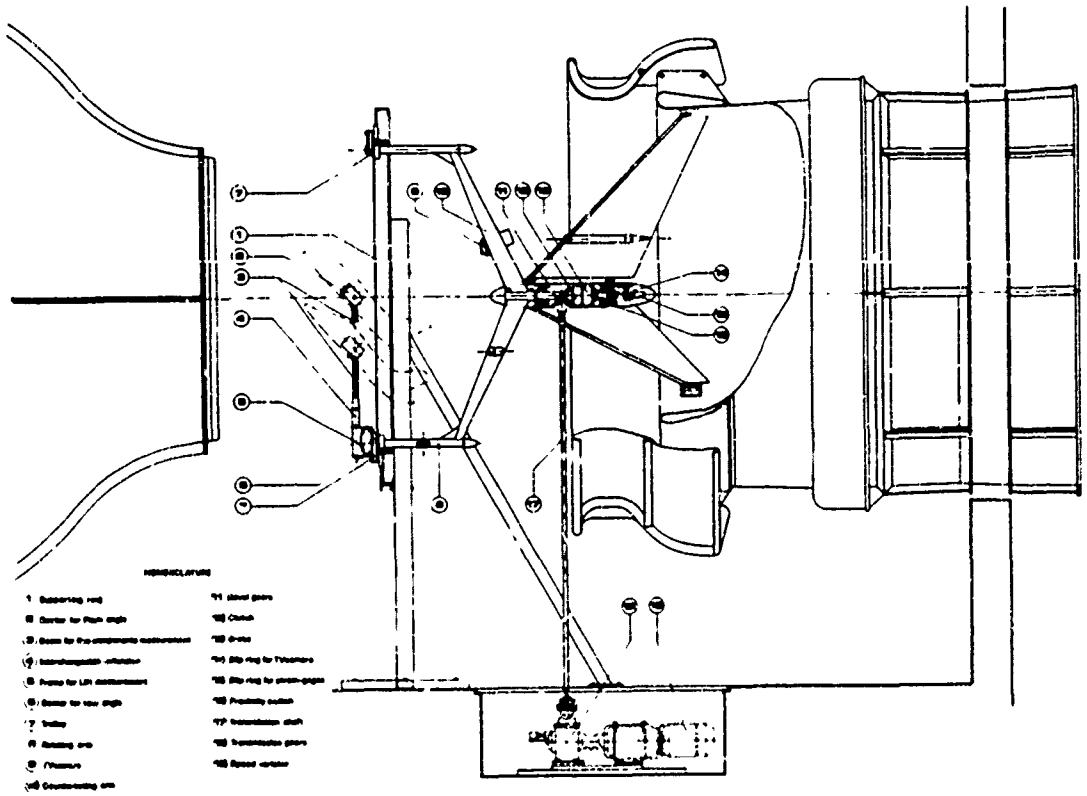

FIGURE 6. SIX-COMPONENTS BALANCE

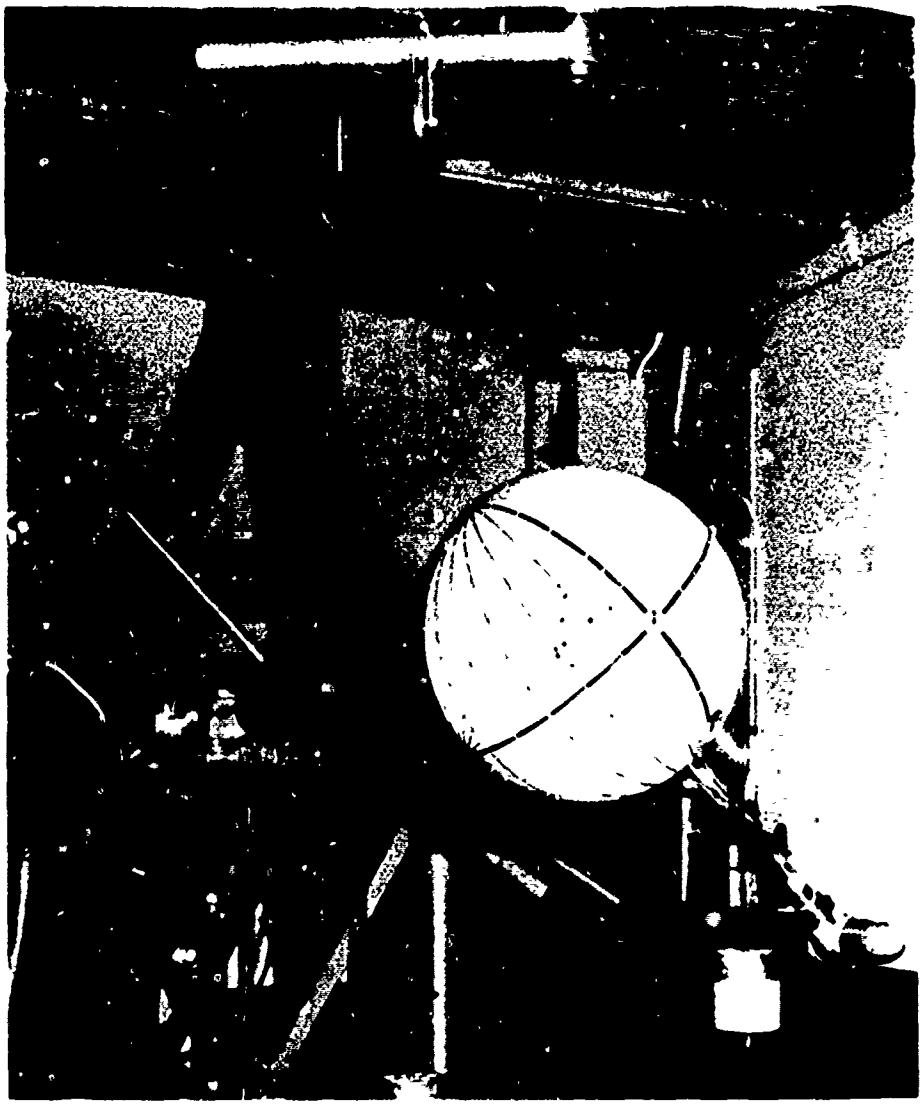

FIGURE 7.
SPHERE FOR FORCE
TRANSDUCERS CALIBRATION

Stall attitudes

a. Aircraft stalling behaviour; visualization of the stall propagation with increasing or decreasing pb/2V. Discovery and study of hysteresis phenomena.

b. Measurement of C_l and C_n as a function of pb/2V, autorotation and damping with and without sideslip.

c. Effects of deflection of the ailerons and lateral control devices.

Attitudes beyond the stall

a. Exploration of the attitudes beyond the stall, including estimated spin attitudes.

b. All tests considered in the preceding paragraphs can be repeated to explore in detail the evolution of the autorotation and damping characteristics and the variation of the lateral-directional stability coefficients

Tests for the analytical study of the spin

In order to develop an analytical study of the spin in accordance with the method of ref. 3, the coefficients obtained from the tests with zero radius of spin can be used in first approximation.

Once the attitudes and ranges of possible spin development have been identified, the tests may be repeated by introducing in the balance the calculated radius of spin.

With the availability of this new aerodynamic information, it is possible to develop a more detailed study of the probable spin conditions, in addition to the spin entry and recovery.

8. EXAMPLE OF PRESENTATION OF THE EXPERIMENTAL RESULTS

A few examples of presentation of the obtained data are given hereafter.

At fig. 8 is given the rolling moment due to the rate of roll as a function of pb/2V, for different angles of attack α. An autorotation sector and a damping sector are perceivable.

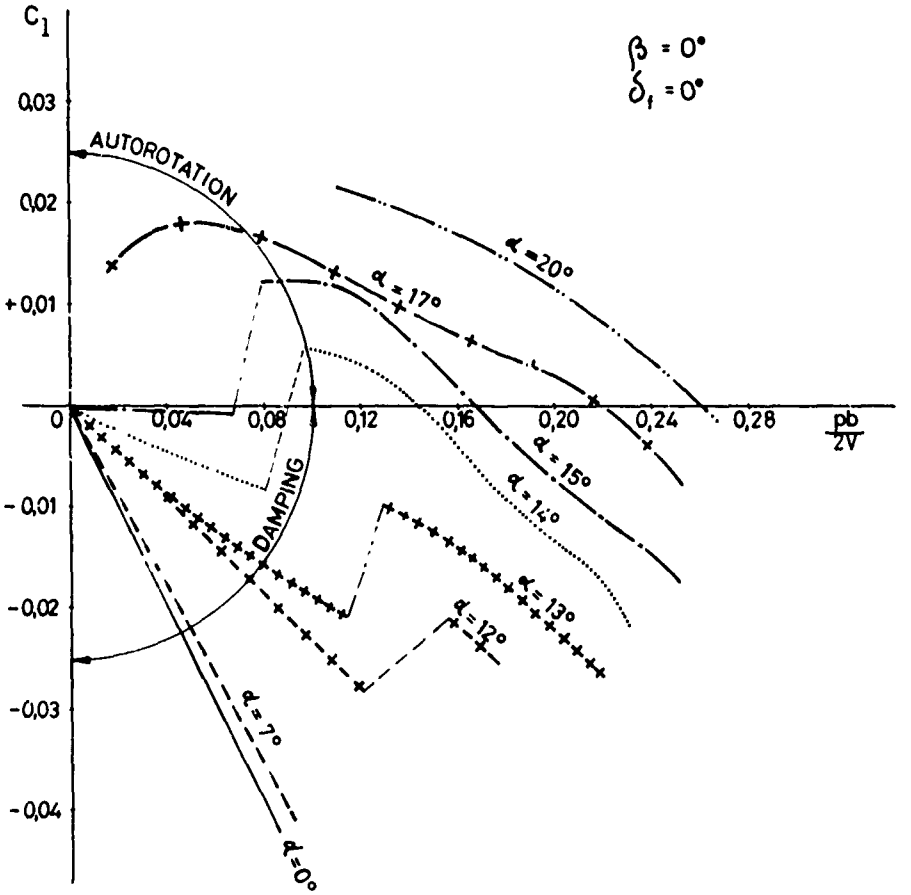

FIGURE 8. ROLL DAMPING

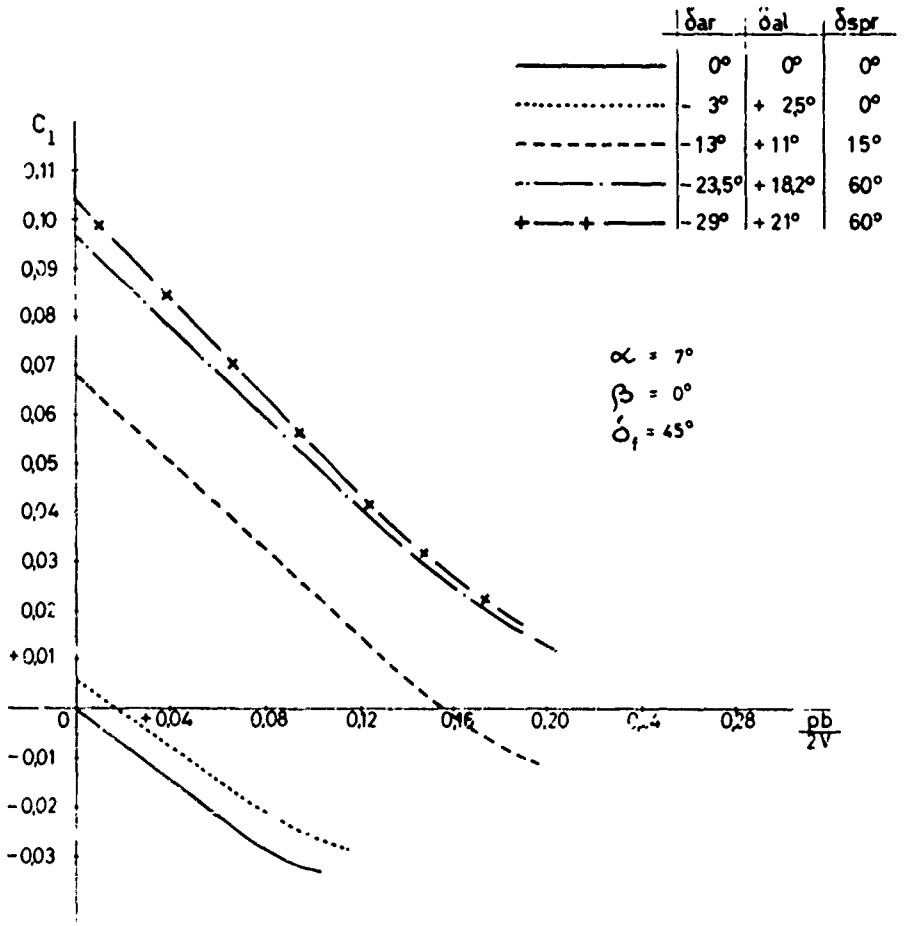

FIGURE 9. LATERAL CONTROL POWER, FIXED INCIDENCE

It is noted that at small angles of attack α the moment is damping but it becomes less damping as α increases.
For α = 12° and pb/2V = 0.12, a discontinuity is experienced due to local stall on the down-going wing. For α = 14° (corresponding to the stall in static conditions) this discontinuity increases and between pb/2V = 0.08 and pb/2V = 0.1 an autorotation range is present. At larger angles of attack, the autorotation range broadens, indicating the likelihood of an incipient spinning condition.
At fig. 9 is given the effect of the aileron deflection in favour of the turn, at constant incidence.
It should be noted that with increasing aileron and spoiler deflection, the achievable rolling moment does not increase proportionally to the deflection; the steady rolling velocity can also be established.
At fig. 10 is given the variation of the rolling moment at various incidences with a given aileron deflection.
Diagrams similar to those in figures 8, 9 and 10 (which refer to a transport aircraft with AR = 8) allow a full study of the lateral controllability and an analysis of possible problems at the approach of the stall.
Fig. 11 and 12 refer to a STOL aircraft with rectangular wing with AR = 7.5.
Fig. 11 shows the influence of stall propagation on the rolling moment. Abrupt changes in the rolling moment are caused by partial stalls on different areas of the highly twisted wing.
Fig. 12 shows, for the same aircraft, the effects of hysteresis on the recovery from autorotation although undoubtedly affected by Reynolds number considerations, the presence of this type of phenomenon might indicate the existence of more than one equilibrium condition in the spin.
To make these discontinuities apparent and locate them, the visualization method, as discussed before, has been very effective.
Fig. 13 refers to a model with a 25° sweptback wing with AR = 5. The angle of attack is α = 8° and 24°.
The C_l is damping for all experimented values of pb/2V for α = 8°, but beyond the stall at α = 24°, the roll damping is very low, and there is an autoration condition above pb/2V = 0.085.
At fig. 13 is also given the pitching moment coefficient C_m. It is interesting to note that the pitching moment coefficient C_m is relatively unaffected by pb/2V.

9. ANALYTICAL STUDY OF THE SPIN

As mentioned in paragraph 7, the rotating balance provides the aerodynamic information required to develop an analytical study of the spin, spin entry and recovery. The method has been dealt with in reference 3.
The application of this method to the MB-326 aircraft, the satisfactory spin behaviour of which has been thoroughly proven in flight, is described here.
In this method, the spin is considered steady and is reduced to the diagram of figure 14. Transient phases and oscillating spin conditions are obtained as discussed later.
The aircraft rotates with steady angular velocity ω around the spin vertical axis U with a radius R measured to the center of gravity, with an angle of attack α and an angle of tilt θ.
In the steady spin, the resultant of the aerodynamic and inertia forces must lie in the plane formed by the body axis Z and the spin axis U.

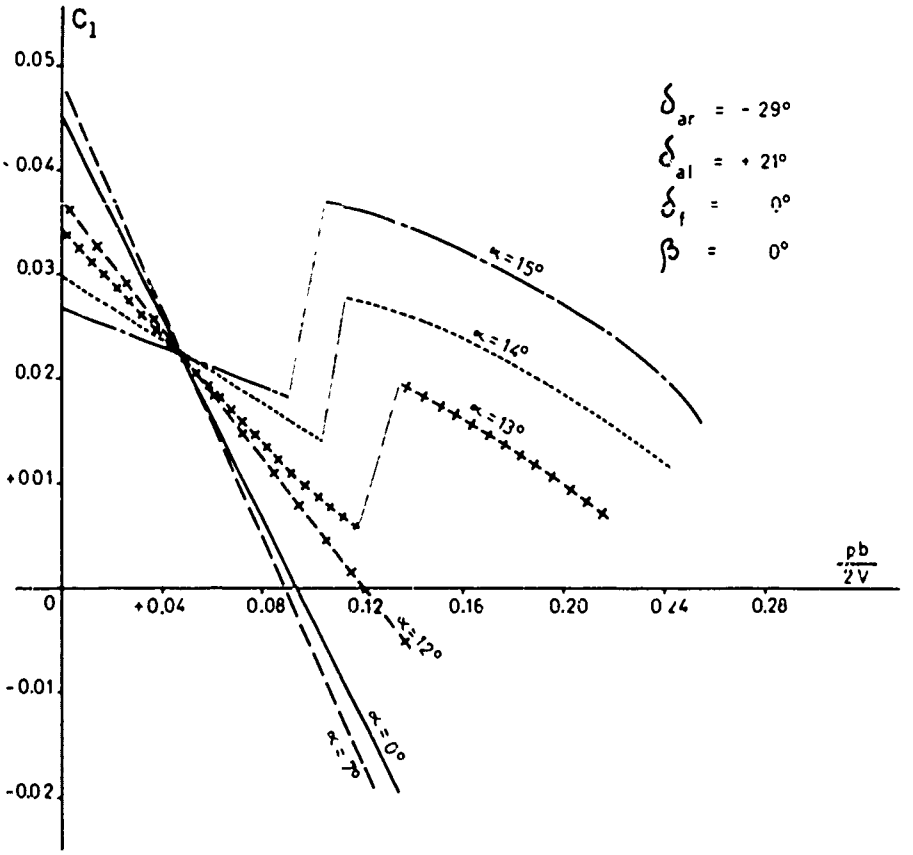

FIGURE 10. LATERAL CONTROL POWER, VARIABLE INCIDENCE

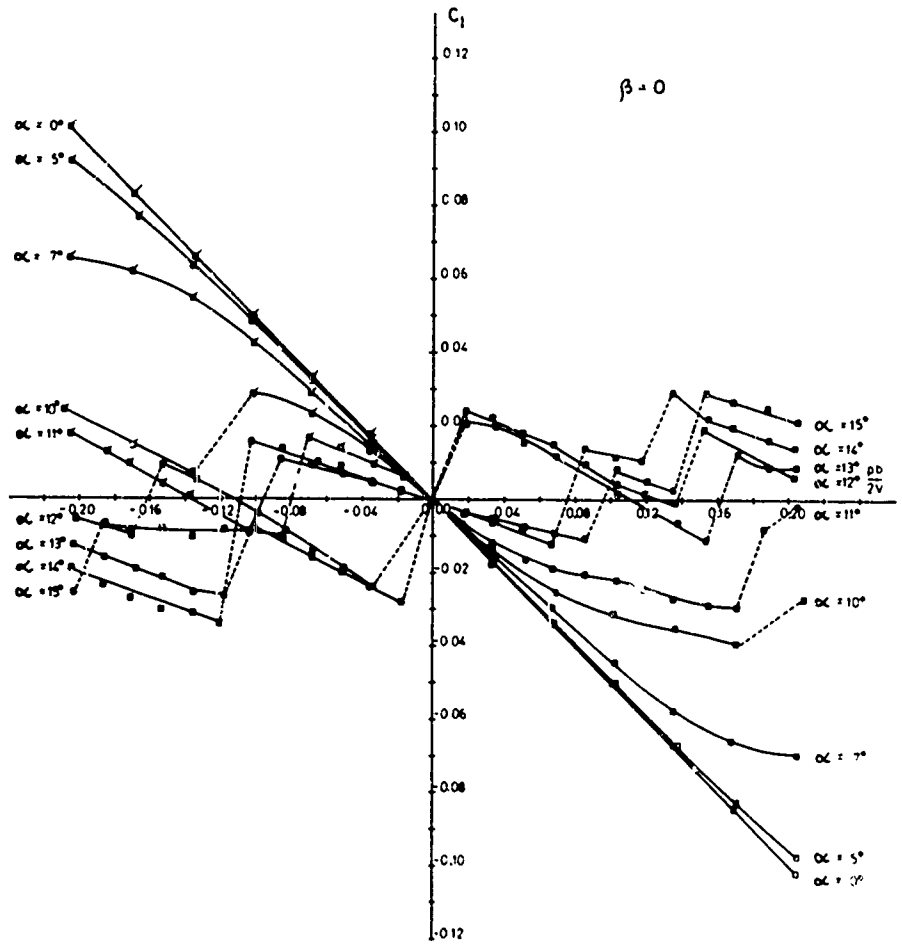

FIGURE 11. INFLUENCE OF STALL PROPAGATION ON ROLL DAMPING

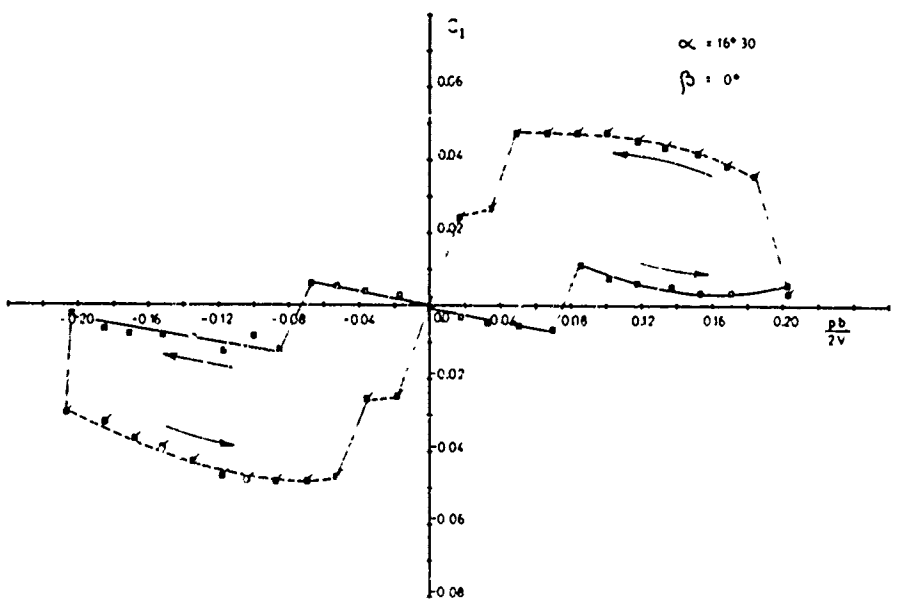

FIGURE 12. HYSTERESIS OF ROLL DAMPING AFTER STALL

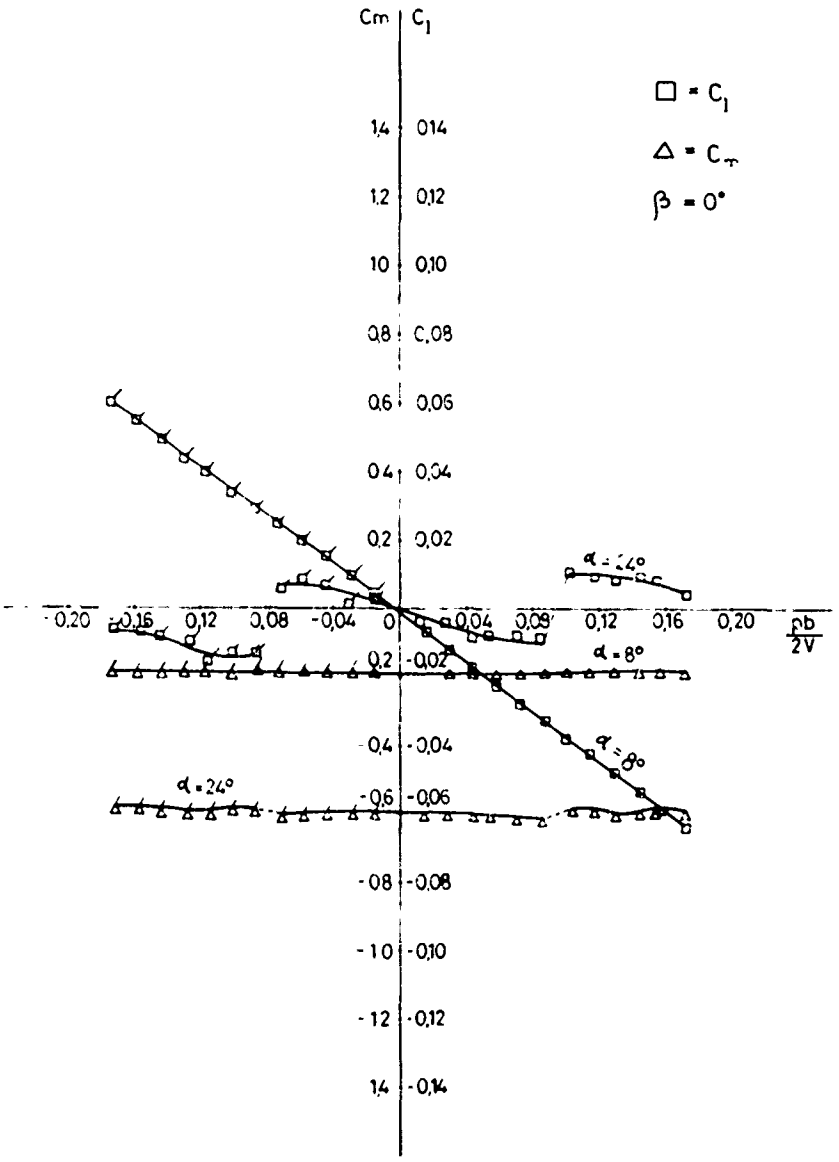

FIGURE 13. VARIATION OF ROLL DAMPING AND C_m WITH INCIDENCE

For a steady spin condition to be obtained, all forces and moments must be balanced out.
For the balance of forces, it is necessary to have:

$$W = D = \tfrac{1}{2}\rho SV^2 C_D$$

$$\frac{Ml}{j}\omega^2 R = L = \tfrac{1}{2}\rho SV^2 C_L$$

$$F_y = 0$$

For the balance of moments, it is necessary to have:

$$L_a + L_i + L_e = 0$$

$$M_a + M_i + M_e = 0$$

$$N_a + N_i + N_e = 0$$

The above equations can be solved for all possible combinations of inertial and aerodynamic configurations, controls surface deflections, etc., to find all the possible spin regimes. However, this method requires a very extensive computer effort, and it is advisable to define approximately the ranges of configurations likely to produce a spin by a first approximation graphical study based on the method of ref. 3.
This method consists essentially of the independent solution, for a limited number of conditions, of each of the three equations expressing the equilibrium around each axis, and superimposing the curves thus obtained. It is easy to determine the likelihood of an equilibrium in the spin, expressed by a simultaneous crossing of the three curves.

Assuming the reference axes as defined in fig. 14, fig. 15 shows, for a given condition (elevator and rudder deflection, inertial configuration fixed and a selected value of the longitudinal attitude), the pitching moment coefficients (aerodynamic, inertial and engine gyroscopic couple) as a function of $\lambda = \omega b/2V$, with the angle of tilt as parameter. Imposing the equilibrium around the pitching axis will provide a relationship between angle of and λ (fig. 16).

Similarly, fig. 17 shows, for a given angle of attack, the equilibrium conditions around axis T and fig. 18 the equilibrium around the axis U (It should be noted that, if the spin radius is zero, these axes coincide respectively with the wind yaw and roll axes). Superimposing the loci of the equilibrium around each of the three axes, we can find, for each angle of attack, the possibility of a steady spin, expressed by a simultaneous crossing of the three curves (fig. 19).

In general, the crossing will not be simultaneous, but the intersections will define a triangle, whose size will be indicative of the remoteness of the condition studied from a steady spin. The spin regimes so identified can then be fully explored with the computer, introducing systematic variations of inertia, control deflections, etc.

Stability of the spin or its tendency to become oscillatory can be evaluated by the examination of the slopes of each partial equilibrium curve, which shows in which direction a perturbation of the spin parameters is most likely to occur, and in which axes the restoring moments are most powerful.

The results of this type of investigation are quite good, as it can be seen from fig. 20, which correlates the computed spin parameters with the flight test results.

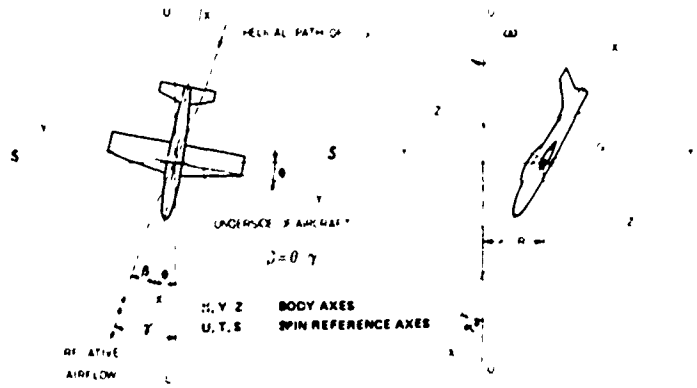

STEADY SPIN	
BALANCE OF FORCES	BALANCE OF MOMENTS
$W = D = \frac{1}{2}\rho SV^2 C_D$	$L_a + L_i + L_e = 0$
$\frac{W}{g}\omega^2 R - L = \frac{1}{2}\rho SV^2 C_L$	$M_a + M_i + M_e = 0$
$F_y = 0$	$N_a + N_i + N_e = 0$

FIGURE 14. SPIN REFERENCE AXES

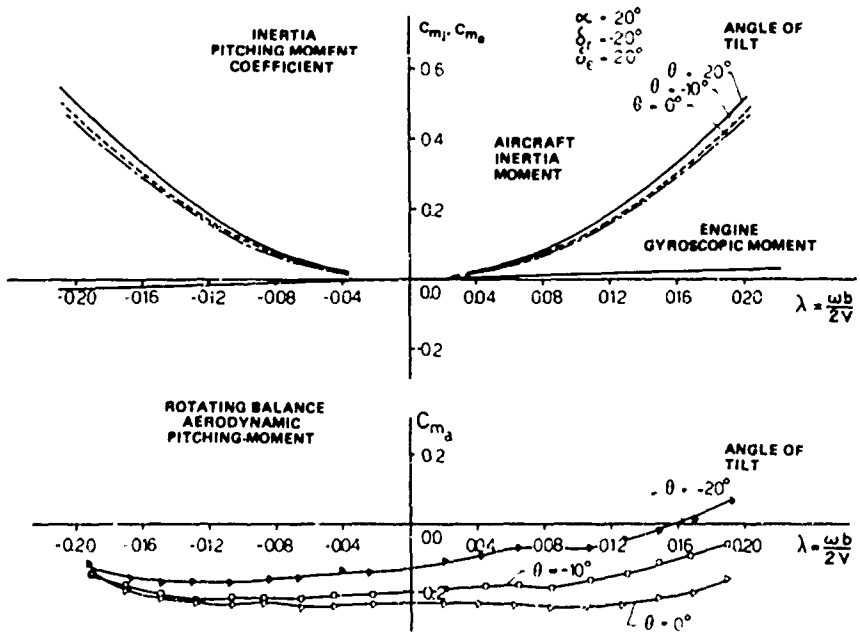

FIGURE 15 LONGITUDINAL (PITCHING) MOMENT COEFFICIENTS

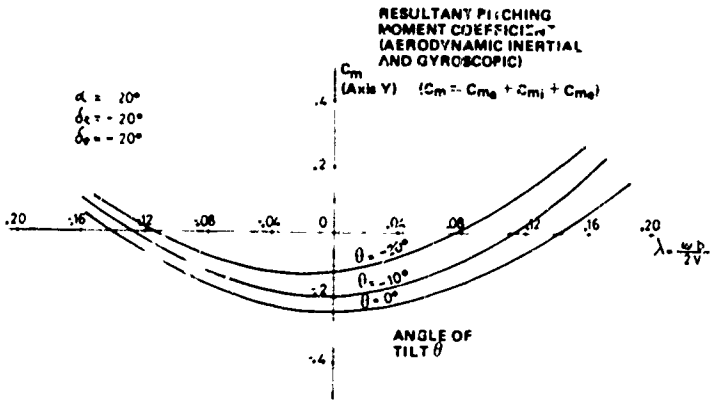

FIGURE 16. RESULTANT PITCHING MOMENT COEFFICIENT

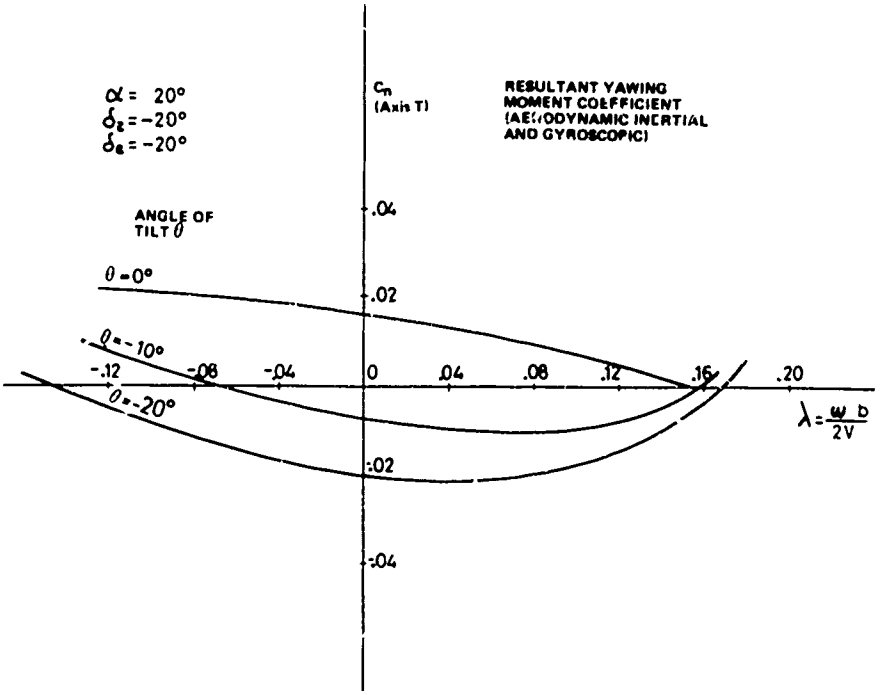

FIGURE 17. RESULTANT YAWING MOMENT COEFFICIENT

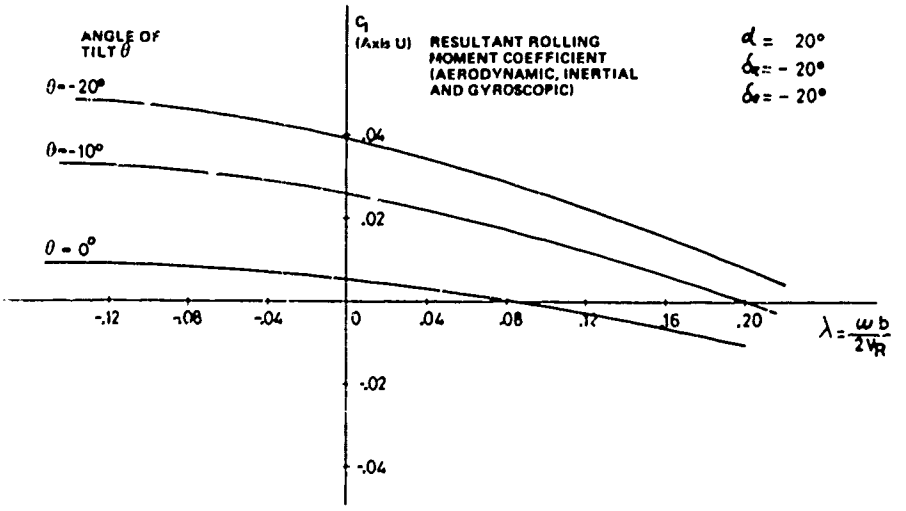

FIGURE 18 RESULTANT ROLLING MOMENT COEFFICIENT

10. CONCLUSIONS

The purpose of this paper is to provide information on testing methods and equipment that can provide some specific results not readily achievable with other methods

Even considering the significant influences of the scale effects, it is believed that the test methods described are a valid source for the design of a modern aircraft.

Especially in the non-linearity ranges of the aerodynamic phenomena, wind tunnel testing is practically the most effective means of analysis and the described investigation methods permit an enlargement of the research areas.

In particular the analytical study of the spin, made possible by the obtainment of otherwise unmeasurable aerodynamic coefficients, permits an evaluation of the influence of the many factors that affect the complex phenomenon of the spin. Vertical wind tunnel and model free-flight test provide synthetic information which do not allow the separate evaluation of the influences of each design parameter.

Up to date at Aeronautica Macchi almost 3000 runs have been carried out with rotating balances in connection with different projects as listed below:

Aermacchi MB-326 and MB-339	600
Aermacchi AM3 and C4	300
Aermacchi various projects	200
Aeritalia G-222	450
Panavia MRCA	1300
Embraer EMB120	30

11. ACKNOWLEDGEMENTS

I wish to thank and acknowledge the help of my assistants; in particular Mr. Sergio Comoretto, responsible for wind tunnel tests and Mr. Renato Caula responsible for flight test analysis.

I am also grateful to Aeronautica Macchi for the permission granted to present this paper.

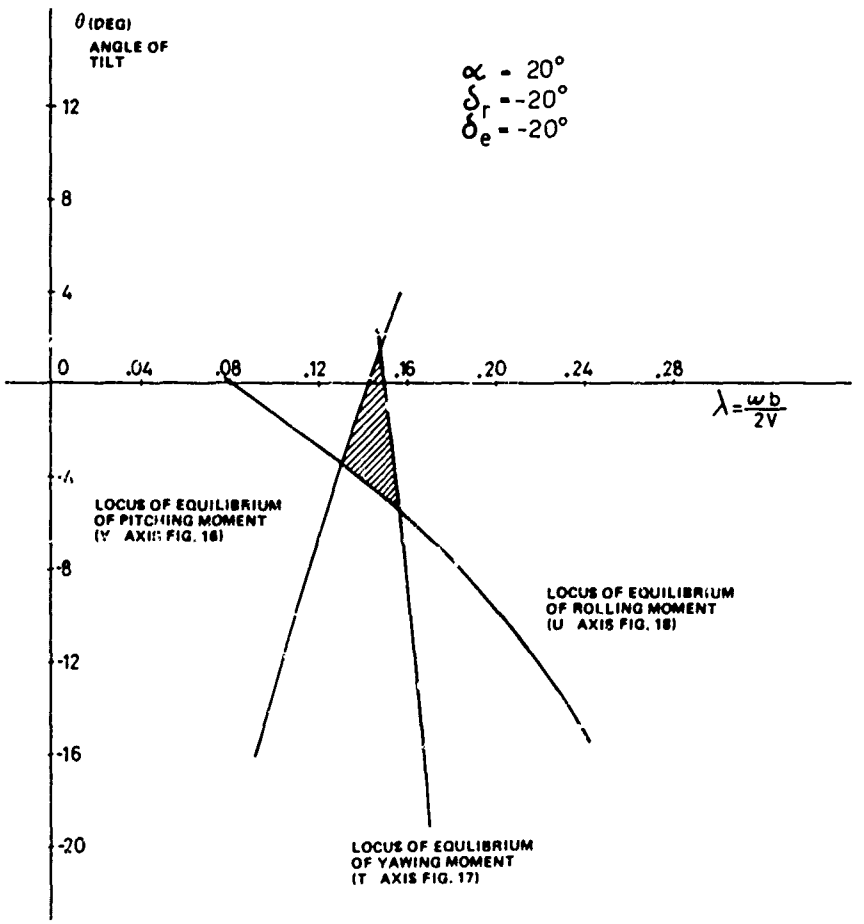

FIGURE 19. SPIN EQUILIBRIUM BOUNDARY

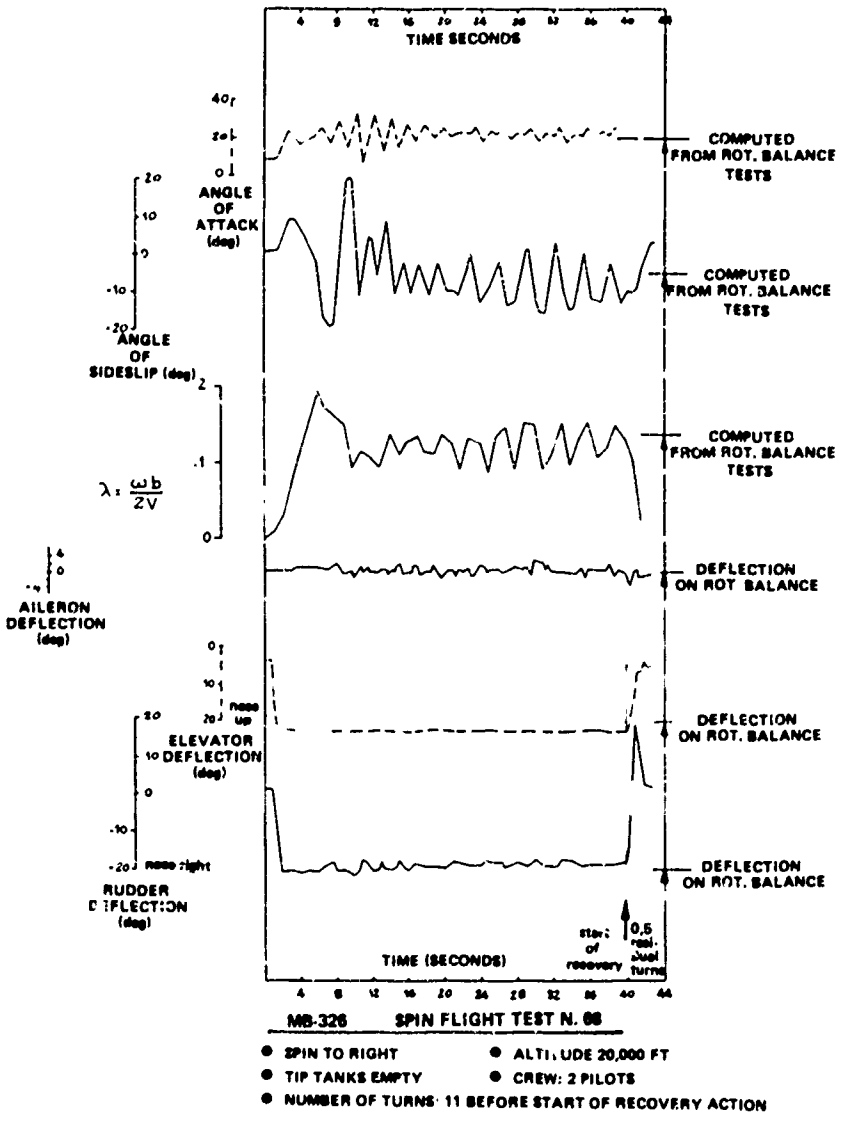

FIGURE 20. TIME HISTORY OF SPIN

12. REFERENCES

1. Allwork, P.H.. Continuous rotation balance for measurements of yawing and rolling moments in a spin. A.R.C. R & M 1579, 1934.
2. Anglin, Ernie L., Scher, Stanley H.. Analytical study of aircraft-developed spins and determination of moments required for satisfactory spin recovery. NASA TN D-2181, 1964.
3. Bazzocchi, Ermanno. Etude analytique de la vrille en utilisant des données à la soufflerie horizontale et methode d'essai des modèles à l'air libre. Proceedings of the Second European Aeronautical Congress, Scheveningen, 1956.
4. Determination of the spinning characteristics of Macchi MB-326H aircraft. Royal Australian Air Force, Aircraft Research & Development Unit, Report No. TS 1956, 1971.
5. Philips, W.H.: Effect of steady rolling on longitudinal and directional stability. NACA TN No. 1627, 1948.
6. Stone, R.W., Klinar W.J.. The influence of very heavy fuselage mass loadings and long nose lengths upon oscillations in the spin. NACA TN No. 1510, 1948.
7. Bowman, J.S Free spinning tunnel investigation of gyroscopic effects of jet-engine rotating parts (or of rotating propellers) on spin and spin recovery. NACA TN 3480, 1955.
8. Klinar, W.J. Spinning and related problems at high angles of attack for high speed airplanes. NACA RM L55L23a, 1956.
9. Marx, A.J.. Some results of comparison of model and full scale spinning tests. AGARD Report 26, 1956.
10. Gough, M.N. Notes on correlation of model and full-scale spin and recovery characteristics. AGARD Report 27, 1956.
11. Dennis, D.R. Model spinning tests on a jet trainer (Macchi MB 326) R.A.E., Farnborough, Tech. Note Aero 2489, 1956.

12. Neihouse, A.I. et al: Status of spin research for recent airplane design. NASA TR R-57, 1960.

13. Granthan, W.D., Grafton S.B.. Effects of aircraft relative density on spin and recovery characteristics of some current configurations. NASA TN D-2243, 1965.

14. Chambers, J.R. Bowman J.S., Anglin E.L.: Analysis of the flat-spin characteristics of a twin-jet swept-wing fighter airplane. NASA TN D-5409, 1969.

15. Casteel, G.R., Weyl, C.J.: A design approach to provide satisfactory spin characteristics for a modern fighter aircraft. AIAA Paper No. 70-928, 1970.

16. Reparto Sperimentale di Volo, Aeronautica Militare Italiana Velivolo MB-326: Studio sulle prove di vite. Relazione N. 28-1969.

17. Bowman, J.S.: Summary of spin technology as related to light general-aviation airplanes. NASA TN D-6575, 1971.

18. Weissman, R.: Preliminary criteria for predicting departure characteristics/spin susceptibility of fighter-type aircraft. J. of Aircraft, Vol. 10, No. 4, 1973.

19. Young, J.W.: Optional and suboptimal control technique for aircraft spin recovery. NASA TN D-7714, 1974.

20. Boyden, R.P.: Subsonic roll-damping characteristics of a series of wings. NASA TN D-7827, 1974.

21. Layton, G.P., NASA/Edwards FRC, USA: Experimental remotely-piloted research vehicles. AGARD F.M. Panel, Valloire/Modane, 1975.

22. Gobeltz, J.: I.M.F. Lille: Flight simulation with free models. AGARD F.M. Panel, Valloire/Modane, 1975.

23. Anonym: Stall/post-stall/spin flight test demonstration requirements for airplanes. USAF Military Specification MIL-S-83691, 1971.

STABILITY OF HELICOIDAL MOTIONS AT HIGH INCIDENCES

F.C. HAUS

Retired Professor at the Universities of
Ghent and Liège
Vice President of the Board of Directors
of the von Karman Institute for Fluid Dynamics

1. INTRODUCTION

Advances in experimental aerodynamics make it possible to obtain numerical values of aerodynamic coefficients as functions of the state variables of aircraft motion. This is even true for high angles of incidence.

It is possible in the present state of the art, to find mathematical solutions of three kinds of problems :

1°) To compute the equilibrium condition of steady motion, when the aircraft follows a helicoidal descending path around a vertical axis ;
2°) To establish the linear equations governing perturbations about the steady state, and to determine the characteristic modes of the resulting motion ;
3°) To integrate, in the most general case, the non-linear equations of motion and to determine the manner in which an aircraft can reach a steady state motion, or depart from it - (entry into or recovery from a spin).

Such mathematical operations provide insight into the mechanics of spinnning motion even though aerodynamic coefficients are not known very accurately at the present time.

2. COEFFICIENTS

The aerodynamic coefficients used in this report have been obtained from NASA TN.D.6670 for Aircraft C, and from TN HSA 137 of the Australian Defense Scientific Service for an aircraft referred to here as Aircraft Au, which is in fact similar to the Mirage. (See Appendix 2 and Ref. 1 & 2).

They provide mathematical models of the aircraft. Such models consist of a number of coefficients of the type :

$$C_i \ (\alpha,\beta,p^x,q^x,r^x,\delta_a,\delta_e,\delta_r) \quad \text{for } i = X,Y,Z,l,m,n.$$

(The control settings $\delta_a,\delta_e,\delta_r$ are represented by $\delta_l,\delta_m,\delta_n$ if ISO symbols are used).

In the simplest model each coefficient C_i may be represented by the series expansion :

$$C_i \ (\alpha,o,o,o,o,o,o,o) + \frac{\partial C_i}{\partial \beta}\ \beta + \frac{\partial C_i}{\partial p^x}\ p^x + \ldots\ldots + \frac{\partial C_i}{\partial \delta_a}\ \delta_a + \ldots\ldots$$

the function C_i and all its derivatives being non-linear functions of α.

Such coefficients form the mathematical models of Aircraft C and Aircraft Au1.

The data given in the Australian report allow us to define a more complicated model, characterising Aircraft Au2, where the C_i are :

$$C_i\ (\alpha,\beta,o,o,o,o,o,o) + \frac{\partial C_i}{\partial p^x}\ p^x + \ldots + \frac{\partial C_i}{\partial \delta_a}\ \delta_a + \ldots$$

which implies a non-symmetrical flow around the aircraft, as $C_i\ (\alpha,\beta,o,o,o,o,o,o)$ may be non-zero when β equals zero.

3. GEOMETRICAL AND INERTIAL DATA

The numerical data concerning both aircrafts are extracted from the previously quoted reports. During the research, it was also useful to consider the model of a "Synthetic Aircraft" in which all the aerodynamic, geometric and inertial data are arithmetic means of the characteristics of aircraft C and aircraft Au1.

4. PATH AND COORDINATES

The path followed in steady state motion is a helix described on a vertical cylinder of radius R, with an angular velocity Ω and a vertical velocity W. The slope of the trajectory is γ. The trajectories corresponding to a non-steady state do not satisfy this condition. (Fig. 1)

The set of body axes x,y,z is assumed to coincide with the principal inertial axes. Their position in space is defined by 3 rotations, starting from an arbitrarily chosen initial position. Two different conventions have been used :

First Convention

The set of body axes is referred to an initial set, such that :

x_h is horizontal and tangential to the considered cylinder

y_h is directed along the radius R (for a right hand spin)

z_h is vertical

The angular displacements necessary to rotate the axes from their initial to their final position, are the classical angles ψ,θ,ϕ.

Second Convention

The body axes are referred to an initial set of axes, where :

x_o is the direction of the resultant velocity V

$V = W^2 + \Omega^2 R^2$

y_o is in the direction of the normal

z_o is in the direction of the binormal

The rotations are made in the following sequence :

ν around axis x_o

β around the intermediate position of axis z

α around the final position of axis y

The relations between the two series of coordinates have been calculated and used when necessary.

5. EQUATIONS OF MOTION

The 6 classical equations of motion are used. They take different forms, according to which of the problems previously referred to is considered.

In the case of equilibrium, the time derivatives are zero and the equations reduce to an algebraical system.

The equilibrium equations, with the aircraft position defined by ψ,θ,ϕ have been solved by Adams. (Ref. 3). The same equations, with the aircraft position defined by ν,β,α are presented in Appendix 1. They are easy to solve.

In the study of the linear differential equations of motion, we have a system of 6 + 2 = 8 equations, with constant coefficients. The two last equations are only kinematical relations. In this part of the study, we prefer to represent the aircraft position by the angles ψ,θ,ϕ.

The study of the non-linear differential equations is nevertheless the main part of our work. The convention ψ,θ,ϕ is also used. The treatment of the equations consists always in a numerical integration using the Runge-Kutta method.

6. RESULTS OF CALCULATIONS

6.1. Determination of steady state motions

There are 6 equilibrium equations and 9 variables :

V,Ω,γ defining the trajectory

ν,α,β defining the aircraft position in relation to the trajectory

$\delta_a,\delta_e,\delta_r$ defining the setting of the 3 main controls

Manipulation of the throttle is not considered. The mathematical model refers always to only one position of the throttle (engine idle in our case).

It is imperative to chose arbitrarily 3 of the variables, in order to allow the calculation of the 6 others. The easiest way to resolve the equations is to choose the variables ν,α,β and to calculate the 6 remaining ones.

This gives us information as useful as if we had chosen the control settings $\delta_a,\delta_e,\delta_r$ and calculated the other variables.

This method of calculation allows us to determine trajectories of large radius (50 km) as well as to study trajectories with a radius < 10 m and even as low as 1 m.

The resolution of the algebraic equations shows that for each of the mathematical

models which were used there are many combinations of variables, each with realistic control settings, which satisfy equilibrium conditions in the spin. Graphs have been established which show the evolution of the state variables when one of the arbitrarily chosen parameters varies.

The values of the state variables which satisfy the equilibrium conditions are shown :

- for Airplane C, in the range $62° \leq \quad \leq 69°$
  with a constant elevator setting of -30° (Fig. 2)

- for Airplane Au1, in the range $67° \leq \quad \leq 85°$
  with a constant elevator setting of -20° (Fig. 3)

6.2. Linear Systems

We are concerned with 8th order systems which define the evolution in time of the perturbations of $V,\alpha,\beta,p,q,r,\theta,\phi$ around their equilibrium values.

The linearization process presented some unexpected difficulties. After some initial errors have been corrected, we found a set of coefficients which were in good agreement with the coefficients indicated in Ref. 3.

6.2.1. Eigen values and Eigen vectors

Linear equations provide eigen values and eigen vectors. Each combinaison of an eigen value and its corresponding eigen vector, defines a mode.

Let us first consider a set of trajectories described at the same incidence $\alpha = 30°$ and sideslip $\beta = 0°$ with decreasing ν.

The radius depends on the angle ν. Increasing ν means decreasing radius R. Root loci have been calculated when ν and R vary slowly. (Fig. 4)

For nearly rectilinear trajectories, the phugoid, short period longitudinal mode and Dutch Roll lateral mode, are clearly identified. In many cases, the 2 roots corresponding to roll and spiral motion are real, but in some cases, as on Fig. 5, these motions are replaced by a slow lateral oscillation. (called also lateral phugoid).

With decreasing radius, a new mode develops from either the longitudinal phugoid and the real roll and spiral roots, or the longitudinal phugoid and the slow lateral oscillation. The loci shown on Fig. 5 have been calculated for the synthetic model.

For real spins at large incidence, the equations indicate either
3 oscillatory short-period modes, together with
2 subsidences
or 4 oscillatory modes - three of short period and one with a very long period. The 3 short period modes are, in many cases, characterised by eigen values of the same order of magnitude.

Fig. 6 shows the root locus for Aircraft Au1 with α in the range 67-85 degrees, and with a constant elevator setting of -20 degrees. The rudder setting is unimportant as, in this particular mathematical model, the rudder does not produce any moment for the range of incidence considered.

It has been possible to identify the 3 curves. One is a continuation of the short period longitudinal root, another is the continuation of the Dutch Roll roct, while the third one refers to a mode which is the same as the 3rd mode identified in the preceeding figure.

At the incidence of 78° with δ_e = -20° and δ_a = 5,33°, the roots correspond to the following periods and damping.

	T	t1/2 *
Third root	3,69 sec	7,5 sec
Short period (incidence)	2,90	6,45
Dutch Roll	2,34	6,08

The Dutch Roll root becomes instable at α = 83°.

Inspection of the 3rd root shows that the imaginary part ω of its eigen value tends towards the angular velocity Ω of the spin, as the radius tends to zero. We call this mode the synchronous oscillation. If the system is reduced to the sixth order by suppressing the variables ϕ and θ, this last mode disappears while the other modes are maintained nearly unchanged. This suggests that the mode is due to the effect of changes in the components of the weight.

The investigation of linear systems has demonstrated the existence of a domain where the spins of Aircraft A1 are asymptotically stable whereas those of Aircraft C are unstable in all cases.

The intermediate mathematical model has been used to investigate the factors which contribute either to stability or instability.

The components of the eigen vectors indicate how the different state variables contribute to the different modes. When the radius decreases, it is no longer possible to separate the longitudinal and lateral modes. Each mode consists of a mixture of longitudinal and lateral components.

We think the linear study can contribute to the understanding of some results obtained by the integration of the non-linear equations.

6.2.2. Time Histories

The integration of the linear equations has been performed on an analogue computer. The results are, of course, only valid for small initial perturbations or small changes in the control settings.

The curves show the existence of beats due to superposition of modes with nearly the same period. Fig. 7 shows the time history after a perturbation in side slip.

---

*t1/2 = time to damp to half amplitude.

6.3. Integration of non-linear equations

We report here only the results obtained with mathematical models Au1 and Au2.

Some of the calculations have been made independently using respectively a digital and a hybrid computer operated by different people. (digital computer at the VKI, hybrid computer at the University of Ghent).

The results were essentially the same but there was a tendency for the hybrid solution to show less well damped oscillations.

The results shown on Fig. 8 to 10 are obtained by digital computation.

The air density ρ has been assumed constant. It would of course be possible to calculate the altitude h by integration of the vertical velocity, and to consider ρ as a function of h. However, our main purpose being to find an explanation of the mechanical properties of the spin, this refinement has not seemed necessary.

The spins are spins to the right, unless otherwise indicated.

The following calculations have been made using model Au1.

6.3.1. Excitation of a single mode

A. Starting from a stable spin, the system is excited by a set of initial perturbations which correspond to the components of the eigen vector of each of the modes as defined by the linear system.

Fig. 8 shows the free oscillations following such perturbations. Inspection of the curves shows clearly the relative amplitudes of θ, α, $\emptyset$, β for the different modes.

B. Starting from a stable spin, the system is excited by a harmonic motion of one of the controls (either aileron or elevator) the frequency being the eigen frequency of one of the modes.

If this is done successively, using the frequencies of the 3 oscillatory modes, a synchronized harmonic response is invariably obtained, but the amplitudes of the variables are different in each case, for the same excitation amplitude.

Fig. 9 shows the comparative amplitudes of the state variables when the elevator provides a harmonic excitation of $\pm$ 3° around -20°. The same computations have been made with harmonic motion of the ailerons.

6.3.2. Excitation of multiple modes

A. Starting from initial conditions, chosen arbitrarily but however not too far from a spin, the controls are given settings which correspond to those of a spin. If the spin is stable, the calculations converge to the steady state. This procedure has been used to verify the results provided by the algebraic equations in the case of stable spins.

B. Starting from a stable spin, a step input is given to the setting of one control.

During a spin at α = 78°, with the following control settings

δ_e = -20° $\qquad$ δ_a = +5,33°

one of the control settings is changed.

a)

δ_a remaining +5,33°, the stick is pushed forward, δ_e becoming 0°.

The characteristics of the spin are gently modified as indicated on Fig. 10. The final motion is a stable spin.

The modes characterising this final state have the following periods and damping.

	T	t1/2
Third root	3,14 sec	7,09 sec
Incidence	2,63	5,00
Dutch Roll	2,29	10,12

More than one mode is excited by the change of elevator setting. Beats are identified in the response of some variables.

b)

δ_e remaining -20°, the aileron setting becomes δ_a = +3°.

Here also, the final motion is a stable spin. The transition from one to the other is smooth.

c) The elevator setting δ_e = -20° is maintained but the aileron setting is inverted. δ_a becomes -5,33° instead of +5,33°.

Although such a setting is compatible with a stable spin in the opposite sense, the computations do not predict reversal of the direction of spin. They show that the final motion is a gyration at moderate incidence.

This problem is one of those which have been solved in two different ways. Fig. 11 where V, α, β are replaced by u, v, w, shows that there is good agreement between the digital and the hybrid computer.

6.3.3. Entry into a spin

Starting from rectilinear flight conditions at low incidence, the controls are set to the positions corresponding to a stable spin.

A. Mathematical Model Au1

The computer shows that such an aircraft would not enter into a spin, but would describe a path called post-stall gyration.

On the other hand, the calculations converge to the steady spin if, at the beginning of the motion, the rudder setting is temporarily increased above that corresponding to the equilibrium state. Careful inspection of the results indicates the mechanical reason for this behaviour.

B. Mathematical Model Au2

In the case of Aircraft Au2, the calculations show that the aircraft goes into a left hand spin if the control settings corresponding to such a steady spin are applied

while flying straight and level at low incidence. (This result has also been obtained in Australia and in Lille).

The aircraft having the same mathematical model will not enter a right hand spin, if equal but opposite control settings are applied.

7. FINAL REMARKS

7.1. Definition of the Mathematical Model

The scientist making use of a Mathematical Model is bound to accept the model as it is provided by the aerodynamicist. He is not always in a situation to evaluate its validity.

Derivatives obtained with rotating balances seem more suitable than derivatives obtained from oscillatory tests.

7.2. Symmetrical and non-symmetrical models

The important difference between the motions computed using symmetrical models and slightly unsymmetrical models, shows the importance of unexpected non-symmetrical flows.

7.3. Conclusions reached with symmetrical models

7.3.1. Steady State

When the aircraft is assumed to be symmetrical, it is easy to determine the combinations of control settings which satisfy the equilibrium conditions.

7.3.2. Linear theory of motion

The modes defining the evolution of perturbations around a steady state spin may be stable or unstable, as indicated by classical linear methods.

In our calculations, instability in the spin has been found to affect the incidence oscillation, the Dutch Roll oscillation or one of the subsidences.

No case of unstable "synchronous oscillation" has been found, but it should be noted that a very limited number of cases have been studied.

The synchronous oscillation seems to be a characteristic of spinning motion. It may depend on the position of the axis of the cylinder on which the path described by the aircraft center of gravity lies.

Inclination of the cylinder axis to the vertical may be at the origin of the oscillation.

7.3.3. Integration of the non-linear equations

Integration of the non-linear equations of aircraft motion at large incidence was first performed more than ten years ago. Some of the results presented here show that when the input is such as to energize only one mode of the lienar equations, the

the non-linear system reacts in the same way as the linear system.

The linear modes appear clearly in the non-linear solutions.

7.3.4. Where Research is needed

A. Up to the present time, it has not been possible to determine the physical causes of the stability or instability of the modes for configurations situated at the boundary between stable and unstable spins.

Calculations were primarily considered as a test to determine if all the roots are negative, rather than providing an explanation of the facts. A discussion of stability conditions should be undertaken.

B. Studies with the aim of relating the occurence of a spin, or the case of stopping a spin - with one or other characteristic of a non-linear mathematical model have been made in the U.S. (Ref. 4 to 7)

Perhaps it would be rewarding to try to correlate the spin entry or recovery with the stability or instability of the linearized equations.

ACKNOWLEDGEMENT

The author is very grateful to MM. J.C. CATALA and F. DE SCHUTTER for their help in performing the computations.

During discussions, Professor P. HABETS contributed to clarify some points.

Professor VAN STEENKISTE allowed the author the use of a hybrid computer at the University of Ghent.

Professor SANDFORD was kind enough to correct the English redaction.

REFERENCES

1. W.P. GIBERT and C.E. LIBBEY
Investigation for an automatic spin prevention system.
NASA - TN D 6670

2. R. WILSON
Analytical investigation of spinning behaviour and recovery using a high speed digital computer.
Australian Defense Scientific Service
TN HSA 137

3. W.M. ADAMS, Jr.
Analytical prediction of airplane equilibrium spin characteristics.
NASA - TN D 6926

4. J.W. YOUNG and W.M. ADAMS, Jr.
Analytical prediction of aircraft spin characteristics and analysis of spin recovery.
AIAA Paper N° 72-985

5. W. BIHRLE, Jr.
Influence of the static and dynamic characteristics of the spinning motion of aircraft.
Journal of Aircraft, Vol. 8 - N° 10

6. R. WEISSMAN
Criteria for predicting spin susceptibility of fighter type aircraft.
Technical Report ASD-TR-72-48

7. E.L. ANGLIN
Analytical study of effects of product of inertia on airplane spin entries, developed spins and spin recoveries.
NASA - TN D-2754

8. G. VAN STEENKISTE and F. HAUS
Analysis of aircraft developed spins by digital computations using analogue subroutine.
Symposium on Hybrid Computation in Dynamic Systems Design.
Rome, November 1974.

APPENDIX 1

SOLUTION OF THE EQUATION OF MOTION FOR A STEADY SPIN

I. Data

The aircraft is defined by the following quantities :

$\bar{l}$, S, r_x, r_y, r_z, μ

where $\bar{l}$ is an arbitrary reference length

$$\mu = \frac{2m}{S\bar{l}\rho}$$

The coefficients C_i are expressed in terms of a reference area S and the same reference length $\bar{l}$.

The equilibrium conditions for translational motion are :

$$j_x = \frac{V^2}{\mu\bar{l}} C_x + g_x \qquad \text{where} \qquad j_x = qw - rv$$

$$j_y = \frac{V^2}{\mu\bar{l}} C_y + g_y \qquad \text{where} \qquad j_y = ru - pw$$

$$j_z = \frac{V^2}{\mu\bar{l}} C_z + g_z \qquad \text{where} \qquad j_z = pv - qu$$

p, q, r, being components of Ω

The equilibrium conditions for rotational motion are :

$$(r_z^2 - r_y^2)\, qr = \frac{V^2}{\mu} C_l$$

$$(r_x^2 - r_z^2)\, rp = \frac{V^2}{\mu} C_m$$

$$(r_y^2 - r_x^2)\, pq = \frac{V^2}{\mu} C_n$$

Vector j is horizontal.
Vectors g and Ω are vertical.
Their components, relative to the aircraft axes, must be computed.

II. Angular Transformation

The orientation of the aircraft in space is defined by the rotations ν, $-\beta$, α.

The convenience of this system of angular transformations is due to the fact that it uses the angles α and β which determine the magnitude of the aerodynamic forces and moments.

The corresponding transformation matrix is :

$$A = \begin{bmatrix} a & h & b \\ c & k & d \\ e & l & f \end{bmatrix}$$

where

$a = \cos\alpha \cos\beta$

$b = -\cos\alpha \sin\beta \sin\nu - \sin\alpha \cos\nu$

$c = \sin\beta$

$d = \cos\beta \sin\nu$

$e = \sin\alpha \cos\beta$

$f = -\sin\alpha \sin\beta \sin\nu + \cos\alpha \cos\nu$

$h = -\cos\alpha \sin\beta \cos\nu + \sin\alpha \sin\nu$

$k = \cos\beta \cos\nu$

$l = -\sin\alpha \sin\beta \cos\nu - \cos\alpha \sin\nu$

It enables us to find the components of a vector with respect to the aircraft body axes x,y,z, when its components with respect to x_o, y_o, z_o, are known.

In particular, the components of a horizontal vector representing the acceleration are :

$$\frac{j_x}{j} = h$$

$$\frac{j_y}{j} = k$$

$$\frac{j_z}{j} = l$$

Let η be the angle between the resultant velocity vector and the horizontal plane, considered to be positive for descending flight. (In fact, $\eta = -\gamma$)

The acceleration is given by :

$$j = \Omega V \cos\eta$$

The components of the vertical vectors are :

$$\frac{g_x}{g} = \frac{p}{\Omega} = a \sin\eta + b \cos\eta$$

$$\frac{g_y}{g} = \frac{q}{\Omega} = c \sin\eta + d \cos\eta$$

$$\frac{g_z}{g} = \frac{r}{\Omega} = e \sin\eta + f \cos\eta$$

<u>New Formulation of the Equations</u>

From the preceeding remarks, it follows that the 6 equations of steady motion may be written :

$$\Omega V h \cos\eta = \frac{V^2}{\mu l} C_x + g(a \sin\eta + b \cos\eta)$$

$$\Omega V k \cos\eta = \frac{V^2}{\mu \bar{l}} C_y + g(c \sin\eta + d \cos\eta)$$

$$\Omega V l \cos\eta = \frac{V^2}{\mu \bar{l}} C_z + g(e \sin\eta + f \cos\eta)$$

$$(r_z^2 - r_y^2)\,\Omega^2 (c \sin\eta + d \cos\eta)(e \sin\eta + f \cos\eta) = \frac{V^2}{\mu} C_l$$

$$(r_x^2 - r_z^2)\,\Omega^2 (e \sin\eta + f \cos\eta)(a \sin\eta + b \cos\eta) = \frac{V^2}{\mu} C_m$$

$$(r_y^2 - r_x^2)\,\Omega^2 (a \sin\eta + b \cos\eta)(c \sin\eta + d \cos\eta) = \frac{V^2}{\mu} C_n$$

The aerodynamic coefficients depend non linearly on α and β, and linearly on δ_a δ_e δ_r. The moments coefficients depend also on p^* q^* r^*.

$$p^* = \frac{p\bar{l}}{V} = \frac{\Omega}{V} \bar{l} (a \sin\eta + b \cos\eta)$$

$$q^* = \frac{q\bar{l}}{V} = \frac{\Omega}{V} \bar{l} (c \sin\eta + d \cos\eta)$$

$$r^* = \frac{r\bar{l}}{V} = \frac{\Omega}{V} \bar{l} (e \sin\eta + f \cos\eta)$$

The set of equations can be solved only if 3 variables are arbitrarily chosen. The computation is very straightforward if v, β, α, are so chosen, and the equations solved for

$$\begin{matrix} V & \Omega & \eta \\ \delta_a & \delta_e & \delta_r \end{matrix}$$

A particular case which occurs for Aircraft Au1 is that in which $C_{l\delta r}$ and $C_{n\delta r}$ are zero. There are then too many equations, and the computation must proceed differently by determining the values of δ_a which satisfy separately the rolling and yachting equations. The solution sought is then that for which the independently calculated values of δ_a are equal.

APPENDIX 2

The Aerodynamic characteristics of model Au1 are shown on Fig. 12.

The numerical values of the moment coefficients, extracted from Ref. 2, are based on 4 different reference lengths :

$$c, b, \frac{c}{2}, \frac{b}{2}$$

As we used, in our computations, only one reference length $\bar{l} = b$, these coefficients were converted before being introduced in the equations.

The C_y, C_l, C_n coefficients of model Au2 are shown on figures 13,14,15, extracted from Ref. 2.

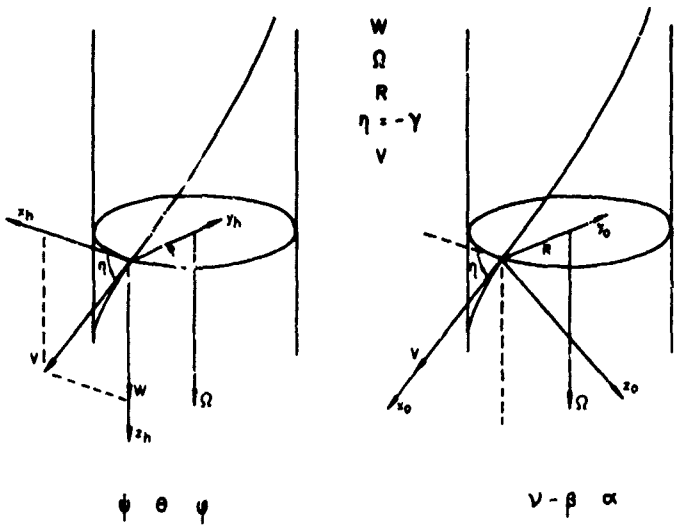

FIG 1

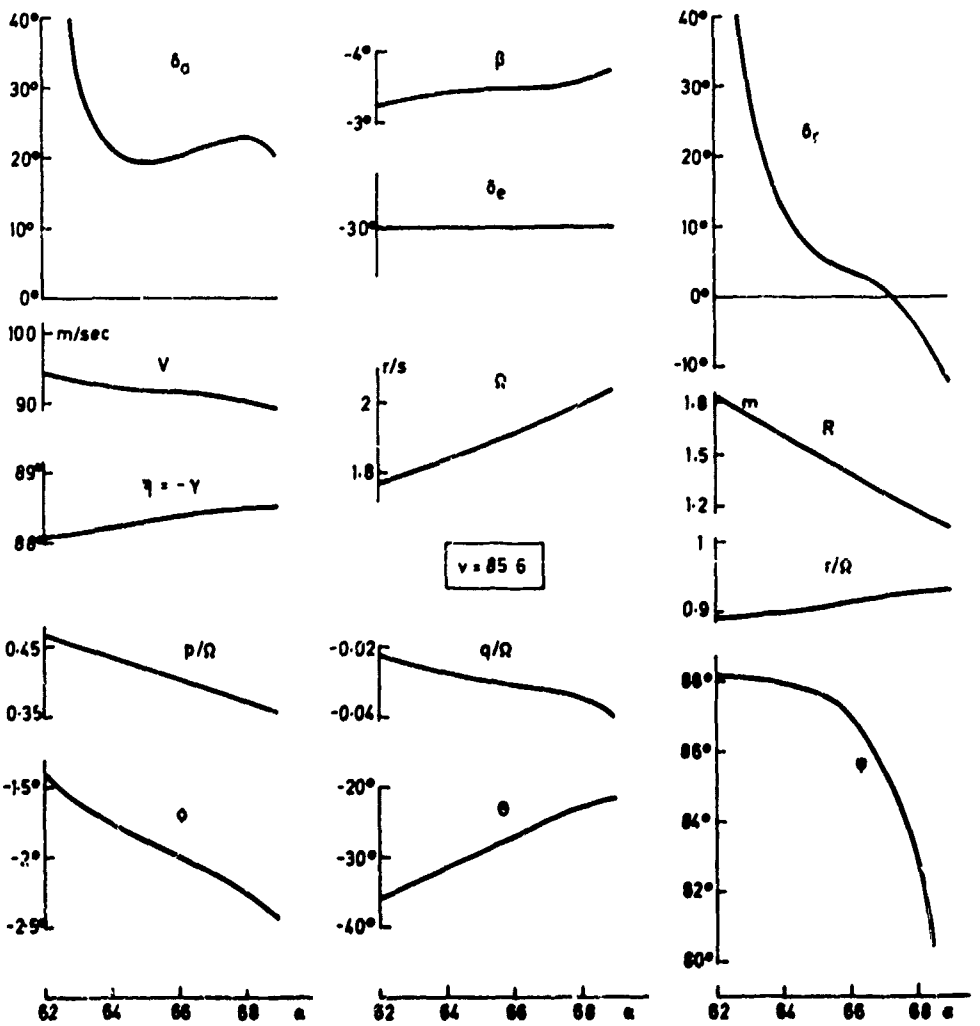

FIG. 2

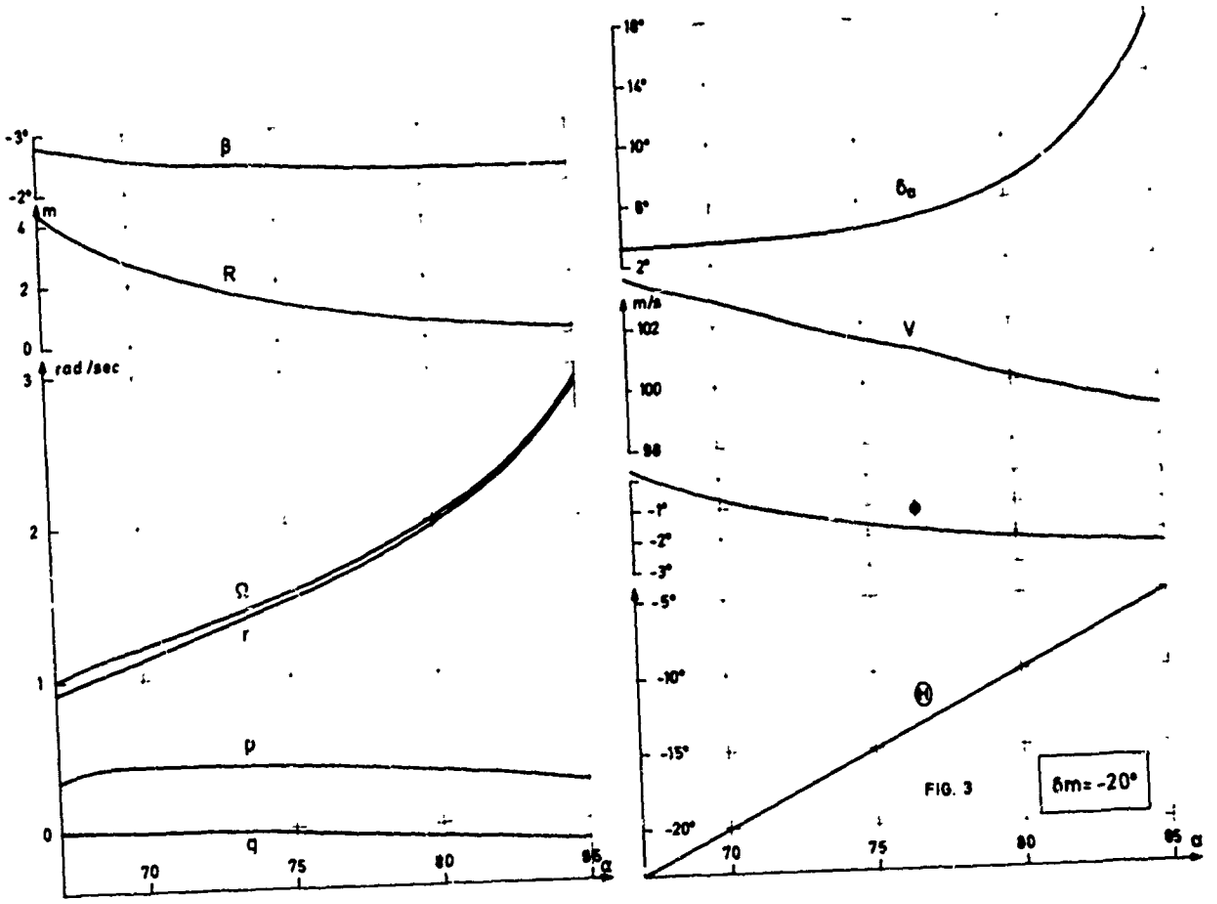

FIG. 3

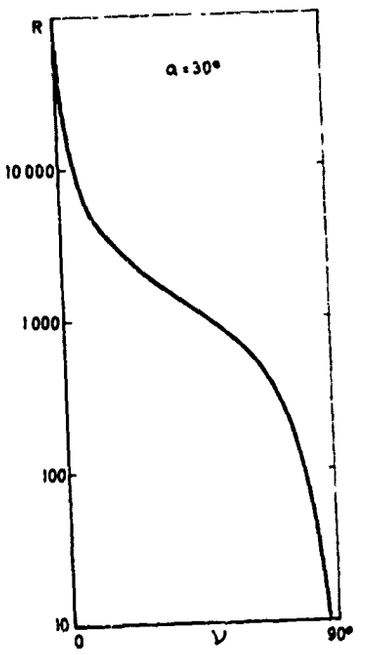

FIG 4

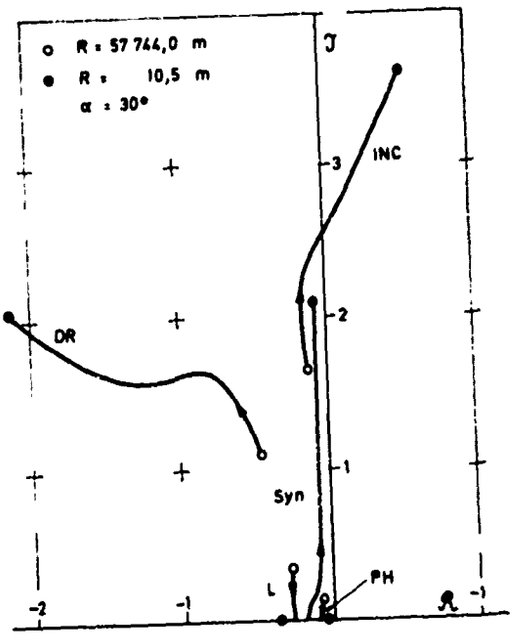

FIG 5

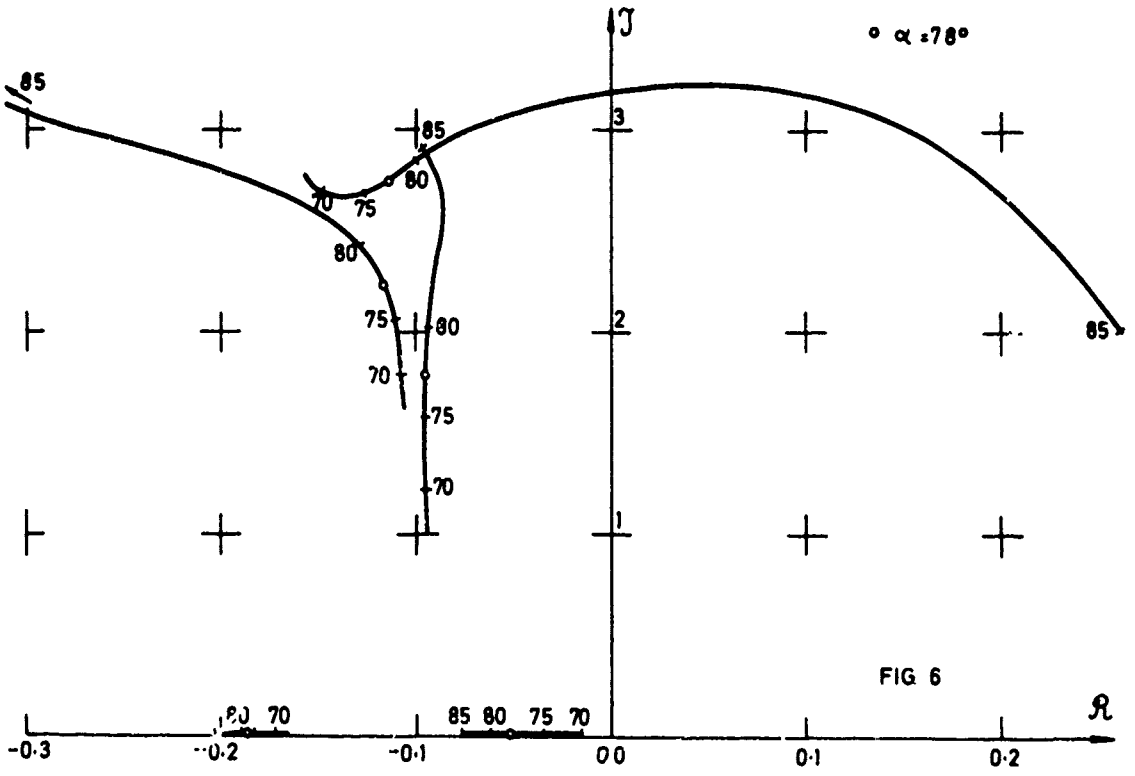
ℑ
∘ α =78°
85
85
80
75
70
80
75
80
70
75
70
3
2
1
85
FIG 6
ℜ
80 75 70
85 80 75 70
-0·3
-0·2
-0·1
0 0
0·1
0·2

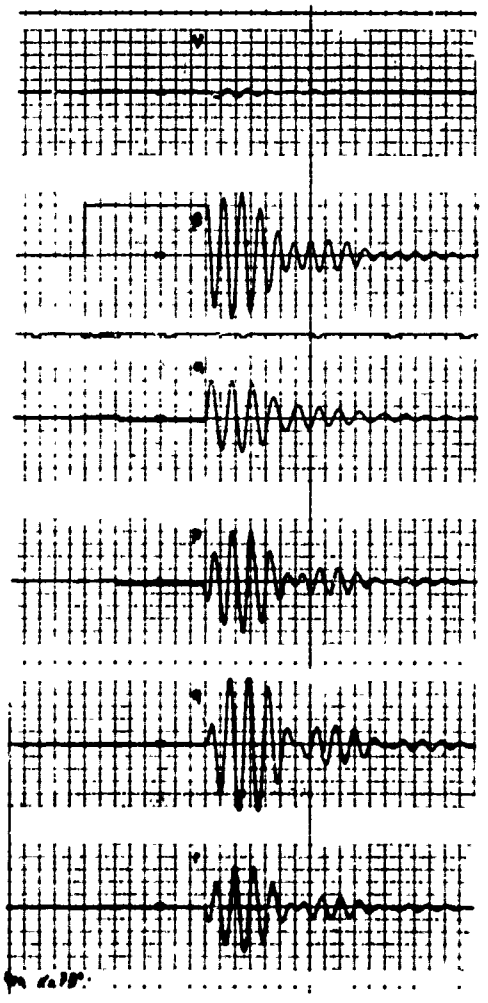

FIG.7

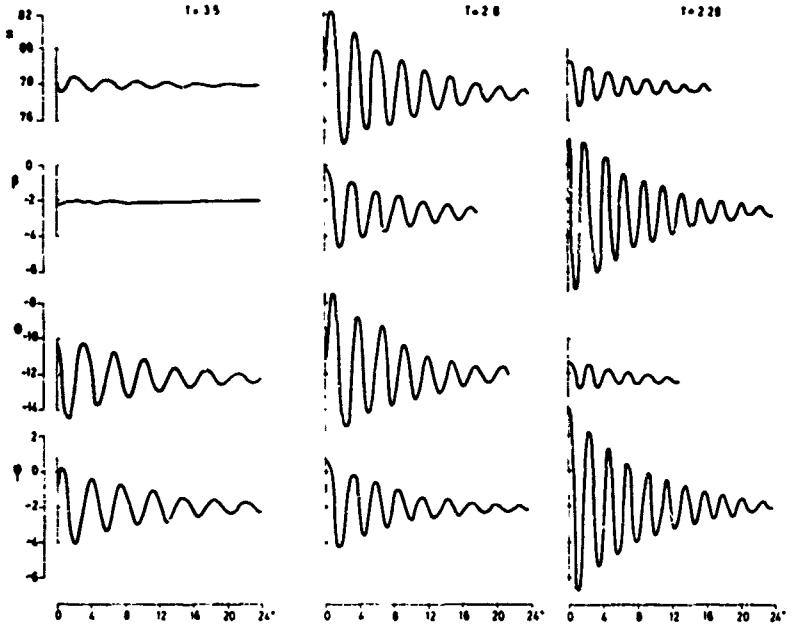

FIG. 8

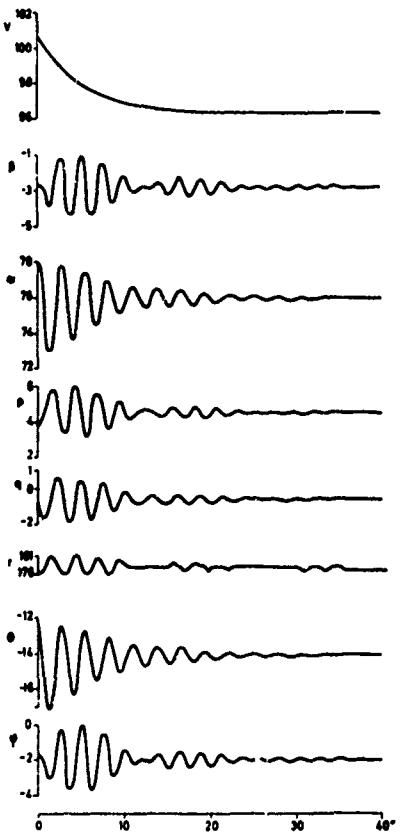

FIG.10

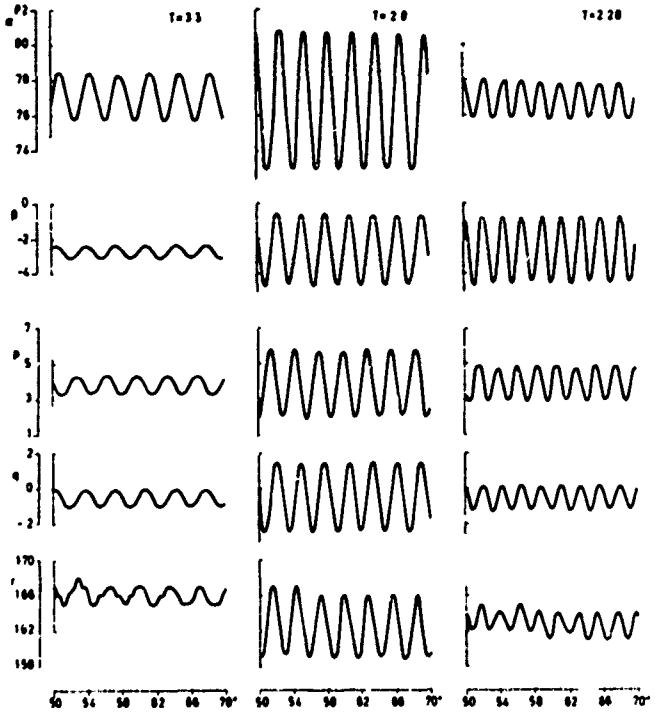

FIG. 9

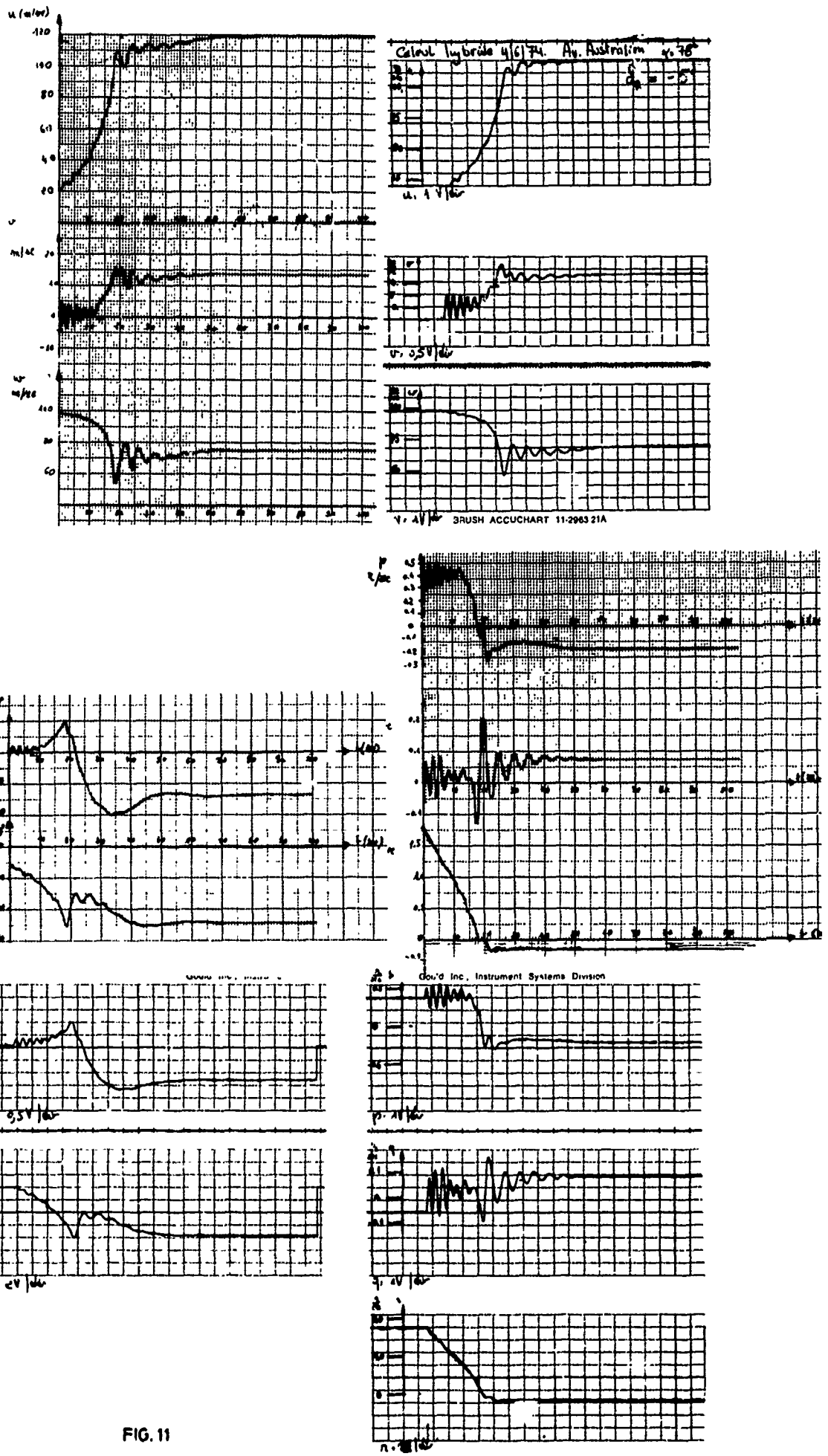
Calcul hybride 4/6/74. Av. Australien
BRUSH ACCUCHART 11-2963 21A
Gould Inc., Instrument Systems Division

FIG. 11

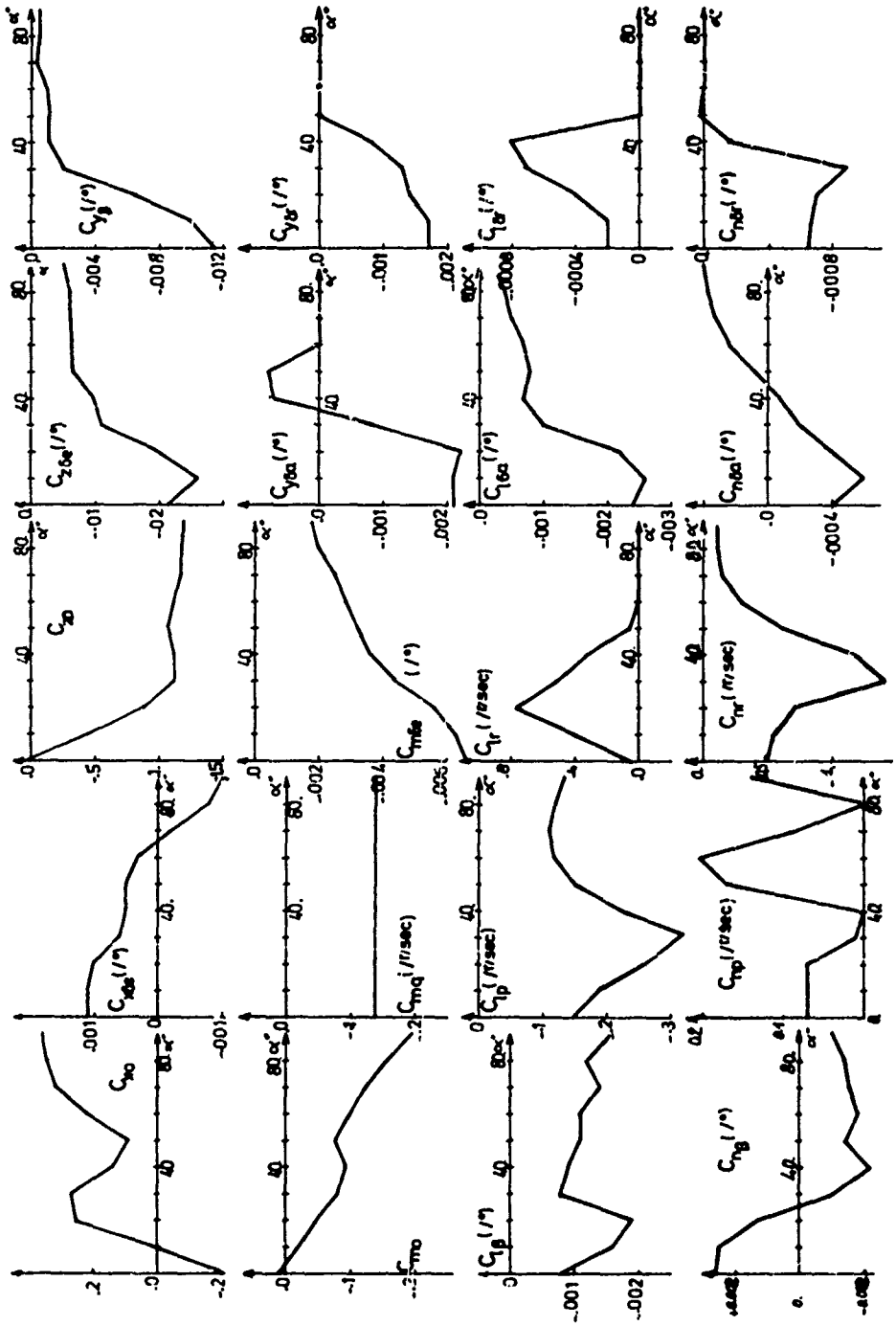

FIG. 12

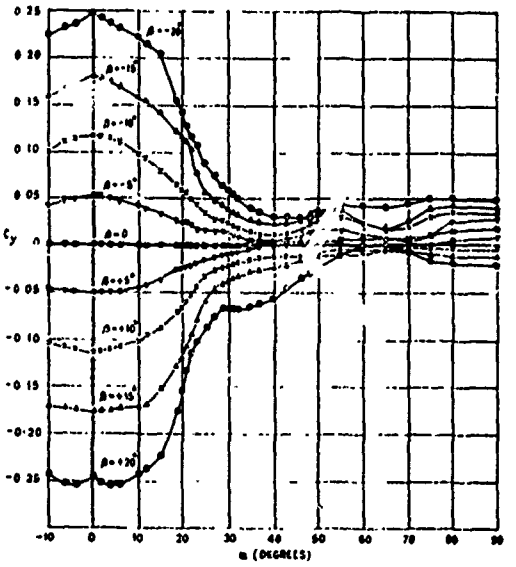

FIG. 13a - Side force coefficient

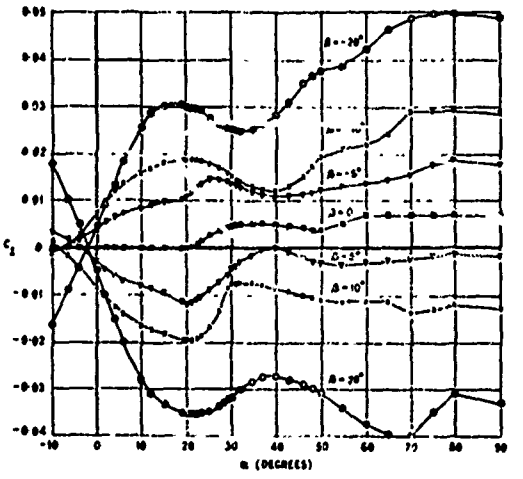

FIG. 13b - Rolling moment coefficient

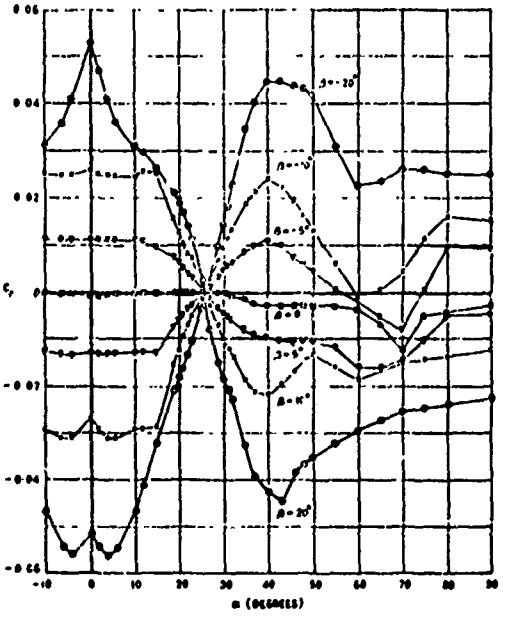

FIG. 13c - Yawing moment coefficient

EVOLUTION DES CARACTERISTIQUES DE LA VRILLE EN FONCTION DE L'ARCHITECTURE DES AVIONS

par Jean Gobeltz
Directeur technique
Institut de Mécenique des Fluides de Lille
5,bd Paul Painlevé, 59000 - LILLE (France)

TABLE DES MATIERES

1 - Introduction
2 - La vrille en fonction des époques
- 2.1 - Avions lents à hélice
- 2.2 - Avions rapides à hélice
- 2.3 - Premiers avions à réaction
- 2.4 - Accroissement de la flèche des avions à réaction
- 2.5 - Allongement, vers l'avant, du fuselage des avions à réaction
- 2.6 - Remarque

3 - Action des diverses variables - Résultats généraux
- 3.1 - Présentation du chapitre
- 3.2 - Effet des surfaces mobiles
  - 3.2.1 - La direction
  - 3.2.2 - La profondeur
  - 3.2.3 - Le gauchissement
  - 3.2.4 - Les volets hypersustentateurs
  - 3.2.5 - Les becs
  - 3.2.6 - Les aérofreins
  - 3.2.7 - Les trappes
- 3.3 - Effet de surfaces complémentaires
  - 3.3.1 - Quilles
  - 3.3.2 - Virures
- 3.4 - Effet des formes géométriques générales
  - 3.4.1 - Voilure - Flèche
  - 3.4.2 - Voilure - Autres caractéristiques
  - 3.4.3 - Fuselage - Longueur
  - 3.4.4 - Fuselage - Forme de la section
  - 3.4.5 - Les empennages horizontaux
  - 3.4.6 - L'empennage vertical
- 3.5 - Les caractéristiques d'inertie
  - 3.5.1 - La masse
  - 3.5.2 - Le centrage
  - 3.5.3 - Les moments d'inertie
- 3.6 - Les charges extérieures
  - 3.6.1 - Effet selon les positions
  - 3.6.2 - Les masses
  - 3.6.3 - Les encombrements géométriques
- 3.7 - Le contrôle des agitations
- 3.8 - Le contrôle des vrilles plates
  - 3.8.1 - Vrilles plates et lentes
  - 3.8.2 - Vrilles plates et rapides
- 3.9 - Le vrille dos
- 3.10- Le parachute
- 3.11- Les fusées

4 -Ebauche d'étude de corrélation
- 4.1 - Présentation
- 4.2 - Résultats

5 - Modification des vrilles selon les versions d'un même avion
Exemples de limite d'emploi des résultats généraux
- 5.1 - Présentation du chapitre
- 5.2 - Mirages III Delta
  - 5.2.1 - Place relative des vrilles des Mirages III
  - 5.2.2 - Les vrilles des premières versions C et E
  - 5.2.3 - Les vrilles en vol des autres versions
  - 5.2.4 - Comparaison des vrilles des diverses versions
- 5.3 - Lightning

1 - INTRODUCTION.-

La communication est dans sa totalité relative à l'étude globale de la vrille ; le terme "étude globale" est ici utilisé en opposition avec le terme "étude analytique" réservé au traitement des équations de la mécanique du vol en vue de calculer la vrille. Le terme étude globale est employé indifféremment pour des études sur maquettes ou en grandeur réelle.

A chaque époque un sous-ensemble de l'ensemble complet des avions en conception correspond à des formules nouvelles ou tout au moins à des formules sensiblement différentes de celles dont elles sont l'extrapolation. Si l'on considère les vrilles de ce sous-ensemble on constate alors que leurs caractéristiques sont une fonction du temps. De là il faut conclure immédiatement que la vrille n'est pas tout à fait n'importe quoi, mais qu'elle a des caractéristiques liées à l'architecture des avions. Certes le nombre des variables déterminant la vrille est très grand, parfois même des variables ne devant avoir, à priori, que peu d'effet s'avèrent très actives ; il n'en reste pas moins que ceux qui ont l'occasion de suivre pendant des dizaines d'années le sujet en retirent des impressions générales.

Il en est ainsi pour l'équipe de l'I.M.F.L. qui est actuellement composée de quelques personnes ayant suivi le sujet de la vrille sans discontinuer depuis 1947. Son expérience s'étend ainsi sur toutes sortes d'avions depuis environ 30 ans. Cette équipe n'a, par contre, qu'une connaissance de seconde main sur les avions d'avant et de pendant la guerre 39-45. Mais les possibilités de l'homme en stockage et en tri sont très limitées, c'est pourquoi nous avons entrepris une étude de corrélation sur calculateur. Il est bien sûr loin de notre pensée de prétendre en tirer la définition de la vrille d'un avion futur. Une prévision avec le maximum de probabilité est seule envisageable.

Pour traiter ce sujet, la communication est décomposée en quatre parties.

En premier lieu on tente de dégager comment a évolué au long des années la vrille des avions de formules nouvelles.

En second lieu on cherche à exposer ce que les personnes qui, en France, ont accumulé une large expérience, pensent pouvoir tirer comme résultats généraux relativement à l'action d'un certain nombre de variables sur la vrille.

Après ces chapitres relatifs à l'analyse humaine, on traite de l'ébauche d'analyse statistique entreprise sur calculateur.

La dernière partie est destinée particulièrement à montrer les limites d'emploi des résultats généraux. Sur le cas particulier de deux avions construits en série durant de nombreuses années, selon des versions apparemment très voisines, il est montré comment les caractéristiques de vrille peuvent être très sensibles à des grandeurs dont l'action échappe totalement à l'étude statistique entreprise.

2 - LA VRILLE EN FONCTION DES EPOQUES.-

2.1 - Avions lents à hélice (figure 1)

Si l'on remonte très loin avant 1940, les vrilles semblent toujours avoir été décrites comme calmes. La vrille plate était à ces époques fréquente ; il semble que cette vrille plate ait été aussi rapide et l'on peut penser maintenant que l'attitude plate était consécutive à une action du couple centrifuge de tangage. Les avions étaient alors à aile droite et le plus souvent leurs empennages, particulièrement le vertical, étaient largement sous dimensionnés. Les consignes étaient alors mal étudiées et se réduisaient souvent à une extrapolation du vol normal ; pour chercher à réduire l'incidence on poussait alors le manche. Depuis, on a pu mettre en évidence qu'une telle consigne fut souvent très néfaste. Le Tail Damping Power Factor est un coefficient qui, inventé depuis, rend très bien compte de cela.

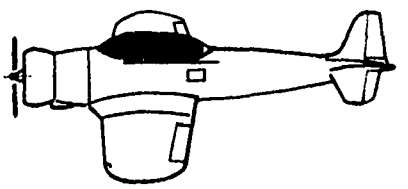

Fig. 1 - Avions lents à hélice

2.2 - Avions rapides à hélice (figure 2)

Pendant la guerre 39-45, s'est alors généralisée une autre consigne de sortie de vrille qui tenait compte de ce qui vient d'être dit : pied contre et, environ un demi-tour après, manche en avant. Cette consigne a alors très souvent donné satisfaction. Les avions, encore à hélice, étaient pourvus d'empennages plus grands que précédemment et l'avant de fuselage était moins court. La majorité des vrilles restèrent calmes pendant des années, les vitesses de rotation étaient supportables, les attitudes étaient moyennes entre les vrilles très plates et très piquées.

Fig. 2 - Avions rapides à hélice

2.3 - Premiers avions à réaction (figure 3)

Puis sont apparus les avions à réaction à flèche faible ; au début leurs entrées d'air en pitot conduisirent à des longueurs de fuselage à l'avant relativement modérées. Les vrilles restèrent alors peu différentes de celles des derniers avions à hélice ; par contre se dessinèrent dès ce moment des modifications nettes sur la consigne de sortie de vrille. Le fuselage arrière à cause de la présence du réacteur devint beaucoup plus gros. En vrille, son sillage sur l'empennage vertical diminua considérablement l'action de la gouverne de direction qui devint alors incapable de contrer la rotation. C'est à cette époque que l'on fut obligé de faire appel au gauchissement qui était alors entièrement contrôlé par des ailerons ; ceux-ci étaient à cette époque largement dimensionnés. La sortie de vrille imposa alors l'usage des ailerons mis Avec (Avec le virage de même sens que la vrille). Si précédemment la sortie de vrille s'opérait à dérapage faible (assiette transversale très faible), par un piqué progressif de l'avion, la sortie de vrille en utilisant le gauchissement prit alors une autre allure. L'aile marchante (ou aile extérieure) se relevait en sorte qu'apparaissait un dérapage (l'avion tendant à glisser vers l'intérieur de la vrille) ; mais les avions de cette époque avaient une très grande réserve de stabilité de lacet et le dérapage se résorbait. L'incidence tendait ainsi à décroître au profit d'un dérapage qui disparaissait de lui-même. Les récupérations étaient alors très franches, l'avion reprenant largement de la vitesse. C'est la reprise de vitesse qui était toujours le signe indiscutable du retour aux incidences de vol normal, même si les ailerons étant Avec, la rotation de vrille s'était transformée en rotation de tonneaux verticaux.

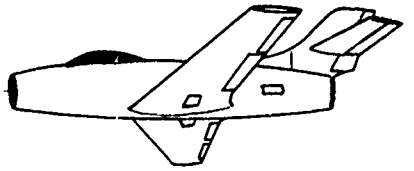

Fig. 3 - Premiers avions à réaction

2.4 - Accroissement de la flèche des avions à réaction (figure 4)

Les avions destinés à voler à des vitesses plus grandes eurent alors des voilures à plus forte flèche ; c'est à ce moment qu'apparurent des vrilles agitées. Les agitations les plus fréquentes et les plus amples étaient des agitations de roulis. On vit apparaître les vrilles à agitations divergentes, la vrille cessant alors au profit d'une autorotation autour de l'axe de roulis, baptisée par nous auto-tonneau ; l'axe de roulis est au départ de cette autorotation voisin de 90° avec la vitesse. Mais les avants de fuselage n'avaient pas à ce moment-là assez grandi pour détruire la reserve de stabilité de lacet, en sorte que, quelles que soient les caractéristiques de tangage, l'avion piquait très vite et redevenait contrôlable.

C'est aussi à cette époque que les avions, si les phénomènes agités ne l'emportaient pas, redevinrent aptes à la vrille plate et rapide bien que les empennages soient largement dimensionnés.

Fig. 4 - Accroissement de la flèche

2.5 - Allongement, vers l'avant, du fuselage des avions à réaction (figure 5)

Les évolutions suivantes des vrilles semblent liées surtout à l'allongement de l'avant des fuselages. Conjointement on a assisté à une tendance à l'accroissement du masque porté sur l'empennage vertical par l'aile, le fuselage ou des réacteurs extérieurs. Les vrilles sont à ce stade devenues souvent très agitées ; les agitations ne sont plus seulement que du roulis, mais ont aussi des composantes de lacet et de tangage ; souvent le mouvement obtenu n'est pas une vrille organisée mais plutôt un mouvement désordonné. Le pilote est alors très désorienté, il est souvent presque incapable de reconnaître un sens moyen du mouvement ; l'application d'une consigne non systématique n'est pas certaine. La répartition des surfaces de fuselage entre l'avant et l'arrière est alors telle que la réserve de stabilité latérale de lacet est très fortement en[illegible] ; la récupération n'est pas assurée lorsque, la première fois, l'avion atteint une attitude où, à priori, on aurait pu le penser récupéré.

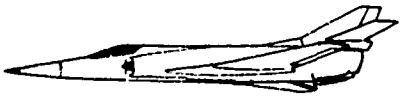

Fig. 5 - Allongement, vers l'avant, du fuselage.

2.6 - Remarque.

La description historique qui vient d'être faite est évidemment très incomplète ; y ajouter d'autres points aurait consisté à l'alourdir et aurait masqué l'essentiel.

3 - ACTION DES DIVERSES VARIABLES - RESULTATS GENERAUX.-

3.1 - Présentation du chapitre.

Si le chapitre 2 était relatif à la relation des phénomènes apparus au cours des années, le présent chapitre a pour but d'énoncer des conclusions générales au sujet de l'effet d'un grand nombre de variables sur l'ensemble des vrilles étudiées tant en soufflerie qu'en vol grandeur. Les résultats utilisés sont donc simultanément relatifs à des avions de tous types, d'armes ou non, et cela pour toutes les époques à la fois.

Il est important de mettre, avant de commencer, en garde le lecteur de prendre pour absolu tout ce qui est écrit. Rares sont les cas où les propos sont des affirmations sans restrictions ; il est nécessaire de bien tenir compte des nuances mises dans l'expression des résultats généraux car pour bon nombre de ceux-ci des exemples contraires pourraient être présentés.

Le chapitre porte successivement sur :

- effet des surfaces mobiles et des surfaces complémentaires,
- considérations sur les formes géométriques générales,
- géométrie et masse des charges extérieures,
- divers aspects particuliers des vrilles, successivement :
  - les vrilles agitées,
  - les vrilles plates,
  - les vrilles dos.
- effet de moyens de secours.

3.2 - Effet des surfaces mobiles.

3.2.1 - La direction.

Lorsque la gouverne de direction a un effet sur la vrille, celui-ci est toujours de même sens : Direction Avec favorable à la vrille stabilisée et Direction Contre favorable à la sortie de vrille. Mais la presque totalité des avions d'armes depuis 15 à 20 ans ont une direction tout à fait inopérante en vrille ; l'effet est nul parce que l'empennage vertical est dans le sillage de l'empennage horizontal, de réacteurs arrière extérieurs, de la voilure ou plus simplement du fuselage (voir figure 6). Des essais de soufflerie effectués en supprimant l'empennage vertical ont souvent donné des résultats semblables à la forme complète. Les avions à empennage en T, très minoritaires, ne sont pas inclus dans les résultats de ce paragraphe.

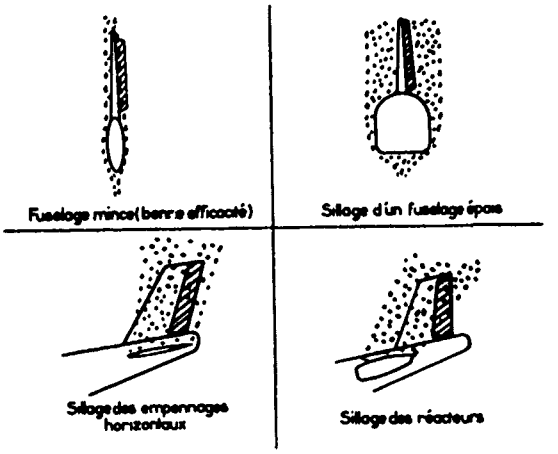

Fig. 6 - Gouverne de direction

3.2.2 - La profondeur.

Il est difficile de donner des indications générales relatives à l'action de la profondeur sur les vrilles, en excluant bien sûr la phase de déclenchement. Le braquage de la profondeur, ou de l'ensemble de l'empennage horizontal, introduit, en plus d'une modification des efforts sur le plan horizontal lui-même, une modification de l'écoulement autour de l'arrière du fuselage et de l'empennage vertical ; c'est la diversité des modes d'action qui en disperse les effets.

Si une vrille maintenue est relativement calme, passer de manche tiré à manche poussé tend en général à rendre la vrille plus établie. En moyenne, la vitesse de rotation croît, le rayon de vrille se réduit, l'attitude devient plus plate (voir figure 7) ; cela ne veut pas dire que, manche tiré, il n'y ait pas aussi des vrilles plates et rapides.

Si par contre il s'agit d'une vrille agitée, souvent les agitations deviennent encore plus amples. Certains avions peuvent avoir, selon les circonstances, des vrilles calmes ou des vrilles agitées, ce qui conduit à des effets divers du braquage de la profondeur.

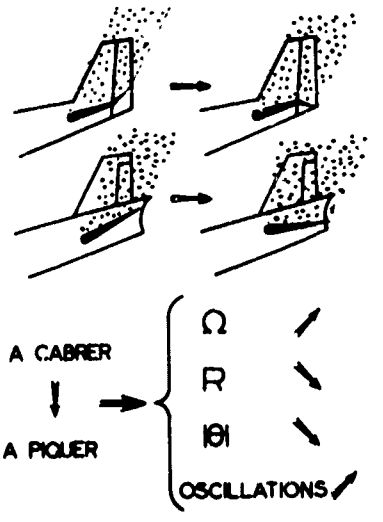

Fig. 7 - Gouverne de profondeur

3.2.3 - Le gauchissement.

Trois types de gauchissement sont à considérer : les ailerons, les spoilers, le braquage différentiel des empennages horizontaux. On peut tout de suite éliminer les spoilers qui n'ont pas d'action appréciable sur la vrille hormis son déclenchement. Le braquage différentiel des empennages horizontaux a une action de nature très voisine de celle des ailerons, elle est cependant

souvent moindre ; une limitation de l'effet provient souvent de la limitation des braquages globaux, profondeur + gauchissement.

Dans la très grande majorité des types d'avions, la vrille est favorisée par le gauchissement Contre et la sortie favorisée par le gauchissement Avec. Les types d'avions qui n'ont pas cette caractéristique ont alors une vrille piquée.

Le domaine de gouvernes qui permet les vrilles plates et rapides, si elles existent, contient toujours gauchissement Contre. Si une sortie à partir d'une vrille plate et rapide est possible par les gouvernes, c'est toujours le gauchissement Avec qui le permet le mieux.

Lorsque les vrilles sont agitées de façon presque systématique, les agitations sont plus fréquentes et plus amples gauchissement Contre ; c'est dans ces conditions que la vrille dégénère le plus en auto-tonneaux. Il existe aussi des vrilles agitées gauchissement Avec, elles sont beaucoup plus rares. Si les agitations prépondérantes, gauchissement Contre, sont celles de roulis, il semble qu'en passant à gauchissement Avec cela fasse disparaître cette prépondérance et on peut alors observer de nettes agitations de tangage.

3.2.4 - Les volets hypersustentateurs.

Il est malaisé de tirer des lois générales sur l'effet des volets hypersustentateurs. Leur action passe notamment par l'interaction sur l'écoulement au droit des empennages, en sorte qu'elle est très fonction des formes générales de l'avion ; la dispersion des résultats imposerait une analyse plus fine. Malgré cela, on peut cependant dire que le braquage des volets s'est en moyenne avéré légèrement défavorable à la sortie de vrille. Souvent, l'effet est nul ; il n'est pratiquement jamais favorable.

3.2.5 - Les becs.

Nous ne disposons sur avions d'armes que de trop peu de résultats pour en dégager une action type de la sortie des becs. Sur avions légers par contre, si les becs repoussent le point d'entrée en vrille, les becs semblent défavorables à la sortie de vrille.

3.2.6 - Les aérofreins.

La disposition des aérofreins est beaucoup trop diversifiée pour que l'on puisse attendre une action typique de ces surfaces.

3.2.7 - Les trappes.

Les trappes qui peuvent avoir une action sont surtout celles du train avant. Si les trappes se composent de deux éléments symétriques, on recueille un effet d'amortissement très sensiblement moindre qu'avec une surface unique placée dans le plan de symétrie et qui aurait la surface totale des trappes ; l'effet d'amortissement peut non seulement être considérablement réduit mais parfois être inversé.

Une seule trappe latérale peut avoir un effet de sens variable selon le sens de la vrille.

3.3 - Effet de surfaces complémentaires.

3.3.1 - Quilles (figure 8)

Sous le nom de quilles, nous rangeons les surfaces qui sont sous le fuselage, dans le plan de symétrie et pour les implantations arrière également des surfaces symétriques. Sous l'avant du fuselage les quilles ont pour effet de freiner la rotation des vrilles plates et rapides. Elles peuvent mettre l'avion complètement à l'abri de ces vrilles. Pour que ces quilles avant soient efficaces, il est nécessaire qu'elles soient placées très à l'avant ; le premier avantage est évidemment le gain au sujet bras de levier, mais ce n'est pas le seul gain. Si la quille est placée à une certaine distance de l'avant, elle se trouve placée dans un écoulement de contournement déjà organisé et son action de conditionnement de l'écoulement est moindre.

Des essais en remplaçant tout l'extrême-avant d'un fuselage avec sa quille par sa projection dans le plan de symétrie ont conduit à un amortissement moindre que par la forme normale fuselage + quille. Pour qu'une quille soit efficace, elle doit avoir une certaine hauteur sous une surface quasi-horizontale. Le fonctionnement d'une quille en deux éléments symétriques verticaux fait perdre de l'efficacité.

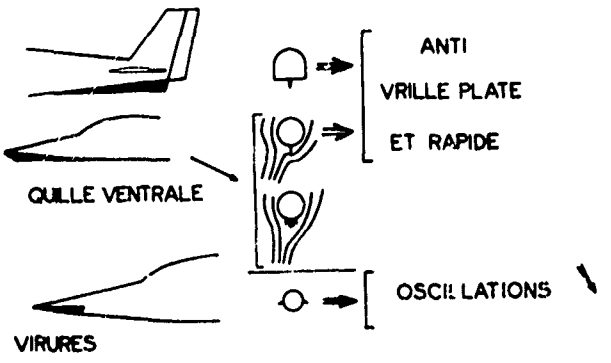

Fig. 8 - Surfaces complémentaires

Sous l'arrière du fuselage, l'effet des quilles est beaucoup moins systématique. Pour des avions légers, on recueille un amortissement de lacet. Pour des avions d'armes, les effets sont dispersés ; mais parfois ces effets sont importants.

3.3.2 - Virures (figure 8)

L'expérience que nous avons sur les virures concerne essentiellement les avions d'armes actuels (résultats maquette et avion).

Les virures sont des surfaces qui se placent perpendiculairement, ou presque, à la peau du fuselage, à l'avant de celui-ci. Elles sont toujours symétriques et très écartées. Le but de ces surfaces est de créer des singularités dans les conditions initiales de l'écoulement autour de l'avion. Ces singularités fixent l'écoulement et empêchent notamment des dissymétries aléatoires bien qu'intenses. Ces dissymétries s'installent même à dérapage nul ; elles débutent autour de l'avant du fuselage puis s'amplifient autour de l'ensemble de l'avion. Les vrilles sont d'autant plus agitées et les sorties sont d'autant moins sûres que ces dissymétries s'installent. L'effet des virures est alors, grâce à la fixation de l'écoulement, de calmer la vrille et de rendre la sortie plus sûre. Pour que cet effet soit obtenu, il est nécessaire de placer les virures très en avant et qu'elles fassent entre elles au moins 90°. Les conditions de positions et de dimensions ne peuvent pas être plus généralisées. Par contre, une condition générale de la définition des virures est de passer par des essais préalables. D'une part, calmer une vrille agitée fait apparaître une vrille calme (qui pourrait être sévère) qui était totalement masquée par les agitations qui en empêchaient l'établissement. D'autre part, les virures mal placées et mal dimensionnées pourraient, par exemple, faire naître des moments de lacet pro-vrille ou des agitations anti-vrille ; lorsque la rotation introduit du dérapage, l'une des virures est masquée.

3.4 - Effet des formes géométriques générales.

3.4.1 - Voilure - Flèche.

L'augmentation de la flèche n'est pas une cause systématique de l'aggravation des vrilles. En effet, on peut constater que plus la flèche est forte, moins il y a de probabilités de rencontrer des vrilles plates et rapides, sans que cela puisse être attribué à l'apparition d'agitations qui nuiraient à la vrille plate et rapide. C'est par un amortissement général de la rotation que la vrille tend à être moins rapide.

Par contre, les attitudes longitudinales, sans même action d'une forte vitesse de rotation, sont, toujours en moyenne, plus plates si la flèche est plus grande. A mêmes vitesses de rotation, les attitudes moyennes à flèche nulle sont à 45-50° de l'horizontale, à flèches modérées, elles sont voisines de 30° et aux fortes flèches elles sont voisines de 20°.

Si l'on compare les types de vrille des avions à flèches différentes, on constate qu'en moyenne les vrilles sont moins souvent agitées à faible flèche et que ces agitations sont aussi plus ordonnées. Cependant, on peut penser que les modifications citées ne sont pas dues spécifiquement à la flèche car sur des avions à flèche variable, on ne retrouve pas cet effet.

3.4.2 - Voilure - Autres caractéristiques.

Si des cas isolés ont montré l'action de l'allongement, de l'effilement, ou du dièdre, par contre rien ne permet d'en tirer des résultats généraux.

3.4.3 - Fuselage - Longueur.

La longueur du fuselage vers l'arrière joue sur l'efficacité des empennages ; par contre, cette longueur accroît le couple centrifuge de tangage, ce qui absorbe une partie de l'efficacité des empennages horizontaux. Avec de longs fuselages arrière, les vrilles, si elles peuvent être encore peu piquées, sont alors rarement simultanément rapides.

La longueur du fuselage avant est sans doute une des variables qui a, le plus, agi ces dernières années sur la vrille. Les longs nez ont eu pour effet de réduire considérablement le domaine incidence - dérapage où il y a stabilité de lacet. D'autre part, ils sont à l'origine de nombreuses vrilles agitées et ils ont aussi pour effet de rendre ces agitations plus désordonnées. Sur les reprises de contrôle, les longs nez ont une action importante ; l'approche au cours du mouvement ou même la pénétration à une certaine vitesse du domaine incidence - dérapage de vol stable, ne permettent pas une reprise de contrôle systématique ; l'avion peut fort bien ressortir du domaine stable et réatteindre des incidences et des dérapages très élevés.

3.4.4 - Fuselage - Forme de la section (figure 9)

A l'arrière, une forme aplatie, à grand axe vertical, conduit à un meilleur amortissement de lacet, elle réduit le masque sur l'empennage vertical et parfois aussi sur l'empennage horizontal. Inversement, une forme aplatie, à grand axe horizontal, réduit considérablement l'amortissement propre du fuselage et nuit aussi largement à l'amortissement de l'empennage vertical. Une mention particulière est à faire au sujet de certains avions légers à fonds plats et qui présentent des arêtes ou des arrondis à très faibles rayons de courbure entre les fonds et les flancs latéraux ; ces formes génèrent des

sillages très épais qui nuisent fortement à l'amortissement propre du fuselage et à l'amortissement de l'empennage vertical, et par suite, à l'action de la gouverne de direction.

A l'avant du fuselage, on retrouve l'effet amortisseur propre au fuselage qui varie considérablement selon qu'il est aplati verticalement ou horizontalement. Mais d'autres effets existent. Il a été vu dans les paragraphes précédents que des écoulements très dissymétriques pouvaient prendre naissance autour de l'avant du fuselage et que l'on pouvait faire disparaître ces dissymétries par des singularités. On conçoit alors aisément que les courbures de la forme des cadres et que l'évolution de ces formes en fonction de l'abscisse sont aussi capables d'agir très fortement. Par contre, il est absolument impossible, à l'heure actuelle, de donner des résultats généreux sur ce point. Le chapitre 5 de la communication fournit un exemple d'action des formes de l'avant d'un fuselage.

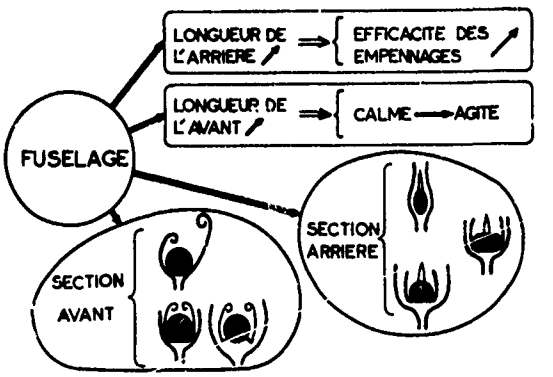

Fig. 9 - Forme de la section fuselage

3.4.5 - Les empennages horizontaux.

Il est possible d'affirmer que la taille des empennages horizontaux en elle-même ne peut pas conditionner le type de la vrille ; il existe en effet avec de grands empennages horizontaux des vrilles piquées ou plates, rapides ou lentes, calmes ou agitées.

Pour un avion donné, la modification de la taille de l'empennage horizontal peut, par contre, agir de façon sensible ; mais le sens de l'action n'est pas simple. Pour expliquer cela, il suffit de rappeler ce qui en a été déjà écrit au cours du paragraphe 3.2.2 relatif à l'action de la gouverne de profondeur : l'empennage horizontal agit pour son propre compte et agit indirectement par l'interaction qu'il a sur les effets de l'empennage vertical. Si l'on veut apprécier l'action isolée de l'empennage horizontal, il faut se reporter à la communication de MM. GOBELTZ et BEAURAIN* (I.M.F.Lille) et y considérer l'effet de fusées en tangage ; on constate alors que pour modifier fortement l'attitude de vrille, des variations de surface importantes seraient nécessaires. Or ces variations entraînent en plus des actions importantes sur le fonctionnement des surfaces verticales.

3.4.6 - L'empennage vertical.

Si à l'amont de l'écoulement autour de l'empennage vertical ne se trouvent pas des volumes ou des surfaces ouvrant des sillages qui baignent cet empennage, l'empennage vertical par sa taille peut alors conditionner très fortement le type de vrille. Il n'existe pas de vrilles plates et rapides, ni de vrilles très agitées si l'empennage vertical, suffisamment grand, est correctement alimenté. De la même façon, l'action de la gouverne de direction est grande si elle n'est pas masquée. Le T.D.P.F. relatif à l'action de la direction (voir figure 10) supposait implicitement que le masqué ne pouvait venir que de l'empennage vertical. Il était adapté à des avions anciens ; pour les avions à réaction il n'est alors adapté, au plus, qu'à ceux ayant leurs moteurs sous la voilure, largement détachés du fuselage.

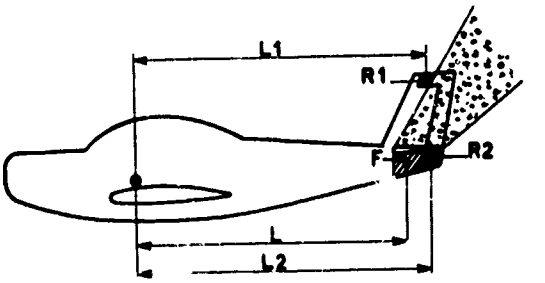

$$T.D.P.F. = \frac{F \cdot L^2}{S\left(\frac{b}{2}\right)^2} \times \frac{R1\,L1 + R2\,L2}{S\frac{b}{2}}$$

Fig. 10 - Tail Damping Power Factor

3.5 - Les caractéristiques d'inertie

3.5.1 - La masse.

Aucune action systématique ne peut être attribuée à la masse en elle-même.

3.5.2 - Le centrage.

On a coutume, au sujet du centrage, de penser exclusivement au centrage longitudinal ; or le déplacement latéral doit être considéré avec encore plus de soin.

Longitudinalement, la position du centre d'inertie a évidemment une action fondamentale sur le déclenchement des mouvements conduisant à la vrille ; par contre, une fois la vrille entamée, le

---

* Titre de la communication : Action sur la vrille, par moment "statique", de fusées et de chargements dissymétriques.

centrage longitudinal perd rapidement de son importance ; les vrilles ne sont pas transformées par une variation de quelques % de corde de la position longitudinale du centre d'inertie.

Pour les mouvements qui suivent l'arrêt de la rotation, il est bien évident que le centrage longitudinal reprend toute son importance ; importance qui est fondamentale pour les avions sujets au deep-stall.

Le déplacement transversal du centre d'inertie peut agir sur les vrilles de façon considérablement plus rapide que le déplacement longitudinal. Certains avions y sont très sensibles. De façon systématique, le centre d'inertie vers l'intérieur favorise la sortie de vrille et vers l'extérieur favorise le maintien de la vrille (voir figure 11 a). La communication de MM. GOBELTZ et BEAURAIN (I.M.F.Lille), déjà citée, traite en détail du sujet.

3.5.3 - Les moments d'inertie (figure 11 b)

Pour les avions dont les moments d'inertie de roulis et de tangage sont voisins, on peut observer des variations des résultats en fonction de la valeur respective de ces deux moments. Par contre, pour les avions d'armes de ces dernières années, le moment d'inertie de tangage est tellement supérieur à celui de roulis que l'action des valeurs respectives de ces moments est largement masquée par l'action des autres variables.

Pour les avions à moments d'inertie de tangage ——— et roulis voisins, on observe des modifications non pas tellement sur les caractéristiques moyennes des vrilles mais plutôt sur les actions des gouvernes favorables à la sortie de vrille. Le résultat général est que, ailes lourdes, les sorties sont favorisées gauchissement Contre, et fuselage lourd elles sont favorisées gauchissement Avec.

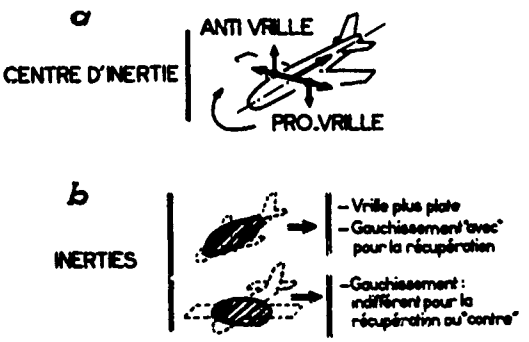

Fig. 11 - Caractéristiques dynamiques

Lorsque les avions sont à fuselage très lourds, les attitudes sont en moyenne plus plates ; une faible rotation de vrille aplatit rapidement celle-ci.

3.6 - Les charges extérieures.

3.6.1 - Effet selon les positions.

Les charges extérieures sous le fuselage, souvent placées trop près du centre d'inertie de l'avion, n'ont pas d'effet systématique.

Les charges extérieures sous voilure peuvent avoir un effet important. Si elles sont peu distantes du plan de symétrie, elles peuvent avoir des dimensions importantes et agir par leur géométrie. Loin du plan de symétrie, elles ont une action par les moments d'inertie ajoutés ; elles peuvent aussi avoir une action très importante si elles sont dissymétriques, introduisant alors de sensibles déplacements latéraux du centre d'inertie ; ces déplacements agissent alors plus que l'accroissement de l'inertie de roulis.

3.6.2 - Les masses (figure 12 a).

On n'observe pas de modification systématique importante des caractéristiques des vrilles due aux masses symétriquement disposées des charges extérieures. Même lorsqu'elles introduisent des moments d'inertie importants, les moments de tangage des avions d'armes récents restent encore largement supérieurs à ceux de roulis. Sur les vrilles calmes, les actions sont faibles. Sur les vrilles agitées, en roulis principalement, l'action est une tendance à réduire les agitations. Si les vrilles sont agitées de façon désordonnée, les actions ne sont en rien systématiques.

De façon tout à fait inverse, les masses des charges extérieures deviennent très actives si elles sont dissymétriques : voir à ce sujet la communication de MM. GOBELTZ et BEAURAIN (I.M.F.Lille) déjà citée.

3.6.3 - Les encombrements géométriques (fig.12b)

En moyenne, les caractéristiques des sorties de vrille sont moins bonnes avec de volumineuses charges extérieures sous voilure.

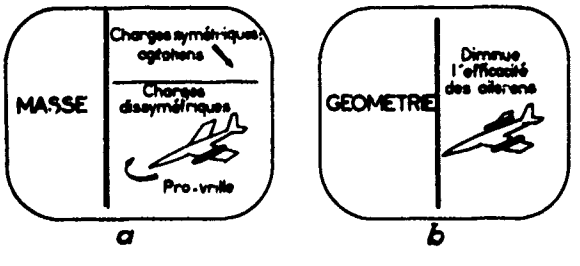

Fig. 12 - Charges extérieures

Hormis cette tendance sur la qualité des sorties de vrille, il n'est pas possible de tirer des résultats généraux au sujet de l'action de la géométrie des charges extérieures sur la vrille. La détérioration de la qualité des sorties peut être attribuée à ce que des charges volumineuses, ou des ailettes de charges plus discrètes en elles-mêmes, peuvent perturber l'écoulement devant des gouvernes de gauchissement réduisant par là les actions de celles-ci.

3.7 - Le contrôle des agitations.

Les agitations désorientent souvent les pilotes. Si elles sont surtout composées de roulis, elles sont encore analysables. Si par contre, ce sont des mouvements désordonnés, elles ne sont plus analysables et même la reconnaissance d'un sens de vrille est problématique.

Pour tous les avions, dont les vrilles sont agitées en roulis presque exclusivement, il est possible de définir des consignes de sortie de vrille. Si les agitations peuvent dégénérer en auto-tonneaux, les consignes doivent être appliquées avant que les agitations ne soient devenues trop amples, sinon la divergence s'opère sans possibilité d'action. La sortie s'opère cependant parce que les auto-tonneaux sont instables. Il y a donc toute une période pendant laquelle rien ne peut être fait pour accélérer la sortie.

Pour les avions qui sont agités de façon désordonnée, la récupération ne s'opère pas selon un processus systématique comme après des agitations de roulis divergentes cédant la place à des auto-tonneaux. La sortie peut durer, pour des conditions de départ très voisines, des temps très divers, certains redéparts pouvant même s'opérer après une sortie presque atteinte. Il faut donc systématiquement se prémunir contre l'entrée en mouvements désordonnés ou fournir des moyens auxiliaires au pilote pour que ces mouvements cessent sans faire appel à un pilotage humain.

Un résultat général sur les agitations est qu'elles empêchent l'établissement de vrilles calmes qui pourraient être dangereuses ; elles ne sont donc pas systématiquement à amortir.

3.8 - Le contrôle des vrilles plates.

3.8.1 - Vrilles plates et lentes (figure 13 a)

Les vrilles plates et lentes sont celles qui ont une attitude plate par action du moment aérodynamique statique sans aide du couple centrifuge de tangage. Ce sont les plus incontrôlables par les gouvernes ; même l'arrêt de la rotation ne les fait pas piquer et les commandes de profondeur sont inefficaces pour faire piquer. Seuls des moyens de secours extérieurs peuvent conduire à la sortie.

3.8.2 - Vrilles plates et rapides (figure 13 b)

Les vrilles plates et rapides deviennent toujours en même temps plates d'une part et rapides d'autre part et elles ne le deviennent que rarement en très peu de temps ; c'est l'accroissement progressif du couple centrifuge de tangage qui les aplatit. Ces vrilles laissent, avant d'être totalement établies, un délai au pilote pour appliquer la consigne ; des départs dynamiques en vrille peuvent cependant réduire fortement ce délai.

Pour tous les avions, de tous types, la vrille simultanément plate et rapide est contrée par le gauchissement mis Avec ; si le gauchissement Avec est insuffisant, les autres gouvernes ont peu de chance de l'aider à le devenir.

Si une vrille plate et lente peut être, modérément du moins, agitée et pourtant se perpétuer, par contre une vrille plate et rapide n'est jamais agitée. Si elle a tendance à s'agiter, elle se ralentit et pique. Inversement, si, légèrement agitée, elle se calme, alors elle s'accélère et s'aplatit.

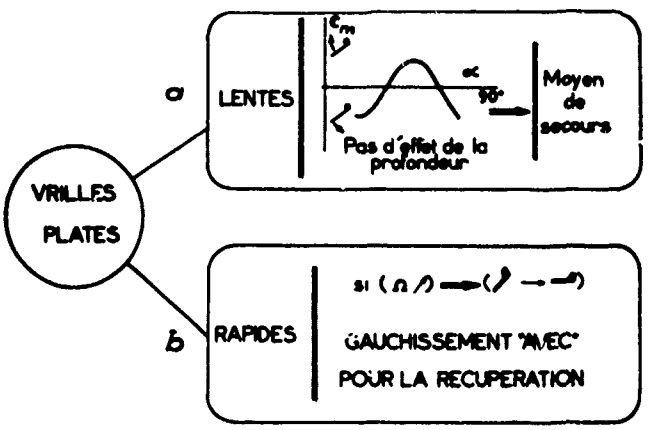

Fig. 13 - Vrilles plates

3.9 - La vrille dos (figure 14)

La vrille dos est beaucoup moins étudiée que la vrille ventre. En vol elle se rencontre beaucoup moins. Elle est presque toujours plus facilement contrôlable que la vrille ventre. Pour les avions d'armes le gauchissement est prépondérant sur le ventre ; il reste actif aussi sur le dos et cela dans le même sens. Mais le gauchissement cependant ne reste pas prépondérant, c'est le gouverne de direction qui le devient. Le plus souvent, une consigne tout au neutre est suffisante pour opérer une sortie à partir de la vrille qui est toujours plus piquée. Seuls font exception à ces règles les avions à configurations d'empennages en T ou en V.

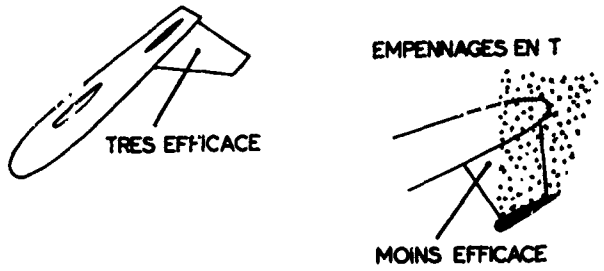

Fig. 14 - La vrille dos

3.10 - Le parachute (figure 15 a)

Dans la très grande majorité des cas, le parachute anti-vrille n'est pas requis. Cependant, il peut être utile lorsque les attitudes sont plates et plus spécialement lorsque simultanément la vrille est lente, c'est-à-dire lorsque l'on est en présence d'un problème de tangage purement aérodynamique. Lorsque la vrille est simultanément plate et rapide, son action ne peut être que lente et n'est pas certaine.

Lorsque la vrille est fortement agitée et que les gouvernes ne sont plus capables d'accélérer la sortie ou, à fortiori, plus capables de l'entraîner, le parachute pourrait s'avérer utile si tout au moins il peut ne pas être dangereux en accrochant son câble à l'avion. Pour des avions présentant de tels risques de vrille, il faudrait une utilisation très précoce du parachute, ce qui est difficile à réaliser.

Enfin, un résultat tout à fait général, au sujet des parachutes, est relatif à la longueur du câble. En dessous d'une demi-longueur de fuselage, le parachute est inopérant et a toutes les chances d'accrocher sa coupole à l'avion. En dessous d'une longueur de fuselage, le parachute a une efficacité au m2 ou au kg qui est faible et les risques de retombée existent encore. Pour avoir une efficacité convenable, la longueur du câble doit atteindre une longueur et demie du fuselage.

Pour agir correctement sur des vrilles, où il est utile, un parachute a une coupole dont la surface est en moyenne le quart de la surface de la voilure de l'avion.

3.11 - Les fusées (figure 15 b)

Puisque le parachute présente des risques d'accrochage avec l'avion, il est logique de penser à des fusées. Si l'on veut contrer une vrille avec des fusées agissant symétriquement, celles-ci doivent développer des poussées très importantes. Comme dans le paragraphe relatif au centrage longitudinal, il faut faire ici une mention spéciale à propos des avions sujets au deep-stall. Pour ces avions, lorsque la rotation de vrille est arrêtée, une fusée agissant en tangage pourrait être très efficace ; elle n'aurait pas à être aussi forte que pour arrêter une vrille puisque le couple centrifuge de tangage ne serait plus à vaincre.

Si l'on utilise des fusées agissant de façon dissymétrique, on constate qu'elles peuvent être très efficaces avec des poussées faibles. MM. GOBELTZ et BEAURAIN (I.M.F.Lille) déjà cités, traitent de cela dans leur communication.

Si l'on pense aux fusées, on peut être tenté aussi de penser aux réacteurs, mais à ce sujet deux remarques générales sont à faire. D'une part, un réacteur en vrille n'est pas apte à fournir une poussée substantielle ; d'autre part, dans la mesure où un réacteur serait capable de fournir une forte poussée, il n'en serait pas pour autant capable de faire sortir de vrille, car pour sortir de vrille il faut disposer de moments et non pas de forces ; l'effet des moteurs à hélice n'est pas assimilable à celui d'une fusée ; il s'agit d'actions aérodynamiques.

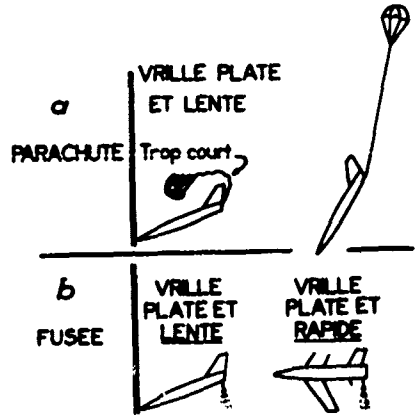

Fig. 15 - Dispositifs de secours

4 - EBAUCHE D'ETUDE DE CORRELATION.-

4.1 - Présentation.

Cette étude, à l'état d'ébauche actuellement, est faite en décrivant par un certain nombre de critères, d'une part les avions, d'autre part les vrilles.

Les critères de description des avions peuvent être très nombreux. Leur définition est faite à priori, mais ensuite c'est la façon dont ils se corrèlent qui guidera les retouches nécessaires, le but étant de définir les critères avions qui se corrèlent le mieux. Ces critères avions portent sur la géométrie générale, sur des géométries de détail et sur l'inertie.

Les critères de définition de vrille sont, soit qualitatifs, soit quantitatifs ; ils portent sur la définition du mouvement et les actions possibles.

La population étudiée est formée de 117 avions différents de tous types ; sur ces avions, 27 sont des avions d'armes ; les autres sont soit des avions légers, soit école, soit transport. Le nombre d'avions brut est en fait accru par le fait que les avions d'armes notamment ont des versions suffisamment différentes pour être comptabilisées séparément. De plus, lorsqu'un même avion a plusieurs vrilles pour une même combinaison de gouvernes, il est aussi comptabilisé plusieurs fois.

Cette etude débute seulement ; les avions pris en compte correspondent aux 20 dernières années ; nous ne sommes pas encore remontés au-delà. Par ailleurs il est évident que plus la population sera grande, plus il sortira de renseignements ; aussi il serait souhaitable d'y ajouter toutes les données complémentaires que pourraient fournir les personnes qui en détiendraient.

4.2 - Résultats.

Afin de présenter quelques résultats, nous avons choisi de nous limiter à un très petit nombre de grandeurs soit pour les caractéristiques avion :

- flèche,)
- hauteur sur fuselage,) de la voilure
- dièdre,)
- longueur relative de l'avant du fuselage,
- moments d'inerties,

et pour les caractéristiques de vrille :

- niveau des agitations,
- attitude longitudinale,
- durée d'un tour.

Dans le tableau de la figure 16 se trouvent classées, par ordre d'importance, les corrélations, d'une part pour l'ensemble Σ "Tous avions" et, d'autre part pour le sous-ensemble M "Avions d'armes". Le coefficient de corrélation est calculé pour chacune des 27 combinaisons de gouvernes (3 positions pour chaque gouverne). L'importance relative est jugée en tenant compte de la moyenne des 27 valeurs et de la valeur extrême parmi les 27.

Dans le tableau ne sont présentés que les 10 premiers (classés par ordre d'importance décroissante) parmi les 15 coefficients possibles. Les 5 restants sont d'importance quasi-nulle. On voit immédiatement que le caractéristique de vrille qui se corrèle le mieux est le degré d'agitations. Dans le chapitre précédent, nous avions noté que pour la voilure, l'analyse humaine n'était capable de sortir une action qu'au sujet de la flèche ; or on voit tout de suite dans la figure 16 apparaître les limites de l'analyse humaine puisque le dièdre et la hauteur de l'aile semblent avoir plus d'effet moyen.

Parmi ces coefficients, faisons maintenant quelques remarques sur $\Sigma_2 - \Sigma_6 - \Sigma_7$ d'une part et $M_1 - M_3 - M_5$ d'autre part.

ENSEMBLE Σ Tous avions	ENSEMBLE M Avions d'armes
Σ_1 Longueur AV fuselage / Agitations	M_1 Longueur AV fuselage / Assiette longitudinale
Σ_2 Dièdre / Agitations	M_2 Longueur AV fuselage / Agitations
Σ_3 Flèche / Agitations	M_3 Hauteur de l'aile / Agitations
Σ_4 $I_x - I_y$ / Agitations	M_4 Dièdre / Agitations
Σ_5 Hauteur de l'aile / Agitations	M_5 $I_x - I_y$ / Agitations
Σ_6 Longueur AV fuselage / Assiette longitudinale	M_6 Longueur AV fuselage / Durée de 1 tour
Σ_7 Flèche / Durée de 1 tour	M_7 Flèche / Agitations
Flèche / Assiette longitudinale	Hauteur de l'aile / Durée de 1 tour
Longueur AV fuselage / Durée de 1 tour	Dièdre / Assiette longitudinale
Dièdre / Assiette longitudinale	Hauteur de l'aile / Assiette longitudinale

Fig. 16 - Etude de corrélation
Classement

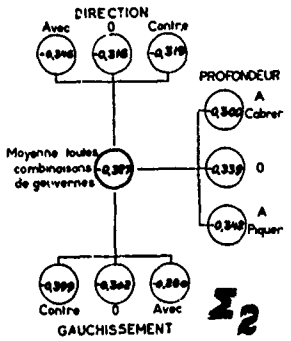

Fig. 17 - Corrélation Dièdre / Agitations

TOUS AVIONS

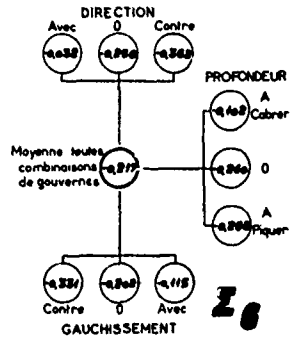

Fig. 18 - Corrélation Longueur AV Fuselage / Attitude longitudinale

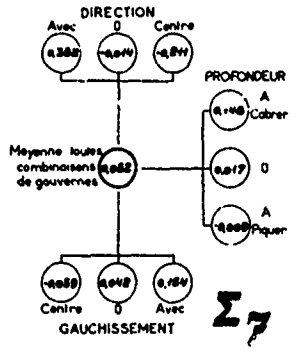

Fig. 19 - Corrélation Flèche/Durée de 1 tour

La figure 17 est relative à Σ_2 effet du dièdre sur les agitations, tous avions confondus. La valeur au centre est la moyenne des coefficients pour les 27 combinaisons de gouvernes. La ligne supérieure est la moyenne pour chaque position de la direction. La colonne de droite correspond à la profondeur et la ligne du bas au gauchissement. Le signe correspond à dire que plus le dièdre est élevé, plus la vrille est calme. On constate ici que l'action est peu influencée par la position des gouvernes, les valeurs sont assez uniformes dans tout le domaine.

L'exemple (donné dans la figure 18) de l'effet de la longueur relative du nez sur l'attitude longitudinale se présente différemment. En effet, on note que les valeurs sont affectées par la position des gouvernes et, ici, par les trois gouvernes. C'est ici le module de l'assiette qui est pris en compte de sorte que plus le nez est long, plus l'attitude est plate. Pour définir s'il y a action par le couple centrifuge de tangage ou par pur effet aérodynamique, il faudrait encore comparer avec un tableau relatif à la vitesse de rotation.

Si dans la figure 18 nous avons vu des dispersions dans le domaine de gouvernes, celles-ci étaient encore telles que le signe reste toujours le même ; par contre, l'exemple présenté dans la figure 19, relatif à la flèche-durée d'un tour, présente des signes opposés. On notera que la valeur moyenne générale est très faible, mais que des modules relativement importants sont obtenus avec les deux signes. On observe ainsi que direction Avec la vrille est ralentie par la flèche et accélérée direction Contre. Il faut sans doute lier cela en partie à une uniformisation des vrilles vis-à-vis de la direction, c'est-à-dire à une moindre action de celle-ci sur la sortie. Il sera alors indispensable de définir la part que l'on peut attribuer, pour cela, aux formes arrière de l'avion masquant la dérive et liées à l'augmentation de la flèche.

Les trois exemples suivants (figures 20 - 21 - 22) sont relatifs aux avions d'armes seulement. Une constatation générale : les valeurs sont plus faibles que pour l'ensemble général ; cela peut être dû à une dispersion naturelle mais aussi à une population trop peu étendue. Dans le tableau de la figure 20 on constate que même à l'intérieur du groupe des avions d'armes, la longueur relative du nez joue sur l'attitude qui est d'autant plus plate que le nez est long. Précédemment, pour l'ensemble général, on observait plus de variations vis-à-vis des gouvernes.

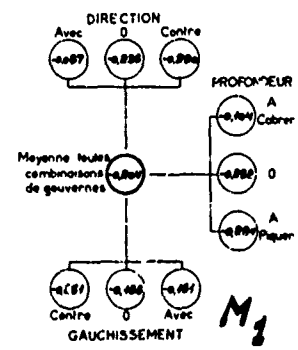

Fig. 20 - Corrélation Longueur AV Fuselage / Attitude longitudinale

AVIONS D'ARMES

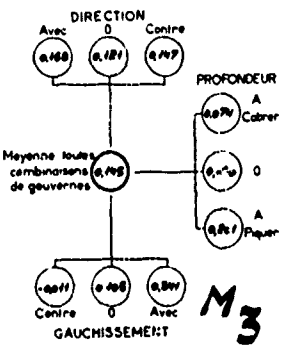

Fig. 21 - Corrélation Hauteur voilure / Agitations

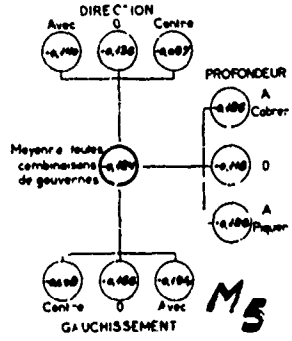

Fig. 22 - Corrélation $\frac{I_x - I_y}{mb^2}$ */ Agitations*

Si nous avons retenu de présenter le tableau de la figure 21 c'est tout d'abord parce que l'on ne s'attendait pas à trouver si bien placée la corrélation hauteur de l'aile-agitations et ce qui étonne encore plus, c'est le sens. En effet, le signe correspond à dire que plus l'aile est haute, plus le phénomène est agité en moyenne. Gauchissement Contre, l'action moyenne est nulle ; au contraire, gauchissement Avec elle est très marquée, ce qui conduit donc à dire que plus l'aile est haute, moins les sorties de vrille sont pures. Ce résultat mériterait comme bien d'autres, une étude plus approfondie.

Le dernier exemple (figure 22) concerne les moments d'inertie et les agitations. Le signe moins correspond à dire que plus le moment d'inertie de tangage est grand, plus les agitations sont grandes ; cela est presque insensible à la direction et à la profondeur, mais par contre on retrouve une action de même type que celle de la hauteur de l'aile en fonction du gauchissement : effet nul gauchissement Contre et effet net gauchissement Avec où les phénomènes sont plus agités si I_y est grand. A nouveau donc les sorties en sont moins pures.

Les quelques exemples qui viennent d'être donnés montrent bien qu'une étude de corrélation sera une aide substantielle pour appréhender au mieux les résultats généraux.

5 - MODIFICATION DES VRILLES SELON LES VERSIONS D'UN MEME AVION. EXEMPLES DE LIMITE D'EMPLOI DES RESULTATS GENERAUX.-

5.1 - Présentation du chapitre.

Lorsqu'un avion a une longue carrière, il est évident que voient le jour successivement différentes versions. Un certain nombre de ces versions sont suffisamment différentes des précédentes pour que l'on pense, à priori, que leur vrille peut en être changée. Par contre, il peut exister toute une famille de versions qui ne présentent entre elles que des différences mineures. Ces différences peuvent être des modifications de forme locale pour loger et permettre l'emploi de tel équipement ; ce peut être aussi l'adjonction d'appendices discrets. A coté des différences dues au passage d'une version à l'autre, il faut aussi prendre en compte les configurations de charges extérieures. A certaines dates de la carrière d'un avion, on peut choisir lui faire emporter des charges plus volumineuses ou plus lourdes ; on peut aussi choisir de le faire voler avec des charges extérieures dissymétriques. Enfin une autre cause de novation est le changement du domaine de missions et d'emploi au cours de ces missions de l'avion.

L'ensemble des points évoqués peut ainsi, au cours de la vie opérationnelle d'un avion, modifier considérablement les risques de départ en vrille, la sévérité de la vrille et les aptitudes à la sortie. C'est ainsi qu'un même avion de base peut rester des années en opération avant que n'apparaissent des problèmes de vrille.

5.2 - Mirages III Delta.

5.2.1 - Place relative des vrilles des Mirages III.

Pour illustrer le point de vue qui vient d'être présenté on a choisi, en premier lieu, le cas de l'avion Mirage III Delta. Dans l'histoire des Mirages Delta, nous ne remonterons pas tout à fait à l'origine ; il sera exclu le Mirage III A qui n'eut pas de vie opérationnelle réelle. Cette première version avait une voilure ne comportant pas de bord d'attaque cambré. Ce fut la seule qui eut cette caractéristique. En conséquence, les versions dont il sera question ici ont toutes la même forme de voilure.

Le fait d'être muni d'une aile delta ne classe pas du tout le Mirage III à part des autres avions au sujet vrille. Il entre dans une des familles décrites au chapitre 2, dans le paragraphe ayant pour titre "Accroissement de la flèche des avions à réaction". C'est un avion qui, selon les conditions, peut avoir pour une même configuration aussi bien une vrille plate et rapide qu'une vrille agitée. Le type d'agitations est caractéristique ; les agitations sont presque exclusivement composées de roulis. Ces agitations ordonnées ne posent pas en elles-mêmes de problèmes.

5.2.2 - Les vrilles des premières versions C et E.

Les premières versions étudiées en vrille furent les versions C et E (voir figure 23). Ces deux versions ont un nez de révolution presque conique ; l'avant du III E étant un peu plus long que celui du III C. Sous l'avant du III E il y a un renflement abritant un doppler. Les essais en soufflerie avaient sur ces versions mis en évidence une très nette prédominance des agitations vis-à-vis de la vrille plate et rapide. Même si la maquette était lancée en vrille plate et rapide avec toutes les précautions nécessaires pour que le mouvement imposé soit calme, des agitations finissaient toujours par apparaître. Ces agitations freinaient la vrille. A la suite des agitations on pouvait obtenir une sortie ventre ou bien les agitations dégénéraient en auto-tonneaux. Ces auto-tonneaux étaient toujours instables ; l'axe longitudinal, au début voisin de l'horizontale, plongeait rapidement. Si une vrille calme s'agitait, l'inverse n'était pas possible, une vrille agitée ne se calmait pas ; de cela on conclut alors que la vrille plate et rapide ne serait que difficilement observable en vol. Lors des campagnes d'essais en vol faites sur ces deux versions, on retrouva les agitations nuisibles au maintien de la vrille et, vu leur nature, favorables à la récupération.

5.2.3 - Les vrilles en vol des autres versions.

Les études de développement de l'avion firent naître des versions très voisines des versions initiales ; ces nouvelles versions répondent à divers impératifs de nouvelles utilisations. Les modifications apportées par les services chargés du développement de l'avion étaient apparemment si petites que ceux-ci n'eurent absolument pas conscience de ce qu'elles pourraient avoir un quelconque effet. C'est ainsi que diverses variations de forme furent apportées à l'avant du fuselage (seules zones de l'avion où il y eut des modifications) ; elles peuvent se classer en trois types (voir fig.23)

a) allongement du fuselage,
b) agrandissement du cockpit pour passer à une version biplace,
c) apparitions de singularités diverses.

c-1 : sur les versions biplace B et BE, il existe des carénages en forme de boudins placés comme des virures de part et d'autre du bas du fuselage au droit du cockpit.

c-2 : sur la version M5 la perche anémométrique est non plus en avant de la pointe mais en-dessous de celle-ci et implantée dans un carénage longitudinal

c-3 : les versions BE - R et RD présentant des troncatures de l'avant du nez.

Ces relations de l'utilisation opérationnelle des versions n'ayant pas fait directement l'objet d'études de vrille mirent en évidence que l'ensemble des types de vrille rencontrés n'était pas entièrement inclus dans l'ensemble des vrilles prévues par les essais des premières versions. En particulier, furent rencontrées des phénomènes suffisamment calmes pour que la vrille plate et rapide puisse s'établir ; les gouvernes étaient moins efficaces pour contrer cette vrille et les accélérations vers l'avant au niveau pilote étaient trop élevées.

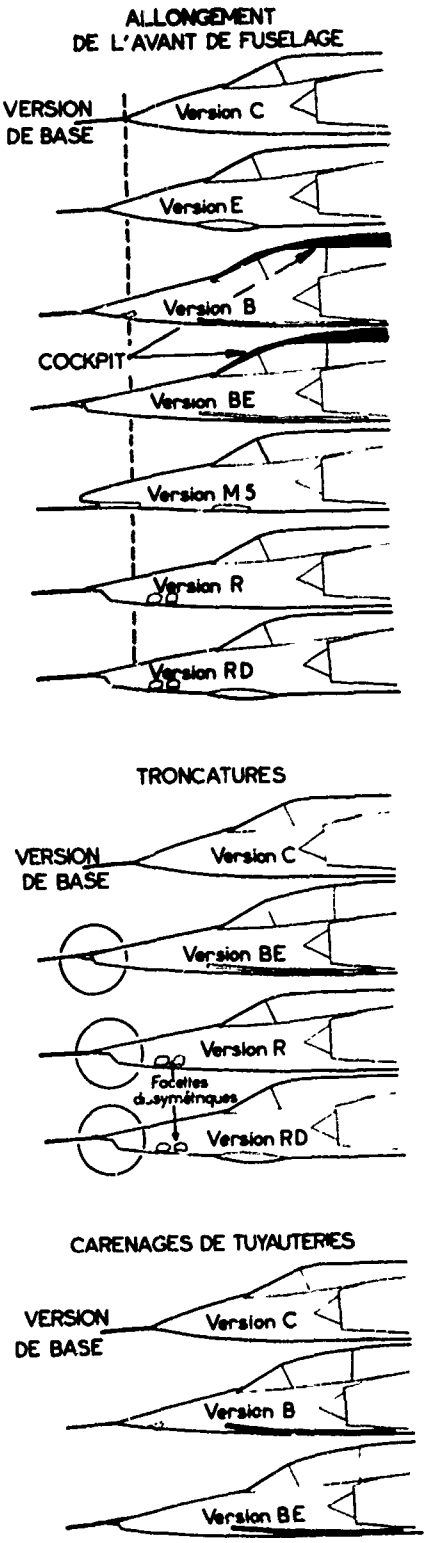

Fig. 23 - Différentes versions du Mirage Delta

5.2.4 - Comparaison des vrilles des diverses versions.

Une nouvelle campagne d'essais de vrille en soufflerie fut entreprise pour situer les vrilles des versions récentes par rapport à celles des premières versions.

La première conclusion qui fut tirée de cette nouvelle étude fut que les versions primitivement étudiées en soufflerie et en grandeur (soit E et C) se trouvaient être les seules versions qui ne présentaient pas de problèmes de vrilles et cela grâce aux agitations. Pour toutes les autres versions, à des degrés plus ou moins marqués, une tendance à des phénomènes calmes fut constatée ; à partir de vrilles agitées, de façon encore modérée cependant, on pouvait observer l'établissement d'une vrille calme. Par suite de la diminution ou de l'absence des agitations une vrille plate et rapide pouvait s'établir. Lorsque cette vrille était parfaitement établie, la récupération par les gouvernes était possible mais longue, et une sortie trouvée longue en soufflerie doit être classée parmi les vrilles. En effet, pour le pilote, le mouvement semble ne pas évoluer et il aura alors tendance à ne pas poursuivre l'application de la consigne. De plus, la marge d'erreur entre essais en soufflerie et en vol doit être toujours considérée dans le sens pessimiste, en sorte qu'une sortie laborieuse en soufflerie ne doit pas être considérée comme transposable en vol. Dans la marge d'erreur il faut inclure des paramètres, tels que le centrage latéral, dont on sait qu'il peut très facilement transformer une sortie en 4 tours en une vrille maintenue.

Ainsi, certaines modifications de la forme de la pointe avant du nez, en fait peu importantes, s'avérèrent capables de modifier notablement le caractère de la vrille. Mais les modifications du nez proprement dit ne furent cependant pas les seuls paramètres en cause. En effet, pour les versions biplace, l'influence anti-agitations et donc pro-vrille plate et rapide, s'est trouvé accentuée par la présence des carénages de tuyauteries extérieures. Un essai fait en soufflerie a nettement mis en évidence l'effet de ces carénages ; placés sur la maquette d'une version (la version E) qui, en géométrie

normale avait une vrille agitée, donc sans problèmes, ces carénages ont calmé la vrille et ainsi amené une vrille plate et rapide. D'autres essais concernant toujours l'effet de ces carénages ont amené des résultats également intéressants ; nous avons prolongé ces carénages vers l'avant et, à la limite, jusqu'à la pointe avant. Au fur et à mesure que les carénages étaient allongés la vrille plate et rapide s'établissait plus facilement et lorsqu'elle était parfaitement établie, ses caractéristiques étaient plus sévères, comme le montrent les résultats ci-dessous :

- Carénages normaux	2,5 sec/tour	3 à 3,5 g au pilote
- Carénages prolongés de 1 mètre ou plus	1,9 sec/tour	6 g au pilote

Pour les versions biplace, les carénages normaux ont donc aggravé les phénomènes ; mais ceux-ci auraient pu être encore plus graves si, par nécessité, les tuyauteries avaient été plus longues sur l'avion.

5.3 - Lightning.

Le Lightning, comme le Mirage Delta, est un avion de carrière longue ; il eut ainsi plusieurs versions entre lesquelles il existait certaines différences géométriques portant sur divers éléments de l'avion. Ainsi, par rapport à une version dite de base,certaines versions avaient :

- une dérive plus grande (corde de base inchangée, corde extrême haute doublée, hauteur inchangée),
- un cockpit plus volumineux (version biplace),
- une voilure agrandie (envergure conservée mais corde agrandie vers l'avant à partir de la moitié de l'envergure environ),
- un fond de fuselage plus bombé (passage d'un réservoir de 250 gallons à un réservoir de 600 gallons) : le réservoir de 250 gallons portait une quille unique à l'arrière, tandis que le 600 gallons avait deux quilles inclinées à peu près au même endroit que la quille unique en longitudinal. La surface d'une quille inclinée était environ double de celle de la quille unique.

Pour certaines versions, ces modifications étaient combinées les unes avec les autres de telle sorte qu'en face de changements de la vrille, il était impossible de définir la modification qui avait provoqué ce changement.

Pour toutes les versions du Lightning, la vrille la plus fréquemment rencontrée était notablement agitée en tangage et roulis ; il s'agit toutefois d'agitations ordonnées.

En plus de la vrille agitée, un autre type de vrille a été trouvé (en soufflerie et sur avion) mais seulement pour certaines versions. Par rapport à la première vrille, cette dernière vrille était sensiblement moins agitée, moins piquée et plus rapide, sans qu'il s'agisse toutefois d'une vrille qui puisse être qualifiée de plate et rapide.

A partir d'une vrille agitée, l'arrêt s'obtenait en manoeuvrant une seule gouverne : il faut entendre par là que les autres gouvernes, laissées à un braquage quelconque, n'empêchaient pas l'arrêt. Stopper une vrille calme était moins simple puisqu'une manoeuvre supplémentaire sur une autre gouverne s'avérait nécessaire.

Une ou plusieurs modifications géométriques apportées au Lightning avaient donc détérioré, mais modérément, sa vrille. Définir cette ou ces modifications était évidemment impossible par des essais avion.

En soufflerie, en étudiant séparément chacune des modifications citées ci-dessus, il a pu être mis en évidence que c'était le remplacement de la quille unique par les deux quilles inclinées (voir figure 24) qui avait, le plus, changé le caractère de la vrille. Là encore on se trouve manifestement devant un cas qui impose de ne considérer les résultats généraux que comme des indications et non des certitudes.

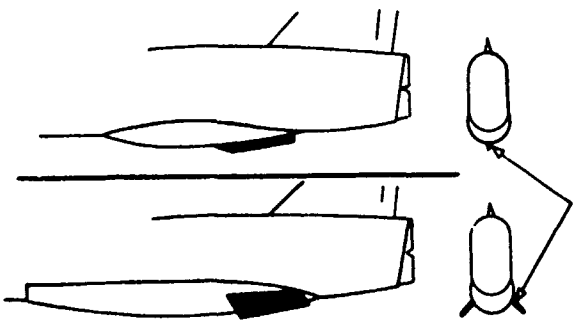

Fig. 24 - Lightning - Formes du fond de fuselage

LIMITINC FLIGHT CONTROL SYSTEMS

by

David K. Bowser
Group Leader
Air Force Flight Dynamics Laboratory
Wright-Patterson Air Force Base, Ohio 45433
USA

SUMMARY

The use of automatic flight control systems for the improvement of an aircraft's high-angle-of-attack flight dynamics as well as the prevention of loss of control is becoming a more commonplace practice. Implementations range from relatively simple stick pushers as on the F-104 to more complex stability augmentation and limiting systems where state information is used to compute switching boundaries as a function of several variables such as angle of attack, sideslip angle, and pitch rate. Augmentation of this sort has been used as a fix for problems of existing aircraft and more recently has been incorporated early in the design stage as on the control-configured vehicles. This paper addresses the development and application of various types of automatic flight control systems for high-angle-of-attack augmentation and limiting. Considerations included are improved handling qualities for maximum tracking effectiveness, reduced pilot workload, control-configured vehicles, stall inhibitors, and departure prevention systems.

LIST OF SYMBOLS

C_i - ith switching boundary coefficient

C_ℓ - Dimensionless rolling moment coefficient

C_n - Dimensionless yawing moment coefficient

K_i - ith control law coefficient

L - Rolling moment

L_r - Dimensional rolling moment coefficient due to body-axis yaw rate

N - Yawing moment

N_p - Dimensional yawing moment coefficient due to body-axis roll rate

p - Body-axis roll rate

q - Body-axis pitch rate

r - Body-axis yaw rate

r_3 - Stability-axis yaw rate

S - Laplace operator

V_o - Free-stream velocity

Z_α - Dimensional normal force coefficient due to α

α - Angle of attack

α^* - Departure boundary

$\dot{\alpha}$ - Angle of attack rate

β - Sideslip angle

δ_{a_d} - Aileron command due to departure preventer

δ_{e_d} - Elevator command due to departure preventer

δ_{r_d} - Rudder command due to departure preventer

INTRODUCTION

Limiting flight control systems have evolved chiefly as a means to provide a solution to loss-of-control problems occurring at high angles of attack. Due to rapidly changing stability and control characteristics in the near-stall flight regime, degraded and/or dangerous flying qualities may result.

Degraded flying qualities may be caused by buffet buildup, reduced aircraft damping, nonlinear aerodynamic effects, and/or pronounced dynamic coupling effects with increasing angle of attack. These effects can cause poor tracking performance and poor ride qualities at high angles of attack.

Dangerous flying qualities can result from rapid changes in bare airframe forces and moments encountered with increasing angle of attack. Uncontrollably large forces and moments may exist in certain ranges of angle of attack so that phenomena such as pitch up, nose slice, wing rock, and/or spin may be exhibited if the pilot allows the aircraft to enter that flight regime. Limiting systems are designed to guard against inadvertent entries into such flight regimes.

The above phenomena would appear to be open loop in nature for the most part, however evidence exists that wing rock may be both an open-loop (Reference 1) and potentially a closed-loop phenomena. Nose slice has been thought of as primarily an open-loop phenomena, but Reference 2 has shown that in one instance pilot closure of a pitch attitude to elevator tracking task can cause an open-loop lateral-directional pole to migrate with increasing pilot gain near stall angles of attack toward a strongly unstable right-half plane real zero. This right-half plane zero was caused primarily by the complex coupling terms L_α and N_α. Consideration of only bare airframe characteristics predicts an oscillatory divergence whereas flight experience shows an initial exponential divergence as predicted by the pilot-in-the-loop analysis of Reference 2.

Since there is evidence that both open-loop and closed-loop phenomena exist, careful consideration of control system structure and gain selection can be used to eliminate or at least attentuate some of the closed-loop, high-angle-of-attack, loss-of-control problems if their nature can be sufficiently identified. However, when the point is reached where the destabilizing forces and moments acting on the airplane exceed the control forces and moments available for stabilization, loss of control will result no matter how smart the flight control system or pilot. The only ways to prevent such loss of control are to reduce the destabilizing forces and moments, increase the control forces and moments available for stabilization, and/or to limit aircraft attitudes and angular rates to insure that the aircraft will not enter the region of loss of control.

Depending upon the aircraft and its mission, even if dangerous loss-of-control conditions are known to exist, they may be so far removed from the normal flight regime that a limiting system is not warranted. A simple warning system such as lights, audible tone, stick shaker, etc., or even natural warning through aerodynamic buffet may be more than adequate. However, if the aircraft, its mission and loss-of-control characteristics warrant a limiting system, a switching boundary must be established to trigger the limiting system. Thus comes the concept of a loss-of-control boundary.

The computed loss-of-control boundary which will be used to trigger the limiting system should be established to insure that all likely loss-of-control situations are covered. In actuality, the true loss-of-control boundary can be a complex nonlinear function of many parameters such as angle of attack, pitch rate, roll rate, sideslip angle, external store complement, etc. However, a switching boundary which is a complex function of all of these variables is not practical. In many cases, the switching boundary which has been selected for limiting systems has been simply a fixed value of angle of attack led by pitch rate to guard against dynamic overshoot. This fixed angle of attack is chosen small enough so that loss of control will not be induced by adverse values of other influencing parameters.

A simple example of the influence of factors other than simply angle of attack and pitch rate is shown in Figure 1. Above the loss-of-control boundary shown is a known region of pitch up which is primarily a function of angle of attack. However, as higher roll rates are achieved, the angle of attack at which pitch up can occur reduces due to inertia coupling effects. Shown on this figure is a switching boundary for a simple angle of attack limiter. If chosen as shown, this limiter will not protect against pitch up at extreme roll rates and at low to moderate roll rates it sacrifices maneuverability due to reduced load factor and turn rate capability. One could limit roll rate at high angles of attack but this also directly limits maneuverability. If maneuverability is a dominant consideration for the aircraft and its mission, then a loss-of-preventer triggered as shown in Figure 1 as a function of both angle of attack and roll rate would allow for maximum maneuverability while still protecting against loss of control.

As is evident from the above simple example, loss of control prevention and maneuverability may be two conflicting concepts. Careful consideration as to the choice of the switching boundaries to be used with the limiting flight control system should be made with the aim of getting the best of both worlds.

The remainder of this paper deals with a short and by no means complete history of limiting flight control systems beginning with simple stick pushers and ending with limiting systems triggered as a complex function of several state variables including multi-axis feedback loops. This is followed by a discussion of a current concept for a limiting flight control system tailored for the A-7D which will not only provide a limiting function but will also improve high-angle-of-attack flight by delaying loss of control. The paper is then concluded by a discussion of a recommended approach to loss-of-control problems and limiting. This discussion also includes some interesting problems and possibilities for control-configured vehicles (CCV).

HISTORY

High-angle-of-attack limiting systems have been around since the most early days of manned flight, when it was recognized that aerodynamic buffet felt by the pilot was a prelude to loss of control and appropriate action had to be taken to increase airspeed (reduce angle of attack) or loss of control would ensue. This, in a fundamental sense, is a limiting flight control system where the switching boundary is the aerodynamic buffet and the pilot recognition of the warning and his subsequent action are the limiting function. However, many current aircraft such as the A-7 and F-4 exhibit aerodynamic buffet onset so far before loss of control occurs and the buffet intensity buildup is stretched over such a large range of angle of attack, that it cannot effectively be used as a warning of impending loss of control.

Lights and/or audible tones triggered on some threshold of angle of attack have been developed and used as a loss-of-control warning system for a large complement of aircraft and are effectively in use for many current aircraft. However, in combat situations when pilot workload is great, other audible tones are in use and the situation calls for chiefly head-out-of-the-cockpit maneuvering, lights and/or audible tones

can easily be ignored.

In situations where aerodynamic buffet cannot be relied upon and pilot workload makes doubtful the effectiveness of lights and/or audible tones for warning, stick shakers and rudder pedal shakers have been developed and used as effective warning devices. However, rudder pedal shakers are useless when the pilot is maneuvering with his feet on the floor.

In situations where more than loss-of-control warning is required, devices such as stick pushers have been developed to provide a nose down pitching moment to reduce angle of attack when some maximum allowable angle of attack has been reached. To guard against dynamic overshoot in angle of attack, pitch rate has been used to lead the limit angle of attack in some stick pusher implementations. The systems are normally implemented so that they can be overriden by a large pilot breakout force. However many pilots tend to dislike such systems, even if what the pilot is trying to do is wrong, since the system tends to take control of the aircraft from the pilot. To handle high-angle-of-attack pitch-up problems, stick pushers have been developed for the F-101 and F-104 aircraft and have been effectively in use for many years on these aircraft.

In more recent years, Honeywell developed what they called a Boundary Control System for the Air National Guard F-101 aircraft to handle the previously mentioned pitch-up problem. This system is similar to a stick pusher but with one particularly important difference. Rather than pushing the stick forward at the switching boundary, the Boundary Control System acts as a moving-stick stop in that once a limit value of angle of attack and weighted pitch rate is reached, further aft motion of the stick is not possible unless the pilot applies a sufficiently large pull force to override the automatic system. This system is more readily acceptable to pilots since it appears to be a natural characteristic of the vehicle rather than the artificial feeling of the stick pusher pulling the stick from the pilot's hands.

In 1959, in time between the development of the stick pusher and the Boundary Control System, the Cornell Aeronautical Laboratory (CAL) performed a particularly noteworthy effort with regards to a high-angle-of-attack, loss-of-control problem on the F-7U aircraft (Reference 3). Rather than limiting aircraft motions within some prescribed loss-of-control boundary, CAL took the approach of changing the loss-of-control boundary through use of a control law tailored for high-angle-of-attack flight. A large forward vertical canard was installed on the aircraft to provide directional control power at high angles of attack for use in stabilization of the aircraft through an open feedback loop. This is stability axis yaw rate. By closing the directional axis loop in this manner, the aircraft tended to roll about its velocity vector rather than an axis near the aircraft longitudinal body axis. In this way, during high-angle-of-attack rolling flight, sideslip angle is held near zero. By minimizing sideslip excursions in high-angle-of-attack rolling flight in this manner the post-stall gyration problem of the F-7U was effectively handled at least on an experimental basis.

In 1971, NASA Langley Research Center demonstrated the concept of an automatic spin preventer on one of their F-111 free-flight drop models (Reference 4). The system was triggered when fixed levels of angle of attack and yaw rate were exceeded. The system was attempting to sense the incipient spin. When the boundary was exceeded, normal spin recover controls were automatically applied. A normal accelerometer sensed whether the incipient spin was erect or inverted and the sign of the yaw rate determined the sense of the lateral and directional controls required. Spin recovery controls were automatically held until angle of attack and yaw rate had returned to levels consistent with controlled flight at which time the automatic system returned control of the drop model to the operator. This system was demonstrated to be effective in preventing the spin of the dynamically-scale free-flight drop model of the F-111 aircraft.

In the early 1970's General Dynamics developed and tested on an F-111 aircraft a Stall Inhibiting System (SIS) (Reference 5). This system was designed to inhibit loss of control at high angles of attack and was triggered on angle of attack alone. The SIS consisted of two basic parts. One part was called an Angle-of-Attack Limiter and the other was called a Beta Reducer. The Angle-of-Attack Limiter was activated when the switching boundary had been exceeded and the stabilator was then driven in proportion to the difference between the measured angle of attack and the switching boundary to eventually limit angle of attack. This system operated in conjunction with the normal longitudinal command augmentation system (CAS) of the F-111 and reduced CAS gains above the switching boundary. The Beta Reducer was also triggered when another switching value of angle of attack had been exceeded. At this time additional augmentation loops (rolling tail to rudder interconnect with angle of attack and stability axis yaw rate to rudder feedback) were activated to heavily damp the directional axis to drive sideslip angle near zero. The total system was implemented to drive the control surfaces, not the stick, so that again the characteristics appear to be the natural characteristics of the aircraft. However, since CAS gains are reduced and angle of attack to elevator feedback is initiated above the switching boundary, stick forces are increased and CAS nose-up authority is reduced. The system was refined and worked well during the flight test program.

In 1973 the Calspan Corporation performed a design study and manned simulation of an automatic departure prevention system for the A-7D aircraft (Reference 6). In one fundamental aspect this system is different than all of the limiting systems described above. It not only provided a limiting function, but it also improved high-angle-of-attack stability and allowed the simulator pilots to take advantage of an expanded usable maneuver envelope. The approach taken during the study phase of the effort was to establish the sensitivity of aircraft loss of control to variations in parameters such as angle of attack, sideslip angle, Mach number, roll rate, turn rate, and center-of-gravity position. Based upon wind tunnel data analysis, digital simulation, and existing flight test information, a definite trend of angle of attack required for loss of control decreasing with increasing sideslip angle was established for the A-7D. Based upon this analysis a switching boundary was formulated for the limiting flight control system. The boundary was a function of not only angle of attack biased by weighted pitch rate but also a function of the magnitude of the sideslip. This approach was in consonance with the concept of allowing for the maximum level of maneuverability while guarding against loss of control. The control laws developed during this effort were similar in concept to those developed for the SIS. Angle of attack was retarded in proportion to state variable excursions beyond the switching boundary, and at the switching boundary heavy directional augmentation was initiated to reduce sideslip angle toward zero. The directional augmentation added to the normal A-7D augmentation beyond the switching boundary was based upon sideslip angle, the

integral of sideslip, and stability axis yaw-rate feedback. All of the system and switching boundary gains were left as variables during the simulation to allow for optimization of the system with the pilot in the loop. This system, its implementation, the simulation, and results will be discussed in detail in the next section.

As can be seen, there is a great range of limiting flight control systems that have been designed to address the myriad of problems that are classed as high-angle-of-attack loss-of-control problems. Such factors as pilot acceptability, system effectiveness, system cost, and complexity must be considered when choosing the approach to solving such problems. A system that is interruptive will not likely receive pilot acceptance. A system which operates in a manner to appear to the pilot to be the natural response of the aircraft can more readily obtain pilot acceptance if it is also reliable and effective. The system described in the next section has promise of being such a system. The final proof of such a concept has to be flight test demonstration.

A CURRENT CONCEPT

Reference 6 documents the conceptual design, breadboard development, and pilot-in-the-loop evaluation of an automatic departure prevention system for fighter aircraft. Using the A-7D as the study aircraft, a departure boundary characterized by angle of attack and sideslip angle was determined from the available data. The departure boundary was then used to help design an automatic departure preventer. The departure preventer provides automatic control inputs to the pitch and yaw axes. Based upon analysis and simulation results, the automatic departure prevention device works smoothly and will benefit the A-7D aircraft. With the departure preventer, the pilots could maneuver freely, with great confidence, and use the full capability of the airplane well beyond the present departure boundary. The program documented in Reference 6 consisted of five phases: analysis, design, digital simulation, fabrication of breadboard hardware, and piloted ground simulation.

The goal of the departure preventer was to deter the pilot from departing the aircraft from controlled flight without degrading its full operational flight envelope. In the study and simulation effort, this goal was exceeded since the departure preventer designed was not only capable of preventing loss of control but it was also capable of expanding the A-7D's flight envelope. To achieve this goal the system was designed to permit the aircraft to fly along the departure boundary rather than to force the aircraft from it. Clearly, the determination of the departure or loss-of-control boundary is the first step toward designing such a system. The departure boundary is considered analytically to be a stability boundary. Determination of the boundary was based upon the use of semi-analytical methods relying heavily on digital computer simulation and physical considerations. A stability criterion based on an autonomous system description with initial conditions but without control inputs was selected in that it was readily amenable to digital computer simulation.

The stall approach and departure characteristics of the A-7D are as follows. For normal 1 "g" stalls in the cruise configuration, buffet onset occurs at 11.5 to 13.5 degrees of angle of attack and increases in intensity until stall, which occurs at approximately 21 degrees of angle of attack. The stall characteristics of the A-7D are fairly independent of external store arrangement and Mach number. From buffet onset to the stall, a relatively wide range of angle of attack exists (as high as 10 degrees). As the angle of attack is increased beyond buffet onset, the intensity of the buffet slowly increases for a while then stays constant, providing inadequate stall warning. The A-7D stall is defined as a directional divergence (nose slice) in either direction accompanied by a wing drop in the direction of yaw. Recovery during departure is immediate if the stick is returned to neutral and released while simultaneously applying opposite rudder provided this action is taken before approximately 20 degrees of yaw is reached.

In determining the departure boundary, the available flight test data were first surveyed to see if there existed general trends of the major state variables such as angle of attack, sideslip angle, yaw rate, etc., at the departure. The high-angle-of-attack wind tunnel data were then analyzed with the primary emphasis placed on the lateral-directional static derivatives, C_{n_β} (α, β) and C_{ℓ_β} (α, β). Calculations using the high-angle-of-attack wind tunnel data showed that the lateral and directional static derivatives were strongly affected by the angle of attack as well as the angle of sideslip. These characteristics are shown in Figures 2 and 3. Examination of stall approach flight test time histories and full-scale spin evaluation tests on the A-7B/A and the A-7D revealed a general trend of angle of attack versus sideslip angle in the vicinity of departure. When the sideslip angle was large, the angle of attack at the departure tended to be smaller. Other variables such as angular velocities and aileron position were also studied for a recognizable correlation with departure; however, there was no definable trend for these variables.

A nonlinear six-degree-of-freedom digital computer program incorporating the A-7D wind tunnel data for high angles of attack was used to establish the departure boundary by applying several values of the initial sideslip angle from some isolated equilibrium conditions in the vicinity of departure. As shown in Figure 4, the six-degree-of-freedom digital simulation verified a general trend of angle of attack versus sideslip angle at the departure. The α-β departure boundary is defined by

$$\begin{aligned} \alpha^* &= C_1 - C_2\,|\beta| && |\beta| < 30^\circ \\ &= C_1 - 30\,C_2 && |\beta| \geq 30^\circ \end{aligned} \qquad (1)$$

where $C_1 = 20$, $C_2 = 0.2$. The effects of the c.g. location, gross weight, and turn rates (up to 15 deg/sec and 3.5 "g" level turns) were determined and were found to be relatively insignificant.

An attempt was made in the program to correlate the wind tunnel data with the flight test data available. Because of the relatively low quality of the flight test data, no further attempt was made to identify the stability and control parameters of the A-7D aircraft to achieve a better representation of the aerodynamic coefficients for computer simulation. However, to allow for possible discrepancy of the wind tunnel data and the full-scale A-7D aircraft aerodynamic characteristics, the coefficients, C_1 and C_2, were varied in the digital program and their effects were evaluated in the design of the departure preventer.

Thus, the theoretical basis used in establishing the loss-of-control boundary was the stability of the autonomous system at some isolated equilibrium states in the near-departure region. Relying on physical considerations and digital computer simulation, a simplified departure boundary described by only two major state variables, angle of attack and sideslip angle, was determined.

The design objectives of the departures preventer were twofold. The preventer must be able to prevent the aircraft from departing the full operational flight envelope of the aircraft. The preventer must be automatic, simple, and readily adaptable to the existing A-7D flight control system.

To meet the second design objective, the preventer must work within the existing automatic flight control system (AFCS) of the A-7D. Schematic diagrams of the pitch axis and yaw axis of the A-7D automatic flight control system are shown in Figures 5 and 6 respectively. The departure preventer inputs are also shown in the schematics.

A schematic for the lateral axis is not shown. Early in the design of the departure preventer, consideration was given to the neutralization of the lateral control upon activation of the departure preventer. A scheme utilizing a proportional plus integral nullification of pilot and AFCS lateral commands was mechanized on the breadboard of the departure preventer. However, with the longitudinal portion of the departure preventer which tends to limit the excursion of angle of attack beyond the departure boundary, and with the directional portion of the departure preventer which nullifies the sideslip, the lateral control portion of the departure preventer became unnecessary. This allowed the pilot to freely use the lateral control for roll maneuver upon activation of the departure preventer.

To meet the first design objective cited above, and in view of the previously determined departure boundary, the device should command a longitudinal control action necessary to regulate the aircraft motion at the departure boundary. At a given angle of attack in the stall/departure region, a nose-down moment must be automatically applied to reduce the angle of attack whenever the angle of sideslip exceeds the boundary. In addition, at a given sideslip angle, a nose-down moment must be automatically applied to reduce the angle of attack whenever the angle of attack exceeds the boundary. The sideslip should be reduced or eliminated in the stall/departure region to increase the maximum usable angle of attack to its full capability for the aircraft. To achieve this, the directional stiffness of the aircraft should be augmented at the stall/departure boundary, and furthermore the aircraft should be restricted to roll about its flight path.

To regulate the angle of attack along the departure boundary, a simple proportional control law for the longitudinal control may be used.

$$\delta_{e_d} = K_1 (\alpha - \alpha^*) \qquad \text{if } \alpha - \alpha^* \geq 0$$

$$= 0 \qquad \text{if } \alpha - \alpha^* < 0 \tag{2}$$

where α^* is the relation for the departure boundary previously given. With proper selection of K_1, the steady state offset resulting from the proportional control will permit the pilot to use the full capability of the aircraft well beyond the previous departure angle of attack towards the conventional aerodynamic stall. For the A-7D, maximum lift coefficient occurs between 28 and 30 angle of attack, depending on the unit horizontal tail (UHT) position. Based upon the above control law and the departure boundary relation, once activated, the departure preventer will command a trailing-edge-down UHT whenever α or $|\beta|$ or both increase, thereby achieving the desired function. Notice that as defined, the control law for the longitudinal portion of the departure preventer will cause no transient with its activation or deactivation.

To the directional control, the main departure prevention function is to keep sideslip angle small. This is accomplished by use of a proportional plus integral feedback of sideslip angle to the rudder in addition to the feedback of stability-axis yaw rate, r_s, to the rudder.

$$\delta_{r_d} = K_4\beta + K_5 \int \beta \, dt + K_6 r_s \qquad \text{if } \alpha - \alpha^* \geq 0$$

$$= 0 \qquad \text{if } \alpha - \alpha^* < 0 \tag{3}$$

The use of the stability axis yaw rate feedback to the rudder is to restrict the airplane to roll about its flight path. It also tends to minimize the effect of inertia coupling from the longitudinal to lateral-directional motions which is a very desirable feature. The use of the proportional plus integral feedback of sideslip angle to the rudder was aimed at keeping sideslip angle near zero in the near-departure region, since there are no known maneuvers that call for intentional sideslip in the post-stall region. As a matter of fact, since rolling is not restricted, integral of sideslip angle feedback is required when the bank angle is large (~90). With large bank angle, the gravitational force can develop substantial side force and thereby generate a large sideslip. Through use of integral of sideslip angle feedback, the angle of sideslip can be reduced.

Some modifications of the above set of simple control laws were required to achieve better departure prevention. First, the switching boundary that activates the departure preventer was modified to include an anticipation term, $C_3\dot{\alpha}$, to account for rapid changes in angle of attack during maneuvers. The modified switching boundary became

$$\alpha^* = C_1 - C_2 |\beta| - C_3\dot{\alpha} \tag{4}$$

In the presence of turbulence, the anticipation term could become excessively large, thereby causing "premature" activation and deactivation of the departure preventer. Neglecting the effect of speed changes, which are slow by comparison, the rate of change of angle of attack may be approximated by

$$\dot{\alpha}(S) = \frac{S}{S - \frac{Z_\alpha}{V_o} q(S)} \tag{5}$$

Subsequent digital simulation showed that substitution of the lead term (S/S+.25)q(S) for a direct $\dot{\alpha}$ term proved to be adequate and desirable. The switching boundary became in final form

$$\alpha^* = C_1 - C_2 |\beta| - C_3 (S/S+.25)q \tag{6}$$

The longitudinal control law remained

$$\delta_{e_d} = K_1 (\alpha-\alpha^*) , \quad \alpha-\alpha^* \geq 0$$
$$= 0 , \quad \alpha-\alpha^* < 0 \tag{7}$$

where α^* as defined above gives the elevator control in final form

$$\delta_{e_d} = K_1 [\alpha-C_1-C_2|\beta| + C_3 (S/S+.25)q] , \quad \alpha-\alpha^* \geq 0$$
$$= 0 , \quad \alpha-\alpha^* < 0 \tag{8}$$

The modifications and refinement of the directional control law were pursued in the following two areas: the yaw rate feedback and the proportional gain of the sideslip angle feedback. To provide better steady-state performance in a coordinated turn, the pure proportional gain for the stability-axis yaw rate feedback loop was replaced by a high-pass circuit with a washout time constant of approximately one second. This time constant and gain were determined from a root locus analysis using the linearized lateral-directional equations of motion. The directional control law for the departure preventer finally took the following form:

$$\delta_{r_d} = \left(K_4 + \frac{K_5}{S}\right) \beta + \frac{K_7 S}{S+1} (r - \alpha p), \quad \alpha-\alpha^* \geq 0$$
$$= 0 , \quad \alpha-\alpha^* < 0 \tag{9}$$

It should be noted that the integrator in the above expression does not start to integrate until $\alpha-\alpha^*$ exceeds zero. If $\alpha-\alpha^*$ becomes less than zero, the integrator resets the zero output, thus assuring that the integrator has a zero initial condition when the departure preventer is activated. The form of the proportional gain of the sideslip angle feedback to the rudder, K_4, is modified to be a function of $\alpha-\alpha^*$ rather than just a constant such as K_5 and K_7. Two factors were considered in this modification: (1) to prevent the undesirable transients in the lateral-directional motion of the aircraft associated with the activation and the deactivation of the departure preventer because of nonzero sideslip angle and (2) to compensate for C_{n_β}, which is a function of both α and $|\beta|$.

The initial determination of departure preventer gains was based largely on physical considerations. For example, K_4 was chosen so that when $\alpha-\alpha^* = 2 - 4^\circ$, the value of the augmented directional static stability, $C_{n_\beta}(\alpha) + K_4 C_{n_{\delta_r}}(\alpha)$, would achieve the level of C_{n_β} at low angles of attack, say at $\alpha = 0$ to 10°. The stability-axis yaw rate feedback gain K_7 was initially determined such that at Dutch roll frequency and above, the augmented effective cross coupled damping N_p and L_r would be predominantly aerodynamic and the effect of inertial coupling due to the pitch rate would be minimized. These gains and others were finally determined using six-degree-of-freedom nonlinear digital simulation. The nominal values along with the switching boundary are listed in Table 1.

The Calspan ground-based simulation that was used in the Reference 6 study is a fixed-base simulator with an outside view display and a full instrument panel display. The aileron and elevator control is a standard stick with a two-degree-of-freedom electrohydraulic feel system. The rudder pedals are loaded with a mechanical spring. The elevator-aileron system is able to simulate breakout forces and hysteresis characteristics and control system dynamics. Summing points are provided to permit signals for simulation of bobweights, etc.

A full instrument panel is provided with aircraft and engine instruments. Full maneuvering capability is simulated in that the equations are scaled for outside view display, a "line drawing view" is computer-generated and presented on a large CRT with intensity modulation. A high-resolution TV camera views the oscilloscope presentation and transmits it to a 1,000 line, high-intensity TV projection tube which projects the image on the rear of a translucent screen. The screen is in front of the simulator. The field if view is $\pm 30^\circ$ horizontal, 37° vertically up and 7° vertically down.

For the computations, a hybrid computer facility is used. The aerodynamic data and equations of motion are solved by the digital computer. The control system dynamics and associated nonlinear functions are solved on analog computers which also drive the instruments.

A flyable target airplane image was generated for the heads-up pursuit tracking. The target airplane aerodynamics are simplified and only a stick is needed to manually fly the target airplane. The target airplane image represented a delta wing airplane, presented to the pursuing pilot always in a proper perspective.

A rigorous pre-evaluation of the departure preventer was performed prior to any formal evaluations. These pre-evaluations examined the characteristics of the device and determined the most efficacious gain settings to prevent departures while not reducing the pilot's capabilties with the simulated A-7 airplane. Initially, many maneuvers were flown, purposely entering the departure region and also using pro-spin control inputs. During this phase many gain levels were explored until departure-free maneuvering was attained.

As a result of the pre-evaluation tests, the following characteristics were chosen for the formal evaluation:

a. Switching Boundary:

$$\alpha^* = C_1 - C_2 |\beta| - C_3 (S/(S+.25)q \quad (10)$$

where C_1 = Switching boundaries at 18° and 20° and 22° angle of attack for zero sideslip

C_2 = A switching slope of 0.2 deg/deg

C_3 = 0.1 deg/deg/deg

b. Departure Preventer:

$$\delta_{e_d} = 1.0 (\alpha-\alpha^*) \quad (11)$$

$$\delta_{a_d} = 0 \quad (12)$$

$$\delta_{r_d} = (K_4 - \frac{0.5}{S})\beta + \frac{1.5S}{S+1} (r - \alpha p) \quad (13)$$

where

$$K_4 = - .14 (\alpha-\alpha^*) \quad (14)$$

The rating scale and comment card for the formal evaluations were as follows:

Rating Scale:

a. Much improved over A-7, can use full capability of airplane with confidence.

b. Better than A-7, but with some shortcomings.

c. No improvement over A-7.

d. Worse than A-7.

Comment Card:

a. Does departure preventer operate smoothly and satisfactorily?

b. Do you have confidence in the total system?

The planned evaluation matricies were as follows:

		SWITCHING BOUNDARY 1 : C = 18					
		DEPARTURE PREVENTER WITH ELEVATOR AFCS AUTHORITY OF 4.8°		DEPARTURE PREVENTER WITH ELEVATOR AFCS AUTHORITY OF 9.6°		DEPARTURE PREVENTER WITH ELEVATOR AFCS AUTHORITY OF 14.4°	
PILOT	EVAL	ON	OFF	ON	OFF	ON	OFF
1	1						
	2						
	3						

In the matrix, the starred runs were all nominal airplane with an elevator AFCS authority of 4.8 degrees.

An identical matrix was made for Switching Boundary 2, C_1 = 20 degrees, and it was planned that each pilot would experience the same matrix of runs.

For the evaluation runs, a pursuit tracking task was performed. The target airplane was initially two miles directly ahead of the pursuing airplane and both airplanes were at the same altitude and identical airspeed in trimmed flight. The pursuing pilot would fly the simulated A-7 to a relatively close position (100 to 300 ft) behind the target airplane at which time the target airplane was maneuvered in climbing turns which the pursuit pilot followed. This resulted in a scissors maneuver between the two airplanes and gradual loss of airspeed that took the pursuing aircraft into the departure region.

The results of the formal evaluation stabilized very rapidly as is indicated by the relative ratings which are presented in Table II.

There are several points that can be gleaned from the pilot's comments.

From the ratings it appears that the pilots were insensitive to the difference in switching boundary. They were able to discern the difference in switching boundary, but except for one case, the difference had an insignificant effect on the rating.

As formal evaluations proceeded, the test conductors quickly became aware that the pilots' comments and ratings were consistent and very stable. Because of the attained stability of comments and ratings, an opportunity to deviate from the planned matrix was taken in order to expand the formal evaluations.

The A-7 has an AFCS cut-out in the lateral mode for angles of attack above eighteen degrees. One of the pilots did ten evaluations where the automatic cut-out feature was inactivated. No changes in the pilot comments or pilot ratings were observed.

The analytical and experimental studies of Reference 6 led to the following conclusions:

a. The simplified departure boundary, which is characterized by only the two major parameters, the angle of attack, and the angle of sideslip, has been shown to be desirable and adequate for use in the design of the departure preventer for the A-7D aircraft.

b. A switching boundary based upon the $\alpha - |\beta|$ departure boundary and the time rate of change of α (or its substitute using pitch rate passing through a high pass filter) for activation and deactivation has provided a natural means to design a departure preventer. The nonlinear longitudinal control law is a function of the magnitude of the sideslip as well as of the lateral-directional state variables, and the nonlinear directional control law is a function of the angle of attack as well as the lateral-directional state variables. Furthermore, the concept permits these devices to be deactivated outside the dangerous stall departure region.

c. The evaluation pilots consider the departure preventer, which when activated automatically commands the longitudinal control (UHT) and the directional control (rudder), has been shown to be very desirable. It works smoothly, and it permits the pilot to use an expanded maneuvering capability of the aircraft with confidence.

RECOMMENDED APPROACH TO LOSS-OF-CONTROL PROBLEMS AND LIMITING

The potential for loss of control at high angles of attack should be addressed by the aircraft designer from the very beginning of conceptual design. Steps should be taken to insure that the data necessary to determine high-angle-of-attack flight dynamics is available as early as possible so that if a serious problem or design deficiency is uncovered, the designer has a chance to solve the problem during the design phase before a costly retrofit program and/or acceptance of operational limitations are required.

In general, greater attention should be paid to aerodynamic design practices tailored for good high-angle-of-attack characteristics. The fundamental concept is to get the best high-angle-of-attack characteristics through fundamental aerodynamic design practices that can be afforded when weighed against performance, cost, and complexity. Improvements in this area are likely to directly benefit maneuverability and flight safety.

Having arrived at a basic aerodynamic design, flight control design practices can be used to further enhance high-angle-of-attack flying qualities. Attention has to be paid to the nonlinear and highly-coupled phenomena normally encountered at high angles of attack when formulating the augmentation system control laws and sufficient aerodynamic control power must be provided for the control system to effectively do its job. If a departure or loss-of-control boundary exists for the bare airframe, proper control system design may eliminate the loss-of-control problem without limiting.

At this point, the augmented aircraft high-angle-of-attack characteristics can be established. If a serious loss-of-control problem is still expected, at this time a limiting system should be incorporated into the design. The limiter should be incorporated only if necessary.

The general trend for limiting systems has been to add them on an ad hoc basis once a problem has been identified through flight test or operational experience. Not until recently, with the advent of CCV aircraft which are statically unstable over a relatively wide range of flight conditions, has the incorporation of a limiting system during the aircraft design phase been seen. However, if the instabilities for a particular CCV design are strong enough at high angles of attack and the associated aerodynamic control power available at these angles of attack is not sufficient to return the aircraft to lower angles of attack, the limiting system must not allow transients to these angles of attack or the aircraft may be locked into an uncontrollable trim condition much as the deep stall condition. However, consider the tail-slide maneuver. If the pilot wants the aircraft to go dead in the air during a vertical maneuver, he can do it against any current limiting system concept. In this situation the aircraft will slide back and encounter angles of attack near 180° and may never return to low angles of attack due to control power deficiencies versus aerodynamic instabilities at high angles of attack. Future CCV design trends towards strongly statically unstable aircraft may require the incorporation of a V_{min} limiting system to insure that the aircraft will not go dead in the air and to insure that sufficient dynamic pressure is available to allow the limiting flight control system to do its job. A V_{min} limiting system could be designed through use of engine thrust and pitch attitude as the control variables.

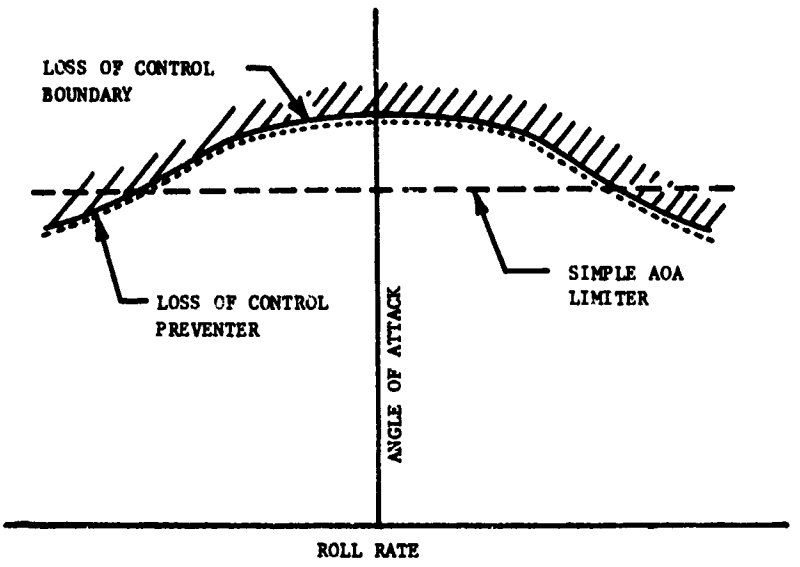

FIGURE 1 DEPARTURE PREVENTER SCHEMES

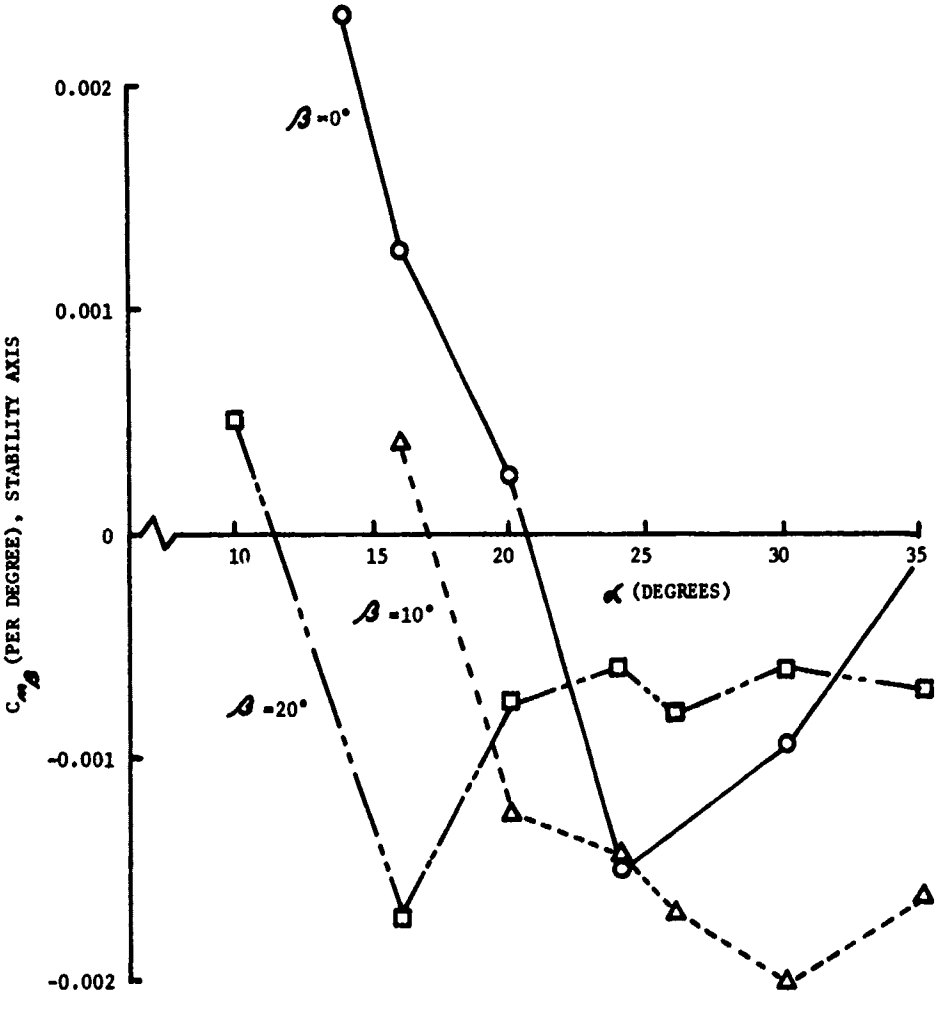

FIGURE 2 $C_{m_\beta}(\alpha)$ AT β= 0°, 10°, AND 20°

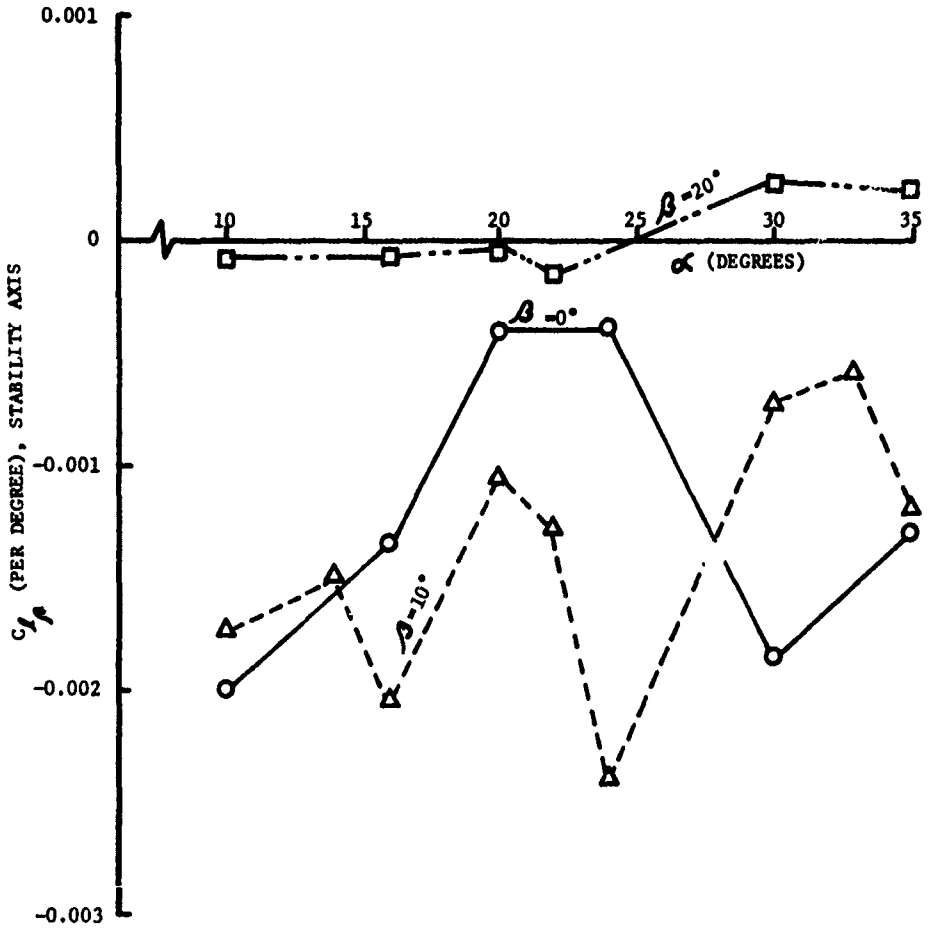

FIGURE 3 $C_{l_\beta}(\alpha)$ AT β= o°, 10°, AND 20°

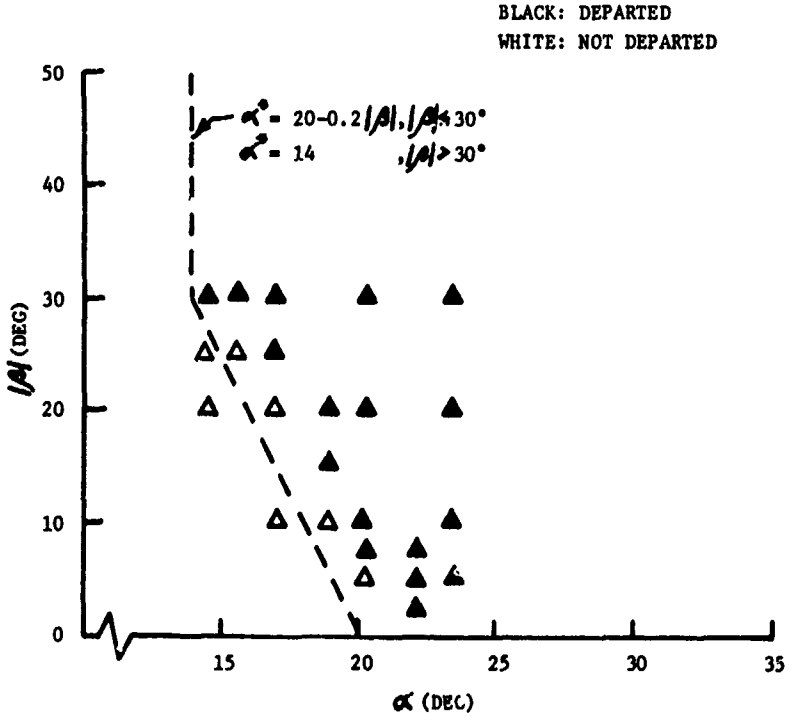

FIGURE 4 A-7 DEPARTURE CHARACTERISTICS OBTAINED FROM COMPUTER SIMULATION

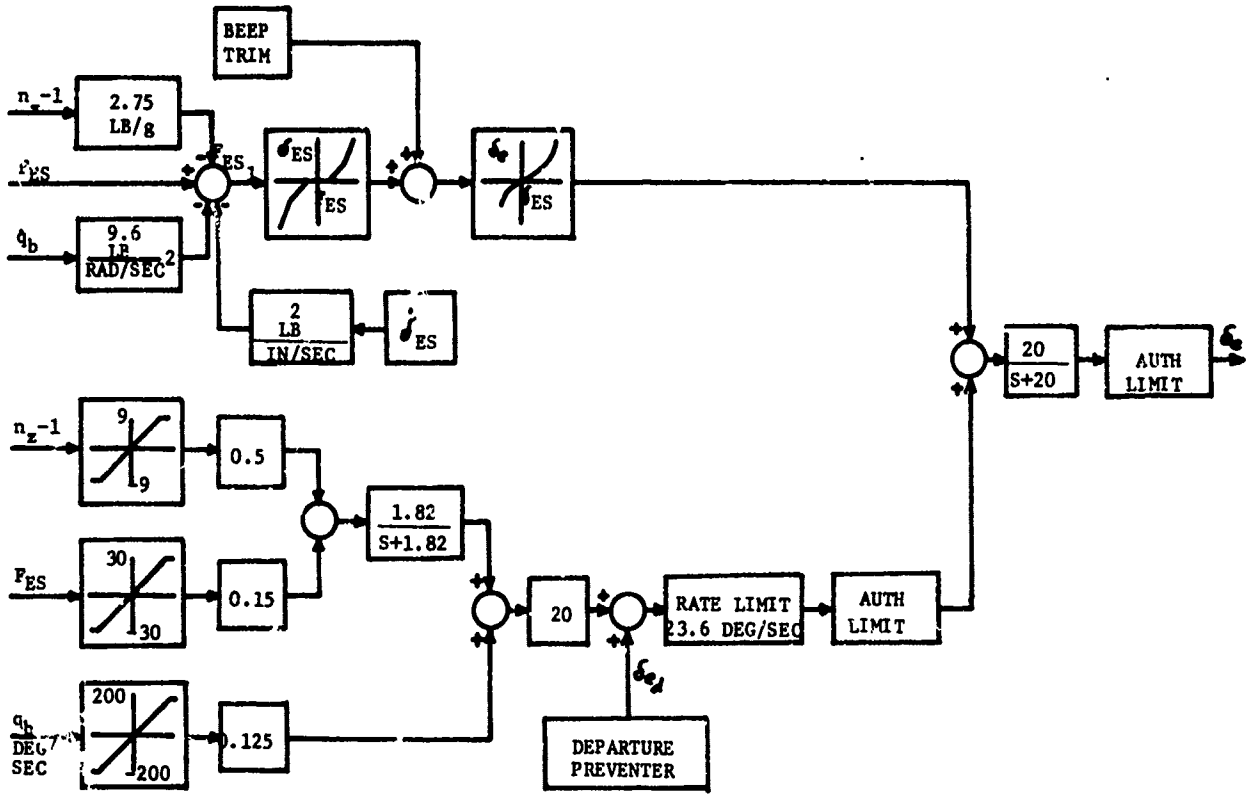

FIGURE 5 PITCH AXIS --CRUISE CONFIGURATION

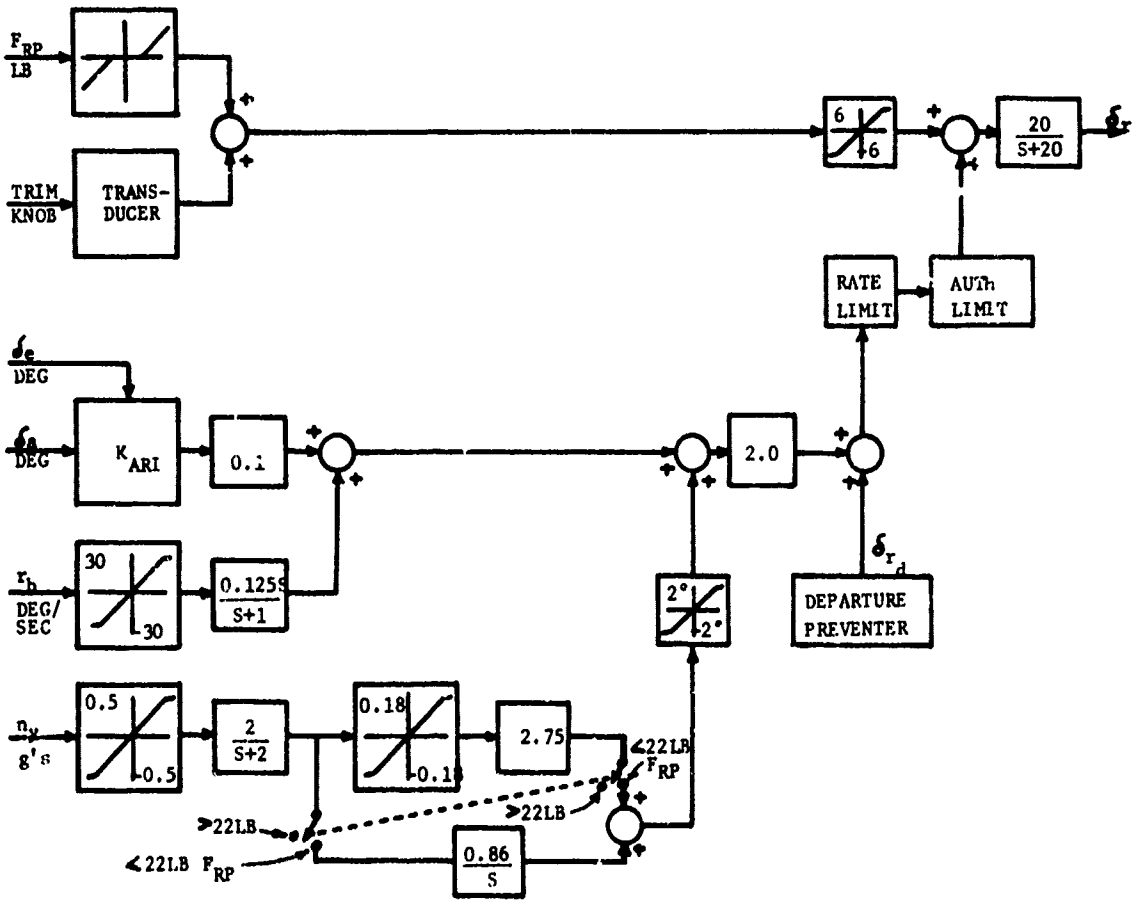

FIGURE 6 YAW AXIS -- CRUISE CONFIGURATION

TABLE I

SWITCHING BOUNDARY COEFFICIENTS
AND DEPARTURE PREVENTER GAINS

PARAMETERS		NOMINAL GAINS
SWITCHING BOUNDARY	C_1	18 - 20 (deg)
	C_2	.13 - .20 (deg/deg)
	C_3	.10 - .30 (deg/deg/sec)
DEPARTURE PREVENTER	K_1	1.0 - 3.0 (deg/deg)
	K_4	$-.14(\alpha-\alpha_0)$ (deg/deg)
	K_5	-.5 (1/sec)
	K_7	1.5 (deg/sec/sec)

TABLE II

RELATIVE RATINGS (* IS NORMAL AIRPLANE)

		SB_1					
		DP_a		DP_b		DP_c	
PILOT	RUN	ON	OFF	ON	OFF	ON	OFF
1	1	A+	C*	A+	C*	A+	C*
	2	A+	C*	A+	C*	A	B*
2	1	A	C*	A	C*	A	C*
		SB_2					
1	1	A+	C*	A+	C*	A+	C*
	2	A	C*	B	C*	A+	C*
2	1	A	C*	A	C*	A	C*
SUMMARIZED COMMENTS FROM BOTH PILOTS							
Primary reason for rating		Great, smooth, can use full capability of airplane with confidence	Seems no different than normal A-7	Great, smooth, can use full capability of airplane with confidence	Seems no different than normal A-7	Great, smooth, can use full capability of airplane with confidence	Seems no different than normal A-7

REFERENCES

1. Cord, T. J., AFFDL-TM-75-76-FGC, Hysteresis Induced Wing Rock, June 1975.

2. Johnston, D. E., Ashkenas, I. L., and Hogge, J. R., Systems Technology, Inc., AFFDL-TR-74-61, Investigation of Flying Qualities of Military Aircraft at High Angles of Attack, June 1974.

3. Schuler, J. M., CAL Report No. TB-1132-F-2, Flight Evaluation of an Automatic Control System for Stabilizing the Large Uncontrolled Motions of Airplanes in Stalled Flight, October 1958.

4. Gilbert, W. P. and Libbey, C. E., NASA TND-6670, Investigation of an Automatic Spin-Prevention System for Fighter Airplanes, March 1972.

5. Anderson, Charles A., AGARD Fluid Dynamics Panel, Specialists Meeting on Fluid Dynamics of Aircraft Stalling, Lisbon, Portugal, Stall/Post-Stall Characteristics of the F-111 Aircraft, 26-28 April 1972.

6. Chen, R. T. N., Newell, F. D., and Schelhorn, A. E., Calspan Corporation, AFFDL-TR-73-29, Development and Evaluation of an Automatic Departure Prevention System and Stall Inhibitor for Fighter Aircraft, April 1973.

ASYMMETRIC AERODYNAMIC FORCES ON AIRCRAFT FOREBODIES AT HIGH ANGLES OF ATTACK - SOME DESIGN GUIDES

by

Gary T. Chapman, Earl R. Keener and Gerald N. Malcolm
Ames Research Center, NASA
Moffett Field, California 94035

SUMMARY

This paper reviews the problem of aerodynamic side forces on forebodies produced by two types of flow: asymmetric vortices on bodies of revolution and nonuniform flow separation on square bodies with rounded corners under spinning conditions. Steady side forces that can be as large as the normal force are produced by asymmetric vortices on pointed forebodies. This side force has a large variation with Reynolds number, decreases rapidly with Mach number, and can be nearly eliminated with small nose bluntness or strakes. The angle of attack where the side force first occurs depends primarily on body geometry. The theoretical techniques to predict these side forces are necessarily semi-empirical because the basic phenomenon is not well understood. The side forces produced by nonuniform flow separation under spinning conditions depend extensively on spin rate, angle of attack, and Reynolds number. The application of simple crossflow theory to predict this side force is inadequate much below angles of attack of 90°.

1. INTRODUCTION

The flow field about an aircraft at high angles of attack is very complex. Typical of this flow are extensive, nonuniform areas of separated flow, wing vortices that may have burst and forebody vortices that may be asymmetric. All of these features can lead to highly nonlinear aerodynamic characteristics, and some are potentially disastrous for maneuvering aircraft.

Traditionally, studies of aircraft stall/spin problems have focused on the wing and tail flow fields. Early investigations (in the 1950's) of the effect of forebody shape ahead of the wing (ref. 1) concentrated on two-dimensional testing of the cross-sectional shape. It was found that forebody shape could have considerable influence on the spin and spin-recovery characteristics and that the Reynolds number could have considerable influence on whether the nose provides damping or autorotational moments. One of the first studies of the autorotational effect of the forebody under spinning conditions using a rotary model (Clarkson, ref. 2) revealed that the fuselage nose, rather than the wing, can be the major source of autorotative moment. For about 10 years, until the late 1960's, the fundamental aerodynamics of the stall/spin problem remained unexplored, although great progress was made in reducing the number of accidents by spin-testing aircraft models. In the meantime, the problem was magnified with the advent of high-performance aircraft designed to operate at high angles of attack, conditions that were encountered only inadvertently by previous aircraft. Continual loss of high-performance aircraft due to control problems resulted in an extensive wind-tunnel study of these aircraft. Generally, such studies found that strong side forces and yawing moments occurred at zero sideslip when the angle of attack was large, as illustrated in figure 1 (results from Chambers et al., ref. 3). This side force was shown to be a result of an asymmetric vortex system, which was first discovered in flow studies on long bodies by Allen and Perkins (ref. 4) and first measured by Letko (ref. 5). In the last few years, this phenomenon has received considerable study (refs. 6-14). The resulting side force and yawing moment can be large and could contribute to loss of control of high-performance aircraft.

This paper examines asymmetric forces associated with aircraft forebodies. Primary emphasis will be put on the forces and moments produced by asymmetric vortices on circular or near circular shapes. A brief discussion of the side forces produced by nonuniform separation on spinning forebodies having square cross sections with rounded corners will also be given. Further details of the data presented can be obtained from references 12 to 14.

2. ASYMMETRIC VORTEX FLOW

The basic phenomena considered here can best be described by referring to figure 2. At low angles of attack, the vortex flow around a pointed body of revolution is symmetrical (fig. 2(a)). The aerodynamic forces and moments on the body are readily calculated by semi-empirical methods such as given in Nielsen's book on missile aerodynamics (ref. 15). When the body is pitched to higher angles of attack, the symmetric vortex system is unstable and the vortex sheet tears, leading to a series of alternating free vortices (like a Karman vortex street but stationary), with those near the body still connected by a feeding sheet (fig. 2(b)). The number of alternate vortices depends on the angle of attack and length of the body. In the crossflow plane, the flow resembles the flow about an impulsively started cylinder. (See reference 7 for details of this flow on long bodies.) For aircraft where only the forebody exists (wings prevent afterbody vortices), there are only three to five of these vortices.

An extensive study of forebody aerodynamics is underway at Ames Research Center. This study has two basic objectives: first, to better define the flow phenomena to allow better theoretical modeling and, second, to provide design guidelines to determine under what conditions the phenomena occur and how it can be eliminated or reduced in strength. Figure 3 shows the forebody configurations that have been studied (refs. 12,13). Base diameters were 15.24 cm for models 1, 2, and 3; 18.82 cm for model 4; and 13.21 - 18.87 cm for model 5. Wind-tunnel tests have been conducted over a wide range of Reynolds numbers, Mach numbers, and angles of attack.

A typical example of the side force vs. angle of attack for the $\ell/d = 3.5$ tangent ogive is shown in figure 4. For comparison, the result from Coe et al. (ref. 9) on a geometrically identical body tested at Langley Research Center is shown. Although the direction (sign) of the side force is different (there is no reason that they should be the same), the basic shape and magnitude are similar. Also shown is the normal-force curve. Note that the side force is larger than the normal force at some angles of attack.

Three main features of this side-force variation with angle of attack will now be considered in more detail: (1) the angle of attack at which the side force first occurs, to be called angle of onset; (2) the maximum value of the side force; and (3) the upper limit of angle of attack where the side force returns to zero, to be called the upper limit. In addition, consideration will be given to methods of alleviating the side force, the stability of the asymmetric vortex system, and finally methods of predicting the side forces.

2.1 Angle of Onset

The geometry was found to be the primary variable that affected the angle of onset. Figure 5 shows side forces vs. angle of attack for the four bodies of revolution and the elliptical body. Note that the angle of onset varies from 20° to 35° depending on body geometry, with high fineness-ratio bodies having lower angles of onset (compare the ℓ/d = 3.5 and 5.0 tangent ogives). No other variable (Reynolds number, Mach number, etc.) had a significant impact on the angle of onset.

It was found that the angle of onset could be correlated with the forebody half angle (fig. 6). Data from several sources are included. Although there is some scatter, the data for pointed circular forebodies (fig. 6(a)) falls along the line given by $\alpha_{onset} \approx 2.5N$. Note in figure 6(b) that the angle of onset for the elliptic tangent ogive tested in both positions of major axis horizontal and vertical is significantly lower than that of the corresponding circular tangent ogive with the same planform length/span ratio. For forebodies with afterbodies, onset occurs at lower angles of attack depending on body length (fig. 6(c)). Data points for three aircraft configurations are also shown. For the aircraft, onset generally occurs at angles of attack similar to forebodies alone or higher, indicating that the wings may suppress the formation of asymmetric vortices.

2.2 Maximum Side Force

As noted earlier, the maximum side force can be as large as the normal force for the forebody alone. The side force, once it starts to build up, can switch directions (see the cone data in figure 5). This can be a result of either an instability of the vortex system (there is no reason that it should be left or right) or the vortex feeding sheet may be tearing, forming a new free vortex and starting a new bound vortex. (This point on vortex stability is discussed later.) Besides being generally dependent on geometry, as shown in figure 5, the maximum side force is also strongly dependent on Reynolds number and Mach number. The effect of Reynolds number on C_Y is shown in figure 7. Not only the maximum value of C_Y changes with Reynolds number but the shape of the curve changes as well. As noted before, the one point that does not change significantly is the angle of onset. At this time, the behavior of C_Y with Reynolds number is not understood.

The influence of Mach number is such that the maximum side force decreases with increasing Mach number, as illustrated in figure 8 where it is also seen that the maximum Mach number at which a side force occurs is higher for the more slender forebodies.

2.3 Upper Limit

As shown in figures 4, 5, and 7, the side force has decreased to zero near an angle of attack of about 70°, with small variation, depending on flow conditions and geometry. Above this angle of attack, the flow characteristics have most likely changed to those of a wake-type flow.

2.4 Alleviation of Side Force

The potentially disastrous effects that the large side force and yawing moment could have on aircraft control has led to an extensive study of methods to alleviate the side force. Two different methods have generally been used: blunt the tip of the forebody and attach small strakes near the tip. Both techniques seem to be effective. For example (fig. 9), three different degrees of bluntness were tried on the ℓ/d = 3.5 tangent ogive. The intermediate bluntness (r_w/r_d = 0.084) gave the best results, practically eliminating the side force. Too much bluntness might result in a sizeable side force (ref. 6). These results were not significantly altered by the other flow variables or by geometry. Similar results were obtained with small strakes. The drastic change from asymmetric to symmetric flow in the flow pattern with additional bluntness or strakes is illustrated by the oil flow pictures in figure 10. Since many aircraft use nose booms for air data sensors, a simulated nose boom was tested and also found to greatly reduce the side force.

2.5 Stability of Asymmetric Vortices

We have thus far assumed that the asymmetric vortices are stable and have deferred questions concerning the direction of the asymmetric force, left or right. Various tests were performed to determine the stability of the asymmetric vortex pattern, particularly to assess the sensitivity of its orientation to the body. These tests are described briefly.

Two means of mounting the model in the tunnel were used to assure that results were independent of mounting. Most of the low-speed data were obtained with the model mounted from the floor, the standard high-angle-of-attack test procedure used in the 12-Foot Pressure Tunnel at Ames Research Center. One set of tests was conducted with the model mounted on a bent sting from the blade strut. The results at low speed were basically the same.

To check the effects of the flow around the base of the forebodies, particularly at high angle of attack, an afterbody 3.5 diameters long was attached to the sting but not to the forebody. Again the data were basically the same as for the forebody alone. These facts, along with the good agreement with the Langley data (fig. 3), indicate that reliable data could be obtained on this rather unusual phenomenon.

Next a series of tests was performed to determine the origin of the asymmetric vortices. First, the model was tested with the entire body in various roll positions. Then it was tested with only the

removable nose tip (the forward 19%) of the body rolled. The latter results are shown in figure 11. The results are basically the same as for rolling the complete model, indicating the importance of the nose region. Previous studies have shown and these data also show that small imperfections at the tip are responsible for establishing the direction of the asymmetry.

Next, to determine if the unsymmetric vortex system were stable, several different tests were conducted. First, the model was sideslipped when there was a strong side force. An example of these data is shown in figure 12. Here we see that it takes a sideslip angle greater than 5° to change the side force to the opposite direction. The results are very repeatable with no hysteresis. Second, a canopy was added to the $x/d = 3.5$ tangent ogive to see if its presence would upset the asymmetry. The results were identical to the case without a canopy.

Finally, two sets of tests were run recently with a model spinning. First the model was spun about the velocity vector at $\alpha = 45°$ (simulating a coning motion or a steep spin). The results of this test are shown in figure 13 with a small insert sketch showing the model. The side force was measured separately on the tangent ogive ($x/d = 3.5$) forebody portion of the model and on the cylindrical afterbody. The data are plotted vs. the dimensionless spin parameter ($\xi = \omega\ell/V$), where ω is the spin rate, ℓ is the reference length, and V is the freestream velocity. At zero spin, we have the static side force similar to that observed in the earlier test results just presented. Note that the side force is not altered by the spin motion, indicating a very strong tendency to retain its asymmetric configuration.

The second spin test about the body axis was done on a 10° half-angle cone. Here the side force behaved much as it did when the model was tested at various roll positions. As the roll velocity was increased, the waveform of the side force as a function of roll angle was basically the same with only small irregularities being eliminated with higher speed and the overall amplitude of the side force became smaller. Reversing the direction of roll produced essentially the same result, but in reverse sequence. The lack of an effect of rotation was also noted by Clark et al. (ref. 6).

In summary, the symmetric vortices, once formed, represent a very stable flow configuration.

2.6 Theoretical Predictions

Theoretical predictions of the phenomena of asymmetric vortex formations and the resulting asymmetric forces are at an early stage of development. The earliest attempt was that of Thomson and Morrison (ref. 7), who performed a creditable series of experiments which they analyzed by means of the so-called impulsive crossflow analogy, which has subsequently been widely referenced.

Briefly, they correlated their observed vortex spacings and vortex strengths on long bodies to data from a two-dimensional cylinder. The result was a prediction of the vortex crossflow drag force; asymmetric forces were not considered. Several attempts (refs. 16-21) have since been made to predict asymmetric forces using the impulsive crossflow analogy as formulated by Thomson and Morrison. The approach of Wardlaw (ref. 17) was to use the basic vortex tracking ideas of Bryson (ref. 22) which involves a solution in the crossflow plane, but modified to remove the symmetry constraint in a manner similar to that used by Kuhn et al. (ref. 23) to calculate the vortex positions on a body spun about the velocity vector. A more recent paper by Wardlaw included some refinements by treating the vortex as composed of elemental vortices (ref. 18). All of these theoretical approaches are semi-empirical, although the most recent one of Wardlaw (ref. 18) has removed some of the empirical inputs. In the final analysis, however, none of these methods are satisfactory in computing the magnitude of the side force, although there is some indication that they may be useful in predicting the angle of onset.

In closing the discussion of the theoretical prediction of the asymmetric vortex phenomena, a word of caution is in order. All of the efforts to predict this phenomenon have drawn heavily on the impulsive crossflow analogy. As powerful as this analogy is in comparing the phenomenalogical observations, it does not have an analytical foundation. The methods get around this by simple empirical inputs, such as separation points, vortex strengths, etc. A true theoretical model for this difficult flow problem is a big challenge and must include the boundary-layer characteristics.

2.7 Some Design Guides

The foregoing material can be summarized in a few design guides. Figure 14 shows the angle-of-attack boundaries for the side-force phenomena for pointed forebodies. At the lowest angle of attack is the angle of onset boundary that is independent of Mach number and Reynolds number but dependent on geometry ($\alpha = 2\delta_N$). The upper limit decreases with increasing Mach number from a maximum of 80° at low speed to 60° at $M = 0.3$. Finally, as the Mach number increases, the side force goes to zero (solid points), which is approximately bounded by $M \sin \alpha = 0.5$. Within this boundary, we can expect side forces as large as the forebody normal force. Finally, this side force can be extensively reduced with small amounts of bluntness or small strakes.

3. NONUNIFORM SEPARATION ON NONCIRCULAR FOREBODIES

Flow separation on noncircular bodies is now discussed, called "nonuniform separation" to distinguish it from asymmetric separation on circular bodies. The simplest way to describe the difference between nonuniform separated flow and asymmetric vortex flow is to use the illustrations in figure 15. Figure 15 illustrates an asymmetric vortex flow pattern as it might be observed in the crossflow plane of a circular cylinder or circular cross-section forebody (as described previously). The flow separation characteristically occurs near the maximum diameter on both sides if the angle of sideslip is zero, but can be asymmetric when asymmetric vortices are shed which lead to side forces (shown by C_y). Nonuniform flow separation for noncircular bodies is illustrated in figure 15(b), which shows a body with square cross section and rounded corners. The flow field for this type of body at zero sideslip angle (i.e., zero roll angle about the body longitudinal axis for the two-dimensional case) is normally symmetric (exceptions occur in the critical crossflow regime). However, with small amounts of sideslip (or body roll) two-dimensional tests (ref. 24, 25) have shown that at subcritical Reynolds numbers, the flow

attaches at the near corner (windward side) and separates on the far corner (leeward side) and at supercritical Reynolds numbers the flow is attached on both windward and leeward sides. This very nonuniform flow behavior results in strong side forces that can either be into ($+C_y$ as shown in Fig. 15(b)) or away from ($-C_y$) the cross wind velocity component.

Some recent tests on models with this type of cross section have been conducted in the Ames 12-Foot Pressure Wind Tunnel on a rotary spin apparatus (fig. 15(c). The nose cross section was a 7.62 cm (3 in.) square with rounded corners of 1.9 cm (0.75 in.) radius. The total length of the nose was approximately 26.7 cm (10.5 in.) including the hemispherical tip. A more detailed description is given by Clarkson et al. (ref. 14). Force and moments were measured on the nose section alone and also for the entire model, including the circular center and tail sections, by use of force balances located in both the nose and the rotating sting. In addition to tests at angles of attack of 90°, where the flow is essentially two-dimensional, tests at angles of attack of 45°, 60° and 75° were also conducted.

3.1 Angle of Attack and Reynolds Number Effects

A set of side-force coefficient data measured at two angles of attack (45° and 90°) and over a range of Reynolds numbers from subcritical to supercritical is shown in figure 16 as a function of the dimensionless spin parameter (sometimes referred to as the reduced frequency). Two important points should be noted. First, at $\alpha = 90°$, the side force on the nose changes from a strong pro-spin contribution at low or subcritical Reynolds numbers to a strong antispin contribution at the higher or supercritical Reynolds numbers. It is also possible to get asymmetric flow with resulting side forces with no spin motion, particularly in the critical Reynolds number range. The second major point is that at $\alpha = 45°$ the side force is antispin for all Reynolds numbers including the low Reynolds numbers. This is not what one would expect on the basis of simple crossflow analogy concepts since the crossflow Reynolds number at $\alpha = 45°$ is 0.7 of the crossflow Reynolds number at $\alpha = 90°$ for the same freestream Reynolds number.

3.2 Comparison of Measured and Calculated Spin Coefficients

To assess the ability to predict spin coefficients, a comparison was made between the measured spin coefficient at $\alpha = 90°$ and a calculated spin coefficient based on two-dimensional static force data determined at a variety of Reynolds numbers and body roll angles (at $\alpha = 90°$, the body roll angle in a static test would correspond to the local body helix angle in a spin model). The method for computing these coefficients is shown in reference 14. Computations were made for both supercritical and subcritical flow cases (fig. 17). Two supercritical comparisons are shown in figure 17(a), one for an initial body roll angle of 0° and one for 10°. The agreement between measured and calculated coefficients is very good. Figure 17(b) shows a subcritical comparison at zero body roll and, although the agreement is not as good as for the supercritical flow case, it does have the correct trend.

If one were to apply this comparison technique to the body at 45° using the crossflow Reynolds number to determine the proper force calculation, there would obviously be total disagreement (fig. 16). At any given freestream Reynolds number, the decrease in angle of attack from 90° to 45° results in a decrease of the crossflow velocity vector and, consequently, crossflow Reynolds number. This means that flow characteristics should look even more subcritical than at 90°. However, the data show that at $\alpha = 45°$ at low Reynolds numbers, the side force indicates supercritical flow as was observed at high Reynolds numbers at $\alpha = 90°$. The strong influence of axial flow and the resulting complex three-dimensional flow field are the subjects of an active research program presently under way at Ames.

3.3 Some Design Guides

Unfortunately, there are not as yet many design guides available for nonuniform separated flows. Some words of warning may be in order, however. First, testing at subcritical Reynolds numbers in free-spin tunnels and on captive spin test apparatus as used here can lead to erroneous conclusions if one were to directly apply the results to spin prediction of full scale aircraft with supercritical flow. Second, the application of simple crossflow ideas to calculate body forces on spinning aircraft near $\alpha = 90°$ (flat spin case) may be valid, but for angles of attack less than that encountered in a very steep spin the calculation would be totally inadequate. This reinforces the point made in an earlier section that application of crossflow analogy ideas in many cases may be misleading.

4. CONCLUDING REMARKS

Two basically different types of forebody flow have been examined. The state of our understanding of the side forces and moment resulting from these flows has been discussed and some design and testing guides proposed. Although much testing of these flows has been performed and much empirical understanding exists, a considerable amount of basic knowledge is still lacking. Detailed flow measurements and pressure distributions must be made to improve the state of knowledge. Finally, the crossflow analogy ideas may be hindering an examination of these data with a completely open mind. The analogy has been a valuable aid, but other flow models need to be considered.

REFERENCES

1. A. L. Neihouse, W. J. Klinar, and S. R. Scher: Status of Spin Research for Recent Airplane Designs. NASA TR R-57, 1960.

2. M. H. Clarkson: Autorotation of Fuselages. I.A.S. Aero. Rev., Feb. 1958, pp. 33-35.

3. J. R. Chambers, E. L. Anglin, and J. S. Bowman, Jr.: Effects of a Pointed Nose on Spin Characteristics of a Fighter Airplane Model Including Correlation with Theoretical Calculations. NASA TN D-5921, 1970.

4. H. J. Allen and E. W. Perkins: A Study of the Effects of Viscosity on Flow Over Slender Inclined Bodies of Revolution. NACA TR 1048, 1951.

5. W. Letko: A Low-Speed Experimental Study of the Directional Characteristics of a Sharp-Nosed Fuselage Through a Large Angle-of-Attack Range at Zero Angle of Sideslip. NACA TN 2911, 1953.

6. W. H. Clark and J. R. Peoples: Occurrence and Inhibition of Large Yawing Moments During High Incidence Flight of Slender Missile Configurations. AIAA Paper 72-968, 1972.

7. K. D. Thomson and D. F. Morrison: The Spacing, Position, and Strength of Vortices in the Wake of Slender Cylindrical Bodies at Large Incidences. Journal of Fluid Mechanics, vol. 50, part 4, 1971, pp. 751-783.

8. G. S. Pick: Investigation of Side Forces on Ogive-Cylinder Bodies at High Angles of Attack in the M = 0.5 to 1.1 Range. AIAA Paper 71-570, 1971.

9. P. L. Coe, Jr., J. R. Chambers, and W. Letko: Asymmetric Lateral-Directional Characteristics of Pointed Bodies of Revolution at High Angles of Attack. NASA TN D-7095, 1973.

10. J. R. Krouse: Induced Side Forces on Slender Bodies at High Angles of Attack and Mach Numbers of 0.55 and 0.8. NSRDC Test Rept. AL-79, May 1971.

11. K. J. Orlik-Ruckemann, J. C. LaBerge, and S. Iyengar: Half- and Full-Model Experiments on Slender Cones at Angle of Attack. AIAA Journal of Spacecraft, vol. 10, no. 9, Sept. 1973, pp. 575-580.

12. E. R. Keener and G. T. Chapman: Onset of Aerodynamic Side Forces at Zero Sideslip on Symmetric Forebodies at High Angles of Attack. AIAA Paper 74-770, 1974.

13. E. R. Keener and J. Taleghani: Wind-Tunnel Investigation of the Aerodynamic Characteristics of Five Forebody Models at High Angles of Attack at Mach Numbers from 0.25 to 2. NASA TM X-62,502, 1975.

14. M. H. Clarkson, G. N. Malcolm, and G. T. Chapman: Experimental Determination of Post-Stall Rotary Derivatives for Airplane-Like Configurations at Several Reynolds Numbers. AIAA Paper 75-171, 1975.

15. J. N. Nielsen: Missile Aerodynamics, McGraw-Hill Book Co., Inc., 1960.

16. K. D. Thomson: The Estimation of Viscous Normal Force, Pitching Moment, Side Force and Yawing Moment on Bodies of Revolution at Incidences up to 90. Australian W.R.E. Rept. 782 (WR&D), 1972.

17. A. B. Wardlaw, Jr.: Prediction of Yawing Force at High Angle of Attack. AIAA Journal, vol. 12, no. 8, 1974, pp. 1142-1144.

18. A. B. Wardlaw, Jr.: Multivortex Model of Asymmetric Shedding on Slender Bodies at High Angle of Attack. AIAA Paper 75-123, 1975.

19. E. L. Fleeman and R. C. Nelson: Aerodynamic Forces and Moments on a Slender Body with a Jet Plume for Angles of Attack up to 180 Degrees. AIAA Paper 74-110, 1974.

20. J. E. Fidler and M. C. Bateman: Asymmetric Vortex Effects on Missile Configurations. AIAA Paper 75-209, 1975.

21. H. C. Kao: Side Forces on Unyawed Slender Inclined Aerodynamic Bodies. Journal of Aircraft, vol. 12, no. 3, March 1975, pp. 142-150.

22. A. E. Bryson: Symmetric Vortex Separation on Circular Cylinders and Cones. Journal of Applied Mechanics, Dec. 1959, pp. 643-648.

23. G. D. Kuhn, S. B. Spangler, and J. N. Nielsen: Theoretical Study of Vortex Shedding from Bodies of Revolution Undergoing Coning Motion. NASA CR-1448, 1969.

24. E. C. Polhamus, E. W. Geller and K. J. Grunwald: Pressure and Force Characteristics of Noncircular Cylinders as Effected by Reynolds Number With a Method Included for Determining the Potential Flow About Arbitrary Shapes. NASA TR R-46, 1959.

25. E. C. Polhamus: Effect of Flow Incidence and Reynolds Number on Low-Speed Aerodynamic Characteristics of Several Noncircular Cylinders With Applications to Directional Stability and Spinning. NASA TR R-29, 1959.

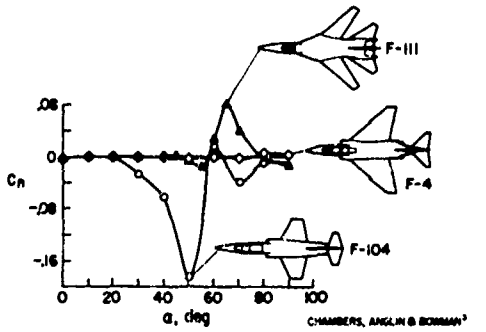

Fig. 16-1 Yawing moments at high angles of attack and zero sideslip for three aircraft models.

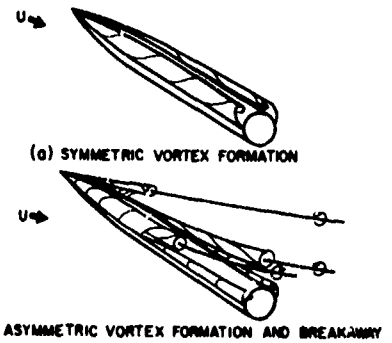

Fig. 16-2 Schematic of symmetric and asymmetric vortex formations on a body of revolution at moderate and high angles of attack.

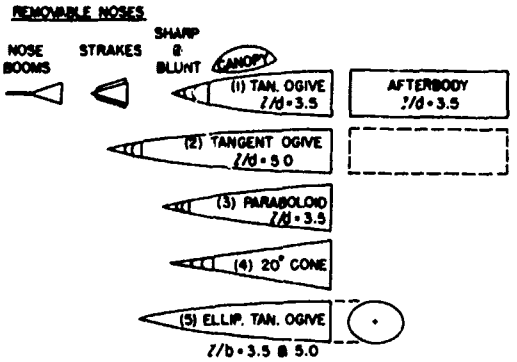

Fig. 16-3 Sketch of forebody configurations for asymmetric force studies.[12]

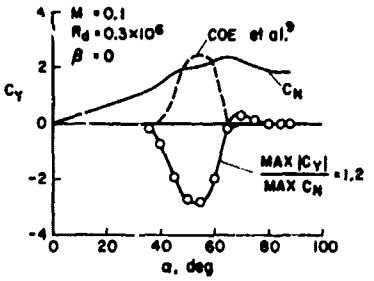

Fig. 16-4 Typical forebody side-force curve, including a comparison of results from separate facilities, for an ℓ/d = 3.5 pointed tangent ogive.

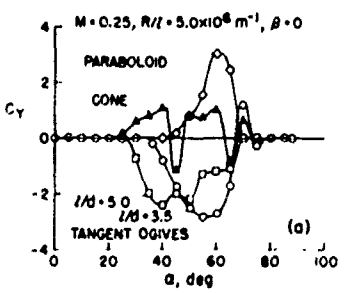

(a) Pointed circular forebodies

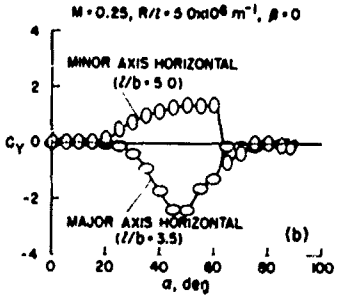

(b) Pointed elliptic forebody

Fig. 16-5 Effect of forebody shape on side-force curves for the forebody models with pointed noses.

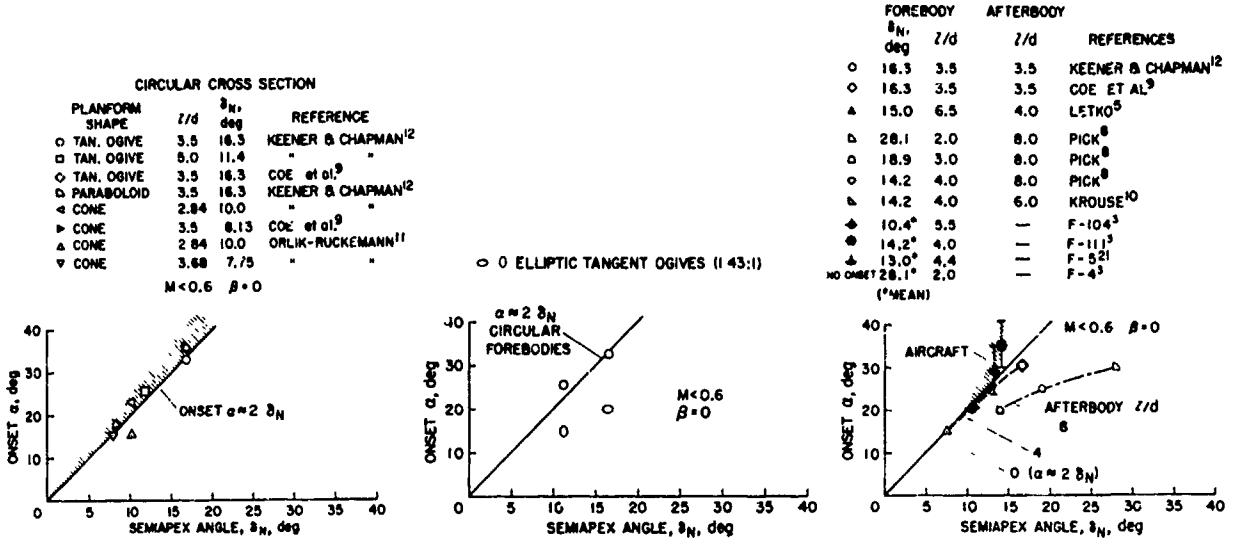

(a) Pointed circular forebodies (b) Pointed elliptic forebodies (c) Effect of afterbody and wings

Fig. 16-6 Angle of attack for onset of side force for pointed forebodies.

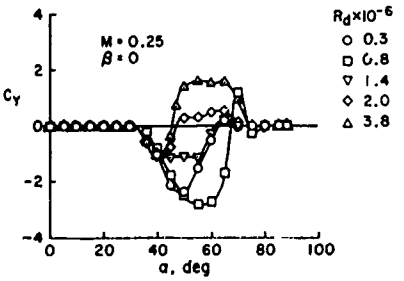

Fig. 16-7 Effect of Reynolds number on side-force curves for ℓ/d = 3.5 pointed tangent ogive.

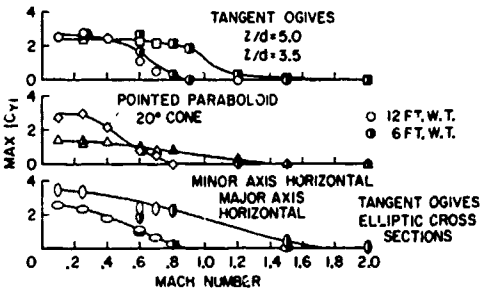

Fig. 16-8 Variation of maximum side-force coefficient with Mach number.

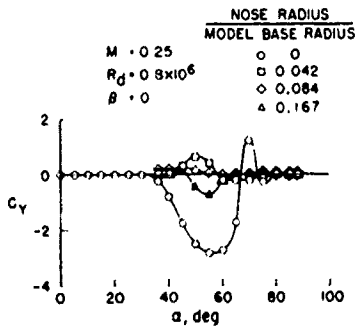

Fig. 16-9 Effect of nose bluntness on side force for ℓ/d = 3.5 pointed tangent ogive.

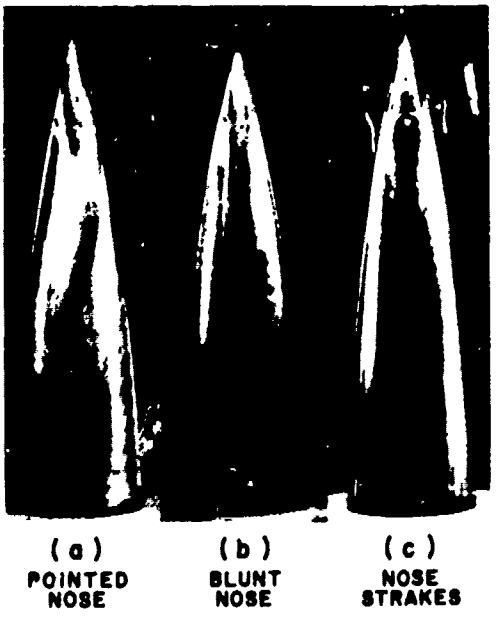

Fig. 16-10 Oil-flow photographs of top surface of ℓ/d = 3.5 tangent ogive.

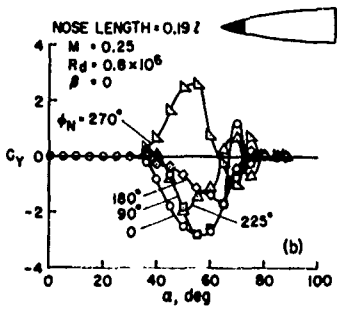

Fig. 16-11 Effect of roll-angle position of removable-nose-tip section on side force for ℓ/d = 3.5 pointed tangent ogive.

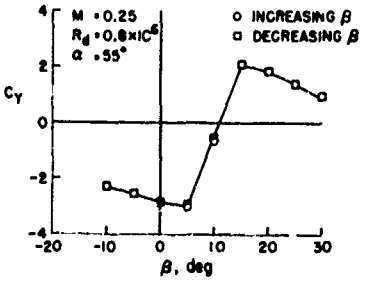

Fig. 16-12 Effect of sideslip on side force for ℓ/d = 3.5 pointed tangent ogive.

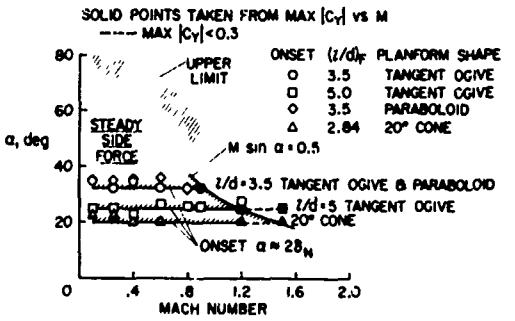

Fig. 16-14 Angle of attack/Mach number boundaries for steady side force for pointed circular forebodies.

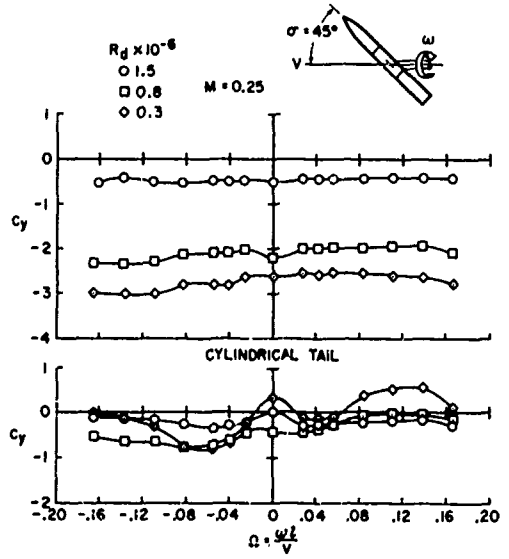

Fig. 16-13 Effect of Reynolds number and spin rate on side force for ℓ/d = 3.5 pointed tangent ogive.

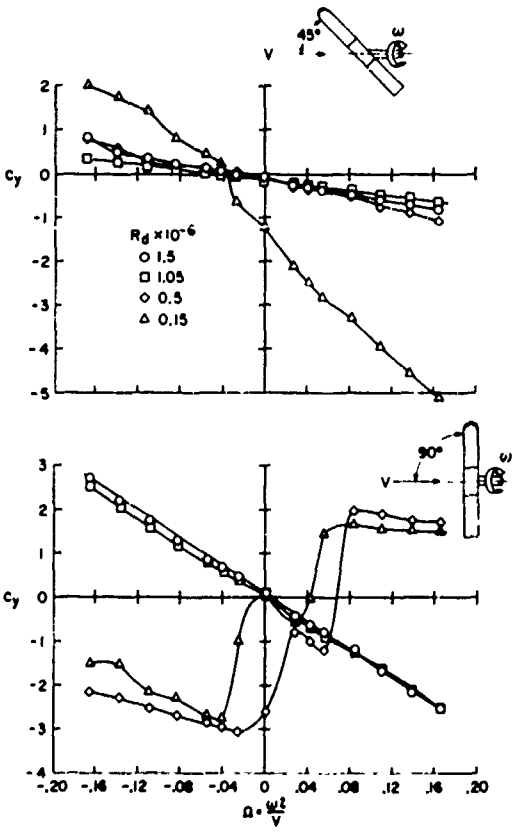

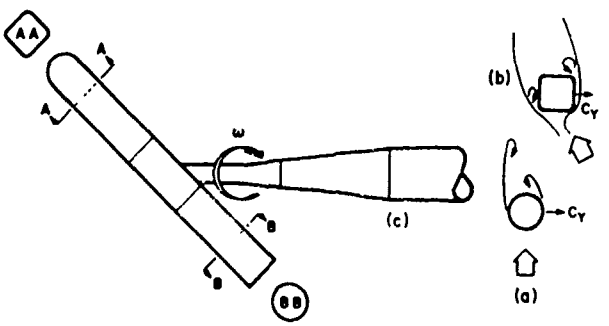

Fig. 16-15 Asymmetric flow mechanisms in a spin motion.

Fig. 16-16 Effect of Reynolds number and angle of attack on nose section side force in spin motion.

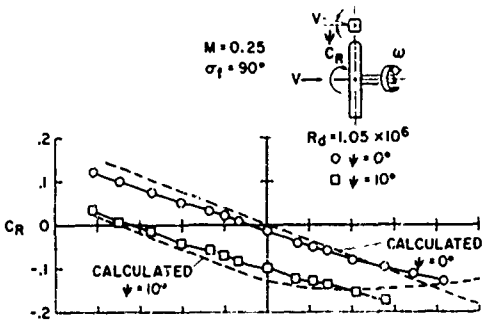

(a)

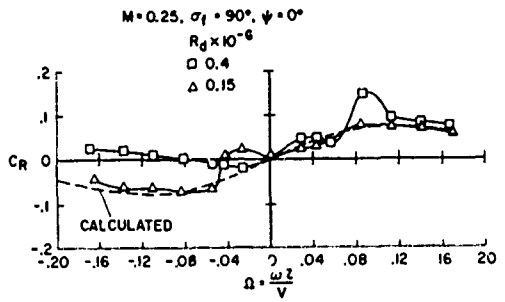

(b)

(a) Supercritical Reynolds numbers
(b) Subcritical Reynolds numbers

Fig. 16-17 Comparison of calculated and measured spin moment coefficients.

STALL/SPIN TEST TECHNIQUES USED BY NASA

Joseph R. Chambers and James S. Bowman, Jr.
Aeronautical Engineers
NASA Langley Research Center
Hampton, Virginia 23665
U.S.A.

and

Gerald N. Malcolm
Aeronautical Engineer
NASA Ames Research Center
Moffett Field, California 94035
U.S.A.

SUMMARY

The National Aeronautics and Space Administration has developed several unique test techniques and facilities which are used to predict the stall/spin characteristics of highly maneuverable military aircraft. The paper discusses three of the more important test techniques used at the Langley and Ames Research Centers, including the objectives, advantages, and areas of application of each technique. The techniques are (1) flight tests of dynamically scaled models, (2) rotary-balance tests, and (3) piloted simulator studies.

As a result of the shortcomings of theoretical methods, the most reliable source of information on stall/spin characteristics prior to full-scale flight tests has been tests of dynamically scaled models. The dynamic model techniques used by NASA are (1) the wind-tunnel free-flight technique, (2) the outdoor drop model technique, and (3) the spin-tunnel test technique.

The results of rotary-balance tests conducted for several current fighter configurations indicate that the aerodynamic characteristics of these vehicles during spins are extremely complex phenomena which tend to be Reynolds number dependent and which vary nonlinearly with spin rate. Computer studies of spinning motions have indicated that data obtained from rotary-balance tests will be required for the development of valid theoretical spin prediction techniques.

Recent experience has indicated that the extension of piloted simulation techniques to high angles of attack provides valuable insight as to the spin susceptibility of fighter configurations during representative air combat maneuvers. In addition, use of the technique is an effective method for the development and evaluation of automatic spin prevention concepts.

SYMBOLS

b	Wing span, m (ft)	c_y	Body side-force coefficient	Ω	Spin rate, rad/sec
C_n	Yawing-moment coefficient	V	Free-stream velocity, m/sec (ft/sec)		

INTRODUCTION

Perhaps the most valuable contribution to an analysis of the stall/spin characteristics of a modern military airplane is an accurate prediction of these characteristics at an early design stage. Unfortunately, standard design procedures which are usually applied with success to conventional unstalled flight are severely limited in application to the stall/spin area because of the relatively complex aerodynamic phenomena associated with stalled flow. Experience has shown that the aerodynamic factors which influence the stall and spin may be nonlinear in nature and dependent on interference effects. In addition, many factors tend to be extremely configuration-oriented. These complexities have been a major deterrent to the development of design procedures for the stall/spin area.

In view of the general lack of understanding of the stall/spin problem, NASA has developed several unique test techniques and facilities for stall/spin studies. For example, the only operational spin tunnel in the U.S. is located at the NASA Langley Research Center. As a result of these specialized techniques, much of the stall/spin research for military aircraft and virtually all of the dynamic model flight tests related to stall/spin are conducted by NASA.

These studies involve the use of a wide matrix of tools including conventional static wind-tunnel force tests, dynamic force tests, flight tests of dynamic models, theoretical studies, and piloted simulator studies. The present paper describes three of the more important techniques: (1) flight tests of dynamically scaled models, (2) rotary-balance tests, and (3) piloted simulator studies.

DYNAMIC MODEL TECHNIQUES

As a result of the complexity of the stall/spin problem, and the lack of proven alternate predictive methods, the most reliable source of information on stall/spin characteristics prior to actual flight tests of the particular airplane has been tests of dynamically scaled airplane models. A properly scaled dynamic model may be thought of as a simulator with the proper values of the various aerodynamic and inertial parameters.

The NASA has developed several unique dynamic model test techniques for stall/spin studies. This paper will describe three of the more important test techniques including the objectives, advantages and limitations, and area of application of each technique. The techniques are: (1) the wind-tunnel free-flight technique, (2) the outdoor radio-controlled model technique, and (3) the spin-tunnel test technique.

Before discussing the techniques, however, a brief review of model scaling laws is in order to properly introduce the reader to dynamic model testing and to clarify some of the reasons for the test equipment and procedures.

Model Scaling Considerations

Dynamic models must be scaled in each of the fundamental units of mass, length, and time in order to provide test results that are directly applicable to the corresponding full-scale airplane at a given altitude and loading condition. Units of length are, of course, scaled from geometric ratios; units of mass are scaled from those of the full-scale airplane on the basis of equal relative density factor; and time is scaled based on equal Froude number. As a result of scaling in this manner, the motions of the model are geometrically similar to those of the full-scale airplane and motion parameters can be scaled by applying the scale factors given in Table I.

Some limitations of the dynamic model test techniques are apparent from an examination of the factors given in Table I. For example, the model is tested at a value of Reynolds number considerably less than those of the full-scale airplane at comparable flight conditions. A 1/9-scale dynamic model has a Reynolds number only 1/27 that of the corresponding airplane. It should also be noted that, although the linear velocities of the model are smaller than full-scale values, the angular velocities are greater than full-scale values. For example, a 1/9-scale model has a flight speed only 1/3 that of the airplane, but it has angular velocities that are three times as fast as those of the airplane.

The discrepancy in Reynolds number between model and full-scale airplane can be an important factor which requires special consideration for stall/spin tests. For example, during spin-tunnel tests, large Reynolds number effects may be present which cause the model to exhibit markedly different characteristics than those associated with correct values of Reynolds number. This point will be discussed in detail in a later section on spin-tunnel testing.

The fact that the angular velocities of the model are much faster than those of the airplane poses special problems with regard to controllability of the model for certain techniques. Because the human pilot has a certain minimum response time, it has been found that a single human pilot cannot satisfactorily control and evaluate dynamic flight models. It will be shown in subsequent sections how this control problem is overcome by use of multiple pilots.

The stall and spin of an airplane involve complicated balances between the aerodynamic and inertial forces and moments acting on the vehicle. In order to conduct meaningful tests with dynamic models, it is important that these parameters be properly scaled. It is, therefore, mandatory that the scale factors given in Table I be used to arrive at a suitable dynamic model. Simply scaling dimensional characteristics without regard to other parameters (as is the case for most radio-controlled hobbyist models) will produce erroneous and completely misleading results.

The Wind-Tunnel Free-Flight Technique

Each of the model test techniques to be discussed in this paper has a particular area of application within a broad study of stall/spin characteristics for a given airplane configuration. The first technique to be discussed, known as the wind-tunnel free-flight technique, is used specifically to provide information on flight characteristics for angles of attack up to and including the stall. The test setup for this model test technique is illustrated by the sketch shown in Figure 1. A remotely controlled dynamic model is flown without restraint in the 9.1- by 18.2-meter (30- by 60-ft) open-throat test section of the Langley full-scale tunnel. Two pilots are used during the free-flight tests. One pilot, who controls the longitudinal motions of the model, is located in an enclosed balcony at one side of the test section while the second pilot, who controls the lateral-directional motions of the model, is located in an enclosure at the rear of the test section. The model is powered by compressed air, and the level of thrust is controlled by a power operator who is also located in the balcony.

The cable attached to the model serves two purposes. The first purpose is to supply the model with compressed air, electric power for control actuators, and control signals through a flexible trailing cable which is made up of wires and light plastic tubes. The second purpose of the cable is concerned with safety. A portion of the cable is a steel cable that passes through a pulley above the test section. This part of the flight cable is used to catch the model when a test is terminated or when an uncontrollable motion occurs. The entire flight cable is kept slack during the flight tests by a safety-cable operator who accomplishes this job with a high-speed pneumatic winch.

The model incorporates limited instrumentation for measurements of motion and control deflections. The instrumentation consists of control-position indicators on each control surface and a three-axis rate gyro package. The output of the instrumentation is transferred by wires to the location of the test crew in the balcony, where the data are recorded in time history form on oscillograph recorders. Motion picture records from several advantageous positions are also made during the flights.

Although it is possible for a single human pilot to fly the model by operating all control simultaneously, such an arrangement is not suitable for research purposes because the pilot must concentrate so intently on the task of keeping the model flying satisfactorily that he is not able to evaluate its flight characteristics in sufficient detail. This intense concentration is required for several reasons, one of which (the high angular velocities of the model) was indicated earlier in the section on model scaling considerations. Another factor contributing to the difficulty of control is the lack of "feel" in flying a model by remote control. In this technique the human pilot does not sense accelerations as the pilot of an airplane does, and he must, therefore, fly with sight cues as the primary source of information. This lack of cues results in lags in control inputs which become very significant when attempting to fly a model within a relatively restricted area within the tunnel test section. These control problems are especially aggravated during tests of airplane configurations at high angles of attack, where lightly damped lateral oscillations (wing rock), directional divergence (nose slice), and longitudinal instability (pitchup) are likely to occur.

In the wind-tunnel free-flight technique, each pilot concentrates only on the phase of model motion for which he is responsible. As a result, he is able to fly the model with greater ease and relaxation and can thoroughly evaluate the characteristics of the model. In this manner, the control difficulties inherent in the free-flight technique are largely compensated for. The control problems are also minimized by the use of a fast actuating full-on or full-off (bang-bang) control system. The rapid response produced by this type of control enables the pilot to maintain relatively tight control over the model.

The wind-tunnel free-flight technique can produce valuable information during studies of flight motions at high angles of attack and at the stall. Various phases of a typical investigation would include: (1) flights at several values of angles of attack up to and including the stall to evaluate dynamic stability characteristics, (2) an evaluation of pilot lateral control techniques at high angles of attack, and (3) an evaluation of the effects of stability augmentation systems.

Studies of dynamic stability characteristics at high angles of attack and at the stall are conducted by varying the tunnel airspeed, model thrust, and the angle of attack of the model in steps in order to trim the model at several values of angle of attack and noting the resulting dynamic stability characteristics at each trim condition. By simultaneously reducing the tunnel airspeed and increasing the model angle of attack and thrust, the model can be flown through maximum lift, or if the model exhibits a dynamic instability, it can be flown to the point where loss of control occurs. As a result of this type of study, instabilities which could seriously limit the maneuvering capability and endanger the safety of the full-scale airplane are easily and safely identified.

An evaluation of the effect of lateral control inputs at high angles of attack is made by using the lateral-directional controls both individually and in various combinations. These tests give an indication as to the relative effectiveness of the controls at high angles of attack, including an evaluation of adverse yaw characteristics. These tests are important because it is possible for a configuration which is otherwise dynamically stable to experience an out-of-control condition because of lack of adequate control power or excessive adverse yaw.

The model is equipped with a simplified stability augmentation system in the form of artificial angular rate damping in roll, yaw, and pitch. Air-driven rate gyroscopes are used in conjunction with proportional-type control servos to produce artificial variations in the aerodynamic damping of the model. The effect of stability augmentation about each individual axis is evaluated as part of the free-flight program.

The wind-tunnel free-flight technique has several inherent advantages: (1) because the tests are conducted indoors, the test schedule is not subject to weather conditions; (2) the tests are conducted under controlled conditions and a large number of tests can be accomplished in a relatively short period of time; (3) airframe modifications are quickly evaluated; and (4) models used in the technique are relatively large (1/10-scale for most fighter configurations) and can, therefore, be used in force tests to obtain static and dynamic aerodynamic characteristics for analysis of the model motions and as inputs for other forms of analysis, such as piloted simulators.

The Outdoor Radio-Controlled Model Technique

A significant void of information exists between the results produced by the wind-tunnel free-flight test technique for angles of attack up to and including the stall, and the results produced by the spin-tunnel test technique, which defines developed spin and spin-recovery characteristics. The outdoor radio-controlled model technique has, therefore, been designed to supply information on the post-stall and spin-entry motions of airplanes. The technique used at Langley has been used for a number of years, and the equipment and overall operation is much less sophisticated than those involved in recent drop model techniques developed by the NASA Flight Research Center and the Air Force Flight Dynamics Laboratory. The Langley radio-controlled model technique consists of launching an unpowered, dynamically scaled, radio-controlled model into gliding flight from a helicopter, controlling the flight of the model from the ground, and recovering the model with a parachute. A photograph showing a typical model mounted on the launching rig of the helicopter is shown in Figure 2.

The models used in these tests are made relatively strong to withstand high landing impact loads of 100 to 150 g's. They are constructed primarily of fiberglass plastic, with the fuselages in this case being 0.64-cm- (0.25-in.) thick hollow shells and the wings and tails having solid balsa cores with fiberglass sheet coverings. The model weights vary up to about 890 N (200 lb) for simulation of relatively heavy fighters at an altitude of 9114 m (30,000 ft). Radio receivers and electric-motor-powered control actuators are installed to provide individual operation of all control surfaces and a recovery parachute. Proportional-type control systems are used in this technique.

The instrumentation for the radio-controlled models usually consists of a three-axis linear accelerometer package, a three-axis rate gyro package, control position indicators, and a nose boom equipped with

vanes to measure angle of attack, angle of sideslip, and velocity. The signals from the instrumentation are transmitted to the ground via telemetry.

Two ground stations are used for controlling the flight of the model. The control duties are shared by two pilots, since this technique is also subjected to the control difficulties previously discussed for the wind-tunnel flight tests. Each ground station is provided with a radio-control unit, communications equipment, and a motorized tracking unit equipped with binoculars (to assist the pilots in viewing the flight of the model). A photograph of the tracking and controlling equipment is shown in Figure 3. All phases of the test operation are directed by a test coordinator. In addition, magnetic tape recorders on the ground are used to record voice communications between the helicopter, coordinator, and the model pilots.

The models are trimmed for approximately zero lift and launched from the helicopter at an airspeed of about 40 knots and an altitude of about 1524 m (5000 ft). The models are allowed to dive vertically for about 5 seconds, after which the horizontal tails are moved to stall the model. After the stall, various control manipulations may be used; for example, lateral-directional controls may be moved in a direction to encourage any divergence to develop into a spin. When the model has descended to an altitude of about 152 m (500 ft), a recovery parachute is deployed to effect a safe landing.

The outdoor radio-controlled model technique provides information which cannot be obtained from the other test techniques. The indoor free-flight tests, for example, will identify the existence of a directional divergence at the stall, but the test is terminated before the model enters the incipient spin. In addition, only 1-g stalls are conducted. The radio-controlled technique can be used to evaluate the effect of control inputs during the incipient spin, and accelerated stalls can be produced during the flights. At the other end of the stall/spin spectrum, spin-tunnel tests may indicate the existence of a flat or nonrecoverable spin mode, but it may be difficult for the airplane to attain this spin mode from conventional flight — the difference being that models in the spin tunnel are launched at about 90° angle of attack with a forced spin rotation. The radio-controlled test technique determines the spin susceptibility of a given airplane by using spin entry techniques similar to that of the full-scale airplane.

During a typical study using this technique, a complete study will be made of the effects of various types of control inputs during post-stall motions. For example, the ability of a configuration to enter a developed spin following the application of only longitudinal control (with no lateral-directional inputs) will be compared with results obtained when full prospin controls are applied. Recovery from the incipient spin is evaluated by applying recovery controls at various stages of the post-stall motion; for example, controls may be neutralized at varying numbers (or fractions) of turns after the stall. The radio-controlled technique, therefore, determines (1) the spin susceptibility of a configuration, (2) control techniques that tend to produce developed spins, and (3) the effectiveness of various control techniques for recovery from out-of-control conditions.

There are several limitations of the radio-controlled technique that should be kept in mind. The first, the most obvious, limitation is the fact that the tests are conducted out-of-doors. The test schedule is, therefore, subject to weather conditions, and excessive winds and rain can severely curtail a program. Another limitation to the technique is that it is relatively expensive. Expensive flight instrumentation is required to record the motions of the model; and the large size of these models requires the use of more powerful and reliable electronic equipment than that used by hobbyists. Costs are compounded by the fact that the model and its electronic equipment frequently suffer costly damage on landing impact. Because of this higher cost and the slow rate at which radio-controlled drop model tests can be accomplished, this technique is used only in special cases where the simpler and cheaper wind-tunnel and spin-tunnel techniques will not give adequate information. For example, when it is necessary to know whether an airplane can be flown into a particular dangerous spin mode, or when one wants to investigate recovery during the incipient spin. Conversely, most of the exploratory work, such as developing "fixes" for a departure at the stall or investigating a variety of spin-recovery techniques, is done in the wind tunnels.

The Spin-Tunnel Test Technique

The best known test technique used today to study the spin and spin-recovery characteristics of an airplane is the spin tunnel test technique. The present 6-m (20-ft) Langley spin tunnel has been in operation since 1941, when it replaced a smaller 4.5-m (15-ft) spin tunnel. An external view of the spin tunnel is shown in Figure 4, a cross-sectional view is shown in Figure 5, and a view of the test section is shown in Figure 6. In this tunnel, air is drawn upward by a fan located above the test section. Maximum speed of the tunnel is about 30 m/s (97 ft/sec), resulting in a maximum value of Reynolds number of about 0.18×10^6/m (0.6×10^6/ft). Models are hand-launched at about 90° angle of attack, with prerotation, into the vertically rising airstream. The model then seeks its own developed spin mode or modes. For recovery, the tunnel operator deflects the aerodynamic controls on the model to predetermined positions by remote control. Motion-picture records are used to record the spinning and recovery motions.

The models tested in the spin tunnel are normally made of fiberglass construction and, for fighter airplanes, are usually made to a scale of about 1/30. In a spin-tunnel investigation, the program consists of (1) determination of the various spin modes and spin-recovery characteristics, (2) study of the effect of center-of-gravity position and mass distribution, (3) determination of the effect of external stores, and (4) determination of the size and type parachute required for emergency spin recovery.

In a typical spin-tunnel test program, tests are made at the normal operating loading condition for the airplane. The spin and spin-recovery characteristics are determined for all combinations of rudder, elevator, and aileron positions for both right and left spins. In effect, a matrix of both the spin and spin-recovery characteristics are obtained for all control settings for the normal loading operating condition. Using these data as a baseline, selected spin conditions are treated again with incremental changes to the center of gravity and/or mass conditions. Then, based on the effects of these incremental changes, an analysis is made to determine the spin and spin-recovery characteristics that the corresponding airplane is expected to have. Also, the effectiveness of various control positions and deflections

are analyzed to determine which control techniques are most effective for recovery. After the spin-recovery characteristics for the normal loading conditions have been determined, additional tests are made to determine the effects of other loading conditions, store configurations (including asymmetric stores), and other items of interest such as speed brakes and leading- and trailing-edge flaps.

The parachute size required for emergency spin recovery is determined for the most critical spin conditions observed in the spin-tunnel tests, and is checked at other conditions throughout the test program. If the parachute size is found to be too small for other conditions, the size is adjusted so that the parachute finally recommended for use on the spin demonstration airplane will be sufficient to handle the most critical spins possible on the airplane for any loading.

As a result of the combination of the relatively small scale of the model and the low tunnel speeds, spin-tunnel tests are run at a value of Reynolds number which is much lower than that for the full-scale airplane. Experience has shown that the differences in Reynolds number can have significant effects on spin characteristics displayed by models and the interpretation of these results. In particular, past results have indicated that very significant effects can be produced by air flowing across the forward fuselage at angles of attack approaching 90°. These effects are influenced by the cross-sectional shape of the fuselage forebody and may be extremely sensitive to Reynolds number variations. Particular attention is, therefore, required for documentation of this phenomenon prior to spin-tunnel tests. This evaluation has been conducted in the past with the aid of static force tests over a wide Reynolds number range as described in the following discussion.

Shown in Figure 7 is a plan view of an airplane in a right spin. The arrows along the nose indicate the relative magnitude and sense of the linear sideward velocities along the fuselage due to the spinning rotation. The sketch on the right-hand side of the figure illustrates the sideslip angle at a representative nose location due to the spin rotation. As can be seen, the airplane rate of descent and the sideward velocity at the nose of the airplane combine vectorially to produce a positive sideslip angle β at the nose. It has been found that sideslip on the nose of an airplane at spin attitudes can produce large forces, and these forces in turn produce large moments, because the length between the nose and center of gravity of modern military airplanes tends to be relatively large. If, in the case of a right spin (as shown in Fig. 7) positive (nose-right) yawing moments are produced by the nose due to the effective sideslip angle, then the nose is producing prospin, or autorotative moments. If, on the other hand, negative (nose-left) values of yawing moment are produced by the nose, then the nose is producing an antispin, or damping moment.

The sense of the moment actually produced by a particular nose configuration may be very sensitive to the value of Reynolds number. For example, shown in Figure 8 is the variation of static yawing-moment coefficient C_n with Reynolds number for a representative fighter configuration at an angle of attack of 80° and a sideslip angle of 10°. Recalling the information given in Figure 7, a positive value of β would be produced at the nose in a right spin, and positive values of C_n are therefore prospin, while negative values are antispin. Two regions of Reynolds number are of interest: A low value which is typical of spin-tunnel tests, and a high value, indicative of the conditions for the full-scale airplane. As can be seen, the values of C_n (which at this angle of attack are produced almost entirely by the nose) tend to be prospin at the spin-tunnel test condition, and antispin for the full-scale airplane flight condition. Also shown are data indicating the effect of nose strake on C_n. The effect of the strake was to modify the airflow around the nose and to make the aerodynamic phenomenon produced by the nose at low Reynolds number similar to that produced at higher Reynolds number.

It has been found during several spin-tunnel investigations that this type of Reynolds number effect did exist for some configurations. The results showed that the model exhibited a nonrecoverable fast-flat spin without corrections for Reynolds number because of the prospin moments produced by the nose. When strakes were added, satisfactory recoveries from the developed spin were obtained and the model results could be extrapolated to full scale with some confidence. Because of concern over the possible existence of such Reynolds number effects, it is required that a series of static wind-tunnel force tests be conducted to insure that adequate simulation of the airplane is provided by the spin-tunnel model. These tests are usually performed in the 3.7-m (12-ft) pressure tunnel at the Ames Research Center.

As discussed in the next section of this paper, a rotary-balance test rig has recently been put into operation in the Ames tunnel, thereby providing for the analysis of aerodynamic characteristics during spinning motions at high values of Reynolds number. It is anticipated that this apparatus will ultimately be used for the preliminary Reynolds number investigations required for spin-tunnel tests.

ROTARY-BALANCE TESTS

One test technique which has been used to produce much significant information regarding the complex aerodynamic characteristics of airplane configurations during spinning motions is the rotary-balance test technique. In this technique, six-component measurements are made of the aerodynamic forces and moments acting on a wind-tunnel model during continuous 360° spinning motions at a constant angle of attack. Such tests were initially conducted many years ago, and the past studies identified some of the major factors which influenced spin characteristics for configurations at that time, such as the autorotative tendencies of unswept wings and certain fuselage cross-sectional shapes. The use of the technique, however, has not kept pace with the rapid evolution in fighter configurations. As a result, little information of this type is available for current fighter configurations which feature long pointed fuselage noses and blended wing-body arrangements.

Shown in Figures 9 and 10 are photographs of rotary-balance test rigs recently put into operation by NASA in the 9.1- by 18.2-meter (30- by 60-ft) full-scale tunnel at the Langley Research Center and the 3.7-meter (12-ft) pressure tunnel at the Ames Research Center. Both rigs are capable of providing measurements of six-component data over a range of angle of attack of 45° to 90° and a range of nondimensional spin rate $\frac{\Omega b}{2V}$ of $\pm$ 0.3.

The apparatus at Langley is designed for tests of the relatively large-scale drop models used for flight tests described in an earlier section of this paper. Thus, aerodynamic data can be measured for the drop model at the same value of Reynolds number as that obtained in flight tests, and the data can then be used together with conventional static force data as inputs to theoretical spin prediction programs for correlation with the results of flight tests. In this manner, the validity of theoretical techniques can be evaluated without the usual complications arising from differences in Reynolds number between wind-tunnel tests and flight tests. The apparatus is currently being used extensively for measurements of data for several current military configurations. Tests are conducted to determine the characteristics of the basic configuration, the effects of individual and combined control deflections, the effects of tail surfaces and nose strakes, and the effects of spin radius and sideslip. The foregoing tests are limited to relatively low values of Reynolds number up to 3.3×10^6/m (1×10^6/ft).

The rotation-balance apparatus presently operational at the Ames Research Center is a modification of an apparatus originally built for testing axisymmetric bodies in the Ames 1.8- by 1.8-m (6- by 6-ft) supersonic wind tunnel. It has just recently been put into operation for conducting basic studies of simple airplane-like configurations and is the forerunner to a new rotation-balance apparatus now under construction. The new apparatus will allow testing of complex model configurations at angles of attack from 0° to 100° and angles of sideslip up to $\pm 30°$ in either the Ames 3.7-m pressure tunnel or 3.4- by 3.4-m (11- by 11-ft) transonic tunnel. As a result of the pressurization capability of both tunnels, data may be obtained for Reynolds numbers up to about 29.5×10^6/m (9×10^6/ft). The existing modified rig has been used initially for tests to determine the effects of Reynolds number, angle of attack, and spin rate on the aerodynamic characteristics of airframe components such as pointed noses, various fuselage cross-sectional shapes, and drooped horizontal tail surfaces.

The two test rigs are used in a coordinated research program between the two NASA Centers. Tests at Langley are directed at an understanding of the types of aerodynamic phenomena exhibited by military configurations during spins, the mathematical modeling of such phenomena, and theoretical evaluations of the effects of the phenomena on spinning motions using the results of dynamic model tests for correlation with theory. Studies at Ames are directed toward an evaluation of the effects of Reynolds number on aerodynamic characteristics and verification of phenomena observed during tests at Langley.

As discussed in References 1 to 3, the results of these tests have identified several configuration features which can have large effects on the aerodynamic characteristics of modern aircraft during spins. Figure 11 illustrates some of the prospin flow mechanisms which have been identified in these tests. The sketch at the left of the figure indicates the well-known tendency of certain noncircular fuselage cross-sectional shapes to produce autorotative moments for certain values of Reynolds number. This particular phenomenon may be caused by the cross-sectional shape of either the forward or aft fuselage, and configurations are particularly susceptible to this condition for angles of attack corresponding to the flat spin ($\alpha \approx 90°$). The second sketch of Figure 11 illustrates a prospin flow mechanism found to exist for a current fighter configuration with drooped horizontal tails. The phenomenon has also been found to be most pronounced near $\alpha = 90°$, but deflection of the horizontal tail as an all-movable control surface has been found to affect spin damping for angles of attack from $\alpha = 45°$ to about $\alpha = 80°$. The third and fourth sketches illustrate prospin flow mechanisms commonly exhibited by airplane configurations with long pointed noses for angles of attack between 30° and 70°. As shown by the third sketch, asymmetric vortices shed off the pointed nose create prospin yawing moments, even for zero rotation rate. Finally, the fourth sketch illustrates that long pointed noses with certain elliptical cross-sectional shapes produce large prospin moments as a result of a large contribution of the nose to static directional stability. This particular phenomenon is a three-dimensional flow mechanism in contrast to the largely two-dimensional mechanism illustrated by the sketch at the left of the figure. The magnitudes of the moments produced by pointed noses are affected by Reynolds number; however, these moments have occurred at the highest values of Reynolds number tested for some configurations.

The results of the tests have also indicated that the aerodynamic moments (particularly yawing and pitching moments) exhibited by current military configurations during spins vary nonlinearly with spin rate. For example, as shown in Figure 12, the results of tests (Ref. 3) for a current configuration with drooped horizontal tails show a markedly nonlinear variation with nondimensional spin rate. A detailed discussion of the importance of such nonlinear data on theoretical studies of spins is beyond the scope of this paper; however, it should be pointed out that recent studies (Ref. 4, e.g.) have shown that nonlinear moments have a large effect on calculated spin motions, and that good agreement is obtained with dynamic model tests for smooth, steady spins when such data are used as inputs for the calculations. On the other hand, use of conventional calculation techniques which use conventional linearized static and dynamic stability derivatives produce completely erroneous results. It appears, therefore, that rotary-balance tests are mandatory for the development of valid mathematical models for spin analysis.

It will be appreciated that the foregoing discussion has been concerned with smooth, steady spins. Experience has shown that many modern military aircraft exhibit large-amplitude oscillatory spins, and more sophisticated wind-tunnel test techniques are required to measure the complex aerodynamics produced by the combined rotary and oscillatory motions.

SIMULATOR STUDIES

The model test techniques previously discussed have several critical shortcomings. For example, the inputs of the human pilot have been minimized or entirely eliminated. In addition, the use of unpowered models and space constraints within the wind tunnels do not permit an evaluation of the spin susceptibility of airplanes during typical air combat maneuvers. Finally, the effects of sophisticated automatic control systems are not usually evaluated because of space limitations within the models. In order to provide this pertinent information, a piloted simulation test technique has been developed as a logical follow-on to the model tests.

A sketch of the hardware used in this technique is shown in Figure 13. The tests are conducted using the Langley Differential Maneuvering Simulator (DMS) which is a fixed-base simulator with the capability of simultaneously simulating two airplanes as they maneuver with respect to one another, including a full,

wide-angle visual display for each pilot. Two 12.2-m (40-ft) diameter projection spheres each enclose a cockpit, an airplane image projection system, and a sky-Earth-Sun projection system. A control console located between the spheres is used for interfacing the hardware and the computer, and it displays critical parameters for monitoring the hardware operation. Each pilot is provided a projected image of his opponent's airplane, showing the relative motions and range of the two airplanes by use of a television system with range and attitude of the target image controlled by the computer program.

A photograph of one of the cockpits and the target visual display during a typical engagement is shown in Figure 14. A cockpit and instrument display representative of current fighter aircraft equipment are used together with a fixed gunsight for tracking. A sophisticated hydraulic control feel system is used which can be programed to simulate a wide range of characteristics. Although the cockpits are not provided with attitude motion, each cockpit does incorporate a buffet system capable of providing programmable buffet accelerations as high as 1-g.

The visual display in each sphere consists of a target image projected onto a sky-Earth-Sun display. The sky-Earth-Sun scene is generated by two point light sources projecting through two hemispherical transparencies, one transparency of blue sky and clouds and the other of terrain features. No provision is made to simulate spatial motions with respect to the sky-Earth scene (such as altitude variation), however, a flashing light located in the cockpit behind the pilot is used as a cue when an altitude of less than 1524 m (5000 ft) is reached. The target-image generation system uses an airplane model mounted in a four-axis gimbal system and a television camera with a zoom lens to provide an image to the target projector within the sphere. The system can provide a simulated range between airplanes from 91.4 m (300 ft) to 13,716 m (45,000 ft) with a 10-to-1 brightness contrast between the target and the sky-Earth background at minimum range.

Additional special effects features of the DMS hardware include simulation of tunnel vision and blackout at high normal accelerations, use of an inflatable anti-g garment for simulation of g-loads, and use of sound cues to simulate wind, engine, and weapons noise as well as artificial warning systems. Additional details on the DMS facility are given in Reference 5.

The application of the simulator to the stall/spin area is, of course, dependent on the development of a valid mathematical model of the airplane under consideration. In view of the present lack of understanding of aerodynamic phenomena at spin attitudes, the simulation studies are currently limited to angles of attack near the stall, and fully developed spins are not simulated. Rather, the studies are directed toward an evaluation of the spin susceptibility or stall/departure characteristics of the airplane during typical air combat maneuvers and the effects of automatic control systems on these characteristics.

Recent studies using the simulation technique have indicated that it is an extremely valuable tool for stall/spin research. Correlation of results with those obtained from full-scale flight tests for several current fighters has indicated good agreement, particularly with regard to the overall spin resistance of the configurations. In addition, valuable insight as to the effects of various automatic spin prevention concepts has been obtained.

It is hoped that current research will ultimately result in valid theoretical methods for stall/spin analysis, which in turn will permit an extension of the simulator technique to studies of the developed spin and spin recovery. A readily apparent application of such a technique would be the development of a procedures trainer for pilot training. This application is deemed especially important, inasmuch as current flight restrictions prohibit intentional spinning of most fighter aircraft, thereby depriving the pilot of training for an emergency which may well be difficult to overcome.

CONCLUDING REMARKS

In this discussion of stall/spin test techniques used by NASA, an effort has been made to describe the techniques and to indicate the most appropriate uses for each technique. These techniques have proven to be especially valuable tools, and a large amount of significant information can be obtained in a relatively safe, cheap, and realistic manner.

REFERENCES

1. Clarkson, Mark H., Malcolm, Gerald N., and Chapman, Gary T.: Experimental Determination of Post-Stall Rotary Derivatives for Airplane-Like Configurations at Several Reynolds Numbers. AIAA Paper 75-171, AIAA 13th Aerospace Science Meeting, Pasadena, California, January 20-22, 1975.

2. Chambers, Joseph R., Anglin, Ernie L., and Bowman, James S., Jr.: Effects of a Pointed Nose on Spin Characteristics of a Fighter Airplane Model Including Correlation With Theoretical Calculations. NASA TN D-5921, 1970.

3. Chambers, Joseph R., Bowman, James S., Jr., and Anglin, Ernie L.: Analysis of the Flat-Spin Characteristics of a Twin-Jet Swept-Wing Fighter Airplane. NASA TN D-5409, 1969.

4. Bihrle, William, Jr.: Effects of Several Factors on Theoretical Predictions of Airplane Spin Characteristics. NASA CR-132531, 1974.

5. Ashworth, B. R., and Kahlbaum, William J., Jr.: Description and Performance of the Langley Differential Maneuvering Simulator. NASA TN D-7304, 1973.

TABLE I. SCALE FACTORS FOR DYNAMIC MODELS

[Model values are obtained by multiplying airplane values by the following scale factors where N is the model-to-airplane scale ratio, σ is the ratio of air density to that at sea level (ρ/ρ_o), and ν is the value of kinematic viscosity]

	Scale factor
Linear dimension	N
Relative density ($m/\rho\ell^3$)	1
Froude number ($V^2/\ell g$)	1
Weight, mass	$N^3\sigma^{-1}$
Moment of inertia	$N^5\sigma^{-1}$
Linear velocity	$N^{1/2}$
Linear acceleration	1
Angular velocity	$N^{-1/2}$
Time	$N^{1/2}$
Reynolds number ($V\ell/\nu$)	$N^{1.5}\frac{\nu}{\nu_o}$

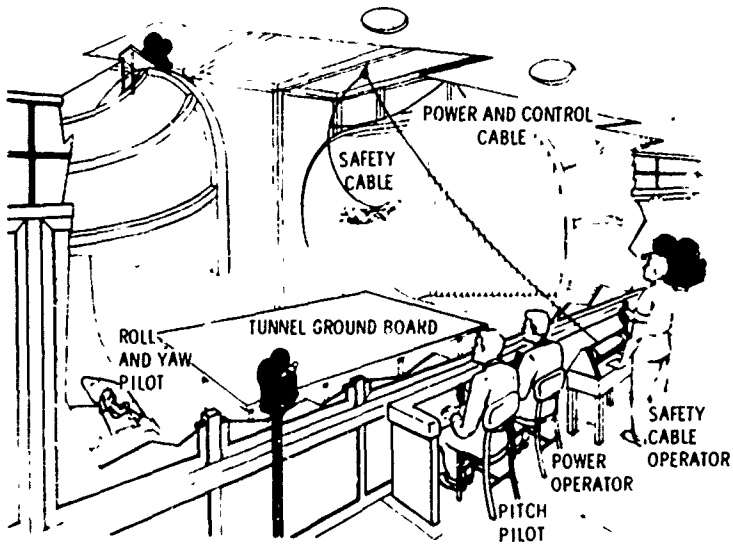

Figure 1. Test setup for wind-tunnel free-flight tests.

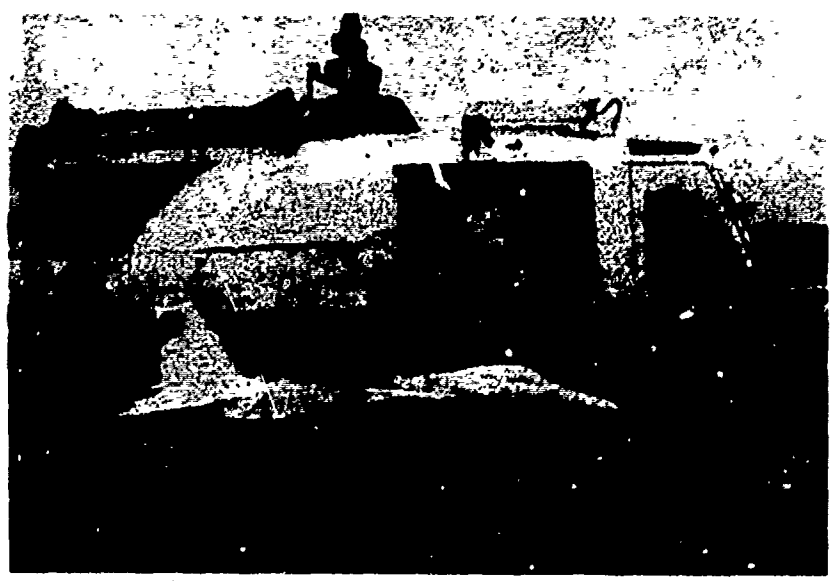

Figure 2. Phot graph of drop model mounted on helicopter.

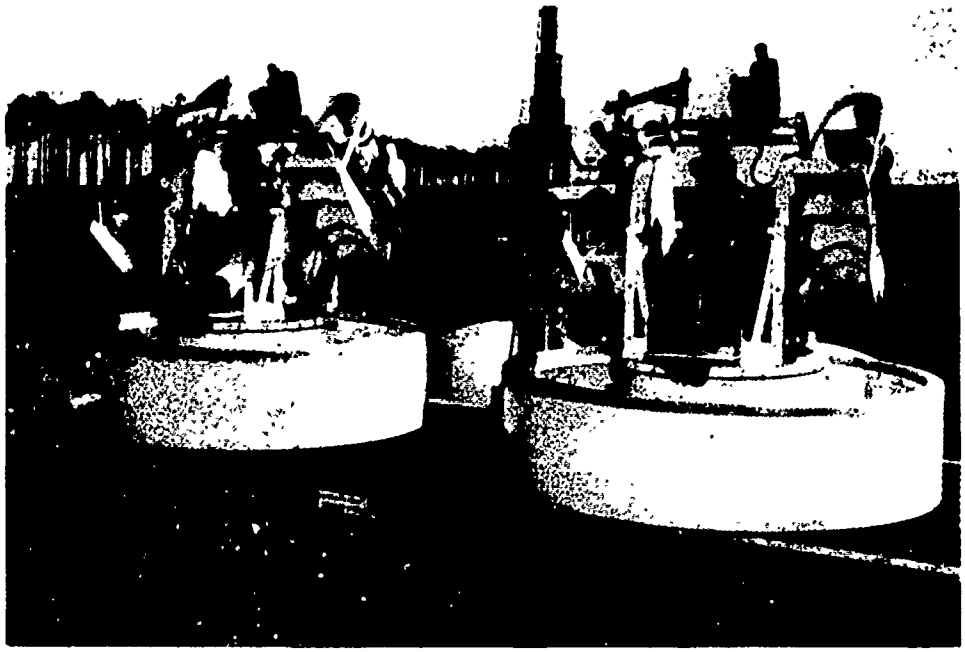

Figure 3. Photograph of ground control unit.

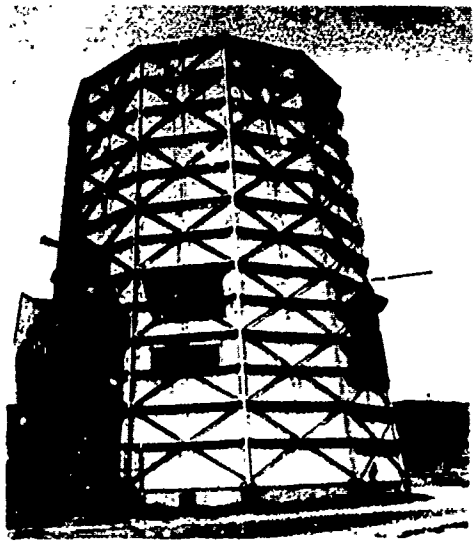

Figure 4. External view of the Langley spin tunnel.

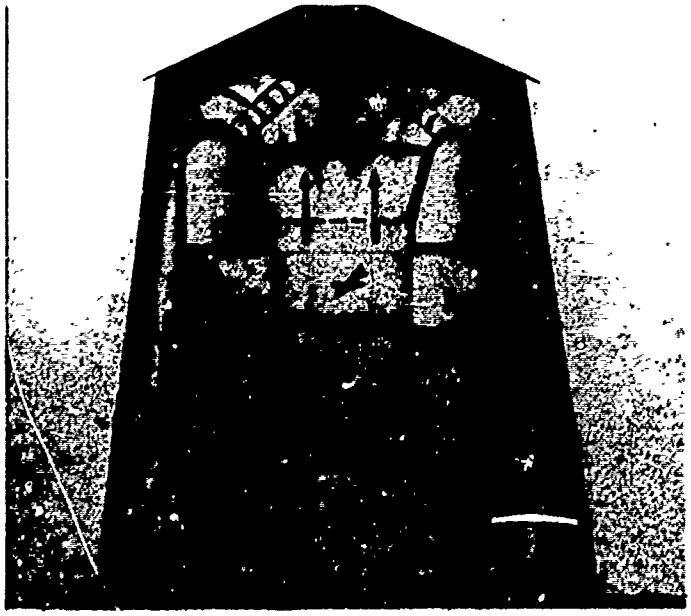

Figure 5. Cross-sectional view of the spin tunnel.

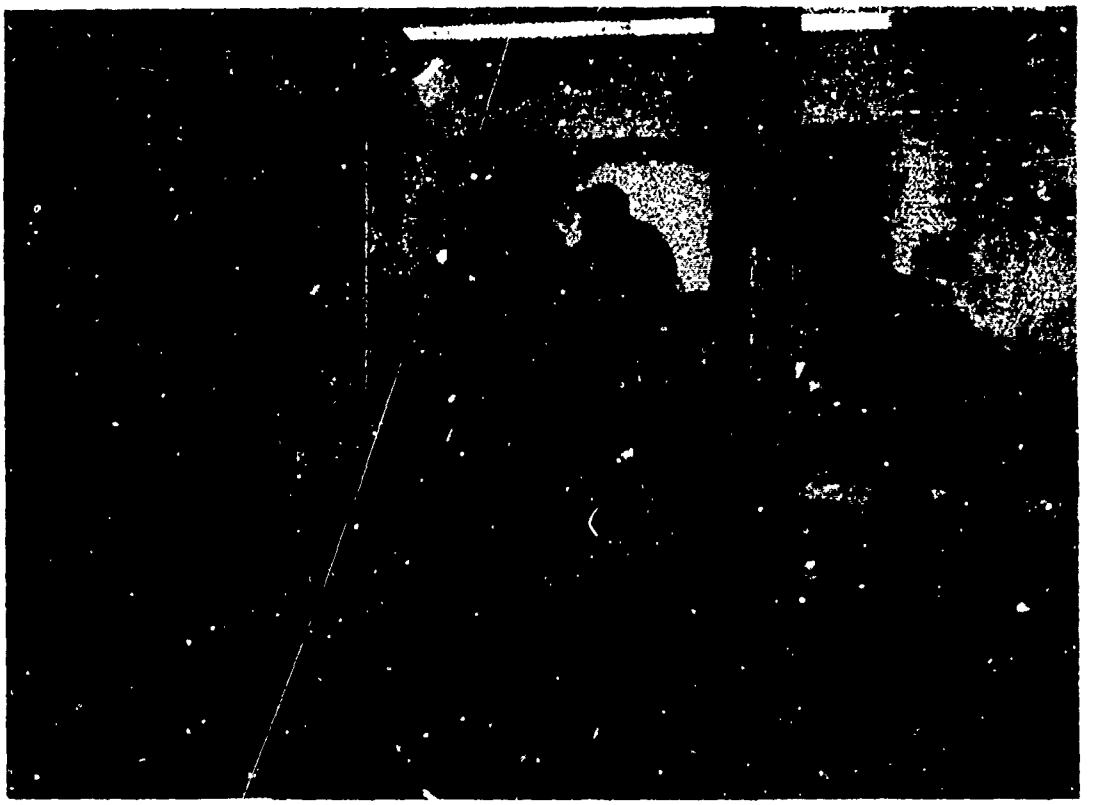

Figure 6. Interior view of the spin tunnel.

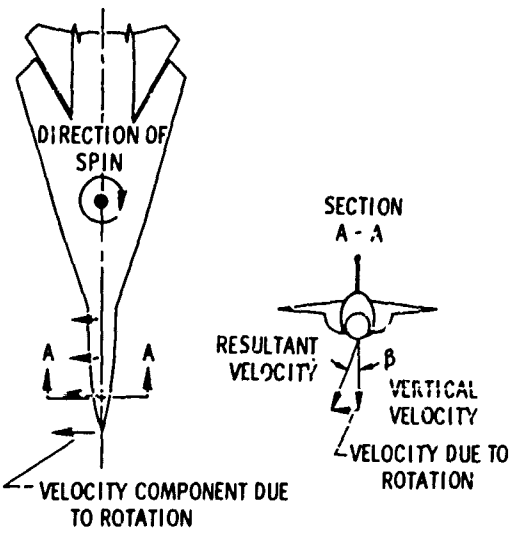

Figure 7. Sideslip angle generated at nose of airplane during right spin.

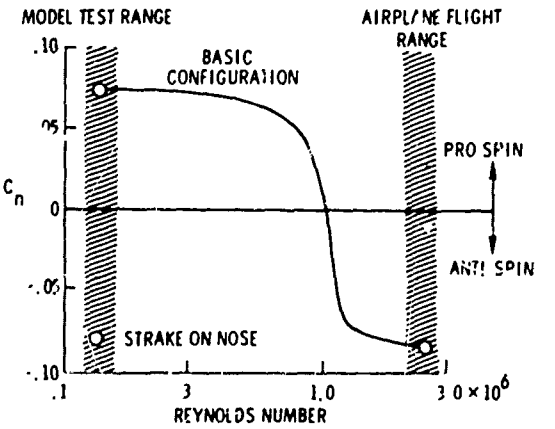

Figure 8. Effect of Reynolds number on yawing-moment coefficient. $\alpha = 80°$, $\beta = 10°$.

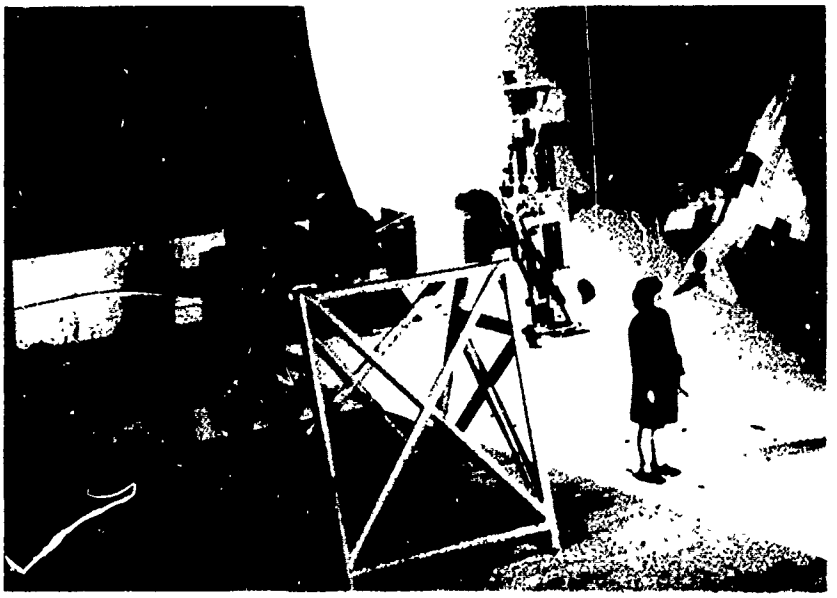

Figure 9. Photograph of rotary-balance apparatus in the 9.1- by 18.2-m (30- by 60-ft) full-scale tunnel at Langley.

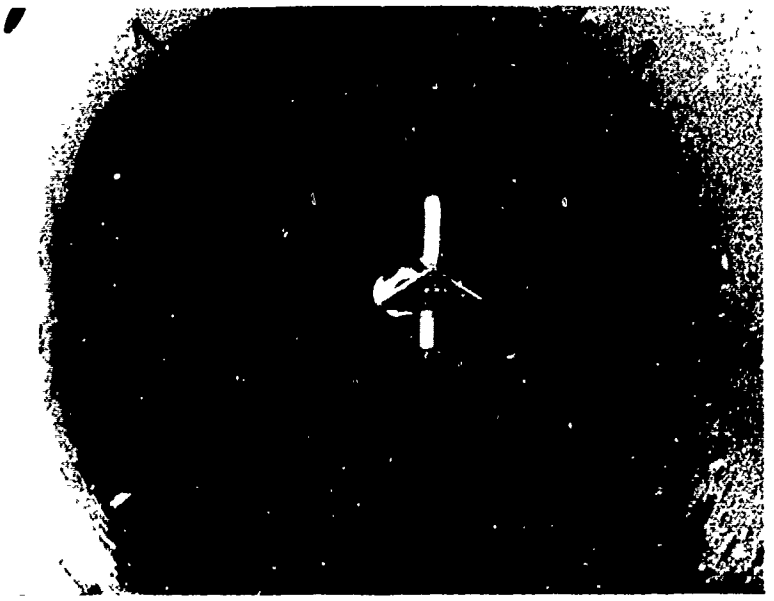

Figure 10. Photograph of rotary-balance apparatus in the 3.7-m (12-ft) pressure tunnel at Ames.

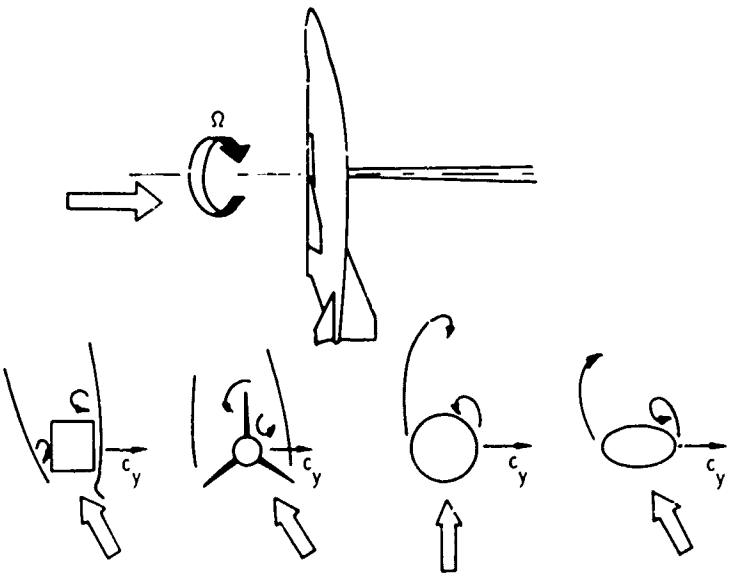

Figure 11. Flow mechanisms which produce prospin moments.

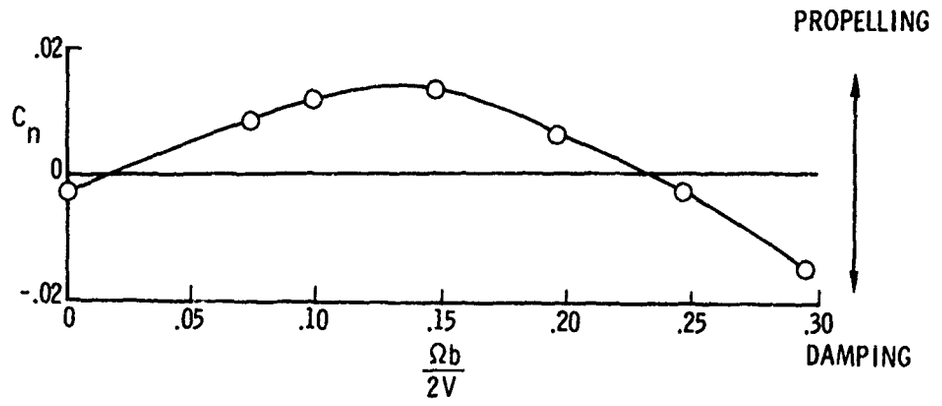

Figure 12. Typical nonlinear variation of yawing-moment coefficient with spin rate.

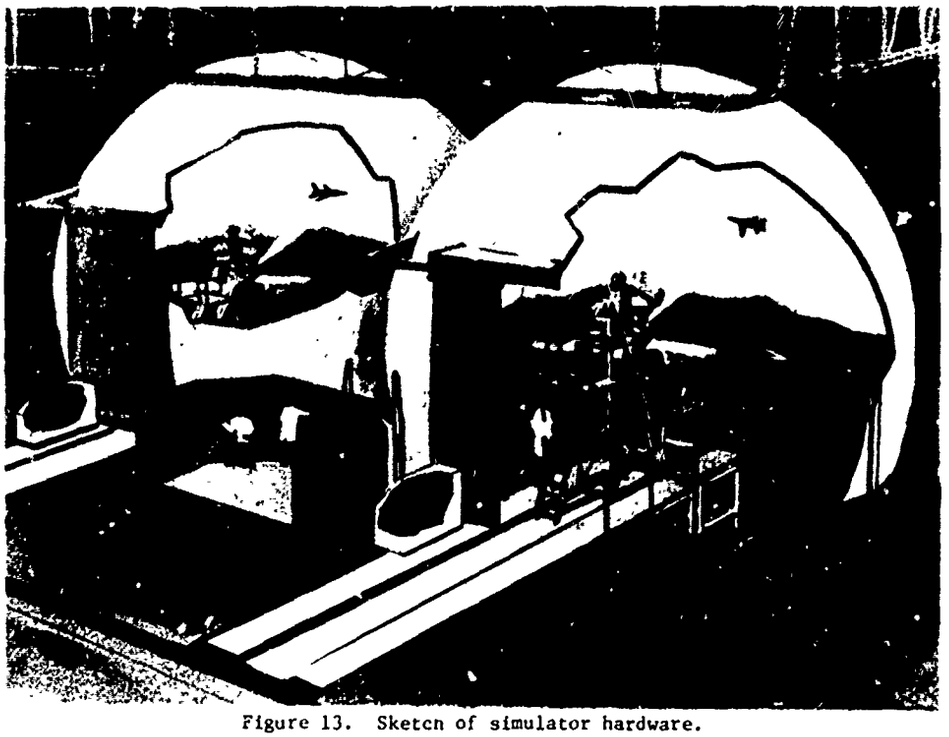

Figure 13. Sketch of simulator hardware.

Figure 14. View of cockpit and visual display within one sphere of OMS.

ACTION SUR LA VRILLE, PAR MOMENT "STATIQUE", DE FUSEES ET DE CHARGEMENTS DISSYMETRIQUES

par Jean GOBELTZ
Directeur technique

et Lucien BEAURAIN
Chef de la Soufflerie Verticale

Institut de Mécanique des Fluides de Lille
5,bd Paul Painlevé, 59000 - Lille (France)

RESUME.-

Le présent document traite de résultats d'études à caractère général qui furent faites à l'Institut de Mécanique des Fluides de Lille sur diverses maquettes en soufflerie de vrille.

Le premier sujet abordé concerne l'action de fusées utilisées en tant que dispositif de secours pour la vrille ; l'étude a, jusqu'ici, été limitée aux avions légers ; cependant certaines conclusions peuvent être valables, du moins qualitativement, pour d'autres types d'avions, avions d'armes en particulier.

Le second sujet concerne l'influence d'une dissymétrie de chargement sur la vrille d'avions de tous types : armes, légers, transport. La dissymétrie considérée est une dissymétrie purement massique telle que celle qui peut être créée par le carburant dans la voilure. Cependant, pour les avions d'armes une dissymétrie, causée cette fois-ci par des charges extérieures (donc dissymétrie à la fois massique et géométrique), est également prise en considération.

1 - FUSEES ANTI-VRILLE

1.1 - Introduction.

Le but de l'étude était de rechercher s'il était envisageable d'utiliser un dispositif fusée susceptible d'être installé rapidement sur tout avion léger pour sa campagne d'essais de vrille. Pour être acceptable la fusée ne devait pas avoir de caractéristiques prohibitives (notamment une poussée trop importante).

Au cours de l'étude sur maquettes, diverses orientations furent données à la fusée afin de définir le sens d'action optimal ; de l'ensemble des résultats, nous ne retiendrons ici que les principaux, à savoir ceux qui furent obtenus avec une fusée agissant successivement en pur tangage, en pur roulis puis en pur lacet.

Outre la valeur intrinsèque des résultats, l'étude a permis aussi de tirer des enseignements concernant le type de modifications qu'il aurait lieu d'apporter à un avion léger ayant une vrille critique.

1.2 - Maquettes utilisées.

Deux maquettes furent retenues pour l'étude des fusées ; comme le montre la figure 1 leurs caractéristiques, tant géométriques que massiques, sont assez différentes. Les maquettes ont été volontairement modifiées dans le but d'obtenir différents types de vrille, entre autres la vrille plate et rapide dont il n'est pas besoin de rappeler les problèmes que cette vrille soulève (cela ne signifie pas pour autant que toute vrille non plate est automatiquement sans problèmes).

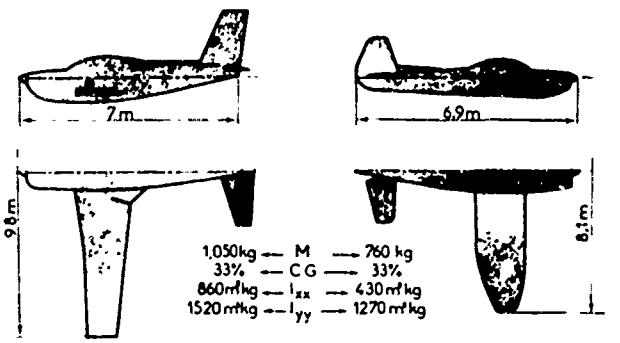

Fig. 1 - MAQUETTES UTILISEES (CARACTERISTIQUES DONNEES EN VALEUR AVION)

Le principe du moteur fusée utilisé est le suivant : un allumeur assure l'inflammation d'un pain de poudre, lequel conditionne, suivant ses caractéristiques chimiques et géométriques, la poussée et la durée de fonctionnement de la fusée ; les gaz émis par la combustion du pain de poudre parcourent un tube jusqu'à l'endroit où on désire appliquer la poussée (la figure 2 précise ces endroits). Cette solution permet de placer le bloc-moteur près du centre d'inertie de la maquette, ce qui rend possible l'équilibrage de cette dernière.

Un dispositif de radio-télécommande est installé dans la maquette ; il permet simultanément la mise à feu de la fusée et une modification de braquage des gouvernes (modification par tout ou rien et de façon prédéterminée).

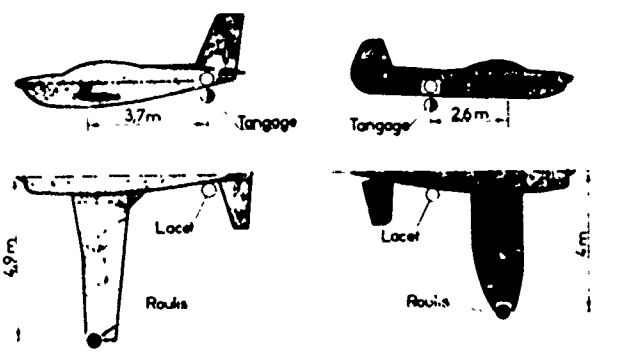

Fig. 2 - POSITIONNEMENT DES FUSEES

1.3 - Conditions d'essais.

L'effet de la fusée a été recherché à partir de différents types de vrille, mais plus particulièrement à partir de la vrille plate et rapide (Fuselage presque horizontal - moins de 2 secondes/tour à l'échelle avion). D'ailleurs les résultats qui sont présentés ici sont surtout ceux qui furent obtenus avec ce type de vrille.

Lors de la mise à feu de la fusée, les gouvernes étaient soit laissées pro-vrille, soit recentrées ; gouvernes laissées pro-vrille est, bien entendu, un cas non réaliste mais qui présente l'avantage de très bien mettre en évidence l'effet du dispositif. Gouvernes recentrees, pour les deux maquettes la vrille se maintenait ou presque, sans fusée.

Les caractéristiques des fusées qui furent essayées sont très variables et comprises entre les valeurs extrémales suivantes (à l'échelle avion) :

- poussée de 8100 newtons agissant pendant environ 2 secondes
- poussée de 200 newtons agissant pendant environ 6 secondes.

Ces poussées représentent respectivement 80 % à 100 % (selon l'avion) et 2 % à 3 % du poids de l'avion, soit pour la première, une valeur nettement prohibitive et non envisageable pour l'avion et pour la seconde une poussée très faible.

Dans les résultats qui vont être présentés, il a paru souhaitable de donner la poussée de la fusée rapportée au poids de l'avion et non pas son module ni le moment qu'elle crée ; notons aussi que les résultats donnés sont ceux qui seraient obtenus avec le bras de levier le plus grand possible pour l'avion soit :

- pour la fusée roulis : fusée placée en extrémité d'aile
- pour les fusées tangage et lacet : fusée placée à l'extrême arrière du fuselage.

1.4 - Résultats.

1.4.1 - Fusée tangage.

Il est évident qu'une fusée agissant en tangage est la solution la plus séduisante puisque son action est indépendante du sens de rotation de la vrille. Sur l'avion une seule fusée serait à installer.

Malheureusement, une fusée tangage est peu efficace du moins si on reste dans les limites raisonnables de poussée. En effet, en recentrant les gouvernes, une récupération n'est possible avec une fusée tangage que si sa poussée est supérieure à 50 % du poids de l'avion et si elle agit, pendant 4 secondes ou plus. Une poussée égale à 80 % du poids de l'avion et agissant pendant 2 secondes conduit à un résultat identique. De telles poussées ne sont pas envisageables pour l'avion ne serait-ce que par les problèmes de résistance de structure que cette fusée poserait.

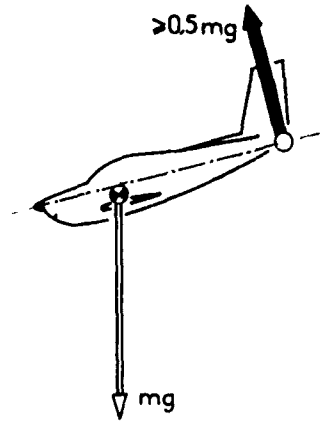

Fig. 3 - FUSEE AGISSANT EN TANGAGE

1.4.2 - Fusée roulis.

Nous avons d'abord recherché s'il était possible de sortir de vrille avec une fusée roulis quel que soit son sens d'action, c'est-à-dire faisant baisser ou relever telle aile. Ce résultat a pu être obtenu, mais il faut préciser qu'une fusée faisant relever l'aile extérieure (aile qui avance pendant la vrille) est plus efficace que la même fusée mais faisant baisser la même aile, et cela dans le rapport 3/1.

Si on prend le sens d'action le plus favorable (donc fusée faisant relever l'aile extérieure) une fusée roulis de l'ordre de 10 % du poids de l'avion et agissant pendant 5 à 6 secondes provoque la sortie en environ 3 tours même gouvernes maintenues pro-vrille ; à impulsion identique ou presque, la sortie est meilleure (plus rapide) si la poussée est doublée. Pour fixer les idées, disons que la poussée d'une fusée roulis appliquée en extrémité d'aile doit être de l'ordre de 15 % du poids de l'avion pour être suffisamment efficace (voir figure 4).

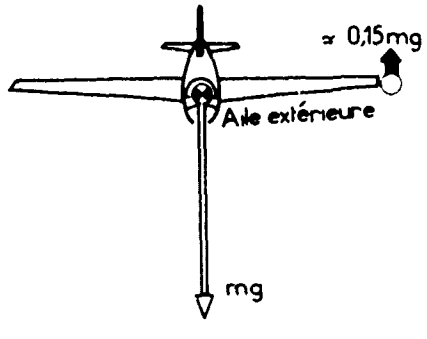

FIG. 4 - FUSEE AGISSANT EN ROULIS

Lorsqu'il y a récupération par fusée faisant relever l'aile extérieure, cette récupération est pure : basculement transversal modéré pendant le freinage et mouvement piqueur amenant l'avion à une attitude verticale ; cela n'est pas le cas lorsque la fusée agit dans le sens opposé (aile extérieure abaissée) ; en effet, l'arrêt de la vrille s'opère avec un basculement transversal parfois suffisamment ample pour amener un passage sur le dos ; il y a effectivement récupération mais après des mouvements peu classiques pour un avion léger, susceptibles de désorienter le pilote. Notons enfin que, en ce qui concerne la fusée faisant baisser l'aile extérieure, si sa poussée est trop faible elle peut aplatir la vrille de façon passagère, c'est-à-dire approximativement pendant le temps de

sa durée de fonctionnement. La fusée peut donc avoir, selon ses caractéristiques, un effet pro-vrille (poussée faible) ou un effet anti-vrille (poussée forte).

1.4.3 · Fusée lacet.

Un résultat déjà très intéressant est obtenu avec une très faible poussée (2 % du poids de l'avion) agissant pendant 7 secondes et gouvernes recentrées ; dans ce cas une sortie est obtenue en 5 à 6 tours ; cette sortie est, bien entendu, encore très longue, mais néanmoins deux fois moins longue que celle obtenue avec gouvernes recentrées et sans fusée.

Une poussée de l'ordre de 5 % du poids de l'avion et agissant pendant 4 à 6 secondes amène une sortie de 2 à 3 tours à partir d'une vrille plate et rapide. Compte tenu du caractère de la vrille à partir de laquelle la manoeuvre est faite, une sortie en 2 à 3 tours peut être considérée comme étant un résultat satisfaisant.

Une fusée lacet est donc très efficace ; un autre résultat caractérise très bien cette efficacité ; il s'agit d'une sortie rapide (1 à 2 tours) obtenue avec une fusée de 12 % agissant pendant 4 secondes, les gouvernes ayant été laissées pro-vrille. Dans ce cas l'effet des gouvernes devient secondaire en regard de celui de la fusée.

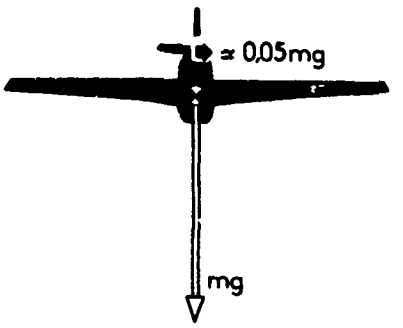

Fig. 5 - FUSEE AGISSANT EN LACET

1.5 - Efficacité relative des fusées.

Les quelques résultats qui viennent d'être présentés, montrent nettement que si l'on classe les fusées selon leur efficacité, on obtient l'ordre suivant :

- fusée tangage (la moins efficace)
- fusée roulis
- fusée lacet

De l'ensemble des résultats de l'étude, en faisant intervenir les paramètres suivants :

- module de la poussée)
- durée de fonctionnement) de la fusée
- bras de levier)
- durée de sortie

nous avons pu définir un rapport approximatif d'efficacité entre les fusées ; ce rapport est

- environ 15 entre les fusées lacet et tangage
- environ 6 entre les fusées lacet et roulis (dans le cas le plus favorable pour cette dernière, c'est-à-dire celui où la fusée tend à relever l'aile extérieure).

1.6 - Remarques relatives à l'arrêt de la vrille.

Nous prenons ici en considération certaines difficultés qui pourraient survenir lors d'un arrêt de vrille consécutif à l'action d'une fusée. Nous nous limitons au cas de la fusée la plus efficace, c'est-à-dire celle agissant en lacet.

Il est évident que si le dispositif était adopté pour les avions, il serait très souhaitable que la durée de fonctionnement de la fusée soit contrôlable ; cette durée serait en effet à ajuster selon certains paramètres, entre autres la position de la fusée (bras de levier) et le type de vrille à vaincre (qui peut ne pas être systématiquement plate et rapide, comme ce fut souvent le cas dans nos essais).

Examinons ici le cas d'une fusée de caractéristiques bien définies et non modifiables (telle qu'une fusée à poudre). Il peut alors arriver que l'efficacité de la fusée soit trop forte en ce sens que la vrille soit stoppée avant que la fusée n'ait cessé de fonctionner ; dans ce cas sous l'action de la fusée on peut craindre un départ en vrille de sens inverse ou, dans le cas d'un passage dos, un départ en vrille dos. Nous pouvons apporter des enseignements à ce sujet par l'exemple suivant :

A l'I.M.F.L. nous avons déjà utilisé les résultats relatifs aux fusées pour l'implantation d'un tel dispositif sur un avion déterminé. La fusée envisagée pour cet avion était à poudre. Etudiée sur la maquette de cet avion, la fusée s'est avérée nettement trop efficace si elle était placée en bout de fuselage (et agissant en lacet bien entendu) ; en effet, gouvernes maintenues à fond pro-vrille, la fusée amenait une sortie très rapide (< 1 tour) suivie d'un non moins rapide départ en vrille inverse ; remarquons que les gouvernes étant inchangées, celles-ci étaient alors à fond anti-vrille en ce qui concerne la vrille inverse, ce qui n'empêchait pas cette dernière de s'établir. Ne pouvant modifier les caractéristiques de la fusée, nous avons réduit son efficacité en diminuant son bras de levier ; nous avons ainsi trouvé une position optimale de la fusée telle que l'efficacité de celle-ci soit suffisante pour stopper la vrille et insuffisante pour lancer une vrille inverse.

Précisons que cette fusée agissait pendant 4 secondes et avait une poussée égale à 20 % du poids de l'avion ; le résultat obtenu avec cette fusée était en accord avec ceux de l'étude générale ; en particulier sa trop forte efficacité lorsqu'elle était placée en bout de fuselage, ne nous a pas surpris.

Cet exemple montre nettement que si, qualitativement, les conclusions tirées de l'étude générale relative aux fusées sont valables pour tout avion léger, dès l'instant où une certaine fusée est envisagée pour un avion, la sécurité impose que le dispositif soit préalablement étudié sur maquette en soufflerie verticale, surtout lorsque la durée de fonctionnement de la fusée n'est pas contrôlable.

1.7 - Enseignements pour modifications géométriques.

Le présent paragraphe concerne les enseignements qui ont pu être tirés de l'étude des fusées, enseignements relatifs au type de modifications qu'il aurait lieu d'apporter à certains avions présentant une vrille critique, vrille plate et rapide en particulier.

Lorsqu'en soufflerie on passe à l'étude de modifications géométriques susceptibles d'améliorer la vrille d'un avion léger, en général les modifications envisageables pour l'avion se localisent à l'arrière ; ce peut être à titre d'exemples :

- un agrandissement de la dérive (modification 1 dans la figure 6)
- une quille (2 dans la figure 6)
- un agrandissement des empennages horizontaux (3 dans la figure 6).

(Le cas du parachute qui, d'ailleurs, n'est pas une modification, sera traité plus loin).

Si on situe ces modifications par rapport à des fusées, on peut considérer que l'effet des modifications 1 et 2 est du même type que celui d'une fusée lacet, c'est-à-dire effet de freinage.

L'effet d'un agrandissement des empennages horizontaux, par contre, est comparable à celui d'une fusée agissant en tangage, c'est-à-dire accroissement du moment de tangage aérodynamique piqueur.

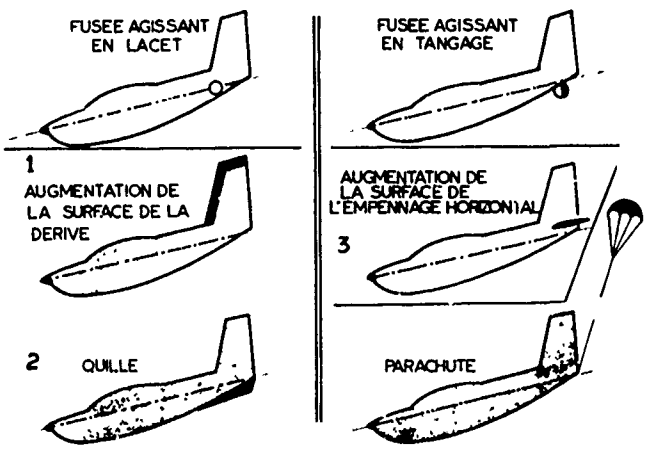

Fig. 6 - MODIFICATIONS ET DISPOSITIF

En ne tenant compte que de l'effet propre de la modification (c'est-à-dire en excluant toute éventuelle interaction de cette modification sur un autre élément de l'avion), étant donné le rapport d'efficacité qui existe entre les fusées tangage et lacet, il est évident qu'un agrandissement de la dérive ou l'implantation d'une quille est, de beaucoup, préférable à une augmentation de surface des empennages horizontaux.

Dans la remarque ci-dessus nous avons exclu une éventuelle interaction de telle modification sur un autre élément de l'avion ; en précisant cela nous pensions plus spécialement à un effet nuisible d'une augmentation de la surface des empennages horizontaux par augmentation de la corde. En effet pour certaines positions relatives de la dérive et des empennages horizontaux il peut arriver que des empennages plus grands masquent plus la dérive ce qui lui fait perdre de l'efficacité vis-à-vis de l'amortissement de lacet. A la limite, l'effet propre de la modification qui est favorable, peut devenir secondaire en regard de son effet nuisible sur la dérive. Le résultat est alors que la vrille avec modification est plus sévère (plus rapide donc plus plate) que celle trouvée avec la géométrie d'origine.

En ce qui concerne un agrandissement de la surface de la dérive, il est nécessaire que cet agrandissement se situe en haut de la dérive, c'est-à-dire à un endroit où la modification a le plus de chances d'être en dehors du sillage du fuselage et/ou des empennages. En fait à surface identique une quille (parce que jamais interactionnée par un autre élément) est souvent plus efficace qu'un agrandissement de la dérive.

Dans la figure 6 nous avons également représenté un parachute ; on peut traiter son cas en considérant, qu'à priori, son action est du même type que celui d'une fusée agissant en tangage. D'après les résultats de fusée pour qu'un parachute ait une action, ses dimensions devraient être très grandes, d'où éventuels problèmes de résistance de structure pour la fixation du câble à l'avion. Mais une remarque importante est à faire au sujet de l'attitude du parachute pendant la vrille ; comme le montre la figure 7 le câble est légèrement incliné par rapport au plan de symétrie ce qui crée une légère composante de lacet ; en nous basant sur le rapport d'efficacité des fusées tangage et lacet, pour le parachute, la composante de lacet, bien que très petite en regard de celle de tangage, peut être aussi efficace, sinon plus, que cette dernière.

Ainsi, pour ce qui concerne le parachute, son action n'est que partiellement là où l'on penserait à priori qu'elle soit essentiellement, c'est-à-dire dans le tangage.

Ces remarques diverses concernant les modifications et le parachute sont surtout valables pour certains types de vrille critique : vrille calme à vitesse de lacet prépondérante. C'est souvent le cas des vrilles critiques d'avions légers. Si on envisage d'autres types de vrille incontrôlables (mais qui, généralement, n'existent pas pour les avions légers) tels que phénomènes très agités ou problèmes de deep-stall, les conclusions précédentes n'ont pas de valeur. En particulier pour le deep-stall, caractérisé par un maintien à incidence décrochée même en l'absence de toute rotation de vrille, il est évident que le choix du dispositif de secours doit se porter sur le parachute ou sur une fusée tangage et leurs caractéristiques (dimensions de la coupole pour le parachute et module de la poussée pour la fusée) dépendront de l'importance du problème. Quant aux phénomènes très agités (qui concernent surtout les avions d'armes) l'utilisation d'une fusée paraît délicate ; même le choix du sens d'action de la fusée n'est pas évident.

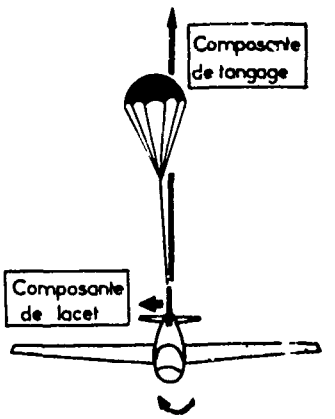

Fig. 7 - ATTITUDE DU PARACHUTE EN COURS DE VRILLE

1.8 - Conclusion.

Des résultats obtenus lors de l'étude de fusées sur maquettes d'avions légers, nous pouvons conclure qu'un tel dispositif est très envisageable comme moyen de secours contre la vrille. Les caractéristiques (poussée, durée et donc impulsion) sont très acceptables et telles qu'elles ne devraient pas présenter de difficultés d'implantation du dispositif sur l'avion, étant bien entendu que la fusée doit agir en lacet.

Une fusée de durée contrôlable est très souhaitable ; une fusée de durée non contrôlable peut aussi être envisagée mais elle impose de s'entourer de précautions ; en particulier, avant son utilisation sur un avion déterminé, elle devrait faire l'objet d'une étude en soufflerie sur la maquette de cet avion.

Dans un ordre d'idées plus général, certaines conclusions du présent document peuvent être valables, du moins qualitativement, pour d'autres types d'avions, avions d'armes par exemple, pour autant toutefois que la vrille critique soit une vrille exempte d'agitations : vrille plate et rapide par exemple.Pour ces avions nous pensons que la fusée agissant en lacet est encore la solution la meilleure. En effet :

- sur des avions d'armes on a pu interdire une vrille plate et rapide grâce à une quille verticale (dont l'action est du même type que celui d'une fusée lacet)
- la géométrie des avions d'armes actuels est telle qu'une fusée lacet peut avoir un bras de levier plus grand qu'une fusée roulis ; cela est un argument supplémentaire qui intervient en faveur de la fusée lacet.

Il est toutefois évident que ces hypothèses se devraient d'être vérifiées par des essais sur maquettes en soufflerie. Ces essais amèneraient de plus des conclusions quantitatives.

2 - INFLUENCE D'UNE DISSYMETRIE DE CHARGEMENT SUR LA VRILLE

2.1 - Introduction.

Au cours d'une étude de vrille faite en soufflerie verticale pour un avion déterminé, il est d'usage de rechercher l'effet des divers paramètres géométriques et massiques afin de couvrir au mieux tous les cas de l'avion ; cependant, en ce qui concerne la position du centre d'inertie, pendant longtemps seules furent prises en considération sa position longitudinale et, à un degré moindre, sa position en hauteur.

A l'I.M.F.L. une étude à caractère général fut entreprise afin de définir l'influence sur la vrille, de la position latérale du centre d'inertie ; l'étude a surtout porté sur un déplacement du centre d'inertie causé, par exemple, par du carburant dans la voilure. Il s'agit donc d'une dissymétrie de chargement purement massique. Cependant, pour les avions d'armes, il est également tenu compte de l'effet d'un décentrage latéral causé, cette fois-ci, par des charges extérieures, donc dissymétrie à la fois massique et géométrique. Le présent document donne les principaux résultats de cette étude.

2.2 - Conditions d'essais.

Environ 25 maquettes d'avions de tous types (armes, légers, transport) furent retenues.

Les décentrages latéraux que nous avons représentés sur ces maquettes sont souvent compris entre

- 4 % et 12 % si on les rapporte à la corde moyenne aérodynamique
- 1 % et 2 % si on les rapporte à l'envergure (voir figure 8). (Quelques décentrages étaient supérieurs ou inférieurs à ces valeurs).

Comme le montre la figure 8 les dissymétries représentées sur les maquettes sont, du moins pour certaines d'entr'elles, inférieures à la dissymétrie maximale envisageable sur l'avion.

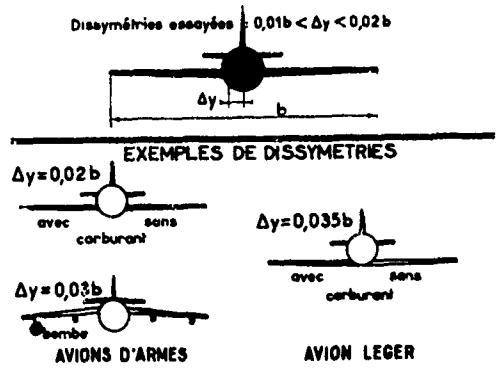

Fig. 8 - DISSYMETRIES ESSAYEES ET EXEMPLES DE DISSYMETRIES ENVISAGEABLES SUR CERTAINS AVIONS.

L'étude a été limitée à la vrille ventre ; pour la majorité des maquettes essayées, des essais ont été faits avec le centre d'inertie placé successivement :

- du coté de l'aile extérieure (aile qui avance pendant la vrille)
- dans le plan de symétrie
- du coté de l'aile intérieure.

2.3 - Résultats.

2.3.1 - Aspect général.

Dans les limites de ce qui fut étudié, l'effet d'une dissymétrie massique est très variable : de nul à important selon certaines conditions d'essais ; il faut cependant préciser que lorsque l'effet n'est pas nul, il est presque toujours de même sens pour toutes les maquettes essayées ; seuls échappent à cette remarque deux cas pour lesquels il y a inversion du sens d'action ; cette inversion trouve son explication dans les agitations comme nous le verrons plus loin.

Comme il est indiqué dans la figure 9 il y a effet :

- pro-vrille quand le centre d'inertie est placé vers l'aile extérieure
- anti-vrille, centre d'inertie vers l'aile intérieure.

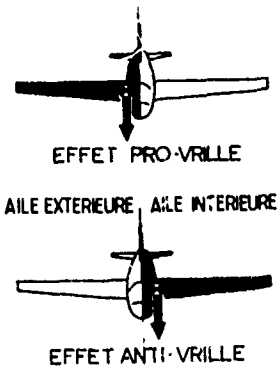

Fig. 9 - EFFET D'UNE DISSYMETRIE DE CHARGEMENT

L'effet du décentrage latéral se manifeste de diverses façons :

- sur l'étendue du domaine des gouvernes où la vrille se maintient (et par voie de conséquence sur les possibilités de récupération)
- sur certaines caractéristiques de la vrille : attitudes longitudinale et transversale et vitesse de rotation, ainsi que sur les agitations.

Ces différents points sont repris en détail dans les prochains paragraphes.

2.3.2 - Effet sur le domaine des vrilles.

Selon la figure 10, l'action d'une dissymétrie de chargement est :

- nulle dans ≃ 20 %
- faible dans ≃ 25 %
- modérée dans ≃ 35 %
- importante dans ≃ 20 %

) des cas étudiés

L'influence de la dissymétrie massique est donc variable ; cela dépend en partie du decentrage qui n'est pas le même pour toutes les maquettes, mais aussi et surtout, d'autres paramètres tel que le type de l'avion (léger, armes, transport) ; des précisions seront données ultérieurement à ce sujet.

La planche 10 montre que, par rapport au cas chargement symétrique, le domaine des

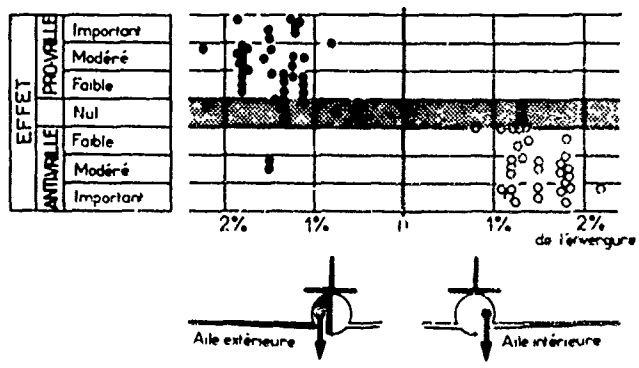

Fig. 10 - EFFET SUR LE DOMAINE DES VRILLES

gouvernes à l'intérieur duquel la vrille se maintient est plus grand quand le centre d'inertie est vers l'aile extérieure ; l'inverse est constaté pour le centre d'inertie placé du coté de l'aile intérieure.

A titre d'exemple, pour une maquette dont l'effet s'est avéré important, cet effet peut se caractériser de la façon suivante (voir figure 11) :

- en chargement symétrique la vrille se perpétue dans la moitié du domaine des gouvernes,

- avec le centre d'inertie déplacé vers l'aile extérieure, la vrille se perpétue, ou se maintient longtemps, dans la presque totalité du domaine des gouvernes ; les sorties deviennent donc très difficiles

- centre d'inertie vers l'aile intérieure, il n'y a presque plus de vrilles maintenues.

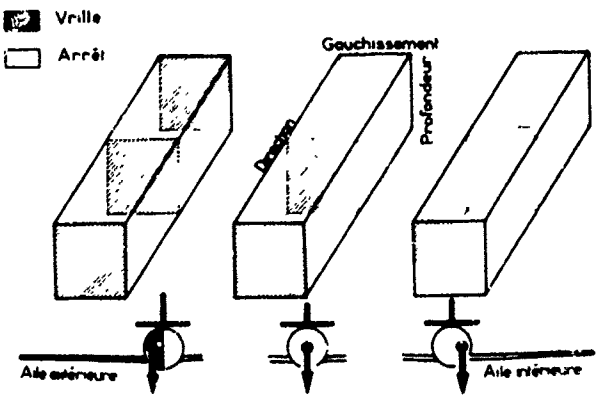

Fig. 11 - EXEMPLE D'UN EFFET IMPORTANT

Pour certains avions, et c'est là notre première conclusion, la position latérale du centre d'inertie se place parmi les paramètres qui influencent le plus la vrille ; à la limite il peut être le plus influent à un point tel que, par exemple, l'effet des gouvernes devient secondaire. En tout état de cause, pour certains avions, tel déplacement en latéral du centre d'inertie a nettement plus d'influence que le même déplacement mais en longitudinal.

2.3.3 - Effet sur certaines caractéristiques de la vrille.

Etudions maintenant l'effet d'un décentrage latéral sur certaines caractéristiques de la vrille ; nous excluons pour l'instant l'effet sur les agitations.

On peut envisager que, initialement un chargement dissymétrique affecte les attitudes transversales ; cela est vrai, mais de façon modérée, puisque dans nos essais, les variations d'assiette transversale ont rarement dépassé 10° bien que certains décentrages qui furent représentés, aient été importants.

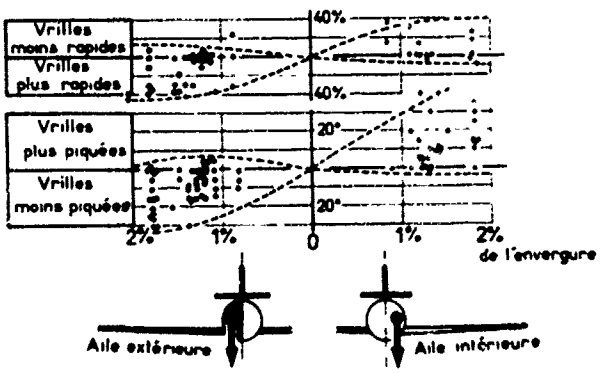

Fig. 12 - EFFET SUR L'ATTITUDE LONGITUDINALE ET LA VITESSE DE ROTATION.

En fait, un décentrage latéral modifie l'équilibre de la vrille de façon telle que son action est plus visible sur des caractéristiques autres que l'assiette transversale ; nous voulons parler de l'attitude longitudinale et de la vitesse de rotation (ces caractéristiques sont d'ailleurs souvent liées car une modification de la vitesse de rotation, de par son action sur le moment de tangage centrifuge, modifie l'assiette longitudinale).

Dans la figure 12 on voit que pour un décentrage latéral égal à 1,5 % de l'envergure, en moyenne :

- quand le décentrage est pro-vrille, la vrille est plus rapide de 20 % et moins piquée de 15°
- quand le décentrage est anti-vrille, la vrille est moins rapide de 15 % et plus piquée de 15°.

Mais ce ne sont là que des valeurs moyennes tirées de la totalité des résultats ; or certaines valeurs peuvent être très éloignées de ces valeurs moyennes. A titre d'exemple la vitesse de rotation peut varier de 40 % et l'assiette longitudinale de 30° ou plus. Ainsi, et toujours pour exemple, par l'action d'un décentrage latéral pro-vrille, une vrille moyennement piquée et moyennement rapide en chargement symétrique peut devenir plate et rapide, c'est-à-dire à fuselage horizontal ou presque et à $\leq$ 2 secondes/tour (du moins pour les avions d'armes et les avions légers) en chargement dissymétrique.

En général, pour un avion déterminé, la vrille est d'autant plus difficile à maîtriser par les gouvernes qu'elle est plate et rapide. En d'autres termes, l'étendue du domaine des gouvernes à l'intérieur duquel la vrille se perpétue est d'autant plus grand que la vrille est plus rapide et plus plate. Cette remarque fournit, du moins pour certains avions, une explication à l'extension du domaine des vrilles qui a été constatée précédemment (voir paragraphe 2.3.2).

De ces résultats on retiendra surtout qu'un chargement dissymétrique peut provoquer une vrille plate et rapide qui n'existait pas en chargement symétrique ; en plus des problèmes de récupération, cette vrille peut amener des problèmes de centrifugation du pilote ; c'est le cas pour un grand nombre d'avions d'armes où le pilote se trouve relativement loin en avant du centre d'inertie ; or au cours d'une vrille plate et rapide bien établie, l'axe autour duquel tourne l'avion passe approximativement par le centre d'inertie de l'appareil.

2.3.4 - Effet sur les agitations.

De façon générale :

- les vrilles d'avions légers sont calmes, c'est-à-dire exemptes d'agitations,
- les vrilles d'avions de transport sont calmes ou agitées mais modérément,
- les vrilles d'avions d'armes peuvent être calmes ou, à l'opposé, fortement agitées. Un même avion peut d'ailleurs avoir différents types de vrille. Lorsque la vrille est fortement agitée, les agitations peuvent avoir une amplitude suffisante pour transformer la vrille en un autre phénomène décroché : auto-tonneaux (auto-rotation autour de l'axe de roulis), fins sur le dos par basculement transversal ou longitudinal, ou encore, mouvements désordonnés.

Dans la figure 13 on voit que lorsqu'en chargement symétrique, la vrille est calme ou peu agitée, elle reste calme ou peu agitée en chargement dissymétrique quel que soit le sens du décentrage ; cela apparaît dans le graphique relatif aux avions légers et aussi, mais de façon moins marquée, pour les avions de transport.

Pour les avions d'armes, l'effet d'un décentrage latéral peut être sensible sur les agitations ; ainsi quand le centre d'inertie est placé du coté de l'aile extérieure les vrilles à agitations divergentes sont plus fréquentes qu'en chargement symétrique. A l'opposé centre d'inertie vers l'aile intérieure, les phénomènes sont systématiquement calmes ou peu agités.

Il y a lieu de s'étendre sur ce point.

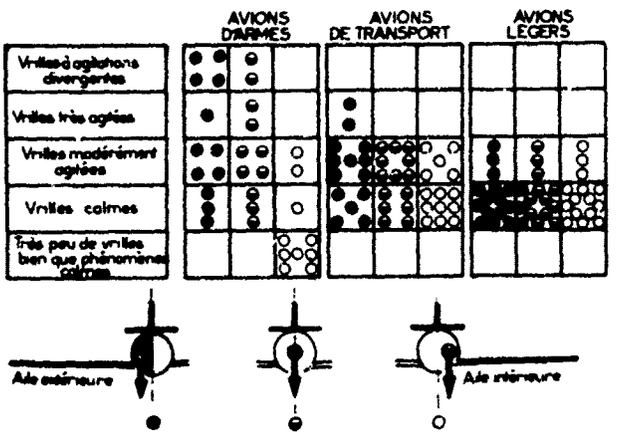

Fig. 13 - EFFET SUR LES AGITATIONS

Décentrage vers l'aile extérieure a, comme nous l'avons vu précédemment, souvent un effet pro-vrille (pro-rotation) ; mais dans le présent paragraphe il ressort que ce décentrage peut aussi avoir un effet pro-agitations, ces dernières, à la limite, pouvant diverger.

Or, il arrive que l'effet pro-agitations l'emporte sur l'effet pro-rotation ; les vrilles maintenues deviennent alors moins nombreuses qu'en chargement symétrique ; cela explique l'existence des deux points particuliers inclus dans la figure 10 pour lesquels le sens d'action du décentrage vers l'aile extérieure n'est pas le même que celui des autres cas ; pour ces deux points il y a moins de vrilles parce que les agitations sont plus fréquentes et plus amples ce qui fait stopper la vrille ; on peut néanmoins affirmer pour ces deux points, que s'il n'y avait pas d'agitations, l'effet du décentrage aurait été de même sens que pour les autres maquettes.

Toujours pour les avions d'armes mais cette fois-ci avec le centre d'inertie vers l'aile intérieure, d'après la figure 13, il apparaît que, sur aucune maquette, il n'a été rencontré de phénomènes fortement agités et pourtant les arrêts de vrille sont fréquents. L'effet du décentrage est effectivement ici un effet pro-freinage et non pas pro-agitations.

De ces résultats relatifs aux avions d'armes on peut alors envisager qu'il puisse exister, pour un avion déterminé, un décentrage latéral optimal pour le maintien de la vrille et ce décentrage peut varier selon l'avion, bien entendu en module, mais aussi en sens. En effet, dans le cas où, en chargement symétrique :

- la vrille est suffisamment calme, le décentrage serait optimal quand le centre d'inertie serait du coté de l'aile extérieure
- la vrille est fortement agitée, la vrille pourrait être mieux maintenue quand le centre d'inertie serait vers l'aile intérieure ; le module du décentrage latéral devrait alors être à la fois suffisant pour calmer la vrille et insuffisant pour la faire stopper.

En conclusion de ce paragraphe, comme toute règle, celle concernant l'influence d'une dissymétrie de chargement comporte des exceptions ; dans le cas présent ces exceptions s'appellent agitations.

2.3.5 - Effet du type d'avion.

Dans les précédents paragraphes les résultats nous ont imposé de déjà faire apparaître, sur certains points, l'action d'une dissymétrie massique selon le type d'avion. Le présent paragraphe apporte d'autres précisions à ce sujet.

Comme le montre la figure 14 l'action d'un décentrage latéral est plus ou moins marqué selon le type de l'avion :

- effet souvent important pour les avions d'armes,
- effet en moyenne modéré pour les avions de transport
- effet souvent faible ou nul pour les avions légers.

Or il faut noter que la gouverne prépondérante :

- pour un avion d'armes, est souvent le gauchissement
- pour un avion de transport, est, selon l'avion, le gauchissement ou la direction
- pour un avion léger, souvent la direction.

En tenant compte de ces remarques il a paru intéressant d'analyser l'effet d'une dissymétrie de chargement en tenant compte de la gouverne prépondérante.

Nous avons ainsi obtenu les résultats qui sont portés dans la figure 15 où l'on constate que :

- dans 90 % des cas où le gauchissement est la gouverne prépondérante, l'effet d'un décentrage latéral est modéré, nu, le plus souvent, important. Le pourcentage serait de 100 s'il n'y avait pas les deux cas particuliers (vrilles à agitations divergentes) dont il a été question au paragraphe précédent.

- dans 70 % des cas où la direction est la gouverne prépondérante, l'effet du décentrage est soit nul, soit faible ; il n'est jamais important.

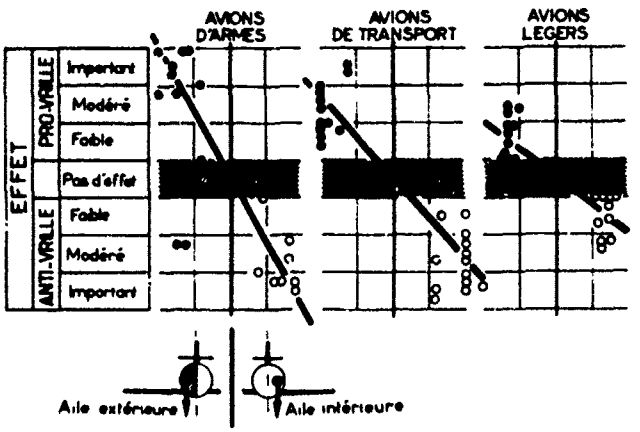

Fig. 14 - EFFET SELON LE TYPE D'AVION

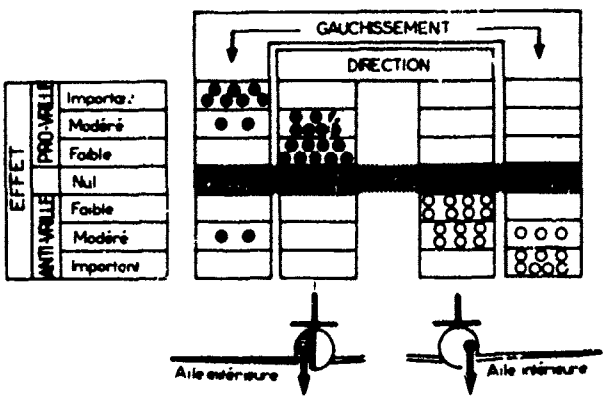

Fig. 15 - EFFET SELON LA GOUVERNE PREPONDERANTE

Un cas qui apparaît dans la figure 14 confirme ces remarques : il s'agit d'un avion d'armes qui est le seul, parmi ceux que nous avons étudiés, pour lequel la gouverne ayant le plus d'influence sur la vrille, est la direction ; pour cet avion l'effet d'un chargement dissymétrique s'est avéré faible ou nul.

L'effet d'un décentrage est donc à classer plus en fonction de la gouverne prépondérante qu'en fonction du type de l'avion.

Remarque : il arrive parfois que la gouverne prépondérante pour la vrille d'un avion est le profondeur. Ce cas ne s'est présenté sur aucune des maquettes retenues pour l'étude présente ; cela explique que dans le présent paragraphe, seuls furent pris en considération la direction et le gauchissement.

2.4 - Effet de charges externes dissymétriques.

Par charges externes, nous entendons ici, charges lourdes et non pas légères du type : réservoir vide. Ces cas ne concernent bien entendu que les avions d'armes pour lesquels l'effet d'une dissymétrie purement massique est souvent important.

De l'ensemble des résultats d'essais faits avec charges externes dissymétriques, il ressort que, très souvent, une charge sous l'aile extérieure a un effet pro-vrille. Inversement une charge sous l'aile intérieure favorise la récupération.

Les résultats sont donc, du moins qualitativement, de même type quand le centre d'inertie est déplacé vers un certain coté, que le décentrage soit causé par une dissymétrie interne ou par

une dissymétrie externe. On peut aussi conclure que dans le cas de charges externes dissymétriques, l'effet de la dissymétrie géométrique est secondaire en regard de celui de la dissymétrie massique.

2.5 - Relation entre effet d'un décentrage latéral et effet du gauchissement.

Lorsque, pour la vrille d'un avion le gauchissement est la gouverne prépondérante :

- gauchissement Contre (c'est-à-dire braqué Contre un virage de même sens que la vrille) favorise le maintien de la rotation, pour autant toutefois que les phénomènes ne soient pas trop agités. Gauchissement Contre a donc généralement un effet pro-vrille.

- gauchissement Avec, souvent la vrille se freine et stoppe même en l'absence d'agitations.

Il semble que l'on puisse mettre en parallèle l'effet du gauchissement et l'effet d'un chargement dissymétrique vis-à-vis de la vrille. Ainsi, si on considère l'effet de ces deux paramètres sur, par exemple, le point concernant l'équilibre transversal, on peut admettre que (voir figure 16)

- d'une part le gauchissement mis contre
- d'autre part le centre d'inertie placé vers l'aile extérieure

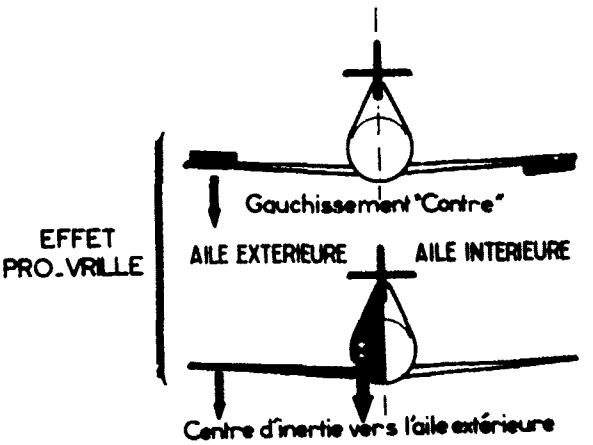

Fig. 16 - COMPARAISON EFFET DECENTRAGE ET EFFET GAUCHISSEMENT

ont tous deux même sens d'action puisqu'ils tendent à faire baisser l'aile qui avance pendant la vrille.

Les ailerons (paramètre géométrique) et le décentrage (paramètre massique) auraient donc un effet du même type sur l'attitude transversale et, comme semble le confirmer la présente étude, par voie de conséquence, sur le phénomène global. Cela pourrait expliquer que l'effet du décentrage soit plus marqué lorsque, pour la vrille d'un avion, la gouverne prépondérante est le gauchissement.

Dans le même ordre d'idées on pourrait également préciser ici certains résultats qui furent obtenus lors des essais qui ont fait l'objet de la première partie de ce document, à savoir essais sur maquettes équipées de fusées. Il s'agit du cas de fusée agissant en roulis.

Nous avons vu dans le paragraphe 1.4.2 qu'une fusée suffisamment forte pouvait déséquilibrer la vrille et la faire stopper même dans le sens d'action où la fusée fait baisser l'aile extérieure. Mais nous avons vu également que, pour ce sens d'action, si la poussée de la fusée est relativement faible, la fusée a pour effet d'aplatir la vrille, du moins passagèrement c'est-à-dire pendant la durée de fonctionnement de la fusée. Cette dernière peut donc avoir un effet pro-vrille lorsque, répétons-le, elle tend à faire baisser l'aile extérieure. Si nous regroupons ici plusieurs conclusions, nous trouvons donc que faire baisser l'aile extérieure :

- soit par le gauchissement
- soit par une dissymétrie de chargement
- soit par une fusée (de poussée relativement faible)

conduit à même résultat, à savoir : favorise le maintien de la vrille.

2.6 - Conclusion.

De l'étude de l'influence d'une dissymétrie de chargement sur la vrille d'avions de tous types, diverses conclusions peuvent être tirées :

1 - L'effet d'un chargement dissymétrique (dissymétrie purement massique) peut varier de nul à important selon, entre autres, le type de l'avion ; mais lorsque cet effet n'est pas nul il est pratiquement toujours de même sens soit : quand le centre d'inertie est déplacé vers :

- l'aile extérieure : effet pro-vrille, c'est-à-dire, augmentation du domaine des gouvernes à l'intérieur duquel la vrille se maintient
- l'aile intérieure : effet anti-vrille

2 - Effet pro-vrille peut signifier de plus : apparition ou augmentation de risques de vrilles plates et rapides au cours desquelles, pour certains avions, le pilote serait soumis à des accélérations inconfortables sinon insupportables.

3 - L'effet d'un décentrage latéral est plus marqué pour les avions dont la gouverne prépondérante pour la vrille est le gauchissement ; or, gauchissement prépondérant est :

- très souvent le cas pour les avions d'armes
- parfois le cas pour les avions de transport
- rarement le cas pour les avions légers.

4 - Un décentrage dû à une charge extérieure sous une aile a le même sens d'action que le décentrage, vers la même aile, provoqué par une dissymétrie interne.

5 - Dans le cas de phénomènes très agités, l'effet d'un décentrage latéral vers l'aile extérieure peut être diminué, annulé ou même changer de sens par un accroissement des agitations qui peuvent alors conduire à une récupération mais par l'intermédiaire de phénomènes divers, auto-tonneaux par exemple ou fin sur le dos.

En conclusion générale il faut surtout retenir que le centre d'inertie placé hors du plan de symétrie peut se classer parmi les paramètres qui influencent le plus la vrille ; à la limite son action peut être notablement plus importante que celle de tout autre paramètre massique ou géométrique. Aussi, est-il nécessaire que ce paramètre soit pris en considération au cours des campagnes d'essais de vrille tant en soufflerie que sur l'avion lui-même.

UNE NOUVELLE ANALYSE DE LA VRILLE
BASÉE SUR L'EXPÉRIENCE FRANCAISE SUR LES AVIONS DE COMBAT

par Claudius LA BURTHE *
Centre d'Essais en Vol
91220 Brétigny-sur-Orge (France)

RÉSUMÉ

Chez les utilisateurs français, les pertes d'avions de combat par enfoncement, décrochage ou vrille, sont relativement peu nombreuses. Entre autres raisons, on peut attribuer ce résultat favorable à un effort particulier d'instruction des pilotes sur les hautes incidences. Néanmoins, l'influence défavorable de la charge alaire fait craindre une détérioration de cette situation sur les avions nouveaux. Un certain nombre de résultats d'essais sont analysés sous l'angle de la nature des pertes de contrôle. On démontre ainsi la prépondérance des phénomènes d'inertie, et on en déduit les limites de crédibilité des avertisseurs liés à l'incidence. Pour les avions futurs, on propose de compléter la protection par un détecteur de couple gyroscopique.

A NEW ANALYSIS OF SPIN, BASED ON FRENCH EXPERIENCE ON COMBAT AIRCRAFT

SUMMARY

Relatively few aircraft are lost by French users, owing to sinking, stalling or spinning. Among other reasons, this favourable result may be attrib · to a particular emphasis put on pilot instruction about aircraft behaviour at high angles of attack. Bu in view of ·ne unfavourable influence of wing loading this situation might deteriorate with new aircraft. Some test results are analysed as regards the nature of losses of control. The major influence of inertia is thus demonstrated. Limits of credibility for stall warning systems, based upon angle of attack measurement, are then deduced. For future aircraft, it is proposed to improve protection by adding a gyro torque detector

NOTATIONS

E	ellipsoïde principal d'inertie de l'avion
E'	ellipsoïde déduit de E par une affinité de centre G
G	centre d'inertie ou de gravité
$\vec{H}$	vecteur moment cinétique
ι	$\epsilon\rho$ π, π'
I_x	moment d'inertie autour de l'axe principal $x'x$
I_y	moment d'inertie autour de l'axe principal $y'y$
I_z	moment d'inertie autour de l'axe principal $z'z$
P	plan tangent à l'ellipsoïde d'inertie et perpendiculaire à $\vec{H}$
	est fixe dans l'espace, et détermine les mouvements de E par rapport à des axes fixes
p	vitesse de roulis
q	vitesse de tangage
r	vitesse de lacet
	} composantes de $\vec{\Omega}$
T	énergie de l'avion en rotation
$x'x$	
$y'y$	} axes principaux d'inertie de l'avion
$z'z$	
α	incidence
β	dérapage
τ	période d'un mouvement oscillatoire
φ	
θ	} angles d'Euler
ψ	
π, π'	plans limites du problème d'Euler-Poinsot inclinés de l'angle i sur le plan Gxy
$\vec{\Omega}$	vecteur rotation instantanée de l'avion.

◊

L'expérience permet de classer les incidents ou accidents qui surviennent à haute incidence en deux catégories : les pertes de contrôle partielles et les vrilles.

Les pertes de contrôle partielles peuvent revêtir un degré de gravité très variable selon la durée et la sévérité du mouvement incontrôlé de l'avion

- minimes et brèves : échappées en roulis ;
- violentes : départ en roulis, départ en lacet, pitch-up ;
- prolongées : décrochage, enfoncement. . .

Dans cette gamme continue, toutes les possibilités existent, et les pilotes le savent, de sorte qu'il est difficile pour eux de décider si tel ou tel incident mérite de faire l'objet d'un compte rendu. En revanche, les cas de vrille sont plus aisément identifiables.

En France, le nombre d'avions de combat perdus en vrille n'est pas très élevé. Les utilisateurs français considèrent la vrille proprement dite comme un problème mineur pour la sécurité des vols. Ils attribuent ce bon résultat autant à la qualité du matériel, qu'à celle de l'instruction.

Cependant, cette situation pourrait se dégrader sur les avions actuels, en raison de l'augmentation des charges. En effet, la figure 1 semble montrer une corrélation entre les taux de perte et la charge

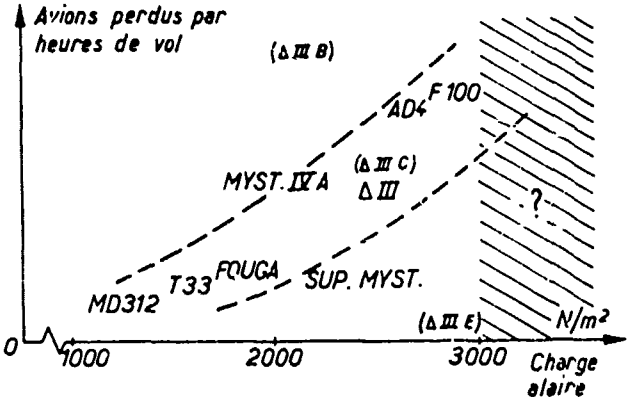

Fig. 1 – Armée de l'Air française (1965/1974)
Pertes d'avions en vrille caractérisée

* *actuellement à l'ONERA – 92320 Châtillon (France)*

alaire à la masse de combat Il ne faut cependant pas exagérer la portée de ce graphique, qui couvre dix ans d'utilisation, mais un nombre d'avions perdus très modeste. Malgré cette réserve, on peut craindre que les charges alaires pratiquées sur les avions nouveaux ne contribuent à augmenter le risque de vrille.

La mise en service d'avions de plus en plus lourds doit logiquement conduire à renforcer l'effort de protection contre la mise en vrille.

HISTORIQUE DE LA PROTECTION

Celle-ci a été d'abord assurée par des limitations portant sur la vitesse, le facteur de charge, ou certains mouvements de gouvernes. Mais la vrille n'étant pas formellement interdite, la meilleure protection restait une bonne connaissance du comportement de l'avion en évolutions serrées. L'apparition de vrilles à grand développement vertical, avec des sorties difficiles, a conduit à l'interdiction complète de vrilles délibérées. Cette interdiction s'est d'autant plus facilement généralisée que la vrille a perdu sa valeur tactique en raison des difficultés de toutes sortes qui l'accompagnent : orientation, fonctionnement moteur, intégrité cellule etc. . . Afin de faciliter l'application de cette consigne, on a conçu des alarmes lumineuses puis sonores, liées à une détection d'incidence (Mirage III).

Mais ces alarmes ont été jugées insuffisantes parce qu'elles représentent des informations discontinues On a donc décidé d'équiper les avions les plus récents d'un indicateur d'incidence linéaire et paravisuel. En outre, cet instrument peut être utilisé dans presque toutes les autres phases de vol. Cependant, il a été jugé nécessaire de conserver l'alarme sonore, pour sa contribution à la sécurité.

CHOIX DES NIVEAUX D'ALARME

Cette question est délicate et doit être examinée en détail. Le niveau d'alarme est choisi évidemment plus bas que les plus faibles incidences de pertes de contrôle Les éléments qui guident ce choix sont de deux ordres

- technique : qualités de vol de l'avion à haute incidence . stabilités, amortissement, pitch-up éventuel, efforts etc .
- opérationnel . politique d'utilisation du matériel, considérations d'entraînement du personnel etc . .

Ainsi, l'écart d'incidence qui sépare l'alarme de la perte de contrôle (que l'on appelle improprement le domaine en "overshoot", notion qui reste ambigue dans la cas de l'incidence) résulte en partie d'une décision de commandement.

Mais il est malheureusement évident qu'une limitation d'incidence est beaucoup plus difficile à respecter que celles portant sur l'altitude ou la vitesse par exemple, même en temps de paix. Or l'analyse technique montre que le pilote qui dépasse une incidence-limite peut rencontrer des comportements d'une extrême diversité sur un même avion. Ceci est dû à l'influence, parfois très forte, des autres paramètres dont dépend le mouvement $\dot{\alpha}$, β, Mach, configuration, couples gyroscopiques etc .

Il serait très compliqué et peu sûr de concevoir une alarme liée à tous ces paramètres. Mais l'analyse qui va suivre permettra de proposer une solution.

COMPARAISON DE QUELQUES VRILLES D'AVIONS DE COMBAT

Les figures 2, 3, 4 et 5 montrent les vrilles de quelques avions volontairement choisis pour leurs différences d'architecture, d'âge et d'origine

Ces vrilles ont un certain nombre de caractéristiques communes :

- mouvement oscillatoire pseudo-permanent, période de l'ordre de grandeur de 3 à 4 secondes,
- durées aléatoires, avec des sorties difficiles, car les gouvernes sont peu efficaces ; grandes pertes d'altitude,
- roulis et lacet généralement synchronisés,
- tangage en avance de phase de 90° dans une vrille à gauche (ou en retard, dans une vrille à droite),
- composante continue importante sur le lacet, faible sur les autres axes

Ces similitudes frappantes montrent que les mouvements sont dominés par un élément commun.

Le calcul des niveaux d'énergie en rotation, qui est élevé (≃ 100 kjoule) par rapport à celui des évolutions normales (quelques kjoules), suggère qu'il s'agit des couples gyroscopiques.

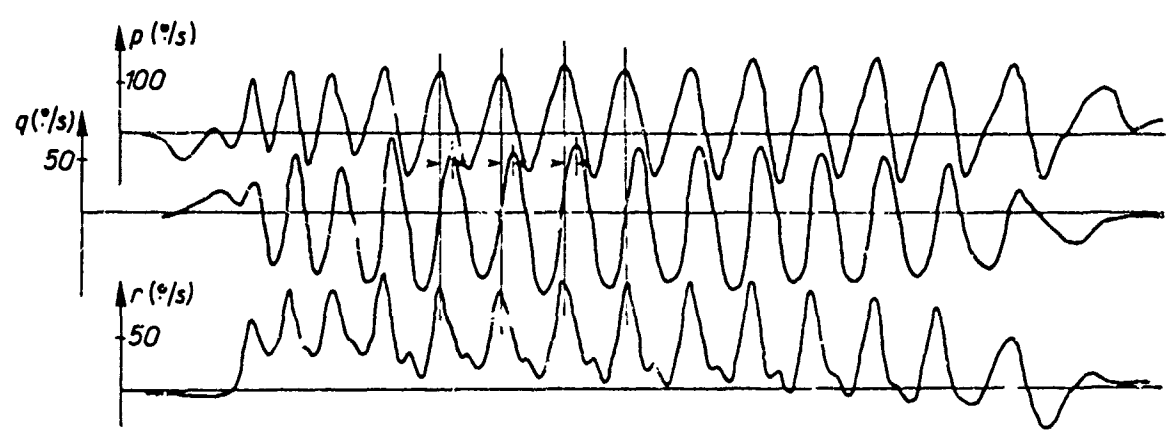

Fig. 2 – Vrille Jaguar monoplace. $\tau \sim 3{,}2$ secondes.

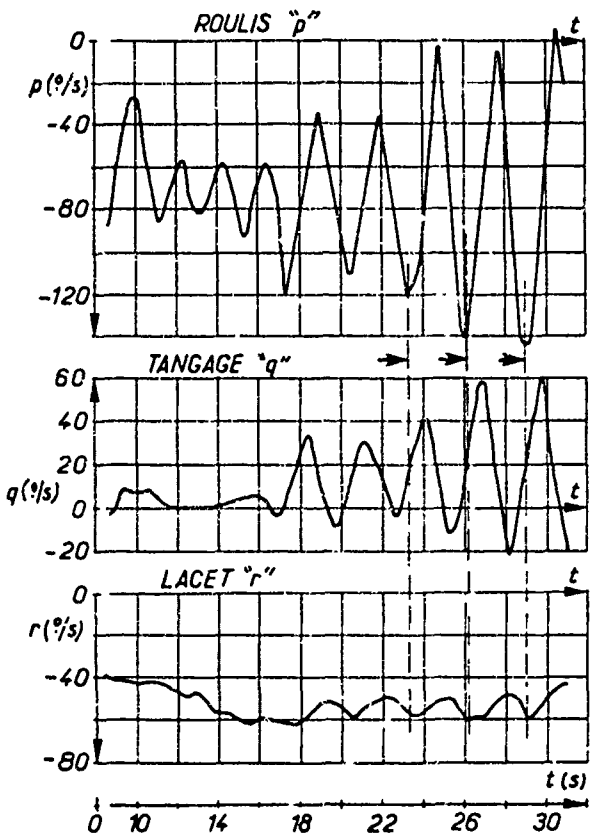

Fig. 3 - Vrille du Fouga CM 170.
réf. Leconte, Mécanique du Vol, Dunod.

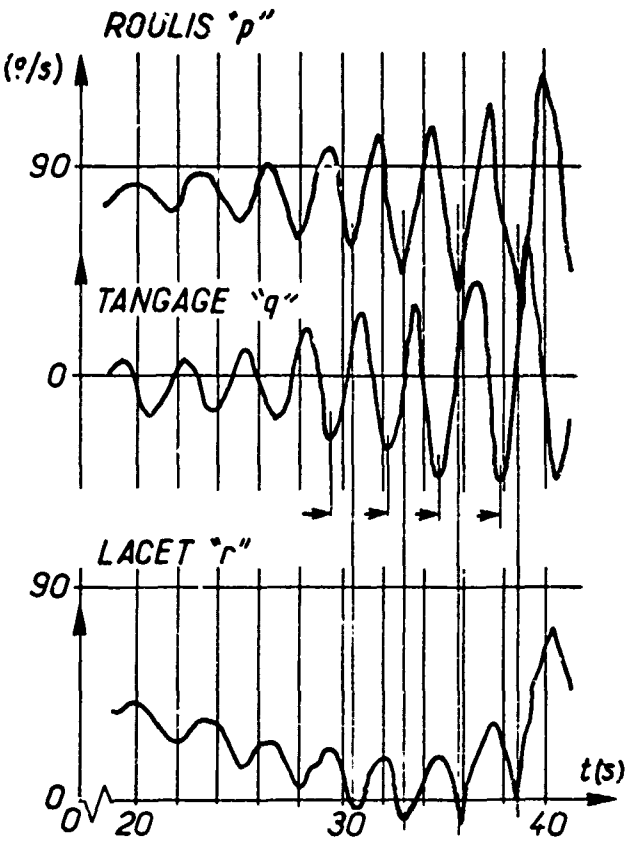

Fig. 4 – Vrille du Viggen.
réf 74 Report of Society of Exp. Test Pilots

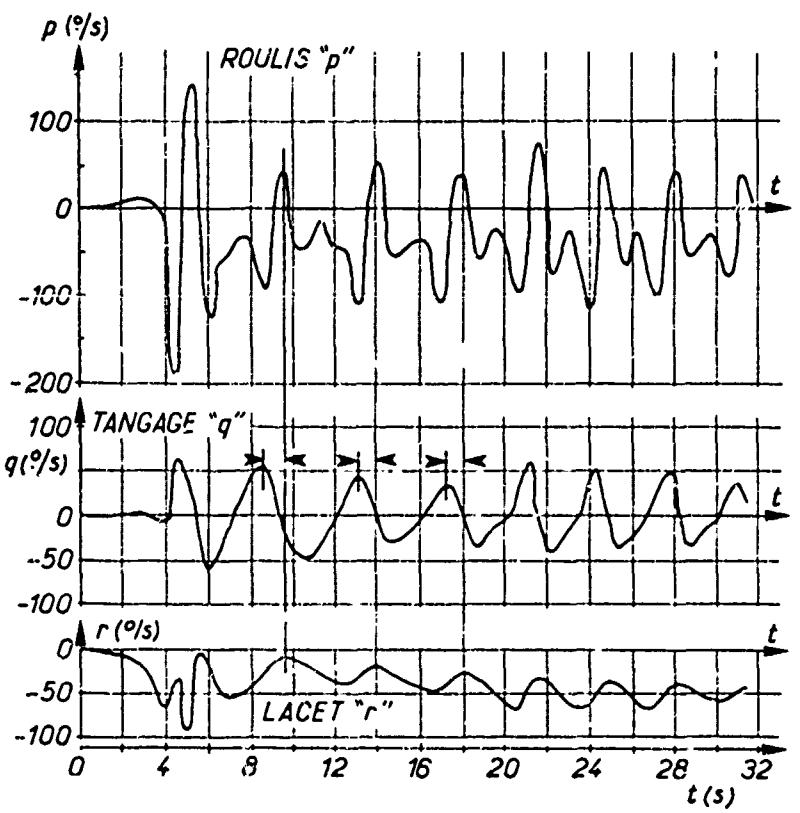

Fig. 5 – Vrille calculée du F5.
réf Weissman ASD TR.72 48

MOUVEMENT D'EULER-POINSOT

Les équations d'Euler-Poinsot représentent le modèle mathématique des mouvements d'un satellite, ou d'un avion sur lequel les moments aérodynamiques ou de propulsion exerceraient une action négligeable. En revanche, on ne fait aucune hypothèse sur les forces aérodynamiques :

$$(1)\quad \begin{cases} I_x \dot{p} + (I_z - I_y)\, q r = 0 & L = 0 \\ I_y \dot{q} + (I_x - I_z)\, r p = 0 & M = 0 \\ I_z \dot{r} + (I_y - I_x)\, p q = 0 & N = 0 \end{cases}$$

$$p = -\dot{\Psi} \sin\Theta + \dot{\Phi}$$

avec $$q = \dot{\Psi} \cos\Theta \sin\Phi + \dot{\Theta} \cos\Phi$$

$$r = \dot{\Psi} \cos\Theta \cos\Phi - \dot{\Theta} \sin\Phi$$

La solution analytique de ce système dépend fortement des conditions initiales. Elle fait appel aux intégrales elliptiques qui sont d'un maniement peu rentables pour les physiciens. La solution géométrique est d'accès plus facile.

Dans un premier temps, on peut écrire que l'énergie en rotation de l'avion est constante, puisqu'il n'y a pas de moment des forces extérieures (ce qui n'empêche pas celles-ci d'agir, comme on le verra, sur l'énergie totale, au sens cinétique et potentielle).

$$I_x p^2 + I_y q^2 + I_z r^2 = 2T = cte$$

On démontre ainsi que l'extrémité du vecteur rotation $\vec{\Omega}$ appartient à un ellipsoïde E', affine de l'ellipsoïde principal d'inertie de l'avion.

Il est clair d'autre part, que dans un mouvement sans intervention extérieure, le vecteur moment cinétique $\vec{H}$ est constant en grandeur et en direction.

Les conditions initiales sont fixées par la position de $\vec{\Omega}_0$ dans E (ou E'). A chaque position de $\vec{\Omega}_0$ correspond une position de $\vec{H}$ (fig. 6). On démontre facilement, par une étude des variations instantanées de $\vec{\Omega}$, que le lieu de l'extrémité de $\vec{\Omega}$ sur E' s'obtient en faisant rouler E' sans glissement, sur le plan P' qui est fixe dans l'espace et perpendiculaire à $\vec{H}$.

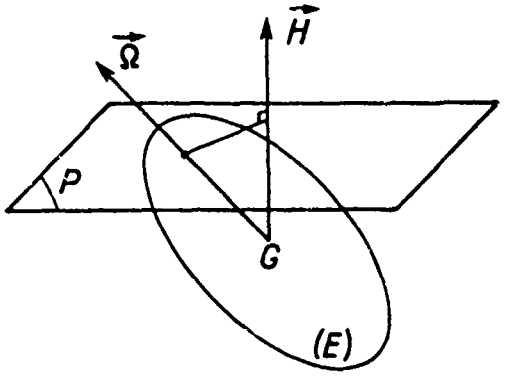

Fig. 6 – Mouvement d'Euler-Poinsot général.

Les courbes obtenues sont appelées "polhodies" et sont présentées figure 7. Elles se décomposent en quatre familles, symétriques deux à deux, qui entourent les pôles de roulis et de lacet. Cette symétrie reflète celle des mouvements gauche/droite.

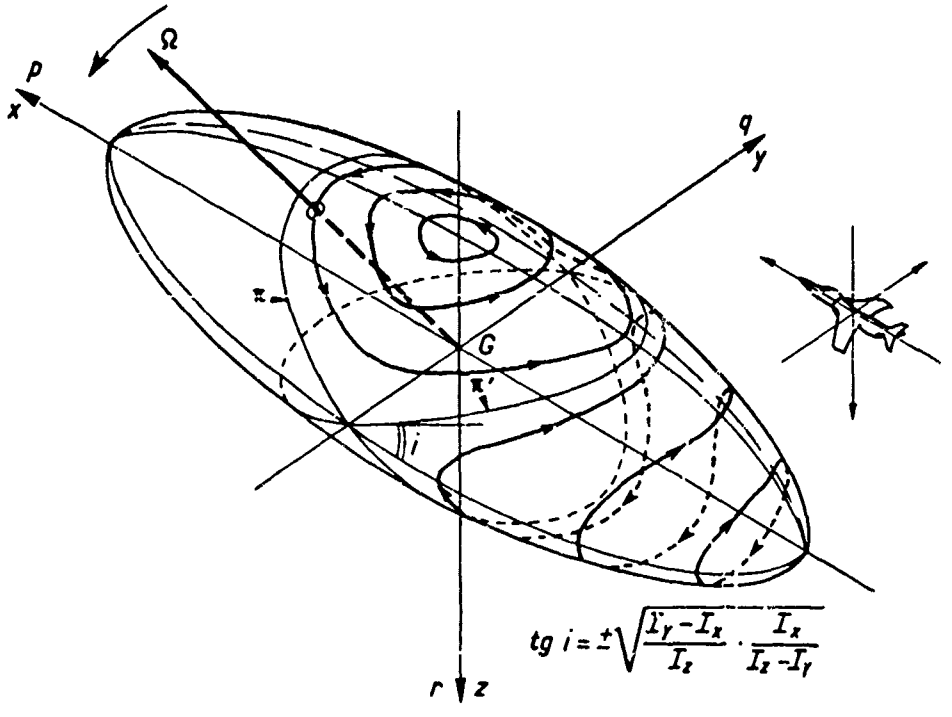

Fig. 7 – Mouvement d'Euler-Poinsot – Polhodies.

Ces courbes sont des biquadratiques qui ont évidemment les mêmes plans de symétrie que ceux de l'ellipsoïde. Elles se projettent sur ces plans selon des arcs de coniques dont on obtient très facilement les équations : on divise membre à membre les équations du système (1) et on les intègre. La solution donne deux familles d'ellipses et une famille d'hyperboles : (fig. 8)

$$\frac{p^2}{\kappa_1} + \frac{q^2}{\kappa_2} = \lambda_3 \qquad \kappa_1 = \left|\frac{I_z - I_y}{I_x}\right|$$

$$\frac{q^2}{\kappa_2} + \frac{r^2}{\kappa_3} = \lambda_2 \qquad \text{avec} \qquad \kappa_2 = \left|\frac{I_x - I_z}{I_y}\right|$$

$$\frac{r^2}{\kappa_3} - \frac{p^2}{\kappa_1} = \lambda_1 \qquad \kappa_3 = \left|\frac{I_y - I_x}{I_z}\right|$$

On constate que l'axe de tangage joue un rôle privilégié, qui doit être attribué à l'inégalité $I_x < I_y < I_z$.

Les deux paires de familles de courbes présentées figure 7 sont séparées par des plans π et π' dont l'inclinaison i sur $x G y$ est donnée par les asymptotes de l'hyperbole ci-dessus .

$$\operatorname{tg} i = \pm\sqrt{\frac{\kappa_2}{\kappa_1}}$$

Il se trouve que pour beaucoup d'avions cet angle est de l'ordre de grandeur de $\frac{\pi}{4}$.

Dans le cas particulier où $I_y = I_z$, l'ellipsoïde est de révolution, (fig. 9) les plans sont confondus avec $y G z$, et les quatre familles de cercles centrés sur $x'x$.

L'explication géométrique met en évidence le fait important que le mouvement d'Euler-Poinsot est permanent. Mais la durée d'un cycle dépend des conditions initiales et peut varier de zéro à l'infini En outre, la vitesse de défilement de $\vec{\Omega}$ le long d'une quelconque des biquadratiques peut varier dans des proportions importantes. Sur la figure 10, on a porté trois exemples de périodes 1, 3 et 10 secondes. Sur cette figure, l'épaisseur des trajectoires est en raison inverse de la vitesse.

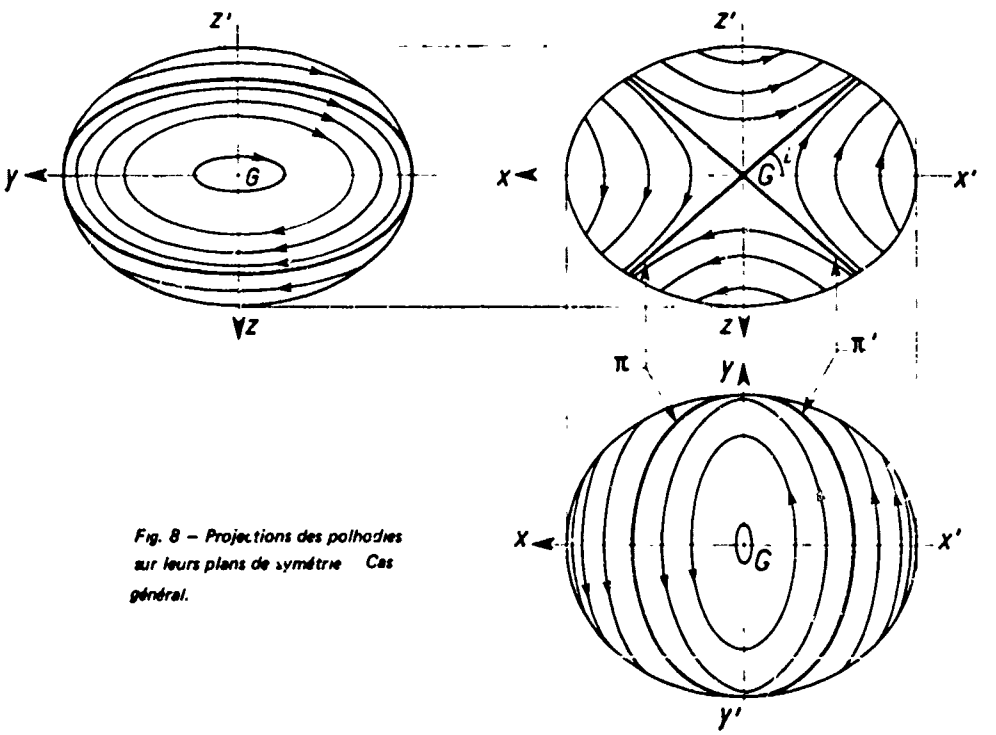

Fig. 8 – Projections des polhodies sur leurs plans de symétrie Cas général.

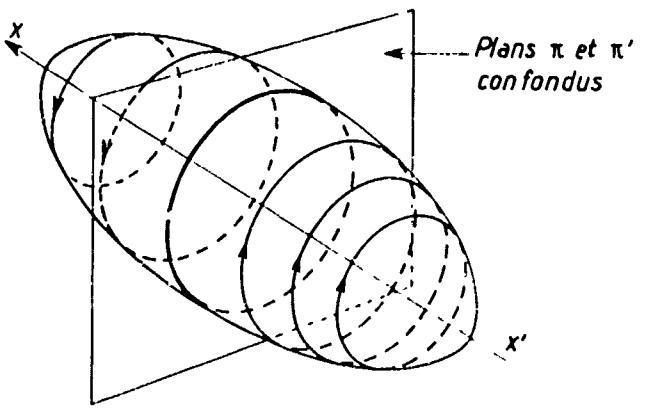

Fig. 9 – Polhodies d'un ellipsoïde de révolution

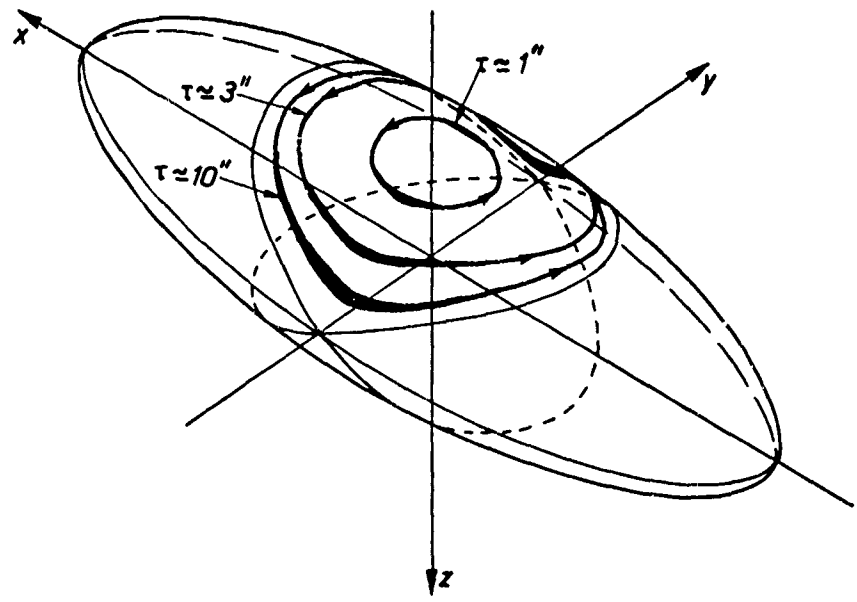

Fig. 10 – Exemples de polhodies de durées différentes.

Les variations de vitesse sont à l'origine des formes particulières des enregistrements de vitesses angulaires p, q, r. Un exemple obtenu sur machine analogique est fourni figure 12 (schéma de câblage fig. 11). Cet enregistrement donne le résultat obtenu à partir de conditions initiales qui conduisent à une courbe de la famille entourant un pôle de lacet. On voit que

- le mouvement est permanent,
- roulis et lacet sont synchrones, fréquence double sur le lacet, roulis en dent de scie,
- le tangage est déphasé de $\pi/2$, forme très carrée,
- il n'y a de composante continue que sur le lacet.

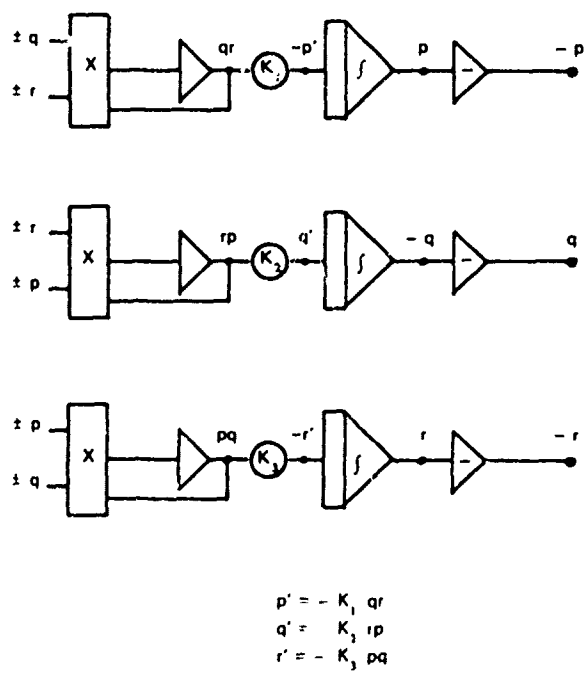

$$p' = -K_1\, qr$$
$$q' = K_2\, rp$$
$$r' = -K_3\, pq$$

Fig. 11 – Machine analogique. Schéma de câblage du problème de Poinsot.

On remarquera l'analogie avec l'enregistrement de la vrille du Jaguar.

Toutefois, si les conditions initiales avaient fait choisir une courbe d'une famille entourant le pôle X, on aurait échangé les comportements qualitatifs du roulis et du lacet.

Ainsi, compte tenu de l'existence du plan de symétrie $\alpha = 0$, on retiendra que chaque courbe de l'une quelconque des familles peut être obtenue sans ambiguïté à partir de conditions initiales exprimées sous la forme

$$\overrightarrow{\Omega_0} = (p_0, r_0) \qquad \text{avec} \quad q_0 = 0$$

La période du mouvement défini dépend à la fois du module et de la position de ce vecteur. Elle diminue lorsque $|\Omega_0|$ augmente. A module donné, elle augmente lorsque $r_0/p_0 \to \operatorname{tg} i$, en raison du ralentissement de $\vec{\Omega}$ lorsqu'il passe du voisinage des pôles de tangage sur (E).

ETUDE D'UNE VRILLE RÉELLE

Les similitudes rencontrées entre les figures 2, 3, 4 ou 5, et l'enregistrement figure 12 sont suffisamment frappantes pour que l'on fasse l'étude complète de l'une des vrilles réelles. On choisit la plus typique : la vrille du Jaguar, figure 2.

On présente figure 13 un cycle de cette vrille, en comparaison avec un cycle de celui des mouvements à la Euler-Poinsot de l'ellipsoïde d'inertie de l'avion, qui possède la même période : 3 seconde. L'écart algébrique qui sépare les deux mouvements est obligatoirement imputable aux moments des forces extérieures : aérodynamiques et propulsion. On l'appellera résidu aérodynamique.

La valeur absolue du résidu permet d'affirmer ce résultat fondamental : "les mouvements de cette vrille sont organisés par les couples gyroscopiques, ceux-ci étant perturbés par les moments aérodynamiques".

Cette conclusion devrait pouvoir être généralisée à toutes les vrilles oscillatoires pseudo-permanentes. On remarquera que dans de nombreux cas, la vitesse de tangage est déphasée d'environ $\pi/2$ par rapport à l'ensemble roulis-lacet.

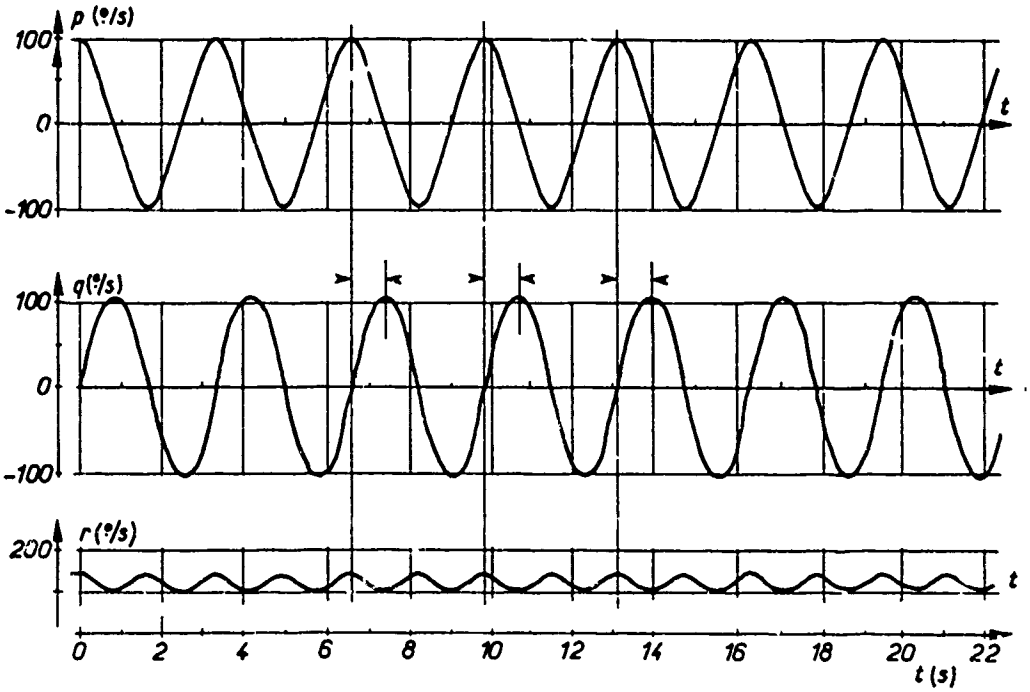

Fig. 12 – Mouvement d'Euler-Poinsot général.

ANALYSE DU RÉSIDU AÉRODYNAMIQUE

Le résidu défini ci-dessus, représente l'image des influences aérodynamiques. On peut donc faire un travail d'identification de coefficients. La figure 14 donne un exemple simplifié. On dérive sommairement les vitesses angulaires. On obtient donc les moments les plus importants. Si on les compare avec les enregistrements d'incidence et de dérapage, on peut tirer les conclusions suivantes .

– le mouvement de tangage est freiné pendant une grande partie de la période cela doit être imputé au coefficient C_{mq} ,

– les mouvements de roulis et de lacet sont affectés simultanément, pendant une courte partie de la période, et précisément lorsque le nez de l'avion est bas (incidence modérée),

– les coefficients responsables d'un tel mouvement sont d'une part un $C_{l\beta} < 0$, d'autre part, un $C_{n\beta} < 0$

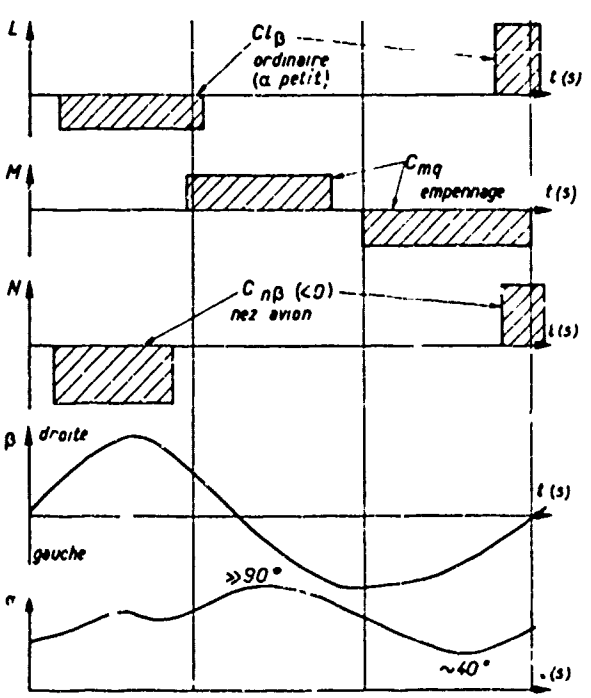

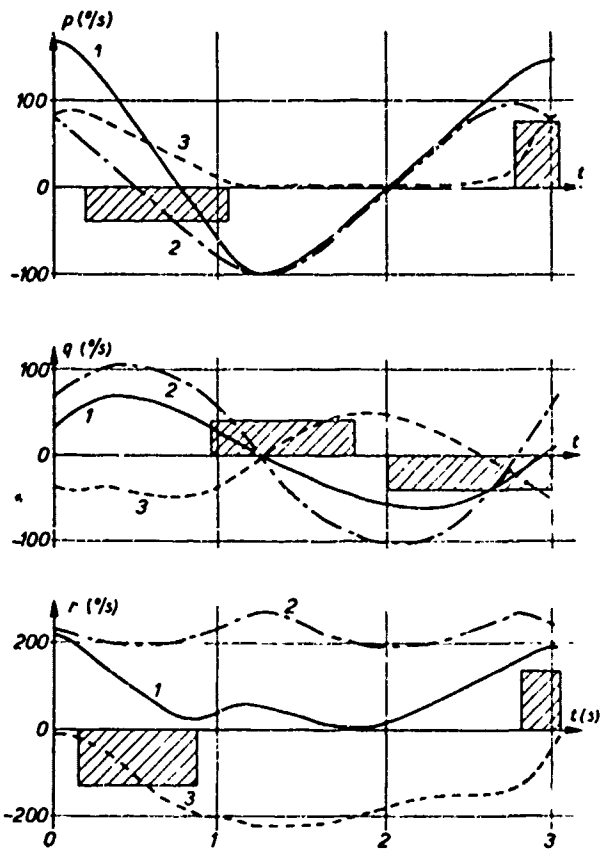

Fig. 13 – Avion Jaguar monoplace
Comparaison vol/Euler-Poinsot sur un cycle de vrille.
1. Vol 2. Euler-Poinsot 3. Résidu aérodynamique

Fig. 14 – Avion Jaguar monoplace.
Interprétation du résidu aérodynamique sur un cycle de vrille.

En résumé, la vrille du Jaguar monoplace peut se décrire comme suit :

- mouvement à prépondérance inertielle,
- influences aérodynamiques modérées en temps et en grandeur. Celles-ci provoquent :
  - un amortissement longitudinal quasi-permanent sur un cycle et, lorsque le nez de l'avion passe en position basse (incidence minimale de vrille) deux impulsions
    - . l'une en effet dièdre de sens conventionnel
    - . l'autre en stabilité de route négative.

On peut en déduire les seules parties de la cellule qui soient actives en vrille :

- empennage horizontal $\longrightarrow C_{mq} < 0$
- voilure en flèche $\longrightarrow C_{l\beta} < 0$ pour α modérée
- nez avion $\longrightarrow C_{n\beta} < 0$ pour α modérée

On remarque que seules les parties frontales de l'avion sont concernées dans l'explication du mouvement transversal.

La solution ainsi proposée n'est peut être pas unique, et mériterait d'être discutée. Mais il faut rester prudent dans la recherche du modèle du résidu, car l'incidence et le dérapage varient énormément, les vitesses angulaires sont très fortes, et il faut s'en tenir aux influences prépondérantes. Sinon, l'identification conduirait à une indétermination concernant les rôles de l'incidence, du dérapage, et des coefficients instationnaires.

GÉNÉRALISATION AUX AUTRES AVIONS

L'analyse du résidu ainsi présentée peut s'appliquer à toute vrille oscillatoire à peu près périodique, même si le déphasage entre tangage et roulis-lacet n'est pas celui du mouvement d'Euler-Poinsot, soit $\pi/2$. Dans ce cas, le résidu est plus important en valeur absolue, il est pulsé, et donc plus difficile à analyser.

Un certain nombre d'entre ces vrilles présente la particularité suivante. Le mouvement de lacet, qui est de fréquence double, est souvent filtré au point d'être à peu près constant. Cette fréquence étant de l'ordre de 1 Hz, il n'y a rien d'étonnant à ce qu'elle soit filtrée par l'aérodynamique, surtout dans des mouvements de grande amplitude. Cette particularité, introduite sous la forme $r = cte$ dans le modèle d'Euler-Poinsot, le rend intégrable, avec des solutions pratiquement sinusoïdales. On constate, en effet, que les caractères de dent de scie du roulis et de mouvement carré du tangage s'atténuent nettement. F1, Alphajet.

La vrille de ce dernier avion est particulièrement intéressante sur le plan pratique, car l'importance du résidu aérodynamique dépend de la position du gauchissement. On peut donc dire, inversement, que le niveau d'agitation est commandé par le pilote (dans une certaine mesure). Cette caractéristique prédispose l'Alphajet à la démonstration des vrilles en vol.

CONSEQUENCES DE L'INTERPRETATION INERTIELLE

Les conséquences de cette interprétation sont extrêmement nombreuses, tant sur le plan théorique que pratique, et semblent pouvoir concerner une très grande population d'avions, que l'on appellera "denses" dans la suite du texte.

En mécanique du vol, on peut proposer une nouvelle définition de la vrille des avions denses :

« La vrille des avions denses est un mouvement organisé par les influences inertielles, et perturbé par l'aérodynamique »

L'étude du mouvement d'Euler Poinsot dans le cas général montre que la composante inertielle de telles vrilles peut être de deux sortes, selon qu'il appartient à l'une ou l'autre des familles entourant les pôles de lacet ou de roulis. Dans les exemples cités, il est manifeste que la vrille du Jaguar est à prédominance de lacet, et que la vrille calculée du F5 (fig. 5) est à prédominance de roulis.

Le cas particulier $I_y = I_z$ mériterait une étude, car un tel avion pourrait présenter une certaine résistance à la vrille, accompagnée d'une tendance aux autotonneaux.

De la nouvelle définition de la vrille, découle une nouvelle définition de la phase transitoire de mise en vrille :

« Le départ en vrille des avions denses correspond à la naissance d'un couple gyroscopique important »

Sur le plan analytique on peut exprimer la perte de contrôle comme : *« la naissance d'une divergence entre le vecteur moment cinétique et le vecteur rotation : $\vec{\Omega} \wedge \vec{H} \neq 0$ »*.

En conséquence, il suffit de mesurer ce produit vectoriel pour créer un système d'alarme.

Pour la protection des avions denses contre la vrille, on propose donc une solution simple, qui permet de compenser les défauts inhérents à la conception des avertisseurs liés à l'incidence. Le calcul du produit vectoriel ci-dessus (qui représente les couples gyroscopiques), est très facile si l'on utilise les gyromètres p, q, r, qui existent sur presque tous les avions. Il suffit alors de déterminer en vol le seuil à partir duquel on règlera l'alarme.

On peut penser que celle-ci surviendrait bien tard dans le processus de la perte de contrôle. Mais l'analyse de très nombreux essais de déclenchés volontaires, non suivis de vrille, et la discussion avec les pilotes, montrent que la durée de la mise en vrille est toujours longue (par exemple 2 à 5 secondes) en regard des délais de braquage des commandes de vol. On peut donc espérer une protection efficace, à condition que celle-ci soit automatique.

Sur le plan pratique, la notion de "tour de vrille" basée sur l'intégration du mouvement de Ω sur un angle de 2π, perd son intérêt. Il y a lieu de la remplacer par la notion de "cycle" du mouvement périodique.

Le problème des sorties de vrille peut être envisagé sous un angle nouveau. Si un avion démontre une vrille à forte composante inertielle, il en sortira toujours difficilement. En réalité, la sortie n'est possible que si les moments aérodynamiques croissent de manière à amortir et à faire "dégénérer" le mouvement d'Euler Poinsot.

L'analyse des sorties réelles montre qu'un certain nombre d'avions présentent une sortie en deux temps :

- transformation d'une rotation à prédominance de lacet (Ω tourne autour de G_z), en une rotation à prédominance de roulis (Ω tourne autour de G_x),
- amortissement du mouvement de roulis.

De telles sorties, appellées autotonneaux trouvent une explication inertielle immédiate, par rapport à laquelle les moments aérodynamiques jouent seulement un rôle perturbateur (qui conduit parfois à l'entretien du mouvement). En particulier, les moments qui font converger le vecteur $\vec{\Omega}$ vers l'axe $x'x$ tendent évidemment à accélérer le roulis (fig. 15).

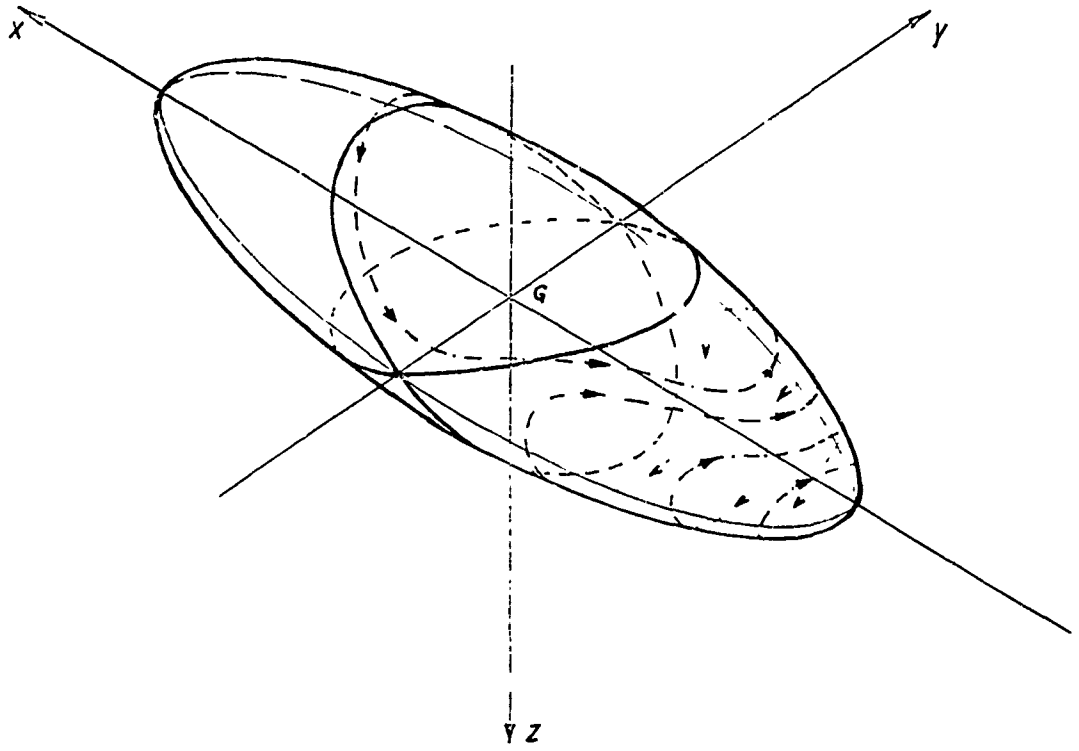

Fig. 15 – Sortie de vrille en autotonneaux.

CONCLUSION

L'expérience française portant sur dix ans d'essais et d'utilisation des avions de combat montre que le risque de perte d'avions en vrille, actuellement peu élevé, pourrait s'accroître dans l'avenir, en raison de l'augmentation des masses et du nombre des configurations.

Simultanément, les systèmes de protection présentent des limitations de performances pour des raisons fondamentales. En effet, l'étude des vrilles d'avions récents montre que la référence à la seule détection de l'incidence ne constitue pas une garantie contre une perte de contrôle essentiellement due au développement d'un mouvement inertiel.

En conséquence, on propose d'améliorer la protection des avions denses, en complétant les avertisseurs d'incidence actuel, par un détecteur de couple gyroscopique.

Plus généralement, on interprète l'entrée en vrille comme une phase de vol transitoire au cours de laquelle se constitue un capital important d'énergie en rotation, dont l'origine ne peut être que cinétique. En conséquence, l'étude de la résistance à l'entrée en vrille peut être abordée sous un angle nouveau : par la recherche des paramètres qui commandent ce transfert d'énergie. D'une telle étude, pourraient découler des explications rationnelles concernant les vrilles pseudo-oscillatoires, mais non permanentes, que le modèle inertiel proposé ne permet pas d'aborder directement.

Egalement, une explication générale de la mise en vrille pourrait être trouvée en cherchant à comprendre la coïncidence suivante : pour l'organisation de leurs vrilles, tous les avions cités semblent "choisir" parmi les mouvements d'Euler-Poinsot, ceux qui possèdent des périodes de l'ordre de grandeur de 3 secondes.

Enfin, si l'on admettait que le phénomène d'autorotation aérodynamique existe pour tout avion, on pourrait envisager la généralisation suivante :

> *« La vrille de tout avion est un compromis entre deux modèles extrêmes : l'autorotation aérodynamique pure, et le mouvement inertiel pur selon le modèle d'Euler-Poinsot ».*

On pourrait ajouter que ce compromis est largement orienté par la "masse spécifique" de l'avion, et son envergure.

☆ ☆ ☆

SPIN INVESTIGATION OF THE HANSA JET

by

Herbert Neppert

Aerodynamics Department
Messerschmitt-Bölkow-Blohm GmbH
Commercial Aircraft Division Hamburg
2103 Hamburg 95, West Germany

SUMMARY

Spin characteristics of the Hansa Jet from calculation, vertical spin tunnel and flight have been compared. As a result of the superstall a special form of flat spin with low rate of rotation is obtained and in the following an analysis is carried out and various recovery methods given.

NOTATION

A. Geometric and mass relationships

X,Y,Z	longitudinal, lateral and vertical axes of aircraft
b	wing span, m
$\bar{c}$	mean aerodynamic chord, m
S	wing area, m^2
l	length of fuselage, m
d	distance of anti-spin 'chute from tail cone, m
R	radius of c.g. about spin axis, m
h	altitude, ft
I_X, I_Y, I_Z	moments of inertia about X, Y and Z body axes, $kg \cdot m^2$
W	aircraft gross weight, N

B. Angular relationships

α	angle of attack at c.g., deg
$\alpha_{C_{Lmax}}$	angle of attack at maximum lift coefficient, deg
β	angle of sideslip at c.g., positive when relative wind comes from right, deg
θ	angle between X body axis and horizontal, positive when aircraft nose is above horizontal plane, deg
ϕ	angle between Y body axis and horizontal, positive when right wing is below horizontal plane, deg
δ_a	aileron deflection, positive when right aileron down (left stick), deg
δ_e	elevator deflection, positive with trailing edge down, deg
δ_r	rudder deflection, positive with trailing edge to left, deg
δ_f	landing flap deflection, positive with trailing edge down, deg

C. Definition of aerodynamic coefficients and derivatives

C_m	pitching moment $(= M / S \cdot q_\infty \cdot \bar{c})$
C_n	yawing moment $(= N / S \cdot q_\infty \cdot b/2)$
C_{m_β}	pitching moment due to sideslip $(= \partial C_m / \partial \beta)$
C_{n_β}	yawing moment due to sideslip $(= \partial C_n / \partial \beta)$
$C_{n_{\delta_a}}$	aileron yawing moment effectiveness $(= \partial C_n / \partial \delta_a)$
$C_{n_{\delta_r}}$	rudder yawing moment effectiveness $(= \partial C_n / \partial \delta_r)$
C_{n_r}	yawing moment due to rate of yaw (damping in yaw) $(= \partial C_n / \partial (r \cdot b/2V))$

D. Definition of rates

V	resultant velocity of c.g., EAS, m/s
V_Z	vertical component of V, EAS, m/s
Ω	rate of rotation about spin axis, radians/s
p,q,r	components of Ω about X, Y and Z body axes, radians/s

E. Miscellaneous definitions

q_∞	dynamic pressure, N/m^2 $(= 1/2 \cdot \rho \cdot V^2)$
q^*	effective dynamic pressure at antispin devices, N/m^2
ρ	density of air, kg/m^3
t	time, s

c.g.	centre of gravity
25	for c.g. at 25 % $\bar{c}$
E	empennage
F	fuselage
W	wing

1. AIRCRAFT DESCRIPTION

Some leading particulars of the aircraft are shown in fig. 1. The forward sweep was chosen for structural reasons so that the main spar of the mid-wing installation would pass behind the passenger cabin. With the relatively low span and aspect ratio destabilising aeroelastic effects are small. An aerodynamic advantage is that, for approximately the same critical Mach No. as for conventional sweep-back, separation begins in the wing root region. However, in order to maintain a clean flow into the engine intakes, this separation is moved outboard by means of a short leading-edge slat and a boundary layer fence. As a result good behaviour in roll at the stall is achieved together with satisfactory intake flow upto and beyond $\alpha_{C_{Lmax}}$.

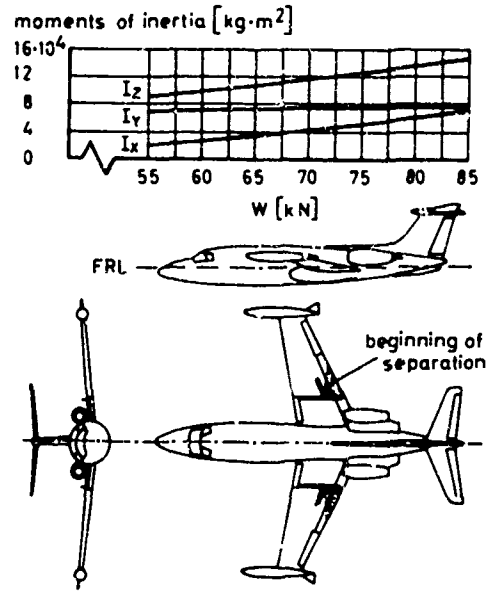

Figure 1: Leading particulars and three-view-drawing of aircraft

S = 30 m²	δ_a = +17,5° to -22,5°
b/2 = 6,73 m	δ_e = + 20° to -25°
$\bar{c}$ = 2,43 m	δ_r = ± 25°
c.g. at 14 to 28 % $\bar{c}$	δ_f = 0° to 60°

2. SPIN DATA FOR THE HANSA JET

2.1 Accident Flight

During the stalling tests carried out to adjust the anti-stall system (stick shaker and pusher) for certification purposes, an aircraft crashed. Fig. 2 shows a trace of the sequence of events As a result of the superstall characteristic the aircraft overshot to the lock-in point at $\alpha_F \simeq 60^0$. During the stable superstall, rotation was most probably initiated by aileron yawing moment since wind tunnel tests show that the controls are otherwise completely ineffective. Resulting from a nose up gyroscopic moment, a flat spin with angle of attack larger than that of the lock-in point developed. An anti-spin parachute had no effect since this did not emerge from the aircraft wake and wrapped itself around the tail. The opening of the cabin door before the exit of the co-pilot is clearly visible from the pressure trace. Although the pressure trace was regained intact, the flight recorder box containing the spin data burst on impact and only about 1,5 turns of the spin could be retrieved.

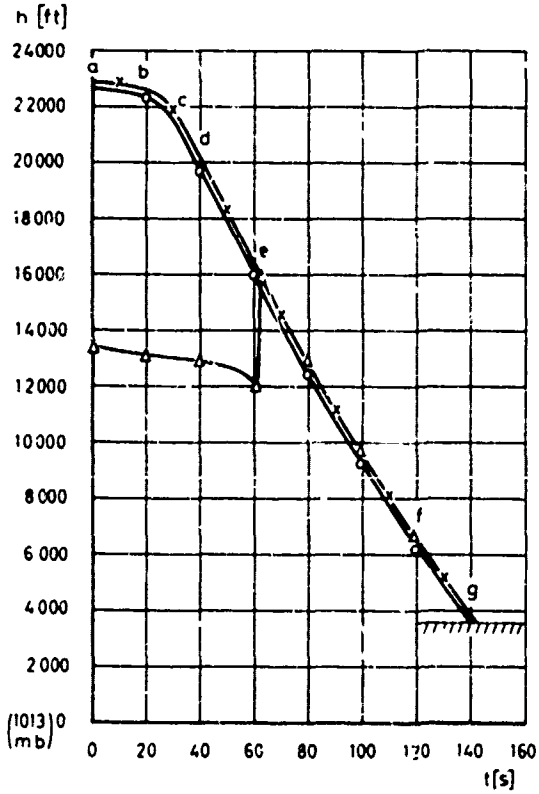

Figure 2. Accident trace of pressure height.
W = 70 kN; c.g. at 22 % $\bar{c}$
o noseboom; x tailboom; Δ cabin pressure
events
a) buffet
b) full stall
c) spin probably produced by $C_{n\delta_a}$
d) drag 'chute out, no effect
e) cabin door opened
f) spin data only retrieved in this region
g) $V_Z \simeq 42$ m/s TAS at impact

2.2 Comparison of Spin Data

Fig. 3 shows a comparison of spin data from

- calculation based on steady-state wind tunnel tests and estimated damping coefficients,
- vertical spin tunnel tests on a 1:25 model in the IMF Lille,
- flight test (accident trace).

Due to the very stable pitching moment characteristic at the lock-in point a slowly oscillating flat spin is developed in the region $\alpha_F \simeq 55^0$ - 85^0. Control and flap positions have practically no effect on the spin form. Also investigation of c.g. and mass distribution in the vertical spin tunnel way beyond the permitted limits showed no appreciable effect on the spin. It can thus be concluded that for this particular type of flat spin with low rotational velocity

the superstall characteristic is the critical factor. The Hansa Jet rotates at a rate of one revolution every 4 to 6 sec. whilst the HS Trident with similar tail geometry rotates at 1 rev. per 6 to 8 sec. [1]. This special form of flat spin is further analysed below and general conclusions are drawn.

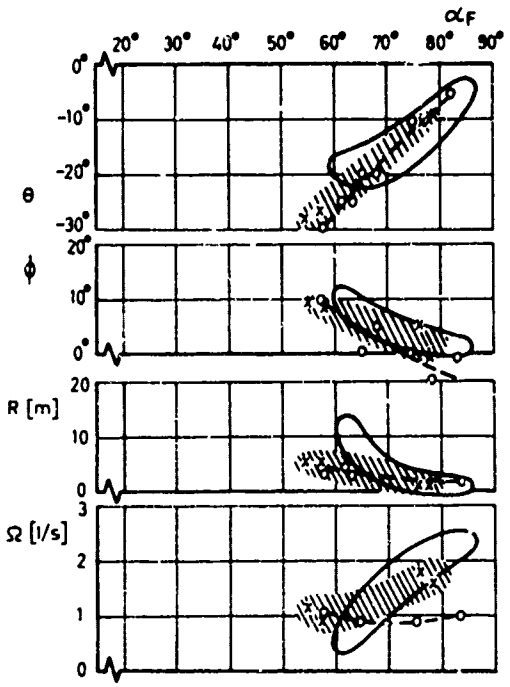

Figure 3: Comparison of data for spin to the right

from:	calculation ———	model test o—o—o	accident trace x (hatched)
W[kN]	80	85	70
c.g.at	25% $\bar{c}$	27% $\bar{c}$	22% $\bar{c}$
h[ft]	6600	16 400	6600
$Re_{\bar{c}}$	$7.0 \cdot 10^5$	$8.4 \cdot 10^4$	$6.6 \cdot 10^6$

└ based on wind-tunnel tests at this Re No.

(for all control and flap deflections)

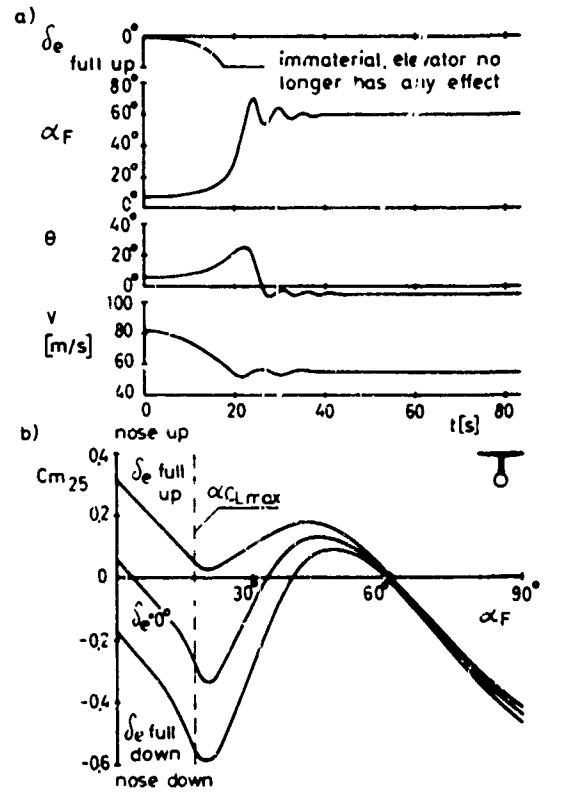

Figure 4: a) Development of a super-stall (δ_a; δ_r; β=0°) and b) super-stall characteristics

a) Aircraft characteristics in the following investigation

wing loading $W/S \approx 2500\ N/m^2$ and moments of inertia in the order of $I_x = 8 \cdot 10^4\ kg \cdot m^2$, $I_y = 8 \cdot 10^4\ kg \cdot m^2$, $I_z = 10 \cdot 10^4\ kg\ m^2$

c.g. at 25% $\bar{c}$ in all cases

b) Spin cases investigated

conventional longitudinal characteristics	super-stall characteristics
case ① satisfactory yaw damping	case ③ not dependent on the yaw damping
case ② insufficient yaw damping	

c) Characteristic spin data

case	type	θ	Ω[1/s]	ϕ	v_Z[m/.]	R[m]
①	"steep"	-50°	2	10°	[illegible]	6
②	flat"	-15°	3	0°	50	1
③	"flat"	-15°	1	0°	50	3

Figure 5: Spin cases investigated

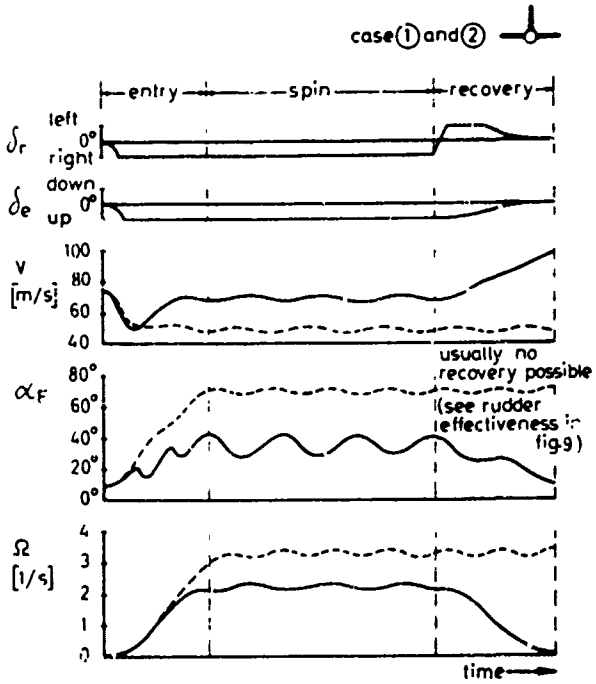

Figure 6: Development of spin with convertional longitudinal characteristics; δ_a=0°
——"steep" with satisfactory yaw damping and
---"flat" with insufficient yaw damping beyond $\alpha C_{L\,max}$ (see fig.5)

3. THE EFFECT OF SUPERSTALL ON THE SPIN CHARACTERISTICS

3.1 The Superstall (fig. 4)

The superstall occurs when a high-mounted tailplane eg. T-tail is enveloped to a greater or lesser extent in the separated wing wake produced by the initial stall. This separated wake can be amplified by rear-fuselage mounted engine nacelles and its core can contain reversed flow. The tailplane which at high incidence normally produces a nose-down pitching moment is then ineffective or actually produces a destabilising moment. An aircraft which either through stall or overshoot enters the nose-up pitching moment range rapidly increases its angle of incidence until it reaches a stable trim condition in the extreme stalled region (lock-in point eg. at $\alpha_F \simeq 60^\circ$). The elevator power available is then usually insufficient for recovery.

3.2 Spin Cases Investigated (fig. 5)

Three typical cases of spin have been investigated and the results from calculation, vertical spin tunnel and flight compared:

case①: steep spin with conventional ie. stable up to $\alpha_F = 90^\circ$, pitching moment curve and adequate yaw damping, see fig. 9.

case②: flat spin also with conventional pitching moment curve but insufficient yaw damping, see fig. 9.

case③: flat spin resulting from superstall. This is independent of yaw damping.

Only similar c.g. positions in the normal range eg. 25 %$\bar{c}$ have been investigated.

A further case with c.g. lieing too far aft so that, even with a conventional pitching moment characteristic and satisfactory yaw damping, a flat spin is produced has not been considered.

3.3 Effect of the Superstall Characteristic

An aircraft with conventional longitudinal characteristics can, dependent on the rotational velocity and therefore yaw damping in the stalled region, enter a steep or a flat spin, fig. 6. However for an aircraft with superstall characteristics only a flat spin is possible with either primary entry immediately after the stall or secondary entry from the trimmed superstall condition, fig. 7. This is determined mainly by the aerodynamic pitching moment ie. by the equilibrium of moments about the Y-axis. Since, in the normal spin range, the gyroscopic moment, $(Iz-Ix)\cdot r\cdot p$, acts in the nose-up sense, equilibrium can only by reached after the trimmed superstall condition when a stable (nose-down) pitching moment characteristic is again achieved, fig. 8b. As a result of the pitching moment due to sideslip in the spin the trimmed condition moves somewhat to the left. It then has to be established if spinning is possible at incidences above the trimmed condition and, if so, whether it is steady-state or oscillatory. In contrast to the conventional flat spin, fig. 8a, it is not necessary to overcome a large aerodynamic pitching moment in order to achieve the flat attitude and a small gyroscopic moment with low rotational velocity is sufficient for

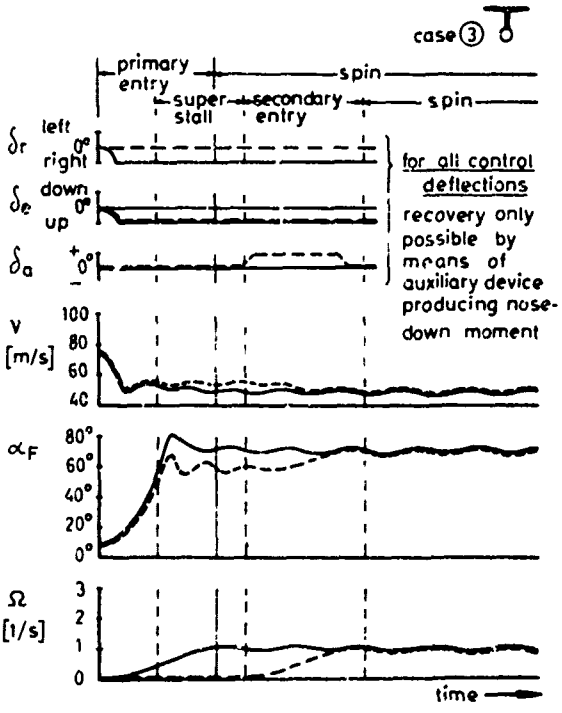

Figure 7: Development of spin with super-stall characteristics
— "flat" with primary entry immediately after the stall and
--- "flat" with secondary entry from a locked-in super-stall, e.g. by aileron deflection ($Cn_{\delta a}$)

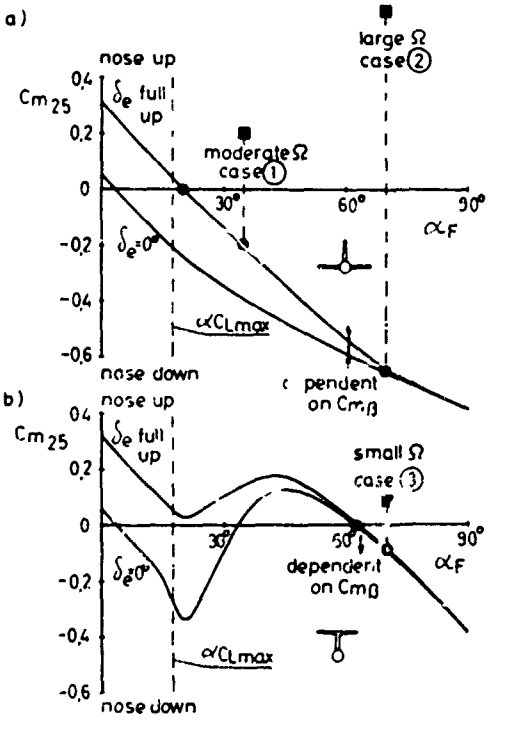

Figure 8: Balance of aerodynamic (⊗) and gyroscopic moments (⊠) about the Y axis for typical spins
a) with conventional longitudinal characteristics "steep" with satisfactory yaw damping ① and "flat" with insufficient yaw damping ② (s. fig 9)
b) "flat" with super-stall characteristics ③

equilibrium conditions. According to [2] the rotational velocity can be expressed as:

$$\Omega^2 = -\frac{M + q\frac{\partial M}{\partial q} + \Omega\frac{\partial M}{\partial \beta} + \delta_e\frac{\partial M}{\partial \delta_e}}{(I_Z - I_X)\sin\theta\cdot\cos\theta\cdot\cos\phi}$$

For the steady-state flat spin, the longitudinal damping can be neglected since $q \approx 0$, the elevator power is almost zero and experiments show that the angular attitude for conventional flat spin and flat spin with superstall is practically the same. Thus, for approximately equal mass distributions, differences in rotational speed can only result from the dissimilar pitching moment curves, (compare fig. 5, case ②and ③). From the above equation Ω is then approximately proportional to $\sqrt{M}$. For the aircraft considered here, the aerodynamic pitching moment in the case of the conventional flat spin is around ten times larger then that for the flat spin with superstall, fig. 8. Consequently the ratio of rotational velocities is of the order:

$$\frac{\Omega_{conv.}}{\Omega_{sup.st.}} \simeq \sqrt{\frac{M_{conv.}}{M_{sup.st.}}} \simeq \sqrt{10}$$

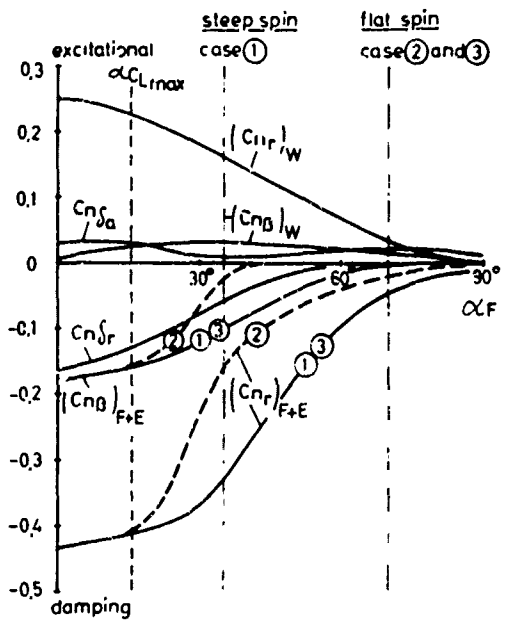

Figure 9: Aerodynamic derivatives about the Z axis for spin cases ①, ② and ③ (valid for all cases except where shown)

3.4 Effect of the Lateral Characteristics

According to investigations such as those in [3], unintentional primary entry is practically impossible for the Hansa Jet. The aileron-alone divergence parameter and $Cn_{\beta_{dyn.}}$ indicate that there will be "no departures", which is in agreement with the separation characteristics already described in section 1, (compare fig. 1).

Secondary entry as a result of aileron yawing moment (see figs. 7 and 9) or some other disturbance is highly likely; rudder deflection at such high values of incidence is, however, usually ineffective. Much smaller excitations are required than for primary entry since the directional stability and the yaw damping at the trimmed superstall condition are also much smaller, fig. 9. Since the fin makes the primary contribution to both, an increase of incidence causes either a gradual or, where shielding occurs, a rapid reduction in those characteristics. In this connection the T-tail is usually advantageous in that the rotational velocity in the case of the flat spin is kept small.

In contrast to the conventional flat spin (case②) which is caused by the high rotational velocity resulting from low yaw damping, the flat attitude of the superstall spin is not influenced by the yaw damping (section 3.3). In that case the yaw damping can only influence the spin equilibrium through the rotational velocity within a relatively small range of incidence above the trimmed superstall condition.

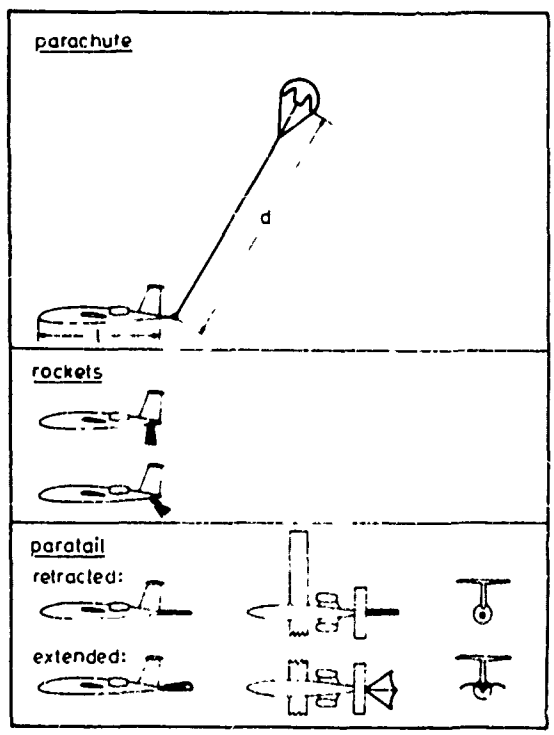

Figure 10: Summary of some anti-super-stall and anti-spin devices

The upper limit of this region in the steady-state case is $\theta = 0^\circ$ ie. $\alpha \leq 90^\circ$. As with the damping, the excitational moments at large incidence are usually small, fig. 9, because during a flat spin both wings are operating well above $\alpha_{C_{L max}}$ where the normal and tangential force coefficients change little with incidence.

3.5 Possible Recovery Methods

With an aircraft which enters a flat spin as a result of an unstable superstall characteristic, the only sure way to effect recovery is normally by influencing the longitudinal motion (ΔC_m). Modification of the lateral motion (ΔC_n) which is normal for steep spins and can also be used for conventional flat spins

produces, at best, a return to uncontrollable superstall with the possibility of renewed spin entry.

However since the elevator is no longer sufficiently effective, fig. 4b, auxiliary devices are necessary, fig. 10, to produce a nose down moment. These devices differ in their effectiveness and reliability, fig. 11, [4].

The parachute configuration requires an extension on the tail cone since otherwise the lines will foul the trailing edge of the elevator. In addition an ejection device is essential since the closed 'chute must be shot out to a distance of at least d = 2 l. Whether the 'chute will then effectively open in the wake turbulence is uncertain. At smaller distances the 'chute is dragged, by means of the reversed flow in the separated wake of the wing, back towards the aircraft.

Current off-the-shelf rockets have the disadvantage of insufficient control over their thrust and its duration. This control is necessary since the recovery time for a spin and a superstall having the same nose-down additional moment requirements is in the ratio 3:1. For this reason a flexible lifting surface, called Paratail, has been used. Over its entire operational range this lies in the full dynamic pressure. It delivers an additional moment dependant on incidence and can be designed to produce its maximum nose-down moment to coincide with the maximum nose-up tendency of the aircraft, fig. 11b. After passing through zero ΔC_m to smaller angles of incidence it provides, by means of the supported fabric surface, a pull-out tendency and produces a minimal out-of-trim moment, fig. 13 and 14.

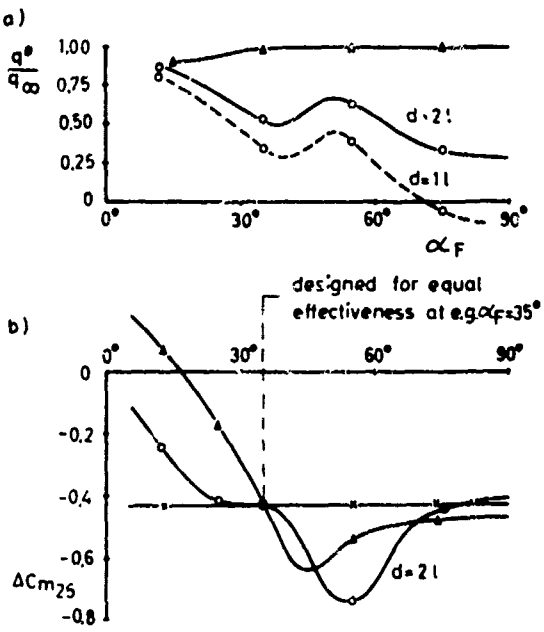

Figure 11: a) Dynamic pressure at the auxiliary devices, b) additional pitching moments produced by the devices, based on aircraft S and $\bar{c}$. o parachute, x rockets, Δ paratail

In the case of spin a nose-up gyroscopic component is present and therefore the additional nose-down moment supplied by the auxiliary device must be appreciable larger than the nose-up moment due to the superstall. This requires an increase in the recovery effectiveness eg. 1,5 times that necessary for the superstall case. Because secondary entry can occur so easily (section 3.4), it follows that the auxiliary device must be laid out for the spin case. The minimum requirements for recovery from the spin are generally accepted as being 2,5 turns after operation of the control or auxilary device, fig. 12. Should the auxiliary device, however, not function in a superstall the crew must escape from the aircraft (preferable in the clean configuration) without attempting any roll or yaw manoeuvres. This is because escape from an aircraft which is not rotating is far safer than from one which is. In a superstall, crew and aircraft separate both horizontally and vertically whereas in a fully developed spin only vertical separation is possible.

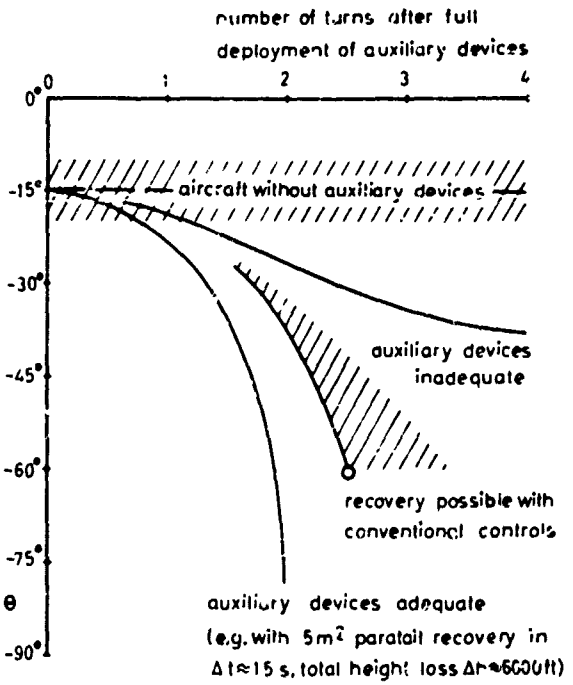

Figure 12: Development of spin recovery using auxiliary devices for nose-down pitching moment; flat spin case ③
(for all initial control and flap deflections)

4. CONCLUSIONS

The flat attitude of the aircraft with superstall is not determined by the yaw damping but by the unstable pitching moment curve. Therefore in the steady-state case, equilibrium conditions are only possible between the trimmed superstall condition appropiate to the given sideslip angle and $\alpha_F = 90^C$. The yaw damping can therefore only effect the equilibrium state through the rotational velocity within that range of incidence. Due to the generally favourable yaw damping qualities of T-tail configurations at large incidence the rotational velocity usually remains small. On the other hand, due to the superstall characteristic, a high rotational

velocity is not necessary for the flat attitude.

It has been determined that, for the flat spin with superstall, both primary entry immediately after the stall as well as secondary entry from the trimmed superstall are possible. Secondary entry can be provoked by disturbances much smaller than those necessary for primary entry because here the directional stability and yaw damping are much smaller. The only sure way to effect recovery with an aircraft that enters a flat spin as a result of a superstall, is to alter the longitudinal motion.

5. REFERENCES

[1] Deep-stall disaster. Points from the report on the Trident test-flying accident in 1966. Flight International, 28 Nov. 1968, pp. 909-911.

[2] H. Neppert — Trudelbeeinflussung durch "Superstall"-Charakteristik (Spin characteristics resulting from the superstall). Zeitschrift für Flugwissenschaften, 20 (1972) Heft 11, pp. 414-421; (in German).

[3] R. Weissman — Preliminary criteria for predicting departure characteristics/spin susceptibility of fighter-type aircraft. Journal of Aircraft, Vol. 10, No. 4, April 1973, pp. 214-219.

[4] H. Neppert — Entwicklung einer Spreizflosse als Antisuperstall-und Antitrudelhilfseinrichtung (Development of a paratail as an anti-stall and anti-spin auxiliary device). Fachtagung Aerodynamik, Berlin 1968. DGLR-Fachbuchreihe Band 3 (1969), pp. 43.1 - 43.36; (in German).

Figure 13: Sideview of extended paratail

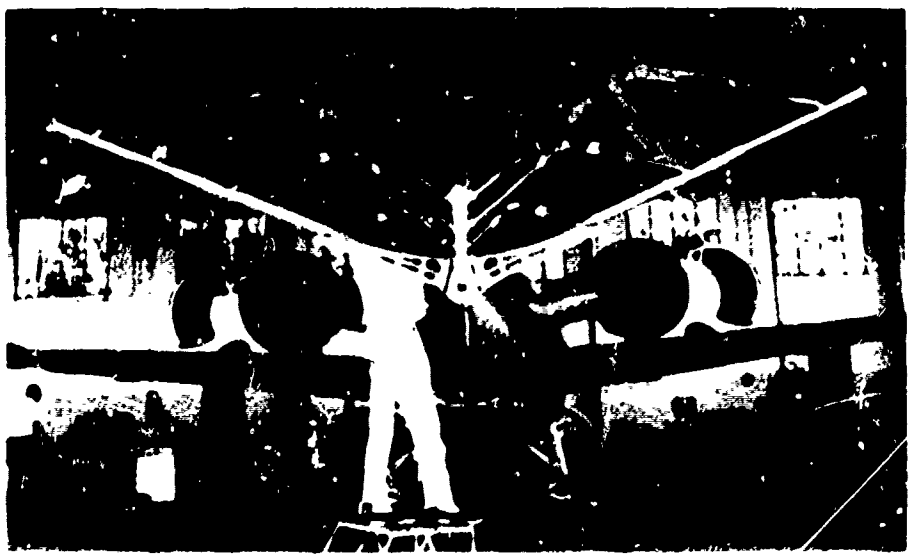

Figure 14: Rearview of extended paratail

METHODES D'ESSAIS DE VRILLES EN VOL

par

J.P. DUVAL

Ingénieur

AVIONS MARCEL DASSAULT - BREGUET AVIATION

ESSAIS EN VOL

B.P. 28

I S T R E S

13 800

France

RESUME :

Une campagne d'essais de vrille nécessite, de la part d'un centre d'Essais en Vol, d'une part la mise en oeuvre de moyens bien spécifiques, d'autre part l'application d'une méthode de travail capable de concilier les impératifs d'efficacité et de sécurité dans un domaine où le comportement de l'avion ne peut pas encore être prédit de façon rigoureuse.

Ce papier présente ces moyens et cette méthode tels qu'ils sont envisagés à l'heure actuelle aux Avions Marcel Dassault - Bréguet Aviation. Les moyens au sol (télémesure, exploitation en temps réel et en temps différé) et sur avion (aménagements des systèmes, caméras...) sont décrits et commentés. La présentation de la méthode de travail sera faite en se référant au cas de l'ALPHA-JET : l'importance des essais préliminaires en soufflerie et la progression logique des essais seront soulignés. Enfin, on donnera quelques résultats obtenus lors des campagnes les plus récentes : durée de la campagne, nombre de vols, etc...

PREFACE : PHILOSOPHIE DES ESSAIS DE VRILLE

Les essais de vrille tiennent une place particulière parmi tous les essais auxquels est soumis un avion prototype. En effet, ils ont pour caractéristique d'emmener l'avion en dehors de son domaine de vol normal, là où l'ingénieur ne sait pas (encore) prédire avec exactitude le comportement de l'appareil par le calcul (ce qu'il prétend savoir faire partout ailleurs), et là où le pilote doit oublier certains réflexes normaux de pilotage et analyser les phénomènes tout en étant soumis, parfois, à un traitement sévère de la part de l'avion. D'autre part, plus que l'obtention de résultats relatifs à l'aérodynamique, le but de ces essais est d'aboutir à une description complète de l'avion en vrille à l'usage des pilotes en formation. Il ne faut donc pas perdre de vue les éléments importants pour ces pilotes : comportement des systèmes et des moteurs, accélérations et rotations peut-être désorientantes, description de la planche de bord pendant le phénomène, problèmes d'éjection éventuelle, et bien sûr, consignes de sortie. Les méthodes et les moyens d'essais doivent être adaptés à ces caractéristiques et à ces buts des essais de vrille.

Que souhaite le pilote d'essais ? D'abord la connaissance la plus approfondie possible de ce qui va se passer. En particulier il prend connaissance des résultats des essais préliminaires en soufflerie et des consignes issues de ces résultats. Ensuite, un avion dont la mise au point initiale est terminée. Enfin, une instrumentation particulière qui lui permette d'une part d'éxécuter les manoeuvres prescrites avec précision, d'autre part de décrire ce qui se passe à l'ingénieur.

Que souhaite l'ingénieur ? D'abord ce que souhaite le pilote ! Ensuite une installation au sol qui lui permette, en temps réel, pendant l'essai, de visualiser et de chiffrer le mieux possible le comportement de l'avion, et d'établir un dialogue fructueux avec le pilote. Enfin, des installations de traitement au sol qui l'aideront à analyser les phénomènes en temps différé, et à les décrire aux utilisateurs futurs.

Ces considérations permettent de dégager les points importants des essais de vrille : étude préliminaire en soufflerie, instrumentation de l'avion en vol et au sol, équipes pilotes - ingénieurs bien rodées pour le maximum d'efficacité en temps réel.

L'INSTRUMENTATION DE L'AVION

La planche de bord est entièrement refondue pour les essais de vrille. En effet, sont fournis au pilote, par l'intermédiaire d'indicateurs, en dehors des instruments habituels au pilotage :

- les positions de gouvernes : 3 indicateurs supplémentaires dans le cas de l'ALPHA-JET par exemple,
- l'incidence "girouette" : l'avion est muni d'une girouette d'incidence pour les grands angles, située sur le côté opposé à la sonde d'incidence normale. Cette girouette est

reliée à un indicateur gradué de -90° à +90°.

La planche de bord étant filmée pendant les essais, les instruments intéressants sont regroupés dans le champ des caméras. On y trouve la boule, l'anémomachmètre et l'altimètre, avec parfois un indicateur du sens de vrille (JAGUAR), et un indicateur de vitesse sensible (JAGUAR). Dans le cas de l'ALPHA-JET, on trouve aussi les paramètres de surveillance des moteurs. Particulièrement importants pour le pilote sont les indicateurs de position des gouvernes : ils ont permis, dans le cas de l'ALPHA-JET, d'étudier l'influence des braquages partiels du gauchissement. Grâce à l'indicateur, le pilote peut afficher avec précision le braquage à étudier.

En dehors des instruments de contrôle de vol, les commandes et contrôles de l'installation d'essais, et les commandes et contrôles des systèmes avion introduites spécialement pour les essais de vrille sont regroupées sur un panneau "vrilles" de façon à ce que le pilote n'ait pas à disperser son attention à droite et à gauche, avant et pendant l'essai. C'est ainsi que dans le cas du JAGUAR, par exemple, on trouve regroupés sur le panneau "vrilles", à la place du viseur : la commande du parachute anti-vrilles, la commande et la signalisation "virures", les commandes du système "électricité", la commande du variateur de sensibilité de direction, la commande du fumigène, la commande de désembuage secours, la commande des caméras, les commandes radio, la commande des bleed-valves. S'ajoutent, bien entendu, les diverses commandes du système de transmission et d'enregistrement des données : télémesure, enregistreurs magnétiques et photographiques embarqués.

Toutes ces commandes supplémentaires sont liées à des modifications des systèmes de l'avion, qui ont pour but d'améliorer la sécurité tant en ce qui concerne les sorties de vrilles que les éventuelles pannes moteurs. Le suivi de l'avion est également renforcé pendant les essais de vrilles. Ces points sont commentés ci-dessous en prenant l'exemple du JAGUAR (une installation analogue étant d'ailleurs reconduite sur tous les avions présentant des caractéristiques analogues à celles du JAGUAR, en particulier en ce qui concerne les moteurs).

MODIFICATIONS DU SYSTEME "HYDRAULIQUE"

L'extinction possible des deux moteurs en cours de vrille a conduit à monter une électro-pompe supplémentaire sur le circuit 1, l'électro-pompe normale de l'avion étant sur le circuit 2. Ces deux électro-pompes sont alimentées par des batteries distinctes. Des accumulateurs supplémentaires ont été montés en amont des servo-commandes des empennages sur chaque génération (planche 1).

Sur le circuit 2, l'électro-pompe a une commande classique par un interrupteur à trois positions ARRET - AUTO - MARCHE. La position normale en vol est "AUTO", c'est-à-dire, qu'elle se met en route lorsque la pression chute en-dessous de 100 bars. Elle est cependant mise sur "MARCHE" pendant les essais de vrilles. Un voyant situé au-dessus de l'interrupteur s'allume quand elle est alimentée électriquement.

L'électro-pompe 1 est commandée par un interrupteur à deux positions ARRET - MARCHE. Elle est systématiquement mise sur "MARCHE" pendant les essais de vrilles, un voyant situé au-dessus de l'interrupteur signalant quand elle est alimentée électriquement. L'indicateur de pressions hydrauliques en position "servo-commandes" donne les pressions après les accumulateurs.

MODIFICATION DE LA GENERATION ELECTRIQUE

Les systèmes électriques sont également modifiés par l'adjonction de batteries supplémentaires. C'est ainsi que sur le JAGUAR, deux batteries supplémentaires ont été montées de façon à pallier à la perte de deux transfo-redresseurs (planche 2).

Sur l'ALPHA-JET, il y a une batterie supplémentaire, et la possibilité de découpler deux barres bus couplées en temps normal. Les commandes de ces systèmes sont groupées sur le panneau "vrilles" (planche 3).

AUTRES SYSTEMES SUPPLEMENTAIRES

- Virures :

Il s'agit de petites surfaces horizontales placées sur le nez de l'avion. Ces surfaces, amovibles sur le JAGUAR, fixes sur la version ECOLE de l'ALPHA-JET, ont pour but de diminuer les agitations et de rendre les sorties plus pures.

- Parachute :

Seul le JAGUAR a été équipé d'un parachute anti-vrilles, à la place du parachute frein normal. Ce dispositif n'a pas eu à être utilisé pendant les essais du JAGUAR monoplace. D'une façon générale, on craint des difficultés possibles au largage, et on évite de le monter (avec l'agrément de la soufflerie).

- Radio :

La voix du pilote passe en permanence par l'intermédiaire du système de télémesure. Le pilote peut, de plus, communiquer avec le sol par l'intermédiaire de deux postes de radio dont les alimentations sont séparées.

- Désembuage :

Les avions sont munis d'une soufflante à air chaud pour le désembuage des glaces frontales.

- Anémométrie et incidence :

En dehors des girouettes d'incidence et de dérapage, étalonnées en soufflerie (F1 et JAGUAR), on peut trouver des dispositifs plus élaborés : c'est ainsi que le F1 était muni d'une perchette à une totale et statique "multi-trous", ainsi que d'une couronne de 12 prises statiques en arrière de la pointe de nez (étalonnage en soufflerie). La statique dite "multi-trous" (12 trous au lieu de 4) permet d'avoir une prise pour laquelle l'erreur ne dépend que de l'angle du vecteur vitesse avec l'axe de la perchette. La couronne en arrière du nez associée à cette perchette permet de calculer l'incidence et le dérapage sans être gêné par un masque éventuel comme c'est le cas pour des girouettes.

Outre ces modifications relatives aux systèmes, l'avion doit recevoir une installation d'essais adaptée aux problèmes de suivi. C'est ainsi que l'on trouve les dispositifs suivants :

- Fumigène :

Les avions en vrille sont filmés depuis le sol par des caméras à longue focale (1000 et 1200 mm). L'acquisition est facilitée par l'émission de fumée un peu avant l'essai. Le système comporte un réservoir d'huile de 30 l environ, une bouteille d'azote gonflée à 150 bars, un détendeur, un électro-robinet et une buse de sortie dans le jet d'air d'un réacteur.

- Caméras :

Les avions destinés aux essais de vrilles sont équipés de deux groupes de caméras : deux caméras qui filment l'horizon, et deux caméras qui filment la planche de bord à travers des tubes optiques.

L'autonomie de chaque caméra est de deux minutes et demi, ce qui fait une autonomie totale de cinq minutes.

Chaque essai est donc filmé par quatre caméras : planche de bord et horizon sur l'avion lui-même, avion d'accompagnement, et caméra sol. Les films obtenus sont destinés à montrer aux pilotes en unité les attitudes de l'avion et les indications lues sur la planche de bord pendant les vrilles.

- Répondeur radar :

Cet appareil facilite l'acquisition, le suivi, et le positionnement précis de l'avion. Les essais de vrille sont en effet initiés en un point précis, situé à quelques nautiques du terrain, au-dessus d'une zone inhabitée. Le radar permet ce positionnement et fournit ensuite les trajectoires.

Les paramètres traités par l'installation d'essais sont transmis par l'intermédiaire d'un émetteur relié à deux antennes disposées sur la pointe avant, à 90° l'une de l'autre.

Le fait d'avoir deux antennes permet de recevoir le signal au sol dans de bonnes conditions malgré les attitudes inhabituelles de l'avion. Les paramètres les plus importants sont passés par voie continue, les autres sont commutés (deux ou trois commutateurs).

Il existe de plus un enregistreur magnétique embarqué sur lequel on trouve les commutateurs, la voix du pilote, la base de temps embarqué et des paramètres relatifs aux qualités de vol : pressions totale et de référence, assiettes et cap, vitesses angulaires. Des enregistreurs photographiques sont affectés éventuellement à l'examen détaillé du comportement des moteurs.

L'INSTALLATION DE SURVEILLANCE AU SOL

Un nombre important de paramètres sont présentés directement (en continu) sous les yeux de l'ingénieur d'essais chargé du vol : altitude et vitesse, position des commandes, vitesses angulaires, incidence, voyants de fonctionnement des caméras et des électro-pompes. Une visualisation très utile est réalisée grâce à un électroscope à mémoire Tektronik 611. Cet appareil permet de suivre instantanément l'évolution de plusieurs paramètres au cours de la vrille, l'ingénieur étant alors capable, dans certains cas, de discerner avant le pilote l'évolution vers la sortie, par exemple, et de donner des indications en conséquence. Les paramètres visualisés sont l'accélération longitudinale, l'incidence et les vitesses angulaires de roulis et de lacet. D'autres pupitres comportent les cadrans et les voyants affectés à la surveillance de la configuration (becs, volets, virures, parachute, etc...) et des moteurs. Enfin, on peut tracer en temps réel jusqu'à vingt paramètres sur un enregistreur à ultra-violets.

A cette installation de surveillance s'ajoutent les appareils de traitement et de stockage des données, avec édition pendant le vol d'un listing et de tracés.

Ces points sont abordés dans les paragraphes suivants.

CONDUITE DES ESSAIS DE VRILLES

Les essais de vrilles d'un avion de combat, pris dans une configuration donnée, sont toujours regroupés en une campagne qui doit être évidemment la plus instructive possible sans pour autant s'étendre sur des mois et des mois. Mais avant le premier vol d'une telle campagne, une certaine préparation a eu lieu.

Il est certain que la théorie ne peut prédire à 100 % le comportement d'un avion en vrille. Une grande initiative est donc laissée aux services d'Essais en Vol. Pourtant entre le stade "Bureau d'Etude" et le stade "Essais en Vol", une étape fondamentale est celle de l'étude en soufflerie, souvent commencée dès les premiers stades de la conception de l'avion. Aux A.M.D. - B.A., cette étude constitue, en fait, la base de tous les essais en vol, et l'orientation des premiers vols d'essais est entièrement déterminée par les conclusions de l'étude en soufflerie.

Ceci est particulièrement important dans le cas de l'ALPHA-JET, puisqu'il s'agit, dans sa version française, d'un avion ECOLE, qui doit présenter une vrille saine assortie de consignes de sortie simples. Cet avion a été soumis à trois campagnes en soufflerie :
- une première étude sommaire, lancée dès 1971,
- une deuxième étude plus complète en 1972, avec différents cas de chargements et diverses modifications aérodynamiques (1500 lancers),
- enfin une troisième étude, simultanée avec les essais en vol, d'un millier de lancers environ en Novembre 1974.

Ceci ne concerne que la configuration sans charges, l'étude des vrilles avec charges a été entreprise en Juin 1975.

A partir du moment où les rapports de la soufflerie sont sur les bureaux des pilotes et des ingénieurs, et où l'avion est équipé de l'installation d'essais et des systèmes adaptés, la phase d'essais en vol proprement dite peut commencer.

Chez A.M.D.-B.A., ces essais en vol de vrilles sont confiés à des équipes bien "rodées" qui maintiennent des relations très étroites avec la soufflerie. Les pilotes entraînés sur divers types d'avion sont également accoutumés aux problèmes de vrilles, car les campagnes reviennent régulièrement. La vrille est en effet un domaine où la connaissance du phénomène lui-même est aussi importante pour le pilote que celle de l'avion : il faut être capable d'analyser les mouvements de l'avion dans une gamme d'attitudes et de vitesses angulaires très étendues et inhabituelles, tout en appliquant en même temps les consignes données depuis le sol. Les pilotes interviennent aussi de façon importante dans la description de la partie non quantifiable de certains essais : facilité d'éxécution de certaines manoeuvres, inconvénients physiologiques liés aux accélérations et aux vitesses angulaires (désorientation, g vers l'avant,...). Ils font d'ailleurs parfois des essais d'accoutumance à la centrifugeuse.

Le rapport de soufflerie constitue la base de travail des équipes chargées des vrilles, surtout pour les premiers vols. Après ces premiers vols, l'orientation des essais doit être déterminée, en partie, d'un vol à l'autre en mettant l'accent sur les points intéressants trouvés. Il en résulte qu'un point fondamental est l'exploitation la plus rapide possible des essais : l'accent est mis sur le maximum d'exploitation en temps réel, élément important de sécurité et d'efficacité.

Le processus de l'exploitation en temps réel est le suivant :

- avant la vrille, il y a traitement en temps réel pour établir un listing de surveillance de l'avion et de l'installation d'essais,

- pendant l'essai, on procède aux opérations suivantes : acquisition de toutes les informations voulues, exécution de certains calculs (incidence, Mach, etc...), stockage sur disque des informations acquises et de celles qui sont nécessaires aux compléments de calcul à terminer,

- après la sortie de vrille, on commande la phase finale d'exploitation : relecture sur disque des informations, achèvement des calculs partiellement réalisés, exécution des tracés sur machine VARIAN couplée à l'ordinateur (Ex. de tracé : planche 4).

Pendant que l'avion est en vrille, l'ingénieur d'essais visualise l'évolution des paramètres sur le scope à mémoire, et donne des indications au pilote s'il y a lieu. Après l'essai, pendant que l'avion remonte à l'altitude de l'essai suivant, il peut analyser les tracés sortant de la machine VARIAN, qui donnent sur papier les paramètres importants : gouvernes, incidence, vitesses angulaires, paramètres moteurs, etc... Ainsi la sécurité du vol repose en grande partie sur l'ingénieur d'essais, l'avion d'accompagnement n'intervenant qu'en cas de perte de la télémesure, ou pour contrôler visuellement un phénomène anormal (déplacement d'une charge, fuite, etc...).

L'exploitation en temps réel est évidemment, de plus, un gage d'efficacité. En effet, tout de suite après le vol, pilotes et ingénieurs peuvent analyser les tracés, et préparer l'ordre d'essais du vol suivant. Ainsi, au cours de la campagne de l'ALPHA-JET, le délai entre deux vols n'a jamais été déterminé par un problème d'exploitation. Un autre avantage est que l'ordinateur n'est occupé que pendant le vol lui-même. En fait, on peut dire que le seul ensemble de résultats qui n'est pas analysable le jour même de

l'essai est constitué par les films (délai de développement).

EXEMPLE D'UNE CAMPAGNE DE VRILLES : CAS DE L'ALPHA-JET

La progression des essais de vrilles de l'ALPHA-JET est caractéristique des campagnes faites aux A.M.D.-B.A. Les premiers essais de perte de contrôle ont lieu en virage, à différentes vitesses. Cette méthode qui correspond d'ailleurs à l'utilisation opérationnelle des avions d'armes, permet de doser le lancement de la rotation. Après avoir déterminé la vitesse optimale, le nombre de tours est augmenté progressivement, et les positions des gouvernes et les consignes de sortie essayées. Ces essais ont lieu aux régimes moteurs qui minimisent les risques d'extinction.

Une fois reconnues les différentes formes de vrilles et les consignes de sortie, on s'oriente vers les conditions d'utilisation en opération : il s'agit de couvrir la perte de contrôle involontaire en virage, à des vitesses de plus en plus élevées, et à tous les régimes moteurs : les derniers essais de déclenchés ont lieu à vitesse ou à Mach élevé, au plein gaz (ou en PC MAX pour les avions qui ont une PC). De plus, sont étudiées les pertes de contrôle en ressource, les décrochages en palier, les figures du type cloche, etc...., toujours dans le souci de cerner les conditions d'utilisation dans une armée de l'air, plus que dans le but de faire des études aérodynamiques. Dans la même optique, on s'attache à étudier l'influence sur la sortie de vrille des erreurs de consigne (pied ou manche "oublié") et des détrimmages (jusqu'au détrimmage défavorable sur deux axes, le cas des trois axes étant considéré comme peu réaliste).

Ce schéma a été appliqué à l'ALPHA-JET, avec un élément supplémentaire : cet avion étant, dans la version française, un avion d'entraînement, il doit présenter une forme de vrille saine, la sortie étant assurée par une consigne simple. De plus, dans la version APPUI comme dans la version ECOLE, il est souhaitable que la reprise de contrôle après une perte de contrôle involontaire se fasse par l'application d'une consigne simple.

Ces impératifs ont conduit d'une part à chercher les conditions de départ (vitesse, altitude, attitude) et les positions de gouvernes les plus favorables à l'obtention d'une telle vrille, d'autre part à essayer plusieurs configurations successives de l'avion. En effet, on s'est aperçu assez vite que la configuration initiale "nez pointu" ne permettait pas d'obtenir facilement une vrille répondant parfaitement aux critères que l'on s'était fixés pour l'école.

Les premiers lancements ont été naturellement entamés à haute altitude : 40.000 ft, entre 130 et 170 kt, et en virage. Cette première partie des essais a permis de mettre en évidence le rôle important du gauchissement dans la vrille de l'ALPHA-JET. Toutefois, l'obtention de la vrille calme du type ECOLE restait assez difficile, la tendance étant plutôt aux agitations.

On a donc, en appliquant les résultats de soufflerie, essayé plusieurs configurations du nez de l'avion : celui-ci a été arrondi, puis des virures ont été ajoutées. Dans ces conditions, l'obtention d'une vrille ECOLE devenait à la portée d'un élève-pilote. (Cf Photo 1 : version ECOLE, Photo 2 : version APPUI).

Dans la configuration retenue, l'étude a été poursuivie en insistant sur les points suivants : consignes de sortie, erreurs d'application des consignes, influence des détrimmages sur la sortie. Parallèlement étaient vues les influences de l'altitude, de la motorisation et du centrage.

Enfin, dans la dernière partie de l'étude, on a insisté sur les points suivants : déclenchés jusqu'à 290 kt/M = 0,8 pour couvrir les déclenchés involontaires, vrilles avec les aérofreins sortis, clochés, etc.... Les vrilles dos ont été l'objet d'une attention particulière : il était en effet intéressant de savoir si un tel type de vrille pouvait être démontré de façon simple en école, et on a pu trouver une procédure permettant d'atteindre ce but.

En ce qui concerne la version APPUI de l'avion, l'optique était un peu différente : il s'agissait surtout d'étudier les pertes de contrôle involontaires et d'autre part de continuer l'étude de certains paramètres tels que le centrage ou l'inertie en roulis. Bien entendu, les essais de l'avion en version APPUI (nez pointu) ont permis de déterminer avec précision l'influence de la forme du nez sur les caractéristiques de la vrille. Dans cette version APPUI, l'accent a été mis sur la recherche d'un domaine d'emploi sûr du gauchissement à grande incidence.

L'ensemble de la campagne a donc nécessité un nombre de vols important : 78 vols, correspondant entre Juillet 1974 et Février 1975, à un peu plus d'un vol tous les deux jours ouvrables. La moyenne du nombre d'essais par vol a été de 5,5.

Pour le F1, la campagne d'essais a nécessité 153 essais répartis en 37 vols, et pour le JAGUAR, 139 essais en 34 vols.

CONCLUSION

La coopération avec la soufflerie et l'exploitation en temps réel constituent deux principes de base des méthodes d'essais de vrilles aux AVIONS MARCEL DASSAULT - BREGUET AVIATION. Les campagnes d'essais récentes ont montré que ces méthodes permettaient d'effectuer et d'exploiter plus de cinq essais par vol, dans le cas de l'ALPHA-JET, avec environ 1,5 vols tous les deux jours ouvrables, et ceci moins de neuf mois seulement après le premier vol du premier prototype.

PHOTO N° 1 - VERSION ECOLE

PHOTO N° 2 - VERSION APPUI

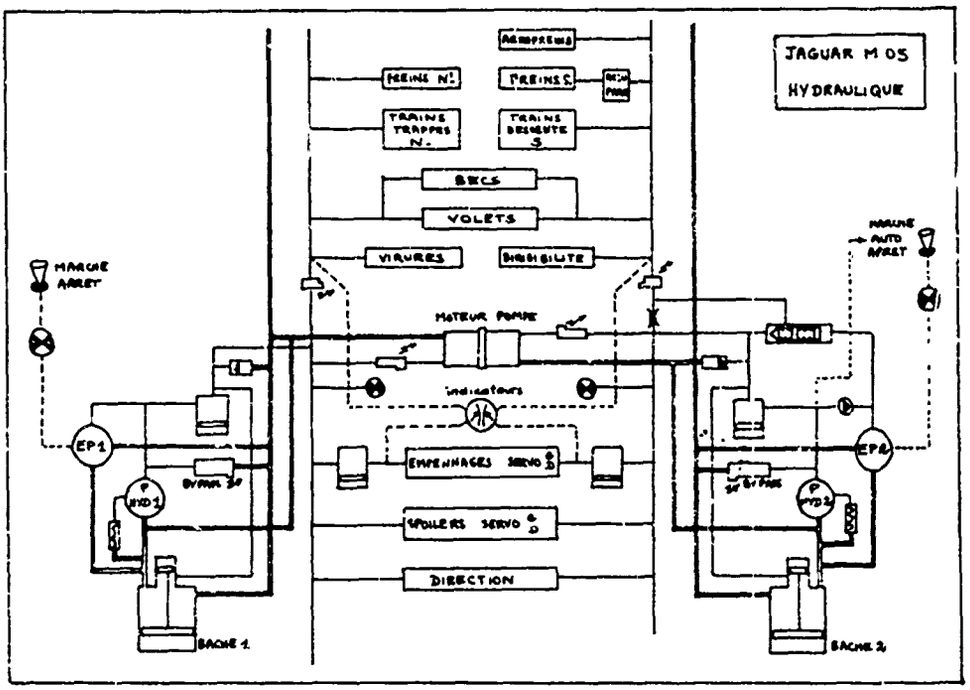
JAGUAR M 05
HYDRAULIQUE
FREINS N°1
FREINS N°2
TRAINS RENTRÉS N.
TRAINS DESCENTE S
BECS
VOLETS
VIRURES
DIRECTION
MARCHE ARRÊT
MARCHE AUTO ARRÊT
MOTEUR POMPE
indicateurs
EMPENNAGES SERVO G/D
SPOILERS SERVO G/D
DIRECTION
EP1
EP2
BACHE 1
BACHE 2

PI 1

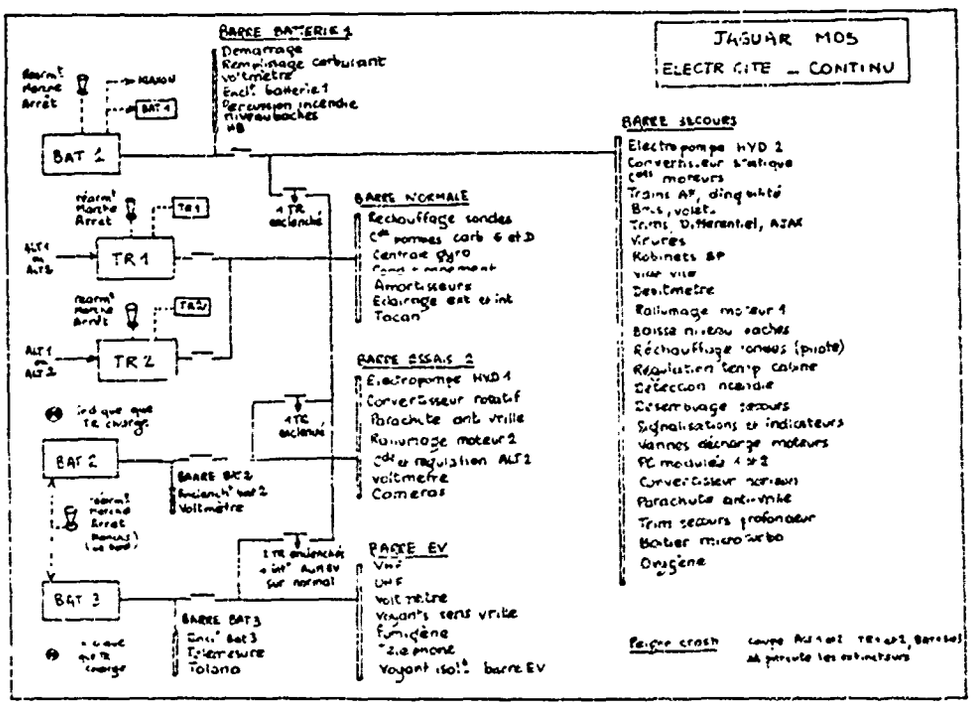
JAGUAR M05
ELECTRICITE — CONTINU
BARRE BATTERIE 1
Demarrage
Remplissage carburant
voltmetre
Encl° batterie 1
Recursion incendie
niveau baches
BAT 1
BAT 2
BAT 3
TR 1
TR 2
BARRE NORMALE
Reschauffage sondes
Cdes vannes carb G et D
Centrage gyro
Amortisseurs
Eclairage ext et int
Tacan
BARRE ESSAIS 2
Electropompe HYD 1
Convertisseur rotatif
Parachute anti vrille
Ramonage moteur 2
Cde et régulation ALT 2
voltmetre
Cameras
BARRE EV
Vmc
UHF
Voltmetre
Voyant sens vrille
fumigène
Voyant isol° barre EV
BARRE BAT 3
BARRE SECOURS
Electropompe HYD 2
Convertisseur statique
Trains AR, dinguité
Becs, volets
Trims, Differentiel, AZAK
Virures
Robinets BP
Densimetre
Rallumage moteur 1
Baisse niveau eaches
Réchauffage sondes (pitots)
Régulation temp cabine
Détection incendie
Déverrouage secours
Signalisations et indicateurs
Vannes décharge moteurs
PC modules 1 et 2
Convertisseur secours
Parachute anti-vrille
Trim secours profondeur
Boiter micro sur bo
Oxygène
Poignée crash

PI 2

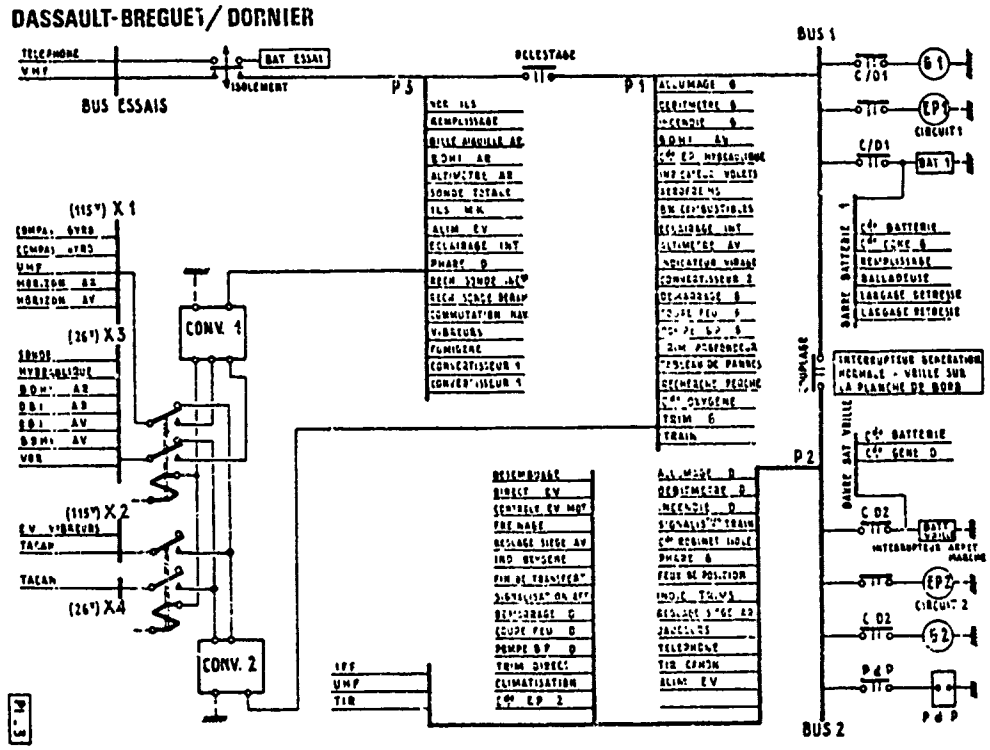
DASSAULT-BREGUET / DORNIER
BUS 1
BUS ESSAIS
BAT ESSAI
ISOLEMENT
DELESTAGE
P3
P1
P2
(115°) X 1
(26°) X 3
(115°) X 2
(26°) X 4
CONV. 1
CONV. 2
BUS 2

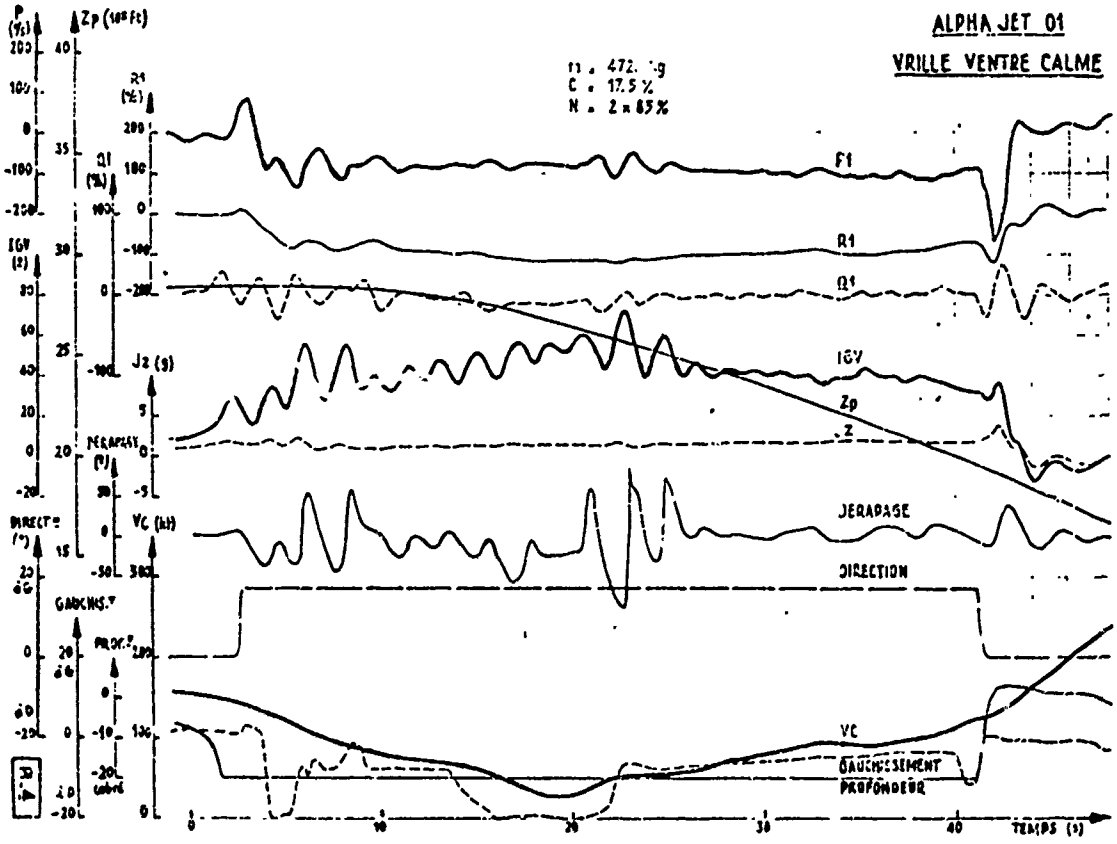
ALPHA JET 01
VRILLE VENTRE CALME
m = 472. kg
C = 17.5 %
N = 2 x 85 %
Zp (100 Ft)
F1
R1
Q1
IGV
Zp
Z
JERADAGE
DIRECTION
VC
BAUCHESSEMENT
PROFONDEUR
TEMPS (s)

F-14A STALL AND SPIN PREVENTION SYSTEM FLIGHT TESTS

Charles A. (Chuck) Sewell, Chief Test Pilot
Raymond D. Whipple, Project Engineer
Grumman Aerospace Corporation
Calverton, New York 11933

SUMMARY

Prior to commencing the traditional spin demonstration program for the F-14 Tomcat, the Grumman Aerospace Corporation obtained U. S. Navy approval to develop, evaluate and demonstrate a spin prevention system for the airplane. The philosophy underlying this decision is discussed.

The evaluation of various spin-prevention design concepts by analytical, simulation, and experimental methods is described

Preparation of the test vehicle is detailed showing unique emergency systems and qualification testing of these systems. Operational aspects of the flight test program including the problem of devising a system flexible enough to permit in-flight optimization of design parameters is treated.

The gradual shift in emphasis from spin-prevention, which was accomplished with relative ease, to departure amelioration for enhanced air combat effectiveness is documented. An overview of the final ARI with associated subsystems is given.

INTRODUCTION

Modern high-performance fighter airplanes are relatively short-coupled, densely packed and of high moments of inertia. This condition generally results in undesirable spin and spin recovery characteristics. An airplane that easily enters a spin compounds the problem while a spin-resistant airplane provides some compensating features. If appropriate recovery procedures are followed promptly after departure from controlled flight, while sufficient aerodynamic control effectiveness remains to counteract the buildup of rotational energy, the development of spins can usually be prevented. Unfortunately, the pilot is seldom able to initiate proper action quickly enough because the departure was very sudden, completely unexpected, violent and disorienting and, more than likely, the first he has ever experienced in that particular type of airplane. There is no tactical advantage to be gained from spinning. The solution then, might well be the use of a spin prevention system in modern tactical airplanes in order that the airplanes can be flown throughout the envelope without fear of encountering a spin.

When the Grumman Aerospace Corporation contracted with the United States Navy to build the F-14A fighter, the classical spin demonstration program was routinely included. The objectives of the spin program were to make every attempt to generate the fully-developed critical spin and demonstrate successful recovery from it.

SPIN TEST PHILOSOPHY

Up to that time the tactical airplanes used by the U.S. Navy and Marine Corps had all been evaluated under a basic Navy program of a Contractor Demonstration followed by a Customer Evaluation; and they had all suffered losses from inadvertent spins. During one seven year period, the U.S. Navy and Marine Corps averaged almost two airplanes per month lost to stalls/spins. There were ninety-six fatalities associated with these losses.

U.S. NAVY/MARINE CORPS AIRCRAFT LOSSES
DUE TO SPINS/DEPARTURES
(1965 - 1972)

TYPE	NUMBER LOST
A-4	20
A-5	3
A-6	11
A-7	15
F-4	44
F-8	34
F-9	23
T-2	17
T-28	2
	169

Five test airplanes were lost during spin programs or in preparation for conventional spin programs.

NAVY AND AIR FORCE
TEST AIRCRAFT LOST DURING SPIN TEST PROGRAMS

o F-4 (USN)	1961
o F-4 (USN)	1967
o F-4 (USAF)	1970
o EA-6B (USN)	1971
o F-111 (USAF)	1972

It was not unreasonable to conclude that this basic program warrented improvement.

This is not to deny that such a program generated accurate information about the spin characteristics of the airplane and established the degree of accuracy of the spin model testing; but, just as out-of-control accidents cannot be prevented by pilot's handbook warnings, neither can they be prevented by pilot's handbook spin descriptions and spin recovery procedures. It should also be noted that control requirements for spin recovery are often well determined long before flight testing. Spin tests "confirm" analytical and spin tunnel results

Spin testing was hazardous, expensive and time-consuming. The upcoming revision to the flight demonstration specification, MIL-D-8708B (Reference 1) contained a greatly expanded spin section. Regardless of whether or not the Contractor had achieved the fast, flat spin, he still must demonstrate no less than five entry techniques at five loading conditions. A complete range of center-of-gravity locations, spin direction and control positions would have to be tested in order that the "critical" demonstration conditions might be selected by the Customer.

This led us to seriously question the underlying philosophy of those Stall/Post-Stall/Spin Demonstration requirements. The airplane could usually exceed its maximum velocity envelope, but no demonstration beyond it was required. The airplane could exceed its maximum load factor envelope, but no demonstration beyond it was required. The airplane could exceed its design landing sink rate, but no demonstration beyond it was required

Why then should we expend vast amounts of time and money demonstrating what might be termed third order failure: the fully developed spin? (The first failure being stalling the airplane, the second aggravating it to the post-stall gyration stage.) Would the money not be better spent helping the pilot recover immediately upon departure from controlled flight, or better yet, preventing departures entirely?

The model tests and analyses and an emergency spin recovery system for the test airplane would still be required. But the spin would no longer be for the test airplane a goal to be attained, rather it would be the non-compliance result showing that the airplane needs a spin prevention system or that the spin prevention system needs improvement.

This would reduce spin losses, a goal which the classical spin program had clearly failed to achieve.

With this philosophy in mind, while proceeding with the standard preparations for spin testing and demonstration, Grumman undertook an intensive campaign to reorient the F-14 program toward spin prevention.

Supported by earlier spin studies conducted at Grumman (Reference 2 and 3) under Naval Air Systems Command (NASC) sponsorship, combined with an increasing quantity of encouraging F-14 wind tunnel data, and a high level of activity on spin prevention systems at the NASA Langley Research Center, in late 1970, NASC gave Grumman approval to develop, evaluate and demonstrate a spin prevention system in the F-14 airplane, with the understanding that the system must in no way compromise airplane tactical maneuvering capabilities, and particularly that there be no longitudinal restriction on the airplane.

In as much as we were faced with the virtually simultaneous tasks of technology development and prototype development under severe time constraints, all available assistance was solicited from research centers and facilities. A centrifuge simulation was undertaken by the Naval Air Development Center. At Langley, tests of a 1/10-scaled free-flight model were conducted in the 30 by 60-foot tunnel; the Differential Maneuvering Simulator (DMS) was programmed with F-14 data, and work on the radio-controlled drop model was greatly accelerated.

In support of the Grumman analytical investigation, additional high angle of attack wind tunnel data were generated at the Ames Research Center 12-foot pressure tunnel and the Langley 12-foot and Grumman 7 by 10-foot low speed tunnels.

PLANNING THE SPIN PREVENTION SYSTEM FLIGHT TESTS

Evaluation of a spin prevention system for a tactical airplane was without precedent. The spin prevention program replaced the classical spin demonstration program and no intentional spins were planned or required. The spin prevention test plan was developed around the following objectives:

Technology Development

- o Develop a system which will preclude spins.
- o Optimize this system such that its operation does not compromise air combat maneuvering capability, and especially that there be no longitudinal restriction on the airplane.

Prototype Development

- o Define the character of the post-stall motions of the airplane with and without the system operating.
- o Determine the optimum techniques for recovery from out-of-control situations for airplanes equipped with the system.
- o Determine critical control inputs, configurations, entry techniques, store loadings and departure direction.
- o Investigate engine operation during post-stall gyrations.
- o Provide necessary information on which to base Flight Manual instructions regarding recovery from out-of-control situations.

The flight test program was structured in three phases. The sequence of test and buildup maneuvers was based on data derived from model testing and analytical work, since no precedents existed. It was acknowledged before the flight test program started that test sequence and maneuvers would be subject to continual revision based on flight test results. To this end, frequent reviews were held, attended by representatives of NASA and the Naval Air Test Center as well as NASC and Grumman.

After preparatory flights to check out the various special test systems, including deployments of the spin recovery parachute at high and low dynamic pressures, Phase I of the Spin-Prevention Program would begin with two candidate systems.

The airplane stall characteristics with and without spin prevention systems were to be explored from conventional entries and in accordance with MIL-D-8708A (WEP), (Reference 4) as amended by a contract addendum (Reference 5). The effects of store loadings, center-of-gravity locations and wing sweep in automatic and at several predetermined fixed wing sweeps would be investigated. Critical maneuvers were to be determined and noted for the formal demonstration.

Phase II consisted of assessment of post-stall gyrations with the system operating, starting with a mid center-of-gravity location and no external stores, and evaluating progressively longer applications of full control deflections, including full pro-spin controls at varied input rates, to a maximum of fifteen seconds. Vertical, inertia-coupled and tactical entry investigations were expected to determine any critical conditions Successful completion of Phase II would establish the viability of the spin prevention system and define the system parameters and thresholds necessary for the F-14A airplane.

In Phase III, selected maneuvers determined to be most critical were selected to substantiate spin prevention system operation at extremes of store loading and center-of-gravity locations. Entries with asymmetric store loadings and asymmetric thrust were planned, as were tests of stability augmentation system effects and trim setting effects Full pro-spin controls held for a minimum of fifteen seconds would be the standard. The results of Phase III tests would determine the critical conditions for the formal demonstration.

TEST AIRPLANE CONFIGURATION

The test airplane, number 2 F-14A was initially used for subsonic stability and control testing For the high angle of attack program all the modifications originally planned for the spin demonstration were incorporated, including:

- o A mortar-deployed 26-foot diameter ring-slot spin recovery parachute on a 102-foot towline Parachute size and towline length were determined in the NASA Langley vertical spin tunnel. The parachute was not locked to the aircraft until after takeoff and was unlocked prior to landing A mechanical jettison device was used and a back-up pyrotechnic jettison provided. Cockpit indications of mechanical and electrical integrity of the system were employed.
- o In order to preclude external structural modifications to the test airplane to sustain loads from a larger parachute, the selected parachute was supplemented by a pair of retractable nose-mounted canard-like devices recommended by NASA. These surfaces were 22-inches wide by 80-inches long and were operated by cockpit control. A back-up deployment system was provided using an air bottle.
- o Lateral stick positioner - an automatic recovery system described under spin prevention systems.
- o A single-crew cockpit configuration permitting operation of all necessary functions from the pilot's station, to avoid unnecessary exposure of a second aircrewman to hazardous conditions.
- o Escape system changes to permit pilot ejection through the canopy (normal ejection from the F-14 is preceded by canopy jettison).
- o A mechanical restraint which limits forward motion of the pilot's head under high "eye-balls out" longitudinal acceleration.
- o Tailored ejection-seat leg restraints to compensate for possible high longitudinal acceleration.
- o An Emergency Power Unit powered by mono-methyl-hydrazine to provide hydraulic power and, through the auxiliary generator, electrical power for 3.5 minutes in case of a double engine flame-out.
- o Additional Cockpit Instrumentation located for immediate pilot reference - yaw rate indicator, calibrated sideslip gauge, g-meter, and expanded range nose-boom angle of attack indicator.

- o Cockpit manual control of the engine Mid-Compression Bypass, 12th stage bleed and Mach-lever shift.
- o Hot mike permitting continuous transmission of pilot voice without the necessity of keying a microphone.
- o Forward-Looking 16 mm color movie camera with the upper instrument panel and windscreen in the field of view.
- o Videotape camera with sound recording.
- o Telemetry - 190 PCM parameters and any one of four analog tracks with 8 parameters per track were telemetered to the ground and recorded. Real-time displays were selected from these and more than 80 critical measurements were continuously limit checked by the computer.
- o Cockpit lights which comprised a visual check-off list prior to maneuver. The functions presented were:

  Parachute in position
  Parachute locked to aircraft
  Mortar armed
  EPU armed
  Instrumentation on
  Cameras on

- o Special advisory lights to indicate the status of unique test systems, such as EPU oil temperature, EPU activated indication, spin chute deployed and jettisoned lights.

FLIGHT TEST SUPPORT

CHASE

All flights were chased by an A-6A airplane flown by a limited number of pilots identified with the program in order to have an effective and safe chase and to insure program continuity. Chase pilots were active participants in briefs and debriefs. A photographer flew in the right seat of the chase A-6A airplane. A hot mike telemetry receiver was installed in the chase airplane to permit the chase flight crew to monitor telemetry voice. This provided the chase flight crew with a continuous flow of information and made it unnecessary for the test pilot to key the UHF to transmit to the chase pilot. This was especially valuable during unexpected situations and emergencies.

GROUND STATION

The flight tests were controlled by an engineering team that was headed up by the Test Conductor and included an aerodynamic engineer, flight test engineer, propulsion engineer, instrumentation engineer and computer systems engineer. Other specialist engineering personnel were included when required for specific tests and conditions. The following displays were available in the flight test control room:

- o Real-time data displays on a CRT
- o Real-time computer monitoring of more than 80 selected parameters for pre-set limits
- o Three strip-chart recorders presenting twenty-four parameters.

All personnel in the control room were linked via hot-mike intercom and each person had the capability to talk directly to the test airplane in an emergency situation. However, the Test Conductor normally provided the voice link with the test airplane.

FLIGHT TESTS

STALL TESTS

Stall tests were conducted with and without the spin prevention systems. In all Cruise and Combat configurations the F-14A does not exhibit any characteristic which a pilot would call a "stall" - no g-break, no wing-rock, no nose-slice, no minimum control airspeed. The flow over the wing certainly separates at some nominal "stall" angle of attack, but the airplane remains controllable.

The stall warning problem therefore became interesting. If there is no stall what do we warn against? Is a warning needed? The F-14 experiences the normal buffet buildup as the wings undergo separation, but then, as higher angles of attack are reached the buffet intensity falls off.

Since warning implies a hazardous condition, perhaps what we really want is some form of angle of attack information. Hopefully, this could assist the pilot in maintaining optimum maneuvering angles of attack. The exact nature of these requirements has yet to be determined. Recovery from all the high angle of attack conditions is easily effected in less than 5,000 feet by releasing aft stick force.

In the high-lift Power Approach configuration, extended speed brakes improve directional stability at high angles of attack. With speed brakes extended, the normal landing configuration, the airplane has been flown at full longitudinal stick deflection, about 40 degrees angle of attack. This means the pilot can exceed the approach angle of attack by almost 30 degrees without experiencing a departure. At this condition, he would have long since lost sight of his landing area --- but he can still get there without encountering disaster. Again, the airplane does not exhibit any characteristic which the pilot would call a stall. In Takeoff and Waveoff configurations some lateral directional divergent oscillations occur at about 27 - 28 degrees angle of attack, more than double the approach angle of attack. This situation does define a stall in that a minimum control airspeed is attained. Recovery is immediate with release of aft stick force.

These oscillations are potentially hazardous and so, although an enormous safety margin existed, an artificial stall warning device was recommended. A rudder pedal shaker was installed and evaluated by several carrier-qualified pilots. The consensus quickly grew to use the device as a warning of exceeding the approach angle of attack rather than of nearing the area of weakened stability.

SPIN RESISTANCE TESTS

The F-14A test airplane was evaluated for basic airframe spin resistance, and it was determined to be much more spin resistant than tunnel and model tests had shown. The airplane was flown, without a spin prevention system, with all air-to-air external loadings, from forward to aft center-of-gravity extremes and at all wing sweeps, to +90 and -50 degrees indicated angles of attack, and to full longitudinal stick deflections in level, banked and inverted flight. With full longitudinal stick deflections (resulting in trim angles of attack of +43 degrees erect, -30 degrees inverted) the airplane is controllable about all three axes. Full lateral stick deflection was held for more than twelve seconds at greater than 40 degrees angle of attack. Full rudder deflection rolls were completed through more than 360 degrees of bank at angles of attack greater than 35 degrees. Full aft stick and full rudder were held simultaneously for more than one minute. Pitch and angle of attack rates greater than 60 degrees per second erect and 30 degrees per second inverted were obtained. The airplane was repeatedly held in a vertical attitude until it slid backwards and pitched nose down making an excellent recovery "hands off".

The airplane did encounter departures from controlled flight. The departures took the form of slow to rapid rolls opposite to commanded roll. Recovery was easily effected by neutralizing lateral stick deflection. A more rapid recovery was effected by using lateral stick in the direction of departure roll.

Air Combat Maneuvering was conducted against several types of airplanes as a part of the basic spin resistance tests, with no restrictions imposed on the F-14A and no serious departures were encountered. But, even though the F-14A apparently possessed a high degree of spin resistance it was realized that there was probably some combination of control deflections that could cause a spin. For this reason it was considered prudent to continue to develop and to evaluate a spin prevention system. Our goal was to provide the U.S. Navy with the world's finest fighter airplane with absolutely no angle of attack restrictions, and to essentially guarantee no departures from controlled flight, or at the very least, no spins.

EVALUATION OF THREE SPIN PREVENTION SYSTEMS

From the earliest analyses, it was realized that the adverse yaw generated by the large differential horizontal tail surfaces at high angle of attack was the major source of pro-spin yawing moments. If necessary, this could also provide powerful recovery moments.

Since the spin-prevention system had not been part of the original design effort, several unique problems were faced by the engineering staff. Most significant was the severe time constraint - extensive analytical studies of various systems were not possible - system gains would have to be optimized in flight tests.

In addition, the device would have to be tailored to work in an already-existing control system with an absolute minimum number of modifications.

To meet these requirements, the candidate systems were equipped with a variable gain calibrator (VGC) for each relevant variable. The pilot could change any gain from the cockpit.

LATERAL STICK POSITIONER (LSP)

At first, it was thought advisable to delay the engagement of the spin-prevention system to as high an angle of attack as possible. This was expected to permit fairly severe departures, so use was made of the strong yawing moment from differential stabilizer as a recovery mechanism.

A Lateral Stick Positioner was installed in the test airplane. Above a threshold angle of attack this system automatically moved the control stick to full lateral deflection when a pre-set yaw rate was encountered and released the stick back to neutral as the yaw rate decreased through another pre-set value.

This system concept was evaluated in the NASA Langley Differential Maneuvering Simulator (DMS). Although the LSP performed its spin-prevention function admirably, it was becoming apparent by observing Fleet usage of the airplane that the F-14 would be used to the limits of its unprecedented high angle of attack capability, and the LSP did permit departures.

ADVANTAGES

- Recovers airplane from departures
- Prevents spins.

DISADVANTAGES

- Departures from controlled flight are not prevented
- Tactical advantage lost through a departure
- The high yaw rates encountered before recovery could possibly result in engine compressor stalls.

This system was discarded as a candidate for incorporation in production airplanes but left in the test airplane to serve its purpose as a spin prevention system.

LATERAL STICK CENTERER (LSC)

The DMS evaluation of the LSP had demonstrated that minimizing lateral control inputs greatly diminished departures. A logical conclusion was to limit lateral inputs above a selected angle of attack. The DMS was programmed to evaluate this concept which we called a LATERAL STICK CENTERER (LSC). It showed tremendous potential.

This system was installed in the test airplane and included deactivation of roll stability augmentation as well as physical centering of the control stick. It could be over-ridden with 25 pounds of lateral stick force. An extensive flight evaluation of this system was completed with all external loadings and center-of-gravity positions and at all wing sweeps in Cruise configuration. It was determined that:

ADVANTAGES

- Recovers airplane from departures
- Prevents spins
- Minimizes frequency and severity of departures
- The airplane could be flown safely to full aft stick deflection at all wing sweeps.
- Roll control through rudder deflection was excellent
- Recovery from high angle of attack was immediate upon release of aft stick force
- Recovery was completed from the worst condition with less than 5,000 feet of altitude loss.

DISADVANTAGE

- Engagement transients under some conditions degraded tactical maneuvering at high angles of attack.

The LATERAL STICK CENTERING system was discarded due to the degradation of high angle of attack maneuvering..

AILERON-RUDDER INTERCONNECT (ARI)

One of the spin-prevention concepts being investigated at Langley was the Aileron-Rudder Interconnect (ARI). This mechanization phased out lateral control surface deflection commanded by lateral stick inputs with increasing angle of attack and simultaneously phased in coordinating rudder. The ARI was programmed for the F-14 on the DMS and the results were extremely encouraging.

The ARI was installed in the test airplane. For maximum flexibility, the test system was designed with independent lateral control (LARI) and rudder (RARI) components. VGC switches permitted variation of:

- RARI angle of attack threshold
- RARI angle of attack interval to full gain
- Lateral stick to rudder ratio
- LARI angle of attack threshold
- LARI angle of attack interval to full gain
- Lateral stick to negative differential tail deflection ratio.

Flight tests quickly determined that the rudder coordination feature of the ARI was beneficial at much lower angles of attack than required for spin/departure prevention. Roll rates were significantly increased by a generous use of rudder.

The spin prevention efficacy of the system was well established. Further work proceeded to refine operation in the air combat maneuvering (ACM) environment, particularly the high subsonic regime.

A rather extreme test technique was developed which seemed to be the "worst case" and served as our standard. It consisted of a rolling dive to maintain target Mach number with maximum practical lateral control held in while an abrupt aft stick displacement was made.

These evaluations revealed the necessity of scheduling the LARI as a function of Mach number. From 0.55 M to 1.0 M the angle of attack threshold decreased linearly.

This system was found to have the following favorable characteristics during evaluations in both the NASA Langley DMS and the F-14A airplane:

- No engagement or disengagement transients
- Airplane is flown the same at high angles of attack as at low angles of attack

- o Systems are easily checked for proper operation before flight and can be checked in flight by observing the rudder indicator as lateral stick is applied above the threshold angle of attack
- o Roll control and rate of roll were improved over the Lateral Stick Centering System at high angles of attack by having some differential horizontal tail available
- o Departures from controlled flight were minimized
- o No spins occurred. Full pro-spin controls were held for as long as 48 seconds.
- o Reliability was excellent
- o Tactical maneuvering was not compromised.

NOSE PROBE ANGLE OF ATTACK SENSOR

One more refinement remained to make the ARI a viable system. The angle of attack vane on the F-14 was of the standard type, located on the side of the forward fuselage. It provided accurate angle of attack information for conventional flight tasks, but proved inadequate for the vast range of extreme airflow angles made possible by the F-14's combat agility.

A nose-mounted differential pressure sensing probe with an expanded range capability was evaluated and proved itself able to meet the stringent demands of the F-14 ACM prowess.

The ARI and this sensor comprise the highly-successful spin/departure prevention system currently installed in the F-14 Tomcat.

CONCLUSION

The first F-14A Tomcat production airplane equipped with the spin prevention system, number 185, is scheduled for acceptance by the U.S. Navy in December 1975.

Despite the enormous obstacles of simultaneous technology development and prototype development tasks under severe time constraints on a configuration already being manufactured, with no precedents or guidance, success was achieved. After a 71 flight high angle of attack flight test program spanning one and one-half years, encompassing over 1200 maneuvers beyond the nominal stall angle of attack, the Grumman Aerospace Corporation is confident that the goal has been accomplished. We are delivering the first Navy fighter with an unrestricted angle of attack capability.

This pioneering effort would not have been possible without the dedicated efforts of hundreds of people - the Grumman Pilots, Engineers and Technicians; the Naval Air Systems Command personnel, both civilian and military; the Honeywell Corporation and other sub-contractors; and NASA personnel with their essential test facilities.

We all hope that the point has been clearly demonstrated that spin prevention is an attainable goal, and it is feasible and economical.

Future spin-prevention programs can build on our early efforts and possibly improve on our methods. Commitment to spin prevention technology development will ensure safer and less costly flight test evaluations and demonstrations. Perhaps increased combat capability is difficult to value quantitatively, but the anticipated savings from reduced airplane and air crew losses should provide striking vindication of the spin prevention approach.

Let us relegate the spin to the devotees of air show aerobatics, no longer to be a sinister bugbear of military aviation.

REFERENCES

1. MIL-D-8708B (AS), Military Specification Demonstration Requirements for Airplanes, dated 31 January 1969.
2. Bihrle, W. and Heyman, A., "The Spin Behavior of Aircraft", GAEC Report No. 394-68-1, December 1967.
3. Bihrle, W., "The Influence of Static and Dynamic Aerodynamic Characteristics on the Spinning Motion of Aircraft", Journal of Aircraft Vol. 8, No. 10, October 1971.
4. MIL-D-8708A (WEP), Military Specification Demonstration Requirements for Airplanes, dated 13 September 1960.
5. Addendum 64A to MIL-D-8708A (WEP), Demonstration Requirements for Model F-14A Airplane, dated 9 September 1970.

ESSAIS DE VRILLES
DU JAGUAR, DU MIRAGE F1 ET DE L'ALPHA-JET

par
Messieurs J. DIFFER, JP. DUVAL, J. PLESSY
Ingénieurs
AVIONS MARCEL DASSAULT - BREGUET AVIATION
ESSAIS EN VOL
B.P. 28
I S T R E S
13 800
France

RESUME

Trois campagnes d'essais de vrilles ont été entreprises récemment par les AVIONS MARCEL DASSAULT - BREGUET AVIATION : JAGUAR, MIRAGE F1 et ALPHA-JET. En fonction des buts fixés au départ et des résultats obtenus, chacune de ces campagnes présente un caractère original propre, l'ALPHA-JET en particulier se distinguant nettement des deux autres avions par sa mission "ECOLE".

Ce papier expose les résultats obtenus au cours de ces campagnes, et les compare avec les prévisions de la soufflerie.

ESSAIS DE VRILLES DU JAGUAR MONOPLACE

HISTORIQUE

Les essais de vrilles du JAGUAR M 05 (monoplace) en configuration lisse ont comporté 139 essais en 34 vols : 8 essais de décrochage en palier, 31 essais pour étude de l'efficacité des gouvernes transversales et 100 essais de déclenchés et vrilles. La progression des essais a été la suivante : recherche des différentes formes de vrilles possibles et définition d'une consigne de sortie, décrochages en palier, déclenchés et consigne de sortie, avec ensuite l'influence des erreurs de consigne, et des essais à différents régimes moteurs. Les départs ont d'abord eu lieu entre 40 000 et 42 000 ft de 150 à 300 kt, puis à 35 000 ft de 150 à 340 kt. Quelques essais pour les moteurs ont été effectués à 30 000 ft.

RESULTATS

Le JAGUAR a un très bon comportement aux incidences élevées, s'améliorant encore avec la coordination des gouvernes.

Déclenchés et vrilles

Les déclenchés et vrilles du JAGUAR se caractérisent par de fortes agitations à caractère périodique en transversal mais aussi et surtout en longitudinal. Ces agitations peuvent être éprouvantes pour le pilote. L'incidence varie entre 50 et 90°, la rotation de lacet est modulée et celle de roulis alternée. Les premiers tours se font autour d'un axe sensiblement horizontal, si bien que l'assiette passe quelquefois de 90° nez bas à 90° nez haut en deux secondes. Dans ces mouvements, la vitesse indiquée oscille en fonction de l'incidence, et progressivement l'axe de la vrille devient plus piqué, indiquant une évolution favorable, jusqu'à la sortie, qui se produit entre 160 et 180 kt.

Les indications de la sortie proche sont : les maxima de vitesse indiquée qui augmentent, les minima d'incidence qui diminuent, l'assiette longitudinale qui decroît.

Il n'y a jamais eu de vrille plate et rapide. Quelques départs ont eu lieu avec une vitesse de lacet régulière, mais dès que l'incidence atteint 70°, les oscillations de dérapage, roulis, lacet sont apparues.

La vrille dos n'a pas été rencontrée; seuls quelques passages dos ont été observés, mais ils n'ont pas duré plus de trois secondes, et sont dûs à une position de profondeur à fond à piquer. Cette position de gouvernes a provoqué quelques sorties en tonneaux lents, mais l'expérience et les calculs montrent que l'avion n'est pas sujet aux auto-tonneaux rapides.

Influence des gouvernes

La profondeur est de loin la gouverne la plus efficace, et si la plupart des lancements ont été réalisés en croisant les gouvernes transversales, quelques vrilles ont été lancées en amenant la profondeur à cabrer un bref instant. La profondeur à fond à piquer donne des agitations plus importantes au cours du déclenché, et une tendance au passage dos, avec des mouvements de roulis à la sortie. La profondeur à cabrer est néfaste dans tous les cas : elle provoque le déclenché, et, bien qu'elle diminue l'amplitude des agitations, freine la sortie.

Le gauchissement et la direction ont peu d'influence en cours de vrille: cela tient vraisemblablement au fait que la vitesse de roulis est alternée et celle de lacet modulée au départ, puis alternée à la sortie. Toutes ces considérations ont conduit à recommander la consigne "gouvernes au neutre" à la sortie, ou même "tout lâcher", étant entendu qu'il n'y a pas d'influence du trim de profondeur dans la plage maximale utilisable en vol.

Décrochages en palier

Des décrochages en palier ont été effectués dans les configurations suivantes: lisse, becs combat, volets 20° + becs, volets 20° sans becs, pleins volets + becs et pleins volets + becs, train sorti.

En toutes configurations on a pu atteindre 30° d'incidence pilote, avec un bon contrôle longitudinal et quelques mouvements de roulis-lacet alternés. Au-delà, l'avion part en roulis-lacet mais le rendu de main est très efficace même si l'incidence est montée à 60°.

Essais en cloche

Il n'y a pas de problèmes particuliers, la VC tombe à 0, l'avion commence à redescendre "la queue la première" puis bascule sur le côté sans déclencher et le contrôle peut être immédiatement repris.

Comportement des moteurs

Les premiers essais ont été effectués un moteur coupé et le deuxième au ralenti; ensuite on a systématiquement gardé un moteur à un régime égal ou supérieur au PG sec. Pour les derniers essais, les deux moteurs furent gardés soit au PG sec, soit en PC mini, soit en PC max.

Sur les réacteurs mis au ralenti avant essai, il se produit en général un décrochage tournant avec pour seuls signes une faible augmentation de TGT et une très légère chute de régime; sur mise des gaz, on note des TGT trop élevées imposant la coupure du moteur. Sur les moteurs à des régimes $\geq$ PG sec, il se produit des décrochages avec ou sans bruit : après une brève augmentation, TGT et régime chutent et lorsque le régime passe en-dessous du ralenti, on observe une montée très rapide de TGT qui impose la coupure du moteur.

Comparaison des résultats essais en vol - soufflerie

La presque totalité des vrilles obtenues en vraie grandeur, et quelles que soient les positions des gouvernes, sont à classer dans le groupe appelé par la soufflerie "vrille peu rapide, calme ou peu agitée". Le recoupement entre les mouvements de l'avion et ceux de la maquette est excellent et la consigne des Essais en Vol correspond à la recommendation de la soufflerie de mettre toutes les gouvernes au neutre en cas de vrille agitée.

Quelques rares vrilles obtenues en vol peuvent être classées dans les vrilles à agitations divergentes et, tout comme en soufflerie, ces vrilles se sont produites avec la profondeur à piquer et direction "pour".

En vol, il n'a jamais été obtenu de vrille plate et rapide même en appliquant les positions de gouvernes trouvées favorables par la soufflerie. La vrille dos n'a jamais pu être stabilisée non plus.

Il est difficile de comparer l'influence des gouvernes entre la soufflerie et les essais en vol étant donné qu'en vol seules les vrilles agitées ont été obtenues. Toutefois, il a été constaté que la profondeur à cabrer ralentissait la vrille ce qui a été trouvé en soufflerie pour la vrille plate et rapide.

ESSAIS DE VRILLES DU MIRAGE F1

HISTORIQUE

Les essais de vrilles du MIRAGE F1 ont été faits, en ce qui concerne la configuration "sans charges extérieures" en 1973, au cours d'une tranche d'essais de 27 vols A.M.D. - B.A. plus 10 vols C.E.V. Au total, 153 essais ont été effectués.

Nous nous proposons de résumer, ici, les premiers essais concernant la configuration "sans charges extérieures".

- Préparation
- Déroulement des essais
- Résultats
- Comparaison Essais en Vol/Soufflerie.

PREPARATION

Essais en soufflerie verticale

L'étude de la vrille du MIRAGE F1 a été faite à la soufflerie verticale de l'IMFL avec une maquette au 1/20ème. Ces essais ont montré que le F1 n'avait pas ten-

dance à vriller "à plat", et, même, qu'une vrille ventre lancée calme ne pouvait pas se maintenir au-delà de 5 tours. Seule, la vrille dos est apparue calme (mais non rapide). Les essais de soufflerie ont permis de préciser l'influence des gouvernes et d'établir une prédiction des mouvements de l'avion au cours de la récupération.

- Sortie de vrille classique.
- Passage dos avec possibilité de vrille dos.
- Auto-tonneaux.
- Mouvements désordonnés (agitation).

Au cours de cette étude qui comporte 1 200 lancers, quelques sorties de vrille ont été interrompues par un re-départ vers les grandes incidences. Ces observations ont motivé des recherches approfondies pour expliquer l'origine de ces évolutions. Ainsi, l'effilement de la pointe de nez est apparu comme très influent sur le comportement transversal de l'avion à grande incidence. Il s'agit de moments de lacet très importants vers 30 ou 40° d'incidence, même à dérapage nul.

A partir de ces constatations, l'étude a été poursuivie pour assurer la reprise de contrôle dans ces cas particuliers, bien qu'ils aient été rarement observés. L'étude a abouti sur la mise en place de surfaces bien définies en forme et position sur les côtés de la pointe avant. Dans cette configuration, le phénomène de re-départ en vrille a été éliminé (symétrisation de l'écoulement autour de la pointe avant).

Préparation de l'avion

Fabrication d'une pointe avant spéciale

Pour tenir compte des expériences faites en soufflerie, une pointe avant a été fabriquée spécialement pour y inclure un dispositif de portes manoeuvrables en vrille. Lorsque ces portes sont fermées, le nez de l'avion est conforme à celui des avions de série.

Installation de sécurité et installation d'essais

Ces installations sont décrites dans l'article: "Méthodes d'essais de vrilles en vol".

DEROULEMENT DES ESSAIS

Les essais ont été faits dans un domaine compris entre 30 000 et 50 000 ft, IAS de 150 à 350 kt. Il y a autant d'essais de perte de contrôle que d'essais de lancement de vrille (environ 70 de chaque), plus quelques essais divers (figure en "cloche", décrochages en palier basse vitesse, inversions rapides).

RESULTATS

Le MIRAGE F1 a des limites de manoeuvre très saines; quand on amène la profondeur en butée cabrée, on peut atteindre des incidences très élevées.

En gardant la profondeur au plein braquage cabré et en laissant les gouvernes transversales au neutre, l'avion peut partir en rotation ou hésiter d'un bord sur l'autre. Si l'on utilise le gauchissement, le départ en lacet/roulis se produit plus franchement et de sens contraire à celui où le manche est mis.

Si on a laissé partir l'avion en déclenché, la consigne est : commandes au neutre. Si elles sont recentrées immédiatement après le déclenché, la rotation s'arrête en 1 ou 2 tours. Le nez de l'avion baisse et le mouvement se termine avec une assiette longitudinale comprise entre 30 et 90° piquée. La perte d'altitude est de 10 000 ft environ, ressource comprise.

La récupération s'effectue bien souvent en une sorte de tonneau, nez bas, avec une augmentation sensible de la vitesse de roulis. En effet, au cours du déclenché, la rotation s'effectue autour d'un axe où l'inertie est importante, par combinaison lacet-roulis-tangage (grande incidence et dérapage). Dans la phase finale de récupération, la rotation se termine autour de l'axe de roulis sur lequel l'inertie est minimale : l'énergie acquise en rotation provoque un accroissement de la vitesse de roulis pur, avant de s'amortir en plusieurs secondes.

Nous n'avons pas pu lancer de vrille ventre stabilisée. Généralement, à partir du 2ème tour, les agitations apparaissent, l'assiette longitudinale devient de plus en plus piquée et le pilote n'a plus qu'à recentrer les commandes pour reprendre le vol normal.

Nous avons observé, plusieurs fois, des transformations de vrille ventre en vrille dos. Elles peuvent s'accélérer et être maintenues si le pilote laisse la direction braquée dans le sens du lacet, ou même direction au neutre. La sortie exige un "contre" à la direction à fond pendant 6 ou 7 secondes, ce qui peut paraître long au pilote. C'est le seul cas de vrille sur F1 qui demande une action positive de la part du pilote pour obtenir la sortie.

Dans tous les autres cas, les récupérations ont été obtenues gouvernes recentrées aux trims de vol et, de ce fait, nous n'avons pas eu à utiliser le système des portes de pointe avant.

COMPARAISON ESSAIS EN VOL/SOUFFLERIE

Dans l'ensemble, les résultats trouvés en essais en vol cadrent bien avec les prévisions faites à l'IMFL.

Les points sur lesquels les recoupements sont excellents se résument ainsi :

- Caractère aléatoire des mouvements à partir de conditions initiales identiques.
- Mouvements agités plus ou moins descriptibles.
- Vrille ventre qui ne se maintient pas, même avec des positions de gouvernes considérées comme favorables au mouvement.
- Vrille dos faiblement agitée et pouvant être maintenue direction "avec" le lacet. Efficacité de la manoeuvre de sortie en mettant la direction "contre" le lacet.
- Influence du centrage non visible.
- Il faut que le facteur de charge dépasse 1 pour qu'il y ait mouvement assimilable à une vrille.
- Il faut que l'incidence soit très élevée pour que l'on puisse lancer une vrille. Ceci est à rapprocher des mesures de moment de lacet faites à l'IMFL : ce moment apparaît pour des incidences comprises entre 30 et 50°.
- Le braquage du gauchissement crée de l'agitation.

Les points montrant quelques différences sont rares :

- Nous n'avons pas observé de mauvaises sorties de vrille telles qu'il en a été vues, parfois, en soufflerie (de ce fait nous n'avons pas eu à utiliser les portes de pointe avant). Cependant, il faut rappeler que nous avons effectué 66 lancements de vrille en essais en vol contre 1 200 en soufflerie. Une fois, nous avons observé des remontées de nez sur l'horizon mais elles ont été forcées profondeur plein arrière et gauchissement à fond contre le lacet.

- Pour l'effet de la profondeur, nous avons eu souvent des mouvements rapides en roulis pur dès que cette gouverne a été mise au plein piqué. En soufflerie, les phénomènes observés étaient plutôt du genre "désordonnés".

ESSAIS DE VRILLES DE L'ALPHA-JET

HISTORIQUE

Un historique des essais de vrilles de l'ALPHA-JET est donné dans l'article "Méthodes d'essais de vrilles en vol".

RESULTATS : LES DIFFERENTES FORMES DE VRILLES DE L'ALPHA-JET

Les résultats exposés ci-dessous sont valables pour les deux versions de l'ALPHA-JET : version ECOLE équipée d'un nez rond avec des virures, et version APPUI équipée d'un nez pointu et d'une perche.

La seule différence importante est que la première forme de vrille (vrille calme) est plus difficile à obtenir avec le nez pointu de la version APPUI. En revanche, la vrille "agitée" est la forme la plus courante.

Vrille ventre calme ou peu agitée

Cette forme de vrille est obtenue profondeur à fond à cabrer, direction à fond dans le sens de rotation désirée. Le départ en roulis - lacet doit être contré à fond au gauchissement pendant 1 à 2 secondes, puis le gauchissement stabilisé entre 30 et 50 % contre la direction.

Elle doit être lancée entre 130 et 170 kt, 20 000 et 30 000 ft, en virage, moteurs à 85 %. Le point classique est : 25 000 ft, 150 kt. Cette vrille s'obtient plus facilement à gauche qu'à droite, un tour dure environ 3 secondes, la perte d'altitude par tour est de l'ordre de 900 ft, et la sortie a lieu, commandes lâchées, en moins de deux tours.

Vrille ventre agitée

Cette forme de vrille est obtenue profondeur à fond à cabrer, gouvernes transversales croisées à fond. On peut la lancer en virage, entre 130 et 170 kt, 25 000 à 35 000 ft, moteurs à 85 %.

Le roulis change brièvement de signe toutes les deux secondes, l'assiette longitudinale est très oscillée, le lacet garde un sens bien net.

Un tour dure entre 3 et 3,5 secondes, la perte d'altitude par tour est de 900 ft. Cette vrille agitée peut passer tos par inversion du roulis. On obtient alors des auto-tonneaux. La sortie se fait dans tous les cas en recentrant les gouvernes. Elle se fait en deux tours environ.

Auto-tonneaux

Il y a essentiellement deux types d'auto-tonneaux :

a/ Les auto-tonneaux obtenus en gardant les commandes transversales croisées après un passage dos en vrille agitée. La sortie se fait en recentrant les commandes, elle est très rapide car la vitesse est alors de l'ordre de 150 kt.

b/ Le deuxième type d'auto-tonneau est obtenu en amenant la profondeur à piquer et les gouvernes transversales au neutre pendant un auto-tonneau du premier type. La sortie se fait, là aussi, en recentrant les commandes.

Vrille dos

Il est possible de démontrer la vrille dos sur ALPHA-JET. En partant d'une vrille agitée, il faut amener, au moment du passage dos, la profondeur à fond à piquer et le gauchissement de 0 à 20 % contre la direction. Les meilleures conditions de lancement sont à 35 000 ft entre 150 et 170 kt. La sortie commandes recentrées, se fait en moins de 7 secondes (soit 2,5 tours, au maximum).

Vrille calme et rapide

Cette forme de vrille se distingue de la vrille calme normale par son incidence plus élevée, et la vitesse de rotation plus rapide. C'est la seule forme de vrille de l'ALPHA-JET pour laquelle il est demandé au pilote d'appliquer le gauchissement "pour" à la sortie. Cette manoeuvre assure alors la sortie en moins de 10 secondes, résultat obtenu simplement en recentrant les gouvernes dans tous les autres cas.

On peut obtenir la vrille calme et rapide en amenant la profondeur à fond à piquer et progressivement le gauchissement à fond contre la rotation au cours d'une vrille calme. Toutefois, dans la plupart des cas, cette manoeuvre amène des agitations, en particulier sur l'avion ECOLE, équipé de virures sur le nez.

Régimes décrochés sans rotation définie

Lorsqu'au déclenché la rotation n'est pas suffisante, ce qui arrive en particulier lorsqu'il n'y a pas assez de gauchissement, l'avion part en roulis - lacet alterné à une incidence voisins de 30°. Profondeur à cabrer, direction au neutre et gauchissement à fond, on obtient également un régime décroché sans rotation définie, caractérisé par des grandes variations d'incidence et des oscillations de roulis. Dans les 2 cas, la reprise de contrôle est immédiate au recentrage des gouvernes.

Déclenchés

Des déclenchés ont été effectués jusqu'à 270 kt de 20 000 à 40 000 ft; on n'a pas cherché à stabiliser de vrilles à partir de ces essais, réalisés dans le but essentiel de couvrir les déclenchés involontaires. En amenant la profondeur à fond à cabrer et en croisant à fond les gouvernes transversales, le déclenché est d'autant plus sévère que la vitesse est élevée, et à même vitesse, d'autant plus que le Mach est plus élevé.

Comportement des moteurs

Le paramètre le plus influent sur le comportement des moteurs est l'altitude; pour N2 = 85 % qui est le régime pour lequel le moteur est le plus tolérant, il n'y a aucun risque d'extinction pour Zp < 30 000 ft.

Au plein gaz, les décrochages s'accompagnent de surchauffe en général brève, ce qui conduit à recommander la réduction des moteurs dès la perte de contrôle quand elle survient alors que les moteurs sont au régime maximal.

Comparaison avec les résultats de soufflerie

L'accord entre les prévisions de la soufflerie et les résultats d'essais en vol est excellent. On ne note, sur l'ensemble des caractéristiques des différentes formes de vrilles, que quelques légères divergences. Ainsi, la consigne de sortie donnée par la soufflerie : gauchissement "pour" et pied "contre" est surabondante dans tous les cas, sauf la vrille rapide. De même, la vrille dos est un peu plus rapide, et tolère une plage de braquage au gauchissement moins étendue que celle donnée par la soufflerie.

Enfin, l'influence de la forme du nez sur les caractéristiques de la vrille, prévue par la soufflerie, a pu être mise en évidence sur avion : le nez "pointu" est plus favorable aux agitations.

CONCLUSION

Les différentes vrilles de l'ALPHA-JET présentent des caractéristiques saines, et la consigne de sortie est simple et efficace. En effet, la récupération se fait en moins de 10 secondes en recentrant les gouvernes. Seule une forme de vrille rapide, très rare, nécessite de la part du pilote une action positive pour sortir en moins de 10 secondes, à savoir l'application du gauchissement dans le sens de la vrille.

Les vrilles sont démonstratives, c'est-à-dire, répétitives sans habileté particulière. On peut ainsi démontrer une vrille calme ou modérément agitée, une vrille

agitée et des auto-tonneaux. La vrille dos est même à la portée des pilotes entraînés.

L'ALPHA-JET offre des possibilités d'entraînement relativement faciles et sans danger à toutes les manoeuvres à grande incidence sur avion de combat moderne. Il permet aux pilotes entraînés de visualiser certains comportements intéressants qu'ils pourront retrouver ultérieurement sur d'autres avions d'armes, comme la vrille agitée du JAGUAR ou le régime sans rotation définie du MIRAGE F1.

YF-16 HIGH ANGLE OF ATTACK FLIGHT TEST EXPERIENCE

by

John P. Lamers
F-16 Stability & Flight Controls
General Dynamics' Fort Worth Division
P.O. Box 748, Fort Worth, Texas 76101

SUMMARY

The objective of YF-16 high angle of attack flight tests was to clear the aircraft for the air combat maneuvering test phase. This was to be accomplished by validation of predicted aerodynamic data, and a comprehensive evaluation of handling qualities and flight control system performance during aggressive simulated tactical maneuvering. The program also included a realistic evaluation of the effectiveness of special automatic control system features designed to enhance high angle of attack maneuverability, handling qualities, and departure resistance. Of particular interest were the effects of the active control system (command and stability augmentation) and relaxed static stability concepts upon stall/spin characteristics and recovery capability. Engine operating characteristics at high angle of attack, high angle of sideslip, low airspeed conditions were also of interest. Results show excellent high angle of attack flight characteristics, good correlation with NASA spin model results, and normal flight control system operation over the range of conditions tested.

LIST OF SYMBOLS

α_R	angle of attack, right hand sensor
α_L	angle of attack, left hand sensor
α_N	angle of attack, nose boom sensor
α_{SEL}	select angle of attack (middle value of α_R, α_L, α_N)
α_{CG}	angle of attack at the center of gravity
$A_{N_{CG}}$, A_N, n_z	normal acceleration at the center of gravity
β_{CG}	sideslip angle at the center of gravity
$A_{Y_{CG}}$	lateral acceleration at the center of gravity
δ_{HE}, δ_e	elevator surface position
δ_{HA}	horizontal tail aileron position
δ_{FA}	flaperon aileron position
δ_R	rudder surface position
F_X, F_E	longitudinal stick force
F_Y, F_A	lateral side force
F_R, F_{RP}	rudder pedal force
P	roll rate
Q	pitch rate
R	yaw rate
P_W	wind axis roll rate
M	Mach number
H, H_C	altitude
c.g.	center of gravity

S_x	aircraft horizontal displacement, +North -South
S_y	aircraft horizontal displacement, +East -West
θ	pitch angle
Ψ	heading angle
ϕ	roll angle
g	pilot's normal acceleration meter reading
Q	angular acceleration in pitch
C_M	pitching moment coefficient
q	dynamic pressure
S_W	wing area
$\bar{c}$	mean aerodynamic chord
I_{xx}	aircraft moment of inertia about the longitudinal axis
I_{yy}	aircraft moment of inertia about the lateral axis
I_{zz}	aircraft moment of inertia about the vertical axis
C_N	normal force coefficient
$C_{m_{.25\bar{c}}}$	pitching moment coefficient referenced to 25 percent $\bar{c}$
δ_{LEF}	leading edge flap deflection
δ_F	trailing edge flap deflection
WUT	wind up turn
ANL	aircraft nose left
ANR	aircraft nose right
TED	trailing edge down
TEU	trailing edge up
LWD	left wing down
RWD	right wing down
TEL	trailing edge left
TER	trailing edge right
V_c	calibrated airspeed
ARI	aileron-rudder interconnect
ANU	aircraft nose up
AND	aircraft nose down

TEST AIRCRAFT DESCRIPTION

YF-16 No. 1 was used in the high angle of attack test program. It is a prototype air-superiority day-fighter, designed with emphasis on high performance, maximum maneuverability, small size, low weight and low cost. It is a single-seat, single-engine aircraft with a relatively low wing loading and a high thrust-to-weight ratio. Wing span is 30 feet and length is 46.5 feet. The aircraft, pictured in Figure 1, is powered by a Pratt and Whitney F100-PW-100 engine, which is identical to that used in the F-15.

Flight path control is achieved through the actuation of an all-movable, differential horizontal tail for pitch and roll control, wing-mounted flaperons for roll control, and a conventional rudder for yaw control. Maneuver capability at high angles of attack is enhanced with a full-span leading edge flap positioned automatically after takeoff as a function of Mach number and angle of attack. Both the leading edge flap and trailing edge flap (flaperon) provide high lift during takeoff and landing.

A full fly-by-wire flight control system provides maximum flexibility for tailoring handling qualities. A pilot-operated controller commands surface actuators via high-response command servos in the proximity of the surfaces, with no mechanical linkage employed between the cockpit and the command servos. Quadrex electronics provide fail-operative performance after two failures in each of the three control axes. Three-axis command and stability augmentation enhance the aircraft's handling qualities.

Spin Recovery Parachute System

For the high angle of attack tests, the aircraft was equipped with a mortar-deployed, 28 ft. diameter spin recovery parachute attached below the rudder and above the heat cone of the engine exhaust. The aircraft was ballasted to compensate for the c.g. shift produced by the spin chute system. Test maneuvers were performed to assess the aerodynamic influence of the chute system. Results showed that the installation was slightly stabilizing both longitudinally and directionally between 10° and 20° angle of attack, and that dihedral effect, C_{ℓ_β}, was increased at high α with the chute installed.

FLIGHT CONTROL SYSTEM DESIGN CHARACTERISTICS

Throughout this report, emphasis is placed on selected topics and events that are of particular interest because of their relationship to the unique flight control system technologies employed in the YF-16 aircraft. Of particular interest in this regard are relaxed static longitudinal stability, angle of attack limitation and the other departure-prevention features of the flight control system.

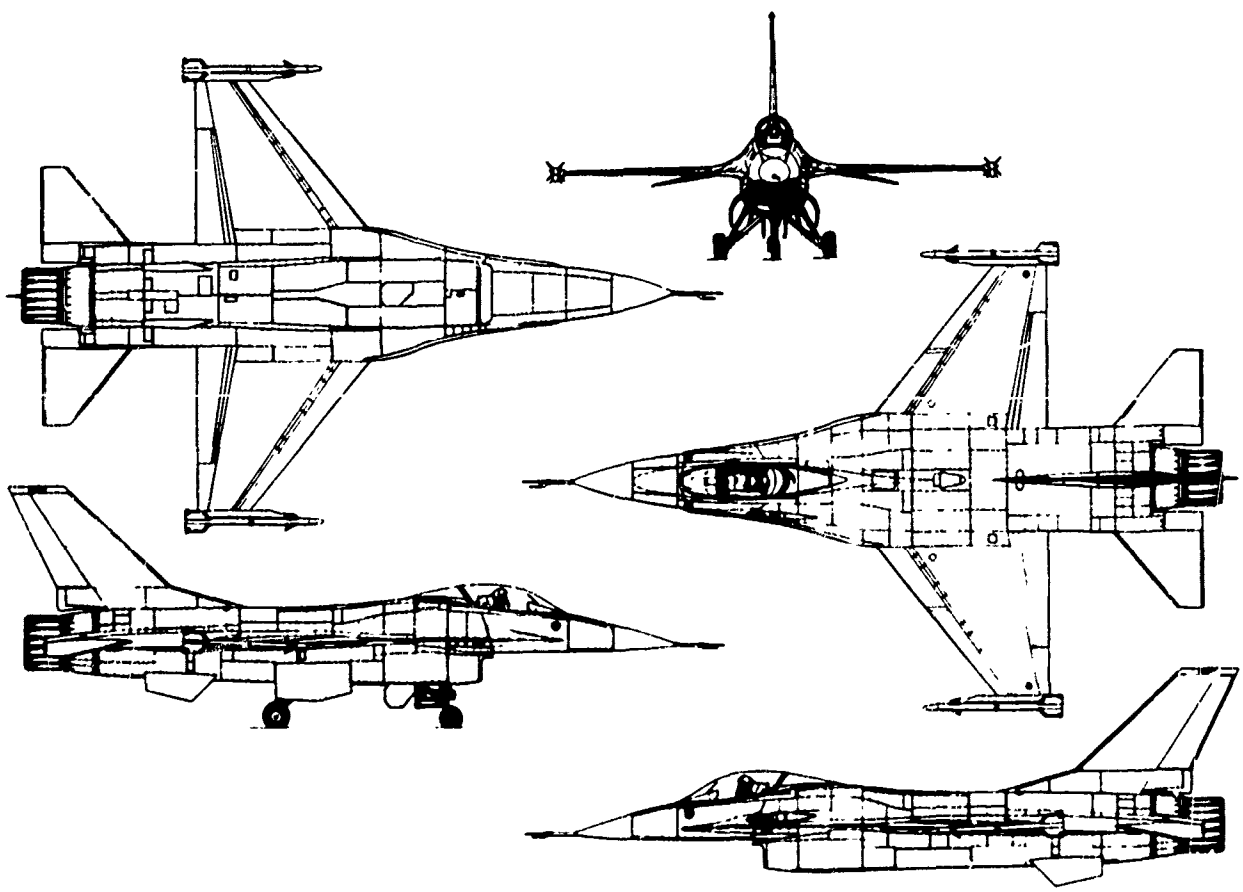

Figure 1 YF-16

Relaxed Static Longitudinal Stability

The control-configured vehicle (CCV) principle of relaxed static stability (RSS) is employed in the longitudinal axis as a part of the basic YF-16 design. RSS provides an aerodynamically efficient vehicle, with exceptional cruise and maneuver performance. Apparent stability is provided to the pilot by the full-time operating, highly reliable stability augmentation system (SAS). Note that the closed-loop aircraft/control system combination is a stable system that requires no special pilot techniques or adaptation.

The aft c.g. limit was established to provide adequate pitch control power for recovery from high angle of attack. (Many other factors also influenced the aft limit; however, these are beyond the scope of this discussion.) In Figure 2 is shown YF-16 normal force and pitching moment data from 1/15-scale and 1/9-scale force model tests, which were used to establish the aft c.g. limit at 35% $\bar{c}$. Note that the 1/9-scale data show that the aft limit could have been set further aft than 35%. A conservative approach dictated use of the 35% limit; however, and flight test data later verified that the 1/15-scale data more closely represents the full-scale aircraft.

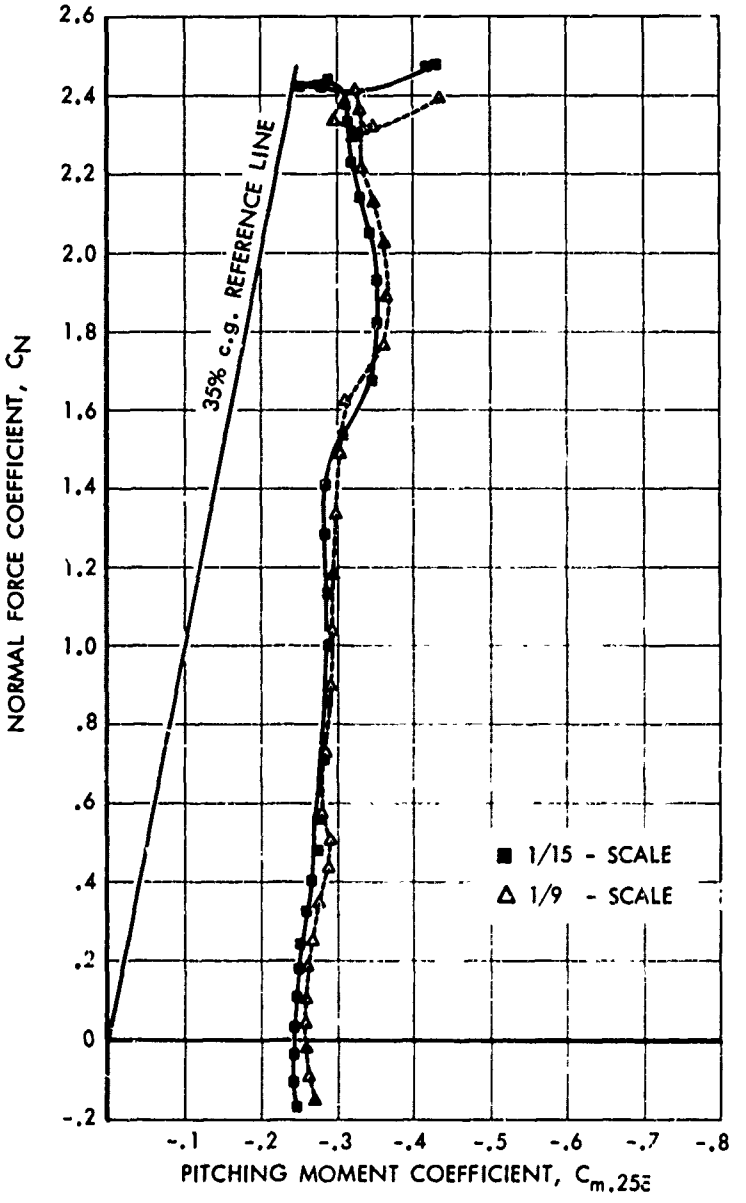

Figure 2 YF-16 Normal Force & Pitching Moment; +25° Elevator

From Figure 2 it may be observed that the aft limit was established to prevent static nose-up aerodynamic pitching moment at any angle of attack, with full trailing-edge down elevator deflection (+25°). A better criterion would have been, "the aft limit will be established such that satisfactory recovery is available from any out-of-control event." The difficulty with such a criterion is, of course, that until a comprehensive high α flight test program has been completed, the actual limit is not precisely definable. One is, therefore, forced to rely on a conservative interpretation of force model and spin tunnel data. Such was the basis for the static trim requirement.

Angle of Attack Limitation

To inhibit loss of control, an angle of attack limiting system was employed. This system used both angle of attack and pitch rate feedback loops to control aircraft angle of attack within preset maximum values. The purpose of the α-limiter was to permit the pilot to maneuver the aircraft safely to the limit of its capability without reference to his cockpit instruments.

A primary test objective was to assess the effectiveness of the α-limiter under aggressive maneuvering conditions.

Aileron-Rudder Interconnect (ARI)

Control of the amount of coupling between the roll and yaw axes is desirable for improved flying qualities and precise tracking. The ARI, which counters the yawing moments produced by the roll control surfaces, was one of two features specifically incorporated to precisely control this coupling. Because of the wide variation in lateral control-induced yaw with angle of attack and Mach number, the ARI was programmed as a function of these two variables.

Stability Axis Yaw Damper

The yaw axis minimizes roll-yaw coupling by providing a roll rate-to-rudder feedback during rolling maneuvers. The roll rate signal is multipled by a signal proprotional to angle of attack in radians and summed negatively with the yaw rate feedback signal. The resulting signal is an approximation of stability axis yaw rate. That is

$$R_{stab} = R_{body} \cos\alpha - P_{body} \sin\alpha$$

$$\cong R_{body} - P_{body}\, \alpha_{rad}$$

This feedback attempts to cause the airplane to roll about the stability axis. Flight test results show that adverse yaw is reduced and roll performance at high angle of attack is improved by this feedback.

In addition, a lateral acceleration-to-rudder feedback is used to augment directional stability.

HIGH ANGLE OF ATTACK TEST PROGRAM DESCRIPTION

A 25 degree α-limiter setting was used during the initial stages of testing to provide an additional margin of safety. All-axis pulses, sideslips, and bank-to-bank rolls were performed at the following conditions:

NORMAL ACCEL., g	ANGLE OF ATTACK, DEG.		
	22	24	25
1	X	X	X
2	X	X	
3	X		

The effectiveness of the 25 degree α-limiter was evaluated by performing a series of maneuvers intended to produce high α, high α rates, and low airspeeds. These maneuvers included

1. 1g, 3g, and 5g idle power slow downs to maximum α
2. A 7g slow down turn from supersonic speed at maximum power

3. High α-rate wind up turns to maximum α.

4. High pitch angle climbs.

Simulated tactical maneuvers such as turn reversals, barrel rolls, vertical and near-vertical slow downs (referred to by test pilots as "hang and look" maneuvers), aileron rolls, and rudder rolls were also performed.

After a thorough evaluation of the envelope allowed by the 25 degree α-limiter, the limiter boundary was relaxed to 26.7 degrees. Three flights were made with the 26.7° α-limiter. All axis pulses, sideslips, and bank-to-bank rolls were made at the following conditions:

NORMAL ACCEL., g	ANGLE OF ATTACK, DEG.	
	26	26.7
1	X	X
2	X	

Maneuvers to evaluate limiter effectiveness and selected tactical maneuvers were also performed with the 26.7 degree α-limiter.

One flight was then made with a 31 degree α-limiter setting primarily to obtain lateral-directional stability data. Roll and yaw pulses were obtained at 26, 27 and 28 degrees α, and sideslips were performed at 26 and 27 degrees α.

It is interesting to note that these maneuvers were not flown primarily to identify limits to be observed by the pilot, but rather to validate the departure prevention features of the flight control system. With the system configured in accordance with test results, it was intended that, immediately after these tests, the aircraft would be flown in an aggressive air-to-air maneuvering test phase.

It is also interesting to note that because of the inherent electrical and hydraulic power supply redundancies of the YF-16 flight control system, it was not necessary to provide the customary emergency hydraulic and electrical power supply for the test aircraft. This saved time and cost during the test program, and provided increased confidence in successful system operation in the event of engine stall/spooldown.

It was also not necessary to install a test nose boom, since the existing air data sensors were adequate, thus YF-16 No. 1 was quickly configured for the high test program and later deconfigured with a minimum expenditure of manhours.

FLIGHT TEST RESULTS

As stated earlier, rather than a detailed discussion of the results of the high-α flight test program, only those specific events and topics of particular interest are addressed. These are intended to illustrate the effect of the unique aerodynamic and control system features of the aircraft on its high-α characteristics.

Angle of Attack Limiter Operation

Various maneuvers were performed in attempts to defeat the α-limiter, that is, to induce an overshoot of the limiter boundary. The α-limiter functioned by using pitching moment from the elevator surface to counter pro-departure aerodynamic or inertial pitching moments. Test results showed that, with certain exceptions, the α-limiter provided excellent protection from loss of control, and enabled the pilot to maneuver safely to very high angle of attack without reference to cockpit instruments. Figure 3 shows normal acceleration and angle of attack data obtained during maximum command wind-up turns at 0.6, 0.8, and 0.9 Mach number at 30,000 ft., illustrating automatic control of angle of attack within safe limits. Figure 4 illustrates excellent α-limiter protection during a 60° stick-free climb to a minimum airspeed of approximately 60 knots.

During the termination of a vertical-entry "hang and look" maneuver on Flight 121, airspeeds below 50 knots were encountered. As shown in Figure 5, the pro-departure inertial moments of the aircraft during this maneuver became predominant over the available stabilizing aerodynamic moments, and an angle of attack of approximately 80° was momentarily encountered. Such predominance of inertial over aerodynamic characteristics is typical of extremely low speed flight in any fixed-wing aircraft, and, in the case of the YF-16, it establishes the limit of protection available from the automatic features of the flight control system. When extremely low airspeeds and angle of attack overshoots were encountered, however, the YF-16 exhibited excellent spin resistance (as illustrated by

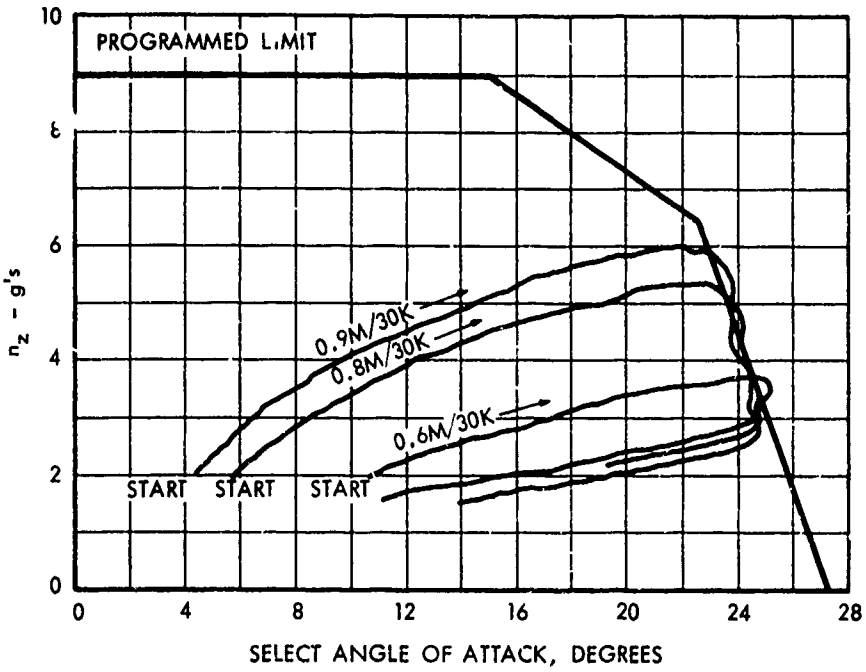

Figure 3 α-Limiter Protection During Rapid Wind Up Turn

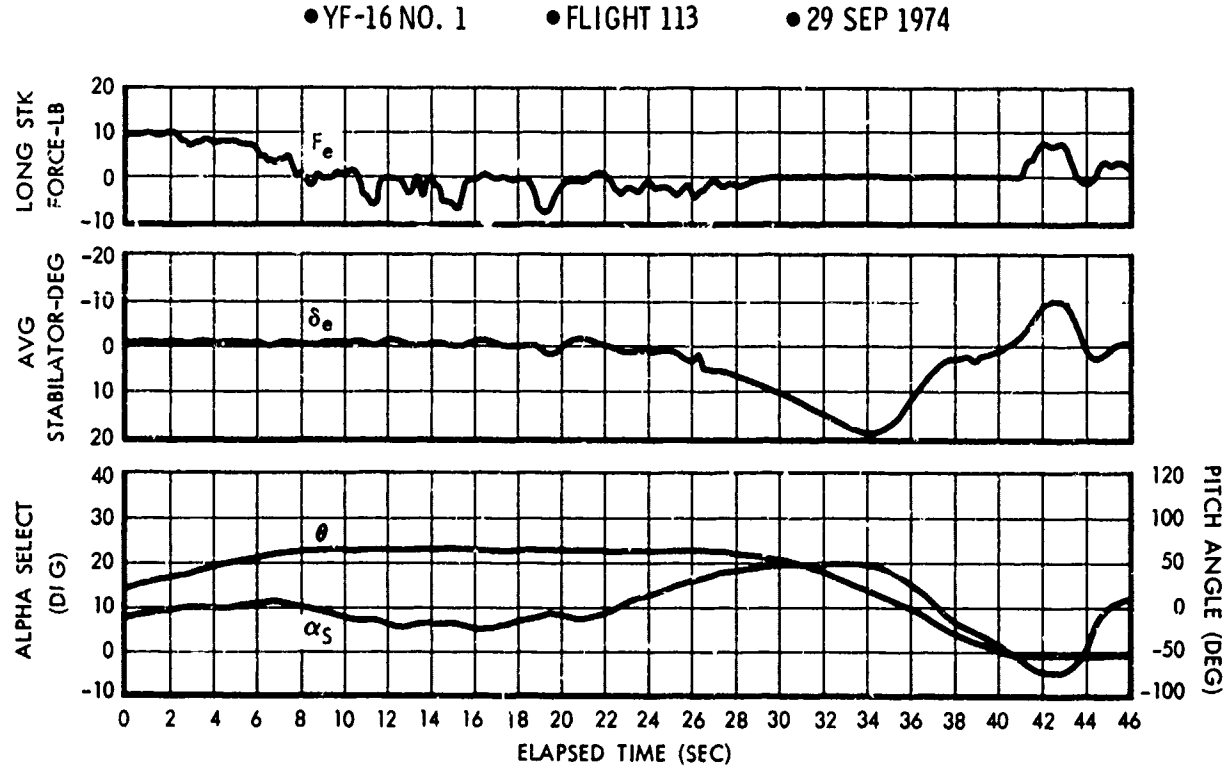

Figure 4 60° Pitch Angle Climb

the data in Figure 5), and a rapid recovery was usually achieved as dynamic pressure increased.

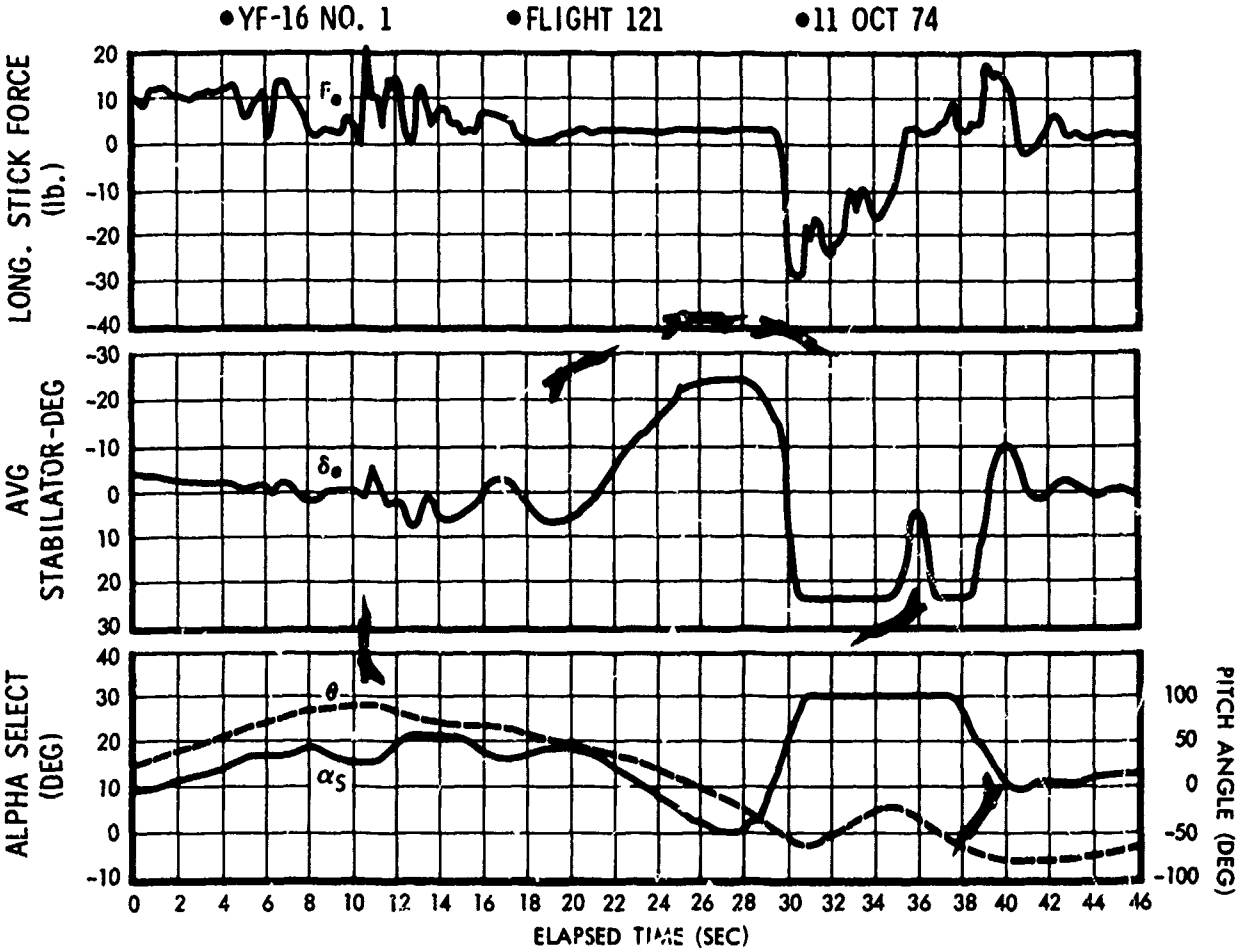

Figure 5 Vertical Climb to Low Airspeed

Aileron-Rudder Interconnect Operation

Figure 6 shows data recorded during a slow deceleration to 29° α_{select} with ARI off during Flight 122 of YF-16 No. 1. (Note: select angle of attack, or α_{select}, is the middle value of the three signals from the three sensors. At 29° α_{select} the test aircraft was at a true angle of attack of approximately 31 deg. Also note that the α-limiter boundary had been relaxed to 31° α_{select} for this particular flight.) As 28° α_{select} is reached, the aircraft begins an uncommanded yawing/rolling motion to the left, which the pilot counters by application of right stick force. However, with ARI off, the aileron-induced yawing moment aggravates the yaw divergence and sideslip angle quickly exceeds 10°, at which time the pilot applies forward stick force, producing a rapid recovery. On an earlier test run during this same flight, however, rudder pulses and sideslips were performed at this same angle of attack, 28° α_{select}, with the aileron-rudder interconnect on. No divergent aircraft motions were noted. The aileron-induced yawing moment, in this case, was cancelled by rudder surface deflection produced by the ARI.

F-16 No. 1 Flight 117 Spin

A spin was encountered on Flight 117 of YF-16 No. 1. This was the only spin that occurred during the high angle of attack flight test program, and it provides a unique example of sustained out of control flight and recovery of a statically unstable air vehicle.

Spin Entry

Spin entry occurred during termination of a sustained, large command, 360 degree rudder-induced roll. This was one of a series of aggressive tactical maneuvers performed during the test program with the objective of clearing the aircraft for the air combat maneuvering test phase that was to follow. It was intended that the test program should include, in addition to the traditional high-α test runs, demonstrations of maneuvers that might be performed during air-to-air combat.

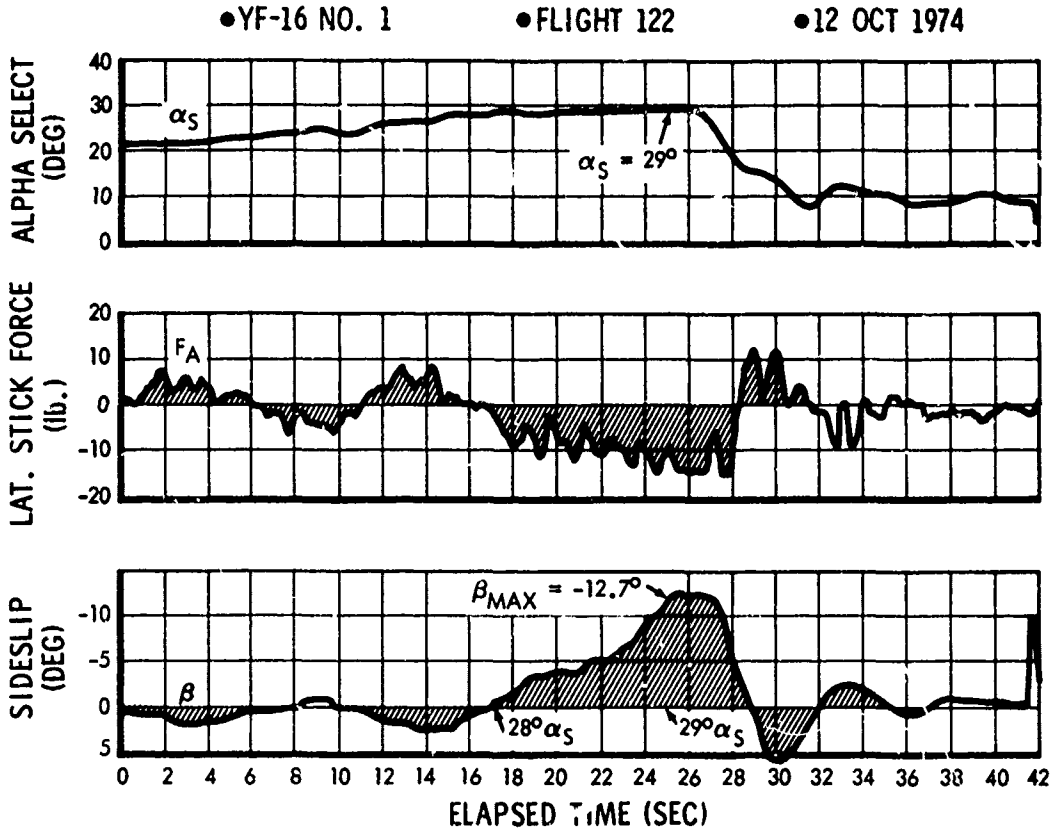

Figure 6 1g Deceleration

The pilot applied approximately 10 lbs. left rudder pedal force to initiate the rudder roll. Maneuver entry was at 34,800 ft. altitude and 150 knots calibrated airspeed. After 4 seconds, having rolled through approximately 90° of bank angle change, rudder pedal force was increased in an attempt to increase roll rate. During this phase of the maneuver the command augmentation feature of the roll axis provided right-wing-down roll command in opposition to the apparently uncommanded left-wing-down aircraft roll rate. This cross-controlling produced an increasing amount of positive sideslip angle (wind from the right side of the nose).

About 6.5 seconds after maneuver entry, the elevator surface saturated in the full trailing-edge-down position as the α-limiter opposed the increasing angle of attack. Figure 7 shows time histories of various flight control system, aerodynamic, and inertial data items, and will be used to illustrate the mechanism of spin entry.

The pitch acceleration of the aircraft was in response to the sum of an aerodynamic moment, an inertial moment, and an engine gyroscopic moment. Theoretical time histories of the components of aircraft pitch acceleration due to each of these three terms are shown in Figure 7. The aerodynamic pitching moment, by itself, would have produced a nose-down or anti-departure pitch acceleration during the entry phase. This term,

$$\dot{Q}_{AERO} = (57.3 \Sigma C_{m_{.35}} q S_W \bar{c})/I_{yy}$$

remained negative until angle of attack reached 38°. The inertial term,

$$\dot{Q}_{INERTIAL} = \left(\frac{I_{zz} - I_{xx}}{57.3\ I_{yy}}\right) RP$$

on the other hand, remained positive (pro-departure) throughout the spin entry, and the sign of aircraft yaw rate during the left rudder roll was such that the engine gyroscopic term,

$$\dot{Q}_{ENG} = -57.3\ \frac{160}{I_{yy}}\ R$$

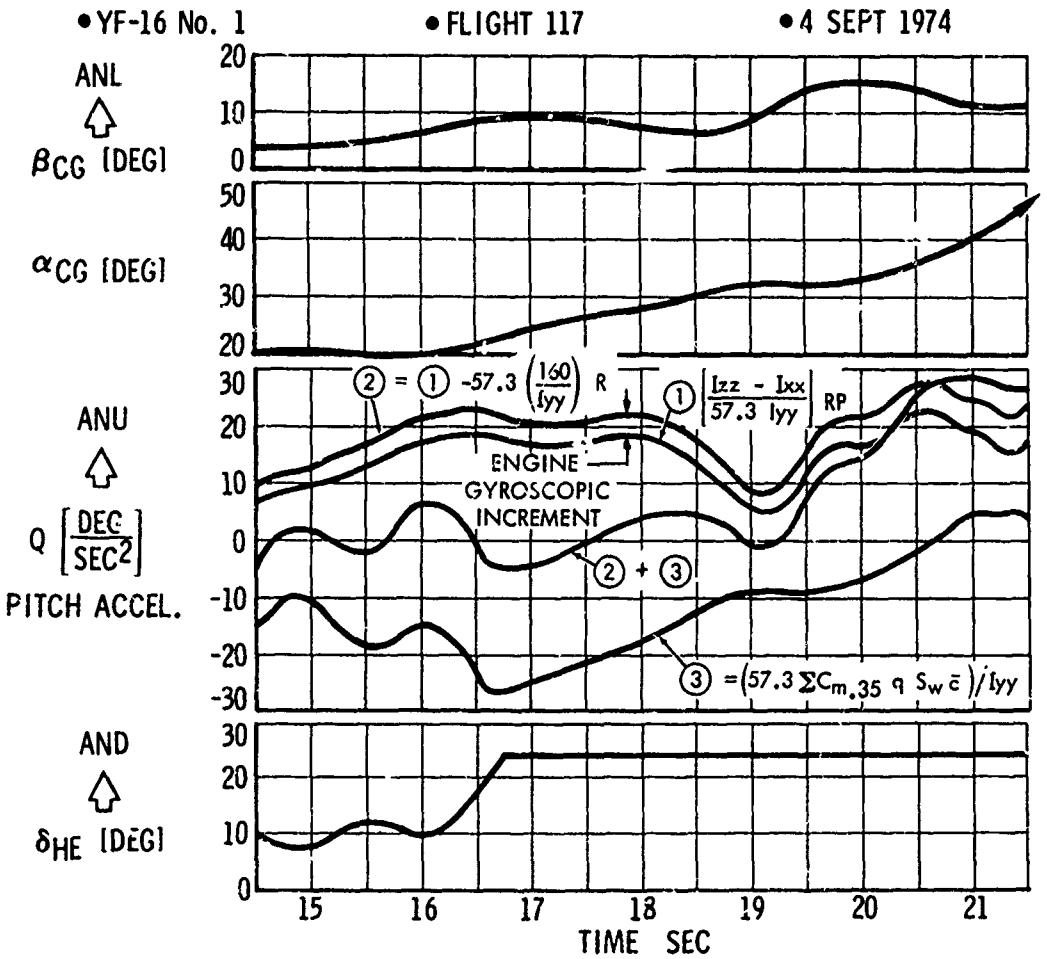

Figure 7 Spin Entry

was also positive, or pro-departure. Figure 7 shows that the inertial and engine gyroscopic effects combined to overpower the aerodynamic effect, causing the angle of attack to exceed 30°. At this condition directional stability had become negative, and a yawing/rolling divergence began. The pilot then applied full lateral command in opposition to the left roll; however, this control application caused further sideslip angle buildup due to aileron yaw, and caused α and β to diverge more rapidly, firmly establishing the aircraft in an out-of-control condition.

Spin

Time histories of various data parameters during the spin are shown in Figure 8. Body angular rates were oscillatory in all three axes. Rotation rate was slow and in close agreement with NASA spin tunnel-derived predictions. Time required for a 360 degree change in heading was 8 to 9 seconds. Angle of attack varied between 42 and 96 degrees during the spin, while angle of sideslip varied between maximum values of $\pm$ 24 degrees.

Elevator surface activity during the spin was primarily in response to the automatic features of the flight control system. Angle of attack was very high, hence the elevator would be expected to remain in the full trailing-edge-down position. However, the surface position time history in Figure 9 shows a definine oscillatory characteristic in response to the oscillatory pitch rate of the aircraft during the spin. Based on YF-16 wind tunnel data at extremely high angles of attack (such as during a spin), the total aerodynamic aircraft pitching moment is relatively independent of elevator surface position and is strongly nose-down. Thus, although the elevator surface position is oscillatory during the spin, it is considered to have little effect on spin characteristics or recovery capability.

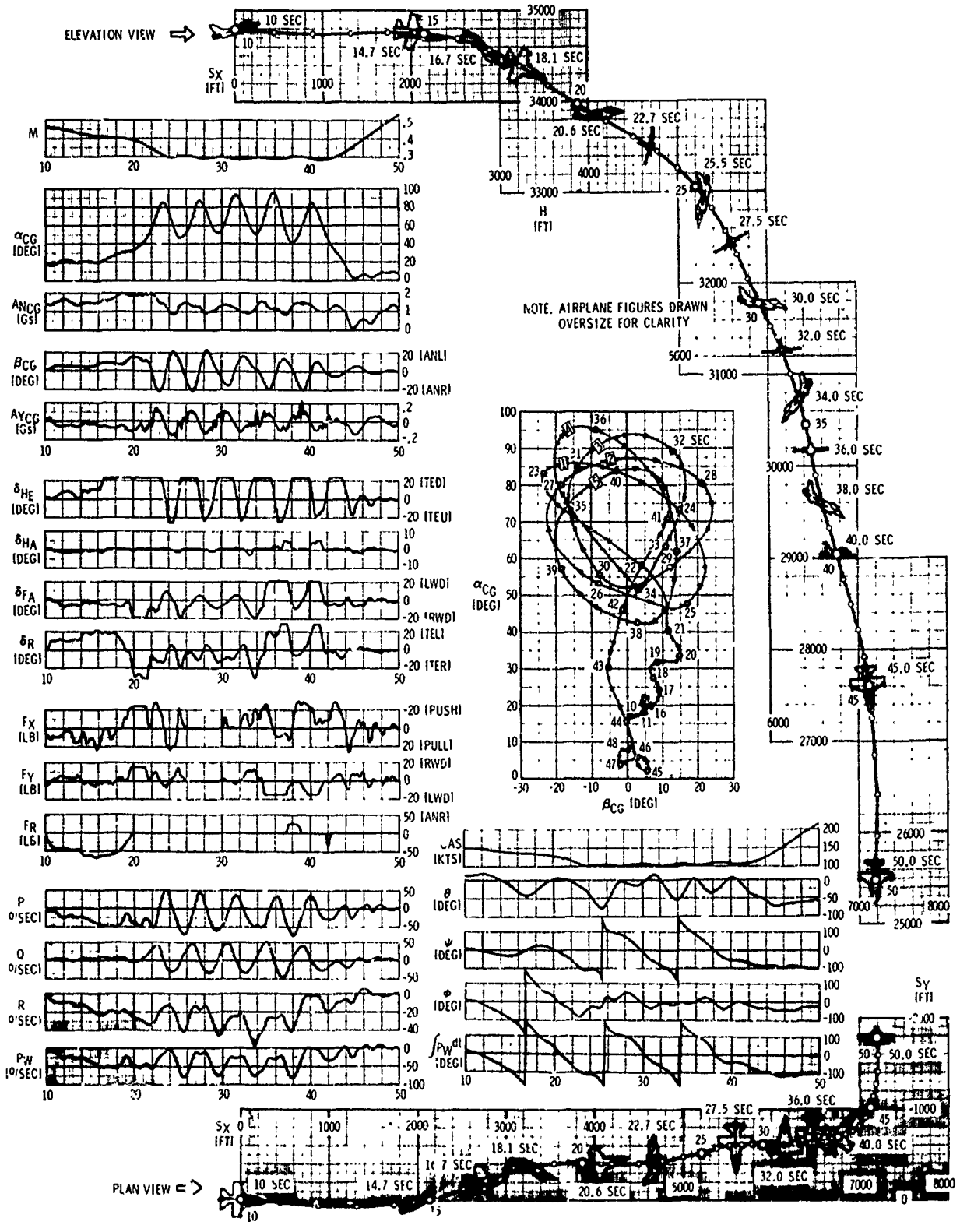

Figure 8 Spin

Spin Recovery

The pilot applied momentary nose down stick force at spin entry, then removed all control inputs while analyzing aircraft motion characteristics. Correctly identifying the left spin, he then applied the pre-briefed recovery controls of left stick force and right rudder pedal force, with neutral elevator input. A rapid recovery to controlled flight was obtained, with less than 2,000 ft. altitude loss between initial recovery control application and full recovery. Lateral stick was very effective in producing an anti-spin yawing moment and a reduction in heading rate, which permitted the nose-down aerodynamic moment to overpower the nose-up inertial moment, followed by a rapid reduction in angle of attack.

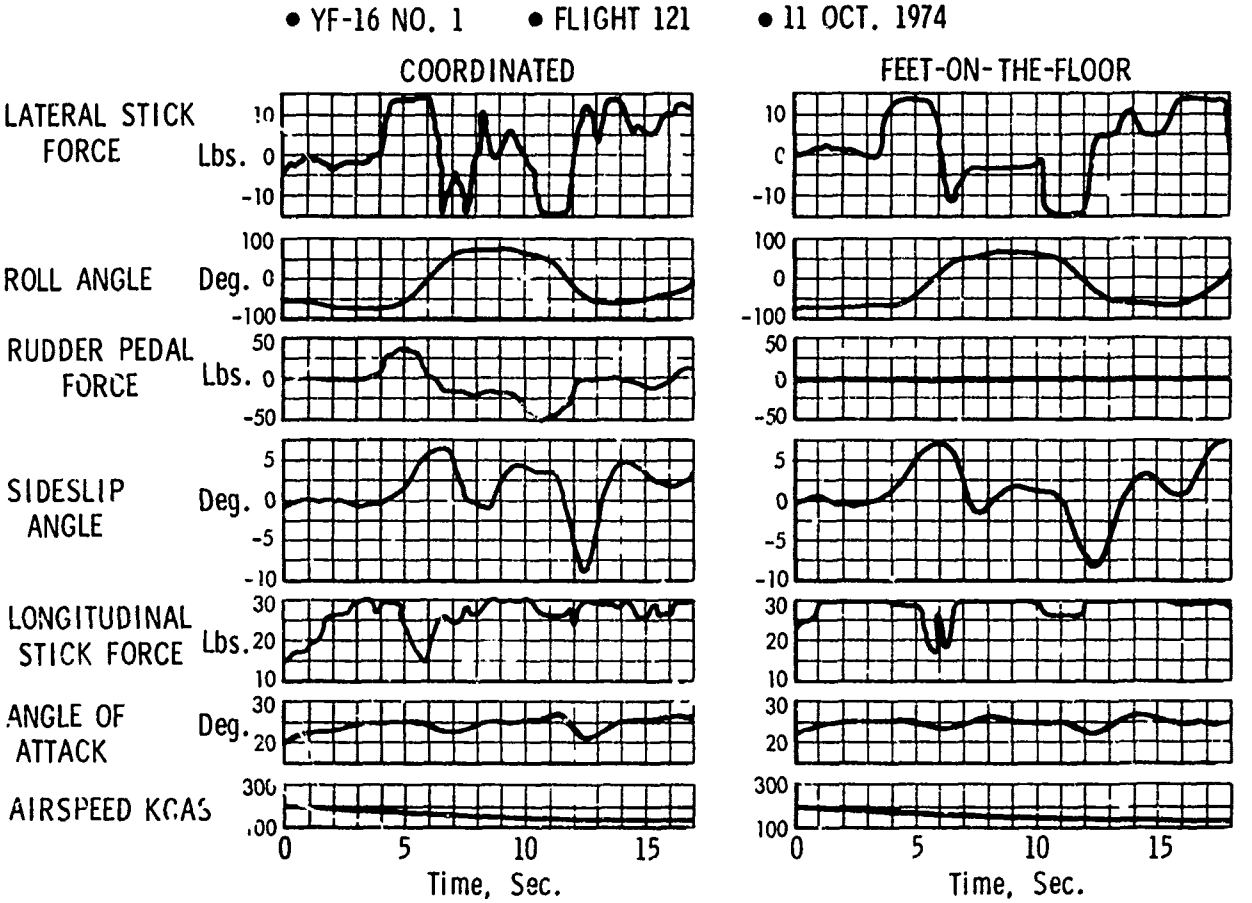

Figure 9 Roll Reversals

Flight control system and engine performance were normal during the spin. The engine remained at the intermediate thrust condition throughout the maneuver. This maneuver was most significant in that it demonstrated that a statically unstable aircraft could be safely stalled, spun, and recovered. YF-16 sustained rudder rolls were prohibited as a result of these tests; however, since they cannot be performed inadvertently, and since roll performance is better with ailerons, sustained rudder rolls are of very limited tactical significance in this aircraft.

Other Maneuvers

Additional test maneuvers performed included coordinated and uncoordinated (no rudder pedal inputs) maximum command bank-to-bank rolls at limit α. In Figure 9 are shown time histories of data obtained during such runs. Note that angle of attack is precisely and automatically controlled during these test runs, and that the aircraft exhibits excellent roll response at high-α . These characteristics of safe and effective high-α maneuverability are of particular importance during a low speed air-to-air engagement.

The time histories in Figure 10 illustrate excellent stability and control characteristics during a low speed, maximum aft stick force barrel roll performed during Flight 121 of YF-16 No. 1. The angle of attack limiter boundary was set at 25° for this particular flight.

Maximum command, 1g entry, 180° and 360° aileron rolls were performed at various entry angles of attack to assess YF-16 roll coupling resistance. These maneuvers were conducted in a buildup series on Flight 118 of YF-16 No. 1. As entry angle of attack was gradually increased, peak values of body axis pitch rate increased correspondingly, and maximum elevator also increased in opposition to the inertial nose-up pitching moment. This maneuver series was terminated in accordance with test ground rules when maximum elevator reached 22° trailing-edge down during a 360° maneuver entered from 17° angle of attack. This maneuver series, along with the "hang and look" series, documents

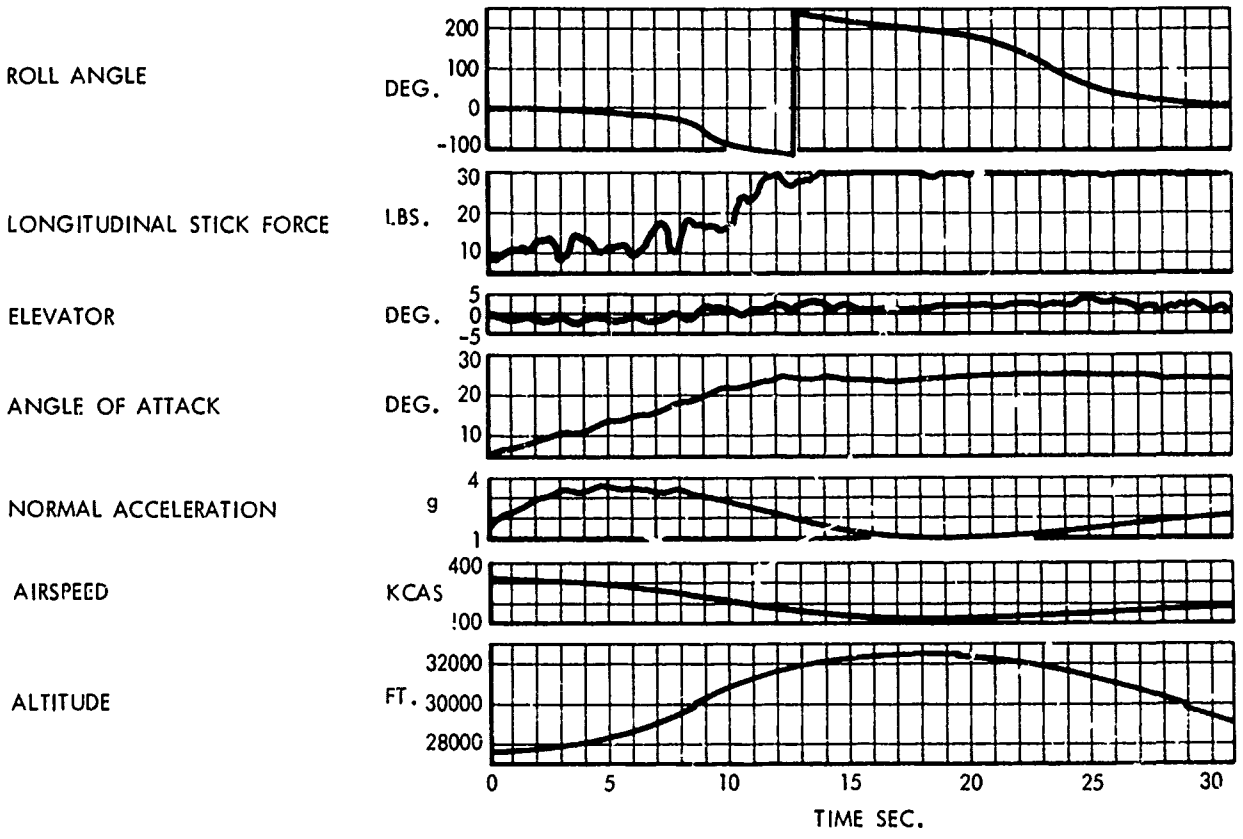

Figure 10 Low Speed Barrel Roll

the fact that the limit of protection available from the departure-prevention features of the flight control system occurs at low airspeed when the anti-departure aerodynamic moments can be overpowered by pro-departure inertial moments. Improvement in low speed protection is, of course, available through a variety of redesign approaches (such as bigger aerodynamic surfaces); however, as with all conventional fixed-wing aircraft, some minimum-control airspeed will still exist unless reaction controls are employed. On the YF-16, this minimum-control airspeed was repeatedly demonstrated to be well below that which would be encountered during normal tactical maneuvering. The aircraft proved to be an exceptional air-to-air fighter, particularly in the low speed region.

An interesting example of the effectiveness of the departure-prevention/maneuver enhancement features of the flight control system is provided by the time histories shown in Figure 11. This data was recorded during Flight 227 of YF-16 No. 1 at Edwards AFB on 24 April 1975. The maneuver is a low speed, maximum aft stick command, maximum lateral stick command, 280° roll to the right immediately after takeoff. Note that angle of attack does not exceed 25°, the α-limiter boundary. Also note that maximum sideslip angle is limited to +5.5° and -4.5°, although body axis yaw rate exceeds +25°/sec.

CONCLUSIONS

The YF-16 demonstrated outstanding high-α flight characteristics during the test program. Control was excellent during aggressive maneuvering at high angle of attack and low airspeeds. The α-limiter functioned as designed. Flight control system and engine operation were normal throughout the tests. One spin was encountered as a result of a low speed. sustained rudder roll. Spin characteristics and spin recovery were demonstrated to be in close agreement with the slow, oscillatory mode predicted from NASA spin tunnel tests. These tests demonstrated that a statically unstable aircraft can be aggressively maneuvered at very low dynamic pressure conditions and can be stalled, departed, spun, and recovered provided adequate control power is available. Since elevator pitching moment is a function of center of gravity location, the aft c.g. limit must be established to insure that sufficient pitching moment is available for recovery from any out-of-control event.

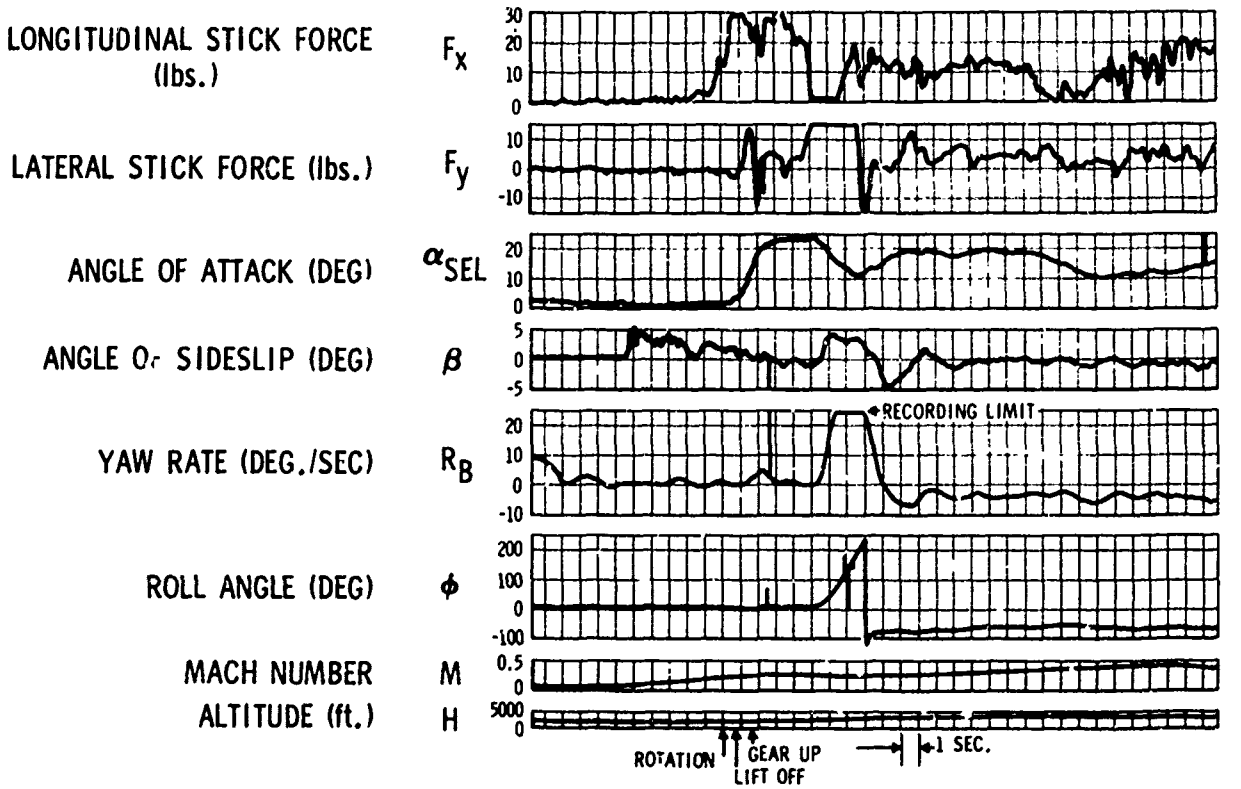

Figure 11 Roll After Takeoff

ACKNOWLEDGEMENT

The author gratefully acknowledges the contribution to this paper of Mr. George E. Sanctuary, Project Aerosystems Engineer, General Dynamics, Ft. Worth Division. Mr. Sanctuary performed the analysis of the spin of YF-16 No. 1, the results of which are presented in Figures 7 and 8.

U. S. NAVY FLIGHT TEST EVALUATION AND OPERATIONAL EXPERIENCE AT HIGH ANGLE OF ATTACK

Alexander F. Money
Stability and Control Engineer
Airframe Division
Naval Air Systems Command
Washington, D. C. 20361
USA

Donald E. House
Supervisory Aerospace Engineer
Attack Branch
Strike Aircraft Test Directorate
Naval Air Test Center
Patuxent River, Maryland 20670
USA

SUMMARY

The operational environment of today's high performance U. S. Navy aircraft is such that the aircraft are frequently flown to the edges of their maneuvering flight envelopes. With the greater use of the high-angle-of-attack flight regime has come an increase in the number of departure-related incidents and accidents. This has brought about renewed support for high-angle-of-attack testing at all command levels and has stimulated widespread fleet interest in the evaluation process, resulting in invaluable feedback from fleet pilots as to their experience in this flight regime.

This paper presents an overview of the problem areas presently considered most significant in the high-angle-of-attack flight regime in U. S. Navy aircraft. The U. S. Navy philosophy of high-angle-of-attack flight testing is also discussed, with examples of some of the more recent programs.

INTRODUCTION

From the designer to the pilot, everyone associated with the flying qualities of high performance military aircraft, particularly of the fighter or attack variety, is or should be aware of the importance of the high-angle-of-attack flight regime. It is here that the aircraft will spend a significant amount of its time when performing the mission for which it was designed. It is here that the aircraft must display its most outstanding performance. It is also here that the aircraft, when pushed beyond its limits of controllability, can seemingly defy all laws of physics and principles of flight with which its surprised and often bewildered pilot is acquainted. The frequency of inadvertent loss of control at high angle of attack is such that many combat aircraft pilots are becoming firmly convinced that all pilots may be divided into two categories: those who have departed controlled flight, and those who will. Most thoroughly convinced are those pilots who fall into the former category.

The unfortunate fact concerning departure from controlled flight at high angle of attack is that many aircraft and pilots are lost each year due to failure to recover from the out-of-control flight condition. The circumstances surrounding the losses are varied. Departures from controlled flight may occur unintentionally during high-g maneuvers or intentionally during a nose-high deceleration to zero airspeed in an attempt to gain an advantage over an opponent in combat maneuvering; the aircraft may spin and the gyration be identified too late for recovery, or a steep spiral may be mistakenly identified as a spin, causing recovery controls to be misapplied. Whatever the circumstances, departures from controlled flight result all too often in catastrophe. A statistical summary of out-of-control aircraft losses since July 1971 which resulted from departures at high angle of attack for four models of U. S. Navy and Marine Corps aircraft is shown in table I. The data were compiled by the U. S. Naval Safety Center.

Table I
U. S. Navy Out-of-Control Losses
FY-72 - FY-75

Aircraft	Number
A-4	3
TA-4	13
A-7	7
F-4	19

Quite understandably, such statistics have drawn interest at all levels of command and participation in the U. S. Naval aviation community. Renewed emphasis on high-angle-of-attack characteristics and support for high-angle-of-attack testing have been generated at high levels of command. The fleet has shown more than casual interest in the design and test and evaluation process. Both the fleet and the test and evaluation communities have demonstrated concerted efforts to identify and solve the problems that lead to statistics such as those shown in table I. Some of the problem areas that have been identified will now be discussed.

SPECIFIC HIGH-ANGLE-OF-ATTACK PROBLEM AREAS

A-4/TA-4 AIRCRAFT

As shown in table I, the A-4 series aircraft (both single- and two-seat versions) have suffered heavy out-of-control losses during the period covered. Significantly, this represents a substantial increase in the rate of out-of-control losses for that model when compared to earlier years. The increase correlates well with the time when the A-4/TA-4 aircraft began to be used extensively in Air Combat Maneuvering (ACM) training. A further breakdown of the nature of the aircraft losses gives additional in-

sight as to the real nature of the problem. Of the thirteen TA-4's and three A-4's lost due to out-of-control flight conditions, seven losses (five TA-4, two A-4) occurred during ACM flights. During the ACM phase every known departure was initiated from the 90 degree vertical (nose-high) attitude, zero airspeed regime.

The introduction of the A-4 to the rigors of ACM has shown us characteristics we had neither seen nor worried about in our twenty-one years' experience with the aircraft. Although we have known for some time the spin characteristics of the aircraft, the propensity of the TA-4, for example, to undergo extremely violent post-stall gyrations following decelerations to zero airspeed in vertical maneuvers, and its tendency to transition rapidly into a fully developed inverted spin with only the slightest misapplication of controls came as a rude awakening. Only in the past two years with extensive flight test effort have we come to an acceptable level of understanding of this problem. Flight tests have also shown that this particular problem is not shared to the same degree by the single seat A-4 aircraft.

Apart from considerations of aircraft usage, there are design deficiencies, known for many years, that contribute to the out-of-control accident statistics. To illustrate two, in three accidents, asymmetrical slat conditions were recorded as contributing factors and there were three accidents where the pilots reported some degree of incapacitation while experiencing negative-g that restricted their ability to effectively manipulate the controls. Asymmetric slat extension in the A-4 aircraft (the slats are extended aerodynamically and each operates independently of the other) has been a known problem area for some time. Solutions have been proposed, but they cost money that has not been available. Two U. S. Navy squadrons, Top Gun, who use A-4's in the Navy Fighter Weapons School combat training exercises, and the Navy Flight Demonstration Squadron (Blue Angels) who recently transitioned to A-4's, lock the slats in a permanently closed position. At some sacrifice in maneuvering performance, this precludes asymmetric slat extension during maneuvering flight. The second example given refers to the lack of adequate pilot restraint. This and other problem areas in the cockpit are not limited to the A-4/TA-4, and are discussed later in this paper.

A-7 AIRCRAFT

The A-7 shows a somewhat better accident record. Although all seven were out-of-control resulting from high-angle-of-attack maneuvering, none are believed to have hit the ground spinning. The A-7 is not a spin-prone airplane; it is a departure-prone airplane, and its departures from accelerated stalls at other than slow decelerations are extremely violent. Aerodynamic stall in the A-7 occurs very close to the optimum maneuvering angle of attack. In the vicinity of the stall angle of attack, lateral-directional stability is weak. Buffet onset and buildup occur too early to serve as acceptable stall warning. Near the stall, buffet intensity is so heavy that it masks the artificial stall warning provided by rudder pedal shakers, particularly at high power settings. The departure may occur anywhere between stall angle of attack and several degrees above. Hence, by exceeding optimum angle of attack, a pilot may suddenly find that he has progressed through stall warning, stall, and departure in such rapid succession that he has no time to react to counter it.

The A-7 departure is characterized by a rapid nose slice accompanied by snap rolls in the direction of the slice. The ensuing motions are violent roll and yaw motions superimposed on milder pitch oscillations, and are extremely disorienting to the pilot. Recovery is consistently accomplished by releasing the controls, and typically results in a near vertical nose-down attitude and excessive altitude loss. This description of the A-7 departure, necessarily simplified for presentation here, is the root of the A-7's problems at high angle of attack. More detailed discussions of A-7 high-angle-of-attack characteristics may be found in references 1 and 2.

It is of significance to note that of the seven accidents that occurred during the reporting period, five occurred at sufficient altitude for recovery. Furthermore, six of the seven were A-7E's. Both of these statistics lead one to the conclusion that lack of training is a problem. In the former, that conclusion is obvious. In the latter, the reasoning is more complex, as follows: further examination of the accident statistics reveals that the departure accident rate (based on flight hours) for A-7C and E models is more than double that of A-7A and B models. Presently, the A/B and C/E readiness squadron syllabus hours are the same. But the C/E models are much more complex weapons systems than the A/B models; therefore, for a C/E pilot to attain the same level of proficiency in his aircraft as an A/B pilot, more syllabus hours are needed. It is believed that the higher accident rates in the C/E models are related to this training deficiency. Further discussion of training aspects of stall/spin problems is presented later in this paper.

F-4 AIRCRAFT

Of the nineteen out-of-control F-4 accidents occurring during the reporting period, nine were maneuvering accidents, while the remainder occurred during takeoff or landing. Four of the total were directly attributed to material failure, and material failure of lesser magnitude is believed to have been a factor in half of the takeoff and landing accidents. Of interest here are those that involved no material failure as a causal or contributing factor.

Of the takeoff accidents reported, two were due to over-rotation. This is a problem that has been with the F-4 all its service life and for which no design solution will ever be incorporated, in spite of the fact that it has accounted for many losses of aircraft over the years. The problem of over-rotation on takeoff can be consistently avoided with proper manipulation of stabilator control. It is interesting to note that no accidents of this type (nor other types of takeoff or landing accidents) have occurred in the past two years.

Departure from controlled flight while maneuvering is a serious problem for the F-4 as it is with many other high performance aircraft (see references 3 and 4). The departures are not as violent as in the A-7. Neither is the aircraft particularly susceptible to rapid transitions from departures to spins, provided the pilot recognizes his situation and applies forward stick to unload the aircraft in a timely manner. Herein, however, lies part of the problem; the fleet pilot is apparently experiencing difficulty in

recognizing the fact that his aircraft has departed, and is driving the aircraft into a regime where recovery is more difficult and more altitude-consuming. Flight test experience in the F-4 indicates that, while natural stall warnings of airframe buffet and lateral instability combined with the rudder pedal shaker provide the pilot excellent warning of impending normal, one-g stalls, the point at which the aircraft stalls is not always apparent to the pilot unless he checks the angle-of-attack indicator. Failure to recognize the stall can allow the pilot to drive the aircraft into a deep stall and bring about large random oscillations about all axes and high rates of descent. On the other hand, impending accelerated stalls are harder to recognize, mainly due to rapidity of entry; but once the aircraft stalls, the fact that departure has occurred is generally unmistakable, with a snap roll opposite to the direction of turn. The types of entries in which the fleet pilots are experiencing recognition difficulties have not yet been determined, but it is suspected that they are at low speeds and low normal accelerations where the departures are milder. Whatever the circumstances, a recommendation from the fleet was made at the U. S. Naval Safety Center Conference on Out-of-Control Aircraft Losses earlier this year to incorporate a "departure warning device," to warn the pilot when preset departure parameters such as combinations of angle of attack and yaw rate are exceeded.

Another problem with the F-4 aircraft is the existence of the flat spin mode. While this mode is seldom entered, when it does occur, it is irrecoverable. None of the nineteen losses reported in table I were thought to involve flat spins. Nevertheless, the existence of such a mode can be a significant factor in seemingly unrelated losses due to the added anxiety a pilot experiences when he loses control of his aircraft.

PILOT FACTORS

The discussion until now has dealt with problems specifically related to the aircraft -- design problems. It has been pointed out that, in the case of the TA-4 for instance, we are still learning new things about an old aircraft through fleet experience and through test and evaluation. Implicit in the preceding discussions has been that the pilot is a large factor in many of the accidents, frequently through no fault of his own. The reason -- insufficient training in the out-of-control flight regime.

Given the less than desirable high-angle-of-attack characteristics of many of today's high performance military aircraft, the largest single contributing factor to the high accident rates appears to be lack of pilot experience in recovery from out-of-control flight conditions. Currently, Navy and Marine Corps student pilots are trained in spin recovery in T-34's in basic flight training, and in advanced jet training receive one flight dedicated to spin practice in the T-2 aircraft. No further formal training in spin and recovery is ever received except in such special cases as Test Pilot School students or for instructor pilots in the training squadrons. It is no wonder that when a pilot suddenly finds that he has departed controlled flight, he experiences some difficulty in handling the situation.

The first problem a pilot is likely to experience following a departure is in recognizing his predicament and properly identifying the motions of his aircraft. In many cases the pilot fails to use the only positive means of identification of the situation, his instruments. The urge to look outside the cockpit is simply too great. Knowing what his aircraft is doing is essential to his successful recovery. In the case of spin, a check of angle of attack and airspeed is of primary importance in determining if the aircraft is in fact spinning. To apply spin recovery controls when the aircraft is only in a steep spiral dive can result in loss of the aircraft just as certainly as failure to apply proper recovery controls in a true spin.

Proper use of the controls, particularly the lateral controls, following departure is another area where pilot training is deficient. At the point of departure, for instance, the pilot's natural tendency is to counter such motions as a wing drop or snap roll with opposite aileron. This holds true for the pilot inexperienced in out-of-control flight even when he has just been briefed on correct procedures and is intentionally departing the aircraft, and is borne out by experience with student pilots at the U. S. Naval Test Pilot School. The proper procedure in most cases is to accept the roll and whatever other gyrations the aircraft experiences with the controls either physically held in the neutral position or, in the case of the A-7, by releasing the controls. Similar difficulties are seen, for example, in using aileron in the direction of the erect spin in order to recover from it. Such actions are unnatural and therefore difficult for the pilot who is intent on controlling his aircraft, and must be ingrained through practice.

A third difficulty experienced by the pilot is that his concept of the passage of time changes radically, by a factor of five, when he loses control of his aircraft. This fact has been established by comparing actual data traces to the statements of test pilots concerning the length of time controls were applied to recover from a spin. Thus, a pilot might think he has held recovery controls for twenty seconds with no apparent results and eject, when in reality he has only held the recovery controls for four seconds and the aircraft has not had time to recover. A discussion of this and other physiological factors may be found in reference 5.

SUMMARY OF PROBLEM AREAS

The preceding discussions provide only cursory treatment of the main problem areas, but the specific examples presented were chosen because they are representative of the type of problems experienced in the U. S. Navy and Marine Corps aviation communities. Before proceeding with further discussion of the problem areas, they should be summarized. The main areas of concern are:

1. Lack of inherent resistance to violent departure and spin in many aircraft designs.

2. The need to fully explore and document, through test and evaluation, the out of-control characteristics and recovery procedures for all high performance aircraft.

3. The need for more adequate training for the fleet pilot in the out-of-control flight regime.

ELEMENTS OF THE HIGH-ANGLE-OF-ATTACK PROBLEM

DESIGN PROBLEMS

The ideal solution to the design problem is of course to simply design aircraft so that they are well-behaved at high angle of attack with no sacrifice in flying qualities and performance in other flight regimes. Such words are easy to say, and perhaps are said on occasion by those not intimately familiar with the problems faced in implementing a task of such magnitude. Those problems are many and range from lack of complete understanding of the mechanisms that trigger violent departure from controlled flight to the unacceptability of known solutions in terms of the price that must be paid in other areas, such as performance. There is no question that one of the greatest obstacles faced in performing the research necessary to solve many of our design problems is lack of funds. But current fiscal policies should not be used as an excuse for poor performance. They simply mean that we in the technical community must rely more heavily upon our ingenuity in accomplishing our work, work more closely with others in our field, and take more calculated risks.

Many advances in aerodynamic design for high-angle-of-attack characteristics have been made in recent years and are continuing. For example, the concepts of wide fuselage, twin vertical tails, and good vortex control provided by a highly-swept wing leading edge at the wing-body juncture contribute to the excellent high-angle-of-attack characteristics of the F-14. Even so, the aircraft can be pushed beyond the limits of controllability and will spin. Perhaps demonstration, through operational experience, of the tactical advantages available to aircraft that perform well at high angle of attack will provide the impetus needed to promote further major advances in basic aerodynamic design.

Since we have not yet mastered the problems associated with basic aerodynamic design, we resort to other means of improving the controllability of our aircraft at high angle of attack. Because we want to minimize the requirements for positive remedial action on the part of the pilot when dangerous flight conditions are approached, we implement artificial compensation for less than desirable bare-airframe characteristics through the use of stability augmentation systems, the function of which is to increase the level of stability about one or more axes through motion of control surfaces in response to motions of the airframe. Such systems have their opponents, particularly in those of the old school where seat-of-the-pants flying was the rule. Indeed, such systems are not without drawback. First of all, they must be reliable -- they must work when they are needed. The added complexity they introduce to the flight control system tends to decrease overall reliability and adds maintenance requirements. In the functional area, while some such systems aid the aircraft in performing at high angle of attack and even expand the safe flight envelope, they often hinder or even prohibit recovery of an aircraft that has exceeded its maneuvering limitations, in some cases even driving it into a spin. Therefore, a positive means of automatic disconnect of the system at the right moment must be provided. again increasing complexity. Variants of stability augmentation systems include such systems as aileron-rudder interconnect, which shifts roll control from aileron to rudder as angle of attack increases while the pilot continues to command roll control with the stick, and systems which respond to limit maximum angle of attack of the aircraft. While not all variants have been proven in operational use, stability augmentation in some form has been accepted for some time as quite suitable for its intended purpose and is of primary importance in assuring that the maximum amount of the flight envelope is available to the pilot.

Even with the best of inherent aerodynamic characteristics and artificial stability devices, there are limits beyond which the aircraft should not be maneuvered. The problem is to warn the pilot when he is approaching these conditions. Natural aerodynamic stall warning is the most desirable means, but is not always available, or occurs too early to be of benefit to the pilot. Therefore, we must provide him with various types of artificial stall warnings. These, too, have drawbacks and in many cases are somewhat ineffective. Popular types of artificial stall warning devices are rudder pedal or stick shakers and aural tone devices. The effectiveness of these systems depends very much upon the characteristics of the aircraft in which they are installed and on compatibility with other aircraft equipment. In the case of the A-7, rudder pedal shakers are masked by heavy buffet which itself appears too early to serve as effective stall warning. Aural tone systems have been found by the Navy to be ineffective in some aircraft due to confusion with other tones providing the pilot with other types of information. Therefore, care must be exercised to ensure that the type of system being incorporated will be compatible with its operational environment. Also, such systems by their nature are not positive deterrents to departure from controlled flight and their usefulness in providing sufficient warning to the pilot in rapid approaches to the stall is doubtful.

Recovery from out-of-control flight conditions can in most instances be virtually guaranteed by the use of devices, usually parachutes mounted on the aft fuselage, designed specifically for the purpose. While such devices are commonly used on aircraft in high-angle-of-attack flight test programs, it is generally impracticable to incorporate them in fleet aircraft. The F-4 drag chute may be used to assist in recovery from out-of-control flight, but is useless in the flat spin mode; increased rudder throw for spin recovery is available in the A-6. Except for these, no other U. S. Navy aircraft have systems which may be used to augment the normal flight controls in out-of-control recovery. Perhaps consideration should be given to incorporation of spin-recovery devices on fleet aircraft dedicated to frequent use in flight regimes where the probability of loss of control is high (i.e., aircraft used in air combat maneuvering training).

A discussion of design problems should not be limited to aerodynamic design. Of equal importance is the cockpit. Two problem areas identified during recent flight test programs, and with which fleet pilots have reported difficulties during attempts to recover from out-of-control flight conditions, are location of instruments and the lack of effectiveness of pilot restraint systems. The importance of reading such instruments as the angle of attack, airspeed, and turn indicators in identifying aircraft motions has already been discussed. In many cases it has been reported that one or more of these instruments could not be readily seen by the pilot during out-of-control flight. Some models of the TA-4, for instance, have the angle-of-attack indicator located beneath the glare shield in such a manner as to be concealed from the pilot's view when he is forced up and out of his seat by negative-g's. This brings us to the second problem area, that of inadequate pilot restraint systems. This problem is common to the

A-4/TA-4, A-7, and F-4 aircraft. Aside from causing difficulty for the pilot in reading his instruments, poor restraint systems unnecessarily complicate proper control inputs, allow the pilot to "rattle around" in the cockpit, which adds to his disorientation, and can leave him dangerously out of position for ejection should it become necessary. One pilot, when asked if he had retarded the throttle after he had departed controlled flight in an A-4, replied, "No, it was the only thing I had to hang on to!"

FLIGHT TEST PHILOSOPHY

In the course of an aircraft development program high-angle-of-attack data are generated in many ways -- by analysis and by various types of aerodynamic testing -- long before a flyable machine is available (see reference 6). But the real proof of design and identification of the true aircraft characteristics at high angle of attack can be obtained only through a well-structured and thorough flight test program such as that described in reference 7. Typically, the U. S. Navy conducts its high-angle-of-attack flight test programs in two phases, the first of which is contractor demonstration, followed by Navy evaluation.

The contractor's role is to investigate and identify any and all attainable motions of the out-of-control aircraft that the fleet pilot might be expected to encounter, and to determine whether or not the aircraft is recoverable from these conditions. The end result is that the most critical conditions are demonstrated to a Navy witnessing authority, usually a team of test pilots and engineers from the U. S. Naval Air Test Center. After the contractor has satisfactorily completed his task, the Navy evaluation can begin. This phase of the flight test program is designed to accomplish many things. Techniques for avoidance of out-of-control conditions are developed. The aircraft is driven repeatedly into the regions where the contractor has demonstrated recoverability to ensure that is it indeed consistently recoverable. Recovery procedures are optimized for the fleet pilot from both the standpoints of minimizing the numbers of different techniques required for recoveries from various conditions and in simplification of the positive pilot actions required. Recommendations are made as to what types of stall, departure, or spin training may be safely performed in the aircraft. The information obtained during the evaluation is fully documented in report form, and is the basis for the information provided the fleet pilot in the flight manual.

This approach to high-angle-of-attack flight testing has been practiced for many years. However, recent programs have seen a shift in basic philosophy; instead of extensive investigation of fully developed spins, more emphasis is being placed on the stall/departure phases of out-of-control flight. Whereas the contractor was once obligated to drive the aircraft into fully developed spins by whatever normal means necessary, he has in more recent programs been allowed to limit his attempts to the use of pro-spin controls for "reasonable" time periods, and has been allowed some relief from the number of turns required once the aircraft enters the spin. Hence, the contractor may now satisfy his obligation to demonstrate his aircraft's high-angle-of-attack characteristics by showing that the aircraft possesses departure or spin resistance. His primary role in the flight test effort, that of demonstrating most critical conditions attainable, has not changed; and the responsibility for developing departure- and spin-avoidance techniques remains with the Navy. The definition of "most critical conditions" has changed, however, and reflects new Navy thinking as to what conditions the fleet pilot might reasonably be expected to encounter. It should be added that the Navy high-angle-of-attack flight test philosophies have been influenced by recent U. S. Air Force thinking as reflected in references 8, 9, and 10 on the same subject. The differences that exist appear to lie in the extent to which the contractor is tasked to develop operational techniques, with the Air Force apparently relying more heavily upon him for these tasks than does the Navy.

TRAINING PROBLEMS

An overwhelming number of out-of-control accidents are a direct result of the inability of the pilot to cope with his aircraft at high angles of attack, either before or after departure. More adequate training in this flight regime would then appear to offer a solution to many of our problems. Except in rare cases involving material failure or pilot incapacitation, a properly trained pilot should be able to avoid or recover from most out-of-control situations. While some basis exists for such a statement, there are obstacles to overcome before it can be truly tested.

The most desirable type of training is, of course, flight training in the type aircraft to which the pilot is assigned, or in an aircraft which demonstrates characteristics representative of his aircraft. But some aircraft are simply not suitable for training in all phases of out-of-control flight -- the F-4 by virtue of its irrecoverable flat spin mode, the TA-4 because of its extremely disorienting inverted spin mode. Even in aircraft that do not exhibit such undesirable characteristics, such a program, no matter how closely controlled, would inevitably result in some aircraft losses in training. Although it is a virtual certainty that operational losses prevented by the training would more than offset training losses, the unfortunate fact is that aircraft lost are much more easily counted than are prevented losses. This is a major obstacle in the justification of post-stall training.

The question of how to best implement high-angle-of-attack flight training also raises problems. In order to remain proficient in the high-angle-of-attack flight regime, a pilot should receive training on a recurring basis, preferably every six months, and certainly no less frequently than once a year. There is no recurrent training now established at such intervals, so incorporation of this type of training into an existing training cycle is not a possibility if the yearly criterion is to be met. The choices are then limited to two: establish separate high-angle-of-attack training units through which all fleet pilots are cycled at regular intervals, or designate instructors to provide the training within the squadrons at specified intervals.

Neither alternative currently appears practicable. The former requires dedicated aircraft and manpower. Such specialized usage of assets is not likely to receive favor in these days of tighter defense budgets. The second alternative, that of training within the squadron presents a problem in the allocation of limited operational flight hours for this purpose and would cause difficulty in maintaining controls over a program where numerous diversities are likely to emerge.

A third alternative exists, but will not provide the desired annual or semi-annual retraining. This is to incorporate high-angle-of-attack syllabi in the readiness squadrons where pilots receive training prior to initial deployments, after tours of duty involving infrequent flying, and when changing aircraft type. Here the pilots would receive exposure to out-of-control flight under close supervision of qualified instructor pilots -- perhaps not at the desired interval, but experience indicates some training of this type is better than none at all.

The last alternative given (training in the readiness squadrons) appears to be the only one which is feasible at this time. In fact, such a program has been implemented on a trial basis in one of the A-7 training squadrons with promising results. In the normal course of training, students are encouraged to depart controlled flight in the A-7, and are emerging with a significantly improved level of confidence in the capabilities of the aircraft and in themselves. This type of training in the A-7 is low-risk in comparison to other aircraft; the A-7 exhibits no motions from which recovery is extremely difficult and is not prone to spin. Perhaps continued success will set a precedent for limited post-stall training in other aircraft types where it is even more desperately needed.

Flight simulation might seem to offer a satisfactory solution to the training problem. Indeed it can be useful in the pre-stall high-angle-of-attack regime, but some difficulty is encountered when attempting to simulate post-stall or out-of-control aircraft characteristics. The problem rests in two areas: formulation of an accurate mathematical model of the aircraft motions and obtaining accurate dynamic stability derivatives at high angle of attack. A further deficiency of flight simulation of out-of-control flight is that the limited motions generated by the device are not truly representative, depriving the student of a very important part of his familiarization with this flight regime. Therefore, while some constituents of the training community maintain that a good job of procedural training in high-angle-of-attack maneuvering and departure avoidance can be accomplished with existing simulators, little promise is seen in the near term for totally satisfactory high-angle-of-attack training in flight simulators.

Narrated spin movies for most U. S. Navy high performance aircraft models now in service are provided to the fleet. These films accurately depict the out-of-control characteristics and avoidance and recovery procedures for the aircraft, and even go into some detail as to why the aircraft reacts as it does. Such films would be a useful classroom supplement to an in-flight departure training program -- they are no substitute.

Other "classroom" activities have included lecture tours by U. S. Naval Air Test Center pilots who had recently completed spin flight test programs. Of two recent tours, held within the A-4 community, the first (discussed in reference 11) included spin demonstration flights in TA-4's. Both the lectures and flights were well received, and highly effective from the standpoint of the direct communication afforded between fleet pilots and spin project pilots on a somewhat mysterious and foreboding flight regime. The demonstration flights generated much enthusiasm for formal spin training in TA-4's for the A-4 community, and effectively reduced or eliminated the apprehension of spinning the aircraft previously held by the participating pilots. In short, the reactions of the pilots to whom spins were demonstrated in TA-4's were very much like those of pilots who have participated in the trial A-7 departure-training program discussed earlier.

Hopefully, this discussion has shed some light on the high-angle-of-attack training deficiencies currently experienced in the U. S. Navy. Diligent efforts are being made to overcome the obstacles which stand in the way of flight training programs. The programs are desperately needed if we are to reduce our out-of-control losses.

U. S. NAVY HIGH-ANGLE-OF-ATTACK FLIGHT TEST

The preceding discussions have dealt with the problem areas faced by the U. S. Naval aviation community in the high-angle-of-attack flight regime. It is important to note that many of the conclusions could not have been reached through testing alone; the importance of the information available through close liaison with the aircraft users in the fleet must not be overlooked. Conversely, neither can we depend solely on operational experience for all the answers. While the fleet-supplied information is very useful in identifying problem areas, flight testing under controlled conditions by highly trained specialists remains an essential tool in solving these problems.

Such a capability is maintained at the U. S. Naval Air Test Center, located at Patuxent River Naval Air Station, Maryland. It is here that the U. S. Navy trains its test pilots, who are typically above-average Navy pilots with approximately 1500 hours flight time and with recent operational flight experience. Upon completion of an intensive eleven-month course of instruction at the Naval Test Pilot School, the pilots then generally serve a two- to three-year tour at the Naval Air Test Center in project work. In addition to the test pilots, a civilian engineering force highly qualified in flight testing is maintained. This team of pilots and engineers provides a necessary mix of recent fleet operational experience provided by the test pilots and a wealth of flight test experience and continuity provided by the engineers.

The Naval Air Test Center maintains an array of up-to-date flight test equipment and continues to expand its capabilities. A most recent addition is the Real-Time Telemetry Processing System, a complex assemblage of transmitting and receiving, data processing, and audio-visual equipment for the purpose of monitoring the progress of various flight test programs as they are being performed. The flight test applications of such a system are limitless, not the least important of which is in high-angle-of-attack testing.

The basic U. S. Navy philosophy of high-angle-of-attack testing has already been discussed. A brief description of test procedures and techniques will now be presented.

FLIGHT TEST PROCEDURES AND TECHNIQUES

There is probably no other type of flight testing which requires a more comprehensive background information gathering program than high-angle-of-attack testing. As previously discussed, U. S. Navy

programs occur only after the contractor has demonstrated the most critical out-of-control conditions of the particular aircraft involved. During the spin demonstrations, a wealth of important information is obtained which is fully exploited and utilized by the Navy test team. In addition, any areas which are not clear or need further amplification are discussed with the contractor pilot who flew the spin demonstration. Other useful information, obtained through analysis and aerodynamic model investigations which are performed prior to the contractor's spin work, are taken into account in finalizing the test plan. Where applicable, experience gained through previous high-angle-of-attack testing of similar configurations is used as a baseline for new testing. Only after all available data have been thoroughly examined can U. S. Navy high-angle-of-attack flight testing begin.

TEST INSTRUMENTATION

A properly instrumented aircraft is of maximum importance in high-angle-of-attack testing due to the rapidity with which the values of critical parameters change in out-of-control maneuvers. An on-board magnetic tape system and a telemetry transmitter and ground monitoring station constitute the primary recording media used at the Naval Air Test Center.

With telemetry data the project engineer is able to monitor in real time all parameters critical to safety of flight. Typical telemetered parameters might consist of the following: altitude, airspeed, angle of attack, aircraft rates (pitch, roll, yaw), aircraft attitudes (pitch, bank, sideslip), azimuth or heading, control positions, and engine operating conditions. The ground-recorder data are presented in a logical format with realistic polarity and with overlays showing parameter calibrations and limits, so that the project engineer can readily interpret the data. The on-board tape recorder greatly expands the data gathering capability, necessary for comprehensive data analysis and for reaching final conclusions. The list of recorded parameters can be increased to include such things as the cockpit control positions and forces, accelerations at the center of gravity and pilot's station, expanded engine monitoring, and many other useful parameters not sufficiently critical to safety of flight to warrant real-time monitoring.

Pilot's-eye-view motion picture coverage from a cockpit mounted camera and film shot from externally mounted cameras are used to record the relative motion of the outside world. The pilot's-eye-view should also include coverage of the cockpit instruments. These films are useful in reconstructing aircraft motions and show to some degree the relative violence of the maneuvers as seen from the cockpit. Motion picture films from phototheodolites (ground cameras) with radar tracking for aircraft acquisition are very useful in showing the real life sequence of the spin and provide the capability of slow motion analysis of aircraft motions. The film is subsequently used along with cockpit films for high-angle-of-attack training films and presentations to fleet pilots. Another feature available at the Naval Air Test Center is a real-time television monitoring capability which is part of the phototheodolite system. With this system the project engineer can visually monitor the aircraft motions in real time in concert with the telemetered parameters. With this information, the project engineer can be very helpful to the project pilot in describing the aircraft motions.

The test aircraft cockpit is configured to provide the pilot with controls for activation of all data recording devices. In addition, there are several devices which may be installed to provide the pilot with orientation cues and warning signals. These devices include oversized turn needle (or roll and yaw lights), single pointer altimeter (such as a glare-shield-mounted cabin pressure altimeter hooked to the regular static source), low altitude warning lights and aural warnings, and direct readouts of any parameters considered critical. However, some discretion must be applied in the addition of such devices; the cockpit should remain as near production as possible. By making the cockpit too non-representative of that to be delivered to the fleet, certain problems may be overlooked in the course of a flight test program that the fleet pilot will face when he encounters similar conditions in a production aircraft.

The project pilot will find it extremely difficult to remember the details of each maneuver long enough to write them on a kneeboard, another psycho-physiological phenomenon discussed in reference 5. Therefore, the pilot is provided with a kneeboard- or cockpit-mounted tape recorder, or a telemetry channel is provided for voice recording. The recording device permits the pilot to make a running commentary of the maneuver as it progresses through its various phases. The recorder is particularly valuable for mission suitability observations.

SAFETY CONSIDERATIONS

A chase aircraft is mandatory on all flights in a U. S. Navy high-angle-of-attack program. The chase aircraft must be compatible with the test aircraft. The use of a chase aircraft that has large disparities in performance with the test aircraft results in unnecessary flight delays while waiting for the chase aircraft to get in position. On the other hand, a chase aircraft with low-speed handling qualities inferior to the test aircraft may cause difficulty in closely monitoring the test aircraft in slow-speed flight and in the spin. The chase pilot is tasked to maintain surveillance of the test area, observe aircraft motion, count spin turns, and act as a safety backup by monitoring altitude and inspecting the test aircraft at frequent intervals for any external signs of damage or stress. A non-single-seat chase aircraft can provide space for a photographer to obtain air-to-air photo coverage of selected maneuvers.

Each aircraft to be tested in a U. S. Navy high-angle-of-attack program is fitted with an appropriate spin-recovery device. This emergency device can be utilized by the pilot when aerodynamic controls are ineffective in recovering the aircraft from spin. Most commonly used is a spin-recovery parachute which is deployed behind the aircraft to slow the yaw rate, lower angle of attack, and thereby force recovery from the spin. Spin-recovery parachutes are of many types and sizes and the requirements for a particular chute are determined through spin tunnel tests. Anti-yaw rockets have also been used as spin-recovery devices. But whatever the type, the spin-recovery device used must have been demonstrated by the contractor during the spin demonstration in the following manner: the device is checked out on the ground and in flight prior to the commencement of the high-angle-of-attack demonstration program to ensure that its mechanism functions properly. If, at the end of the demonstration program, the device has not been used to recover from a critical spin condition, such a condition is set up specifically for the purpose of demonstrating that the spin-recovery device will force recovery. The project team should be thoroughly familiar

with the operation and any possible limitations of the emergency recovery device.

Emergency spin-recovery devices obviously require actuation from the cockpit. The actuation devices must be easily accessible and operated with one pilot movement. Favorite locations are the left top of the glare shield or the left forward instrument panel. A spin-recovery parachute requires jettisoning after spin recovery. The jettisoning can be nearly as critical as the deployment; therefore, the jettison actuator should be designed and located with similar care. A de-arming feature must be provided so that the spin-recovery device is armed only when the high-angle-of-attack testing is in progress. Accidental deployment of a rocket or a parachute during the takeoff or landing could be disastrous.

FLIGHT PROGRAM

There is probably no other type of flight testing which requires a more comprehensive and logical buildup program than high-angle-of-attack evaluations. Program planning begins with a complete study by the pilot and engineer of all previous spin data on the aircraft to be evaluated, as previously discussed, as well as a look at earlier spin reports in order that they appraise themselves of any problem areas which might have occurred in previous evaluations. The project pilot will provide himself with several spin familiarization flights in aircraft cleared for intentional spins.

Having completed the planning phase, the project pilot is ready to begin buildup flights in the aircraft to be evaluated. Prior to commencement of actual high-angle-of-attack tests, the project pilot devotes some flights to dive pull-out at various airspeeds, angle of attack, and power settings with and without speed brake. A dive pull-out table can then be prepared from which decision altitudes can be established. Decision altitudes should include:

1. Altitude at which to stop other than optimum recovery tests;

2. Altitude for spin-recovery device deployment;

3. Ejection or bailout altitude.

It is important for the pilot and the engineer to have these altitudes fixed firmly in their minds prior to proceeding with any high-angle-of-attack testing. If a certain critical altitude is reached, the pilot will have a preplanned course of action to follow and will not delay in making the proper decision as to emergency spin-recovery device actuation or ejection. Should the pilot fail to immediately recognize the criticality of his situation, the project engineer on the ground can provide the warning.

Flying qualities indicators may be present which can help predict the stall or out-of-control characteristics. Static longitudinal and lateral-directional stability testing may provide clues to the type of stall or departure to expect. Stall testing should begin in the least critical loading and center of gravity position as predicted from flying qualities data and wind tunnel studies. Departure and post-stall gyration investigations logically follow the stall testing. A spin may be encountered during this phase of the investigation, so the pilot must be prepared to recover from a spin even at this point. Again, the testing should begin with the least critical loading and center of gravity position. A logical buildup sequence of entry conditions (i.e., power setting, amount of control application, rate of control application, etc.) should be used and repeated for the more critical loadings and center of gravity positions. Having successfully completed the buildup, critical conditions (i.e., maneuvers in critical loadings, fully developed spins, etc.) can be evaluated with a reasonable degree of confidence and safety. A further, more thorough, discussion of buildup techniques may be found in reference 12.

Unusual or erratic engine operation may occur. This is to be expected because of the extreme high angles of attack, high yaw rates, and sideslip angles associated with these flights. The pilot must, therefore, be very familiar with such procedures as clearing compressor stalls, airstarts, and flameout landing pattern. In some cases, it may be necessary to fit the aircraft with some auxiliary power devices. For example, a ram air turbine provided for emergency electrical power may not operate if deployed in a spin. In this case, it may be necessary to install a battery to provide for ignition, critical electrical demands, or possibly even run auxiliary hydraulic pumps to provide adequate flight control. If the aircraft is prone to engine flameouts in a spin, it may be valuable to fit it with a continuous ignition circuit.

DATA REQUIREMENTS

There is a myriad of pertinent data collected during a high-angle-of-attack program. These data are presented in the final report in the form of such time histories as various important rates, positions, control deflections and forces, and altitude. Qualitative data provided by the pilot, however, are among the most important data presented. The description of such things as how it feels in the cockpit and the ability of the pilot to remain orientated in the out-of-control maneuver are among the most important portions of the evaluation from the pilot's point of view. For example, use of angle of attack for dive pull-out following spin recovery may be extremely critical. It is important for the project pilot to define the pull-out limitation in terms of seat-of-the-pants cues. Again, it is in obtaining these types of data that the cockpit tape recorder becomes invaluable. Occasionally, all engine parameters may not be instrumented and it will be important for the pilot to observe engine operating characteristics during the high-angle-of-attack maneuver. It is up to the project pilot to ensure that his important cockpit observations are not lost in a maze of quantitative data. A pilot-oriented, qualitative assessment of the post-stall, spin, and spin-recovery characteristics must be foremost in his mind during the course of the test program.

RECENT U. S. NAVY HIGH-ANGLE-OF-ATTACK FLIGHT TEST EXPERIENCE

TA-4 AIRCRAFT

A U. S. Navy spin evaluation of the TA-4 aircraft was performed not only to define the TA-4 spin characteristics and recovery procedures, but also to evaluate the suitability of the TA-4 as a spin trainer.

The TA-4 aircraft exhibited no tendency to spin inadvertently. The aircraft had to be forced to spin by applying and holding pro-spin controls. With wing tanks containing 2,000 lb or more fuel, the aircraft could consistently be forced into a classic erect spin. While the erect motions were not disorienting, the aircraft easily transitioned from erect to inverted gyrations which were found to be highly disorienting and uncomfortable to the pilot, and could overstress the aircraft. The tests indicated that inverted spins could be avoided in certain configurations through precise manipulation of the controls by the pilot. The Naval Air Test Center recommended in its report that the TA-4 aircraft be cleared for intentional spins by pilots who have been trained to avoid inverted spins. But the existence of the inverted mode led to a concern that long term training objectives could be jeopardized by premature embarkation on a spin training program with a less than satisfactory aircraft. Therefore, further development of the TA-4 will be undertaken in an attempt to define a configuration which will be satisfactory for spin training. To date only minor configuration modifications have been considered. If promising results are indicated from the spin tunnel tests of these candidate configurations, flight testing will be performed, followed by final resolution of a further course of action.

A-4 AIRCRAFT

The A-4M aircraft has been evaluated throughout the high-angle-of-attack flight regime, including intentional spins. Testing was conducted with the aerodynamic slats both free and locked in the closed position to evaluate the high-angle-of-attack characteristics of both wing configurations. The tests were performed using the TA-4 results as a planning guide. Extensive investigation of a particular characteristic was planned only if deviation from that TA-4 characteristic was observed. Few significant deviations of the free-slatted A-4M from TA-4 behavior were encountered whereby it was concluded that the TA-4 could be used to demonstrate the spin characteristics of the single place A-4, should spin training in TA-4's become feasible. However, one deviation from the TA-4 characteristics was that the A-4M did not exhibit the tendency to transition from an erect to an inverted spin. In fact, autorotative inverted spins were not attained during the A-4M evaluation. In the locked-slat configuration the A-4M exhibited increased erect spin susceptibility. Full aft longitudinal control with neutral aileron and rudder was sufficient to achieve erect spins. Optimum spin recovery technique was unchanged from the free-slatted A-4M aircraft.

A-4/TA-4 NOSE-HIGH LOW-AIRSPEED DEPARTURE AND RECOVERY EVALUATION

The number of aircraft losses and near-losses resulting from departure from nose-high low-airspeed conditions during air combat maneuvering led to the conclusion that insufficient knowledge of A-4/TA-4 characteristics in that flight regime was available. Therefore, a flight test program was established for investigation of A-4/TA-4 nose-high low-airspeed departure and recovery characteristics.

Significant conclusions drawn from the TA-4 phase of the tests were as follows:

1. Departures from nose-high low-airspeed conditions were generally mild when entered from aircraft nose-up attitudes less than 90 degrees and greater than 100 degrees.

2. Departures resulting from vertical (90 to 100 degree) attitudes at zero airspeed were very violent and disorienting. Of 33 vertical aircraft nose-up/zero airspeed maneuvers, two unintentional inverted spins resulted.

Of interest in the A-4M phase of the evaluation was that the magnitude and rate of yaw excursions during A-4M departures from nose-high low-airspeed condition was significantly less than the same maneuver in the TA-4 under all conditions tested. The A-4M was more spin resistant than the TA-4 from nose-high low-airspeed departures. No spins occurred during A-4M tests even with small intentional control inputs by the pilot.

A-7 AIRCRAFT

As described earlier in this paper, the A-7 aircraft, while highly resistant to spins, is subject to violent and disorienting aircraft motions following accelerated stalls, combined with excessive altitude loss. The pilot is faced with a difficult task in avoiding departure during vigorous maneuvering. In an effort to improve maneuvering capability and improve or eliminate the adverse stall/departure characteristics, the contractor, Vought Systems Division of LTV Aerospace Corporation, designed and flight tested a maneuvering flap system. Automatic leading- and trailing-edge flap extension and retraction as a function of airspeed/Mach number and angle of attack, and a modified high-angle-of-attack aileron/rudder interconnect were incorporated in a test aircraft to enhance the high-angle-of-attack flight characteristics and improve maneuvering performance. The Naval Air Test Center performed limited flight tests to obtain qualitative and quantitative data and to provide an assessment of the characteristics of the system.

The conclusion of this evaluation was that the A-7 automatic maneuvering flap system displayed an outstanding potential to significantly improve the gear-up high-angle-of-attack characteristics of the A-7 aircraft during both maneuvering and non-maneuvering tasks, and the recommendation for its further development and incorporation into fleet aircraft has been made. Whether fiscal constraints will allow this objective to be pursued remains to be seen.

T-34C AIRCRAFT

The T-34C aircraft is a two-place (tandem), single engine, primary trainer, derived from the T-34B. It is powered by a United Aircraft PT6A-25 turbo-prop engine. The aircraft was evaluated during intentional spins to assess the suitability of spin and spin-recovery characteristics for the primary trainer mission. Spin flight testing of the T-34C by Navy pilots revealed the following unsatisfactory characteristics: the fully developed erect spin was characterized by extremely high spin rates. The slowest steady-state spins, with rates of 140 degrees per second, resulted when pro-spin controls were maintained. The high spin rates caused excessive pilot disorientation and discomfort. Furthermore, complicated sequencing of control inputs was required to recover the T-34C aircraft from fully developed erect spins. The Naval

Air Test Center concluded that the high spin rate and complicated spin-recovery characteristics of the T-34C aircraft would preclude its use for intentional spinning. Beech Aircraft Corporation then started a development program in conjunction with engineers at the National Aeronautics and Space Administration Spin Tunnel facility at the Langley Research Center in an attempt to develop an aerodynamic modification that would reduce the spin rate and improve the spin-recovery characteristics. After many hours of spin tunnel and flight tests, a suitable configuration was established by adding strakes and ventral fins to the empennage. A final Naval Air Test Center evaluation of the modified aircraft revealed that the modified T-34C exhibited a reasonably mild steady erect spin which was easily and consistently recoverable in one turn or less. The overall spin characteriscics of the T-34C aircraft are now repeatable and predictable and it should prove to be an excellent spin training vehicle in the U. S. Navy's basic flight training program.

REFERENCES

1. Donald D. Smith, LCDR, U.S.N., "Spinning the A-7," The Society of Experimental Test Pilots 1970 Report, XIV Symposium Proceedings, 24-26 September 1970, Technical Review Volume 10, No. 2, pp. 245-253.

2. LCDR D. D. Smith, U.S.N., LT E. R. Curtis, U.S.N., Mr. W. G. McNamara, "Model A-7A/B Airplane Spin Evaluation Final Report," Naval Air Test Center Technical Report No. FT-72R-71, 24 September 1971.

3. LT E. W. Clexton, Jr., U.S.N., LT D. A. Sullivan, U.S.N., Mr. J. L. Dunn, "Final Report--Evaluation of the Spin and Recovery Characteristics of the F-4B Airplane," Naval Air Test Center Technical Report No. FT-88R-67, 27 December 1967.

4. Elbert L. Rutan, LT Collet E. McElroy, U.S.A.F., MAJ Jerauld R. Gentry, U.S.A.F., "Stall/Near Stall Investigation of the F-4E Aircraft," Air Force Flight Test Center Technical Report No. 70-20, August 1970.

5. D. A. Schultz, "Physcho-Physiolcgical (sic) Phenomena Encountered in Spins," Wright Air Development Center Airplane Spin Symposium, 27-28 February 1957.

6. W. R. Burris and J. T. Lawrence, "Aerodynamic Design and Flight Test of U. S. Navy Aircraft at High Angles of Attack," AGARD Fluid Dynamics Panel Specialists Meeting on Fluid Dynamics of Aircraft Stalling, Lisbon, Portugal, 26-28 April 1972.

7. Charles A. Sewell and Raymond D. Whipple, "Initial Spin Tests," Pilots Handbook for Critical and Exploratory Flight Testing, Society of Experimental Test Pilots, Lancaster, California, and AIAA, New York, 1972, pp. 36-56.

8. Burt Rutan, "Flight Testing - Spin Test or Spin Prevention Test?," The Society of Experimental Test Pilots 1970 Report, XIV Symposium Proceedings, 24-26 September 1970, Technical Review Volume 10, No. 2, pp. 255-260.

9. Patrick S. Sharp and CAPT Collet E. McElroy, U.S.A.F., "Background Information and User Guide for MIL-S-83691," Air Force Flight Test Center Technology Document No. 73-2, March 1974.

10. Robert J. Woodcock and Thomas J. Cord, "Stall/Spin Seventy Years Later," Air University Review, Volume XXV, No. 4, May-June 1974, pp. 25-36.

11. LCDR Richard K. Pottratz, "Spin It!," Approach Magazine, October 1973, pp. 26-28.

12. LTCOL E. B. Russell, U.S.M.C., J. A. Nial, and LT E. R. Curtis, U.S.N., "The U. S. Navy Stall/Post-Stall/Spin Program," Stall/Post-Stall/Spin Symposium, Aeronautical Systems Division AFFDL, Wright-Patterson Air Force Base, Ohio, 15-17 Dec 1971.

ACKNOWLEDGEMENT

The authors wish to acknowledge the contributions of LT Jack Paschall, USN, to this paper. LT Paschall served as a test pilot at the Naval Air Test Center for a period recently ended during which he participated in many of the high-angle-of-attack flight test programs. Although he was transferred prior to being able to participate in the writing of this paper, his contributions to the test programs as Project Pilot and numerous detailed discussions with him concerning the problems associated with the high-angle-of-attack flight regime provided invaluable information for the preparation of this paper.